

1st Hull Performance & Insight Conference

HullPIC' 16

Castello di Pavone, 13-15 April 2016

Edited by Volker Bertram

Sponsored by



www.jotun.com



DNV·GL

www.dnvgl.com

**HUBERT
PALFINGER
TECHNOLOGIES**
LEGENDARY IN INNOVATIONS.

www.hpalfingertech.com



www.napa.fi



www.hoppe-marine.com



www.kyma.no



www.jsira.jp



www.propulsiondynamics.com



www.eniram.fi



www.hempel.com



www.akzonobel.com

MARORKA

www.marorka.com



www.bmtsmart.com



www.enamor.pl



Index

Volker Bertram <i>Added Power in Waves – Time to Stop Lying (to Ourselves)</i>	5
Eva Herradón de Grado, Volker Bertram <i>Predicting Added Resistance in Wind and Waves Employing Artificial Neural Nets</i>	14
Thilo Dückert, Daniel Schmode, Marcus Tullberg <i>Computing Hull & Propeller Performance: Ship Model Alternatives and Data Acquisition Methods</i>	23
Michel Visonneau, Ganbo Deng, Patrick Queutey, Emmanuel Guilmineau, Alvaro del Toro Llorens <i>High-Fidelity Computational Analysis of an Energy-Saving Device at Model Scale</i>	29
Andreas Krapp, Volker Bertram <i>Hull Performance Analysis – Aspects of Speed-Power Reference Curves</i>	41
Erik Hagestuen, Bjarte Lund, Carlos Gonzalez <i>Continuous Performance Monitoring – A Practical Approach to the ISO 19030 Standard</i>	49
Sergiu Paereli, Andreas Krapp, Volker Bertram <i>Splitting Propeller Performance from Hull Performance – A Challenge</i>	62
Tsuyoshi Ishiguro, Hideo Orihara, Hisafumi Yoshida <i>Verification of Full-Scale Vessel’s Performance under Actual Sea by On-board Monitoring System: A Shipbuilder’s View</i>	70
Dinis Oliveira, Lena Granhag <i>Future Work on Drag and Boundary Layer Properties of Biofouling Collected From Commercial Vessels</i>	82
Ryo Kakuta, Hideyuki Ando, Takashi Yonezawa <i>Utilization of Vessel Performance Management System in Shipping Company</i>	96
Mark Bos <i>How MetOcean Data Can Improve Accuracy and Reliability of Vessel Performance Estimates</i>	106
Michael Haranen, Pekka Pakkanen, Risto Kariranta, Jouni Salo <i>White, Grey and Black-Box Modelling in Ship Performance Evaluation</i>	115
Falko Fritz <i>Practical Experiences with Vessel Performance Management and Hull Condition Monitoring</i>	128
Jan Wienke, Jörg Lampe <i>Energy Efficiency Design Index in View of Performance Monitoring</i>	137
Lars Greitsch, Tom Goedicke, Robert Pfannenschmidt <i>Numerical Towing Tank versus Noon Data – Powering Predictions using RANSE CFD</i>	145

Antti Solonen <i>Experiences with ISO-19030 – and Beyond</i>	152
Angelo Odetti, Marco Bibuli, Gabriele Bruzzone, Massimo Caccia, Andrea Ranieri, Enrica Zereik <i>Cooperative Robotics – Technology for Future Underwater Cleaning</i>	163
Charles Badoe, Stephen Turnock, Alexander Phillips <i>Impact of Hull Propeller Rudder Interaction on Ship Powering Assessment</i>	178
Erik van Ballegooijen, Tiberiu Muntean <i>Fuel Saving Potentials via Measuring Propeller Thrust and Hull Resistance at Full Scale: Experience with Ships in Service</i>	192
Wojciech Górski <i>Role of Reference Model in Ship Performance Management</i>	203
Andrea Orlandi, Riccardo Benedetti, Valerio Capecci, Gianni Messeri, Albert Ortolani, Luca Rovai, Andrea Coraddu <i>Evaluation of the Fuel Saving Potential using High Resolution MetOcean Forecasts and Detailed Ship Performance Models</i>	215
Michael vom Baur <i>Acquisition and Integration of Meaningful Performance Data on Board Challenges and Experiences</i>	230
Geir Axel Oftedahl <i>Advances in Measurements of Hull Performance: Implications for Buyers and Sellers of Performance Enhancing Technologies and Solutions</i>	239
Crystal Lutkenhouse, Brian Brady, Jamaal Delbridge, Elizabeth Haslbeck, Eric Holm, Dana Lynn, Thad Michael, Angela Ross, David Stamper, Carol Tseng, Anthony Webb <i>Baseline Propeller Roughness Condition Assessment and its Impact on Fuel Efficiency</i>	245
Kenichi Fukuda, Yoshihisa Okada, Kenta Katayama, Akinori Okazaki, Masatoshi Nakazaki <i>NAT 5000 - Nakashima Advanced Virtual Tank 5000</i>	263
Yakabe Fumi <i>Observational Study on Powers Estimated by Shaft Torque and Fuel Consumption</i>	271
Ditte Gundermann, Tobias Dirksen <i>A Statistical Study of Propulsion Performance of Ships and the Effect of Dry Dockings, Hull Cleanings and Propeller Polishes on Performance</i>	282
Svend Søyland, Geir Axel Oftedahl <i>ISO 19030 – Motivation, Scope and Development</i>	292
Barry Kidd, Alistair A. Finnie, Haoliang Chen <i>Predicting the Impact of Fouling Control Coatings on Ship Powering Requirements and Operational Efficiency</i>	298
Niels Hentschel, Christoph Rühr, Niklas v. Meyerinck <i>Automated Hull Surface Preparation and Paint Application and the Potential Influence on Ship Performance</i>	312

Giovanni Cusano, Mauro Garbarino, Stefano Qualich, Giuseppe Stranieri <i>Monitoring, Reporting, Verifying and Optimizing Ship Propulsive Performance: A Support System to Ship Management Focused on Energy Efficiency</i>	319
Sigurdur Jonsson, Helgi Fridriksson <i>Continuous Estimate of Hull and Propeller Performance Using Auto-Logged Data</i>	332
Cezary Afeltowicz <i>Performance Monitoring & Hull Performance: A Ship Manager's View</i>	339
Index of authors	349
Call for Papers for next conference	

Added Power in Waves – Time to Stop Lying (to Ourselves)

Volker Bertram, DNV GL, Hamburg/Germany, volker.bertram@dnvgl.com

Abstract

This paper reviews approaches to predict added resistance and added power in seaways. It concludes that there is no practical approach to quantify the required added power in waves for performance monitoring. While heave and pitch motions for conventional ships are predicted well by virtually all approaches, motions in oblique waves and added resistance are much more difficult to predict, especially in short waves. The additional uncertainty from quantifying the seaway as input makes current approaches for correction highly inaccurate.

1. Introduction

Ships in waves require more power at given speed or have lower speed at given power than in calm water. Quantifying the required added power (respectively the imposed speed loss) is an issue for performance monitoring. With sufficiently accurate correction (a.k.a. normalization) for the effect of seaways, we could relax filtering criteria and get trends faster.

ISO 19030 imposes rather strict filtering for wind forces with an upper limit of Beaufort 4. For most ships, the corresponding sea state (see e.g. *Bertram (2012)* for converting wind speed into corresponding fully matured seaway) will induce lower added resistance due to waves than the direct wind force. The standard does not consider swell, i.e. wind sea that was generated at a different time and place and does not correspond to the current wind condition. The standard implicitly assumes that the wind sea that corresponds to the current wind condition can be neglected, this appears reasonable for the imposed limit of Bft 4. However, this strict filtering means that many data sets are lost which is particularly inconvenient for approaches not using continuous monitoring (i.e. the majority of present monitoring approaches).

Better correction procedures generally allow more lenient filtering. Several performance monitoring approaches have implemented more lenient filtering for sea states, either directly or indirectly via wind criteria. As with all such criteria, limits of applicability are fuzzy. Theoretically, applicability limits should be a function of introduced error, which (for added power in seaways) will depend on seaway, ship geometry, speed, angle of attack, chosen approach for correction, etc. In practice, we cannot quantify the expected error. This leaves then qualitative considerations which are often by necessity speculative even for dedicated experts of ship seakeeping. For the typical developer or user of performance monitoring systems, added resistance in waves is a minefield where the best advice is to stay clear (as implicitly done by the standard ISO 19030 approach). But if correction for waves is used a deeper understanding of capabilities and limitations of such correction approaches is advisable.

In the following, I shall discuss required added power in waves, based on my experience and with the perspective of performance monitoring in mind. The statements reflect my personal opinion, and are subject to debate among fellow seakeeping experts and colleagues from DNV GL.

2. General approaches to “hydrodynamic knowledge”

As for other corrections for performance monitoring (e.g. for the effect of draft on required power), we need hydrodynamic knowledge which may be imbedded in formulas, tables or curves. In principle, there are various approaches that may be used:

- Model tests
Classical model tests are time consuming and expensive (due to the many test runs required for parameter studies, the long waiting time between tests before water is sufficiently calm

again, and the relatively rare installations that can investigate oblique waves). For motions with strong viscous effects (yaw, sway and to lesser degree also roll), model test behavior differs from full-scale ship behavior. For practical purposes, seakeeping model tests are not an option to create the knowledge base. They are only used to validate numerical approaches.

- Full-scale measurements on-board ship whilst at sea
Deriving information from such measurements is problematic due to external “noise” in the measurement, but increasingly performed. Ambient noise must then be removed using either filtering. Adding engineering intelligence in the form of theoretical seakeeping models can improve the accuracy of such system identification. The uncertainty concerning the incoming waves introduces the largest errors in this approach.
- Seakeeping simulations
Most seakeeping codes decompose a seaway into regular waves of various wave length, direction and height, then determine ship responses to these regular waves and approximate the response in a natural seaway as sum of the responses to individual regular waves. This classical and popular approach is computationally efficient, but has limited accuracy with increasing errors for higher sea states. The accuracy depends on further details of the computational model. More advanced seakeeping codes allow nonlinear simulations, but are computationally so expensive that they are not considered for performance monitoring purposes.
- “Design formulas” (statistically derived formulas)
Large data sets (generated by whatever approach) may be used to derive simple design formulas that are readily programmed in any IT (information technology) environment. Classically, we used regression analysis to derive such simple formulas, but more recent data fitting approaches such as Artificial Neural Nets might also be used. Typically semi-empirical approaches are used, i.e. some physical insight (“The resistance will depend quadratically on significant wave height”) and some data fitting (e.g. for a single resistance coefficient) will be combined. The information on the original data used to derive the design formula is generally lost. Limits of applicability are either not known or ignored.

For model tests and computational approaches, the input signal “wave height” is assumed to be given exactly and the discussion about accuracy then focusses often only on the accuracy of the predicted added resistance. For performance monitoring, we need to consider the additional uncertainties for the waves (both frequency spectrum and wave heights) and the factors affecting required power (e.g. changes of propulsive efficiency in waves). We will consider these additional uncertainties further below and focus first on the computation of ship motions and added resistance in waves.

2. Computational seakeeping methods

Since the 1950s, a range of computational seakeeping methods has evolved. *Beck and Reed (2001)* and *Bertram (2012)* are recommended for structured overviews. The most important approaches are:

- (Linear) Strip method
Strip methods are the oldest and still most popular approach for seakeeping analyses. The essence of strip theory is to reduce the 3D hydrodynamic problem to a series of 2D problems that are easier to solve. The underwater part of the ship is divided into a number of strips, typically 20-40, Fig.1. Although the underlying physical models are crude, strip methods are able to calculate heave and pitch motions and several other properties of practical relevance accurately enough for “normal” ships. A multitude of software codes based on the strip method approach has been developed over the decades, but mostly in academia and many codes are now obsolete, undocumented and not portable. Commercial strip method codes include OC-TOPUS (Amarcon), VERES (Marintek), and VisualSMP (Proteus Engineering).

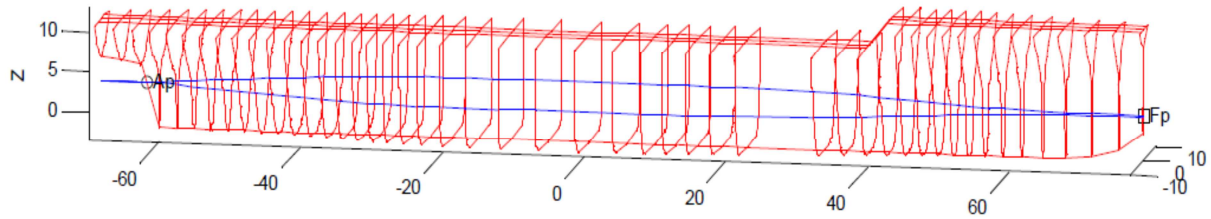


Fig.1: Typical representation of a ship in a strip method, *Alexandersson (2009)*

- **3D Green Function Method (GFM) and Rankine Singularity Method (RSM)**
 For offshore applications, first-order forces and motions are calculated reliably and accurately by 3D GFM, Fig.2. Commercial codes like WAMIT (WAMIT Inc.) and AQWA (ANSYS) are widely used. GFM are less suitable at non-zero speed. All GFMs are fundamentally restricted to simplifications in the treatment of the steady flow which may introduce large errors in local pressures, especially in the bow region. 3D RSM, developed since the 1990s, capture more physics, albeit at a higher computational effort, *Bertram and Yasukawa (1996)*. Both GFM and RSM share inherent difficulties representing flows around immersed transom sterns.

Recently, the RSM codes FATIMA (MARIN) and DNV GL Rankine have presented good results for added resistance in validation studies, outperforming other codes. Both FATIMA and DNV GL Rankine are used for commercially offered analyses, but are not commercially available. The computations required for performance monitoring will require variations of at least wave length and wave direction, but probably also speed and draft. A suitable knowledge based for added power in waves will then require an effort that will range between 10000 and 30000 €, depending on how streamlined processes are and how extensive the considered parameter variations are. This financial commitment is unlikely to come from the market.

- **CFD codes**
 State-of-the-art CFD (Computational Fluid Dynamics) codes solve the Reynolds-Averaged Navier-Stokes Equations (RANSE), modeling turbulent fluctuations by semi-empirical turbulence models, Fig.3. This approach captures all relevant physics, but is computationally expensive; CFD is prohibitively expensive for systematic computations of added resistance in waves.

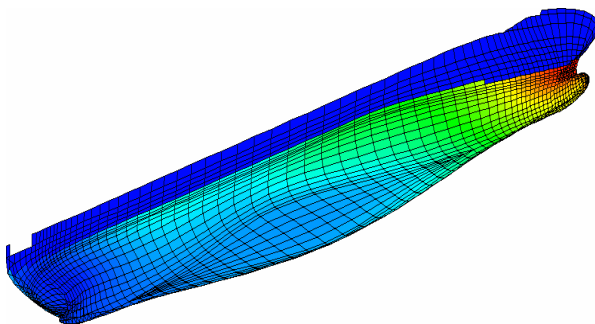


Fig.2: 3D GFM for ship

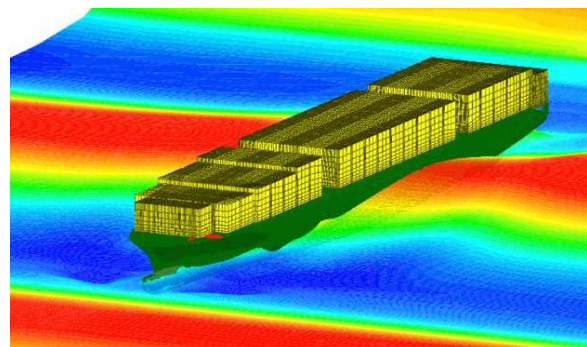


Fig.3: RANSE seakeeping simulation

3. Expect higher errors in performance monitoring applications

With appropriately chosen problems (i.e. ones that match the limitations of a given computational method), all methods work well. In publications, we see always “good agreement”. However, virtually always the presented picture is too optimistic.

Despite decades of research on the topic, added resistance in waves has eluded accurate prediction in short waves ($\lambda/L < 0.5$, where λ denotes the wave length and L the ship length). In addition, we have large uncertainties for the incident waves which propagate quadratically into the added resistance.

Short-coming of assorted approaches are discussed in the following.

3.1. Semi-empirical formulas

Various analytical and semi-empirical formulas to estimate added resistance in waves R_{aw} have been proposed in the course of time; see e.g. *Alexandersson (2009)*. One of the oldest and simplest of these dates back to *Kreitner (1939)*, as given by *ITTC (2005)*, *Hansen (2011)*:

$$R_{aw} = 0.64 \cdot g \cdot H_s^2 B^2 C_B \rho \frac{1}{L_{wl}} \left(\frac{2}{3} + \frac{1}{3} \cos \beta \right)$$

H_s denotes the significant wave height. B the ship's beam, L_{wl} the ship's waterline length, C_B its block coefficient, ρ the sea water density, $g=9.81 \text{ m/s}^2$ and β the encounter angle ($0^\circ = \text{head waves}$).

This formula has been used for many years to correct for added resistance in waves in sea trials. There has been increasing criticism of this practice as such, but let us focus here on applications for performance monitoring. The formula has been intended mainly for ships in head waves ($|\beta| < 10^\circ$).

Prof. H. Yasukawa of Hiroshima University supplied experimental data for two standard test cases: the KVLCC2 tanker hull, and the KCS containership hull. Both test cases have been tested by several ship model basins and have public-domain geometry. The tests were performed in the model basin of Hiroshima University in head waves, using irregular wave spectra following ISSC standard spectra. In each case, 8 runs were performed to ensure low scatter of results. The average of the 8 test runs (scaled to full scale) were taken for comparisons with the Kreitner formula, Fig.4. For the tanker and near design speed (15 kn), the Kreitner formula agrees well with the experiments, with an average error of 10%. But this changes for lower speeds. At 5 kn, where the average error is ~50% (i.e. the Kreitner formula estimates the added resistance by a factor of 2. For the containership, we have an error of 50%, but underestimating the value, for design speed (24 kn) and good agreement for design speed. My conclusion is that we may have up to 50% error irrespective of ship type, on average over realistic operational speed profiles perhaps half that value. The formula will yield speed-dependent variations of errors.

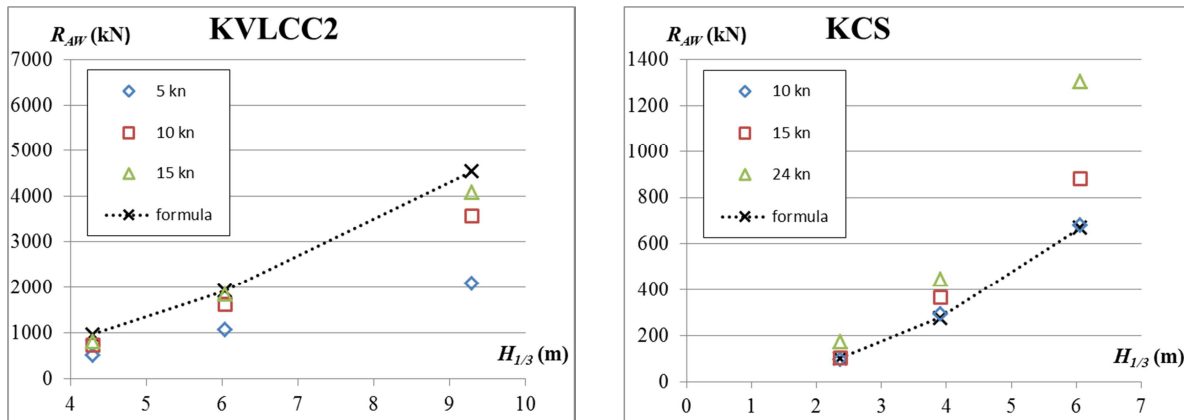


Fig.4: Added resistance for KVLCC2 tanker (left) and KCS containership (right); [Kreitner] formula compared to model test results for 3 speeds.

Dr. V. Shigunov (DNV GL) supplied detailed simulation results of the software “DNV GL Rankine” from a confidential joint-industry project. Again, a tanker and a containership were investigated. In this case, the focus lies on the variation of encounter angle β . Fig.5 shows results for design speed.

For head waves ($\beta = 0^\circ$), the Kreitner formula overestimates the added resistance by 140% for the tanker and 40% for the containership. The relative error increases towards following waves, reaching almost 1000% for the tanker and 200% for the containership.

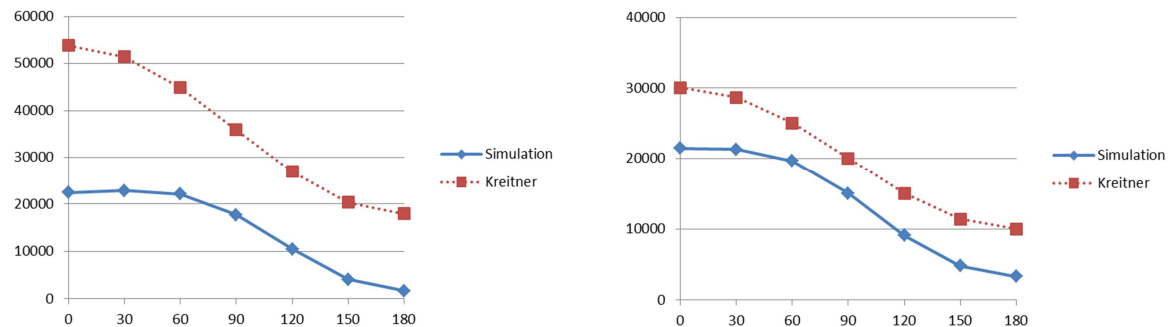


Fig.5: Added resistance for a tanker (left) and a containership (right); Kreitner formula compared to Rankine simulations for design speeds, variation over encounter angle β

A constant error or a Gaussian distributed error with average zero would be easier to accept for performance monitoring. The magnitude of the errors and the dependence on speed and encounter angle limit the applicability of the Kreitner formula. It may be applied for low sea states where the added resistance is a small portion of the overall resistance; but the added accuracy should not be expected to be much higher than if a correction is omitted completely (i.e. accepting a constant error of 100% for the added resistance in waves), as currently recommended for the default method in ISO 19030. If the added resistance becomes significant compared to the calm-water resistance, such a simple formula should not be applied and such data sets should rather be filtered out.

Various researchers have come to similar conclusions for assorted semi-empirical approaches for added resistance in waves, Fig.6:

- *Nabergoj and Prpić-Oršić (2007)* compared five approaches for a ro-ro vessel, with large scatter of results (factor of four (400%) between lowest estimate and highest estimate).
- *Perez Arribas (2006)* discussed various semi-analytical approaches and compares three in more detail against model tests for a ship in head waves. Results showed scatter by a factor 3 (300%).
- *Boom et al. (2008,2013)* compare a different set of empirical wave correction methods coming for a product tanker. Results showed scatter by more than a factor 10 (1000%). “The results were shockingly different”.
- *Söding and Shigunov (2015)* tested a proposal for ISO 15016 (sea trials) and *IMO (2013)* based on *Tsujimoto et al. (2008)*, concluding: “The proposal to IMO for natural seaway [...] appears much too large in all cases.”

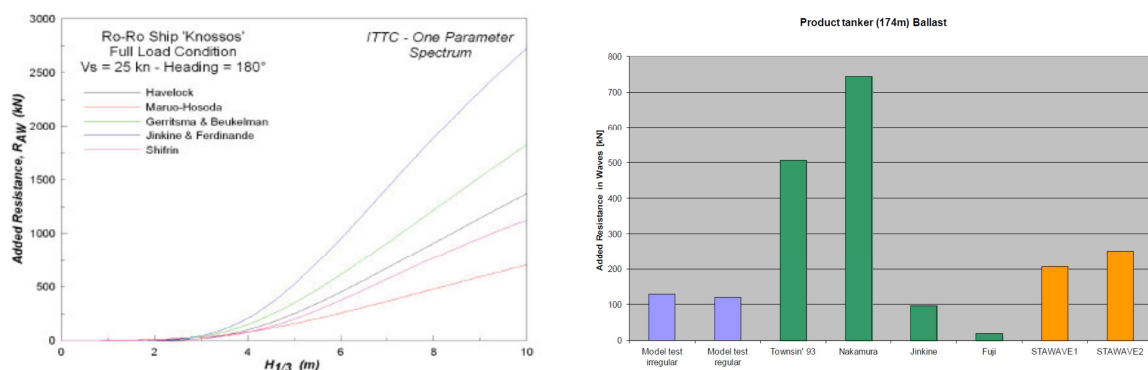


Fig.6: Comparison of semi-empirical added resistance approaches: *Nabergoj and Prpić-Oršić (2007)* (left) and *Boom et al. (2013)* (right), where semi-empirical methods are green bars

For pragmatic purposes, filtering is the only “solution”. A correction based on simple approaches cannot pretend to improve results in performance monitoring significantly.

3.2. Computational approaches

Added resistance in waves is more difficult to compute than motion. Motions are “first-order” quantities (i.e. for small wave height proportional to the wave height), added resistance is a “second-order” quantity (i.e. for small wave height proportional to the wave height squared). Second-order quantities are generally much more difficult to compute than first-order quantities.

The added resistance contains two main contributions:

- Contributions due to the waves generated as a consequence of the ship’s motions (“radiation”)
- Contributions due to reflection and distortion of the incident wave field (“diffraction”)

Some methods omit contributions coming from diffraction, others from ship motions, e.g. Faltinsen’s method for short waves, *Faltinsen et al. (1980)*, *Steen and Faltinsen (1998)*. Such omissions of terms can be justified for certain subsets of problems, e.g. very large ships in short waves, or slender ships in head seas. Unfortunately approaches derived for a specific application are frequently used beyond their realm of applicability.

Most publications show results for head waves, for several reasons:

- Many model basins can measure only head or following seas. Therefore, model test data is more readily available for ships in head waves (where heave and pitch motions dominate).
- Heave and pitch motions are relatively well predicted by all models. They are “computationally friendly”. If you want to show good agreement, show heave and pitch motions.

Ships in oblique waves are much more difficult to compute (and to measure). In oblique waves, the ship has also yaw, sway and roll motions which contribute to added resistance. Yaw and sway motions will create vortex shedding which is not captured by simpler computational approaches and sometimes not even CFD approaches (due to insufficient resolution). In addition, yaw motions depend on the rudder action, particularly at low frequencies. Without a coupled autopilot maneuvering module, motions (and subsequently added resistance) are over-predicted. This introduces large errors for added resistance for low encounter frequencies (i.e. oblique following waves).

Many publications show results for ships without large transom sterns. This may be motivated by published validation data for ship hulls which date back to times when large transom sterns were not customary for ships. Good results are then shown for ships with simpler geometries and simpler flows that can be handled by simpler computational methods. For complex ship geometries (with strongly non-linear hull shape near the average waterline), physics become more complicated and predictions more difficult. The physics may then be captured by a CFD approach, but not the common simpler approaches.

Many publications state implicitly or explicitly that added resistance in waves is highest for head waves, e.g. *Perez Arribas (2006)*, *Hansen (2011)*. This is not true in general. In our experience, the highest added resistance occurs for oblique waves, say 10° - 30° off head waves. All simple approaches using a monotonously decaying function (e.g. cos-function) with angle of encounter will then typically feature higher errors for oblique waves than for head waves.

For accurate pressure integration, the bow region needs to be resolved in much finer detail for added resistance than for motion analyses. *Söding and Shigunov (2015)* show that much finer hull grids are needed for mesh-independent results for added resistance than for motions. Probably, in many cases coarse grid resolution contributes to the error in estimating added resistance.

For practical purposes, added resistance in regular waves is not enough. Whether it is speed loss or added fuel consumption, we need information about power and not “just” resistance. For assessing added power in natural seaways, the following key elements are needed:

- Transfer functions of added resistance (added resistance in a regular wave, divided by the square of the amplitude of the wave)
- Arbitrary spectrum of natural seaway, able to represent wind sea, swell or combination of both
- Resistance due to manoeuvring forces compensating for drift force (both for hull and rudder)
- Consideration of propeller and engine dynamics

While recent progress in our computational capabilities may justify moderate optimism for such computations, computing added power for given ambient conditions is only one half of the equation. We also need then accurate information on wave height or significant wave height.

3.3. Model tests or full-scale system identification

In view of the sobering results of computational approaches (especially for oblique waves and shorter wave lengths), one might be tempted to fall back to “proven” approaches, such as model tests or sea trials. Unfortunately, these do not offer really convincing alternatives as discussed by *Söding et al. (2012a,b)*: Model test methods use either self-propelled or towed models. The former method ensures minimum distortion of model motions by the carriage; however, the influence of motions and waves on thrust deduction factor (required to estimate the added resistance) remains an uncertain factor. Methods with towed models either restrain the model’s surge motion or use springs that connect the model to the towing carriage. Restraining the surge motion may disturb heave and pitch motions and thus influence the added resistance. The arrangement with springs appears more appropriate; however, springs may introduce additional, low frequency oscillations in the longitudinal direction. Another difficulty in model tests is that the added resistance (average force over time) is small compared to the amplitude of the oscillations of the longitudinal force. Thus, errors in the measurement and averaging of these forces in time might be comparable to or even exceed the average force itself. Finally, added resistance is sensitive to the quality of wave generation and wave measurement, especially in short waves. As a consequence, added resistance results from various model basins for the same case often exhibit large scatter, especially for shorter waves and oblique waves.

System identification at full-scale ships comes with its own headaches. As for model tests, the forces to be measured are often much smaller than the calm-water resistance and the fluctuating forces. But the biggest headache is that the incident waves are not known. Estimates from crew are useless in this respect. The remaining uncertainty is simply too large.

4. Our Achilles’ heel – The unknown seaway

Any correction for added power in seaways will require information on the seaway as input. Seaways are often described by a spectrum, i.e. as a mix of many regular waves of different length, propagation direction and height. Often a standard spectrum is assumed. Here the distribution over a mean propagation direction and the distribution over wave length are prescribed. The assumed functions for these distributions come from averaging many, many oceanographic observations. Each individual seaway deviates from the averaged distributions. Unless the actual seaway is measured (e.g. by special radar systems), there is an unavoidable scatter in results even for seaways of same significant wave height. Research is active on methods to obtain the near-field seaway around a ship, but it will take at least a decade before such systems are mature and affordable for commercial shipping.

Significant wave height is not measured in practice for performance monitoring. It may come from crew estimates (worst option), fore-cast or hind-cast weather data or derived from measured wind data assuming fully matured seaway. All approaches have uncomfortably high error margins.

In view of these (at present) unavoidable error margins for the sea state, there is not much sense in paying much money for highly accurate computations of added resistance. At best, such accurate calculation method would allow us to accept Bft 5 instead of Bft 4 in filtering.

5. Conclusions

My own experience as well as the knowledge taken from publications and discussions with experts in the field may be condensed to the following conclusions:

- The fact that heave and pitch motions are “in good agreement” with benchmark results does not mean that added resistance is calculated well.
- The fact that good agreement is shown for head waves and longer wave length does not mean that added resistance is calculated well.
- Added resistance is difficult to predict, regardless what approach is taken, especially in short or oblique waves.
- For performance monitoring, added power and not just added resistance must be considered. This requires at least a simple model of maneuvering forces and propeller characteristics.
- Accurate models for added power in waves make only sense if also more accurate data for the ambient seaway is obtained.

There is no reasonably simple (cheap) and reasonably accurate option to correct for added power requirements in seaways. We should admit this to ourselves and to our customers.

We have the choice between three alternatives, and neither is really attractive and mature at present:

1. strict filtering (\leq Bft 4 resp. sea state 3) with no correction or simple semi-empirical formulas
2. moderate filtering (\leq Bft 5 resp. sea state 4) and relative expensive calculations, where 3d Rankine singularity methods would be my recommended choice. Such calculations make financially only sense if the obtained knowledge is re-used for other applications, such as routing.
3. Possibly type-specific corrections may be developed and supplied using curve-fitting to 3d simulation results. First attempts using Artificial Neural Nets are encouraging in this respect, *Herradon de Grado and Bertram (2016)*, but much more development effort (in the order of several years) will be needed before we see practical applications.

The chosen approach in ISO 19030 – part 2 (default method) is in line with the first option and will remain the commonly adopted approach for the foreseeable future. However, using a fixed filtering limit at sea state 3 or Bft 4 (as recommended at present) may be criticized. Ideally, the limit should be chosen based on the ratio between calm-water resistance and added resistance, or better calm-water power and added power required in waves. Thus filtering should be stricter for lower speed where the added resistance gains in relative importance.

Acknowledgement

I am grateful for the input of many colleagues who shared their special expertise, in particular Hidetsugu Iwashita, Heinrich Söding, Vladimir Shigunov and Hironori Yasukawa.

References

ALEXANDERSSON, M. (2009), *A study of methods to predict added resistance in waves*, Master Thesis, KTH, Stockholm
http://www.kth.se/polopoly_fs/1.151543!/Menu/general/column-content/attachment/Alexandersson.pdf

- BECK, R.F.; REED, A.M. (2001), *Modern computational methods for ships in a seaway*, SNAME Trans. 109, pp.1-52
- BERTRAM, V. (2012), *Practical Ship Hydrodynamics*, Butterworth-Heinemann, Oxford
- BERTRAM, V.; YASUKAWA, H. (1996), *Rankine source methods for seakeeping problems*, Jahrbuch der Schiffbautechnischen Gesellschaft, pp.411-425
- BOOM, H.v.d.; HOUT, I.E. v.d.; FLIKKEMA, M. (2008), *Speed-power performance of ships during trials and in service*, SNAME
<http://www.marin.nl/web/Publications/Papers/SpeedPower-Performance-of-Ships-during-Trials-and-in-Service.htm>
- BOOM, H.v.d.; HUISMAN, H.; MENNEN, F. (2013), *New guidelines for speed/power trials level playing field established for IMO EEDI*, Hansa 150/4
<http://www.hansa-online.de/sta-jip.pdf>
- FALTINSEN, O.M.; MINSAAS, K.J.; LIAPIS, N.; SKJØRDAL, S.O. (1980), *Prediction of resistance and propulsion of a ship in a seaway*, 13th Symp. Naval Hydrodynamics, Tokyo, pp.505-529
- HANSEN, S.V. (2011), *Performance monitoring of ships*, PhD Thesis, DCAMM Special Report S142
http://www.fam.web.mek.dtu.dk/dcamm05/DCAMM_report_S142.pdf
- HERRADON DE GRADO, E.; BERTRAM, V. (2016), *Predicting added resistance in wind and waves employing artificial neural nets*, 1st Hull Performance & Insight Conf., Pavone, pp.14-22
- IMO (2013), *Additional information on revision of ISO 15016:2002*, Paper MEPC 66/INF.7 submitted by ISO and ITTC, Annex, p.51
- ITTC (2005), *Full scale measurements – Speed and power trials – Analysis of speed/power trial data*, Recommendations of the 24th Int. Towing Tank Conf., Edinburgh
- KREITNER, J. (1939), *Heave, pitch and resistance of ships in a seaway*, Trans. Institution of Naval Architects 81
- NABERGOJ, R.; PRPIĆ-ORŠIĆ, J. (2007), *A comparison of different methods for added resistance prediction*, 22nd Int. Workshop Water Waves and Floating Bodies, Plitvice
http://www.iwwfb.org/Abstracts/iwwfb22/iwwfb22_38.pdf
- PEREZ ARRIBAS, F. (2007), *Some methods to obtain the added resistance of a ship advancing in waves*, Ocean Eng. 34/7, pp.946-955
- SÖDING, H.; GRAEFE, A.v.; EL MOCTAR, O.; SHIGUNOV, V. (2012a), *Rankine source method for seakeeping predictions*, 31st Int. Conf. Ocean, Offshore and Arctic Eng. (OMAE), Rio de Janeiro
- SÖDING, H.; SHIGUNOV, V.; SCHELLIN, T.E.; EL MOCTAR, O.; WALTER, S. (2012b), *Computing added resistance in waves – Rankine panel method vs RANSE method*, 15th Numerical Towing Tank Symp. (NuTTS), Cortona
http://www.uni-due.de/imperia/md/content/ist/nutts_15_2012_cortona.pdf
- SÖDING, H.; SHIGUNOV, V. (2015), *Added resistance of ships in waves*, Ship Technology Research 62/1, pp.2-13
- STEEN, S.; FALTINSEN, O.M. (1998), *Added resistance of a ship moving in small sea states*, 7th Symp. Practical Design of Ships and Mobile Units (PRADS), The Hague
- TSUJIMOTO, M.; KURODA, M.; SHIBATA, K.; TAKAGI, K. (2008), *A practical correction method for added resistance in waves*, J. Japan Society of Naval Architects & Ocean Engineers 8, pp.147-54

Predicting Added Resistance in Wind and Waves Employing Artificial Neural Nets

Eva Herradón de Grado, Siport21, Madrid/Spain, eva.herradon@siport21.com
Volker Bertram, DNV GL, Hamburg/Germany, volker.bertram@dnvgl.com

Abstract

Wind and waves cause involuntary loss of ship speed and reduce the propulsive efficiency. In this paper, wind added resistance is obtained through the STA-JIP curves. For the prediction of the added resistance in waves, Artificial Neural Networks are used, albeit for only one containership. The good agreement obtained between the training data and predicted data suggest a potential application of this technology to predict added resistance in performance monitoring or early ship design.

1. Introduction

Wind and waves are generally the main reason for involuntary loss of speed or increased fuel consumption. Added resistance in waves usually constitutes an important part of the vessel's total resistance (often 15–30% of the ship calm-water power), *Pérez Arribas (2007)*. The added resistance in waves is difficult to predict since it depends on many parameters. The main methods used to predict this resistance are based on computational methods, *Bertram and Couser (2014)*. However, often faster and cheaper estimates are required. These will have by necessity lower accuracy.

In this paper, we describe a neural network application to predict added resistance in waves. Many maritime applications of Artificial Neural Networks (ANN) indicate that ANN may be suitable for this task, *Roddy et al. (2006,2008a)*, *Mesbahi and Bertram (2000)*, *Bertram and Mesbahi (2000, 2004a,b,2006)*, *Couser et al. (2004)*, *Cepowski (2011)*. The added resistance (or added power) shall be predicted with generally known values, e.g. main dimensions. The main advantage of the neural network technology is that no initial functions for the relationships between the independent and dependent variables need to be considered.

Added resistance due to wind is based on wind resistance coefficients suggested by ISO 15016. In ISO 15016, these coefficients (coming from STA-JIP (Joint Industry Project regarding Sea Trial Analysis)) are given as curves. This is unsuited for automated procedures. The curves were therefore converted to tabular values and functions (programmed in MATLAB).

2. Wind added resistance

Added resistance due to wind is important for ships with large windage areas, e.g. cruise ships, containerships, car ferries. There are various approaches to determine wind resistance. Wind tunnel tests and CFD are accurate, but expensive and time consuming. For initial design, methods based on empirical formulae are employed, e.g. *Turk and Prpić-Oršić (2008)*.

A very popular approach uses the wind resistance coefficient curves derived within STA-JIP (Sea Trial Analysis - Joint Industry Project). The STA-JIP curves were derived from wind tunnel data and are ship type specific. The curves represent the wind resistance coefficient as function of the apparent wind direction. The data provided is limited to the most common types of ship (container ships, tankers, LNG carriers, car carriers, ferry/cruise ships and general cargo ships). For a proper use of these coefficients, ship type, shape and outfitting shall be considered, *IMO (2013)*. We calculated the wind coefficient from 0° to 180° in steps of 10° using the STA-JIP curves provided by ISO 15016, Table I.

Table I: Wind coefficients for different ship types as function of the angle of attack

	Container ships				Tankers	
	Laden with containers	Laden without containers with lashing bridges	Ballast without containers, with lashing bridges	Ballast without containers, without lashing bridges	Laden	Ballast
0°	-0.671	-0.998	-0.967	-0.861	-0.967	-0.871
10°	-0.749	-1.072	-0.984	-0.830	-0.940	-0.772
20°	-0.738	-1.119	-1.055	-0.873	-0.865	-0.638
30°	-0.656	-1.120	-0.910	-0.703	-0.744	-0.464
40°	-0.487	-1.032	-0.838	-0.702	-0.623	-0.328
50°	-0.344	-0.896	-0.762	-0.687	-0.507	-0.219
60°	-0.259	-0.738	-0.660	-0.607	-0.353	-0.137
70°	-0.227	-0.561	-0.542	-0.520	-0.187	-0.080
80°	-0.234	-0.361	-0.409	-0.416	-0.090	-0.053
90°	-0.269	-0.135	-0.250	-0.287	0.048	-0.001
100°	-0.145	0.132	-0.011	-0.075	0.132	0.069
110°	0.071	0.440	0.245	0.161	0.205	0.158
120°	0.342	0.759	0.500	0.405	0.279	0.269
130°	0.573	0.997	0.793	0.690	0.390	0.346
140°	0.769	1.116	0.951	0.876	0.513	0.444
150°	0.887	1.162	1.021	0.972	0.635	0.549
160°	0.859	1.167	1.056	1.000	0.729	0.581
170°	0.796	1.129	1.039	0.985	0.766	0.623
180°	0.671	0.919	0.903	0.877	0.766	0.608

	Car Carrier	LNG Carrier			General Cargo	Cruise Ferry
	Average	Spherical	Prismatic extended deck	Prismatic integrated	Average	Average
0°	-0.528	-1.114	-0.808	-1.030	-0.592	-0.697
10°	-0.563	-0.921	-0.828	-0.989	-0.882	-0.726
20°	-0.470	-0.759	-0.822	-0.937	-0.998	-0.725
30°	-0.408	-0.708	-0.935	-0.831	-0.998	-0.697
40°	-0.283	-0.623	-0.710	-0.682	-0.866	-0.484
50°	-0.159	-0.513	-0.453	-0.482	-0.850	-0.254
60°	-0.074	-0.374	-0.274	-0.305	-0.654	-0.259
70°	-0.061	-0.226	-0.155	-0.164	-0.430	-0.109
80°	-0.005	-0.003	-0.152	-0.048	-0.275	0.118
90°	0.121	0.292	-0.211	0.032	-0.094	0.063
100°	-0.173	0.477	-0.086	0.090	0.080	-0.048
110°	-0.207	0.667	0.051	0.222	0.481	0.095
120°	0.172	0.819	0.178	0.395	0.843	0.226
130°	0.531	0.657	0.600	0.544	1.148	0.387
140°	0.771	0.636	0.917	0.671	1.368	0.560
150°	0.887	0.775	1.056	0.769	1.468	0.773
160°	0.871	0.914	1.035	0.850	1.322	0.798
170°	0.832	0.913	0.929	0.898	0.913	0.718
180°	0.750	0.734	0.581	0.887	0.808	0.655

The added resistance due to wind R_{AA} is then calculated as:

$$R_{AA} = C_D(\alpha) \frac{1}{2} \rho_a A_F V_R^2$$

$C_D(\alpha)$ is the wind resistance coefficient as function of the wind attack angle as given by Table I; ρ_a is the wind density (1.25 kg/m³); A_F is the frontal projected area of the ship above sea level; V_R relative wind speed in relation with the ship speed at reference height of 10 m above mean sea level.

3. Prediction of added resistance in waves using ANN

The aim was to obtain functions which relate the added resistance in waves (output) with simple ship and weather parameters (input). The employed software and the parameters mainly affecting the added resistance are described in the following.

3.1 Artificial Neural Network (ANN)

ANN is a computational technique for relating input variables to output variables. The ANN software used is ICE (Intelligent Calculations of Equations) provided by William Faller (Applied Simulation Technologies), Appendix A. This code uses Feed-Forward Neural Networks (FFNN) with two hidden layers and sigmoid functions as activation functions. FFNN means that the information moves forward, from the input layer through the hidden layers until the output layer. This type of ANN is called a Multi-Layer Perceptron and it is trained using back-propagation. This learning technique is considered as supervised learning technique since the value of the desired output is needed to train the ANN. The weights and bias connecting the different layers are adjusted in order to produce minimum errors between predicted and desired output.

3.2 Added resistance in waves

Added resistance in waves is attributed to two components:

- Radiation: From radiated waves due to ship motions (mainly heave and pitch)
- Diffraction: Mainly from reflection of waves at the ship hull

Diffraction dominates for large ships and radiation for smaller ships. For added power, we need to consider more than just added resistance: In addition to the second-order longitudinal force (added resistance), we need to compute second-order lateral force (drift force) and yaw moment. Drift and yaw must be compensated by the rudder. Some maneuvering model is required to estimate the associated added resistance from the rudder.

To calculate the added resistance in irregular waves R_{iw} , the superposition principle is used, *IMO (2013)*,

$$R_{iw} = \int_0^{2\pi} \int_0^\infty \frac{R_{rw}(\omega, \mu, V_S)}{\zeta_A^2} E(\omega, \mu) d\omega d\mu$$

$R_{rw}(\omega, \alpha, V_S)$ denotes added resistance in regular waves, ζ_A wave amplitude, ω angular wave frequency, μ encounter angle ($\mu = 180^\circ$ for head waves), V_S ship speed, and $E(\omega, \mu)$ the directional spectrum.

3.3 Methodology

Some experimental or simulation data is needed to train a neural network. The input parameters should be non-dimensional. First, we need to determine the key parameters affecting the added resistance in waves and the best form to express them.

The added resistance is related with the inputs through combinations of sigmoid functions of the form:

$$\sigma(x) = \frac{1}{1 + e^{-x}}$$

The general equation relating the added resistance (output y_o) with the input vector X is:

$$y_o = \sigma [W_{h2o} \cdot \sigma (b_{h1h2} + W_{h1h2} \cdot \sigma (b_{ih1} + X \cdot W_{ih1}))]$$

Subscript i refers to input layer; $h1$ and $h2$ to the first and second hidden layers, respectively; o to the output layer; b is the bias vector and W represents the weight matrixes connecting each layer.

3.4 Parameters affecting added resistance in waves

In a first application, the added resistance of a containership was modelled. We selected the following parameters as being both significant for added resistance and simple:

1. Wave length/ship length λ/L_{pp} : the maximum added resistance is usually obtained near heave resonance. Wave length λ and wave frequency ω are coupled by the dispersion relation, see *Bertram (2012)*: $\omega^2 = 2\pi g/\lambda$ with $g=9.81$ m/s².
2. Encounter angle $\mu/180^\circ$: added resistance is larger in oblique head waves and smaller (possibly even negligible) in following waves.
3. Froude number: Usually ship motions increase with speed and thus also radiated waves. The Froude number is chosen as nondimensional parameter.
4. Ship draft T : For a given ship, only draft changes significantly with loading conditions. The draft is made nondimensional with design and ballast draft. 1 is then design condition and 0 ballast condition:

$$\frac{T - T_{bal}}{T_{des} - T_{bal}}$$

For a general formula, the waterline entrance angle is expected to play a key role. This could be expressed by the beam-to-length ratio B/L_{pp} . However, as we tested our approach first on a single ship, no variation of this parameter was possible.

We used only significant wave height of 1 m then in the simulations. We assume the added resistance to be proportional to wave height squared. This eliminates wave height as an input variable. The output is then a nondimensional added resistance coefficient:

$$X'_{dr} = \frac{X_{dr}}{0.5 \rho V_s^2 L_{pp} T}$$

Negative values of X_{dr} are positive added resistance. The data used to train the ANN was obtained from an in-house 3d Rankine panel code, *Söding et al. (2012)*. The added power in regular waves is obtained through the second-order longitudinal force X_{dr} , drift force Y_{dr} and yaw moment N_{dr} . These were computed for variations of draft, ship speed, wave direction and wave length. Each component of the added power is modelled independently to maximize prediction quality.

4. Results

4.1 Longitudinal second-order force X_{dr}

Fig.1 shows results from the simulations. Some conclusions can be deduced:

- The added resistance increases nonlinearly with draft.
- Oblique waves (160°) produce more added resistance than head waves (180°).

- Following waves ($\mu = 0^\circ$) can be neglected for added resistance.
- For $\mu = 50^\circ$ and at $\omega = 0.7$ rad/s, positive values of the resistance can be observed. This may be explained by small ship motions and thrust from reflected incident waves being larger than resistance from radiated waves.

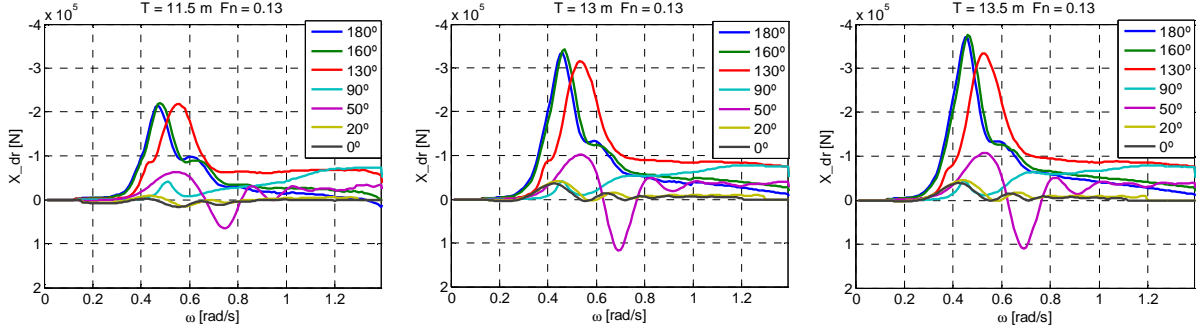


Fig.1: X_{dr} vs. wave frequency ω for $F_n = 0.13$, three drafts T , and various wave directions

Our test containership has $L_{pp} = 317.20$ m, ballast draft $T_{bal} = 7.77$ m and design draft $T_{des} = 12.5$ m. The prediction quality is measured by the Average Angle Measure (AAM), Appendix A, and the correlation coefficient (R). For both measures, a value of 1 indicates perfect agreement. Values above 0.8 are considered as good. The ANN model was trained with 924 values based on the input parameter ranges shown in Table II: 3 drafts T * 4 ship speeds V_s * 7 wave directions * 11 wave lengths. The chosen uneven spacing of the draft values was motivated by available computational data. Longer and shorter wave lengths than covered by the training set can be ignored. For very short waves, the added resistance is zero as the waves also have very low wave height. For very long waves, the ship moves quasi-statically in waves and added resistance approaches again zero.

Table II: Training set

T [m]	11.0, 13.0, 13.5
V_s [kn]	14, 17, 19, 21
μ [$^\circ$]	0, 20, 50, 90, 130, 160, 180
λ/L	0.15, 0.25, 0.50, 0.70, 0.90, 1.10, 1.30, 1.50, 1.80

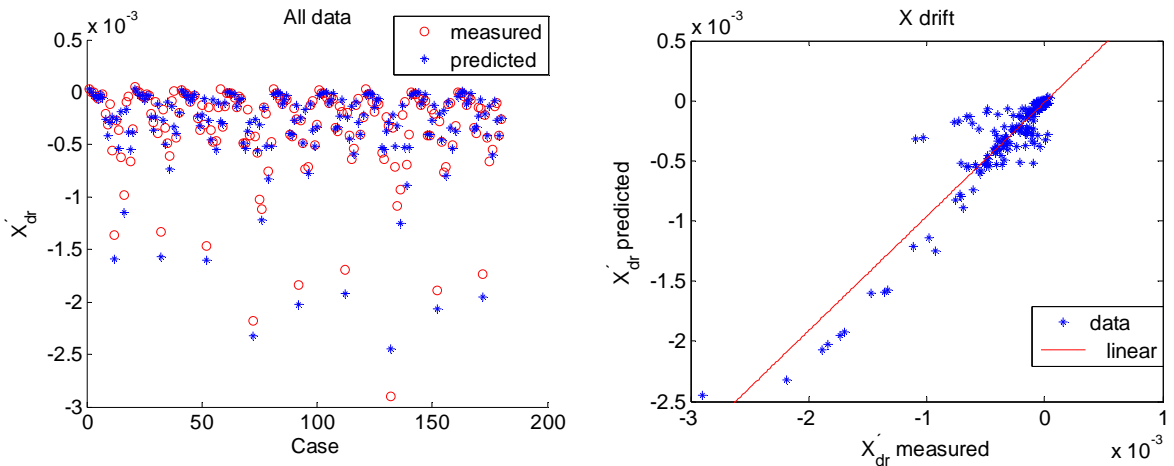


Fig.2: Measured and predicted non-dimensional second-order longitudinal force X'_{dr}

To have a more rigorous representation of the results, both error indicators, AAM and R, are considered only for the validation data. This set comprises 1/3 of the total data and is used to assess the accuracy of the trained ANN to predict similar conditions to the training data. The ANN software varied automatically the architecture and selected finally an architecture with 2 hidden layers with 8

nodes each as best option with AAM = 0.81 and R = 0.93, using arbitrary values of T , V_s , μ and λ/L . The trained neural network thus predicts the added resistance in waves for this ship reasonably well, Fig.2.

The software performs automatically a “lesion analysis”, where input variables are sequentially removed to determine their influence on the output. In our case, all four input variables were found to be significant.

ICE creates automatically a subroutine in Fortran 90 containing the generated ANN architecture, which may then be implemented in other software. As Fortran compilers are rare in Windows environments, we translated the exported subroutine into MATLAB using an automatic converter (<http://engineering.dartmouth.edu/~d30574x/consulting/consultingIndex.html>).

4.2 Second-order drift force Y_{dr} and yaw moment N_{dr}

As for the longitudinal second-force, we used neural nets for the second-order drift force and the yaw moment, training them on the same input data set as given in Table II. Again, nondimensional force parameters are used:

$$Y'_{dr} = \frac{Y_{dr}}{0.5 \rho V_s^2 L_{pp} T} \quad \text{and} \quad N'_{dr} = \frac{N_{dr}}{0.5 \rho V_s^2 L_{pp}^2 T}$$

The lesion analysis showed draft to be a negligible quantity for the force coefficients. Hence, draft was removed, simplifying the network architecture. The trained networks achieved good predictions with AAM = 0.89 and R = 0.98 for Y'_{dr} and AAM = 0.87 and R = 0.97 for N'_{dr} , Fig.3.

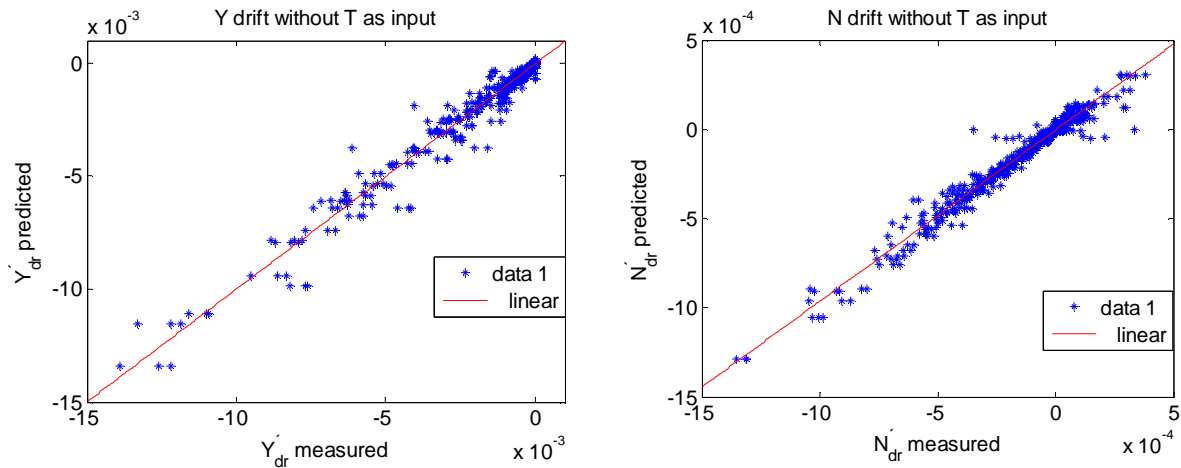


Fig.3: Measured and predicted Y'_{dr} (left) and N'_{dr} (right)

5. Conclusions

Artificial Neural Networks (ANNs) worked well in predicting second-order forces needed to predict added required power in waves. The good correlations indicate that the most important parameters were considered for a single ship. More research is required to extend the approach to other ships. The envisioned extension concerns including more parameters (at least B/L as an indicator of waterline entrance angle) and larger databases covering different ship types.

References

- BERTRAM, V. (2012), *Practical Ship Hydrodynamics*, Butterworth Heinemann, Oxford
- BERTRAM, V.; MESBAHI, E. (2000), *Applications of neural nets in ship design*, Jahrbuch der Schiffbautechnischen Gesellschaft, Springer
- BERTRAM, V.; MESBAHI, E. (2004a), *Simple design formulae for fast monohulls*, Ship Technology Research 51, pp.146-148
- BERTRAM, V.; MESBAHI, E. (2004b), *Estimating resistance and power of fast monohulls employing artificial neural nets*, 4th Int. Conf. High-Performance Marine Vehicles (HIPER), Rome, pp.18-27
- BERTRAM, V.; MESBAHI, E. (2006), *Simple design formulae for SWATH ships derived by artificial neural nets*, 5th Int. Conf. High-Performance Marine Vehicles (HIPER), Launceston, pp.15-24
- BERTRAM, V.; COUSER, P. (2014), *Computational methods for seakeeping and added resistance in waves*, 13th Conf. Computer and IT Applications in the Maritime Industries (COMPIT), Redworth, pp.8-16
- CEPOWSKI, T. (2011), *Application artificial neural networks for predicting wave resistance of Ro-Ro ferry in initial designing stage*, Maritime Univ. Szczecin, Scientific J. 26/98, pp.10-14
- COUSER, P.; MASON, A.; MASON, G.; SMITH, C.R.; KONSKY, B.R. von (2004), *Artificial neural networks for hull resistance prediction*, (COMPIT), Sigüenza, pp.391-402
- IMO (2013), *Air pollution and energy efficiency*, Additional information on revision of ISO 15016:2002, MEPC 66/INF.7
- MESBAHI, E.; BERTRAM, V. (2000), *Empirical design formulae using artificial neural nets*, 1st Conf. Computer and IT Applications in the Maritime Industries (COMPIT), Potsdam, pp. 291-301
- PEREZ ARRIBAS, F. (2007), *Some methods to obtain the added resistance of a ship advancing in waves*, Ocean Eng. 34/7, pp.946-955
- RODDY, R.F.; HESS, D.E.; FALLER, W.E. (2006), *Neural network predictions of the 4-quadrant Wageningen B-screw series*, 5th Int. Conf. Computer Applications and Information Technology in the Maritime Industries (COMPIT), Leiden, pp.315-334
- RODDY, R.F.; HESS, D.E.; FALLER, W.E. (2008a), *Utilizing neural networks to predict forces and moments on a submarine propeller*, 46th AIAA Aerospace Sciences Meeting, AIAA Paper 2008-0888, Reno
- SÖDING, H.; SHIGUNOV, V.; SCHELLIN, T.; EL MOCTAR, O. (2012), *A Rankine panel method for added resistance of ships in waves*, 31st Int. Conf. Ocean, Offshore and Arctic Eng. (OMAE), Rio de Janeiro
- TURK, A.; PRPIĆ-ORŠIĆ, J. (2010), *Estimation of extreme wind loads on marine objects*, Brodogradnja 60/2, pp.147-156

Appendix A: Intelligent Calculation of Equations (ICE)

Intelligent Calculation of Equations (ICE) was developed by William Faller of Applied Simulation Technologies, *Roddy et al. (2006)*. It is composed of five files. First, it is necessary to train the neural network using three files: *ICE.exe*; which consists of the code or executable, *ICE_setup.fi*; where the features of the input data are specified, i.e. number of inputs and outputs, rows and columns where they are located, etc. *T39fs.dat*; constitute the example to apply the code. For the training process, this data file needs to have the dependent (input) and independent (output) variables in order to define the final ANN structure and the value of the weights and bias.

After the training process, it is possible to predict output from some input similar to those used to train the ANN. For that, ICE has another executable, *ICE_Predict.exe* in which you need to enter just the input (file without any header *T39fs_1.dat*) and to obtain the output.

It is possible to export the derived nonlinear equations into other codes using the callable subroutine *ICE_Subroutine.f90*. The subroutine is very similar to the prediction code since it uses the derived ANN structure to get new predictions.

To use the prediction code and the subroutine, you need some files generated after the ANN training. Those files are *gain.dat*; which contains the scaling gains used to normalize the values, *wghout.dat*; containing the value of the final weights and bias, *ice_architecture.dat*; which contains the number of neurons per layer and number of inputs and outputs.

Another important file generated by ICE is a full summary of all the processing steps throughout the determination of the final solution. This file includes:

- The number of training cycles (epochs)
- Final architecture: nodes for the input, hidden and outputs layers (number of parameters and neurons)
- The final inputs (all non-essential inputs removed)
- During training, a lesion analysis is performed. This process successively removes input variables in order to define which are most relevant.
- Two error indicators are used to train the ANN: average angle measure AAM and correlation coefficient R. For both indicators, a value of 1 denotes perfect correlation and a value of 0 complete lack of correlation. R is the covariance of two values divided by the product of their individual standard deviations. AAM is computed for an output variable over a set of N points as:

$$AAM = 1 - \frac{4}{\pi} \left[\frac{\sum_{n=1}^N D(n) |\alpha(n)|}{\sum_{n=1}^N D(n)} \right]$$

$$\alpha(n) = \cos^{-1} \left[\frac{|s(n) + p(n)|}{\sqrt{2} \cdot D(n)} \right]$$

$$D(n) = \sqrt{s^2(n) + p^2(n)}$$

p represents the predicted value and s the “measured” (or training) value. AAM is related with the position of the predicted-measured ordered pair in a predicted-measured space as shown in Fig.5. The 45° line corresponds to perfect match with the measured values. For $p \neq s$, the point will fall on either side of the 45° line. If a line between the origin and this point is extended, it is possible to measure the angle between the new line and the 45° line. This angle gives a measure of the error of the prediction. After, the angles of the entire prediction set are

averaged together, weighted by the distance of each point from the origin. This avoids disproportionately large angles when s is small.

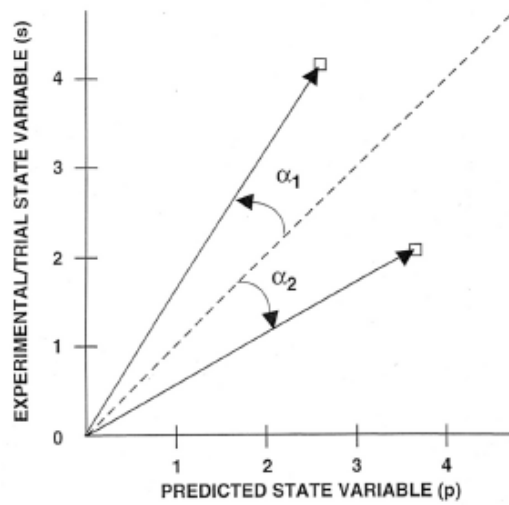


Fig.5: Example graph of predicted versus expected values used to define AAM

The code enables up to 160 different input variables and 20 output variables. The user can modify different features of the code as the learning algorithm, the number of solutions or if the ICE code should remove unnecessary inputs. The initial data used to train the ANN is divided into two sets: training data (recommended 2/3 of all data) used to updating the network weights and gains via back-propagation and validation data (recommended 1/3 of all data) used along with the training data to test the performance of the trained network, avoiding the over-fitting and noise.

Computing Hull & Propeller Performance: Ship Model Alternatives and Data Acquisition Methods

Thilo Dückert, DNV GL, Hamburg/Germany, thilo.dueckert@dnvgl.com

Daniel Schmode, DNV GL, Hamburg/Germany, daniel.schmode@dnvgl.com

Marcus Tullberg, Hempel, Lyngby/Denmark, martu@hempel.com

Abstract

DNV GL's fleet performance management solution "ECO Insight" offers the functionality to compute fouling-related hull and propeller performance based on measurements, corrections for ambient conditions and a ship-specific propulsion power requirement model for operational conditions. Calculations can be performed based on different data acquisition methods and ship model types. For gaining the required measurement data onboard, two options can be applied: semi-manual "snapshot reporting" or fully automated data acquisition. The underlying power requirement models can also be obtained from different sources: model tests, sea trials or CFD. Building upon experience with many client cases, the paper discusses the pros and cons of the above alternatives.

1. Introduction

Performance monitoring of ships has gained in importance with the mandatory introduction of the SEEMP (Ship Energy Efficiency Management Plan) in 2013 and the development of ISO 19030. The particular focus of ISO 19030 lies on the assessment of hull roughness (mainly due to fouling) which increases fuel consumption. The increase of required power (and consequently fuel consumption) can be dramatic. For example, *Schultz (2007)* reports 84% power increase due to heavy fouling. A typical value often quoted and representative for moderate fouling is 30% increase in power requirements. The progression of fouling is difficult to impossible to predict, as it depends on many factors (speed, times of idleness, antifouling used, temperature, salinity, etc.). This leaves then monitoring with trend prediction to derive management decisions, e.g. on cleaning and coating.

The task of performance monitoring is complicated by the ever changing:

- operational conditions (speed through water, draft, trim, ...)
- ambient conditions (waves, wind, ...)

In order to single out the influence of hull and propeller roughness, we need to eliminate (at least approximately) these contributions from converting data to a common baseline. Approaches in data collection and in data correction (normalization) differ in accuracy and required effort. Our experience allows preliminary assessment of the main alternatives as described below.

DNV GL's fleet performance management solution "ECO Insight" (<https://performance.dnvgl.com/>) was introduced in 2014. In its present release, it consists of six modules:

1. **Voyage performance** – fuel consumption, speed, weather, operational profile, EEOI (Energy Efficiency Operational Indicator)
- Engine & Systems performance** – engine or systems degradation identified via SFOC (specific fuel oil consumption), turbocharger speed, pressures, temperatures, loads at main engine, auxiliary engines or other systems
2. **Vessel performance** – hull & propeller degradation, trim adherence and propulsion performance assessed with CFD (computational fluid dynamics) baselines
3. **Fuel quality performance** – performance differences due to fuel quality issues and bunker quality in different ports and from different suppliers can be identified
4. **Environmental performance** – information on emissions to air, disposals, and ballast water management
5. **Onboard data recording ("Navigator Insight")** – voyage, bunker, and performance snapshot data recorded along existing processes without additional hardware effort

For our purposes here, only modules 2 and 5 are relevant. These concern (hull and propeller) vessel performance and onboard (performance) data recording.

2. Getting Data acquisition right – Avoid Garbage In, Garbage Out

The general wisdom, also in ISO 19030, is that “continuous monitoring with high-frequency data density gives better trends in shorter time”. This has been quantified e.g. in *Aldous et al. (2013, 2015)*. We do not question the mathematics used in deriving the uncertainty or error estimates in the ISO 19030. However, the statement assumes that there is no correlation between data frequency and data quality, i.e. that automatic high-frequency data is recorded with same quality as manually logged data. This assumption is questionable.

In the following, we will look more closely at the issue. We may look at two aspects here:

1. data frequency
2. data accuracy

2.1. Data frequency

Data is logged with different frequency (once per day in noon reports or every 15 s in continuous monitoring). For noon reports, the accuracy analysis in ISO 19030 assumed that speed is derived as 24 h average (distance sailed in 24 h divided by 24 h). Operational practice is more complex and varied. E.g. *Krapp and Bertram (2015)* report a case of speed variations over 24 h intervals that caused 3% increase in fuel consumption. Therefore, instead of using 24 h averages, many ship operators use snapshot reports, i.e., using instantaneous (more precisely short-term averaged) readings from onboard sensors. Such snapshot reports lead to much more accurate monitoring than the values given in ISO 19030 for noon reporting. Manual data logging may come with human quality control, e.g. noticing and correcting sensor failures. The accuracy of individual data sets may therefore be higher than that of an automatically logged data set. But the human factor may also lead to errors that do not occur in continuous monitoring.

2.2. Data accuracy

2.2.1. Human factor

A common tale of woe concerns the quality of manually logged data, where the human factor plays an important role. This matches also our experience with evaluating historical noon reports. Fig.1 shows typical examples taken from industry practice. The records shown are blatantly implausible: the fuel consumption remains constant over a large range of speed (left) or varies between near-zero and 30 t per day for 12 kn speed (right). These data errors could have been spotted by simple plausibility checks, but frequently wrong data is more difficult to spot and contaminates performance monitoring efforts.

In our experience, the quality of manually logged data improves dramatically when making the task easier for the crew using human-centric software design. DNV GL’s “Navigator Insight”, <https://www.dnvgl.com/services/voyage-performance-monitoring-navigator-insight-1452>, is an on-board software tool to support crews in their reporting tasks using some simple, but effective guidelines, Fig.2:

- The data input follows a voyage based structuring, i.e. the traditions of seafarers for when to report (noon and event based reporting)
- Data is entered only once and automatically re-used for assorted reports (to owner, charterer, authorities, etc.). This avoids frustration in crew to report frequently the same data and reduces work load considerably. Crews are much more willing to focus then on these few occasions for data reporting.

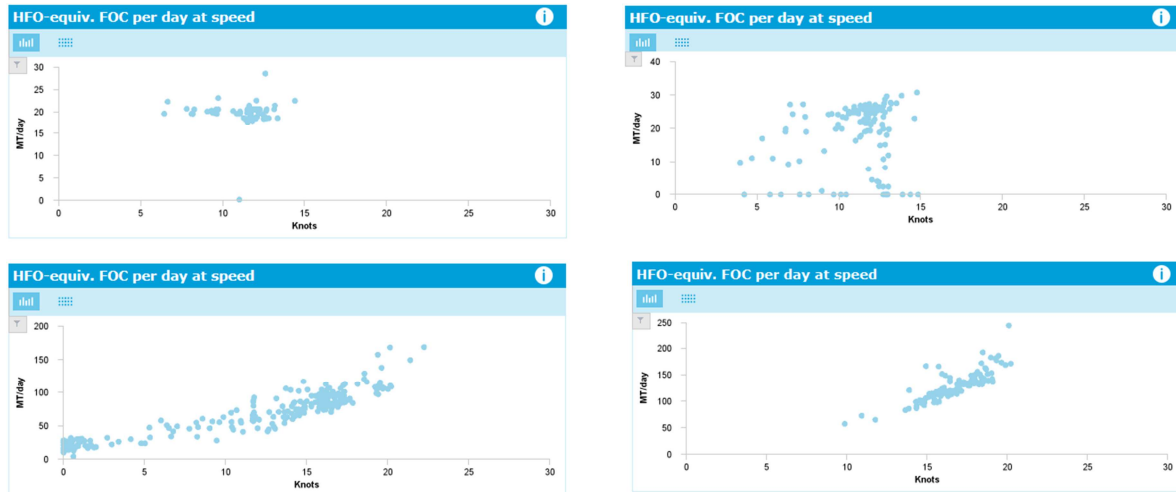


Fig. 1: Crews report often blatantly implausible data which passes unchecked to performance monitoring (top); better manual data capturing using Navigator Insight has proven to lead to significant improvements (bottom)

- Data is immediately checked for completeness and plausibility, eliminating classical error sources such as: inventing data which was initially forgotten to log; transposed numbers; copy & paste of yesterday's or last week's number; etc.
- Smart default numbers reduce entry errors as often the default only needs to be confirmed.

The changes in data quality after introduction of “Navigator Insight” onboard ships are a powerful testimony to the importance of the human factor in performance monitoring.

The screenshot shows the 'Noon (Position) - Sea passage' interface. On the left, there are input fields for 'Sea' (Wind wave height, period, Swell 1 and 2 wave height, period, direction, Current speed, direction) and 'Ice' (Coverage, Situation). Below that is a 'Consumptions' table with columns for Fuel Type, S[%], H2O[%], Visc.[cSt], Dens.[kg/m³], BDN, and Consumed[t]. On the right, a 'CHECK RESULTS' panel is open, listing 7 issues: Machinery operations A/E: incomplete, Fresh water ROB: missing, M/E: work/speed mismatch, M/E: work/consumption mismatch, Machinery operations: work/power mismatch, Sailed distance OG: too small, and Sailed distance TW: too small. A red box highlights the 'CHECK RESULTS' panel.

Guiding crew what needs to be filled in with immediate plausibility checks

Fig. 2: Data capturing from crew can be facilitated by good user interfaces; simpler processes result in better data quality (Navigator Insight)

Data accuracy depends also on sensor accuracy. Sensor accuracy depends on:

- Theoretical sensor accuracy (as specified by the manufacturer and measured under laboratory conditions)

- Correct installation of sensor
- Maintenance / actual condition of sensor

Sensor problems affect both continuous and manual data recording. We recommend plausibility checks once per day with fast feedback to the crew. Ideally, the crew notices at the time of noon (snapshot) reporting any sensor problems and can then repair faulty sensors. However, the issue of sensor calibration is thorny. Constant re-calibration to obtain expected data can lead to self-fulfilling prophecies which give nice-looking, albeit wrong performance monitoring results.

In our experience, plausibility checks and diagnostics at a raw data level works well. Sensor failures (mostly with sensors giving constant zero or non-zero data) are rapidly spotted and rectified with maximum of one day lost in data capturing.

2.2.3. Insight on data acquisition

Data accuracy and data frequency affect performance monitoring insight. The assumption that data accuracy is the same for manual and continuous monitoring ignores the human factor. In industry practice, good manual reporting gives similar results as continuous monitoring, Fig. 3. The investment in crew training and user-friendly data logging has then to be compared with the investment in continuous monitoring.

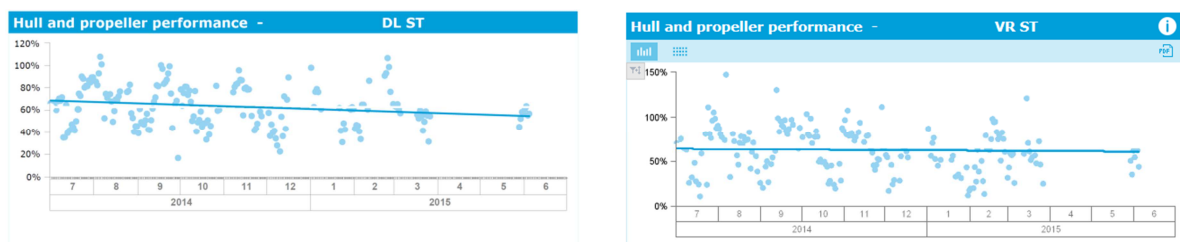


Fig. 3: Continuous monitoring (left) and snapshot reporting (right) for a containership

3. Getting model quality right – Avoid Quality In, Garbage Out

3.1. Effect of changing operational conditions

Key operational parameters that change frequently and affect power requirements are speed (through water), draft and trim. The simplest estimate for speed-power relations is given by the ‘admiralty formula’ or third-power law: $P = \Delta^{2/3} \cdot V^3 / C$. P denotes the required power, V the speed, Δ the displacement (= mass) of the ship and C is a constant. The admiralty formula applies only to “ships that have almost the same [...] F_n , ∇ , etc.”, *Schneekluth and Bertram (1998)*. The Froude number F_n is ship speed, made non-dimensional with ship length and gravity. ∇ is the volume displacement, directly related to the mass by water density. So, in essence we should use this estimate only for minor changes in speed and displacement.

Employing traditional ship design formulas such as Guldhammer-Harvald or Holtrop-Mennen, see e.g. *Schneekluth and Bertram (1998)*, is similarly problematic as using the admiralty formula. These formulas approximate model test data for many ship design projects. The data base consists thus of “best practice” designs of the respective era with a best curve fit to existing data. The problem lies in the term ‘existing data’, as these are all near design speed and design draft (contract condition) and ballast draft (sea trial condition). For lower speeds and intermediate drafts the inherent assumptions are violated and large errors have to be expected.

The speed-power relation is complex over large speed ranges. Expressing this relation by a simple exponential law of the form $P \sim V^n$ is misleading and problematic. Locally, the speed-power curve may be approximated by such a law, but then we will find largely varying n . For low speed, where

frictional resistance dominates, we will find $n < 3$ but near 3. Near design speed we often find values of $n = 4 \dots 6$, due to increasing wave resistance associated with higher speeds, as also discussed by *Kristensen (2010)*.

The influence of draft and trim is complex. For ships with pronounced bulbous bows, intermediate drafts may lead to strong wave breaking. Power requirements then increase with decreasing draft, *Krapp and Bertram (2015)*. In these conditions, ships react very sensitively to trim and required power may reduce by as much as 8% for forward trim vs. level keel at higher speeds.

The admiralty formula is used in ISO 19030 to correct for displacement from a given baseline, provided the actual displacement differs not more than 5% and the trim not more than 0.2% of the ship length from the baseline conditions. For extrapolation outside these narrow bands, ISO 19030 foresees the creation of additional hydrodynamic data by sea trials, model tests or CFD. For some ships, e.g. cruise vessels, the variation in operational conditions (speed, draft and trim) may be small enough to use existing model basin reference curves and the admiralty-formula approach. For most ship types, however, the operational profiles are much wider. Insufficient variation of speed (only upper speed range) or loading conditions (intermediate drafts and variation in trim) will then lead to unacceptable loss of data sets due to the filtering criteria imposed by ISO 19030.

For obtaining a good model of power as function of speed, draft and trim, neither admiralty formula nor simplistic design formulas can be used. ISO 19030, Annex, foresees various alternative options. These have all their pros and cons, as discussed e.g. by *Bertram (2014)*. For containerships, in our experience a total of 250 – 400 combinations of speed, draft and trim are necessary for a good hydrodynamic knowledge base covering all possible operational conditions. This number should be kept in mind when considering required effort. The classical approach for the assessment of ship hydrodynamics employs model tests. In model tests, the creation of the knowledge base involves much more time and cost than in “numerical towing tanks” (CFD). In addition, model tests suffer from scale effects, *Hochkirch and Mallol (2013)*. Full-scale measurements are in principle an option, but for sea trials under controlled ambient conditions, draft variations are almost impossible and the time requirements generally prohibitive; for system identification during regular operation the general caveats for machine learning apply where sufficient encountering training points may take too long and the uncontrolled ambient conditions generate an unavoidable source of error.

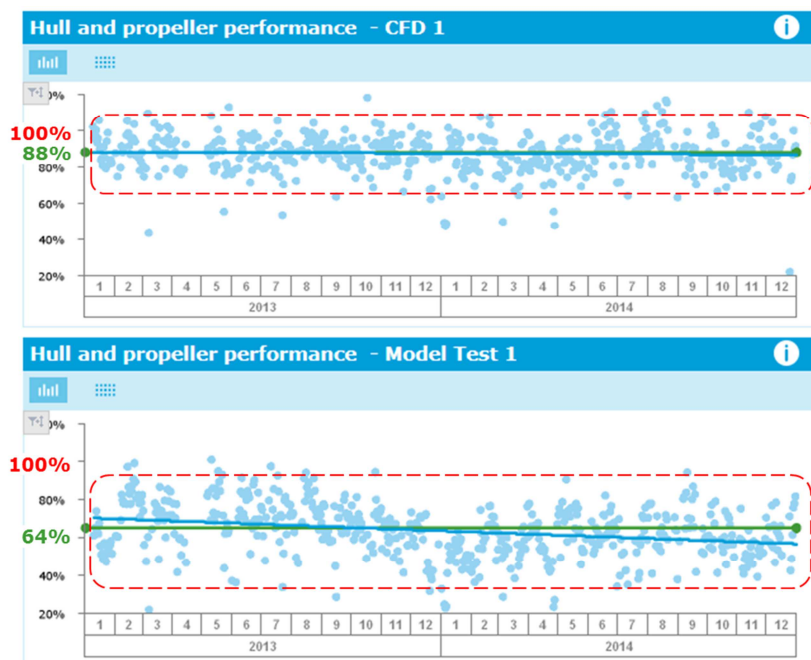


Fig. 4: Hull performance monitoring for one ship; top: based on CFD detailed matrix, bottom: based on model tests (two speed-power curves)

Fig.4 shows results for one ship where the same original data were processed, varying only the underlying hydrodynamic model to correct for different operational conditions. One model was based on a hydrodynamic knowledge base obtained by systematic CFD computations, varying trim, draft, and speed. The other model was based on the available model test predictions for the ship, for ballast and design conditions, losing by necessity trim as an input parameter. The better model not only reduces the scatter in results, it also gives a more realistic trend. The simpler model results in an unrealistic offset; it also gives the wrong trend.

4. Conclusion & Outlook

The quality of performance monitoring depends on the underlying model and on input data. For the underlying model, full-scale CFD is recommended for the correction of varying operational conditions. For input data, ideally both data quality and data frequency should be high. Here, data quality is even more important than data frequency. If in doubt, ship operators should then invest rather in data quality than in data frequency.

Acknowledgements

We thank our customers for giving permission to show the results in this paper (in anonymized form). We thank Erik Heller and Christian Beiersdorf for their shared expertise and Volker Bertram for his merciless pressure without which this paper would never have been finished in time.

References

- ALDOUS, L.; SMITH, T.; BUCKNALL, R. (2013), *Noon report Data Uncertainty*, Low Carbon Shipping Conf., London
- ALDOUS, L.; SMITH, T.; BUCKNALL R.; THOMPSON, P. (2015), *Uncertainty analysis in ship performance modelling*, Ocean Engineering 110, pp.29-38
- BERTRAM, V. (2014), *Trim optimization – Don't blind me with science*, The Naval Architect, July/August, pp.66-68
- BERTRAM, V. (2016), *A simulation-based hull performance monitoring model*, Ship Technology Research 63, paper submitted
- HOCHKIRCH, K.; MALLOL, B. (2013), *On the importance of full-scale CFD simulations for ships*, 12th Int. Conf. Computer and IT Applications in the Maritime Industries (COMPIT), Cortona, pp.85-95
- KRAPP, A.; BERTRAM, V., *Hull performance monitoring – Combining Big Data and simulation*, 14th Conf. Computer and IT Applications in the Maritime Industries (COMPIT), Ulrichshusen, pp.57-63
- KRISTENSEN, H.O.H. (2010), *Model for environmental assessment of container ship transport*, SNAME Annual meeting, Seattle
- SCHNEEKLUTH, H.; BERTRAM, V. (1998), *Ship Design for Efficiency and Economy*, Butterworth & Heinemann, Oxford
- SCHULTZ, M.P. (2007), *Effects of coating roughness and biofouling on ship resistance and powering*, Biofouling 23/5, pp.331-341

High-Fidelity Computational Analysis of an Energy-Saving Device at Model Scale

Michel Visonneau, ECN, LHEEA, Nantes/France, michel.visonneau@ec-nantes.fr

Ganbo Deng, ECN, LHEEA, Nantes/France, ganbo.deng@ec-nantes.fr

Patrick Queutey, ECN, LHEEA, Nantes/France, patrick.queutey@ec-nantes.fr

Emmanuel Guilmineau, ECN, LHEEA, Nantes/France, emmanuel.guilmineau@ec-nantes.fr

Alvaro del Toro Llorens, NUMECA Int., Brussels/Belgium, alvaro.deltorollorens@numeca.be

Abstract

This paper presents a thorough computational study of the flow around the Japan Bulk Carrier (JBC) with or without an Energy Saving Device (ESD) in front of the propeller. This study conducted at model scale was performed in the framework of the Tokyo 2015 Workshop on Numerical Ship Hydrodynamics. Configurations with and without ESD, with and without propeller are compared and analysed and conclusions about the efficiency of this specific ESD at model scale are drawn.

1. Introduction

The Japan Bulk Carrier (JBC) is a Capesize bulk carrier equipped with a stern duct as an energy saving device (ESD). National Maritime Research Institute (NMRI), Yokohama National University and Ship Building Research Center of Japan (SRC) were jointly involved in the design of this ship hull, duct and rudder. Its length between perpendiculars is $L_{pp}=280\text{m}$. Its service speed is 14.5 knots, leading to a Froude number $Fn=0.142$ and a Reynolds number at model scale of $Re=7.46\cdot 10^6$. Towing tank experiments were performed at NMRI, SRC and Osaka University, including resistance tests, self-propulsion tests and PIV measurements of stern flow fields. Several test cases were considered, all with free sinkage and trim; test cases 1.3a (resp. 1.4) are for towing test without (resp. with) ESD, cases 1.7 (resp. 1.8) for self-propulsion tests without (resp. with) ESD. Global force measurements and local LDV velocity profiles at three sections named S2, S4 and S7 before and after the propeller and duct were also provided by the organizers. Figs. 1 and 2 show a view of the stern without and with ESD with the location of the local measurement sections.

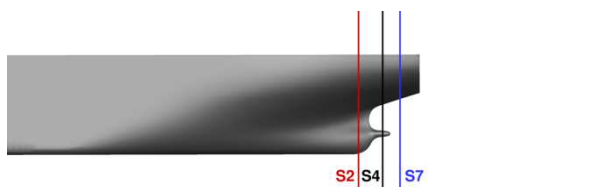


Fig.1: Side view of the hull without ESD

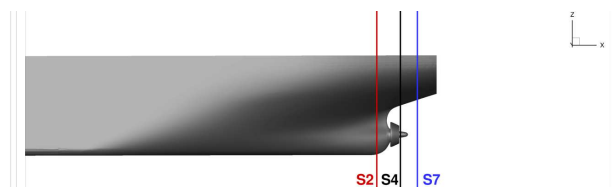


Fig.2: Side view of the hull with ESD

This paper presents a computational study of the flow around this ship with or without these specific appendages in order to analyze the physics of this complex flow configuration. Comparison with available experimental results will be shown. Also a careful verification exercise will be provided to get access to an evaluation of the discretization error.

It is well accepted now that CFD (Computational Fluid Dynamics) is a mature tool for steady-state ship hydrodynamic applications such as resistance in calm water. Accurate enough predictions can be obtained with reasonable resources even for fully appended hulls, both for model and full scale in a routine design procedure. However, rigorous V&V (verification & validation) exercises are seldom performed by CFD users. In most of the cases, one grid and one computation are adopted following guidelines based on recommendations and experience. The recommended setup (such as grid density, turbulence model, etc.) may differ from one institution to another. Comparison with measurement data is often the only criterion when establishing those guidelines. The versatility of a guideline thus

established can be questionable, since a small comparison error can be the result of error cancellation between numerical discretization and physical modeling errors. By performing a careful V&V exercise, one attempts to quantify turbulence modeling error and tries to answer questions such as whether a non-linear turbulence model is more accurate than a linear turbulence model for ship resistance prediction, what is the impact on the accuracy when a wall function is used, etc.

Compared with resistance computations, validation for propulsion computations is much more challenging. To our knowledge, the only approach capable of accurately predicting ship propulsion power is to simulate directly the rotating propeller with sliding grid or overset approaches. Time-accurate simulation with very small time steps is required for such simulation even if time-averaged solution is sufficient. Our experience with V&V exercises show that reliable numerical uncertainty estimations are nearly impossible for this case due to the high iterative error as well as the time discretization error. Self-propulsion simulations may also model the effect of the propeller by body forces in the RANSE solver. With such an approach, propeller thrust can be provided by the RANSE solver. But to determine propeller revolution rate and propeller torque, a simplified model or a coupling approach between RANSE solver and another specific solver simulating the propeller such as RANSE/BEM coupling approach must be used.

2. Numerical approach and case setup

Computations were performed with the ISIS-CFD flow solver developed by our team, also available in the commercial software FINETM/Marine. It is an unstructured finite volume RANSE solver using a free-surface capturing approach. For technical details of the solver, we refer to *Queutey and Visonneau (2007)* and *Wackers et al. (2012)*.

Except for the case when propeller motion is resolved by the RANSE solver, only a half domain is simulated. The inlet boundary is located at $2.5L_{pp}$ from FP (forward perpendicular), the outlet at $3.0L_{pp}$ after AP (aft perpendicular). Bottom and top boundaries are located at $1.5L_{pp}$ and $0.5L_{pp}$ from the waterline, respectively. The lateral boundary is located at $1.5L_{pp}$ from the mid plane. A pressure boundary condition is applied at the bottom and top boundaries, while a far-field boundary condition is applied at the inlet, outlet, as well as the lateral boundary. One relies on the Richardson extrapolation for the V&V exercise. The Richardson extrapolation can be applied only when grid similarity is ensured while the unstructured hexahedral mesh generator HexpressTM available in FINETM/Marine is employed in the present study. With HexpressTM, it is hardly possible to generate a set of rigorously similar grids. But with a special setup, it is possible to ensure grid similarity before the insertion of viscous layer. Our experience shows that grids thus generated usually allow a successful Richardson extrapolation. This grid generation setup is too specific to the grid generator HexpressTM and will not be described here. We refer interested readers to *del Toro (2015)* for details. Table 1 gives the number of grid cells for the different grid sets used here.

Table 1: Number of grid cells for different cases

Cases	Grid 4	Grid 3	Grid 2	Grid 1
1.1a_wm	405K	1.512M	3.143M	5.724M
1.1a_wr	861K	2.632M	5.304M	9.197M
1.2a_wm	725K	2.311M	4.806M	8.750M
1.2a_wr	1.317M	4.269M	8.344M	14.077M
1.5a_wm	2.442M	4.784M	10.247M	18.676M
1.6a_wm	2.513M	6.668M	13.913M	25.332M

In Table 1, case 1.1a (resp.1.2a) stands for the naked hull (resp. hull with ESD) while case 1.5a (resp. 1.6a) stands for hull with propeller (resp. hull with propeller and ESD). "wm" stands for wall modelled simulation for which wall function approach is used, "wr" for wall resolved simulation for which a near wall low-Reynolds turbulence model is employed. For the first case, the same y^+ value of about 30 is applied for all grids, while for the second case, the y^+ value changes from about 0.4 for

the coarsest grid to about 0.16 for the finest grid. Meshes for different configurations have similar grid density. The difference in number of cells is due to the presence of the energy saving device (ESD) and the propeller, additional cells in the viscous layer when using wall resolved approach, and whole domain simulation rather than half domain simulation. Mesh density is not too fine. Mesh size near the free-surface is about $0.0008L_{pp}$ for the fine mesh. Grids 1 and 2 represent meshes commonly used for resistance computation for engineering application. Unless otherwise stated, all computations were performed with the non-linear EASM turbulence model. A second-order upwind blended scheme was employed for spatial discretization except for the case with propeller resolved simulation for which a more stable ALVSMART scheme is used.

4. Results and discussions

4.1 Resistance Results for the JBC test cases

Tables 2 and 3 give main results for total resistance for case 1.1a (without ESD) and 1.2a (with ESD) respectively. We give only the finest grid solution U1, the observed order of convergence p , Richardson extrapolation error RE% defined as $(\delta_{RE}-U1)/\delta_{RE} \cdot 100$, and the comparison error E%D defined as $(D-S)/D \cdot 100$ where D is the measurement data. $S=U1$ is the simulation result. δ_{RE} is the result of Richardson extrapolation. The least squared approach proposed by *Hoekstra and Eca (2008)* is used for Richardson extrapolation. When the observed order of convergence is higher than 2.1, Richardson extrapolation is obtained with assumed second-order accuracy. For both cases, the EASM model gives better prediction than the SST model. Moreover, the numerical discretization error is smaller than the difference due to turbulence model for the fine grid. Hence, when the grid is fine enough, the EASM model should give better prediction for ship resistance for this test case. The reason for the better performance with the EASM model is due to the existence of a relatively strong aft-body vortex for this geometry. When the aft-body vortex is not so strong, the SST model should also be capable to give an accurate prediction for ship resistance as well. Even with a fine grid containing more than 6M cells, numerical discretization error for resistance computation is still about 2% at least. Hence, when the grid is further refined, the EASM model is expected to under-estimate the resistance by about 4% for the case without ESD, and 3% for the case with ESD. This is confirmed by computations with adaptive grid refinement which give a comparison error of 3.1% for the case without ESD, and 2.2% for the case with ESD. For both cases, the use of wall function does not deteriorate too much the predicted result. The predicted resistance differs only by 0.1% and 0.45% respectively, which is much smaller than the discretization error. This observation justifies the use of a wall function for engineering applications due to much lower computation cost. Flow separation is observed on the ESD, Fig. 4. This might explain why the comparison error, the Richardson extrapolation error, and the observed order of convergence are higher for the case 1.4 when the wall function is used.

Table 2: Total resistance for case without duct and propeller (case 1.1a)

Simulation	U1	p	RE%	E%D
easm_wm	4.209	2.07	-2.3	1.87
easm_wr	4.213	1.94	-2.0	1.77
sst_wr	4.087	1.59	-3.2	4.71

Predicting pressure resistance with good accuracy is a challenging task for CFD. Fig. 3 shows the Richardson extrapolation error for pressure resistance for the case without ESD. Even with the finest grid, the error is still about 10% for the EASM model.

Table 3: Total resistance for case with duct but without propeller (case 1.2a)

Simulation	U1	p	RE%	E%D
easm_wm	4.200	2.93	-4.3	1.48
easm_wr	4.219	2.06	-2.3	1.03
sst_wr	4.093	1.67	-3.2	3.99

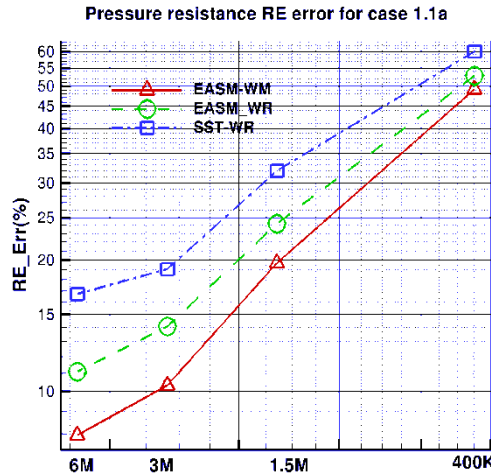


Fig.3: Richardson extrapolation error for pressure resistance

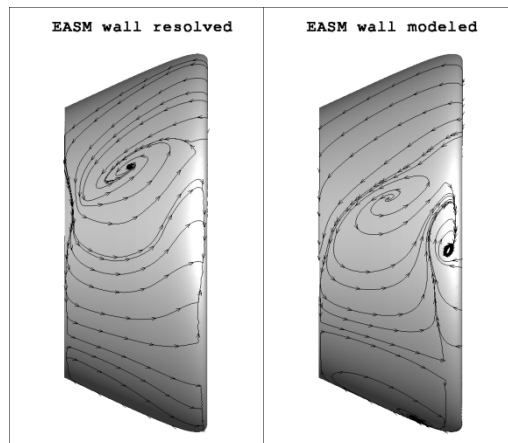


Fig.4 : Local view of the recirculation region on the duct with the EASM turbulence closure without or with wall function

Much higher uncertainty is observed for the SST model. But such high level of numerical uncertainty might be due to observed low order of convergence (1.53). As pressure resistance represents only about 25% of the total resistance, the numerical error observed in total resistance comes mostly from pressure resistance error. For applications where the contribution of pressure resistance becomes more important, e.g. vessels with smaller L/B ratio, higher grid resolution might be needed to achieve acceptable accuracy.

4.2 Self-Propulsion Results for JBC test cases

The most obvious approach to perform a self-propulsion computation is to simulate the rotating propeller with the RANSE solver using sliding grid or overset grid approaches. A sliding grid approach is employed in our computations. With such an approach, time-accurate simulation is required even when only time-averaged results are needed. A rigorous V&V study with such a procedure requires numerical uncertainty estimation on space and time. Due to high computational cost, we did not attempt to assess the time discretization error. Instead, the time step and the non-linear iteration number per time step were chosen according to open-water computations using the same grid for the propeller. A sliding grid approach gives almost the same result for the propeller thrust compared with a computation performed in rotating frame. This "calibration" yields 150 time steps per revolution and 15 non-linear iterations per time step. One performs a first computation with a large time step to accelerate the ship to target speed until convergence. The rotating-frame approach is applied to the propeller domain. Ship trim and sinkage are computed during this computation. Then, in a restart

computation, one switches to a small time step (150 time steps per revolution). Ship motion is frozen during this computation and therefore, during this restart, ship dynamic position is not computed accurately. In our propeller-resolved simulation, computations were performed with the EASM model using wall function only. Computations were performed on 4 grids with different grid density as the cases for resistance computation. Figs. 5 and 6 show the evolution of force imbalance in our simulation for case 1.5a and 1.6a, respectively. 0.5N imbalance represents about 1.2% ship resistance. The force imbalance is expected to vanish under self-propulsion condition. The raw data are highly fluctuating due to rotating propeller. Results shown are smoothed by applying 1000 passes with the smoothing operation available in the Tecplot post-processor. The force imbalance obtained on the coarsest mesh is not shown. It was very high ($\sim 8N$).

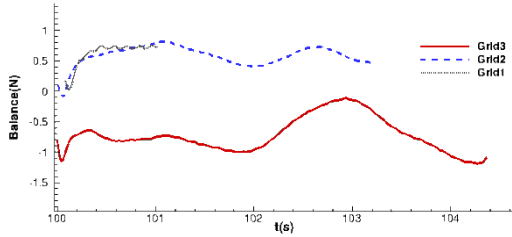


Fig.5: Force imbalance for case 1.5a (with propeller, without ESD)

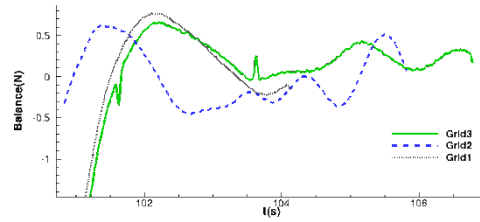


Fig.6: Force imbalance for case 1.6a (with propeller, with ESD)

Such high force imbalance is due to the very strong flow separation at the stern, resulting in a highly asymmetric wake. In our simulation, the propeller revolution rate was prescribed with the measurement value. Propeller thrust is positive. For the case without ESD, the force imbalance has a positive sign on the fine mesh (Grid1), i.e. propeller thrust is too high. We need to reduce propeller revolution rate to satisfy the self-propulsion condition. For the case with ESD, we are close to the self-propulsion condition. For case 1.6a, we performed about 7 seconds physical time, namely more than 50 propeller revolutions. With 150 time steps per revolution and 15 non-linear iterations per time step, the CPU cost is equivalent to about 30 resistance computations. Yet, it is hardly possible to determine a converged value for the force imbalance. Due to this convergence behaviour, we believe that the iterative error in our simulation is much higher than the discretization error. Hence, it is impossible to perform any reliable uncertainty estimation for a discretization error.

Table 4: Comparison error for propeller resolved simulation

	Case 1.5a		Case 1.6a	
	Value	E%D	Value	E%D
Ct*1000	4.661	3.11	4.572	3.99
Kt	0.214	1.47	0.227	2.78
Kq	0.029	-5.55	0.031	-3.52

Table 4 presents the predicted results with the finest grid for Ct, Kt and Kq as well as relative errors compared with measurement data. In spite of the high numerical uncertainty, the predicted results are reasonable. High propeller torque is a typical result for RANSE simulation when turbulence transition is not simulated. But as shown in the following section, the accuracy of the wake flow prediction can be the cause of such an over-prediction as well. It should be stressed that propeller thrust and ship resistance are not clearly defined in a propeller-resolved RANSE simulation. They are evaluated during post-processing using a procedure that is not always clearly defined. Concerning our results, we consider the dynamic axial force acting on the propeller domain as propeller thrust. This choice is justified by the fact that propeller thrust thus obtained agrees with the simulation using actuator disk approach presented later in this paper. With this post-processing procedure, we underestimate propeller thrust and ship resistance compared with measurement data. If we consider axial force acting on propeller blades as propeller thrust, then for case 1.6a, we will overestimate propeller thrust

by 1.2% and underestimate ship resistance by 2%. This results in a better agreement with measurement data, while it is exactly the same simulation result.

We have also performed self-propulsion simulations by using a body-force approach with an actuator disk model. Propeller thrust can be determined directly from the RANSE computation. But to determine other quantities related to propeller performance, such as propeller torque and propeller revolution rate, a special coupling procedure is required. The RANSE solver can be coupled with a BEM code or another type of simplified code to simulate the action of the propeller. In the present study, we employed a simpler approach without using any other simplified code. We only used the open-water K_t - K_q results obtained from the measurements to determine the missing quantities in post-processing. The procedure is as follows. First, we perform a usual RANSE computation with an actuator disk approach to simulate the effect of the propeller. Propeller thrust is adjusted during this computation such that a self-propulsion condition is satisfied. After having obtained the converged solution with the RANSE solver, we compute the total velocity at the propeller plane. The total velocity is computed on a disk with the same size as the propeller diameter. This gives us two conditions: propeller thrust and total velocity. We perform an additional open-water computation using an actuator disk approach based on the open-water K_t - K_q result. In this open-water actuator disk computation, propeller revolution rate and propeller advancing speed are adjusted such that the propeller thrust determined from the K_t - K_q result and the total velocity computed at the propeller plane are the same as the values obtained with the RANSE computation with the hull. With two conditions and two unknowns, the problem is well defined and can be solved iteratively. Compared with more complex coupling procedures such a RANSE/BEM coupling approach, there is no need to compute the propeller induced velocity.

Table 5: Propeller modeled simulation for case 1.5a

	Wall resolved		Wall modeled	
	Value	E%D	Value	E%D
$C_t \cdot 1000$	4.625	3.87	4.620	3.97
K_t	0.214	1.24	0.213	1.84
K_q	0.0291	-4.41	0.0291	-4.19
$n(\text{rps})$	7.60	2.56	7.62	2.31

Table 6: Propeller modeled simulation for case 1.6a

	Wall resolved		Wall modeled	
	Value	E%D	Value	E%D
$C_t \cdot 1000$	4.660	2.14	4.617	3.04
K_t	0.2385	-2.36	0.2327	0.13
K_q	0.0306	-3.66	0.0305	-3.25
$n(\text{rps})$	7.31	2.53	7.33	2.27

Unlike for resistance computations, it is hardly possible to obtain a result with a good convergence behavior with respect to the requirement for Richardson extrapolation. Therefore, only the predicted C_t , K_t , K_q and propeller revolution rate n obtained with the finest grid as well as the relative errors compared with measurement data are shown in Tables 5 and 6 for the cases without and with ESD, respectively, both for wall resolved simulation and for wall modeled simulation using wall function. Unlike for propeller-resolved simulations, propeller thrust and ship resistance are clearly defined in the propeller-modeled RANSE computation. Compared with measurement data, predicted results are slightly better than what we obtained with the much more expensive propeller-resolved simulation presented in Table 4. As the computations are performed with half domain, propeller tangential forces are not taken into account. Errors due to this approximation need to be investigated in a future study. In our simulation, the measured K_t - K_q are employed to determine propeller torque coefficient K_q and propeller revolution rate n . Propeller torque is over-predicted in the propeller-resolved simulation. In spite of the uncertainty about the accuracy of such simplified approach, we believe that such overprediction of propeller thrust can be attributed to the accuracy of the predicted wake. As shown in

the following sub-section, the predicted axial velocity at propeller plane is smaller than the measurement result, especially for the case without ESD. This explains why the estimated propeller revolution rate is lower and the propeller torque higher. In both cases, wall-resolved simulations and wall-modeled simulations give about the same accuracy. This justifies once again the use of wall functions for engineering applications.

4.3 Local Flow Results for JBC

4.3.1 Mesh influence on the flow around the naked hull without ESD or propeller

The mesh set employed in the present study is designed to ensure an accurate enough accuracy for ship resistance and propulsion prediction based on our experiences. Spatial resolution in the wake near the propeller plane is about $0.00086L_{pp}$ with the finest grid. With such a grid resolution, the difference of the predicted axial velocity contours obtained with the two finest grids is still clearly visible as shown in Fig. 4. Thus a grid independent solution for the local flow field has not yet been reached. Therefore, we attempted to obtain a more accurate solution with adaptive grid refinement, first without taking into account the free-surface. Results obtained with a double model computation using wall resolved EASM are shown in Fig. 7. The adaptive mesh contains about 35M cells. Comparison with measurement data is shown in Fig. 8.

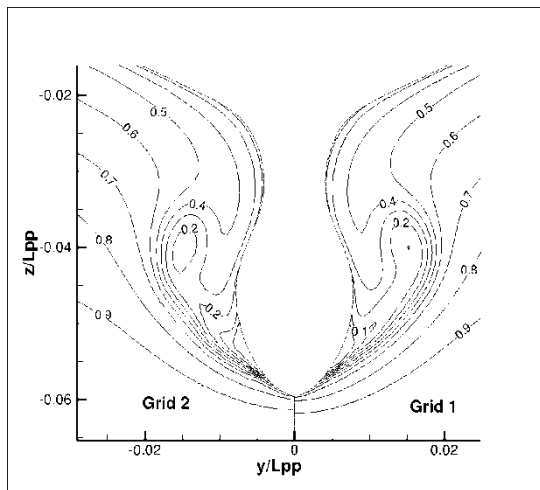


Fig.7: Predicted U velocity contours at section S2

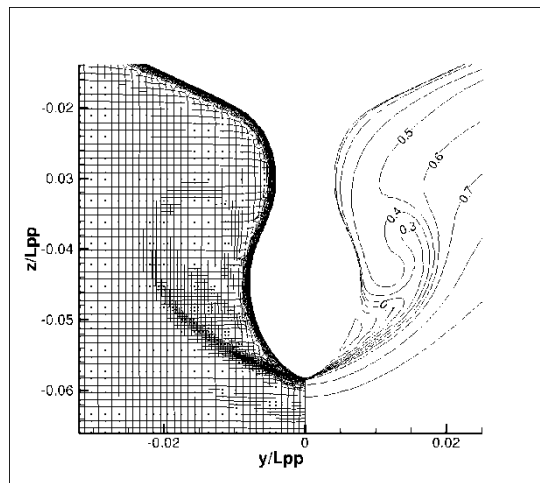


Fig.8: U velocity contours obtained with double model at section S2 with automatic grid refinement

In the core of the aft-body vortex, the predicted axial velocity is higher than measured, while for free-surface computations, the predicted value is lower. This indicates a non-negligible influence of the free-surface deformation on the flow field, despite the low Froude number $Fn=0.142$. To clarify this situation, we have performed another adaptive grid refinement computation with free-surface. The minimum cell size was refined to about $0.00009L_{pp}$. But with such a fine grid, a flow instability develops leading to an unsteady behavior of the large vortex structure. Due to this unexpected unsteadiness, the predicted wake flow is quite different from what we obtained when the numerical solution converged to a steady solution. Such unsteadiness is also observed when the mesh is refined manually in the wake with similar grid resolution, although in that case, the amplitude of the unsteady fluctuation is not exactly the same. The flow around the naked JBC hull appears therefore to be difficult to be predicted accurately because of a likely unsteady behavior of the main vortex structure.

Additional computations based on hybrid LES turbulence models which are essentially unsteady are currently performed and will be presented at the conference. They will hopefully shed some light on this flow with complex physics.

4.3.2 Local flow comparisons with experiments for hull without ESD or propeller

Fig. 9 compares computed and measured longitudinal velocity contours. The computed longitudinal vorticity is slightly weaker than measured. As usually observed, the turbulence anisotropy present in the EASM model contributes to the increase of the longitudinal vorticity (see Fig. 10 which compares at section S2 the isotropic SST and the anisotropic EASM turbulence closures).

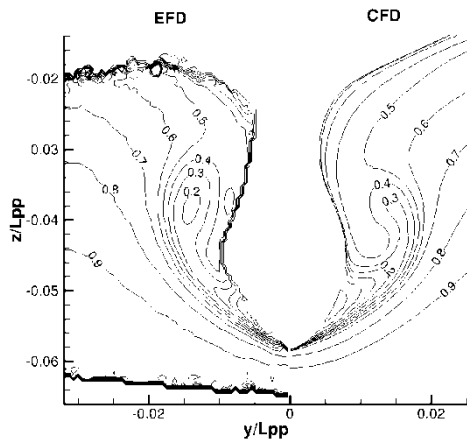


Fig.9: Comparison of U velocity contours at section S2

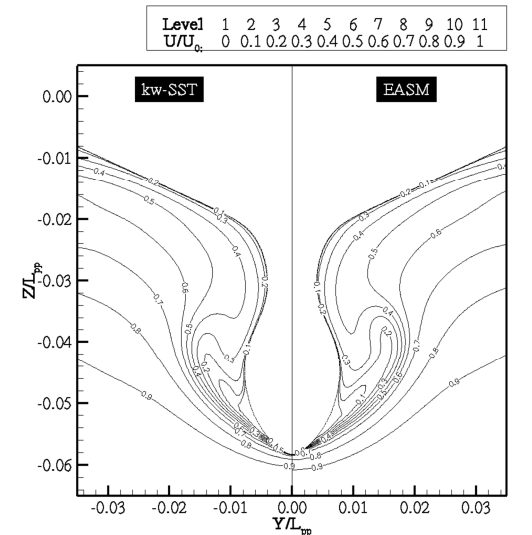


Fig.10: Comparison between SST and EASM model

Figs. 11 and 12 show the wall streamlines on the naked JBC hull without duct or propeller. We can notice a slightly longer line of convergence indicating that the longitudinal bilge vortex is more pronounced with EASM than with SST closures. Moreover, a relatively large zone of recirculation is visible at the stern below the propeller hub, which can be related with the unsteadiness noticed on very fine grids.

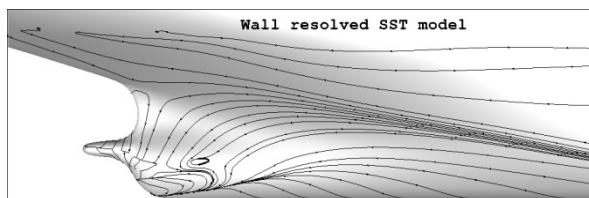


Fig.11: Wall streamlines with SST closure

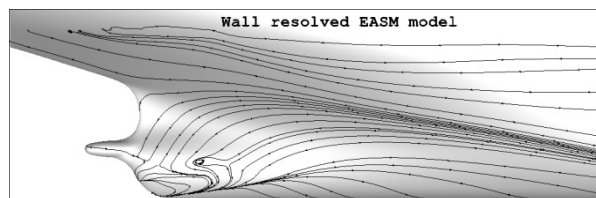


Fig.12: Wall streamlines with EASM closure

4.3.3 Local flow comparisons with experiments for hull with ESD and without propeller

Figs. 13 and 14 show the wall streamlines around the hull with the presence of the duct for two different turbulence closures. The main effect of the duct is a suction effect which removes the spiral vortex which was detected by both turbulence closures just above the recirculation region located at the stern of the hull.

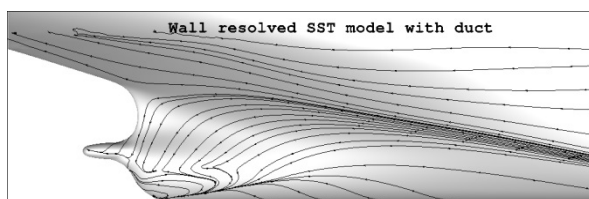


Fig.13: Wall streamlines with SST closure

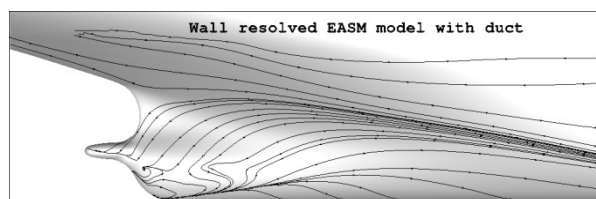
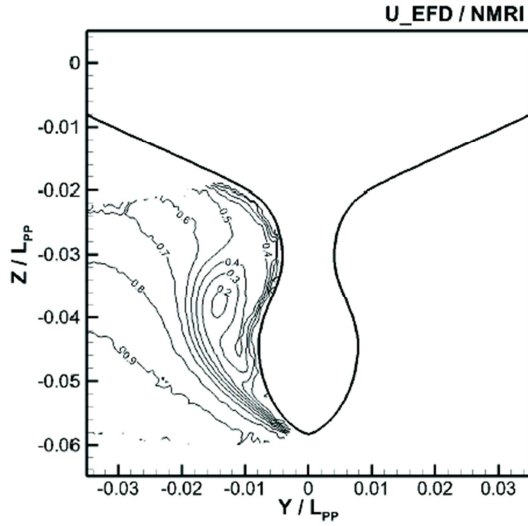


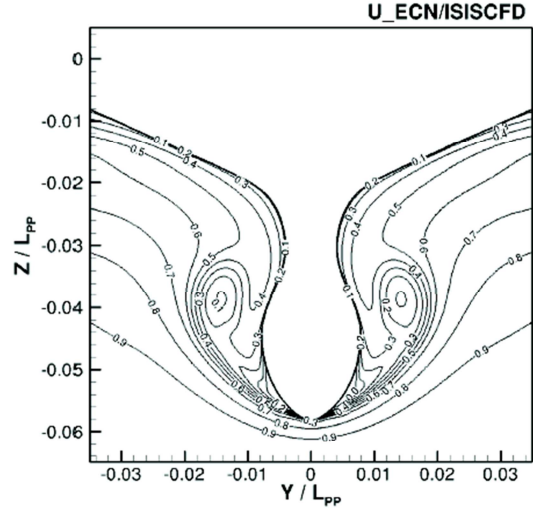
Fig.14: Wall streamlines with EASM closure

Figs. 15 and 16 show the experimental and computed isowake distributions at section S2. We can observe that the presence of the duct increases the computed longitudinal vorticity, leading to an excellent visual agreement between the computations and the measurements at section S2. This agreement is confirmed at section S4 shown in Figs. 17 and 18 although the zone with negative longitudinal velocity seems to be slightly overestimated in the computations.



EFD(NMRI)

Fig.15: Section S2 – Experimental isowake distribution



ECN_CNRS-ISISCFD-LRN_EASM

Fig.16: Section S2 – Computed isowake distribution with EASM closure

5. Propulsive efficiency improvements due to the ESD

In order to conclude on the influence of the ESD on the ship's propulsion system, self-propulsion parameters are computed for both experiments and simulations and compared between hull configurations (see Figs. 19 and 20 for the duct propeller actual configuration). Two additional modeling approaches for the propulsion system, namely actuator disk (AD) and rotating propeller (RP), used in *del Toro Llorens (2015)*, are compared along this assessment. Apart from the already introduced dimensionless coefficients such as J , K_T , K_Q and w_t , we introduce:

$$t = \frac{T + SFC - R_{T,Towing}}{T}$$

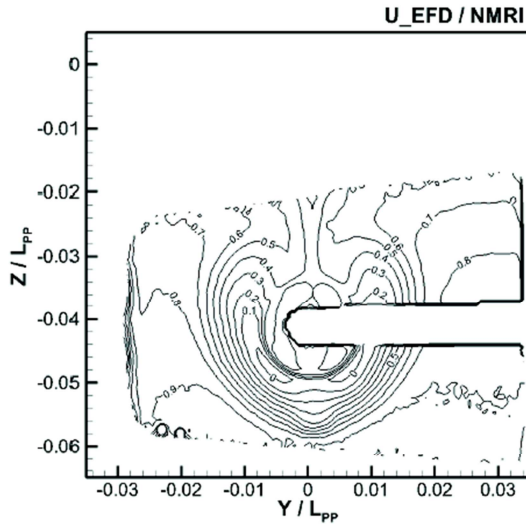
$$\eta_0 = \frac{JK_T}{2\pi K_{Q,OW}}$$

$$\eta_R = \frac{K_{Q,OW}}{K_Q}$$

$$\eta_H = \frac{1 - t}{1 - w_t}$$

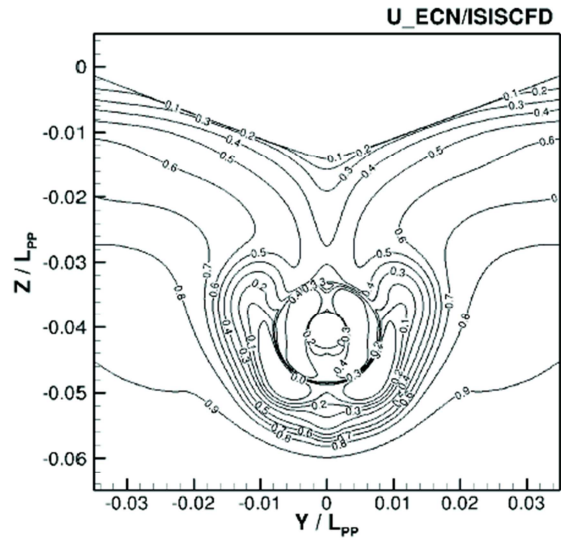
$$\eta_D = \eta_0 \cdot \eta_R \cdot \eta_H$$

t , η_0 , η_R , η_H and η_D are thrust deduction factor, propeller open-water efficiency, relative rotative efficiency, hull efficiency and propeller quasi-propulsive coefficient, respectively. These coefficients are summarized in Tables 7 and 8 which allow comparing the performance of each propulsion modeling approach besides the efficiencies between using or not ESD. The coefficients for both configurations without and with ESD were computed using the simulations with the wall-function modeling approach.



EFD(NMRI)

Fig.17: Section S4 – Experimental isowake distribution



ECN_CNRS-ISISCFD-LRN_EASM

Fig.18: Section S4 – Computed isowake distribution with EASM closure

Table 7: Hull without duct and propeller - Summary of propulsive and efficiency coefficients

Parameter	EFD	AD		RP			
		S_1	$E\%D$	S_2	$E\%D$	S_3	$E\%D$
$K_T \times 10$	2.170	2.130	1.84	2.154	0.74	2.144	1.20
$K_Q \times 10^2$	2.790	2.907	-4.19	2.968	-6.38	2.977	-6.70
$K_{Q,OW} \times 10^2$	2.830	2.958	-4.51	2.835	-0.17	2.826	0.15
n	7.800	7.620	2.31	7.800	0.00	7.800	0.00
T	22.589	20.946	7.27	22.219	1.64	22.113	2.11
$R_{T,Towing}$	36.363	35.668	1.91	35.668	1.91	35.668	1.91
t	0.196	0.166	15.26	0.214	-9.13	0.210	-7.21
w_t	0.448	0.488	-8.92	0.432	3.60	0.429	4.32
J	0.411	0.390	5.06	0.423	-2.93	0.425	-3.51
η_0	0.5013	0.4470	10.83	0.5113	-2.00	0.5134	-2.42
η_R	1.0144	1.0175	-0.30	0.9552	5.84	0.9493	6.42
η_H	1.4575	1.6298	-11.82	1.3845	5.00	1.3833	5.09
η_D	0.7411	0.7412	-0.02	0.6762	8.77	0.6742	9.03

Table 8: Hull with duct and propeller - Summary of propulsive and efficiency coefficients

Parameter	EFD	AD		RP	
		S_1	$E\%D$	S_2	$E\%D$
$K_T \times 10$	2.330	2.327	0.13	2.304	1.12
$K_Q \times 10^2$	2.950	3.046	-3.25	3.097	-4.98
$K_{Q,OW} \times 10^2$	2.977	3.101	-4.18	2.871	3.53
n	7.500	7.330	2.27	7.500	0.00
T	22.435	21.214	5.44	21.966	2.09
$R_{T,Towing}$	36.288	35.752	1.48	35.752	1.48
t	0.189	0.168	11.30	0.196	-3.75
w_t	0.522	0.558	-7.02	0.502	3.86
J	0.370	0.350	5.51	0.386	-4.21
η_0	0.4615	0.4180	9.42	0.4929	-6.82
η_R	1.0090	1.0181	-0.90	0.9272	8.11
η_H	1.6949	1.8837	-11.14	1.6122	4.88
η_D	0.7892	0.8016	-1.58	0.7368	6.63

Despite the fact that the uncertainty related to the previous results is unknown and for both configurations with and without duct, the self-propulsion point was not achieved, the computations performed modeling the propulsion system with a rotating propeller seem to be slightly more accurate than with actuator disk. The full rotating propeller computation is about ten times more expensive than the actuator disk approach. This is the price to be paid if local flow predictions accounting for the complete hull-ESD-propeller interactions are required. Finally, both measurements and simulations reveal an efficiency gain when the ESD is installed, see Tables 7 and 8; so it is working as expected. However, discrepancies appear between EFD and CFD on how much this gain is. EFD gives a gain in propulsive efficiency of 6.5%, CFD around 8.2% - 9.0% depending on the propulsion modeling approach.

6. Conclusions and perspectives

This paper has presented many computations performed on the Japan Bulk Carrier for the last Tokyo 2015 workshop on numerical ship hydrodynamics. A grid influence study was carried out to evaluate the influence of the discretisation error. A preliminary comparison with available experiments was reported for the cases with and without ESD to try to quantify the influence of the duct on the local flow and consequently, on the propulsive efficiency. However, only RANSE computations were performed and the fine grid computations seem to indicate that the flow is not fully steady everywhere. It would be interesting in the future to have recourse to unsteady hybrid LES computations in order to get more physically reliable results and see what the influence of this local unsteadiness on the global flow is. Full-scale computations were not shown due to a lack of time but future studies will be devoted to evaluating the scale effects on the propulsive efficiency associated with the use of this particular Energy Saving Device.

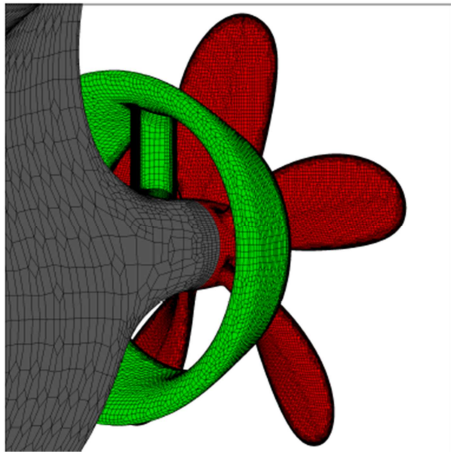


Fig.19: Front view of the propeller + ESD

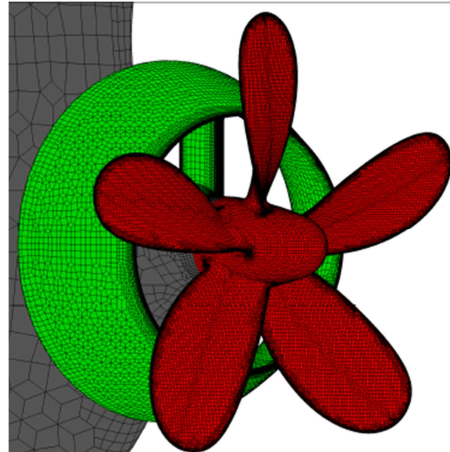


Fig.20: Rear view of the propeller + ESD

Acknowledgement

This work was granted access to the HPC resources under the allocation 2015-2a1308 made by GENCI (Grand Equipement National de Calcul Intensif).

References

- DEL TORO LLORENS, A. (2015), *CFD Verification and Validation for Ship Hydrodynamics*, Master Thesis, Ecole Centrale de Nantes
- HOEKSTRA, M.; ECA, L. (2008), *Testing Uncertainty Estimation and Validation Procedures in the Flow Around a Backward Facing Step*, 3rd Workshop on CFD Uncertainty Analysis, Lisbon

QUEUTEY, P.; VISONNEAU, M. (2007), *An Interface Capturing Method for Free-Surface Hydrodynamic Flows*, Computers & Fluids 36/9, pp.1481-1510

WACKERS, J.; DENG, G.B.; LEROYER, A.; QUEUTEY, P.; VISONNEAU, M. (2012), *Adaptive grid refinement algorithm for hydrodynamic flows*, Computers & Fluids.55, pp.85-100

Hull Performance Analysis – Aspects of Speed-Power Reference Curves

Andreas Krapp, Jotun, Sandefjord/Norway, andreas.krapp@jotun.no
Volker Bertram, DNV GL, Hamburg/Germany, volker.bertram@dnvgl.com

Abstract

This paper discusses the problem of how to deal with variations in draft and trim in hull performance analysis. Dense speed-draft-trim-power relations from computational fluid dynamics simulations are compared to commonly used approaches based on standard model test results for several container ships of different sizes. Most results were found in a joint industry project with a large German containership operator.

1. Introduction

Hull performance analysis of ships recently gained significant focus, triggered by an increased focus on fuel costs and greenhouse gas emissions. The assessment of the impact of hull roughness (mainly due to fouling) on the vessel speed and/or power demand and thereby on the fuel consumption of a vessel is the main objective of hull performance analysis. In general, performance monitoring for ships and hull performance analysis in particular is difficult because there are various other factors influencing fuel consumption, which change in time:

- Different load conditions (draft and trim)
- Different speed
- Sea state
- Current
- Wind
- Shallow water
- Sea temperature and salinity
- Rudder angle
- ...

In order to single out the influence of hull roughness, we need to estimate the contributions from all other significant factors to convert data at different conditions to a common baseline.

All hull performance monitoring systems have a similar basic approach: Raw data acquired on board are filtered and corrected for external influences. The corrections are based on hydrodynamic models which differ in sophistication, accuracy and required effort. Errors in the resulting hull performance rating stem thus from two main sources:

- Input data error: “Garbage in – Garbage out”. Onboard sensors have inherent limited precision. The crew may also be a “sensor” in this sense, adding errors due to faulty estimates, deliberate lies or reporting errors. Data logging is traditionally problematic in performance monitoring, as discussed e.g. by *Pedersen and Larsen (2009)*, *Hansen (2011)*. Continuous monitoring resulting in high data density and cross-referencing data input or sensors for automatic fault detection generally improve data quality.
- Model errors: “Good data in – Still Garbage out”. Models are by definition approximations of reality. Certain influence factors may be omitted completely for convenience, making the model faster and easier to handle. Other factors may be approximated, using for example semi-empirical estimates derived from statistical data for many ships and “representative” or “average”, thus by nature not exact for an individual ship.

Ideally, accurate input data should be processed by an accurate model to obtain good results.

The propulsive power needed to achieve a certain vessel speed depends on the displacement of the vessel and variations in the loading condition have therefore to be accounted for in the model used to analyse the data. During the vessel design process, speed-power curves are predicted and tested in towing tank experiments for two to three different loading conditions – one for ballast load, one for design load, sometimes one for scantling or an intermediate draft. These curves are also the basis for the analysis of speed-trials as part of the vessel delivery process. For many vessels speed trials are performed at light load and the model test results are then used to extrapolate the speed trial results to design load.

In vessel performance analysis, the speed-power curves from model testing or speed trial are commonly used to correct for variations in speed and in loading conditions. The challenge one faces in using model test curves for two or maximum three loading conditions is that they leave high uncertainty on how to deal with intermediate load situations. One commonly used approach to deal pragmatically with this challenge is to interpolate between the curves from model testing. For variations close to a displacement with known speed-power curve, the Admiralty formula is often used. Its applicability is, however, restricted to small variations.

In recent years, computational fluid dynamics (CFD) simulations for use in ship propulsion prediction have reached a high level of maturity and are sometimes referred to as the numerical towing tank. If performed with the necessary level of sophistication, CFD simulations are a real alternative to towing tank experiments, especially if trends are of interest.

The prediction of the speed-draft-trim-power relation by CFD has shown to be of interest to many vessel owners, mainly for operational use as a trim advice tool. DNV-GL delivers CFD-based dense speed-draft-trim-power matrices under the ECO-Assistant label.

2. Model test results versus speed trial results - variations between sister vessels

We compared speed-trial data for 7 sister vessels (container ships) with the model test prediction for this class, Fig.1.

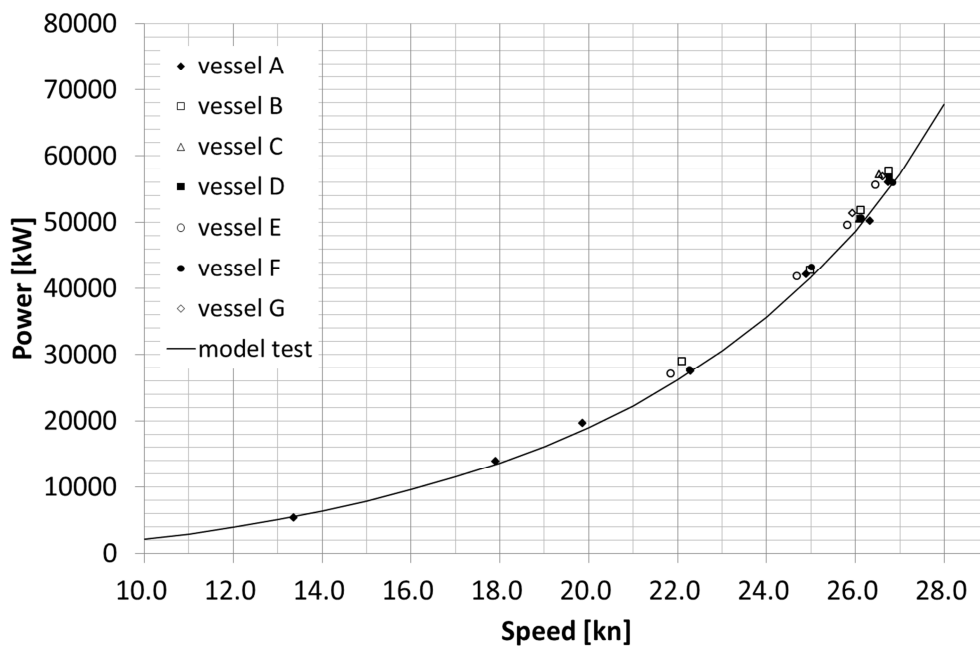


Fig.1: Model test prediction and actual sea trials for 7 sister vessels (containerships)

The ships generally required slightly higher power than predicted from model tests. Sister vessels showed a variation in power of up to 5% (respectively a variation in speed of up to 0.5 kn) in sea trial measurements. This may be due to

- differences in the actually built ships (welding, alignment of bilge keel and other appendages, quality of coating, etc.), *Ciortan and Bertram (2014)*, and
- differences in the sensors on board (alignment of speed log, application of torque meter, etc.) and
- uncertainties in the speed trial analysis procedure (ISO 15016 or similar), which is meant to correct the speed trial measurements to standard conditions (wind, sea state, loading condition)

The first two differences must be expected and accepted. As a consequence, the baseline for performance monitoring should be adjusted according to sea trial data for each ship.

The uncertainty in the speed trial correction schemes is an unfortunate reality that is hard to quantify and which makes it difficult to reliably compare the results of sister vessels.

3. Draft – trim variations

Most hull performance monitoring systems use model test reports to normalize draft, i.e. converting results for arbitrary draft to a benchmark condition. In model test reports, typically only two speed-power curves are available (ballast and design condition) and these cover only the top third of the speed range. For lower speeds, simple extrapolations are employed, e.g. following the Admiralty formula. By necessity, trim is not considered at all in this approach. Some advocate the use of finer draft-trim-speed-power interpolation, e.g. *Hansen (2011)*, *Bertram (2014)*. In this approach, many combinations of trim, draft and speed are investigated, covering the whole operational range of the ship. The required hydrodynamic knowledge base can be taken from trim optimization systems, such as the ECO Assistant of DNV GL.

We investigated the difference between the simplified approach based on model test reports and the advanced approach based on a dense CFD matrix. The hydrodynamic knowledge base of the ECO-Assistant trim optimization software for the test ship was approximated by a 6th-order polynomial expression for the required power as function of trim θ , draft T and speed V. The polynomial had a correlation coefficient of $R^2 = 0.9997$, indicating a very good fit.

For the same speed range and draft-trim conditions as in the model tests, CFD and model test predictions coincide very well. Significant deviations occurred only for ballast draft and low speeds. This can be qualitatively explained as follows: Model tests use a form-factor approach, namely ITTC'78, where the form factor is assumed to be speed independent. Several investigations have shown that this is not (quite) true, especially when there is significant wave breaking and flow separation (ballast condition). Full-scale CFD simulations capture these effects, model tests do not.

Fig. 2 (left) shows the speed-power relation for different draft and trim values (+1m, 0m, -1m). Fig. 2 (right) shows the change in power when increasing draft at constant speed. These graphs are based on CFD simulations. Figs. 3 and 4 show similar graphs for two other vessel classes. All three vessel classes are container ships, vessel 1 is the largest, vessel 3 the smallest.

It becomes obvious that for these three vessel classes, it is not possible to find a straight-forward method of interpolating speed-power curves for intermediate draft over the whole range of speed and draft values. For vessel class 1 and 2, for high speeds and high drafts, the power demand increases approximately linearly with draft, and a linear or quadratic extrapolation seems acceptable. However, for low speeds and lower draft, this does not hold. It is not obvious when the linear extrapolation regime can be applied, when not having access to dense speed-draft-trim-power information. In some instances the power requirement at low speed for a light draft is predicted to be higher than for a

larger draft. This effect can be identified as curve crossing between low and high draft curves in the speed-power curves. For the smallest vessels representing vessel class 3, CFD predicts that the lowest draft shown in Fig. 4 (9.5m) is unfavorable almost over the whole speed range when compared to an intermediate draft of 11.0m and even when compared to the highest computed draft of 12.5m.

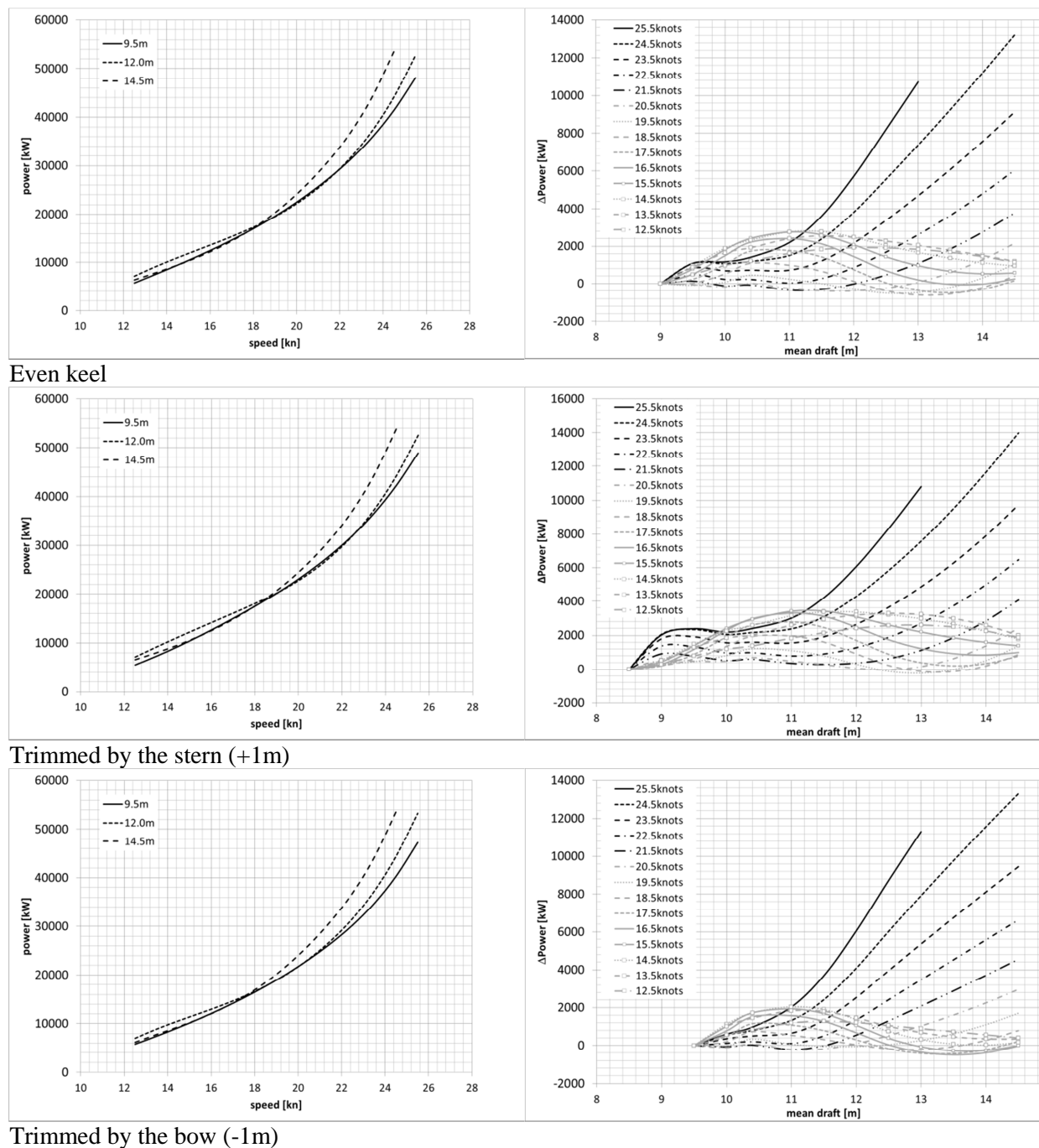
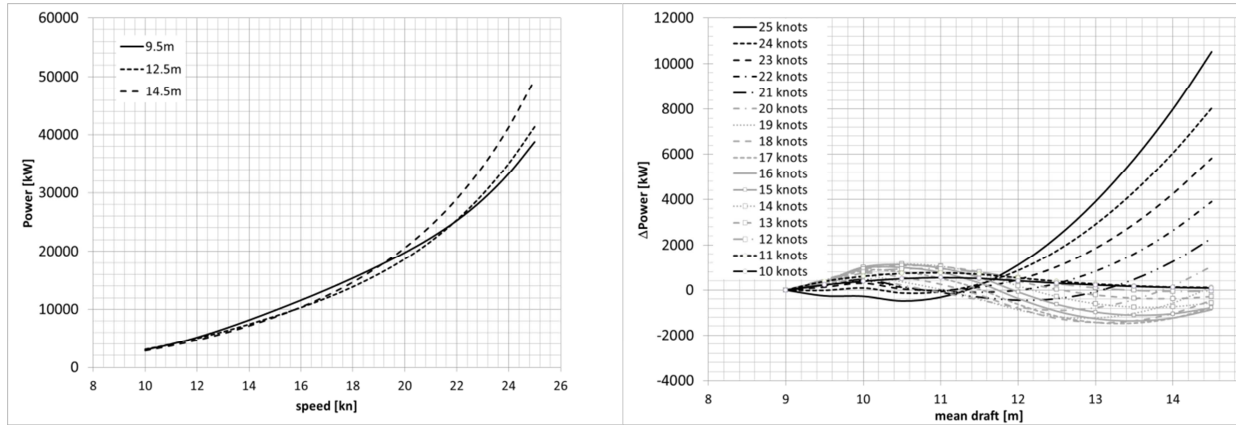
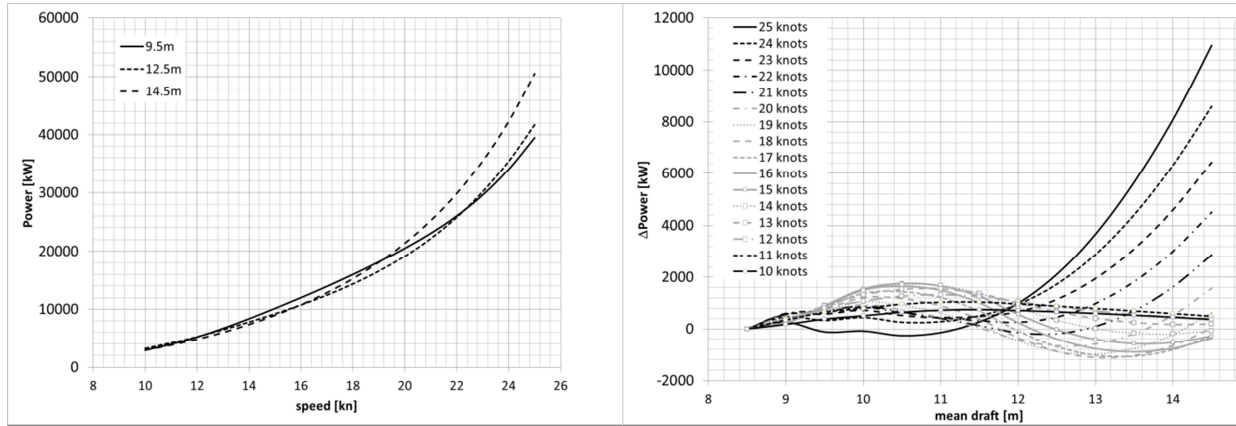


Fig 2: Left: Speed-power curves from CFD simulations for vessel class 1 for different trim (0m, +1m, -1m). Right: Draft-power curves for different speeds for different trim (0m, +1m, -1m)

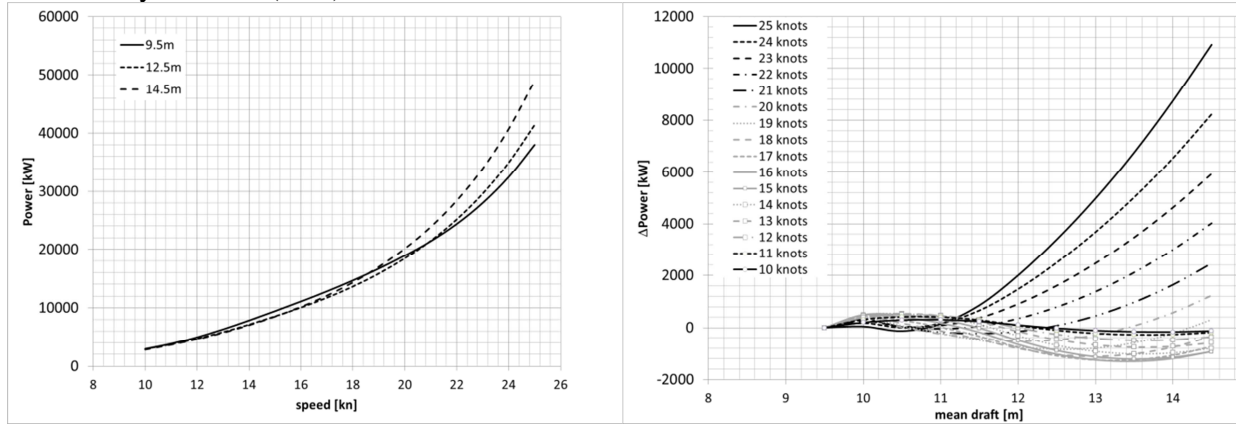
From these three examples of container ships, it seems recommendable to rely on dense speed-draft-trim-power information if one is to correct for draft variations, but also for speed variations. Other vessel types (such as bulk carriers or crude-oil tankers) are less susceptible to these nonlinear variations, due to their hull shape and speed range. But further investigations are needed to quantify whether simple interpolation schemes are sufficient for these ships.



Even keel



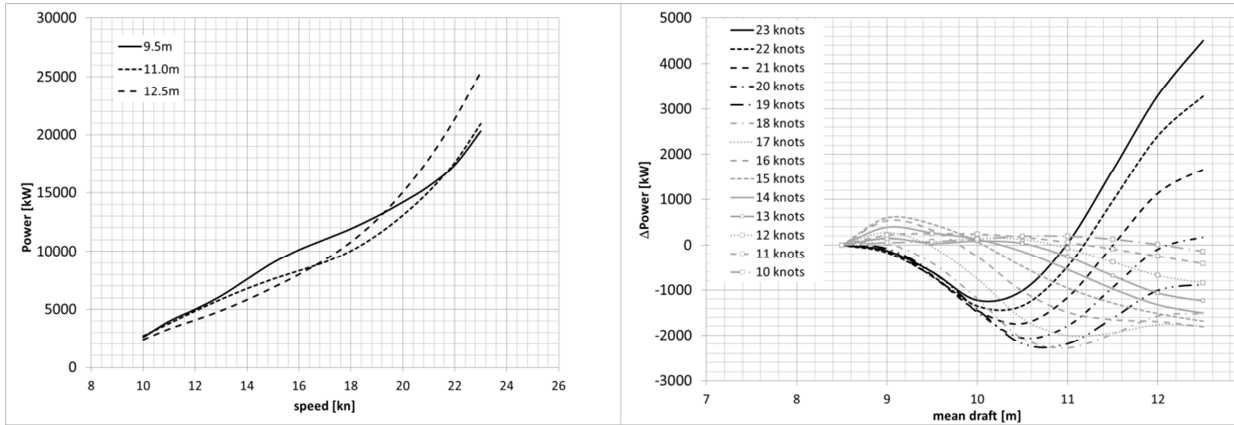
Trimmed by the stern (+1m)



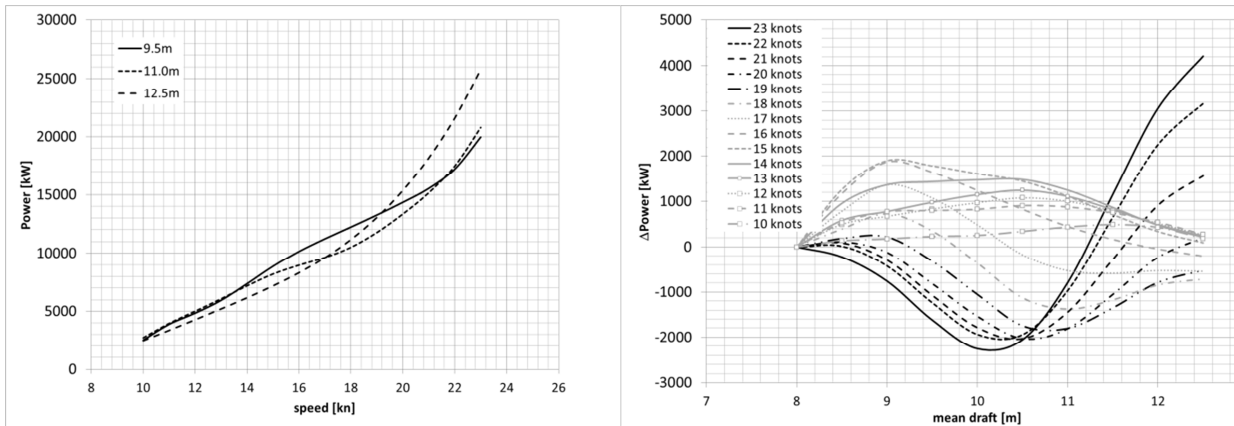
Trimmed by the bow (-1m)

Fig. 3: Left: Speed-power curves from CFD simulations for vessel class 2 for different trim values (0m, +1m, -1m). Right: Change in power by increase in draft for different speeds for different trim values (0m, +1m, -1m)

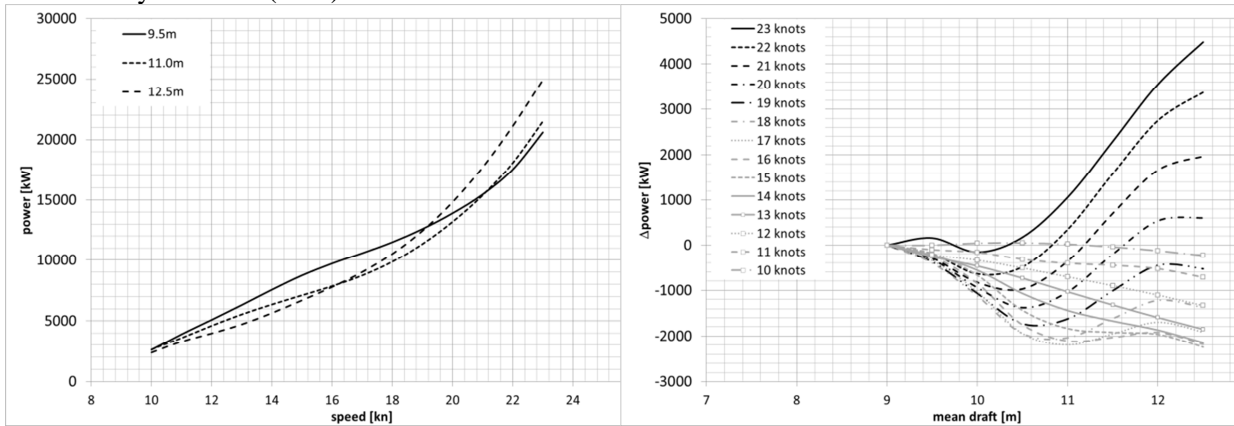
For one vessel of the vessel class 1, we evaluated the difference between power predicted from model tests and from the dense CFD matrix for long-term in-service recordings. Data sets were 15 minutes averages from monitoring. The mean difference between model-test approach with linear interpolation and CFD approach was 9.8%, Fig. 5. Particularly large differences occur for intermediate draft (probably due to surface-piercing bulbous bow) and very low draft, Fig. 6. Differences are also particularly large for low speeds, Fig. 7, probably due to extrapolation errors in the simple approach. In summary, large differences appear for off-design conditions that appear often in operational practice.



Even keel



Trimmed by the stern (+1m)



Trimmed by the bow (-1m)

Fig. 4: Left: Speed-power curves from CFD simulations for vessel class 3 for different trim values (0m, +1m, -1m). Right: Change in power by increase in draft for different speeds for different trim values (0m, +1m, -1m)

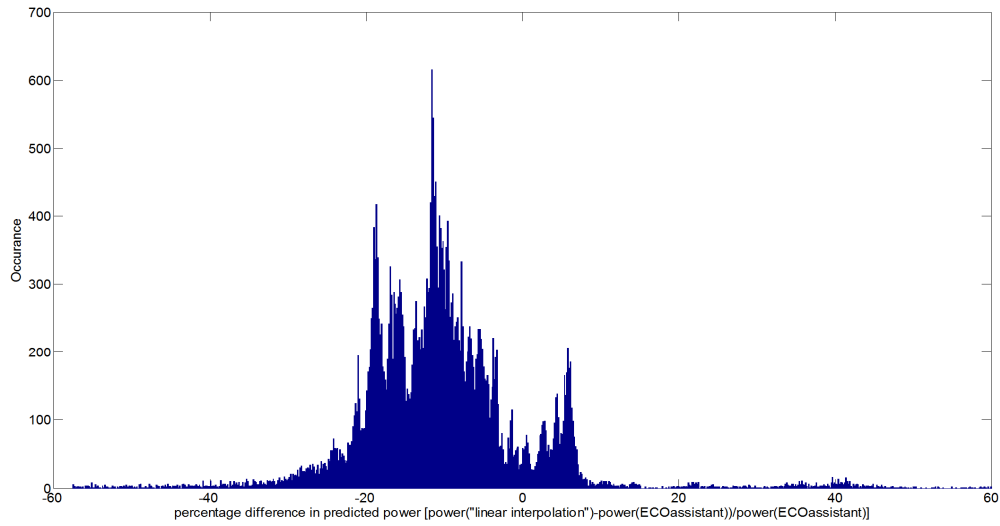


Fig. 5: Difference between model test interpolation and CFD-based fine matrix (ECO Assistant)

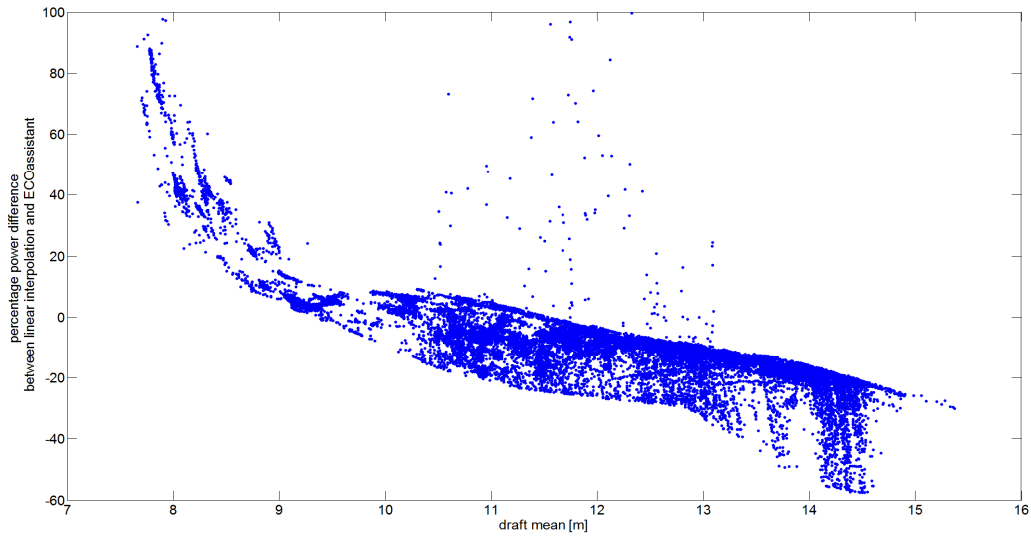


Fig.6: Power prediction for influence of loading conditions; difference between CFD based fine matrix (ECO Assistant) and linear interpolation for two model tests for variations in draft

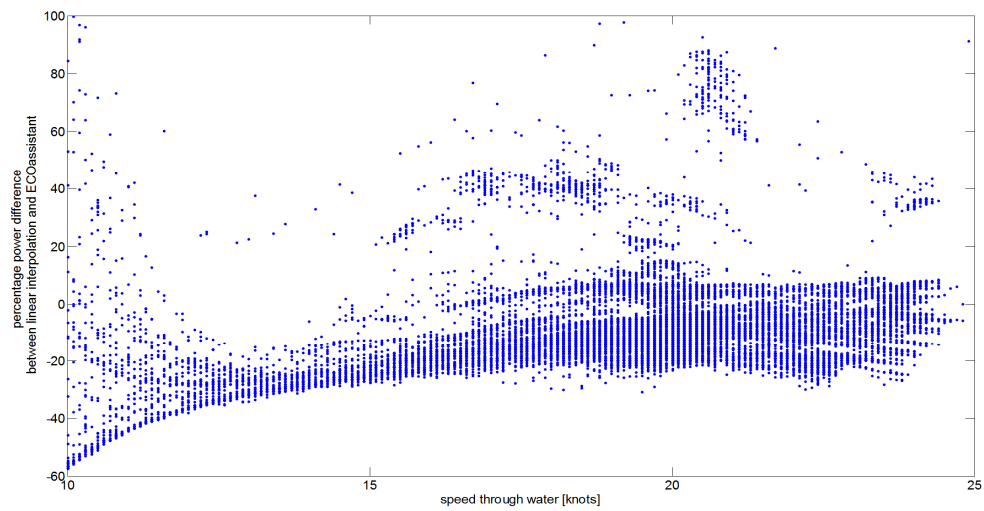


Fig.7: Power prediction for influence of loading conditions; difference between CFD-based fine matrix (ECO Assistant) and linear interpolation for two model tests for variations in speed through water

3. Summary and conclusions

Speed-power curves are used as reference curves to correct for draft, trim and speed variations in vessel performance analysis.

For one class of seven sister vessels the accuracy of model test prediction and sea trial results has been studied and a variability between sister vessels of 5% in power has been observed.

The impact of draft and trim variations on speed-power curves has been studied for three container vessel classes. Based on dense CFD matrices it was concluded that there is no straightforward way to interpolate between speed-power curves for intermediate draft values. Only in the high speed, high draft range a linear or quadratic interpolation between speed-power curves can be used. However, where this range starts is vessel dependant and there is no obvious way to decide from the outside when linear interpolation can be used for a specific vessel.

For one vessel the difference between the predicted power from linear interpolation between model test results and from dense CFD matrices has been studied using real performance data as input. A mean difference of 9.8% has been observed and a clear dependency of the difference on draft and speed was found. This indicates that the use of different approaches to deal with intermediate draft values has a real impact on the analysis of vessel performance and hull performance and care should be taken when choosing the approach to handle intermediate drafts.

Acknowledgements

We are grateful for the cooperation with our joint industry project partners, namely Björn Walther and Niels Kaiser of Norddeutsche Reederei H. Schuldt and Goran Berkes of MAC System Solutions.

References

- BERTRAM, V., *Trim optimization – Don't blind me with science*, The Naval Architect, July/August
- BERTRAM, V.; LAMPROPOULOS, V. (2014), *A hull performance monitoring model for energy efficient operation*, European Conf. Production Technologies in Shipbuilding (ECPTS), Hamburg
- CIORTAN, C.; BERTRAM, V., *RANSE simulations for the effect of welds on ship resistance*, 17th Numerical Towing Tank Symp., Marstrand, https://www.uni-due.de/IST/ismt_nutts.shtml
- HANSEN, S.V. (2011), *Performance monitoring of ships*, PhD thesis, Danish Technical University, Lyngby, [www.dcam.dk/~media/Sites/DCAMM/S-Reports/S142 Søren Vinther Hansen.ashx](http://www.dcam.dk/~media/Sites/DCAMM/S-Reports/S142_Søren_Vinther_Hansen.ashx)
- PEDERSEN, B.P.; LARSEN, J. (2009), *Prediction of full-scale power using artificial neural networks*, 8th Conf. Computer and IT Applications in the Maritime Industries (COMPIT), Budapest, pp.537-550, http://www.ssi.tu-harburg.de/doc/webseiten_dokumente/compit/dokumente/compit2009.pdf

Continuous Performance Monitoring – A Practical Approach to the ISO 19030 Standard

Erik Hagestuen, Kyma a.s, Bergen/Norway, eh@kyma.no
Bjarte Lund, Kyma a.s, Bergen/Norway, bl@kyma.no
Carlos Gonzalez, Kyma a.s, Bergen/Norway, cg@kyma.no

Abstract

This paper presents a recommended solution for setting up a continuous performance monitoring system to comply with the highest tier in the ISO 19030 standard. The system will automatically collect sensor data, apply filtering and statistical analysis, and finally give a meaningful presentation of the current vessel/fleet performance. The paper includes both onboard and onshore applications.

1. Background

In a market where low freight prices are squeezing the margins to a minimum, it is safe to assume that every ship owner would aim to run their fleet as optimum as possible in terms of fuel efficiency. During the operation of a ship, the hull's anti-fouling system will be less efficient. Marine fouling on the hull increases the frictional resistance. The surface of the propeller can also become rough and fouled, making the propeller less efficient. The total resistance, caused by fouling, may increase significantly throughout a docking interval, with a typical speed loss of 2-4 % per year. An increased focus on environmental regulations and smaller profit margins in the shipping industry make fleet performance and efficiency key topics within the maritime world.

For this, a Ship Performance Monitoring (SPM) software with continuous monitoring can be of valuable assistance to the ship crew and the owner. The basic concept and requirement for this system is to measure key parameters onboard, perform processing on these data, and present the results in an easy to understand and intuitive way for the onboard crew and onshore personnel. Based on this continuous monitoring, corrective actions can be planned and performed accordingly. One challenge in this respect is to present a vessels performance status or rather degraded performance correct and adequate, in order to decide when maintenance/repairs are appropriate.

One example could be indication of high fuel oil consumption on the main engine. The C/E have to interpret and evaluate this fuel flow and find out if this measurement is correct. The root cause for an overconsumption could of course be a reduced performance of the vessel. However, a sensor malfunction, wrong or missing manual recordings, adverse weather, or other external factors can also cause it. This is why automatic data collection, filtering, repeatability and transparency in a performance monitoring system are critical elements for the credibility of the SPM system. The combination of displaying instant performance values together with investigating the long trend of important key performance values are keeping the crew and the management continuously updated on a vessel's performance.

2. Sensors and measurements

The ISO 19030 standard outlines in part 1 some general principles on how to measure the performance changes on a vessel. The standard also defines the hull and propeller performance:

“Hull and propeller performance refers to the relationship between the condition of a ship's underwater hull and propeller and the power required to move the ship through water at a given speed. Hull and propeller performance is related to variations in power, because ship hull resistance and propeller efficiency are not directly measurable quantities.”¹

¹ Source: ISO/WD 19030-1:2014(E) chapter 4.1, Definition of hull and propeller performance

In order to measure the hull and propeller performance it is necessary to find the right parameters to monitor and the right sensors that can measure the parameters reliably and accurately. This chapter will discuss a recommended sensor suite to comply with the ISO 19030 standard.

2.1 Recommended measurement parameters

It is obvious from the above definition that propeller shaft power and ship speed through water are two of the most important parameters to monitor. The ISO 19030-2 defines a set of primary and secondary measurement parameters for measuring the vessel performance. The primary parameters are defined as speed through water, propeller shaft power (torque and revolutions), and time and date². To measure these parameters, the ISO standard states a minimum set of sensors, which in this case are a speed log, a shaft power meter and a GPS (giving the UTC time).

In addition to the above-mentioned parameters, it is also recommended adding accurate fuel oil consumption measurements to get the complete performance picture of a vessel. The fuel consumption will ultimately give the current cost and environmental footprint of the vessel. Marine fuel oil cost constitutes a significant part of the vessels operating cost, so a continuous monitoring of the fuel efficiency is essential to cut operating cost. For this reason the engine manufacturers, hull coating manufacturers and propeller designers are constantly trying to develop new products with fuel saving potential. Furthermore, continuous monitoring of the fuel consumption by using high accuracy flow meters, dedicated data acquisition and processing systems makes the fuel consumption one of the key parameters to monitor to evaluate the cost benefit of any possible maintenance or changes to the M/E, hull and/or propeller area.

Monitoring the above primary parameters with correct and reliable sensors will give the ship owner a good continued status of the vessels efficiency. However, we believe that this monitoring setup is not quite enough. The challenge with this minimum set of sensors is that the efficiency will apparently vary quite a lot, because many external conditions will affect the result continuously. To be sure that the monitoring will be as good as possible and unaffected by any external sources like weather, cargo size, depth, etc., adding a few extra sensors to the sensor suite will give the full performance picture.

One of the extra key parameters to monitor continuously should be the draft status. The 'power vs. speed' profile for a vessel is very much dependent on the vessel's draft conditions, which again directly relates to the cargo weight. It is therefore recommended to correct the baseline of the 'power vs. speed' profile of the vessel against the current draft condition. The higher the draft values, (more cargo), the higher necessary power is needed to get the desired vessel speed.

The weather conditions will definitely influence the measurement of a vessel's efficiency. Including measuring the wind speed and direction continuously, and discarding any measured data if the true wind force is above a certain threshold will improve the SPM software. The threshold should be configurable, but the most common threshold used is to discard any performance data when the wind speed is above Beaufort 6. With wind forces above this threshold, it is normally very difficult to estimate the effect on the vessel's performance.

A recommended sensor suite in order to monitor the efficiency of a vessel and to get a good performance acquisition system can be summarized in Table 1.

2.1.1 Shaft Power Meter

One common method of measuring the shaft torque, explained below, is by using strain gauges. Other methods are IR laser beam, or vibrating string transducers for the detection of the shaft twist. There are pros-and-cons with the different methods.

² Source: ISO/WD 19030-2:2014(E) chapter 4.1, Table 1

Table 1 : Recommended sensor requirements

Parameter	Unit	Sensor	Sensor accuracy ³
Shaft torque	[kNm]	Shaft Power Meter	± 0.5 %
Shaft revolutions	[Rpm]	Optical or magnetic sensor	± 0.5 %
Speed through water	[knots]	Speed Log	± 1.0 %
Speed over ground	[knots]	GPS, Doppler log	±1.0 %
Time and date	[Year, month, day, hour, minutes, seconds]	UTC time (from GPS), or local time from vessels master clock.	
M/E fuel oil consumption	[kg/h or litres/h]	Flowmeter	± 0.5 %
Wind speed, and Direction	[knots] [°]	Anemometer	± 0.5 knots ± 5 °
Draft (minimum fwd and aft)	[m]	Draft gauges	±0.1 m
Ship heading	[°]	Gyro Compass, GPS	± 5 °

The shaft material properties i.e. the G-Modulus should be specified in each case by the supplier of the shaft, or if it is not specified, the value of $82\ 400^4$ kN/mm² should be used. The shaft diameter used in the power calculation is the shaft circumference in-situ measured at the location of the torque meter. To get an acceptable accuracy on the measurement it is very important to be very accurate and thorough during the installation of the strain gauges, but once installed, they usually have a lifetime in the same range as the vessel itself.

The relation between shaft power (kW), shaft torque (kNm), and revolutions (rpm) is defined by:

$$P = \frac{M * 2\pi * n}{60} [kW]$$

Where M = Torque, [kNm]
n = revolutions, [rpm]

The surface of a propeller shaft is subject to strain in a direction of 45° when under torsional forces. The mechanical shaft deformation due to this torque is measured by means of strain gauges, and ideally, by a Wheatstone's measuring bridge, which gives the best result, Fig. 1.

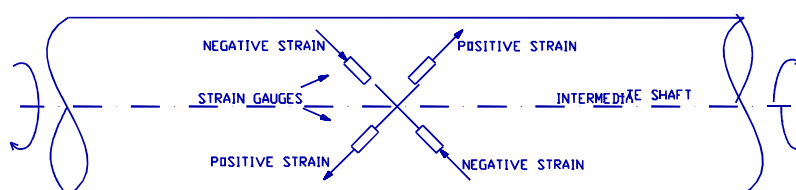


Fig. 1 : Shaft power measurement by strain gauge

A strain gauge consists of parallel thin wires fixed to a piece of plastic. The working principle for a strain gauge is that its resistance will vary proportional to its elongation when stressed mechanically. This change in resistance takes place due to variation in length and cross sectional area of the gauge wire, when an external force acts on it. Over time, the zero adjustment of a strain gauge can drift, so a zero adjustment of the power meter two times a year will keep up the required accuracy of the system.

³ Source : ISO/WD 19030-2:2014(E), chapter 4.1, Primary measurement parameters

⁴ Source : IMO MEPC 68/INF.14

2.1.2 Speed through water

An electromagnetic sensor (EM-Log) can be used to measure the speed through water. The electromagnetic sensor relies upon the principle that any conductor movement across a magnetic field will have induced onto it a small electromotive force (e.m.f.). Assuming that the magnetic field remains constant, the amplitude of the induced e.m.f. will be directly proportional to the speed of movement. In a practical installation, the EM-Log sets up a magnetic field. The induced voltage between the two electrodes measures the magnitude of this voltage signal, which is proportional to the ship speed. The EM-Log must be cleaned and calibrated regularly to keep the required accuracy,

2.1.3 Speed over ground

The speed over ground is measured either by a global positioning system (GPS) or by a Doppler log. The GPS system should operate in the Differential mode to ensure sufficient accuracy. A Doppler speed log can also be used to measure the ship's speed over ground by utilizing the principle of the Doppler effect, which defines that a signal emitted from a moving object is heard with its frequency shifted at stationary locations and the degree of the frequency shift is proportional to the speed of the moving object.

2.1.4 M/E Fuel oil consumption

Depending on the engine(s) fuel oil supply line layout and desired insight, one or more flow meters need to be installed to monitor the fuel oil consumption in real-time. The main principle is to measure the fuel flow before the engine and/or generators and again after.

Coriolis mass flow metering is a well-established technique for industrial flow measurement, and have become more and more the new standard for marine fuel measurements as well. A Coriolis meter consists of a vibrating flow tube through which the process fluid passes. The flowmeter extracts the mass flow and density information based on the vibration frequency of the vibrating flow tube. Coriolis meters offer many benefits, including high accuracy (to 0.1% for static flow rates). Unlike volume measurement, mass measurement is independent of operating pressure and temperature, avoiding the need for density conversions.

2.1.5 Wind measurement

The ship's own anemometer, used for wind measurement, should be located as clear as possible from the superstructure. The true wind speed and direction are calculated based on own ships speed and course.

2.2 Possible additional sensors

In addition to the recommended sensors, Table 2 lists supplemental sensors to the continuous measurement suite.

Table 2 : Possible additional sensors

Parameter	Unit	Sensor	Sensor accuracy
A/E and Boilers fuel consumption	[kg/h or l/h]	Flowmeter	±0.5 %
Wave height and direction	[m], [°]	Wave measuring device (radar, scanner, etc.)	
Propeller pitch (if applicable)	[%]	Synchro unit, etc.	
Sea water density	P [kg/m ³]	Salinity sensor, conductivity sensor	
Sea water temperature	[°C]	Thermometer	

Air temperature	[°C]	Thermometer	
Air pressure	[mBar]	Barometer	
Rudder angle	[°]	Rudder angle indicator	±1.0 %
Water depth	[m]	Echo sounder	± 2.5 % at 100 m

2.2.1 Wave measurements

Preferably, the wave height, wave period and direction of waves due to wind and swell should be determined by using instruments like wave buoys, wave radar or wave scanner. Although less accurate, wave observations may also be determined from observations by multiple observers.

2.2.2 Density and temperature measurements

The recording of the seawater temperature and density enables the calculation of ship's displacement and corrections with regard to viscosity. The water temperature at the seawater inlet level is the preferred measuring point, along with the air temperature and atmospheric pressure, using a calibrated thermometer and barometer.

2.2.3 Rudder angle sensor

The rudders have also some impact on the vessels resistance, even though it is not a very large factor in the overall picture. Quite as expected, the resistance penalty increases with the rudder angle. To obtain a very accurate picture of the vessel performance, the rudder angle's effect on the vessels resistance should be monitored. Normally, the rudder angle sensor connects mechanically directly to the rudder tiller arm or rudder quadrant. This mechanical signal, transformed to an electrical signal, is sent to a rudder angle indicator. The electrical signal can be either a standard analogue signal or a NMEA serial signal.

2.2.4 Depth measurement

Depth of water is another factor that will affect the 'power vs. speed' profile if the vessel enters shallow water. When the depth of water is less than a certain factor of the vessels draft, the hydrodynamic forces may increase, thus subjecting the propeller for a higher load. In general, the shallow water effect is insignificant in water depths of more than ten times the vessel draft. However, even though it is a small factor, a depth-measuring device can be a supplement to get the complete picture of external influencers on the performance.

3. Statistical analysis and filtering

Once the data is gathered from the sensor points, it must be processed, filtered and normalized in order to become more relevant in the statistical analysis and useful for the end users.

3.1 Data logging

The SPM will manage and store large amount of data in order to make a reliable performance analysis. For the performance analysis, the SPM creates the performance observations automatically on a daily basis, using the same set of rules and filtering. All the instant data calculated every logging are filtered and averaged daily, giving a set of reliable performance observations. Each performance observation point is stored in a database for further evaluation. Furthermore, all data points should be stored and backed up in a commonly used format for later processing. A practical solution for backing up the data is to send the data on a regular basis back to the owner for safe onshore storage.

The data from the sensors are not always steady, so in order to get sensible and understandable instant values for the operators, the SPM are applying smoothing algorithms to calculate the average of the

data. Commonly accepted, the logging frequency is set to 15 s (logging time accepted by ISO 19030 Standard). The performance observations, compared with the baseline (design data), will give the deviation point for those variables to be used in the statistical analysis. For the statistical analysis (long trend evaluation), it is established as a reliable frequency of one performance observation per day.

3.2 Performance reference baselines

The SPM software plots the calculated performance observations on different graphs. These graphs are showing the deviation (in percentage) for the key performance indicators. However, to make these observations more useful, a reference base is used to compare them against. Some SPM software uses two different reference levels, one constant and one dynamic.

3.2.1 Constant reference baselines

These reference baselines are the data from the ship's design and they are constant for the complete lifetime of the ship, unless the hull, propeller or main propulsion system undergoes modifications. These baselines designate the 'zero level' in the statistical analysis.

- Constant reference baseline for comparison of speed deviation
One reference level is the design data obtained from the model tank test. The data from the model tank test gives the theoretic relation between the power delivered to the propeller and the ship's speed through the water for ballast and design draft condition. The daily average of speed through the water (performance observation) compared against this theoretic baseline, gives a deviation in percentage, used by the SPM software. Since the speed deviation depends on the ship's cargo, the SPM will automatically interpolate the 'power vs. speed' baseline to any intermediate draft values covering all cargo possibilities. Consequently, the speed deviation value per day takes into account the vessel mean draft, ship speed through the water and the power delivered to propeller. Fig. 2 shows an example of real data obtained from model tank report.

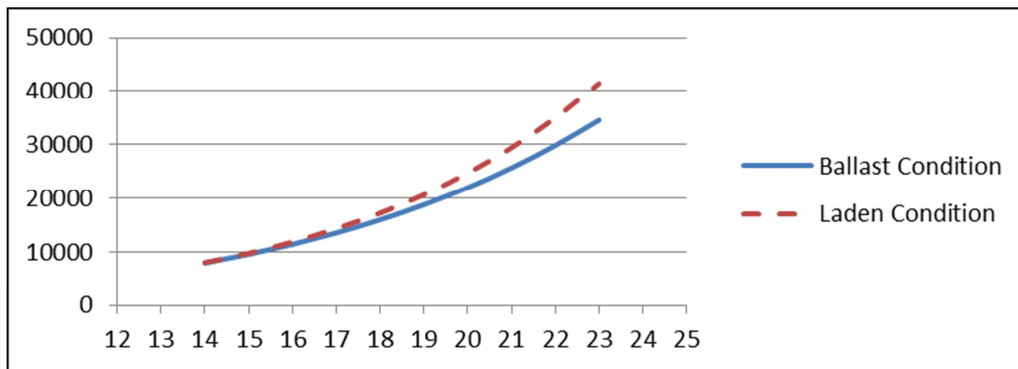


Fig. 2 : Data from model tank test for a container vessel

- Constant reference baseline for comparison of RPM deviation
The reference curve used to calculate the deviation for the RPM is a function of the relation specified in the Propeller handbook⁵:

$$Power = a \cdot (RPM)^{2.7}$$

$$\text{Where, } a = \frac{Power \text{ at } MCR}{(RPM \text{ at } MCR)^{2.7}}$$

⁵ Source: Dave Gerr, Propeller Handbook 1989

The propeller curve contains useful information about the working point of the main engine and the propeller.

- Constant reference baseline for comparison of Specific Fuel Rate (SFR) deviation
This reference curve is obtained from the M/E workshop test report. The fuel type in use by the M/E influences the calculation of the SFR (g/kWh). There are several fuel types onboard with different low heating values (LHV) so the reference baseline shall be at one standard LHV. ISO recommends a LHV reference value of 42,700 kJ/kg.

3.2.2 Dynamic reference baselines

Another reference level is the benchmark level, created with data collected after delivery and/or after any major repair/docking of the ships. Whenever a docking is finished, the operator must set a new ‘trend event’, and the system will automatically use the first months to measure and calculate the current ‘out-of-dock’ condition. This new reference level (benchmark) is created by taking the average of a number of daily observations (i.e. 60-120 performance observations) starting after a major event. These observations, filtered for bad weather and manoeuvring mode (see section 3.4 below), will make up the new benchmark level to compare against for the current operational period until the next trend event.

3.3 Filtering applied in the SPM software

The SPM software is automatically creating performance observations on a daily basis. This requires setting some filtering in the SPM software to avoid useless data to invalidate the long trend analysis. The vessels are operating in varying weather conditions, sea currents, sailing modes (normal navigations, maneuvering, etc.) and cargo conditions (ballast/laden conditions). Due to these changing conditions, the SPM software must apply filtering algorithms to discard data in case of bad weather condition (using the Beaufort scale as reference) or abnormal sailing mode. The performance observation is rejected for use in the statistical analysis if the wind force is above a certain Beaufort level (typically level 6), or the main engine load is less than 30 % MCR.

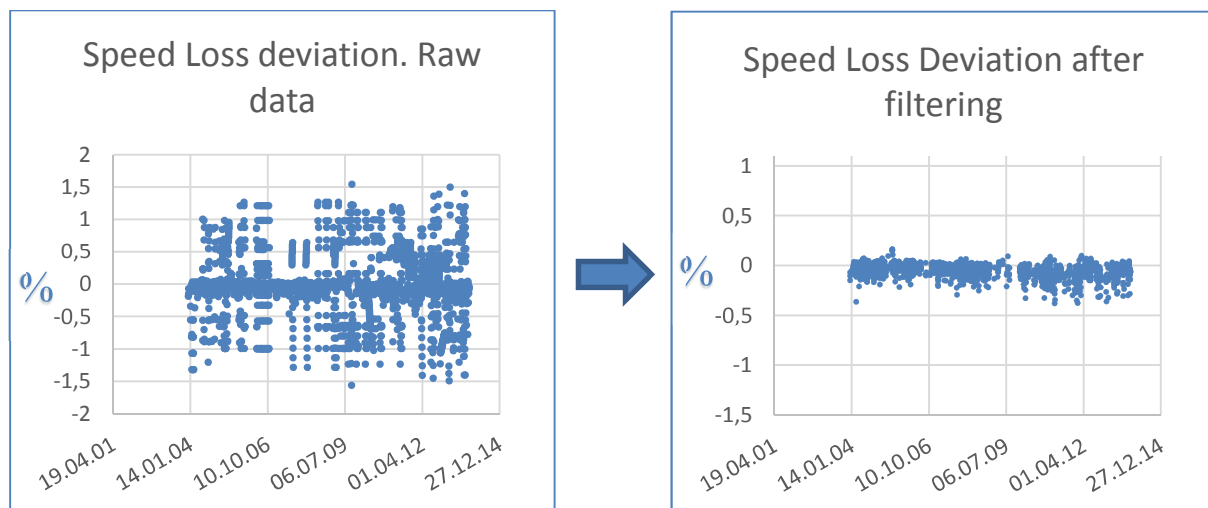


Fig. 3: Left side showing raw data, right side showing data filtered by weather and sailing mode

3.4 Statistical analysis applied by the SPM software

3.4.1 Definition

Per definition, the statistical analysis refers to the methods used to process large amounts of data and report overall trends. Statistical analysis is particularly useful when dealing with noisy data.

3.4.2 Statistical analysis applied

Following the filtering algorithms, the software has a new set of data onto which the statistical analysis is applied. A new trend function on the form $f(x) = ax + b$ based on the filtered data points is plotted along with all the included data points as a solid line. The trend function is calculated from the data points using the linear regression model of least square fit, which is a common method in statistics to find a linear relationship between a set of data points.

4. Presentation of a vessel's performance

After the data is collected, filtered and analyzed, the next step is to display the vessel's performance to the onboard crew and management in the office. There are many different approaches for doing this; some are straight forward, others more complex.

4.1 Instant performance indication

One straight forward approach is to equip the wheel-house with a dedicated instrument indicating if the agreed fuel consumption is exceeded or not. This could be a graphic indication of a target fuel oil consumption of 16 tons/day, and could look like the below example. This works for example for bulk carriers, where the delivery timing is not so time critical, and therefore the vessel can transit in the best fuel efficient speed.



Fig. 4: M/E fuel oil over-consumption and status of generators

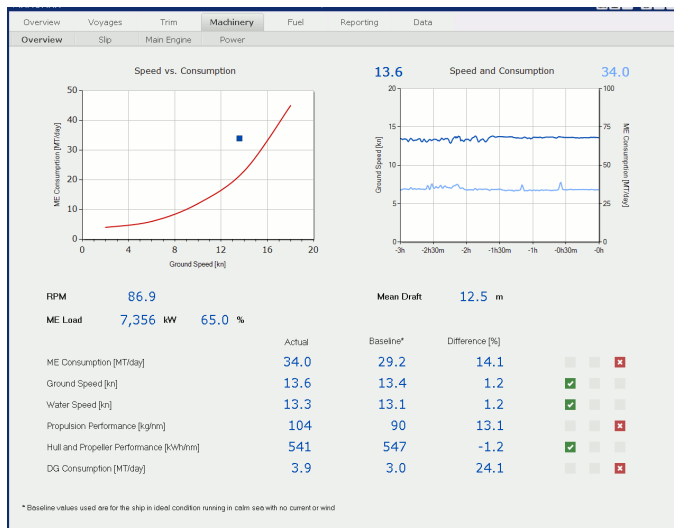


Fig. 5: Example of instant performance dashboard⁶

⁶ Source: Marorka, Iceland

4.2 Performance Trial Report

A welcome feature of a SPM software is to get an instant performance report of the current situation. A Performance Trial of a certain period can give the crew and management a detailed report of the vessel's performance under controlled conditions. Fig. 6 shows a Performance Trial done in good weather conditions and steady state sailing:

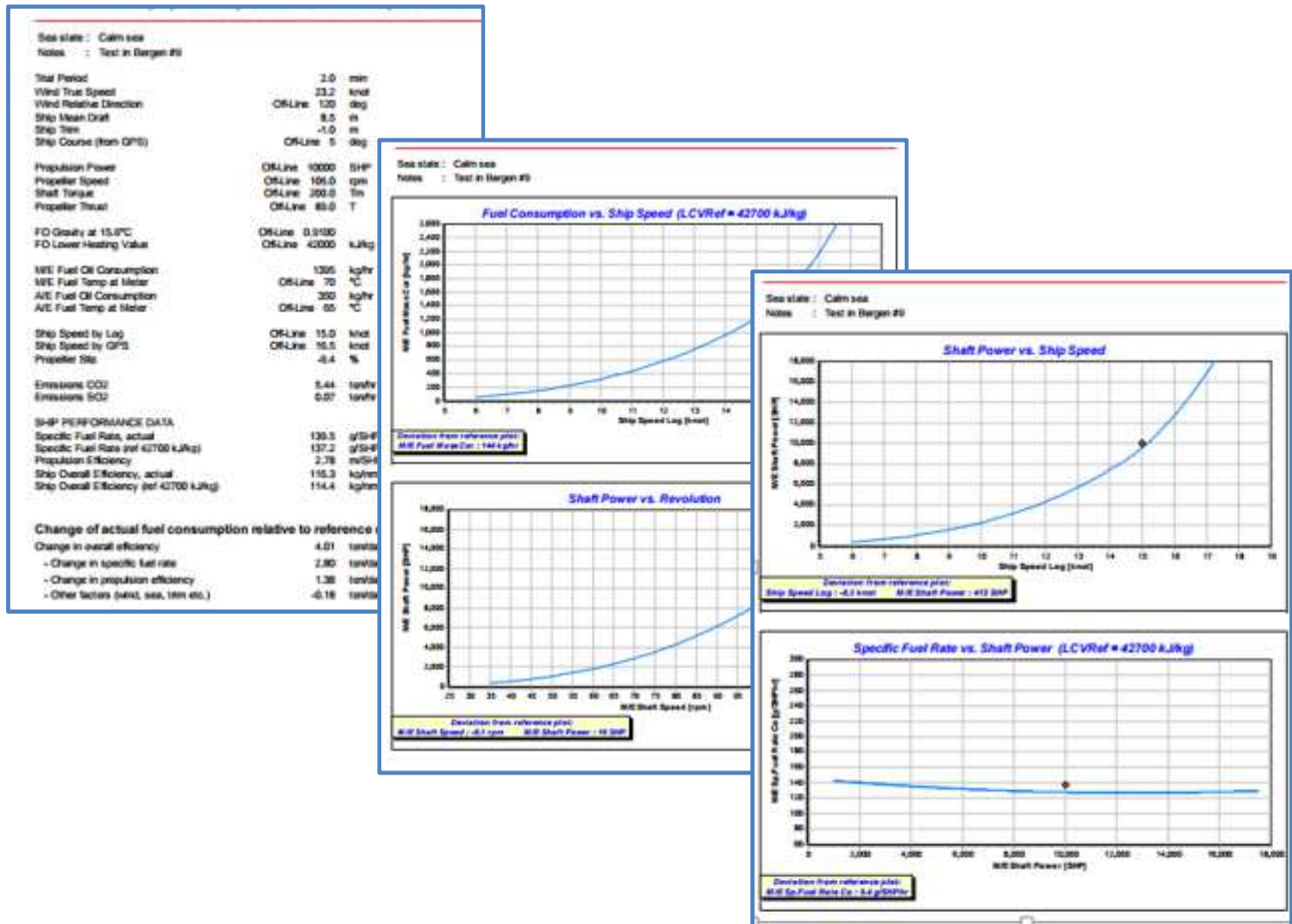


Fig. 6: Performance trial results

4.3 Long trend performance indication

Showing the instant performance can be valuable, but may be influenced by external factors like wind and current. However, looking at the long-term development of the vessels key performance values will statistically give you a more correct picture. With an automated data collection and filtering system in place as earlier described, a performance trend may start to evolve. This trend, shown as the percentage deviation from the design condition, will give the crew and owner a clear picture of the vessel's performance today, shown against earlier performance and design conditions.

The three most important areas of interest are:

- Hull condition (Shaft Power vs. Ship speed through water)
- Propeller condition (Shaft Power vs. Shaft Rpm)
- M/E Specific Fuel Rate (SFR vs. Shaft Power)

Is the performance gradually decreasing, how much, and what does this imply in increased fuel oil consumption? Below are some examples of long trend performance indications available for the user⁷.

⁷ Source: Kyma a.s, Norway

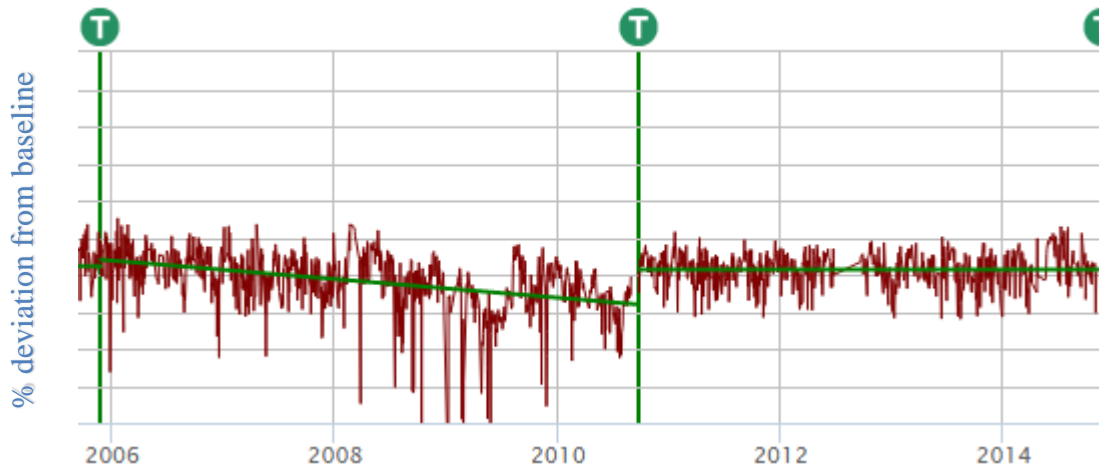


Fig. 7: Speed loss with two different anti-fouling systems.

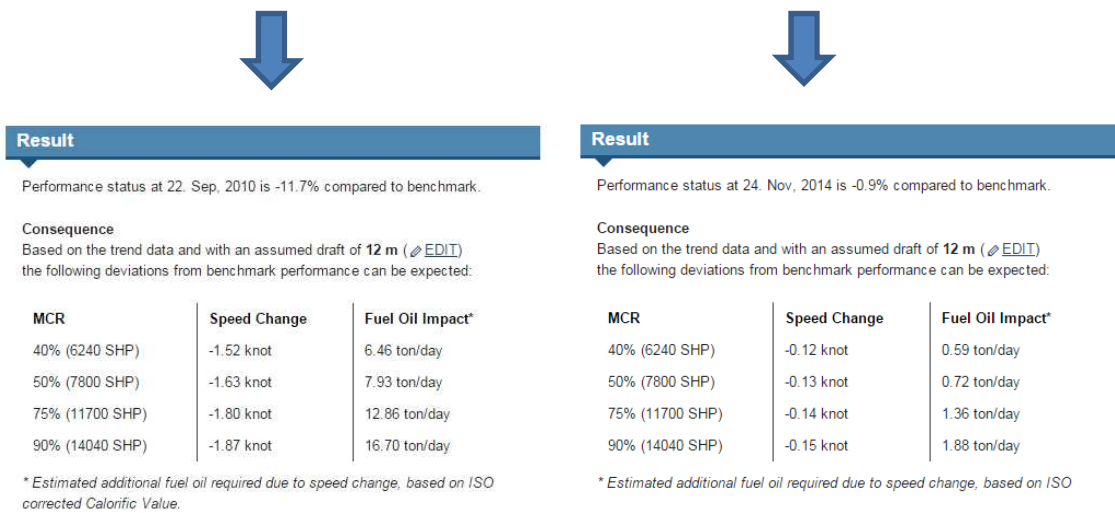


Fig. 8: Large speed loss and increase in fuel oil consumption

Fig. 9: Minimum speed loss and small increase in fuel oil consumption

As Figs. 7-9 clearly indicates, the hull coating system applied after the second docking has a good performance even after 4 years of sailing. Thus saving the owner a significantly amount of fuel oil and reduced emissions compared to the first period. Using traffic light color indications, Fig. 10 shows an LNG carrier with a yearly speed loss of more than 4% (now in the red performance area). Over a period of only 2.5 years this vessel has developed a speed loss of 11.7% compared to 'out-of-dock' condition (benchmark level indicated by blue dotted line), with a theoretical increased fuel oil consumption as indicated in Fig. 11 as a result.

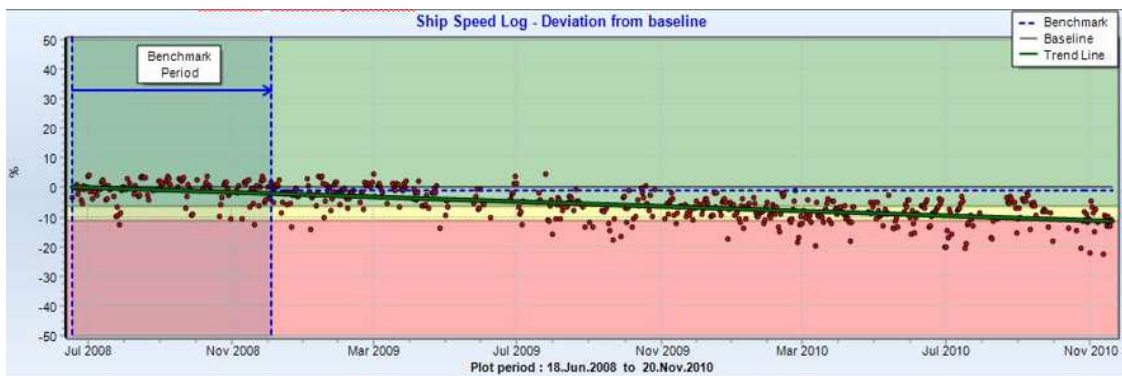


Fig. 10: Speed loss due to deteriorated hull condition

Result

Performance status at 22. Sep, 2010 is -11.7% compared to benchmark.

Consequence

Based on the trend data and with an assumed draft of 12 m ([EDIT](#)) the following deviations from benchmark performance can be expected:

MCR	Speed Change	Fuel Oil Impact*
40% (6240 SHP)	-1.52 knot	6.46 ton/day
50% (7800 SHP)	-1.63 knot	7.93 ton/day
75% (11700 SHP)	-1.80 knot	12.86 ton/day
90% (14040 SHP)	-1.87 knot	16.70 ton/day

* Estimated additional fuel oil required due to speed change, based on ISO corrected Calorific Value.

Fig. 11: Fuel oil impact of the deteriorated hull condition

For the propeller condition, a ‘Shaft Power vs. Shaft RPM’ trend can be as shown in Fig. 12. Again, the long-trend development indicates a substantial loss in performance. The propeller is gradually over 2.5 years becoming heavier, with consequently loss in shaft rpm or increased shaft torque.

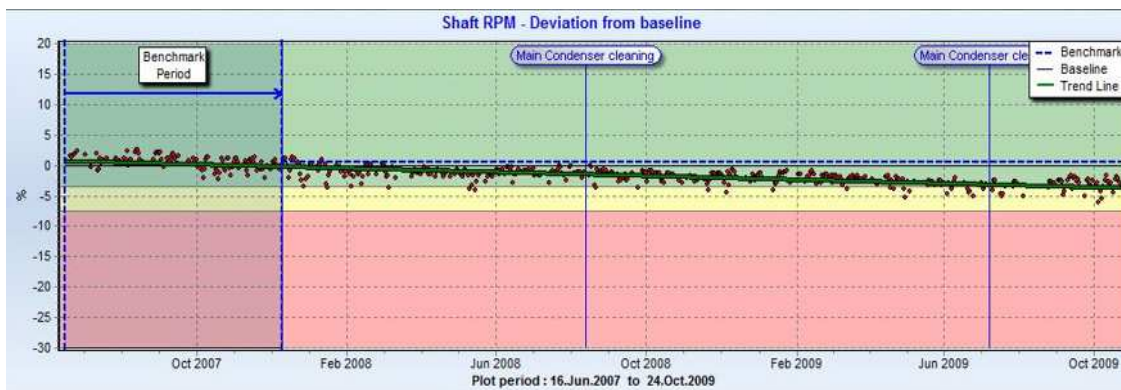


Fig. 12: The propeller is getting 'heavy', indicating a need for a propeller cleaning

4.4 Benefit of docking, is it possible to measure?

There are several options available to the ship owners for improving a vessel's performance. The hull anti-fouling coating could be improved/renewed, the bulb redesigned, propeller area modified, or M/E could be overhauled. These are only some of the options available in the toolbox. However, are they working, and how good? The best way to answer this question is to measure key performance parameters before and after the modification is undertaken. It is important to establish the vessel's performance before a 'Trend Event' (docking, maintenance, modification etc.). By measuring the long trend data from before docking and compare this to data from after docking, the ship owner will be able to check if the promised benefit indeed was achieved or not. Based on these result, the owner can decide if similar modifications should be applied on sister vessels in the fleet.

The screen-shot in Fig. 13⁸ of the long-trend development of the speed through water clearly indicates that a significant benefit was achieved after a new anti-fouling system was applied (a vertical green 'Trend Event' marked with a **T**). Details of the actual saving, Fig. 14, give the owner a cost-saving perspective and could be valuable information when deciding what to do with the rest of the fleet.

⁸ Source: Kyma, Norway

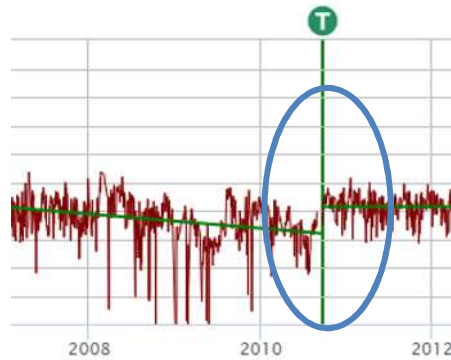


Fig. 6: Benefit achieved in speed through water due to new hull anti-fouling system

Benefit resulting from trend event

23. Sep. 2010 - Finish Docking (w/Hull Cleaning)

Based on the trend data and with an assumed draft of 12 m the following benefit was achieved:

MCR	Speed Change	Fuel Oil Impact*
40% (6240 SHP)	1.34 knot	-5.86 ton/day
50% (7800 SHP)	1.44 knot	-7.20 ton/day
75% (11700 SHP)	1.60 knot	-11.70 ton/day
90% (14040 SHP)	1.66 knot	-15.24 ton/day

Fig. 14: Details of speed change and fuel oil consumption impact at some typical MCR levels

4.5 Fleet performance

Automatic data collecting, filtering and transfer of data to a central database allows the ship owners to follow up the performance on the entire fleet. Furthermore, combining this database with a tailored dashboard system will make key performance indicators of the entire fleet available for the management and for making strategic performance decisions. Comparison within the fleet identifies the low efficiency vessels, making it possible for planning corrective actions accordingly.

5. Summary

This paper presents a practical approach for setting up a continuous ship performance monitoring (SPM) system to comply with the highest tier in the ISO 19030 standard. In addition, the paper recommends adding accurate fuel oil consumption measurements to get the complete performance picture of a vessel. The SPM system uses raw sensor data, filtering and statistical analysis to give the users a clear information about actual status and its progression over time for the main performance indicators.

The ISO 19030 standard defines a reference, and an evaluation period of both a minimum of one year. This paper presents an alternative approach, where the reference period is only 60-120 daily points, and the evaluation period starts after necessary points are collected. This gives a faster benchmark status, and therefore a faster performance overview.

A hype-word in today's ship performance world is 'big data'. The word implies that huge amount of data is stored and available for the user. However, for what purpose, and who should look at all this data? Is the vessels superintendent capable and have the capacity to investigate this? A highly flexible analyzing & dashboard system on top of this 'big data' is maybe the answer here.

Should ship owners have their own performance analysis departments to analyze this mountain of data? For larger ship owners the answer may be yes. To follow up the performance of the fleet is essential to business, and should have a strong focus in every ship owners mind. Some owners may

want to develop their own tailored analysis system, while other may want to team up with suppliers of such systems.

Regardless of the preferred approach; an onboard continuous data collection and performance system combined with an onshore analysis system, will be a valuable tool in order for ship owners to optimize the performance of the fleet, thus saving running costs and reducing emissions of greenhouse gases.

Splitting Propeller Performance from Hull Performance – A Challenge

Sergiu Paereli, Jotun, Sandefjord/Norway, sergiu.paereli@jotun.no
Andreas Krapp, Jotun, Sandefjord/Norway, andreas.krapp@jotun.no
Volker Bertram, DNV GL, Hamburg/Germany, volker.bertram@dnvgl.com

Abstract

This paper discusses the problem of splitting propeller performance from hull performance. Besides discussing the general problem, results from an analysis of in-service performance data are shown. Data from a tanker vessel over 3 years where both shaft power and propeller thrust are monitored are discussed. Even having thrust data available it remains difficult to evaluate the effect of propeller maintenance, underlining the principle challenge one faces when trying to split propeller from hull performance. Alternative approaches to estimate propeller performance without using thrust measurements are discussed.

1. Introduction

The hydrodynamic performance of a ship in service is critically influenced by two factors: the surface character of the underwater hull area (commonly simplified to “Hull Roughness”) and the surface character of the propeller (“Propeller Roughness”). In order to manage and evaluate these two areas for a vessel in service one would need a way to evaluate the performance of the hull and the performance of the propeller separately. This, however, has been and still is a challenging task and therefore most performance measurement approaches deal with both factors combined. The recent work on an ISO standard on “Changes in Hull and Propeller Performance” exemplify this.

In general, in-service performance monitoring for ships is difficult as various other factors than hull and propeller surface condition influence the speed-power performance and vary in time:

- Different environmental conditions (sea state, wind, current, water depth, sea temperature and salinity)
- Different operational conditions (draft, trim, speed, rudder angle, ...)

For the isolation of the effect of the combined hull and propeller surface condition, one has two basic choices. Either one estimates the contributions of all other significant factors and corrects for these, or one filters for comparable conditions given one has enough data available to start from. In practice, most methods (including ISO 19030) rely on a combination of both approaches.

For separating the effect of the hull from the effect of the propeller, one encounters a measurability challenge: propeller thrust is very difficult to measure accurately and is seldom measured on ships in commercial service today. Propeller thrust is, however, a pre-requisite to reliably split hull performance from propeller performance. Alternative approximate approaches, not relying on thrust measurements, have been discussed.

Due to increased focus on hull performance and the broader availability of high-frequency sensor data, the question on how to come to reliable propeller performance indicators has gained some interest recently.

2. Hull Efficiency and Propeller Efficiency

The overall propulsive efficiency of a ship η_D at a certain speed and under certain loading conditions is commonly defined as the ratio of effective propulsive power P_E to delivered power P_D .

$$\eta_D = \frac{P_E}{P_D}$$

The total efficiency can be split in hull efficiency η_H and propeller efficiency in behind condition η_B

$$\eta_D = \frac{P_E}{P_D} = \frac{P_E}{P_T} \cdot \frac{P_T}{P_D} = \eta_H \cdot \eta_B$$

given that the thrust power P_T is measured.

In principle, it should thus be straightforward to get useful performance indicators for hull performance and for propeller performance. However, there are practical obstacles:

- The effective propulsive power P_E is not measurable for a vessel in service. Therefore the hull efficiency cannot be evaluated as such. Instead of the hull efficiency, the ratio of vessel speed (through water) v and thrust power can be regarded as a pragmatic indicator of the efficiency with which the hull moves through the water.

$$\eta_H = \frac{P_E}{P_T} = \frac{R_T \cdot v}{P_T}$$

$$\frac{v}{P_T} = \frac{\eta_H}{R_T}$$

This ratio depends on speed, as the total resistance R_T depends on speed. In practice, one would therefore regard the whole speed-thrust power relation $k(v)$ as the hull efficiency indicator or normalize to a standard speed using speed-thrust power reference curves from e.g. model tests or CFD simulations.

$$v = \frac{\eta_H}{R_T} \cdot P_T = k(v) \cdot P_T$$

- The effect of environmental conditions on the effective power demand has to be dealt with, either by filtering for comparable conditions or/and by estimating their impact and correcting for it.
- Thrust is difficult to measure in service and rarely available. Without thrust measurement, there is no straightforward way to split hull efficiency from the combined hull and propeller effectiveness. If no thrust measurement is available the combined hull and propeller efficiency can be evaluated by analysing the ratio of speed through water and delivered power, in analogy to above:

$$\frac{v}{P_D} = \frac{\eta_D}{R_T}$$

- In order to compute thrust power P_T from measured thrust T , one needs the speed by which the propeller moves through the water behind the vessel (speed of advance). However, as the wake is not normally measured, the speed of advance and therefore the thrust power is not known.
- The wake field behind the hull is influenced by the flow of the water over the hull surface and therefore by the hull efficiency. Thus it is in principle not possible to split propeller efficiency from hull efficiency if the wake is not measured.

In ship design, the propeller efficiency is usually evaluated by conducting open-water tests (i.e. propeller without ship or rudder is measured) leading to characteristic propeller curves. In these curves, the open-water propeller efficiency η_0 is given as a function of the dimensionless advance coefficient J .

$$\eta_0 = \frac{T \cdot V_A}{Q \cdot n \cdot 2\pi} = \frac{K_T \cdot J}{K_Q \cdot 2\pi}$$

$$J = \frac{V_a}{n \cdot d}$$

with the dimensionless thrust and torque coefficients K_T and K_Q

$$K_T = \frac{T}{\rho n^2 d^4}$$

$$K_Q = \frac{Q}{\rho n^2 d^5}$$

with ρ mass density of water
 n propeller speed
 d propeller diameter
 T propeller thrust
 Q propeller torque
 V_a speed of advance of the propeller through the water

For an isolated propeller, the change in efficiency due to varying propeller roughness was studied by *Mosaad (1986)* and the loss in efficiency due to increasing roughness is illustrated in the propeller curves in Fig. 1. It shows a clear impact of increased hull roughness on propeller efficiency, mainly due to an increase in the torque coefficient. The thrust coefficient was hardly affected by the change in roughness. This is to be expected. Torque is largely due to the frictional resistance to moving the propeller blades through water, thrust largely due to the pressure difference between suction and pressure side which is dominated by non-viscous effects.

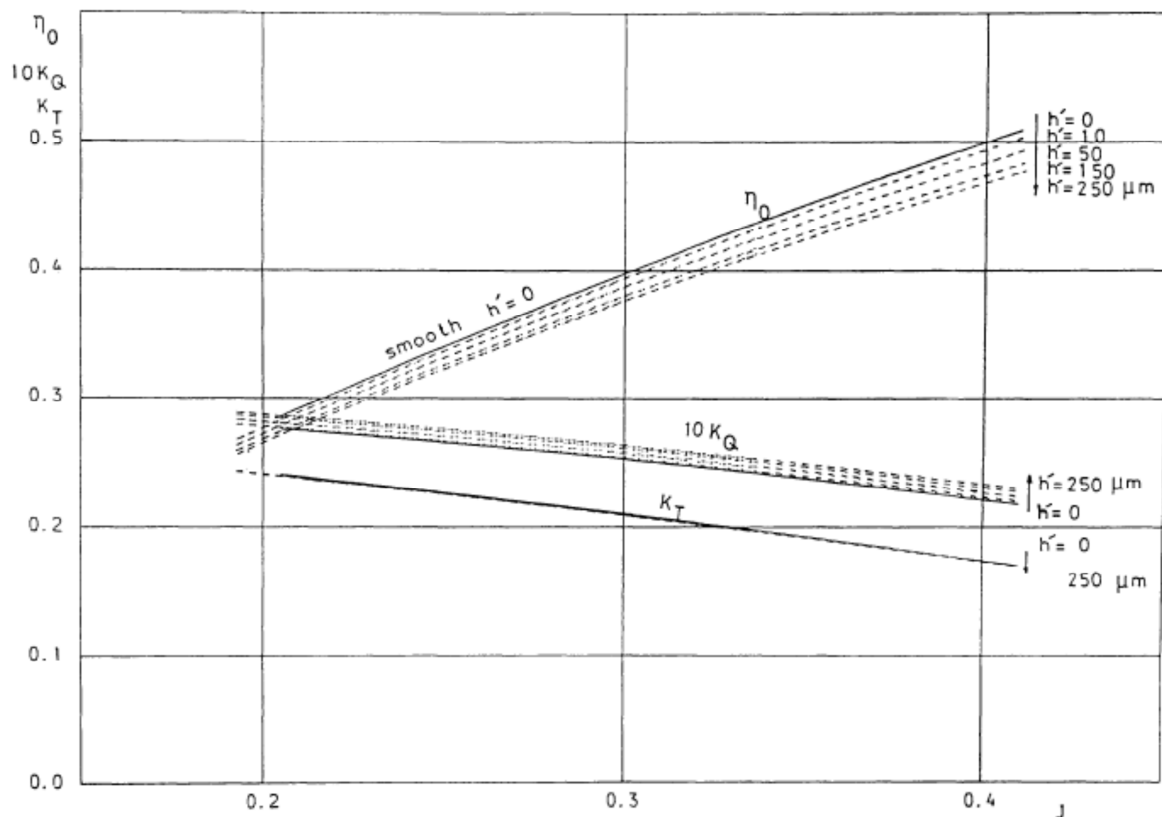


Fig.1: Surface roughness decreases propeller efficiency, *Mosaad (1986)*

For a propeller behind a ship hull, some complications occur, mainly related to the speed of advance. The speed of advance of the propeller is not directly measured, but it is related to the vessel speed through water V_s through the wake fraction w .

$$V_a = V_s \cdot (1 - w)$$

The wake fraction accounts for the effect of the hull, changing the water speed at the position of the propeller. The wake fraction w is a function of draft, trim, speed, propeller rpm and other factors. Comparing or relying on the open-water propeller curves in the evaluation of the in-service propeller efficiency is problematic.

3. In-service data

Despite the fundamental challenge to measure the speed of advance and the practical challenge to measure thrust for a vessel in service, an evaluation of a dataset for a tanker vessel in a regular trade with three years of in-service performance data was performed. The goal was to gain insight into what information a standard measurement setup and a straightforward analysis approach can deliver despite the described challenges.

The vessel was equipped with a data logger acquiring data every 15 s. Speed through water and over ground, propeller rpm, propeller torque and thrust, draft fore and aft and wind speed and direction were measured. Over the monitoring period the vessel underwent several propeller cleanings and after 2 years the vessel was equipped with propeller boss cap fins. These events were expected to affect propeller efficiency significantly and thus to be relatively easily detectable in the datasets.

From the complete dataset, only ballast legs were isolated as there were only small variations in vessel speed and trim in the ballast legs. The data was furthermore filtered for low true wind speeds, below 10 knots. In order to focus on the effect of propeller cleanings and the installation of the propeller boss cap fins, the evaluation focused on comparing two months before and two months after each event.

For the comparison of the propeller efficiency in different periods, but in absence of measured advance speed, the variation of the modified propeller efficiency η_{mod} , the thrust and the torque coefficients with a modified advance coefficient J_{mod} was used. The speed of advance was substituted with the speed through water, thus assuming a constant and unchanged wake.

$$J_{mod} = \frac{V_s}{n}$$

$$\eta_{mod} = \frac{J_{mod} \cdot T}{2\pi \cdot n \cdot Q}$$

While J_{mod} and η_{mod} are not dimensionless, this will not affect the general insight gained in this study.

Averages of the modified advance number, of the modified propeller efficiency and of the thrust and torque coefficients over 17 equally spaced intervals of the modified advance number within the range of J_{mod} between 0 and 0.34 were computed and used for analysis.

Fig. 2 compares the efficiency indicators for two months before a cleaning with those for two months after cleaning. The propeller efficiency as indicated by η_{mod} increased after cleaning. This increase is indicated consistently over the range of J_{mod} values, except for the highest values. This efficiency increase is due to an increase in the thrust coefficient, while the torque coefficient remains unchanged by the cleaning. This is the exact opposite of what was expected from *Mosaad (1986)*, see Fig. 1, where the increase in propeller roughness led to an increase in K_Q , while K_T remained unchanged.

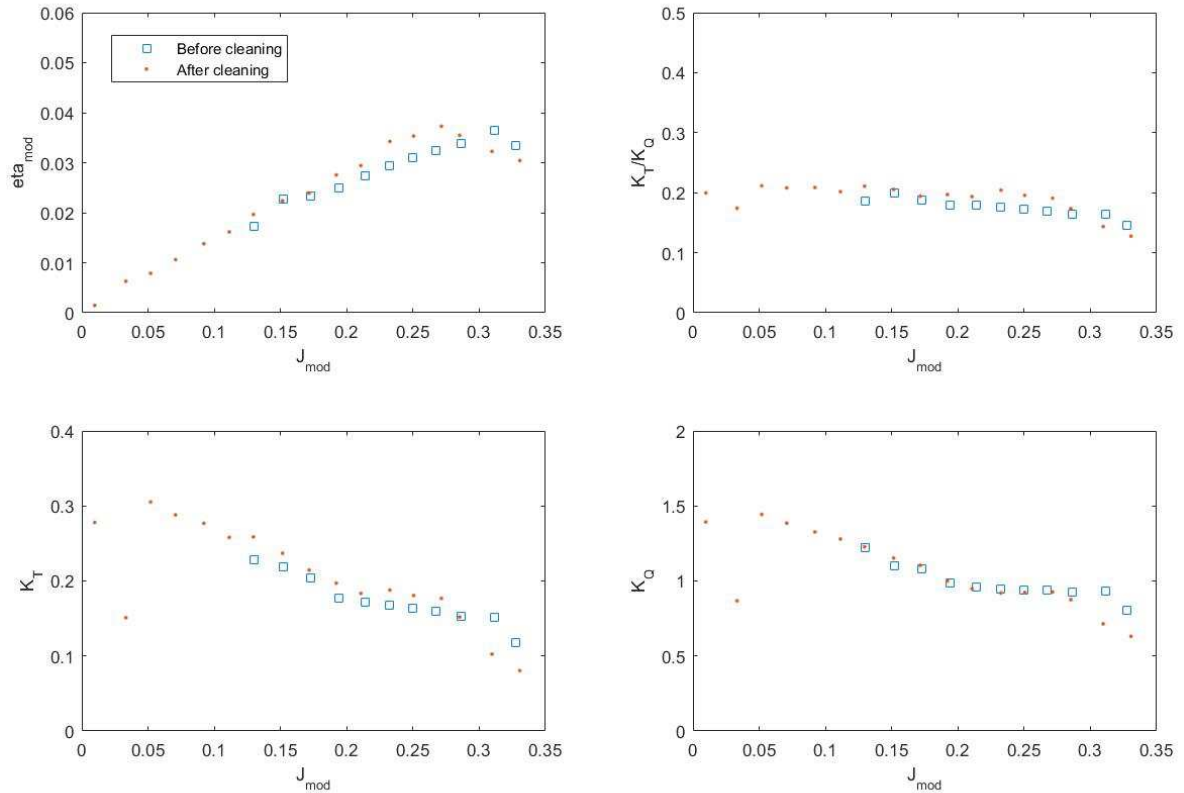


Fig. 2: Modified propeller efficiency, thrust and torque coefficients, and the ratio K_T/K_Q over the modified advance number before and after propeller cleaning 1

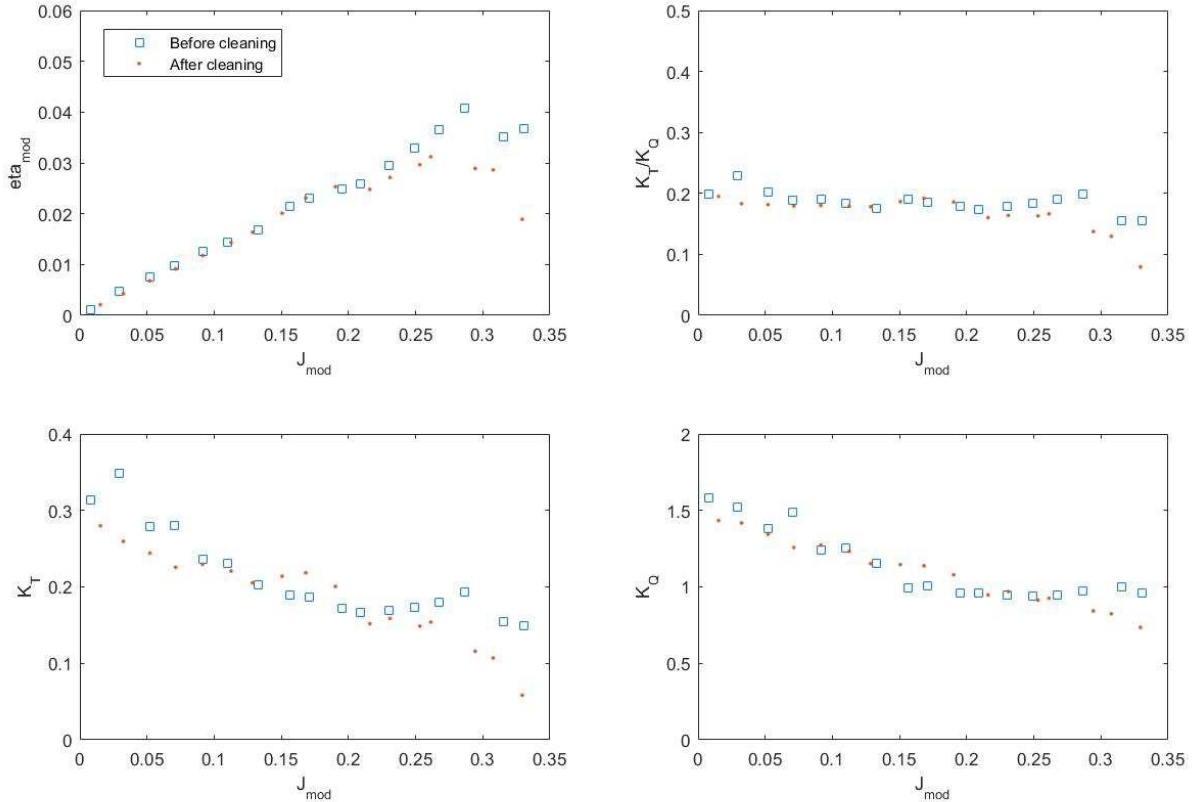


Fig. 3: Modified propeller efficiency, thrust and torque coefficients, and ratio K_T/K_Q over the modified advance number before and after propeller cleaning 4

Fig. 3 shows the results for another cleaning event. In this case, no clear conclusions on the effect of the propeller cleaning can be drawn. This might be due to the propeller having been in a good condition before the cleaning, but other tests with the same dataset for another cleaning event point rather to the fact that the current straightforward analysis approach does not allow reliable evaluation of the effectiveness of changes in propeller efficiency due to cleaning events.

However, the current dataset and the straightforward analysis approach were useful in evaluating the performance gain due to refitting propeller boss cap fins (PBCF) on the vessel. Fig. 4 shows the propeller efficiency indicators after the two cleanings without the PBCF and the indicators after the cleaning and PBCF installation. The PBCF clearly improved propeller efficiency as η_{mod} increased over the whole range of J_{mod} values. The increase in efficiency is higher with increasing J_{mod} . The two periods before the PBCF installation show very similar indicators; this indicates that the overall measurement accuracy is acceptable. The reason for the increase in efficiency by the PBCF is the increase in the thrust coefficient, while the torque coefficient remained essentially unchanged.

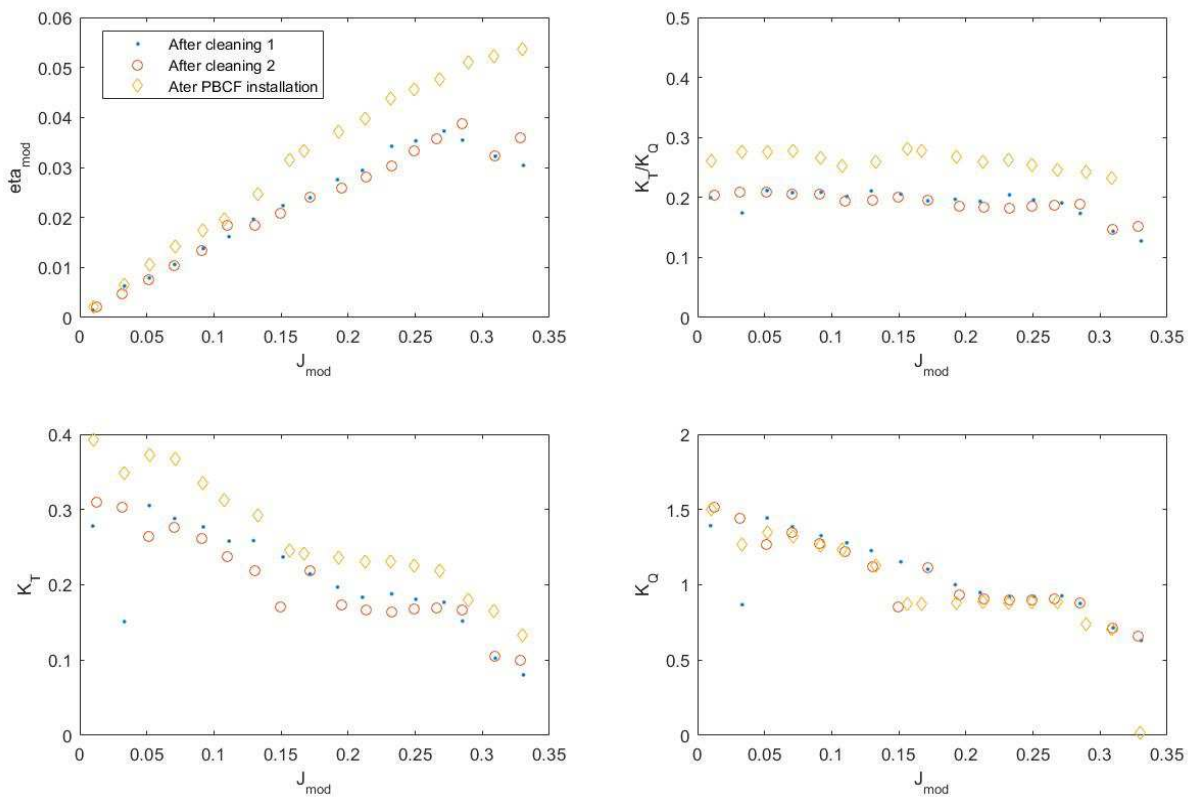


Fig. 4: Modified propeller efficiency, thrust and torque coefficients, and the ratio K_T/K_Q over the modified advance number after cleaning events 1 and 2, and after the installation of the PBCF

From the presented case study, we conclude that the quantifying the effect of propeller cleaning is still challenging, even in the presence of thrust data. The assessment of these cleaning events can only be regarded as indicative. Part of the challenge is due to the variability of environmental and operational conditions. But part of the challenge is also related to sensor uncertainties, mainly from thrust and speed through water. Further uncertainty is linked to the effect of changes in the hull roughness which in turn changes the wake field and thus the advance speed.

On the other hand, a very clear effect of the propeller boss cap fins has been observed. This shows that the general approach to evaluate propeller efficiency changes is useful.

In view of the uncertainties and the current observations, it remains to be seen if approaches not using thrust measurement at all to evaluate the propeller efficiency can deliver better or equivalent insight.

4. An alternative approach to evaluate propeller efficiency changes without measuring thrust

As a starting point for an approach to indicate propeller efficiency changes without relying on thrust measurements and to separate the effect of propeller roughness increase from hull roughness increase, the observations of *Mosaad (1986)* will be used: An increase in propeller roughness will practically not affect thrust, but increase substantially torque. Fig.1 showed this fact for a ship propeller, using nondimensional thrust, torque and rpm, namely K_T , K_Q and J . As torque goes up and thrust remains constant, propeller efficiency η_0 goes down.

Increased hull roughness leads to increased ship resistance. Then for constant vessel speed, higher thrust is needed, which in turn means higher rpm. This will also lead to higher torque. Increased propeller roughness will increase torque, while keeping thrust constant - according to *Mosaad (1986)* -, and for constant speed a constant rpm is required. If above is true, one can use the measured rpm and torque to derive whether propeller or hull degradation cause an observed hydrodynamic performance degradation.

In practice, one could use delivered power (the product of torque and rpm) and a theoretical speed (derived from propeller data) for this purpose. A theoretical ship speed V_{prop} can be calculated based on propeller rpm. This procedure uses data of model test reports; it refers to the original, smooth propeller. The approach requires the measured torque Q_m and rpm n at the propeller shaft, and the propeller open-water curves for the real propeller in the ship. If the propeller characteristics of the real propeller are not known, one may try to use the propeller characteristics predicted for full scale based on the model test (stock) propeller.

Model-test reports give full-scale predictions for advance number J and torque coefficient K_Q . These predicted curves can be used to interpolate an advance number corresponding to a given torque coefficient. With this advance number we can determine the advance speed of the propeller.

The wake fraction w depends on draft and speed. The model-test report typically gives predictions for the wake fraction for design draft and ballast draft. For both load conditions, the wake fraction can be interpolated for an estimated ship speed, e.g. estimated from speed log readings. To obtain the wake fraction w for the estimated speed and the actual draft one interpolates (linearly) for the actual draft between ballast and design draft. Finally one obtains:

$$V_{prop} = \frac{V_a}{(1 - w)}$$

If the final speed differs significantly from the initial estimate, the process can be repeated with the newly obtained value. The process quickly converges. If a detailed power-speed-draft-trim matrix is available from experimental or numerical propulsion tests one can interpolate V_{prop} for a given draft, trim and rpm from this knowledge base instead.

When using this procedure with data from a deteriorated propeller having increased K_Q it will result in a speed V_{prop} which is higher than the measured real speed through water V_{mes} . The theoretical relation is then:

$$\frac{V_{prop}}{V_{mes}} = \frac{K_{Q,actual}}{K_{Q,initial}} = \frac{\eta_{0,initial}}{\eta_{0,actual}}$$

The last expression follows from the usual expression for propeller efficiency

$$\eta_0 = \frac{K_T \cdot J}{K_Q \cdot 2\pi}$$

and the assumption of constant thrust coefficient K_T and rpm n (respectively advance number J).

The approach is based on several questionable assumptions, such as accurate measurement of speed through water, correctly extrapolated (and corrected for ambient weather conditions) wake fraction w , constant ratio of torque values (actual/initial) independent of speed, no influence of the hull roughness changes on the wake etc. As for many other quantities in performance monitoring, it is expected that filtering for selected loading conditions and averaging over many data sets will improve accuracy. First tests of the described approach are currently performed.

5. Summary

Despite the fundamental challenges to evaluate propeller efficiency for a vessel in-service, a dataset for a tanker vessel indicated that it is possible to capture major efficiency changes (such as the installation of propeller boss cap fins) by a straightforward analysis process, relying on filtering and on using vessel speed through water instead of speed of advance. However, propeller cleanings could not be assessed easily and assessment of propeller cleaning remains at best indicative. Further refinement of the approach may reduce the impact of variations in environmental and operational conditions. It remains to be seen if approaches not using thrust measurement to evaluate propeller efficiency changes can bring valuable insight. One such approach is currently tested. In general, a complete split of hull and propeller efficiency is not possible, unless the wake field is measured explicitly.

References

MOSAAD, M.A. (1986), *Marine propeller roughness penalties*, PhD Thesis, University of Newcastle

Verification of Full-Scale Vessel's Performance under Actual Sea by On-board Monitoring System: A Shipbuilder's View

Tsuyoshi Ishiguro, Japan Marine United Corporation, Tokyo/Japan, ishiguro-tsuyoshi@jmuc.co.jp

Hideo Orihara, Japan Marine United Corporation, Tsu/Japan, orihara-hideo@jmuc.co.jp

Hisafumi Yoshida, Japan Marine United Corporation, Tsu/Japan, yoshida-hisafumi@jmuc.co.jp

Abstract

This paper describes the on-board monitoring and analysis system for verifying the full-scale vessel's performance under actual sea with a view to evaluate and feed-back the shipbuilder's design achievement in the performance of new buildings. Corrections for the effect of ambient and operational condition on vessel's performance are essential for the precise verification together with the adequate identification of wave condition. Some examples for design confirmation of Eco-friendly ships are presented and future requirements for the improvement of this system are discussed from a shipbuilder's point of view.

1. Introduction

According to the worldwide demand for environmental protection inspired by global warming, International Maritime Organization (IMO) enforced the regulation for emission control of Green House Gases (GHG) to new buildings by the Energy Efficiency Design Index (EEDI) since January 2013. In parallel, the amount of CO₂ emission for existing vessels shall be monitored and reported by the Energy Efficiency Operational Index (EEOI) based on the Ship Energy Efficiency Management Plan (SEEMP).

To comply with these requests, shipbuilders have focused their efforts on the development and application of new energy-saving technologies to Eco-friendly vessels. To evaluate and feed-back shipbuilder's design achievements, it is essential to verify the full-scale vessel's performance in actual operation. However, since a vessel's performance is affected by both ambient and operational conditions, a sophisticated performance monitoring and analysis system is required to account for these effects.

Therefore, Japan Marine United Corporation (JMU) has developed the voyage support system "JMU Sea-Navi@" which has precise weather routing, performance monitoring and analysis functions. For the precise verification of full-scale performance, key requirements are (a) precise correction for ambient and operational conditions and (b) precise measurement of encountered weather, ocean waves in particular. JMU has long conducted research for precise hydrodynamic modelling of vessel performance with tank testing and verification with an on-board automatic wave measuring system with navigation radar and a wave height meter.

In this paper, the features of the "Sea-Navi" monitoring system including verification of automatic wave measurements are presented. The effects of ambient and operational conditions on the vessel's performance are presented and their correction method is explained. Key issues for design confirmation are described with some examples, including correction of measured performance into ideal condition, confirmation of the accuracy of designed sea margin and the effect of energy saving hull shapes aimed to reduce the sea margin.

2. Description of Sea-Navi system

This chapter outlines the on-board monitoring system "Sea-Navi". The system consists of a high-precision weather routine system, a monitoring and an analysis system for the vessel's propulsive performance in both calm and actual ambient conditions. This paper mainly discusses the latter topics. Details of the weather routine system are described in *Orihara et al. (2010,2014,2015)*.

2.1 System integration

Fig. 1 shows a typical configuration of the “Sea-Navi” monitoring system. This system consists of a suite of sensors (with ship specific combinations) and a system’s PC to acquire, analyse and display monitoring data. Most hull-related data (ship’s speed, course, heading, wind condition, rudder angle etc.) are obtained from the Voyage Data Recorder (VDR) as LAN output data. Machinery-related data (shaft power, fuel-oil flow rate, fuel-oil temperature, etc.) are obtained from the engine-room data logger. Ship motions and encountered waves are optional monitoring items and measured by using dedicated motions sensors and a radar wave analyser (Radar and a wave height meter).

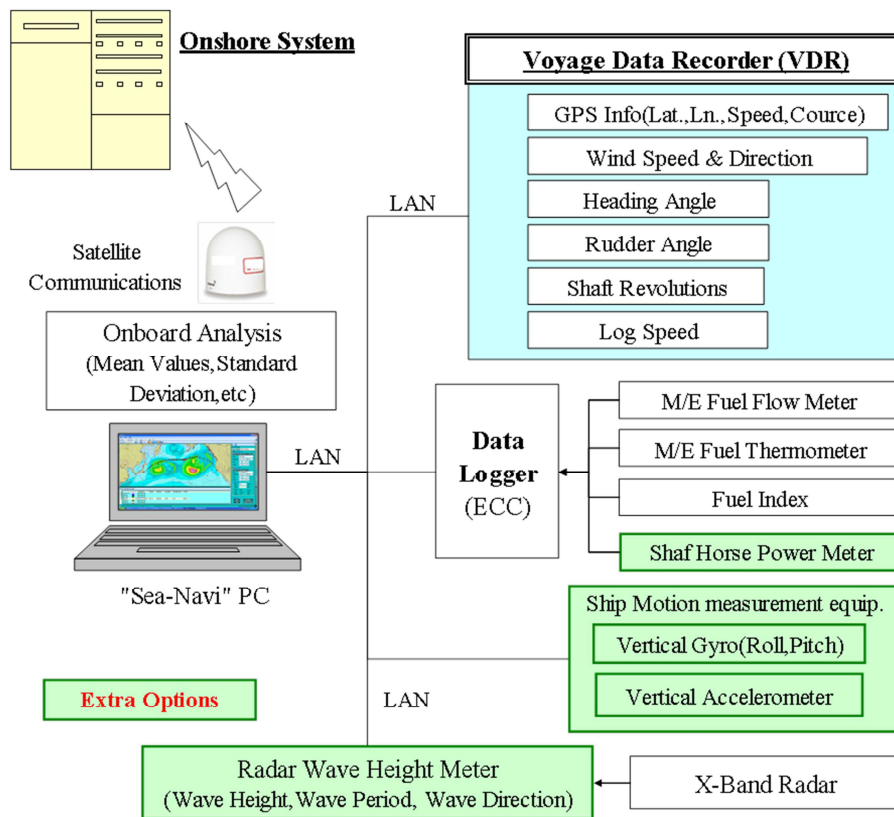


Fig. 1: System configuration of “Sea-Navi” on-board monitoring system

2.2 Accuracy of automatic wave measuring system

Ambient conditions, which play an important role for the evaluation of vessel’s performance in actual operation, consist of wind (speed and direction) and wave data (significant wave height, mean wave period and wave direction). Wind data can be measured directly by the on-board anemometer. Wave data should be obtained either by an automatic measuring device or precise weather forecasting, e.g. a global weather prediction model. This information is essential for the filtering and correction of ambient conditions together with the calculation of the optimum weather routing. Thus it is important to confirm the accuracy of this automatic wave measuring and/or identification system.

To verify the accuracy of this system, automatic wave measurements were carried out for different vessels to compare with weather forecast data supplied by the Japan Meteorological Agency. Fig. 2 shows representative examples of these comparisons for a container vessel in the North Pacific and a large bulk carrier in the Indian Ocean, *Orihara et al. (2010,2015)*. Forecast data correlate fairly well with measurements although the number of measured data is relatively small due to the manual operation of the radar wave analyser. It can be concluded that the weather forecast data employed in “Sea-Navi” can predict actual wave condition with sufficient accuracy for optimum routing calculations and performance evaluation.

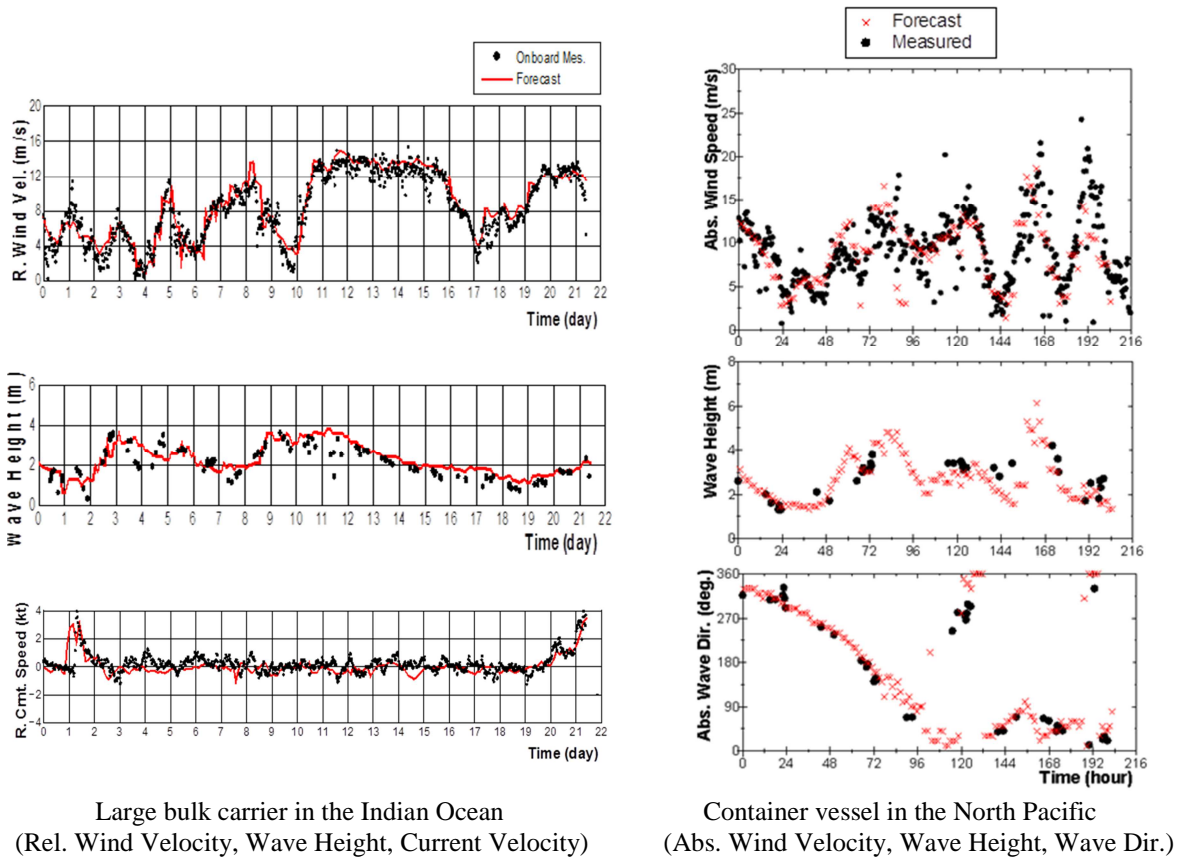


Fig. 2: Comparison of encountered ambient conditions for bulk carrier and container vessel

3. Data collection, filtering and correction for ambient and operational condition

3.1 Data collection and filtering criteria

Monitoring data listed in Fig. 1 are merged as a time-history data file of normally 20-min length (variable for ship type) containing all the data items. Then, a statistical analysis of the time-history data is conducted in the system's PC. Average, minimum, maximum, standard deviation, significant value and zero up-cross periods are calculated for all data items at an interval of 20 minutes. From all the monitored data, adequate data are filtered by the following criteria to extract the performance in calm ambient condition:

- (1) Wind speed is less than 4.0 m/s (Beaufort number less than 3)
- (2) Significant wave height is less than 2.0 m
- (3) Average and Standard Deviation (S.D.) of rudder angle are less than 2.0°
- (4) Shaft revolution is greater than 40 % of maximum revolution
- (5) S.D. of shaft revolutions is less than 5 %
- (6) S.D. of pitch and roll angle are less than 0.25° and 0.50° , respectively

It should be noted that strict filtering criteria tends to scale back the number of remaining data which might lose statistical reliability. Indicated criteria are the standard settings and variable depending on the size of vessel etc.

3.2 Effect of ambient conditions on propulsive performance

Fig. 3 shows the effect of ambient conditions on the propulsive performance for various vessels. The resistance increase due to wind and waves in Beaufort 3 and 4 are estimated based on tank test data and theoretical calculations. The resultant required power in each ambient direction (direction of wind and wave stipulated in Table 1 is assumed to be identical) is plotted as a ratio of power increase over calm-water power. Fig. 4 indicates the proportion of wind and wave resistance among total resistance increase in Beaufort 4.

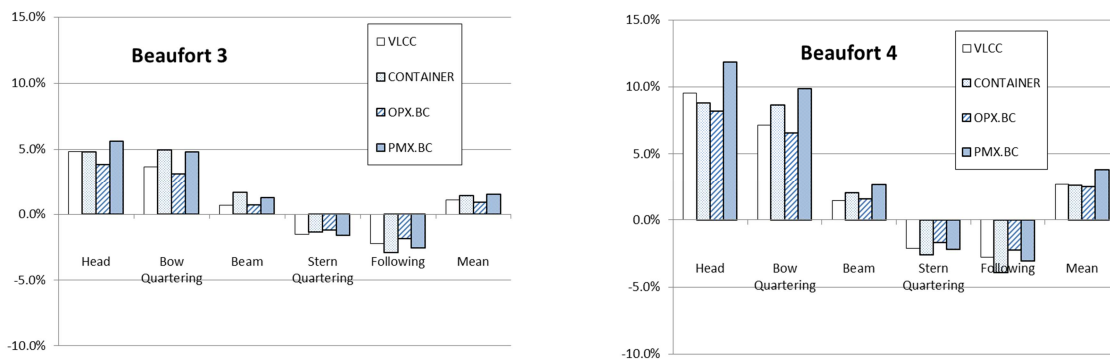


Fig. 3: Ratio of power increase in Beaufort 3 and 4 for various vessels

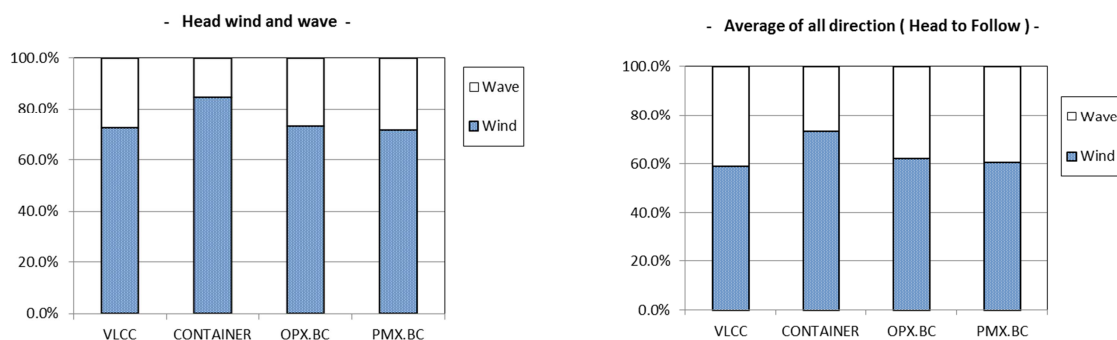


Fig. 4: Proportion of wind and wave resistance among total resistance increase in Beaufort 4

These figures indicate that mean power increase (averaged value of all ambient directions) is 1% in Bft 3 and 3% in Bft 4. Considering that wind resistance contributes 60 to 80% of the total resistance increase, it can be concluded that a major part of the ambient effects can be eliminated by applying the wind correction as specified in *ISO19030 (2016)*.

On the other hand, the power increase can reach up to 5 to 10% especially in head wind and waves. Thus a wave correction is important for a more precise evaluation.

3.3 Outline of correction method for ambient conditions

To carry out a more precise evaluation of performance especially in calm water, the Sea-Navi system has a function for the correction of ambient conditions according to the following steps:

- (1) Determination of propeller working point based on propeller open-water characteristics (POC)

Using the measured delivered power P_d and propeller revolution n , the torque coefficient K_q can be calculated as follows:

$$K_q = \frac{Q_p}{\rho \cdot n^2 \cdot D_p^5} , \quad Q_p = \frac{P_d \cdot \eta_R}{2\pi \cdot n}$$

D_p is a propeller diameter, ρ the density of the fluid and η_R is the relative rotative efficiency determined by tank tests. Based on the POC diagram, the propeller load factor τ_{act} , the advance number J_{p_act} and the propeller efficiency η_{o_act} in actual sea conditions can be identified by way of K_q as illustrated in Fig. 5.

$$J_{p_act} = \frac{V \cdot (1-w_s)}{n \cdot D_p} , \quad \tau_{act} = \frac{R_{act}}{\rho \cdot D_p^2 \cdot V^2 (1-t) \cdot (1-w_s)^2}$$

V is ship speed through water, R_{act} the total hull resistance under actual sea conditions and $1-t$ is a thrust deduction factor determined by tank tests. The wake fraction w_s can be calculated back using determined J_{p_act} as follows:

$$1 - w_s = \frac{n \cdot D_p \cdot J_{p_act}}{V}$$

(2) Calculation of the propeller working point in calm water based on POC

Resistance increases due to wind and wave $\Delta R = R_{wind} + R_{wave}$ are calculated based on wind tunnel tests, seakeeping test and/or theoretical calculation, *Orihara et al. (2016)*. Then, the propeller load factor in calm water: τ_{still} can be calculated as follows:

$$R_{act} = \tau_{act} \cdot \rho \cdot D_p^2 \cdot V^2 (1-t) \cdot (1-w_s)^2$$

$$\tau_{still} = \frac{R_{act} - \Delta R}{\rho \cdot D_p^2 \cdot V^2 (1-t) \cdot (1-w_s)^2}$$

The propeller advance number J_{p_still} and propeller efficiency η_{o_still} in calm water can be identified by way of τ_{still} as illustrated in Fig. 5.

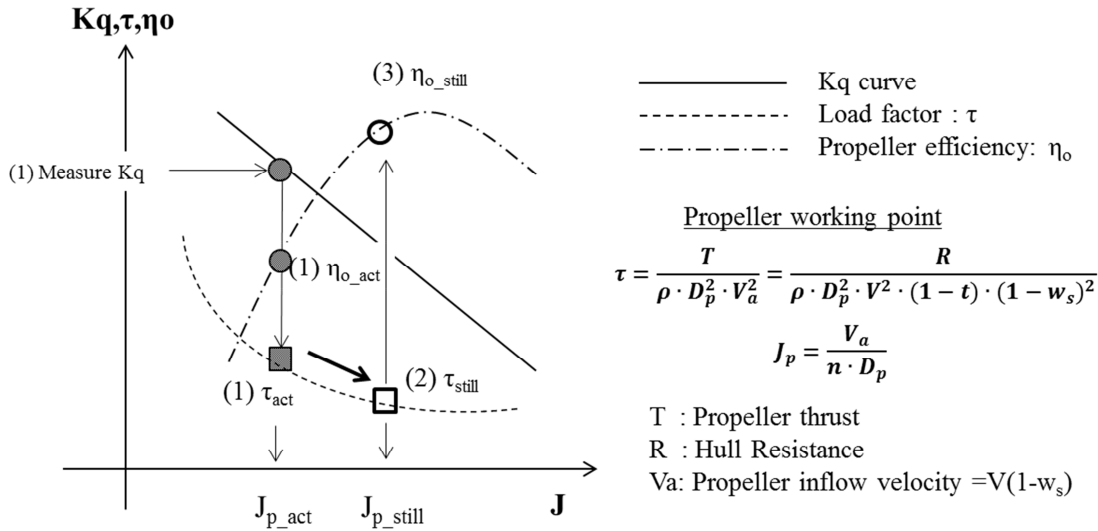


Fig. 5: Schematic diagram for the identification of hydrodynamic properties base on POC

(3) Calculation of required power and propeller revolution in calm water

Using propeller efficiencies in both actual sea and calm water, the required power in calm water P_{still} can be calculated as follows:

$$P_{still} = P_d - \Delta P , \quad \Delta P = \frac{\Delta R \cdot V}{\eta_{qp_still}} + P_d \cdot \left(1 - \frac{\eta_{qp_act}}{\eta_{qp_still}} \right)$$

η_{qp} is the quasi-propulsive efficiency expressed by the propeller efficiency and self-propulsion factors.

$$\eta_{qp_act} = \eta_{o_act} * \eta_R * \eta_H, \quad \eta_{qp_still} = \eta_{o_still} * \eta_R * \eta_H, \quad \eta_H = \frac{1 - t}{1 - w_s}$$

The hull efficiency η_H is calculated by the combination of $1-t$ and $1-w_s$ values which are assumed to be constant in both ambient condition and calm water. Propeller revolution in calm water n_{still} can be calculated as follows:

$$n_{still} = \frac{(1 - w_s) \cdot V}{J_{p_still} \cdot D_p}$$

So called ‘Direct power method’ presented here is applied in *ISO15016 (2015)*. The principle is identical to the wind correction method applied for *ISO19030*.

3.4 The effect of operational conditions on propulsive performance

A vessel’s propulsive performance is affected by operational conditions (speed, draft and trim) and ambient conditions (already discussed in 3.2). Fig. 6 shows an example of an actual operational profile for a VLCC and a container vessel. For the VLCC, the loading conditions are mainly divided into fully loaded and ballast conditions where displacement deviations in each regime will fall within $\pm 5\%$ range. In contrast, the displacements of the container vessel are distributed in a much wider range and trim conditions also vary case by case.

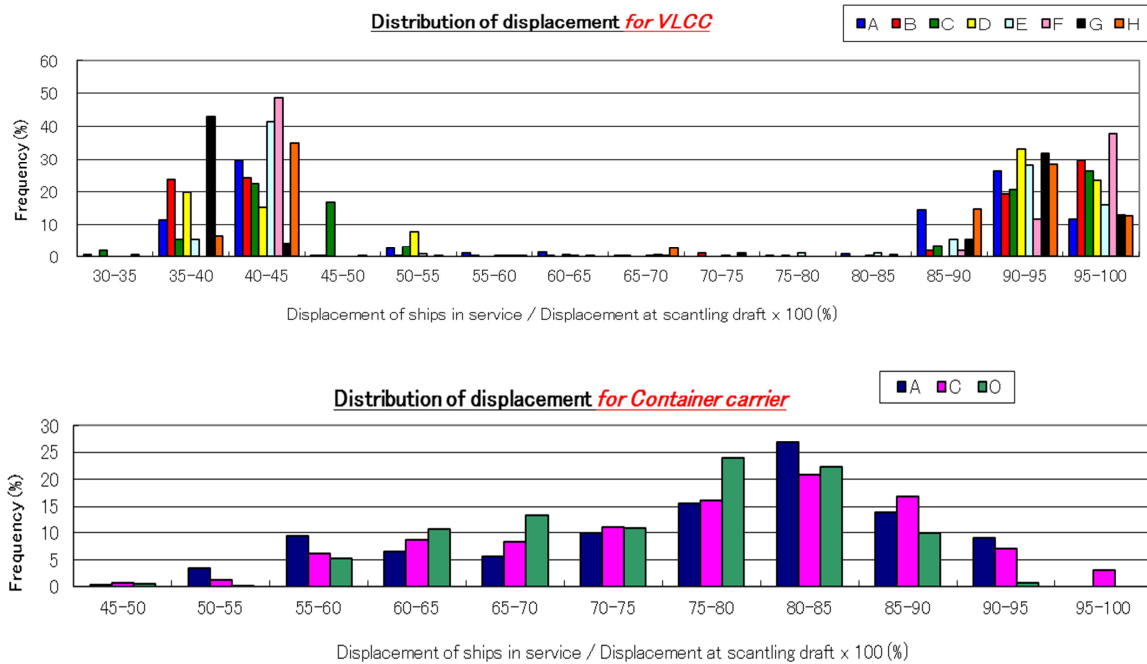


Fig. 6: Distribution of displacement for VLCC and container carrier in actual operation

3.5 Correction method for operational conditions

In general, the correction of propulsive power for different displacements is carried out based on the hypothesis that Admiralty coefficient is constant when deviation of displacement is comparatively small. This correction method is based on the assumption that change of resistance and self-propulsion factors between two displacements are negligibly small and required power is proportional to the change of wetted surface area which roughly corresponds to the two-thirds power of a displacement as follows:

$$C_{adm} = \frac{\Delta^{2/3} \cdot V^3}{P_d}, \quad P_d = \frac{\rho/2 \cdot S_{app} \cdot V^3 \cdot C_t}{\eta_{qp}}$$

$$C_{adm} \propto \frac{\Delta^{2/3}}{S_{app}} \cdot \frac{\eta_{qp}}{C_t}$$

Δ is the displacement, S_{app} the wetted surface area and C_t the total resistance coefficient.

Fig. 7 shows examples of attainable speed as a function of displacement normalized by the design condition for a bulk carrier and a container vessel. In these figures, **[○]** means the attainable speed at constant engine power (normalized by design speed) based on tank test data and **[●]** means the attainable speed based on the Admiralty correction by changes of displacement from design point taking into account. As seen in the figures, the Admiralty correction can be applied to the correction for more than 10% difference of displacement for the bulk carrier. The **[○]** mark for the container vessel case shows a rather complicated tendency and the application of Admiralty correction should be limited in a narrower range.

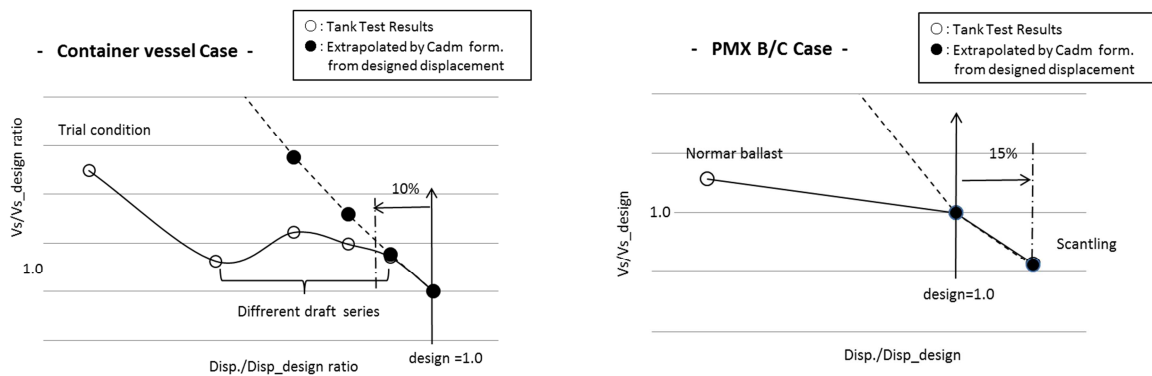


Fig. 7: Attainable speed as a function of displacement based on tank test and Admiralty correction

Fig. 8 shows the measured residual resistance coefficient: rR (normalized at design point) for a container vessel as a function of draft and speed. Fig. 9 shows the effect of trim on rR as a function of draft and trim at design speed for the same vessel, where the vertical axis stands for the percentage increase of rR relative to the even keel condition in each draft.

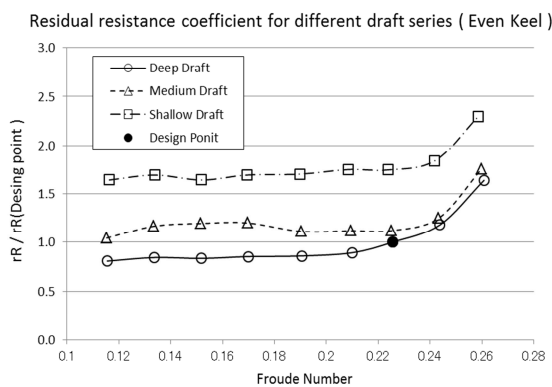


Fig. 8: rR coefficient for container vessel as function of draft and speed

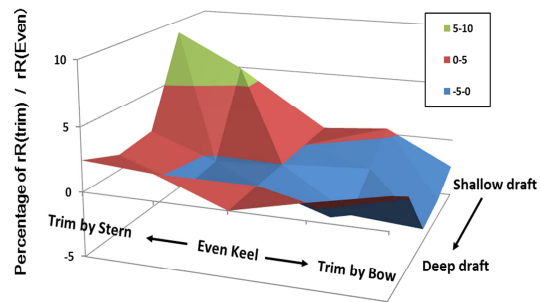


Fig. 9: Effect of trim on rR coefficient as function of trim and draft

Figs. 8 and 9 indicate that hull resistance dramatically varies with operational conditions and particularly increases at low speeds, shallow drafts and aft trims in these cases. One of the major reasons is a characteristic of wave making resistance which varies significantly as a function of ship speed and immersion of bulbous bow. Careful attention must be paid for the correction of operational

condition especially for high speed and fine hull form like a container vessel. In this case, dense power-speed-draft-trim databases should be necessary as recommended in ISO19030. Sea-Navi basically utilizes power curves based on tank test results with different operational profiles to enhance the accuracy of performance evaluation.

4. Evaluation of vessel's performance

This section presents some examples of performance evaluations based on full-scale monitoring data applying the analysis method described in section 3. Examples consist of three parts, correction of measured performance into ideal condition, confirmation of the accuracy on both designed sea margin and the effect of energy saving hull shapes aiming to reduce sea margin.

4.1 Vessel's full load performance under corrected condition

For most of ship types, ship's fully-loaded performance has been confirmed based on the logbook data after her delivery because confirmation by speed trial for this condition is impossible except for tankers. On the other hand, logbook data contain errors such as, averaged or instantaneous values at noon time, manually logged ambient conditions, ship speeds affected by currents, etc.

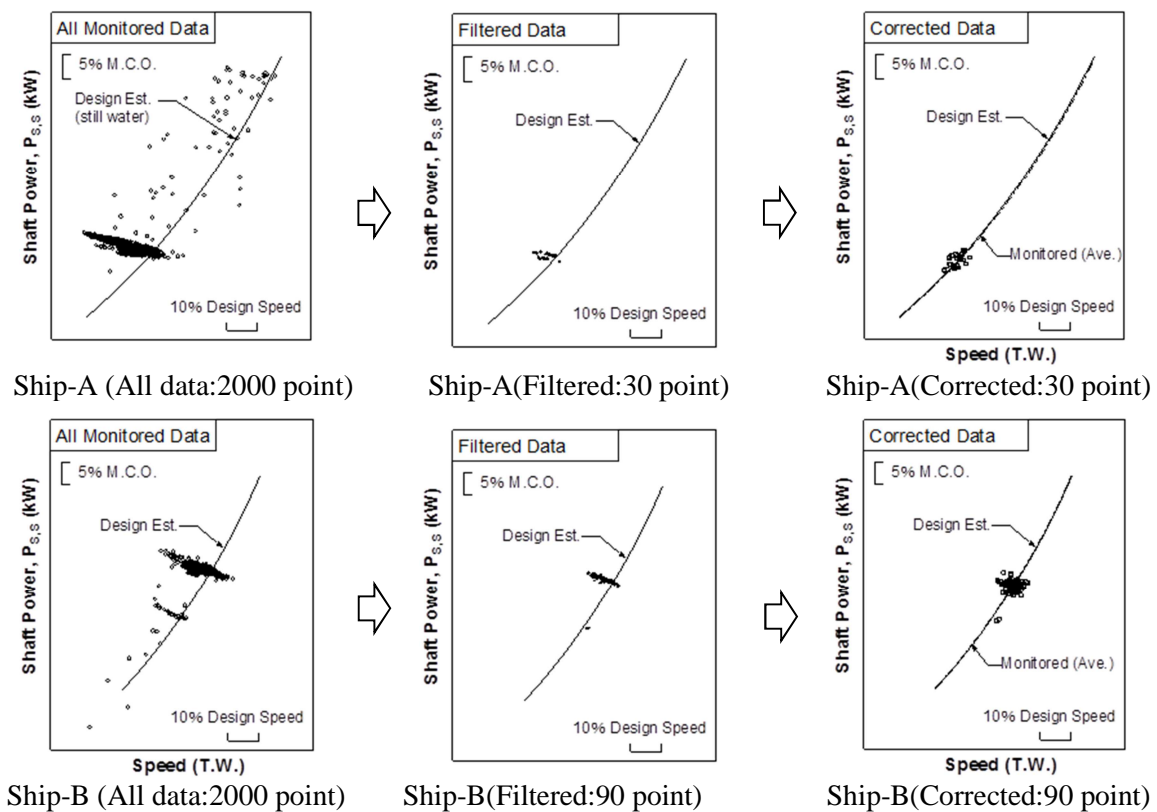


Fig. 10: Comparison of performance analysis in fully loaded condition (bulk carrier)

By means of the on-board performance monitoring and analysis system described in the previous section, ship's performance in fully loaded and calm-water condition are extracted from monitoring data for dry cargo vessels. Fig. 10 shows examples of this evaluation step for two bulk carriers, Orihara *et al.* (2016). In this figure, the left part shows all measured ship speed and shaft power together with designed power curve based on tank test data. By applying the filtering criteria described in 3.1, scattered monitoring data are converged but still contain some discrepancy to the design curve as shown in the middle part. After correcting for ambient conditions, data are concentrated on the design curve which could lead to the conclusion that designed fully-loaded

performance in calm water can be fulfilled. In this connection, monitoring data used for this evaluation is limited to those monitored within six month from their delivery to avoid fouling and aging effects. These favourable results imply not only the correctness of the design performance predictions but also the adequacy of the present procedure of performance monitoring and analysis.

4.2 Estimation accuracy of sea margin

Ship's required power in actual operation is increased by resistance due to wind and waves which is historically called "Sea-margin". Propulsive performance in a seaway represented by EEOI can be improved by reducing this Sea-margin and thus JMU has worked for a long time on energy saving hull forms to reduce sea-margin as presented in 4.3.

To develop these hull forms accurately in the design stage, it is important to evaluate the accuracy of the estimation method of sea-margin. As speed trials are normally conducted in calm sea, this evaluation can only be achieved based on monitoring after delivery.

In this respect, comparison of designed and measured sea margin was carried out for a large bulk carrier. In general, the design sea margin is calculated in Beaufort standard weather condition as tabulated in Table 1 where combination of wind and waves in the same direction is stipulated, *WNO (1995)*. Since measured conditions usually differ from this standard relationship, total resistance is corrected for the difference of the wave effect between actual weather condition and Beaufort standard weather condition. Details of this correction procedure are described in *Orihara et al. (2016)*.

Table 1: Beaufort Standard weather condition

Beaufort Scale	Wind Speed	Wave Height	Wave Period*
Bft 1	0.90 m/s	0.1 m	1.2 s
Bft 2	2.45 m/s	0.2 m	1.7 s
Bft 3	4.40 m/s	0.6 m	3.0 s
Bft 4	6.70 m/s	1.0 m	3.9 s
Bft 5	9.35 m/s	2.0 m	5.5 s
Bft 6	12.30 m/s	3.0 m	6.7 s
Bft 7	15.50 m/s	4.0 m	7.7 s
Bft 8	18.95 m/s	5.5 m	9.1 s

* : wave period (T_m) is calculated from wave height as $T_m = 3.86\sqrt{H_w}$

Fig. 11 shows an example of measured and corrected sea-margin together with designed sea margin on a basis of Beaufort scale, *Orihara et al. (2016)*. From these figures, reasonable agreements between \square corrected results and design value imply that ship's performance under actual sea can be estimated using the present prediction approach. Further, since large deviations between \circ monitored data and corrected results are observed in the case where swell effect is predominant, accurate evaluation of wave condition is crucial in enhancing the accuracy of full-scale performance monitoring and analysis.

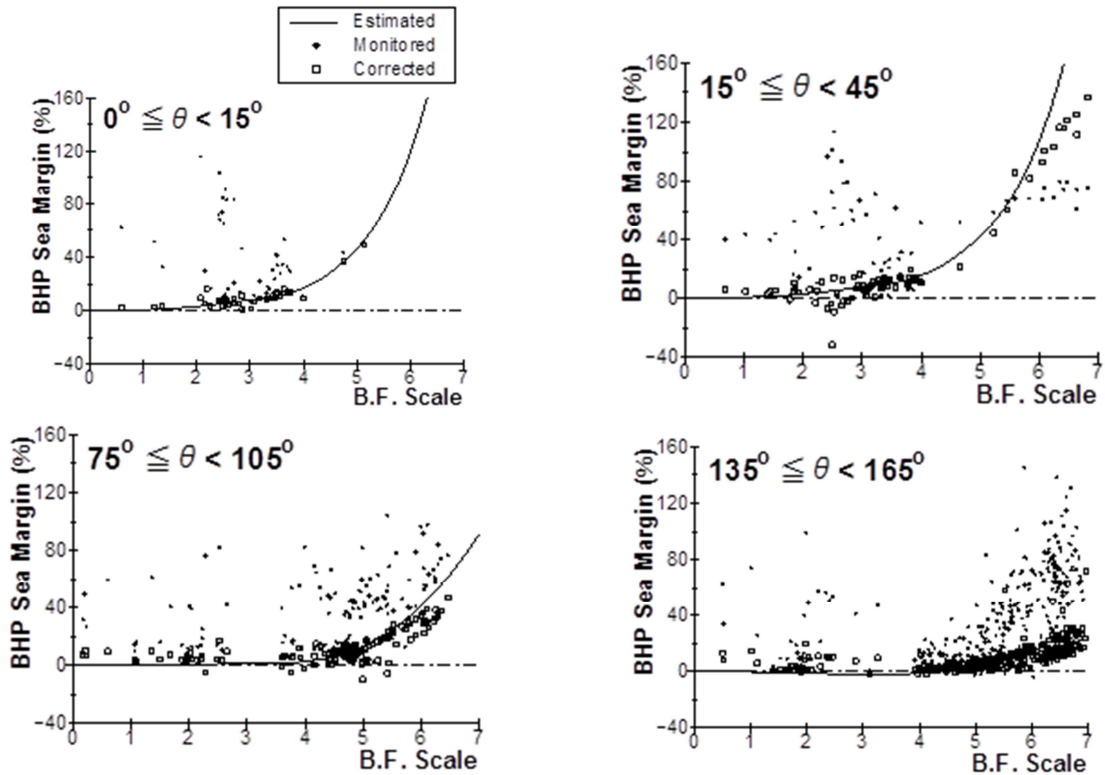


Fig. 11: Comparison of sea-margin in fully loaded condition for bulk carrier

4.3 Energy saving hull form to reduce sea margin

JMU has developed a variety of technologies for reducing resistance increase due to wind and waves, which include Ax-Bow, LEADGE-bow and Low Wind Resistance Type accommodation shape, Orihara *et al.* (2014). Fig. 12 shows a new type bow configuration which reduces the resistance increase due to the diffraction component of the incident wave around the bow. Also, Fig. 13 shows the new deckhouse shape with triangle corner-cut and modified dodger/ pillar configurations to reduce wind resistance.

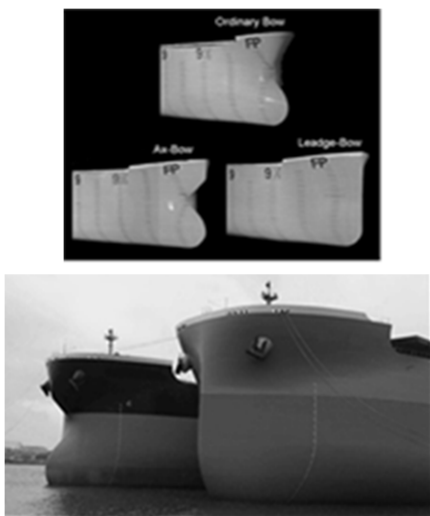


Fig. 12: Ax-bow and LEADGE-bow

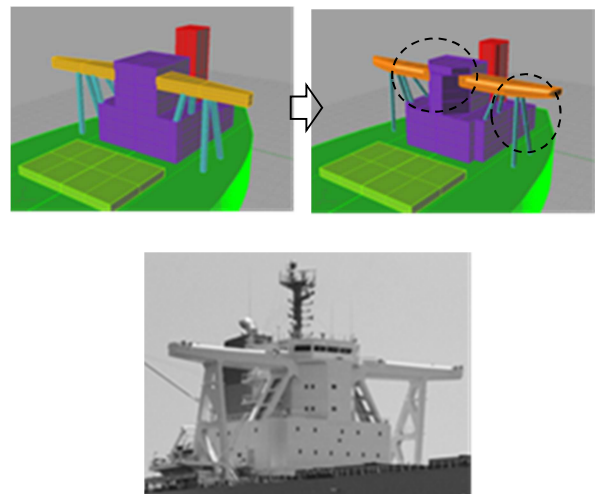


Fig. 13: Low wind resistance deckhouse

These technologies have already applied for many ships built by JMU and their full-scale performance is thoroughly verified by means of on-board performance monitoring. Particularly for the purpose of design verification, analysis of monitoring data was carried out for 3 vessels with different type of technologies as given in Table 2 and relative merits of energy saving technologies in wind and waves are evaluated by comparing measured performance.

Table 2: Particulars of test ships

Name	L(m)×B(m)×D(m)	Bow Shape	Accommodation Shape
Ship A	300×50×25.0	LEADGE	Fully Low W.R. Type
Ship B	300×50×25.0	Ax	Corner-cut only
Ship C	289×45×24.1	Ordinary	Conventional

Fig. 14 compares the power increase ratio ΔP corresponding to the specific engine output for 3 vessel as a function of Beaufort scale specified by wind speed. ΔP for Ship C is corrected for the difference in ship's breadth and length by assuming the same resistance coefficient and length as Ships A and B. Also, added resistance due to waves is adjusted to the Beaufort standard weather condition by applying the approach described in 4.2. This figure demonstrates a clear advantage of the new technologies to reduce the sea-margin, *Orihara et al. (2014)*.

Fig. 15 shows the percentage reduction in ΔP relative to Ship C under the head sea condition based on Beaufort scale for Ships A and B together with the designed value, *Orihara et al. (2014)*. A noticeable power reduction is achieved for Ships A and B and the designed value coincides with measured data within a practical range of accuracy.

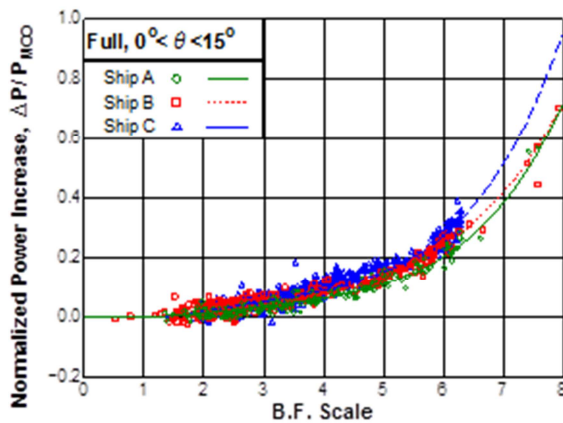


Fig. 14: Analysed power increase in head seas

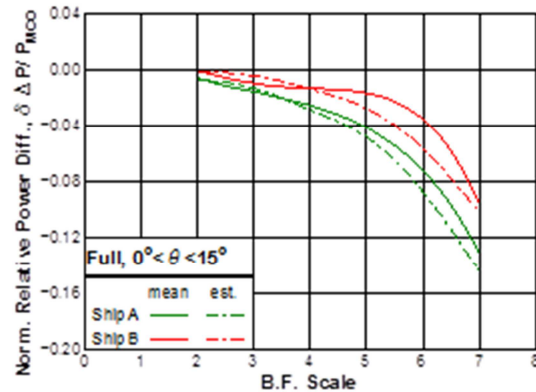


Fig. 15: Power reduction relative to Ship-C in head seas

5. Conclusions

In this paper, importance and availability of on-board monitoring and analysis system as a design tool for performance prediction is described from a shipbuilder's view. Concluding remarks of this study are as follows:

- (1) Full-scale performance of JMU Eco-friendly ships under actual sea can be evaluated by Sea-Navi on-board monitoring and analysis system with high degree of confidence. This system can effectively be used as a design tool to enhance the performance of future Eco-friendly ships.
- (2) Propulsive performance in actual operation is strongly affected by ambient and operational conditions. Correction for these conditions based on a precise hydrodynamic model is essential to evaluate the vessel's performance with higher quantitative accuracy.

- (3) For the correction of the wave effect, precise monitoring of wave conditions by an automatic measurement system or global forecasting with a high degree of accuracy is necessary, together with higher accuracy in the estimation of the resistance increase due to waves.
- (4) A technically sophisticated and practical system for measuring waves is necessary especially to provide a wave spectrum to identify swell whose effect may be greater than that of wind waves.

Acknowledgements

The authors acknowledge the valuable assistance from the experts in the Japanese mirror group for the project of ISO 19030 and sincerely hope that the advanced monitoring and analysis system proposed in this paper might contribute to future improvements of ISO19030.

References

ISO19030 (2016), *Ships and marine technology – Measurement of changes in hull and propeller performance*, ISO, London

ISO15016 (2015), *Ships and marine technology – Guideline for the assessment of speed and power performance by analysis of speed trial data*, ISO, London

ORIHARA, H.; YOSHIDA, H. (2010), *Development of voyage support system “Sea-Navi” for lower fuel consumption and CO2 emissions*, Int. Symp. Ship Design and Operation for Environmental Sustainability, pp. 315-328

ORIHARA, H.; YOSHIDA, H.; HITORA, K.; YAMASAKI, K.; SAITOH, Y. (2014), *Verification of full-scale performance of eco-friendly bulk carriers under actual operating conditions by on-board performance monitoring*, 2nd Int. Conf. Maritime Technology and Engineering, Lisbon, pp.755-763

ORIHARA, H.; YOSHIDA, H. (2015), *Verification of energy saving capability of optimum routing by full-scale trial navigation*, COMPIT Conf., Ulrichshusen, pp.343-354

ORIHARA, H.; YOSHIDA, H.; AMAYA, I. (2016), *Evaluation of full-scale performance of large merchant ships by means of onboard performance monitoring*, ISOPE, Rhodes

WNO (1995), *Manual of Codes, International Codes, Volume I.1, Part A-Alphanumeric Codes*, WNO-No.306 (1995 edition)

Future Work on Drag and Boundary Layer Properties of Biofouling Collected From Commercial Vessels

Dinis Oliveira, Lena Granhag, Chalmers University of Technology, Gothenburg/Sweden,
dinis@chalmers.se

Abstract

This paper presents a method to collect intact biofouling samples from vessels. Magnetic settlement plates (MAGPLATEs) will be attached to ship hulls. In this study, MAGPLATEs will be used to obtain intact biofilm samples, grown and subjected to hydrodynamic conditions similar to those at control patches on the hull. To collect representative samples of fouling in the North Atlantic waters, settlement plates will be deployed on ships with routes in the North Sea. At the end of the sampling period, plates will be analysed regarding composition, topography and drag & boundary layer properties. Future applications of MAGPLATEs are also discussed.

1. Introduction

Biofouling can be defined as the colonization of an interface by living organisms, *Dürr and Thomason (2009, p. xv)*. Marine biofouling ranges from thin biofilms, commonly known as “slime” and composed of microorganisms and their extracellular products to more advanced macrofouling communities, composed of macroalgae and both calcareous and soft-bodied animals, *Schultz and Swain (2000)*, *Woods Hole Oceanographic Institute (1952)*.

Biofouling on ship hulls is well known for its economic and environmental issues. Regarding economic impact for ship operators, drag penalty caused by increased roughness is directly related to fuel consumption or decreased maximum speed and range, *Townsin (2003)*. Also, biofouling leads to increased costs related to hull maintenance and costs associated with accelerated corrosion of the hull, *Schultz et al. (2011)*, *Woods Hole Oceanographic Institute (1952, pp. 14–19)*. In environmental terms, biofouling has an impact on emissions of green-house gases and other air pollutants from shipping. It is estimated that the use of “best available” paint technology to control biofouling would mean a decrease of around 7-10% in current emissions from shipping, circumventing an yearly emission of 70 to 100 million tonnes of CO₂, *IMO (2011)*, *IMO (2014)*. Finally, hull fouling increases the risk of introduction of non-native invasive species (NIS), which is at least comparable to the risk associated with ballast water, posing a threat to ecosystems, human health and local economy, *Bax et al. (2003)*, *Drake and Lodge (2007)*.

Today, international traffic corresponds to over 80% of emissions from shipping, *IMO (2014, p. 24 Table 3)*. Slow steaming has become a popular measure to reduce fuel consumption, *Armstrong (2013)*. However, it is observed that the total resistance at low speeds is almost entirely composed of frictional resistance, part of which caused by biofouling, *Schultz (2007)*, *Woods Hole Oceanographic Institute (1952, Figure 11)*. Still, it is complex to give precise figures regarding the impact of hull condition on fuel consumption, particularly considering required corrections for changes in draft, trim, weather conditions, wind, waves, sea currents, temperature and salinity, *Munk (2006)*, *Munk et al. (2009)*.

A large body of literature deals with the local impact of biofouling on frictional drag. *Lewthwaite et al. (1984)* determined that a thin slime, developed over 240 days and “just detectable by touch”, could lead to an increase in local skin friction coefficient of 25% relative to the clean hull. Results were achieved from sea trials with a 23-meter-long vessel (~12 knots) and using a pitot-type probe. *Leer-Andersen and Larsson (2003)* used experimental results on skin friction (from a pressure-drop pipe system) and proceeded to model the impact of fouling at the ship scale, using CFD (Computational Fluid Dynamics). Hydrodynamic properties of marine biofilms and low-form soft biofouling have been studied in recirculating water tunnels, *Schultz and Swain (1999)*, *Schultz and Swain (2000)*,

Schultz (2000). Laboratory-scale results have been translated into full-scale ship resistance, *Schultz (2007)*. The later results have also been included in economic analysis of fouling control on a naval surface ship, *Schultz et al. (2011)*. Similar turbulent boundary layer studies have been conducted for freshwater biofilms, *Walker et al. (2013)*. However, a much sought-after global relation between physical measurements and increased drag has so far proved elusive. This is aggravated by the fact that biofilms and soft fouling are compliant, i.e. their profile temporarily adapts to flow conditions, *Townsin (2003)*, *Schultz et al. (2015)*. Therefore, hydrodynamic measurements are still required in order to determine drag increases for each specific sample. Still, it is hoped that improved *in situ* surface characterization, together with precise flow measurements, may lead to better insight on the mechanisms leading to increased skin friction, *Schultz and Flack (2009)*, *Schultz et al. (2015)*.

Earlier studies on turbulent boundary layer properties relied on statically-grown biofilm/biofouling samples for their measurements, *Schultz and Swain (1999)*, *Schultz and Swain (2000)*, *Schultz (2000)*. The use of such samples has some limitations, since hydrodynamic conditions on static panels differ significantly from those on actual ship hulls. Furthermore, partial detachment of biofilm during the tests leads to additional uncertainty. Thus, dynamically cultured biofilms have been used in more recent studies on the turbulent boundary layer, *Schultz et al. (2015)*. Also, skin friction has been measured on naturally-occurring biofouling communities, which were dynamically-grown on hull coatings using rotating cylinders installed on ocean rafts, *Lindholdt et al. (2015)*. Although such methods enable to grow fouling under shear-stress values that represent relevant speeds on large commercial vessels (~11 knots), other factors might influence growth on actual hulls, including different fouling pressure in visited ports (route-dependent), the complexity of the flow around the hull (*Larsson and Raven 2010*) and differential exposure to light on different regions of the hull. Additionally, samples from rotating cylinders can only be used in evaluating skin friction alone, *Lindholdt et al. (2015)*, whereas no information can be drawn on drag-increase mechanisms, as obtained from more complete turbulent boundary layer measurements on flat plates, *Schultz et al. (2015)*.

Collecting biofouling samples from actual ship hulls usually meets with significant challenges and restrictions: inspection and collection of samples in the dry dock must be accomplished within the narrow time-window between draining the dry dock and the start of hull cleaning; draining sometimes finishes at night fall; finally, safety rules might restrict access to the dry dock, while in-port inspections are associated with significant safety and security constraints, *McCollin and Brown (2014)* *Coutts et al. (2007)*. Additionally, to the best of our knowledge, there is currently no direct method for *in situ* testing of drag properties on the hull. Therefore, we will in the planned study use a method, enabling to attach settlement plates (area of ~400 cm²) to ship hulls by means of magnets, previously developed by *Coutts et al. (2007)*. These magnetic plates, known as MAGPLATEs, have been used for assessing the survival of biofoulers, which were pre-grown on settlement plates under static conditions and then transferred to the hull for testing survival while the vessel is underway, *Coutts et al. (2010)*. No effect of magnetism on biofouling has been reported using MAGPLATEs, *Coutts et al. (2007)*. The original design of the MAGPLATEs, which were previously built in stainless steel, could withstand vessel speeds of up to 23 knots, in 5-m swell (*Ashley Coutts, personal communication*).

Within the current project, we aim at developing and validating a more direct method for determining the impact of hull fouling on friction, relying on intact biofouling samples collected from actual ship hulls. Also, we aim at gaining insight on drag-increase mechanisms, by determining turbulent boundary layer properties over such samples, along with surface topography measurements. The method relies on MAGPLATEs for sample collection. In this paper, we give a detailed description of planned work, as well as expected outcome and potential future applications of the method.

2. Planned work

We divide the current description into field methods and experimental ones. The former correspond to steps associated with deployment and retrieval of MAGPLATEs, whereas the later correspond to the subsequent lab-based work and analysis.

2.1. Field methods

Within this sub-section, planned field work is described, starting from the MAGPLATE design and settlement plates. Then, other aspects are specified, such as the geographical area, target vessels, data collection, representative sampling of the hull surface and, finally, procedures for deployment, retrieval and transport of samples to the lab.

2.1.1 MAGPLATE: baseplate design and materials

The MAGPLATE consists of an assemblage of a baseplate, which is secured to the hull surface by magnets, and a top settlement plate, corresponding to the flat area exposed to fouling.

The current design of the baseplate is presented in Fig. 1. The baseplate is composed of polycarbonate reinforced with 30% fiberglass, having a set 8 neodymium iron boron (NdFeB) ring magnets on its underside. The current design is based on a previous successful prototype, *Coutts et al. (2007)*. The edges of the plate are bevelled, in order to decrease the disturbance in the flow. The 3-mm thick top settlement plate is bolted to the top of the baseplate (Fig. 1A) and it is flush with the edges of the baseplate.

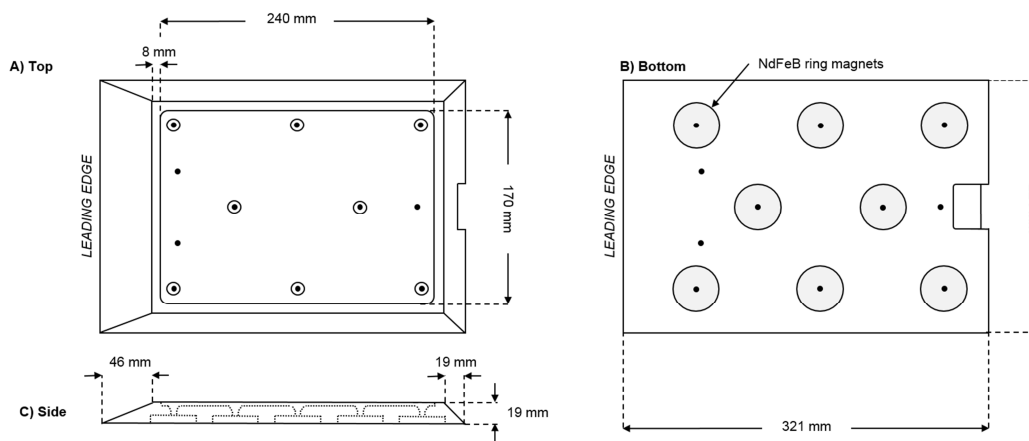


Fig. 1: Base plate of MAGPLATE, as used in the current study: A) top view, B) bottom view, C) side view. The leading edge faces the bow of the ship. NdFeB = neodymium iron boron.

In order to minimize the disturbance caused by the MAGPLATE in the boundary layer, the angle of the leading edge was decreased from the original value of 45° to the current value of 22.5° , while maintaining all other edges unchanged (thus minimizing the weight of the baseplates). This decision is based upon early numerical results, obtained using a commercial CFD code (COMSOL® Multiphysics), that corroborate the hypothesis that, for a longer leading edge (i.e. lower bevel angle), the distribution of shear stresses along the top of the MAGPLATE is more homogeneous (results not shown here). More accurate numerical results on the present geometry would also add a valuable contribution to the validation procedure further detailed in this paper.

2.1.2. Top settlement plates

A 3-mm thick settlement plate is designed to fit the top of the baseplate, flush with the edges. It has a total exposed area of 408 cm^2 . The plates are manufactured in poly(methyl methacrylate) (PMMA). Both top settlement plates and baseplates' edges will be coated at same time as vessel's repainted in dry dock, thus ensuring a similar treatment to both MAGPLATES and the hull (please refer to section 2.1.7. Deployment, retrieval and transport of MAGPLATES).

2.1.3. Geographical area and seasonality

The geographical area of interest is presented in Fig. 2, comprising the North Sea and Baltic Sea. Main ports connected by ferries are marked, as well as currently operating dry docks, used for both shipbuilding and repair/maintenance.

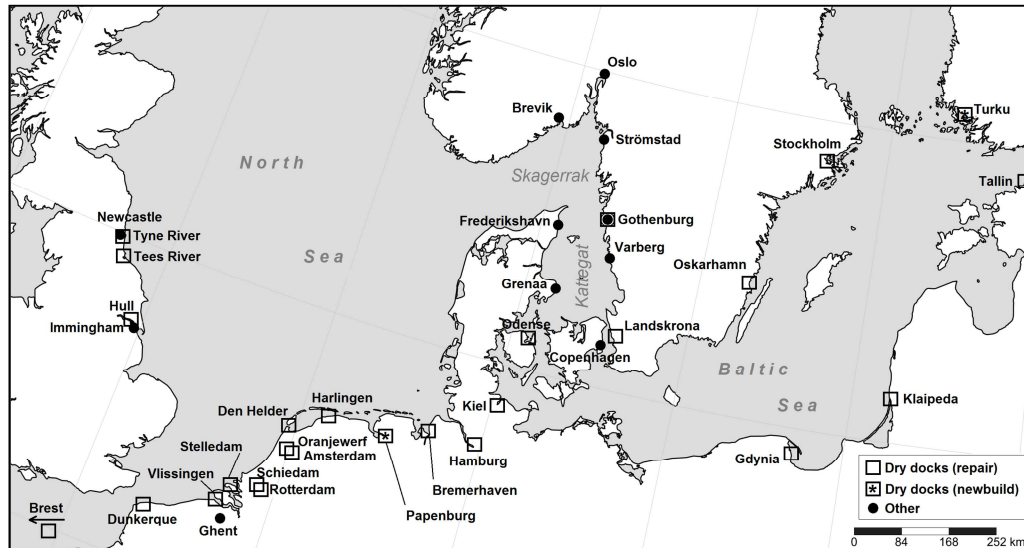


Fig. 2: Geographical area of interest

A considerable number of ferry routes operate in the above geographical area, some of them connecting the west coast of Sweden, where available testing facilities are located, to other main ports around the North Sea and the Baltic. Thus, the current geographical limits are manageable, in terms of transport of samples to the laboratory, as well as available time and resources. It should be noted that conditions vary sharply across the current geographical area, including weather conditions, tidal range, salinity, biodiversity and fouling pressure. However, the vessels to be sampled are expected to follow specific routes, which usually remain unchanged for long periods of time (please see further details below, under sub-sections 2.1.4. and 2.1.5). In the current geographical area, seasonality is another important aspect to consider, as noted in previous studies, e.g. *Berntsson and Jonsson (2003)*. Thus, fouling pressure is higher between April and October, while the abundance of each species is expected to vary throughout that period. Such variations should be taken into account when interpreting results obtained from different seasons.

2.1.4. Target vessels

It is also important to specify the class of vessels to be sampled, especially considering that vessel characteristics vary widely in the North Sea and the Baltic. Thus, target vessels have been selected, taking as reference two sizes of RoRo ferries frequently visiting the west coast of Sweden. Approximate ranges for the particulars of target vessels are given in Table I, enabling to narrow down to 2 specific classes of vessels, while providing a reference frame for our results. The two types of RoRo ferry represent two different ranges of cargo capacities (deadweight), size and speed.

Table I: Target vessels: approximate ranges for two sizes of RoRo ferries.

Particulars	Units	RoRo Ferries I	RoRo Ferries II
Deadweight	[ton]	2,000 – 7,000	10,000 – 15,000
Length Overall	[m]	130 – 190	190 – 250
Breadth	[m]	24 – 30	24 – 30
Draft (loaded)	[m]	5 – 8	5 – 8
Speed	[kn]	10 – 17	15 – 23

2.1.5. Vessel data collection

During the sampling period, vessel data of two kinds will be collected, in order to characterize both the vessel and its operational profile: 1) up-to-date particulars of the vessel, 2) voyage log data (e.g. noon reports), and 3) dry-docking report.

Regarding the particulars of the vessel, the following should be collected, at a minimum: year built, length overall [m], breadth [m] and deadweight [ton].

Regarding voyage data, the following should be collected, at a minimum: distance over ground [nm], logged distance through water [nm], steaming time [h], maximum speed through water [kn], draft [m], displacement [ton], wind [Beaufort scale], relative wind direction [quadrants], visual estimation of wave height [m], port visits [location and date], seawater temperature [°C] and salinity [ppm]. The latter two parameters can be obtained, alternatively, from historical databases. All these variables should be given as a function of date and time (alternatively, time elapsed since out-docking). It should be stressed that voyage data will be used solely in characterizing the operational profile of the vessels; it is therefore not intended for use in any calculation on hull/propeller performance. The steaming time will be used for calculating the cumulative idle time since out-docking, recognized as an important factor contributing to the fouling condition of hull and propeller, *Bocchetti et al. (2015)*. Additionally, the distribution of duration of individual idle periods could be of interest, as it might influence the fouling pattern, according to differences in settlement windows (i.e. time allowed for settlement of fouling organisms).

Finally, the latest dry-docking report should give a description of maintenance activities, extent of repainted external hull [% area, or hull locations] and type of fouling control coating [type and/or product name].

2.1.6. Representative sampling of the hull

In the current study, we aim at obtaining representative samples of hull fouling, i.e. growth that contributes significantly to **total** frictional resistance and, consequently, to the increase in propulsive power or decrease in speed. In this sub-section, hull locations are selected, considering both horizontal and vertical zonation of the hull. Thus, we take into account factors such as hydrodynamics, light and possibility of dislodgement of MAGPLATES near the waterline. The total number of MAGPLATES per vessel is also discussed.

It is well recognized that wall shear stress varies significantly across the hull surface, *Larsson and Raven (2010)*, and this leads to a varying amount of growth and taxonomic diversity between different areas of the hull, according to local hydrodynamic conditions and the varying adhesion strength of different biofouling organisms, *Lewthwaite et al. (1984)*, *Davidson et al. (2009)*, *Hunsucker et al. (2014)*. Therefore, a rational must be carefully considered for selecting locations on the hull, since it is neither practical nor desirable to cover extensive areas of the hull with MAGPLATES.

The distribution of friction on the hull is dependent on both hull design and vessel speed. As a reference, numerical results obtained by Johansson (1984) are presented in Fig. 3, corresponding to the “permissible roughness height” on the underwater hull of a containership. The permissible roughness corresponds to the highest value of sand roughness that represents the limit for a hydraulically smooth surface as given by $h = 5 \cdot v \cdot (\rho / \tau_w)^{1/2}$, being inversely proportional to the square root of the wall shear stress, *Johansson (1984)*. Thus, it is observed that the areas where friction is most significant (lower values of h) are located close to the bow of the vessel and near the waterline. However, it is observed that friction does not vary significantly within a large section of the hull (Fig. 3). The particulars of the vessel, as given in the caption of Fig. 3, correspond to slightly higher values than those of target vessels previously presented in Table I. Thus, having acknowledged that significant differences in shear stress distribution may occur between different hull shapes and speeds,

a qualitative interpretation of the above information suggests a minimum of 1 longitudinal sampling location within the forward half of the hull, roughly at equal distance between amidships and the bow of the ship, i.e. near the forward shoulders. Since in the current study, as opposed to *Coutts et al. (2010)*, there is no specific interest in obtaining data on invasive species, the sheltered areas of the hull (such as the stern) can be left out, and one single longitudinal location is currently regarded as sufficient. This longitudinal location near the forward shoulders apparently represents a significant portion of the hull, thus contributing significantly to total friction (area integral of local shear stresses). For a better estimation on how representative this sampling holds, modelling of the flow for each specific hull design would be required.

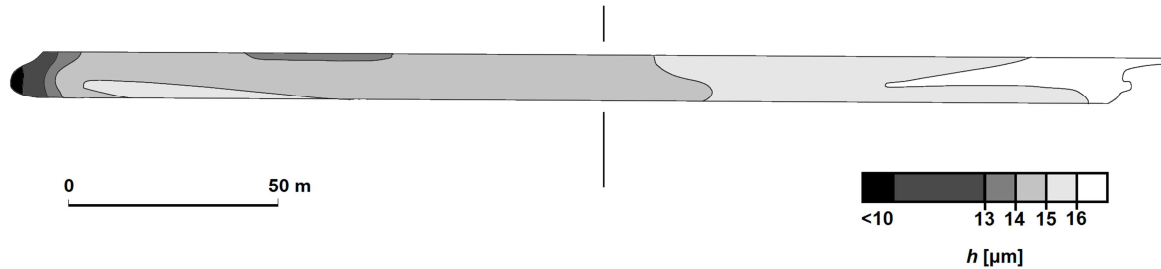


Fig. 3: Computed results obtained by *Johansson (1984)* for permissible sand roughness height h on the hull of a containership with bulbous bow. The contour corresponds to the side view of the underwater part of the hull. High values of h correspond to low values of wall shear stress τ_w , as given by $h = 5 \cdot \nu \cdot (\rho / \tau_w)^{1/2}$. Particulars of the vessel: $L_{pp} = 258$ m, $B = 32.3$ m, $T = 10.7$ m, speed = 28 kn. The vertical line corresponds to amidships. Modified from *Johansson (1984)*.

Next, the sampling depth must be selected. It should be noted that friction varies both longitudinally and with depth, Fig. 3. However, other factors that affect biofouling, such as exposure to light, are also dependent on depth. Furthermore, there are restrictions on how close to the waterline MAGPLATES can be deployed, considering variation in vessel's draft and the action of waves near the waterline. Thus, there must be a compromise between exposure to light, on the one hand, and the possibility of dislodgment of the MAGPLATES or desiccation of samples, on the other hand. Thus, we opt for minimizing/maximizing exposure to light, by selecting two depths: maximum depth that enables safe deployment of MAGPLATES and minimizes exposure to light, and a second, shallower depth that maximizes exposure to light, which is here set to approximately $\frac{1}{4}$ of the minimum draft expected during vessel's operation (including stays in port, as to avoid desiccation between unloading and reloading of cargo). Here it should be noted that both friction and exposure to light decrease with depth, while the two factors are expected to have opposite effects on growth: at maximum depth, a low exposure to light should lead to decreased (micro)algal growth, whereas decreased friction at such depth should enable more intense growth.

Finally, from the above considerations, a total number of 2 MAGPLATES per vessel is proposed: halfway between the bow and amidships, at two different depths, namely: 1) as close as possible to the main keel and 2) at a depth corresponding to $\frac{1}{4}$ of the minimum expected draft. It is assumed that fouling should not vary significantly between the port and starboard sides of the vessels, *Hunsucker et al. (2014)*; otherwise, it would remain a challenge to place each MAGPLATE in the exact corresponding location on each side of the vessel. Variations in fouling between both sides could also arise from the presence of different features on each side of the hull, e.g. cooling water inlets/outlets. The final location chosen for deployment should avoid the proximity of structures such as sea chests and protruding features, which constitute niches and therefore would not be representative in terms of total friction.

2.1.7. Deployment, retrieval and transport of MAGPLATES

Vessels will be selected according to target ranges presented in Table I. MAGPLATES will be deployed just before out-docking of selected vessels. From a total of ~30 dry docks operating in the North Sea and Baltic region, Fig. 2, 23 are currently able to repair those classes of vessels.

All the vessels should have their hulls newly painted before deployment of MAGPLATEs. In the dry dock, assembled plates (i.e. baseplate + top settlement plate) will receive the same treatment as the hull, i.e. the plates will be painted with same number of layers and types of coating. The method of paint application should also be the same between MAGPLATEs and large flat surfaces of the hull. Both top settlement plate and edges of the baseplates will be coated. One additional settlement plate will be coated, for later testing of hydrodynamic properties of a newly-painted, unexposed surface (unfouled), while another plate will be kept without coating (uncoated PMMA).

Since initial coating roughness might have an effect on biofouling patterns, coating roughness readings will be obtained. More specifically, $R_t(50)$ will be measured, i.e. the peak-to-trough distance, in μm , within a linear length of 50 mm, using a hull roughness gauge (TQC Model DC9000; accuracy: $\pm 5 \mu\text{m}$ or $\pm 2\%$, whichever is greater). A minimum of 12 readings (12 \times 50 mm) will be obtained on each MAGPLATE, and also on the corresponding neighbouring area of the hull surface. The latter measurements will be made at a distance of ~ 0.5 m above each MAGPLATE, since this location will also be targeted for analysis of the fouling pattern.

After the exposure period on the hull, which will range from a minimum of 1 month to a maximum of 6 months (depending on port visits and dry-docking schedule), MAGPLATEs will be retrieved by divers, whilst the vessel is at berth. Before retrieval, divers will be asked to capture underwater images of the hull, more specifically covering the MAGPLATEs and neighbouring areas of the hull. A photoquadrat frame will be used in obtaining images that cover a standard area of the hull ($\sim 2000 \text{ cm}^2$). This frame will consist of a PVC structure that keeps an underwater camera centred and at a constant distance from the hull (see *Preskitt et al., 2004*). These images will be later used for determining fouling patterns, using image analysis. The photoquadrats will be targeting 1) fouled MAGPLATEs still in their original hull locations (just before retrieval), and 2) neighbouring control areas of the hull, at a distance of ~ 0.5 m above each MAGPLATE (this location avoids possible effects of flow recirculation downstream from the MAGPLATE, flow stagnation upstream from the MAGPLATE and light shadowing below the MAGPLATE).

The retrieved MAGPLATEs will be placed in containers, kept in seawater from location of collection, and transported to the lab. A larger, thermally-insulated container (filled with ice) shall be used for transporting the inner container at low temperature.

Once in the lab, samples should be kept in a flume, under reduced flow of filtered seawater (FSW), and should preferably be tested within 24 hours, counting from retrieval. Contrary to fouled samples, unexposed newly-painted plates should be kept in FSW for a minimum of 24 hours prior to testing, as to represent hydrated hull surfaces (it has been acknowledged that hull coatings normally absorb water, *Lindholdt et al. (2015)*).

2.6. Experimental methods

In this sub-section, planned lab-based work is described, including fouling pattern (severity, broad taxonomic groups and percentage cover), characterization of surface topography and, finally, skin friction and boundary layer properties. Additionally, aspects dealing with estimation of uncertainties and statistical treatment are also discussed. In every type of analysis (except for hydrodynamic testing in Section 2.6.3), a 20-mm strip measured from the edge of settlement plates will be excluded, considering possible boundary effects, *Coutts et al. (2010)*. The analysed area is thus limited to $260 \text{ cm}^2/\text{plate}$, except for hydrodynamic testing (2.6.3).

2.6.1. Fouling pattern

Upon arrival to the lab, the top settlement plates will be detached from the baseplate, while keeping samples underwater all time. These plates are again photographed underwater, using the same photoquadrat frame previously used by divers in the field (Section 2.1.7). These images will enable to assess the effects of handling, i.e. during retrieval, transport and detachment of settlement plates. The

plates will again be photographed after hydrodynamic testing (Section 2.6.3), following the same procedure.

Subsequently, the Fouling Rate (FR) will be visually determined for each sample, using the U.S. Navy's rating system, *NSTM (2006)*. This FR scale spans from 0 (no fouling detected) to 100 (severe fouling) and it is based on the presence/absence of "slime" (bacterial/diatom biofilm), "grass" (filamentous fouling), tubeworms, barnacles, oysters, mussels and soft sedentary animals. It also takes into account the size of such organisms/colonies. Although the NSTM's FR scale is subjective, it can still provide a rough estimate of increased drag, *Lindholdt et al. (2015)*, *Schultz et al. (2011)*. In the current study, FR is expected to be ≤ 30 , as in most of the results obtained from dynamic testing in the Roskilde Fjord (Kattegat Sea, DK), *Lindholdt et al. (2015)*.

The total percentage cover will be estimated as suggested in the standard *ASTM D6990-05 (2005)*, i.e. by visually comparing the fouling pattern to those of reference diagrams (extent diagrams) and then estimating the percentage cover for each sample. In case macrofoulers are also present, frequency data will be obtained (i.e. counting of individual macrofoulers); still, this is deemed unlikely, considering an expected FR ≤ 30 . Thus, frequency data is no further considered in this paper.

Finally, density and composition of algal fouling will be measured as chlorophyll *a* and group-specific pigments, by fluorescence method, using BenthosTorch (BBE Moldaenke, Germany). In situ measurements on the settlement plates will determine the relative composition of the most common fouling groups of microalga (diatoms and cyanobacteria), as well as green alga.

2.6.2. Surface topography

Recently, *Schultz et al. (2015)* observed that skin friction is dependent on both biofilm thickness and percentage biofilm cover. Here, we further hypothesize that the degree of interspersedness of the biofilm (i.e. distribution of size of biofilm clumps) might also play an important role as a scaling factor: for the same percentage cover, higher interspersedness might lead to higher frictional drag. So far, and to the best of our knowledge, this factor has never been analysed.

Thus, taking a step forward from a qualitative visual assessment of fouling patterns (section 2.6.1), we will determine surface topography parameters, including biofilm thickness, algae layer thickness, percentage cover and degree of interspersedness. It should be noted that the current approach assumes an FR ≤ 30 , i.e. no hard fouling detected.

Biofilm thickness has previously been measured using different approaches. Light section microscopes can be used for this purpose, *Haslbeck and Bohlander (1992)*, *Jackson and Jones (1988)*; however, this method might not be applicable for thicker biofilms, *Jackson and Jones (1988)*. More recently, photogrammetry methods have been suggested, relying on stereo photographs of the biofilm in air, *Walker et al. (2013)*. However, careful use of the later method on fouled surfaces leads to an accuracy of $\pm 240 \mu\text{m}$, *Walker et al. (2013)*, whereas comb-type wet film thickness gauges can be accurate down to $\pm 25 \mu\text{m}$, *Schultz and Swain (1999)*. Therefore, a comb-type gauge will be used in the current study, considering its cost-effectiveness, easy handling and accuracy. Thus, a total of 20 thickness measurements will be taken on each settlement plate, in areas covered by biofilm. These will be obtained only after hydrodynamic testing (section 2.6.3), as to avoid surface damage prior to hydrodynamic testing.

For samples with filamentous algae, the thickness of the algae layer will be estimated using image analysis. Thus, the height will be obtained from profile digital images of the algae layer, *Schultz (2000)*. This thickness will also be determined as a function of mean stream velocity (section 2.6.3).

Finally, photoquadrat images of the fouled plates will be processed and analysed, in order to more accurately determine the percentage cover and degree of interspersedness. An image processing software (ImageJ) will be used for adjusting image contrast and colour threshold. Pre-processed

images will then be analysed in MATLAB® (R2013a, MathWorks®, 2013) for determining percentage cover (area covered by biofilm / total area of image × 100) and degree of interspersedness of the biofilm. The latter is given by an approximation to the perimeter-to-area ratio, here referred to as “edge index”:

$$E [\text{cm}^{-1}] = (N_{\text{edge}} / N_{\text{biofilm}}) \times Res$$

where N_{edge} corresponds to the total number of pixels along biofilm edges (in pixels), N_{biofilm} to the total number of pixels within biofilm clumps (in pixels²), and Res is a scaling factor (in pixels/cm). Thus, E represents the degree of interspersedness of the biofilm, with a higher E value corresponding to a more interspersed biofilm, i.e. higher edge length per area covered by biofilm. It should be noted that the edge index E is only expected to give an estimation of the true perimeter-to-area ratio of the biofilm.

2.6.3. Skin friction & boundary layer properties

For both fouled surfaces (exposed on the hull) and unfouled surfaces (both coated and uncoated PMMA), we aim at determining the local friction coefficient (c_f) as function of Reynolds number based on momentum thickness ($Re_\theta = U_\infty \cdot \theta / \nu$). Also, c_f will be determined as a function of distance from the edge of the sample, to assess stream-wise variations in local friction and to determine the average friction. Additionally, we aim at obtaining the roughness function ΔU^+ (the velocity shift within the logarithmic region of the boundary layer), and relating this to topographic features of the surface (section 2.6.2).

The local friction coefficient (c_f) can be calculated from the wall shear stress τ_w [Pa], using $c_f = \tau_w / (1/2 \cdot \rho \cdot U_\infty^2)$, or, equivalently, from the friction velocity $U_\tau = (\tau_w / \rho)^{1/2}$ [m/s], using $c_f = 2 \cdot (U_\tau / U_\infty)^2$. The wall shear stress (or friction velocity) can be determined using direct or indirect methods, *Goldstein (1996)*. In the current study, we will use an indirect method, relying on velocity measurements within the boundary layer. We rely on the fact that the inner part of the boundary layer adapts rapidly to changes in roughness, *Schultz and G. W. Swain (1999)*, whereas reliable direct measurements of skin friction (e.g. using floating-element balances) are extremely difficult to obtain for such small areas as the present (~400 cm²), *Johansson (1984)*, *Paik et al. (2015)*. Thus, we aim at obtaining velocity profiles along the stream-wise centreline of each sample, in order to be able to determine the wall shear stress using the “Adaptation of the Log Law” method, with virtual origin correction for rough samples, as described in *Lewthwaite et al. (1984)*. The Reynolds number (Re_θ) will be controlled by adjusting freestream velocity. Water properties will be controlled by keeping temperature variations within a narrow interval (to be determined).

The current available facilities for hydrodynamic testing are located in the Sven Lovén Centre for Marine Sciences at Tjärnö (TMBL, Gothenburg University), near Strömstad, on the west coast of Sweden (58.876° N, 11.147° E; Fig. 2). The testing facility consists of an open flume (PMMA tank), in which the flow is set by 2 propellers located in the exit pipe, driven by a 0.75-kW motor (Fig. 4). The working section is located 5 m downstream of two collimating honey-comb panels and it measures 1.5 m × 0.5 m × 0.2 m (stream-wise length × width × depth). Test sample flat plates can be fitted in the working section, flush with the bottom of the flume (Fig. 4). The free surface of the open channel flow is located 20 cm above the sample. Still, free surfaces are known to only affect measurements in the outer region of the boundary layer, whereas the structure of the boundary layer near the wall remains similar to that obtained in a water tunnel, *Andrewartha (2010, pp.50–54)*. In spite of flow conditioning devices (honey-comb panels), the freestream turbulence intensity in this flume is still ~10%. These high values of freestream turbulence will increase uncertainties in determining the boundary layer thickness, *Schultz and Swain (1999)*, but should not otherwise affect the logarithmic region of the boundary layer, *Walker et al. (2013)*, which is used in computing the friction velocity, *Lewthwaite et al. (1984)*. The maximum freestream velocity is ~1 m/s, corresponding to a smooth wall shear stress of 1 – 2 Pa in the working section (i.e., 5 m downstream from the last honey-comb panel). These values of shear stress are comparable to the average skin

friction on a 200-m vessel travelling at a speed of about 2.5 knots (using the ITTC-57 formula, *Larsson and Raven 2010, p.58*). Therefore, the maximum speed in the flume represents the lower range of vessel speeds, e.g. corresponding to a manoeuvring vessel. At a later stage, higher-speed water tunnels could be considered, such as the cavitation tunnel at SSPA, Gothenburg.

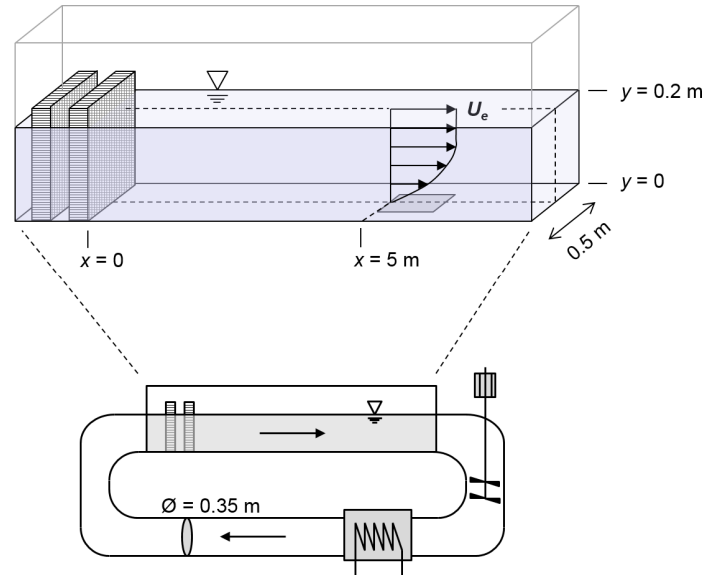


Fig.4: Schematic representation of the open flume at TMBL (Strömstad): on the top, details of the open channel; bottom, overview of the flume (2 propellers coupled to the 0.75 kW motor and a cooling system in the 0.35 m PVC return pipe). Drawings are not to scale.

For velocity measurements, the flume at TMBL is equipped with a Particle Image Velocimetry (PIV) system, which enables flow visualization within a maximum area of $130 \times 180 \text{ mm}^2$. The maximum vector density is 10 vectors/mm. The average seeding particle size, in pixels, is yet to be determined. Reducing the size of the particles normally leads to decreased random error. However, the size should be large enough (normally > 2 pixels), as to avoid the “peak-locking effect”, i.e. biased values of displacement vectors towards integral values, as observed in vector displacement histograms, *Raffel et al. (2007, pp.166–169)*. Precision uncertainties in velocity measurements will be determined by repeatability tests, as suggested by *Schultz and Swain (1999)*, by obtaining replicate velocity profiles and calculating the standard deviation of measurements. Bias uncertainties will be estimated following an approach based on ITTC guidelines for PIV measurement, *ITTC (2008)*.

2.6.4. Uncertainties and statistical treatment

In this sub-section, an outline of uncertainty estimation and statistical treatment is given, regarding the main questions considered in this study, which focuses on the validation of MAGPLATEs for collection of representative biofouling samples from commercial vessels.

For testing whether the initial roughness varies between MAGPLATEs and the hull, the $R_z(50)$ obtained using the hull roughness gauge will be compared. Analysis of variance (One-Way ANOVA) will be performed, in order to test for significant differences (statistical significance $\alpha = 0.05$), using MATLAB® (R2013a, MathWorks®, 2013).

Values of percentage cover, as determined from image analysis, will also be compared. Thus, assuming that the biggest source of error is the pixel resolution of the images, the percentage cover of MAGPLATEs versus Hull, Field versus Lab (i.e. effects of handling of MAGPLATEs) and Pre-versus Post-Hydrodynamic Testing (biofilm detachment during the tests) will all be subjected to testing of significant differences between percentage cover values.

No comparison will be attempted between different vessels, due to complexities introduced by several factors (seasons, weather, operational profile, routes, vessel particulars, etc.). Therefore, results from each vessel will be considered separately. The error associated with velocity measurements and water properties in the hydrodynamic tests will be propagated, in order to determine the uncertainties associated with some of the turbulent boundary layer parameters, such as the Reynolds number (Re_θ), displacement thickness (δ^*) and the momentum thickness (θ). Regarding the friction coefficient c_f , roughness function ΔU^+ and virtual origin correction ϵ , *Lewthwaite et al. (1984)*, confidence intervals will be determined for each parameter (linear regression). Finally, samples will be compared, regarding each of the boundary layer parameters separately: fouled surfaces versus unfouled surfaces and, for fouled surfaces, shallow-depth deployment *versus* maximum-depth deployment.

Additionally, the collapse of results for roughness function ΔU^+ will be evaluated using several available scaling parameters, including biofilm thickness, percentage cover and edge index. However, goodness of fit will probably be unfeasible, due to the expected low number of samples and narrow range of Reynolds number (at least for the moment being).

3. Expected outcome and future applications

In this study, we aim at validating the use of MAGPLATEs for collecting relevant ship fouling. Thus, the outcome should enable us to be state whether the fouling pattern and percentage cover differs between the hull and the MAGPLATE. Additionally, differences arising from the depth of deployment of the MAGPLATE may become evident in the observations (i.e. in the fouling pattern, surface topography, skin friction and boundary layer properties).

In case such validation is successful, another outcome of this study corresponds to the resulting value of increased friction itself. By comparing fouled surfaces to unfouled ones, it is possible to give a figure to the local effects of fouling on that specific vessel, as a way to evaluate the performance of its fouling control coating. Later on, the relevance of the sampled region of the hull to total friction should be evaluated, and, on the other hand, the local effects of friction could be scaled up to total friction.

Additionally, regardless of the relevance of the fouling to total friction on that specific vessel, the study of hydrodynamics over the collected sample might elucidate the mechanisms that lead to increased drag in biofilm and filamentous hull fouling.

Finally, after the present validation, we expect this method to be applicable for testing new coatings and surfaces on ship hulls, enabling to evaluate hydrodynamic performance after a period of exposure on actual ship hulls. Other applications could include the development of a MAGPLATE-inspired method for routine monitoring of skin friction on the hull.

Nomenclature

c_f	Local skin friction coefficient
E	Edge index, $(N_{edge} / N_{biofilm}) \times Res$
h	Permissible roughness height
N	Number of pixels
Res	Pixel resolution, in pixels/cm
Re_θ	Reynolds number based on momentum thickness, $U_\infty \cdot \theta / \nu$
U_∞	Freestream velocity
U_τ	Friction velocity, $(\tau_w / \rho)^{1/2}$
ΔU^+	Roughness function
δ^*	Displacement thickness
ϵ	Virtual origin correction

ν	Kinematic viscosity
θ	Momentum thickness
ρ	Density
τ_w	Wall shear stress

References

- ANDREWARTHA, J.M. (2010), *The effect of freshwater biofilms on turbulent boundary layers and the implications for hydropower canals*, PhD Thesis, University of Tasmania, pp.50-54
- ARMSTRONG, V.N. (2013), *Vessel optimisation for low carbon shipping*, Ocean Engineering 73, pp.195–207
- ASTM D6990-05 (2005), *Standard practice for evaluating biofouling resistance and physical performance of marine coating systems* (Reapproved 2011), p.1-12
- BAX, N. et al. (2003), *Marine invasive alien species: a threat to global biodiversity*, Marine Policy 27/4, pp.313–323
- BERNTSSON, K.M.; JONSSON, P.R. (2003), *Temporal and spatial patterns in recruitment and succession of a temperate marine fouling assemblage: a comparison of static panels and boat hulls during the boating season*, Biofouling 19/3, pp.187–195
- BOCCHETTI, D. et al. (2015), *A statistical approach to ship fuel consumption monitoring*, Journal of Ship Research 59/3, pp.162–171
- COUTTS, A.D.M. et al. (2010), *The effect of vessel speed on the survivorship of biofouling organisms at different hull locations*, Biofouling 26/5, pp.539–553
- COUTTS, A.D.M. et al. (2007), *Novel method for assessing the en route survivorship of biofouling organisms on various vessel types*, Marine Pollution Bulletin 54/1, pp.97–100
- DAVIDSON, I.C. et al. (2009), *The role of containerships as transfer mechanisms of marine biofouling species*, Biofouling 25/7, pp.645–655
- DRAKE, J.M.; LODGE, D.M. (2007), *Hull fouling is a risk factor for intercontinental species exchange in aquatic ecosystems*, Aquatic Invasions, 2/2, pp.121–131
- DÜRR, S.; THOMASON, J.C. (2009), *Biofouling*, Wiley-Blackwell, p. xv
- GOLDSTEIN, R.J. (1996), *Fluid Mechanics Measurements*, 2nd ed., Taylor & Francis, pp.575-648
- HASLBECK, E.G.; BOHLANDER, G. (1992), *Microbial biofilm effects on drag – lab and field*, Proceedings of the Ship Production Symposium, New Orleans, pp.3A11-3A17
- HUNSUCKER, K.Z. et al. (2014), *Diatom community structure on in-service cruise ship hulls*, Biofouling 30/9, pp.1133–1140
- IMO (2011), *A transparent and reliable hull and propeller performance standard*, MEPC 63/4/8, pp.1-6
- IMO (2014), *Reduction of GHG emissions from ships*, Third IMO GHG Study - Final Report, p.24
- ITTC (2008), *Uncertainty analysis: Particle Imaging Velocimetry (7.5-01-03-03)*, 25th International Towing Tank Conference, Fukuoka, pp.1–12

- JACKSON, S.M.; JONES, E.B.G. (1988), *Fouling film development on antifouling paints with special reference to film thickness*, International Biodeterioration 24/4-5, pp.277–287
- JOHANSSON, L.-E. (1984), *The local effect of hull roughness on skin friction*, RINA Transactions, pp.187–201
- LARSSON, L.; RAVEN, H.C. (2010), *The flow around the hull and the viscous resistance*, In J. R. Paulling's (ed.) *The Principles of Naval Architecture Series - Ship Resistance and Flow*, The Society of Naval Architects and Marine Engineers, pp. 51–77
- LEER-ANDERSEN, M.; LARSSON, L. (2003), *An experimental/numerical approach for evaluating skin friction on full-scale ships with surface roughness*, Journal of Marine Science and Technology 8, pp.26–36
- LEWTHWAITE, J.C. et al. (1984), *An investigation into the variation of ship skin frictional resistance with fouling*, RINA Transactions, pp.269–284
- LINDHOLDT, A. et al. (2015), *Estimation of long-term drag performance of fouling control coatings using an ocean-placed raft with multiple dynamic rotors*, Journal of Coatings Technology Research 12/6, pp.975–995
- McCOLLIN, T.; BROWN, L. (2014), *Native and non native marine biofouling species present on commercial vessels using Scottish dry docks and harbours*, Management of Biological Invasions 5/2, pp.85–96
- MUNK, T. (2006), *Measuring hull resistance to optimize cleaning intervals*, Journal of Protective Coatings and Linings 23/6, pp.46–51
- MUNK, T. et al. (2009), *The effects of corrosion and fouling on the performance of ocean-going vessels: a naval architectural perspective*, In C. Hellio and D. M. Yebra (eds.) *Advances in Marine Antifouling Coatings and Technologies*, Woodhead Publishing, pp.148-176
- NSTM (2006), *Chapter 081 – Water-borne underwater hull cleaning of Navy ships*, In *Naval Ship's Technical Manual (Revision 5)*, Washington DC, pp.1-68
- PAIK, B.-G. et al. (2015), *Investigation on drag performance of anti-fouling painted flat plates in a cavitation tunnel*, Ocean Engineering 101, pp.264–274
- PRESKITT, L.B. et al. (2004), *A Rapid Ecological Assessment (REA) quantitative survey method for benthic algae using photoquadrats with scuba*, Pacific Science 58/2, pp.201–209
- RAFFEL, M. et al. (2007), *Particle Image Velocimetry - A Practical Guide*, 2nd ed., Springer, pp.164-176
- SCHULTZ, M.P. et al. (2011), *Economic impact of biofouling on a naval surface ship*, Biofouling 27/1, pp.87–98
- SCHULTZ, M.P. (2007), *Effects of coating roughness and biofouling on ship resistance and powering*, Biofouling 23/5-6, pp.331–341
- SCHULTZ, M.P. et al. (2015), *Impact of diatomaceous biofilms on the frictional drag of fouling-release coatings*, Biofouling 31/9-10, pp.759–773
- SCHULTZ, M.P. (2000), *Turbulent boundary layers on surfaces covered with filamentous algae*, J.

Fluids Engineering 122/2, p.357

SCHULTZ, M.P.; FLACK, K. A. (2009), *Turbulent boundary layers on a systematically varied rough wall*, Physics of Fluids 21/1, Article number 15104

SCHULTZ, M.P.; SWAIN, G.W. (1999), *The effect of biofilms on turbulent boundary layers*, J. Fluids Engineering 121/1, p.44

SCHULTZ, M.P.; SWAIN, G.W. (2000), *The influence of biofilms on skin friction drag*, Biofouling 15/1-3, pp.129–139

TOWNSIN, R.L. (2003), *The ship hull fouling penalty*, Biofouling 19, pp.9–15

WALKER, J.M. et al. (2013), *Turbulent boundary-layer structure of flows over freshwater biofilms*, Experiments in Fluids 54/12, Article number 1628

WOODS HOLE OCEANOGRAPHIC INSTITUTE (1952), *Marine fouling and its prevention*, George Banta Publishing Co., pp.14-19

Utilization of Vessel Performance Management System in a Shipping Company

Ryo Kakuta, Monohakobi Technology Institute, Tokyo/Japan, ryo_kakuta@monohakobi.com
Hideyuki Ando, Monohakobi Technology Institute, Tokyo/Japan, hideyuki_ando@monohakobi.com
Takashi Yonezawa, NYK Line, Tokyo/Japan, takashi_yonezawa@nykgroup.com

Abstract

This paper presents how VPMS (Vessel Performance Management System) is utilized for improving business in shipping company. As an example, the case of SIMS (Ship Information Management System) is described. SIMS automatically collects and processes ship performance data taken from onboard equipment. The processed data is periodically transferred to shore data center. At shore, transferred SIMS data is utilized for various ways such as post voyage analysis to identify the reason and impact of fuel consumption increase. This information is utilized for improving situation awareness of the right person in vessel operation section and fuel saving has been achieved. It is currently planned to share the data from vessel with third party application providers to maximize potential of big data.

1. Introduction

The concern over IoT and big data utilization has risen in any industries. In the field of maritime business, shipping companies has started to utilize the data from vessel performance management system (VPMS) over the few years. Main reason for the spread of VPMS is increased interest in fuel saving. In order to reduce fuel consumption, each shipping company tries to utilize it in different ways. Because the effectiveness of VPMS depends on the degree of utilization in each organization, there still remains controversy regarding the value of VPMS.

In 2008, NYK and its R&D subsidiary MTI started to develop own VPMS, called SIMS (Ship Information Management System) for fuel saving and CO2 reduction. Since then, MTI has been working to support vessel operation in each business section of NYK by utilizing the big data collected from SIMS. After several years of operation, NYK has recognized the value of SIMS and decided to expand installation of SIMS on its fleet. In this paper, how NYK utilizes SIMS to improve vessel operation, how NYK changes organizational process for utilizing big data and future challenge of SIMS are described.

2. Vessel Performance Management System

2.1. VPMS (Vessel Performance Management System)

VPMS (Vessel Performance Management System) is system for supporting vessel performance management. Recently, installation of VPMS has attracted some ship operators or charterers who would like to save fuel consumption. In general, VPMS consists of two systems, auto-logging system on board and data viewer or dashboard for shore office. Auto-logging system collects vessel performance data and sends it to shore data server. VPMS users at shore office monitor the collected data or analysis result by using of data viewer or dashboard.

Table.1 shows examples of VPMS application in shipping company. From a ship operator's point of view, utilization of VPMS for energy saving operation, safety operation and schedule management is demanded. It also can be utilized for fleet planning, service planning and chartering. From a ship owner's point of view, utilization of VPMS for technical management is demanded, which includes safety operation, condition monitoring, environmental regulation compliance, retrofit & modification and design optimization.

Table 1: Examples of VPMS applications

Role	Function	Example of VPMS application
Ship operator	Operation	Energy saving operation Safety operation Schedule management
	Fleet planning	Fleet planning Service planning Chartering
Ship owner	Technical management	Safety operation Condition monitoring and maintenance Environmental regulation compliance Retrofit & modification
	New building	Design optimization

2.2. SIMS (Ship Information Management System)

SIMS (Ship Information Management System) is developed by NYK and MTI, *Ando et al. (2009)*. Fig.1 shows the overview of SIMS. SIMS collects data from on board equipment such as VDR (Voyage Data Recorder) and AMS (Alarm Monitoring System). Collected data is processed in onboard computer and sent to shore server via vessel's satellite communication. The data output from SIMS is basically statistical data, such as average, maximum, minimum and standard deviation. Time interval of data processing in SIMS onboard unit is normally 1 hour, but configurable depending on the intended use. One motion sensor is added to onboard unit to estimate encountered weather.

NYK has installed SIMS on more than 140 vessels including container vessels, PCCs, bulk carriers, tankers and LNG vessels. How NYK utilizes VPMS is described in the following sections.

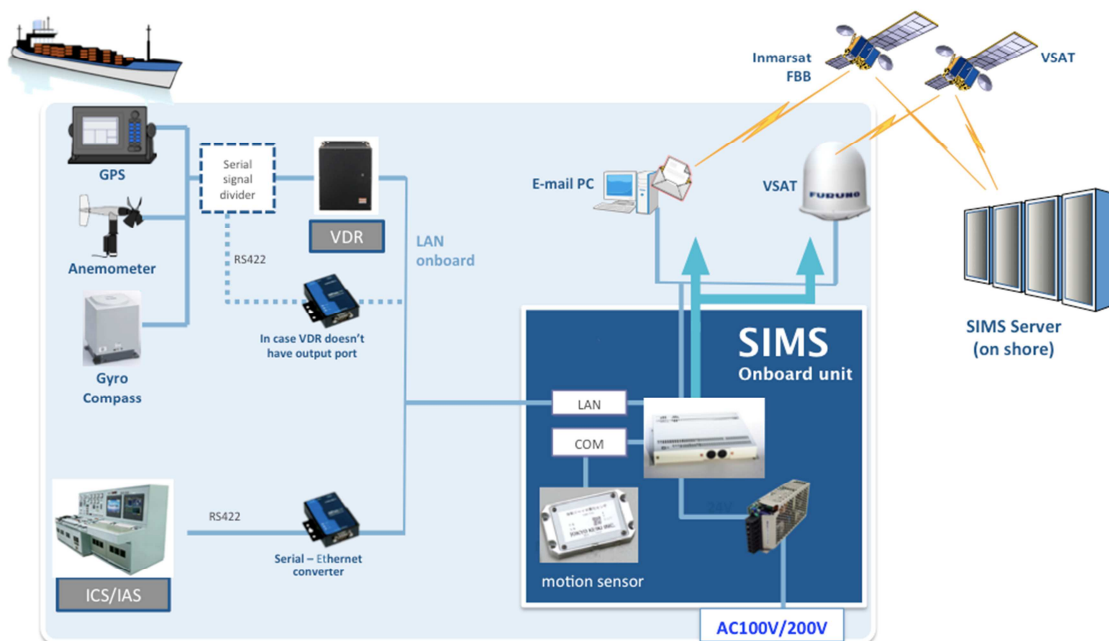


Fig. 1: Overview of SIMS

3. Vessel Performance Model

3.1. Vessel performance in service

Estimation of vessel performance in service is a key problem for shipping company. Ship propulsive performance is affected by several factors, such as wind, wave, displacement, trim, and conditions of

the hull and propeller. Fig.2 shows physical factors affecting vessel performance by draft and trim condition in seaways. All these factors must be considered when developing vessel performance model in service.

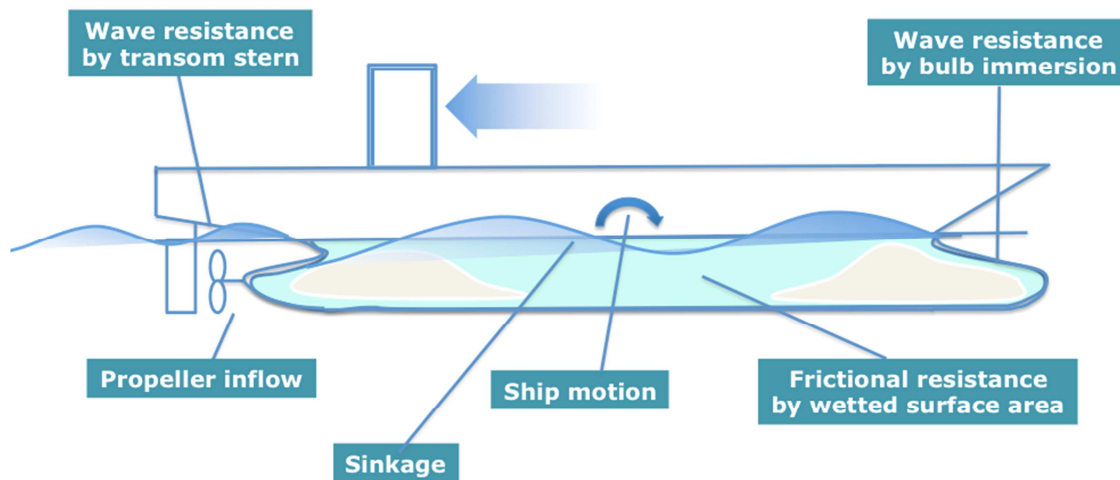


Fig. 2: Factors affected by draft and trim in seaways

3.2. Vessel performance modelling by using of SIMS

Fig.3 shows how vessel performance model in service is developed by using of SIMS. Three methods such as experimental, theoretical and statistical are combined to develop it. Effect of trim, weather and fouling is estimated from experimental, theoretical and statistical methods, respectively.

3.2.1 Experimental method

To understand how trim condition affects each ship, conducting towing tank test is the best way. It is well proven in long history of ship design and helpful to quantitatively identify the elements affecting vessel performance by draft and trim change. Trim tank test result is usually visualized by 2D chart shown in the left of Fig.3.

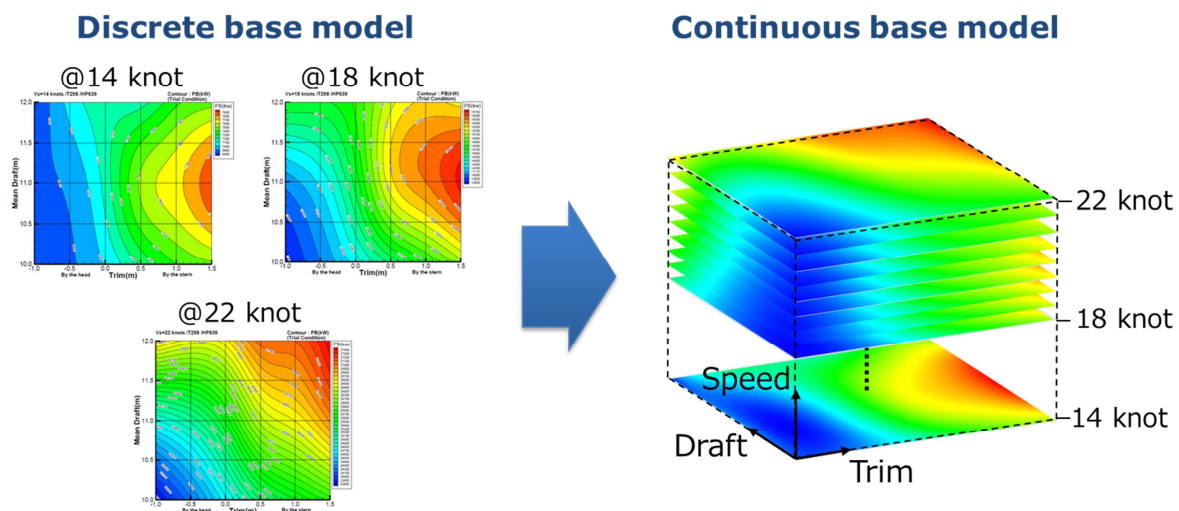


Fig. 3: Conversion from discrete model to continuous model

Because test conditions are limited due to time and cost constraint, obtained chart from the test is discrete. For estimating vessel performance in any trim, draft and speed, the discrete model is

converted to continuous model by using of B-Spline interpolation.

3.2.2 Theoretical estimation

Theoretical estimation is useful for estimating wind and wave effect. It is not realistic to collect vessel performance data in all the possible wind and wave condition. Instead of that, we utilize the performance estimation method developed by National Maritime Research Institute, *Tsujimoto et al. (2013)*. It takes into account the following elements relating to weather:

1. Resistance in still water
2. Hydrodynamic forces and moment due to drift motion
3. Rudder forces and moment
4. Wind resistance
5. Added resistance in short-crested irregular waves

By using of the method, vessel performance model for all-weather condition, which is called performance model in service, can be estimated. The graph in Fig.4 shows an example model which visualizes speed-power curves for head sea condition from Beaufort scale 0 to 9.

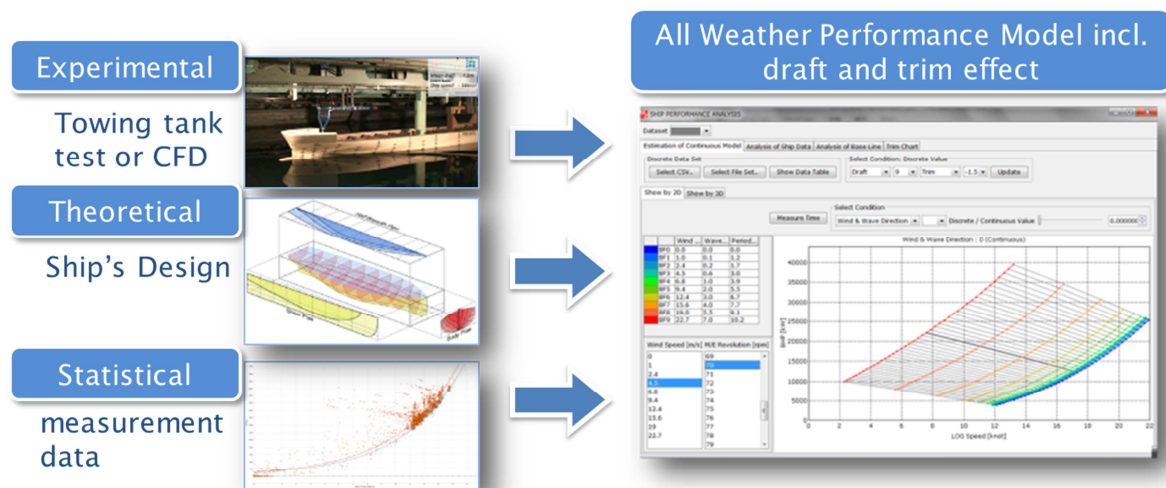


Fig. 4: Vessel performance modelling in SIMS

3.2.3 Statistical approach

Degradation of vessel performance must be considered for estimating vessel performance in all-weather. Change of baseline performance, which means performance in calm sea, affect performance in all-weather to some degree. Fig.5 shows the example of performance degradation analysis and all-weather performance modification based on new baseline. New baseline is obtained from SIMS data in good weather condition. The following data filter is applied for extracting good weather data.

- Beaufort scale is below 2
- RPM change is less than 0.5 rpm
- Max pitch angle is less than 1 degree
- Max rudder angle is less than 3 degree
- Difference between SOG (Speed over ground) and STW (Speed through water) is less than 0.5 knot

Wind and wave correction is applied after data extraction to reduce the weather effect close to zero.

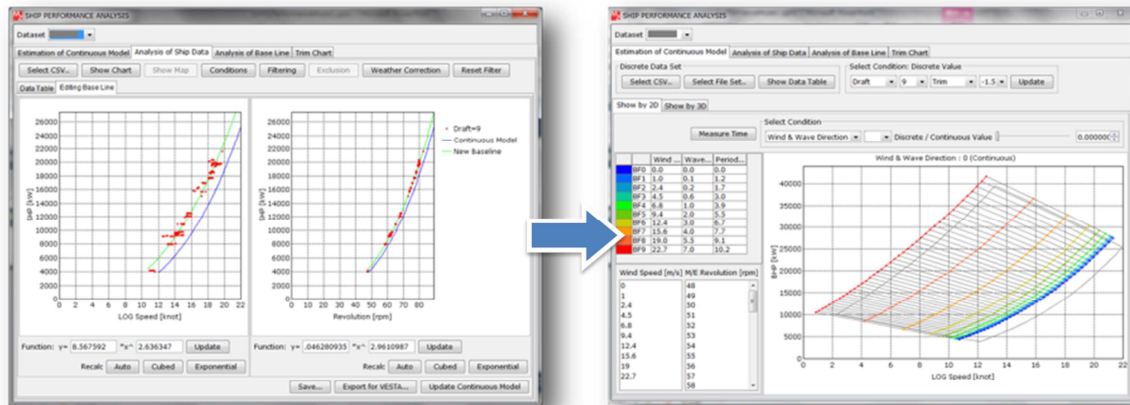


Fig. 5: Vessel performance modification based on SIMS data (left: performance degradation analysis, right: all-weather performance modification)

4. Post Voyage Analysis

4.1. Purpose of post voyage analysis

Post voyage analysis is conducted to identify the reasons and impact of fuel consumption increase. The value of data analysis depends on how much it contributes to better decision making and the importance of decision making. This means that both proper analysis technique and organizational process change for utilizing analysis result are required

Fig.6 shows the process required for utilizing big data for business action in an organization. At first, data must be collected from the target environment by using of IoT or other technology. Then, collected data are converted to information by using of analytics. The information must be recognized by the right person at the right time to improve his or her situation awareness. This step is critical because if the right person has the correct situation awareness at the right time, it results in proper decision-making and right organizational action. Each step requires different skills such as technology, analytics, business knowledge and understanding of organizational management. The way of working must be changed to utilize analysis because whole process is not covered by the conventional job of analyst.

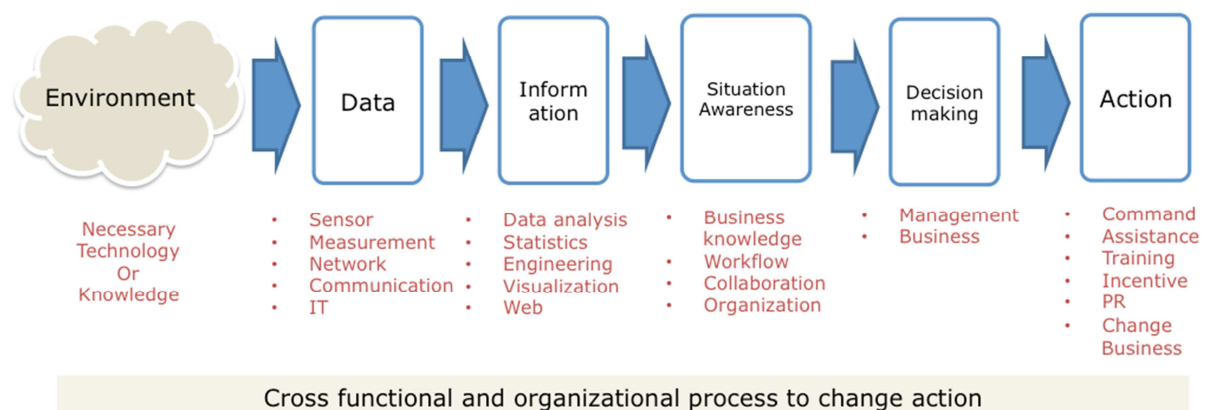


Fig. 6: Organizational process to change action from big data

How collected data is analysed in voyage analysis report of SIMS and how we utilize it are described in the following sections.

4.2. Fuel consumption breakdown

Fuel consumed in voyage can be divided into basic consumption and additional consumption. Basic fuel consumption means standard consumption as a benchmark. Additional fuel consumption can be divided in the following 7 elements.

- FC increase due to weather
- FC increase (save) due to longer (shorter) distance than standard distance
- FC increase (save) due to higher (slower) speed than standard speed
- FC increase (save) due to trim condition compared to even-keel
- FC increase due to deviation from constant power
- FC increase (save) due to current
- FC increase due to hull or propeller fouling

Fig.7 shows the image of fuel consumption breakdown. How to calculate each element is described in the following sections.

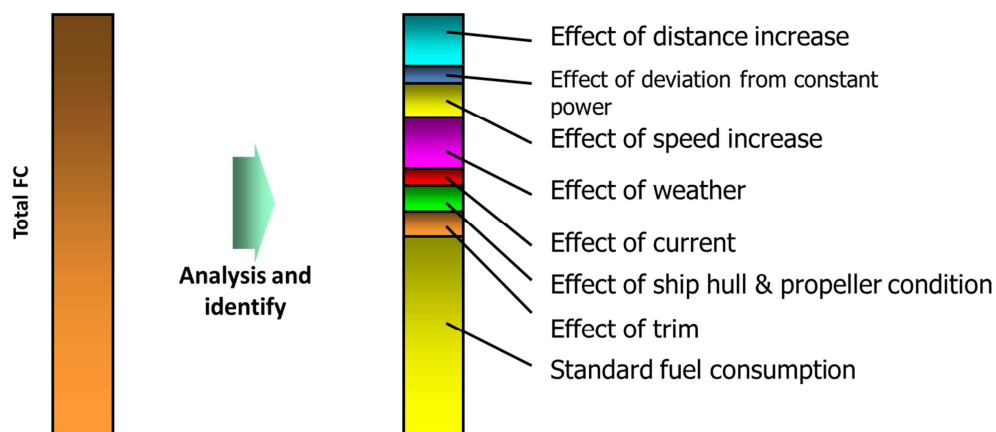


Fig. 7: Fuel consumption breakdown

4.2.1 Basic fuel consumption

Basic fuel consumption is fuel consumption as a benchmark which is calculated from baseline vessel performance and original voyage schedule and standard route. Baseline performance is normally estimated from 3 months data after last dry dock or installation of SIMS. Definition of original voyage schedule depends on vessel type. For example, pro-forma schedule is used for container vessels. Standard route is based on shortest route, but slightly modified by experienced Master considering actual situation.

4.2.2 Hull and propeller fouling

Performance degradation is evaluated by comparing latest vessel performance with baseline to identify the possibility of hull and propeller fouling. Latest vessel performance curve is estimated from SIMS data of target voyage. The same filter and wind-wave correction with baseline estimation are applied to this process. Fig.7 shows comparison of two curves. Based on this comparison, performance degradation ratio can be calculated.

4.2.3 Weather factor

Weather factor is estimated by comparing actual performance with baseline performance. Actual performance data is collected by SIMS and ship performance at actual speed in calm sea condition can be calculated from baseline performance. The difference between two performances shows the effect of weather. By this way, the effect of weather can be calculated for all the SIMS data recorded

during voyage.

4.2.4 Deviation from constant power

Effect of deviation from constant power is calculated from comparison between actual required power and minimum required constant power to keep actual arrival schedule. SIMS voyage analysis searches minimum constant power considering estimated speed loss due to actual encountered weather condition based on in-service performance model.

4.2.5 Speed

Effect of speed shows fuel consumption increase or saving due to higher or slower speed than original speed which is determined by original voyage schedule. The followings are the causes of deviation from original speed.

- Departure delay or earlier departure
- Deviation from standard route
- Engine stop due to troubles
- ETA change during voyage

The effect of speed increase or decrease on fuel consumption per unit time can be estimated from vessel's baseline performance curve.

4.2.6 Distance

Effect of distance shows fuel consumption increase or saving due to longer or shorter distance than distance based on standard route. Deviation from standard route is usually caused by rough sea.

4.2.7 Current

Effect of current shows fuel consumption saving or increase due to sea current. Actual encountered current is calculated from the difference between speed over ground (SOG) and speed through the water (STW). Accordingly, effect of current can be calculated from the difference between fuel consumption per unit at SOG and STW.

4.2.8 Trim

Effect of trim shows fuel consumption increase compared to optimum trim. The effect of trim on vessel performance depends on vessel's speed and draft. Based on speed and estimated draft from SIMS, vessel performance in optimum trim condition and actual trim condition is compared. Fig.8 shows trim chart for draft 9.2 m and 16 knot. When a vessel's actual trim is 0.5 m by the stern, fuel consumption compared to optimum trim is 2.2% higher. The effect of trim can be calculated for all the SIMS data recorded during target voyage.

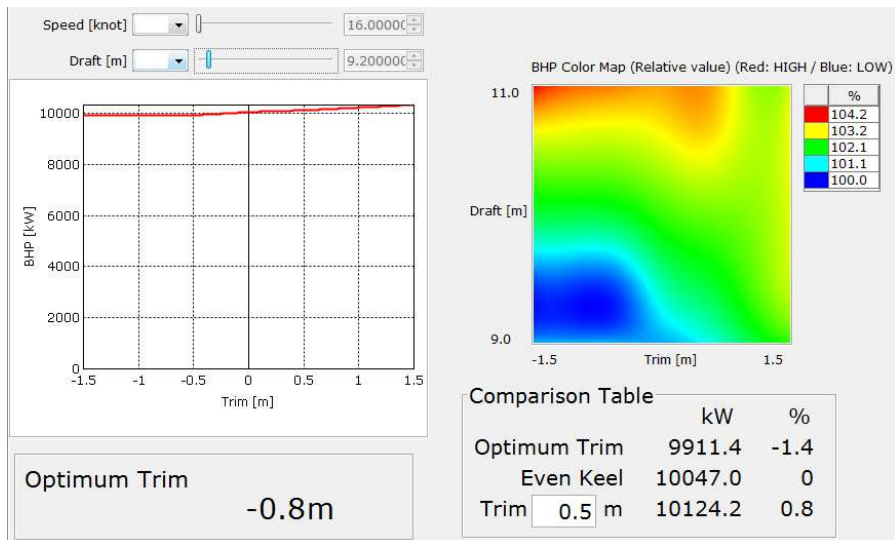


Fig. 8: Estimation of trim effect

4.3. Utilization of analysis result

SIMS voyage analysis report is shared among related stakeholders including operators and vessels. An example of voyage analysis report is shown in Fig.9. Periodical meeting is held for discussing how to reduce the additional fuel consumption for each factor based on the report. Data analysts and people from several sections such as vessel operation or fleet management participate in the meeting to improve their situation awareness and find out corrective action. The following items are discussed:

- Possibility of reducing additional fuel consumption.
- Validity of route or RPM recommendation from weather routing service
- Operator's response to unexpected events
- Vessel performance degradation and chance of conducting under water cleaning
- Feedback to Master and chief engineer for next voyage

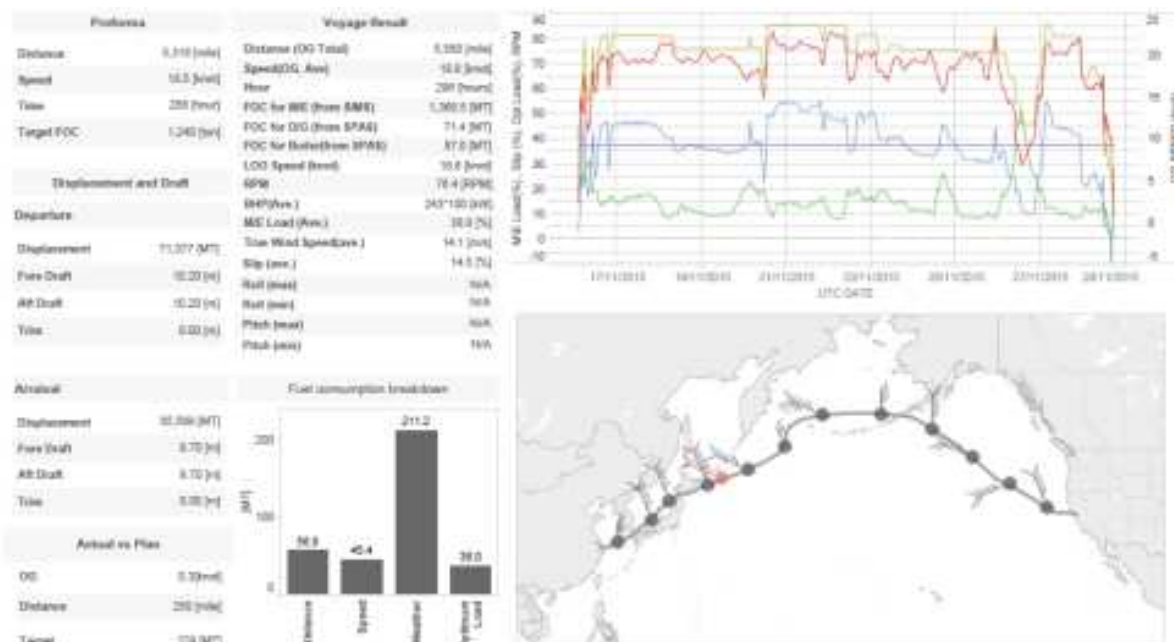


Fig. 9: An example of voyage analysis report

5. Open platform and data sharing concept

To maximize the potential of big data from vessel, platform for open collaboration is required. Fig.10 shows the concept of SIMS open platform. The platform supplier is FURUNO Electric who has global network to install and maintain SIMS. Due to the limited coverage of expertise in a shipping company, collaboration with third parties is required for better utilization of big data. For example, data of ship equipment is utilized by each equipment manufacturer better than by shipping company. If they can access to the data through open platform, they will be able to provide maintenance or diagnosis service based on the data. The followings are the expected third party applications:

- Vessel performance analysis
- Weather routing
- Engine monitoring
- Remote maintenance

For example, weather routing service is one of the applications which data sharing is most expected. Weather routing service needs continuous feedback about current status for understanding the gap between forecasted and actual situation. Quality of weather routing service is potentially to be improved by data sharing through open platform.

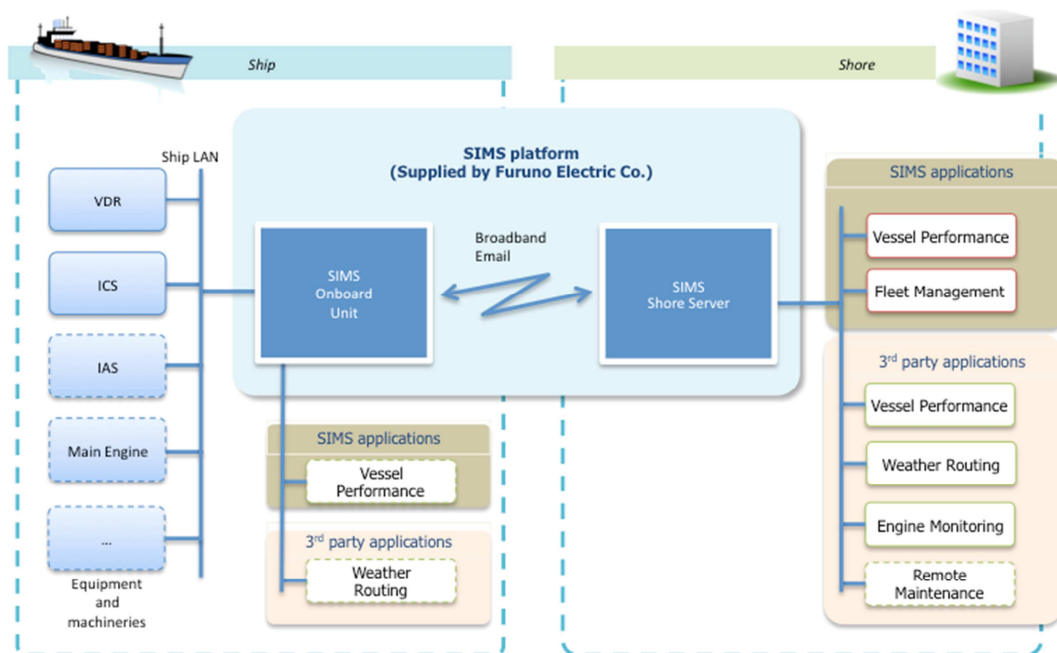


Fig. 10: Concept of open platform

6. Conclusion

The conclusion remarks are as follows:

- A vessel performance management system, SIMS has been developed by NYK and MTI and utilized for business improvement
- Vessel performance model has been developed for estimating the effect of weather and trim.
- Post voyage analysis clarifies the factors and impact of fuel consumption increase and contributes to better decision making through organizational process for big data utilization
- Open platform for data sharing with third party service providers is expected for maximizing the potential of ship big data and improving shipping company's business

References

ANDO, H.; KAKUTA, R. (2009), *Development of Ship Performance Monitoring System for Fleet Operation*, ISSDC2009

TSUJIMOTO, M.; KURODA, M.; SOGIHARA, N. (2013): *Development of a Calculation Method for Fuel Consumption of Ships in Actual Seas with Performance Evaluation*, OMAE2013-11297 pp.1-10

How MetOcean Data Can Improve Accuracy and Reliability of Vessel Performance Estimates

Mark Bos, BMT Smart, Marknesse/Netherlands, mark.bos@bmtsmart.com

Abstract

Vessel performance is assessed from the relationship between the vessels speed through the water and the propulsion power or fuel consumption required to maintain that speed. The vessel performance depends on the operational conditions and is influenced by many factors. The influences of the weather can be significant, but other factors play a role as well. The influence of these factors on vessel performance cannot be assessed separately. In many cases the main driver for assessment of vessel performance is to identify the change in performance for a vessel in calm weather conditions. ISO 19030 highlights the need for accurate data acquisition and provides some guidelines on how to measure and analyse the data to achieve this. Besides the accurate measurement of the speed through water and shaft power a thorough knowledge about the circumstances in which the vessel operates is essential for a proper analysis of vessel performance. Knowing the environment allows to filter out all conditions where the environment is expected to influence the performance or as an alternative the normalisation for these effects.

Meteorologists and oceanographers use sophisticated numerical models to estimate the environment conditions. The data from these models, also known as MetOcean data, can help to understand the environment of the vessel in more detail. The focus in this paper is on using such data for improving the estimate of vessel performance. With the use of real examples we identify some situations where sensor data can result in misleading performance trends and how MetOcean data can help to identify this.

1. Introduction

When monitoring the performance of the vessel over longer periods of time, changes in the performance can be identified. Changes in performance caused by changing fouling conditions of the underwater part of the vessels hull are of special interest. However vessel performance is influenced by many factors and those factors cannot be separately measured. Main factors are the operational conditions of the vessel and the environment in which the vessel operates. It is well known that the weather conditions have a prominent effect on the required shaft power or fuel consumption. Usually vessel performance is understood to be the performance in calm weather conditions. In order to ensure that vessel performance is not biased by the weather conditions the weather effects either need to be corrected for or removed from the analysis. These techniques are called filtering and normalization and a combination of both techniques is also common. In both cases a good knowledge and understanding of the weather conditions is crucial.

Knowledge about the weather conditions can be obtained from visual observations, automatic recording or from numerical simulations. Usually the water temperature, wind speed and wind direction are observed by instruments on board, but other important factors like waves or currents are not so frequently recorded. Satellite observations for winds, water temperature and waves can add value, but this usually is not for the exact location where the vessel is. Numerical simulations of the weather conditions and the oceans can provide a good estimate of the environmental conditions, especially when satellite measurements have been used to validate and improve the simulations. Data from numerical simulations at global and regional scales are made available by several organisations. This study has been conducted using the Copernicus Marine Service Products, in particular its global model for the ocean circulation. For winds the Climate Forecast System products are used, *Saha et al. (2014)*.

2. Speed through water

Speed through water is the most important parameter when analysing vessel performance. The approximately cubic relation between the shaft power and the speed through water indicates that an error in the speed through water has a similar effect on the performance estimate as an error in the shaft power which is only one third as large. Many factors that affect the performance influence the speed through water. This highlights the need for an accurate assessment of the speed through water.

2.1. Speed through water measurement in depth related current

The vessels speed through the water is the relative speed of the vessel with respect to the surrounding water. When currents are absent the water is not in motion and the speed through water is identical to the speed over ground. However when currents are present, the location of the log speed reading and the effects of ship motions, shallow water, waves and wind complicate the measurement.

The strength and direction of the current can differ at spatial scales as small as the size of the vessel. Numerical simulations are particularly good at describing the variations at larger scales and are less suited for variations at smaller scales.

An example to illustrate what can happen is shown in Fig. 1, where measured current velocity and direction at different levels below the water surface can be seen. The currents are measured at an offshore location in 100 m water depth. Suppose a vessel with a draught of 12 meter will sail against such a current with a speed over ground of 12 knots. Then the speed through water measured by the speed log will be higher than the speed over ground by the amount of the current speed at some distance below the bottom of the vessel. In the example the current speed at that depth is about 0.5 knots. The speed through water measured by the speed log will be 12.5 knots. The actual speed through water that the vessel feels is higher and ranges from 12.5 knots at the bottom of the vessel to about 13.0 knots near the water surface. As a result of the gradient in the current it is not so evident what speed through water is representative for the performance in this case, but the actual speed through water that the vessel feels will be several percent higher than that recorded by the speed log. There is also a change in the direction of the current with increasing depth below the surface, which in this case is limited to about 15 degrees over the depth of the vessel. The actual influence of the current speed gradient and current direction twist on the performance of the vessel is not known.

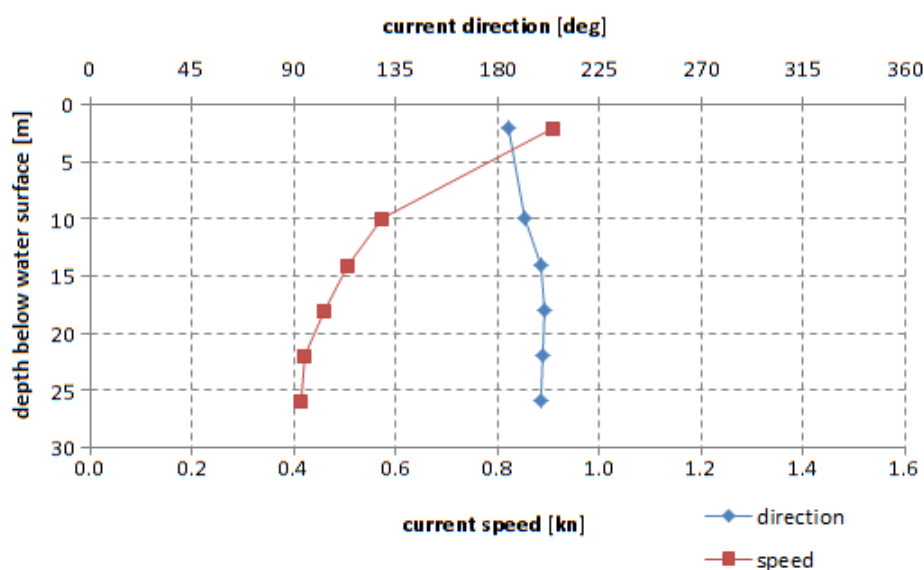


Fig. 1: Layered currents measured at buoy 44034 in the Gulf of Maine

2.2. Assessing the speed through water

The vessels speed through water is measured by the speed log. Some challenges are to be dealt with in order to get an accurate recording of the speed through water. In the first place the accuracy of the instrument itself is important and can differ per type of measurement method. Besides that the conditions during the measurement can cause errors in the readings. Especially the motions of the vessel in waves complicate the accurate measurement of the speed through water.

A speed log needs calibration to avoid a bias in the measurement. Over time the bias can change, also known as sensor drift, as the circumstances change and recalibration of the speed log is required to minimise the bias in the measurements. But it is not obvious how to calibrate the speed log if the actual speed through water is unknown. It is difficult to correctly calibrate the speed log without dedicated speed trials and this is not commonly done when the vessel is in service. Sensor drift causes difficulties when assessing the trend of vessel performance over time. If the actual speed is higher than the speed measured by the log, the vessel performance is under estimated. And vessel performance is very sensitive to such biases.

Another means to obtain the speed through water is the combination of the current vector and the speed over ground vector. Speed over ground is measured by the GPS, and currents can be predicted by numerical models. The measurement of speed over ground by GPS is fundamentally different from measurement of the speed through water by the speed log. Where the speed log measures the speed itself the GPS actually measures the position and the speed is obtained by the change in positions over time. As a consequence the speed over ground does not suffer from sensor drift and biases in the measurement are small when position is accurate.

The two methods of obtaining the speed through water can be used to identify inaccuracies in the measurements from the speed log. Some issues with log speed measurements are illustrated by examples.

2.2.1. Reliability of speed log

In Fig. 2 the speed measured by the speed log and the speed through water obtained from the speed over ground and the currents are both plotted in the same time series graph for a vessel transiting the Mediterranean Sea in relatively calm weather. Large differences in magnitude of the speed through water are observed at times. The differences are so large that this cannot be due to inaccurate estimates of the currents. On average the log speed is lower than the speed through water estimate from the currents and speed over ground. The readings from the speed log are not reliable and would be disregarded in this case and replaced with a derived speed through water from the speed over ground and currents.

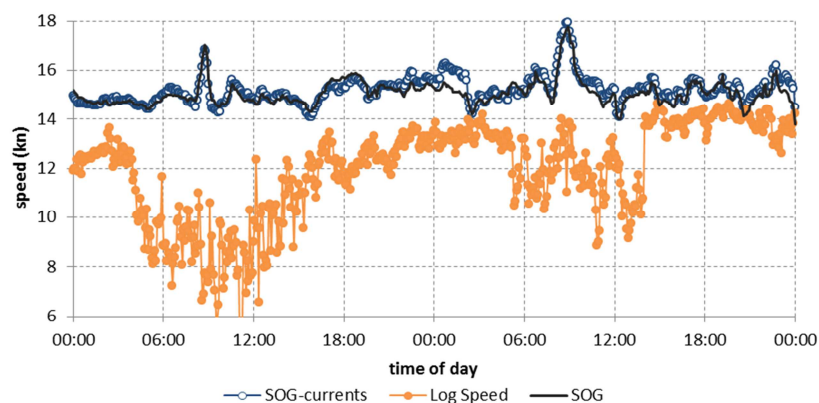


Fig. 2: Large difference between speeds through water obtained by two methods

2.2.2. Speed log bias

Another example is focussed at identifying a possible bias in the measurements. The correlation between the speed through water by the speed log and from speed over ground and currents is assessed to identify systematic errors. The correlation is illustrated in Fig. 3 for a Suezmax tanker. Each data point represents a 5 minute average. The smaller the distance between the data points and the diagonal line, the better the correlation. Ideally all data points are on the diagonal line. Systematic deviation from the diagonal line indicates a bias. In this case, on average the speed through water from the speed log is 3.3% higher than the speed through water from the speed over ground and the currents.

The same analysis is repeated with data for laden conditions only and for ballast conditions only. In ballast condition both estimates of the speed through water are less than 1% different, but in laden condition the speed log gives about 5% higher values. This suggests that the speed log is calibrated correctly for ballast condition, but has a noticeable bias of about 5% in laden condition.

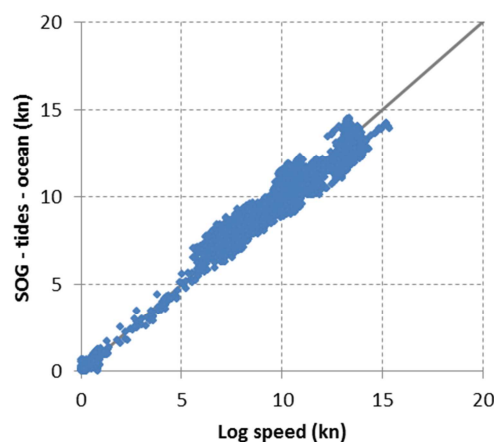


Fig. 3: Systematic difference between log speed and estimated speed through water

2.2.3. Water tracking and bottom tracking

Many log speeds have the option to measure the speed relative to the bottom when the vessel is in shallow waters. It is then in bottom tracking as opposed to water tracking. When in bottom tracking it will automatically switch to water tracking when the vessel comes to deep water where bottom tracking is not possible. When in bottom tracking the speed log does not give the speed through water that we need for vessel performance. The effect is illustrated by an example for a post-Panamax bulk carrier.

Speed log is in bottom tracking mode for the first part of the voyage until 13:00 the first day, then when the water depth gets higher it automatically switches to water tracking mode. In Fig. 4 bottom tracking periods are indicated and are easily observed as the periods where the speed over ground and the log speed are very close to each other. This happens during the first day and at the end of the second day. Water depth is less than about 40 meter in those sections of the voyage. The difference between log speed and speed over ground is close to zero when the speed log is in bottom tracking (see Fig. 5). In this case a better estimate of the speed through water is obtained when the speed through water is calculated from the speed over ground and the currents.

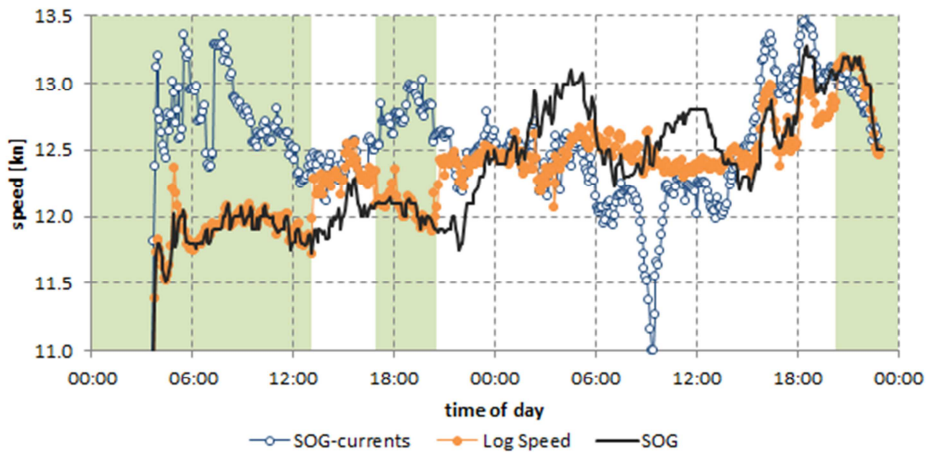


Fig. 4: Speed log in bottom tracking mode (coloured background) and water tracking mode (white background)

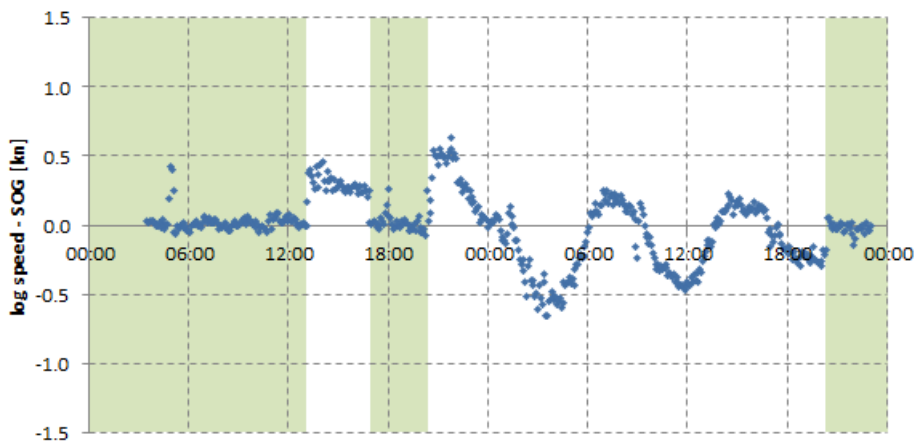


Fig. 5: Difference between log speed and speed over ground. Background is coloured when speed log is in bottom tracking mode.

3. Water temperature

In ISO 15016 it is recognised that water temperature influences ship performance due to a change in viscosity and with that a change in frictional resistance. For bulk carriers and tankers frictional resistance can be 80 to 90% of total resistance. Water temperature differs per region and per season. Average water temperature for June is plotted in Fig. 6. Differences in water temperature between tropics and near the poles can be 30 degrees.

Seasonal differences, identified by the difference in water temperature for January and June, are within 5 degrees for the majority of the oceans surfaces, but can be more than 15 degrees in some regions.

The effect of a change in water temperature is identified by the effect it has on frictional resistance coefficient. We use the ITTC 1957 friction formula and calculate frictional resistance coefficient for a range of water temperatures to quantify the effect on vessel performance for a Capesize bulk carrier sailing at 12 knots. Results are plotted in Fig. 8, where the frictional resistance at a water temperature of 15 degrees is used as a reference.

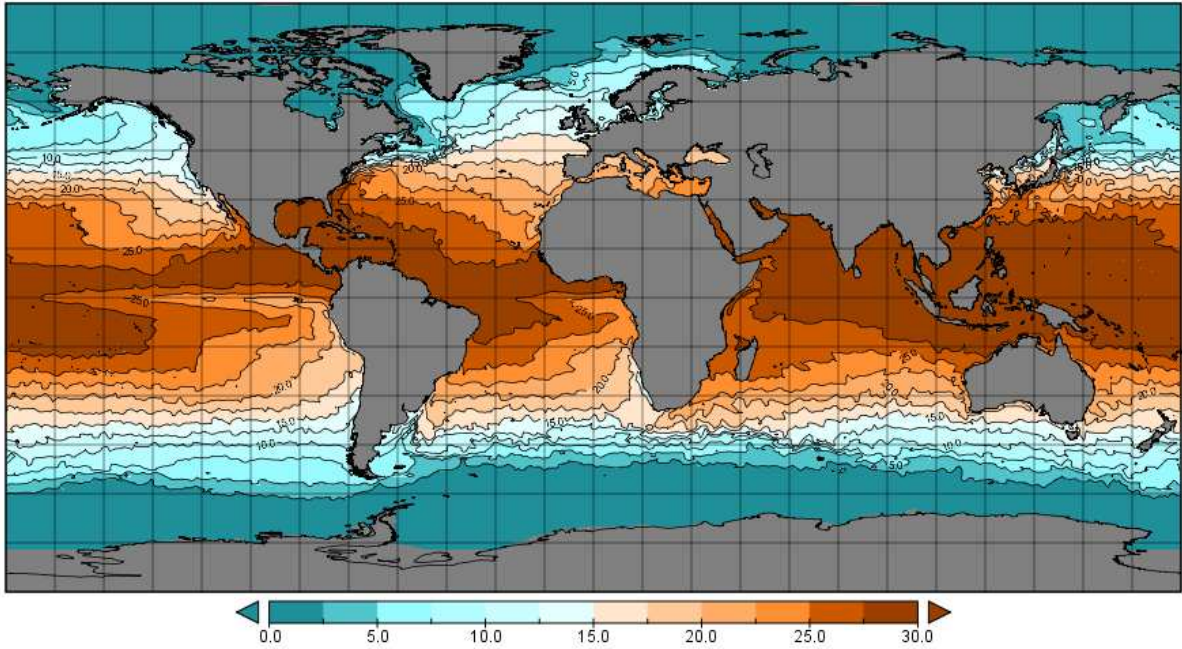


Fig. 6: Average water temperature in June

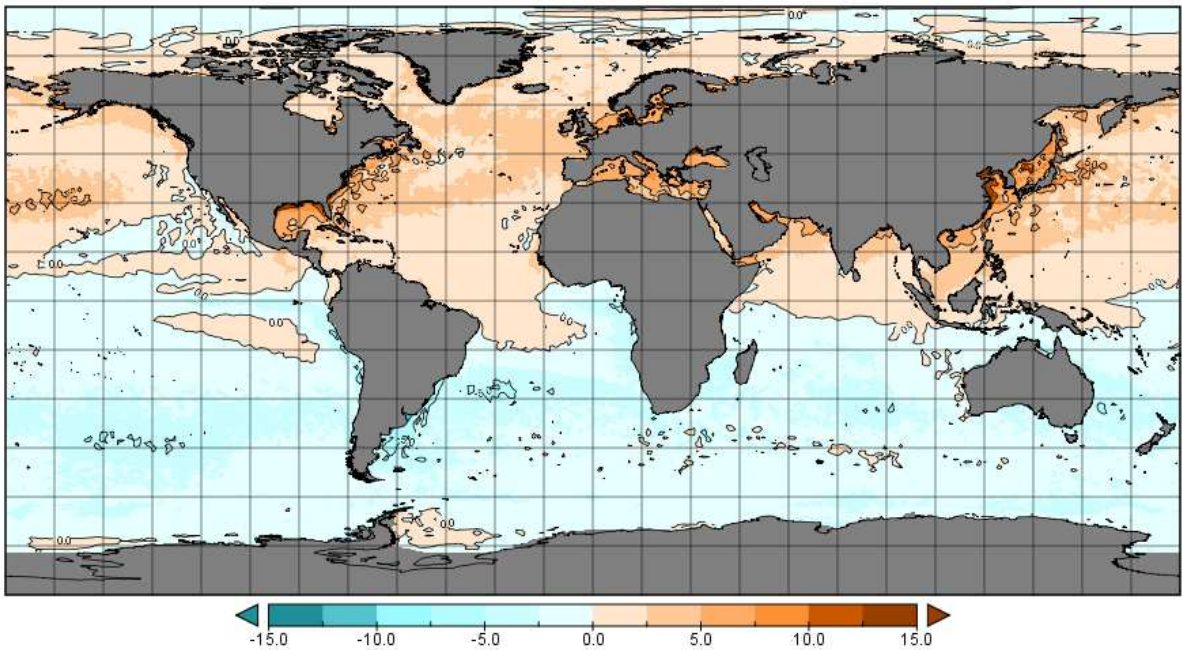


Fig. 7: Difference in water temperature between January and June

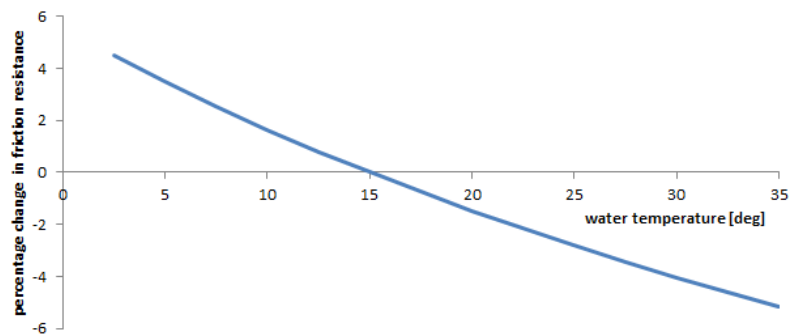


Fig. 8: Effect of water temperature on frictional resistance coefficient

As an example the average water temperature in Mediterranean Sea is about 15 degrees Celsius in January and 22 degrees Celsius in June; a difference of 7 degrees. A vessel operating in that area will have a difference in performance between January and June caused by the difference in water temperature. The isolated effect of water temperature results in a performance improvement of about 2 percent from January to June. If the vessel from then on operates in the Baltic Sea, where the water temperature is 10 degrees Celsius, the performance worsens by 3 to 4 percent.

4. Wind speed

The effect of wind on vessel performance is well understood and a correction method is defined in ISO 19030 and ISO 15016 to normalise for the effects of wind. The correction method uses an estimate of the additional resistance of the ship in wind.

$$R_W = \frac{1}{2} \rho_a A_T C_W(\psi_{WR}) U_{WR}^2 - \frac{1}{2} \rho_a A_T C_W(0) V_{OG}^2$$

With:

- R_W : additional wind resistance
- ρ_a : air density
- A_T : transverse projected area above water line
- C_W : wind resistance coefficient, dependent on the wind direction relative to the ship
- ψ_{WR} : relative wind direction; 0 indicates head wind
- U_{WR} : relative wind speed
- V_{OG} : ship speed over ground

Air density depends on the conditions of the atmosphere, especially air pressure and air temperature. Both can be measured or estimated from numerical models, but those effects are usually not accounted for. Much more important is the accuracy of the estimate for the wind speed and direction. Wind is measured by the anemometer mounted on the vessel and is also available from the MetOcean data. MetOcean winds are calibrated with satellite observed winds and have low bias. The anemometer is particularly good in identifying changes in wind conditions, but it may be biased. The anemometer measures the flow at a location of the ship where the presence of the ship itself may have influenced the air flow. The air is accelerated in certain areas around the ship and decelerated in other areas. How measurements are affected depends on the location of the anemometer, the above water shape of the vessel and wind direction relative to the vessel. It is reported by Yelland et al. (2001) that errors in the wind speed measured by the anemometer due to flow distortion can be as high as 30% for a tanker in headwind. We identify the magnitude of possible distortions of the flow at the location of the anemometer by analysing a multi-year time series of anemometer wind speed measurements and comparison with MetOcean wind speeds. The true wind speed is calculated from the measured wind speed and then divided by the MetOcean wind speed and the ratio is averaged for small ranges of apparent wind direction. To avoid possible influences from nearby obstacles all data where the ship was not moving or at very low speed were excluded from the analysis.

Fig. 9 gives the results of the analysis for a laden Suezmax tanker. On average for all wind directions the anemometer wind speed is 20 % higher than the MetOcean wind speed. A higher wind speed by the anemometer is expected because it is located at a height of approximately 35 m, which is much higher than the reference height of 10 m for which the MetOcean wind speed is valid. The effect of the difference in heights is estimated from the equation from ISO 15016 and is 1.196.

$$\frac{V_{WT}}{V_{WTref}} = \left(\frac{Z_a}{Z_{ref}} \right)^{1/7}$$

Where:

- V_{WT} : true wind speed from the anemometer
- V_{WTref} : true wind speed at the reference height

Z_a : vertical position of the anemometer above water surface
 Z_{ref} : reference height for the MetOcean wind speed

For apparent wind directions close to zero – wind coming from the bow – the flow at the anemometer location is accelerated and has a wind speed error of about +20 %. With the wind coming from the stern the flow is decelerated and the error is about -30 %. The wind speed ratio is not symmetric for starboard and port side wind directions. Most remarkable is the lower value at -90 degrees apparent wind direction. This is probably because the anemometer is downwind of the mast for that wind direction.

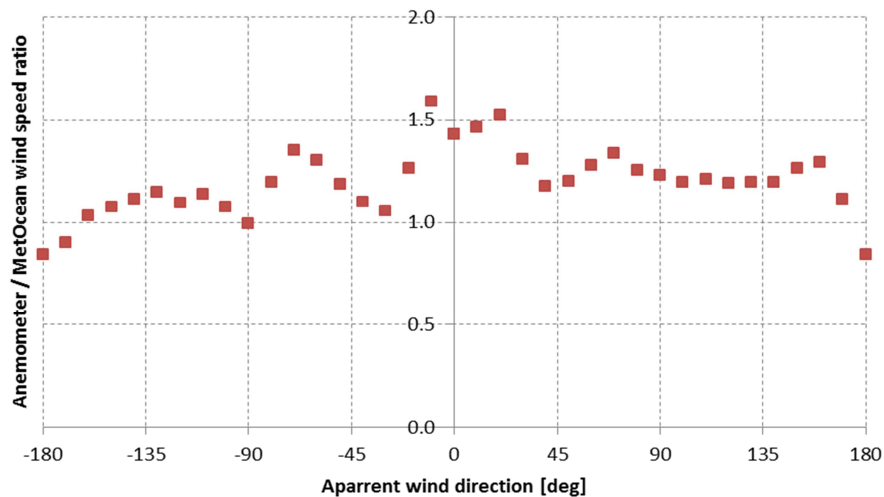


Fig. 9: Ratio between wind speed measured by anemometer and wind speed from MetOcean as a function of apparant wind direction for a laden tanker

The same analysis is applied to an LNG Carrier. The results are given in Fig. 10. On average for all wind directions the anemometer wind speed is 52 % higher than the MetOcean wind speed. The height of the anemometer is approximately 50 meter above water level. A wind speed ratio of about 1.26 is expected for this height. The wind is accelerated for most of the apparant wind directions, but not for winds coming from the bow. In head wind the wind speed from the anemometer is about 12 % lower than expected. Strongly accelerated flow for side wind is observed and differs for winds coming from the starboard side or port side.

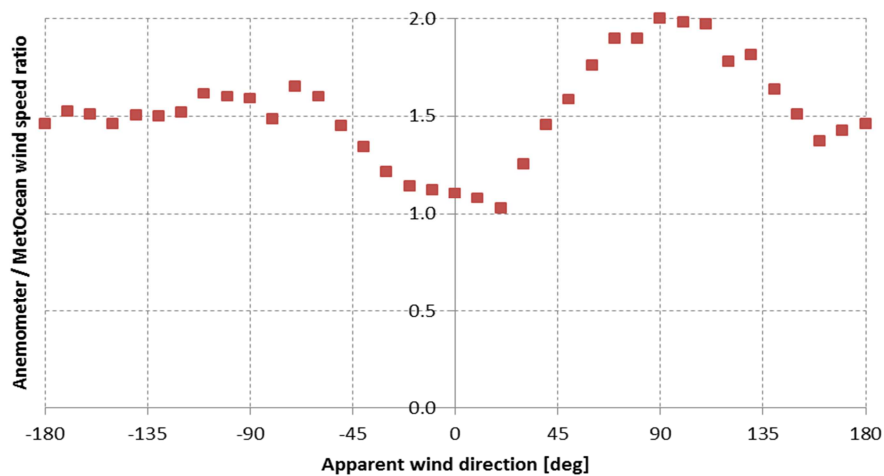


Fig. 10: Ratio between wind speed measured by anemometer and wind speed from MetOcean as a function of apparant wind direction for a laden LNG Carrier
 Especially in case the vessel performance is normalized for the effect of wind, an accurate estimate of

the wind speed is required. Knowledge of the flow distortion for the location of the anemometer can help to improve the estimate of the wind speed and more accurately normalize for the effect of the wind.

5. Conclusions

MetOcean data can provide a much better understanding of the environmental conditions for the vessel. Especially information about the wind, waves, currents and water temperature can be very helpful when analysing vessel performance, especially when such data was not recorded on board. A direct benefit is that it can help to identify periods where the performance may be influenced by the weather, so that those periods can be excluded from the analysis.

Several examples illustrate that the speed through water measured by the speed log is not always reliable. Without a separate source of information to compare with it is difficult to identify when the speed log may give misleading estimate of speed through water. Speed over ground from GPS and currents from MetOcean data can provide an estimate of the speed through water to compare with. This can help to identify a systematic bias in the log speed for instance.

The effect of water temperature on vessel performance is identified theoretically. Differences in performance due to a change in operational area or season can be several percent. If not accounted for it can lead to a misleading performance trend.

MetOcean wind was successfully used to identify air flow distortion at the location of the anemometer. Knowledge of the air flow distortion can improve the accuracy of the wind speed and improve normalisation for the effect of wind on performance.

References

SAHA, S.; MOORTHY, S.; WU, X.; WANG J. et al. (2014) *The NCEP Climate Forecast System Version 2*, J. Climate 27, pp.2185-2208

YELLAND, M.J.; MOAT, B.I.; TAYLOR, P.T. (2001) *Air Flow Distortion over Merchant Ships* Southampton Oceanography Centre, Southampton, UK, 32pp.

White, Grey and Black-Box Modelling in Ship Performance Evaluation

Michael Haranen, NAPA Ltd., Helsinki/Finland, michael.haranen@napa.fi

Pekka Pakkanen, NAPA Ltd., Helsinki/Finland, pekka.pakkanen@napa.fi

Risto Kariranta, NAPA Ltd., Helsinki/Finland, risto.kariranta@napa.fi

Jouni Salo, NAPA Ltd., Helsinki/Finland, jouni.salo@napa.fi

Abstract

Today, on-board data collection opens up new possibilities for technical performance evaluation. The analyst does not necessarily need physical formulas, but can use dynamically updating corrections based on measurements. In practice, the difference between the models lies mainly in the level of physical assumptions in the performance model. The closer to a physical the model is, the greater the need for initial information about the ship's predicted performance to obtain a valid result. Conversely, the less the model relies upon the physical assumption, the more data on varying operational conditions it requires. In this paper, NAPA Ltd. explains different kinds of modelling techniques and the pros and cons of white, grey and black box models in different uses. Using a case study the results of the analysis with various modelling techniques is demonstrated.

1. Introduction

There is a great deal of discussions and scientific articles devoted to different techniques that focus on ship technical performance evaluation and ship operational optimization. The concept of ship performance might have many different meanings, but most of the time the concept is understood as a relation between the ship speed, or traveled distance, and the corresponding energy consumption. This relation is usually described in the form of a model, which may be physical, statistical or something in-between depending on the selected approach. On the other hand, ship operational optimization deals with operational cost savings and revenue maximization. In general, this process employs the available performance model taking into consideration all possible factors that influence the ship performance and selects the model parameters so that the optimization criteria are met.

The process of the ship performance evaluation usually starts at the early stage of ship design because of its high impact to the costs of ship operating. The accurate estimation of the ship performance is a very challenging process because the ship design has to also fulfill the safety requirements, cargo capacity, low construction and operation costs, Logan (2011). At the stage of the ship design there is no sensor data available and only a limited amount of model testing data can be utilized. Therefore, the physical law or deterministic modeling approach is almost the only way to assess the ship performance.

The situation changes after the ship is constructed and starts operating. Nowadays the collection and storing of high frequency on-line data from hundreds or even thousands of sensors is available. The issues that need to be addressed at this stage are how to control the reliability of the data and how to deal with high levels of measurement noise. The high amount of collected data enables the development that employ soft computing and computational intelligence techniques to create a new basis for the ship performance evaluation. This means that the concept of statistical modeling can be very effective method of ship performance evaluation, because the statistical model can deal with noisy data very well.

The three different approaches, which are often mentioned in the world maritime community discussion, are white, grey and black box modeling methods. In this paper we would like to elaborate on the roles of different types of modeling techniques and give some examples from real life applications developed by NAPA Ltd.

1.1 White box

A white box model is a model in which the structure is perfectly known and it has been constructed entirely from prior knowledge and physical insight, *Ljung (2001)*. This modeling approach has been used for decades for ship design and performance evaluation. It is based on a ship resistance calculation by employing physical and hydrodynamics laws, and naval architecture principles as well as the results of model tests. The methods are well described in books and scientific papers such as *Bose and Molloy (2009)*, *Harvald (1983)*, *Holtrop (1977)*, *Holtrop and Mennen (1982)* and *Holtrop (1984)*. A very good overview of many different methods is given in *Schneekluth and Bertram (1998)*.

There are many research efforts devoted to hull and propeller condition analysis and monitoring based on white box modeling approach *Aas-Hansen (2011)*, *Logan (2011)*, *Hansen (2012)*. For example, a very interesting method for analysis and verification of ship performance has been developed by Japan Marine United Corporation *Orihara (2015)*.

The main idea of the white box modeling for ship performance evaluation can be summarized as follows; the ship total resistance is divided into components like still-water resistance and added resistance due to wind, waves, shallow water, maneuvering, etc. After evaluating all components, the measured values for the propulsion power and speed can be corrected to standard conditions, for example calm weather, deep water, design draft, zero trim, etc. After the data correction, any trends and time related deviations in the still-water resistance can be attributed to biological fouling of hull and propeller, engine aging or possible system faults.

The main problems in usage of the white box modeling are well summarized in *Logan (2011)*. All existent methods rely on a set of resistance components. The resistance components are usually separated models and do not take in account possible interactions, which makes modeling inconsistent. The method requires high amount of coefficients and values estimated from the model tests. These coefficients are also calculated in a statistical manner and include errors. The coefficients are then scaled by using Froude laws of comparison, which is not rigorous. Possible errors in model tests and further coefficient scaling also provide additional sources of error and increase the uncertainty of the model. Finally, uncertainty related to the physical model itself also incorporates additional uncertainty into the final results, *Bose and Molloy (2009)*.

1.2 Black box

Black box model is a model for which no physical insight is used or available, but the chosen model structure is selected from a known model family, is flexible and has been “successful in the past”, *Ljung (2001)*. The “black box” terminology was mentioned in works of Isaac Newton. He used this term to describe any phenomena that hides the internal workings from view and prevents explanation. On the contrary, phenomena that can be explained may be called a “white box”. The term black box is widely used in computer science, especially in soft computing and machine learning mostly to refer sophisticated learning algorithms, like regression techniques and neural networks. Most of the time these models can be considered as a system, which describes the relations between some input variables and related outputs. The main goal of such models is to predict or simulate the model output or outputs for any desirable inputs combination.

On the other hand, all such models are very complex to understand which makes them “black boxes”. Technically speaking, within the computer science society not all statistical models are usually called black box techniques. For example, linear regression models are usually considered a white box models because they are based on understandable behavior and good explainability. However, all these statistical “black box” models are parametric models, whose parameters have to be identified from the data, *Hastie et al. (2003)*.

There are many works that demonstrate the use of black box modeling for prediction of ship performance parameters, such as the propulsion power, fuel consumption and speed. Different

techniques have been tested, such as artificial neural networks, Gaussian processes with impressive results, *Pedersen and Larsen (2009)*, *Pedersen and Larsen (2009b)*, *Petersen et al. (2011)*, *Petersen et al. (2011b)*.

Although at one point in human history, statistical models, especially neural networks, were considered as a universal solution for any kind of science and engineering problems, they have disadvantages. All statistical models need to be trained and their parameters need to be estimated from the data, thus, they all depend highly on the data quality. When measurement data is not reliable model uncertainty will be high, which means that data used in model training, testing and validation needs to be carefully selected and preprocessed. Additionally, the uncertainty of any flexible statistical model also depends on the model structure, training and testing strategy, and selected variables, *Hastie et al. (2003)*. There is a problem concerning neural networks, which according to a mathematical viewpoint, there do not exist well founded theory for their convergence especially for high dimensional cases with presence of noise, *Hauth (2008)*. In some statistician circles neural networks belong to the list of the worst predictive modeling techniques, (www.analyticbridge.com), (www.datasciencecentral.com), because they are extremely difficult to interpret, unstable and subject to over-fitting.

1.3 Grey box

Grey box model is a model for which some physical insight is available but some parameters need to be estimated from the observed data, *Ljung (2001)*. Grey box methods can be considered a combination of white and black box approaches together and they are something in-between of those two. The theoretical principles and physical laws of white box models are complemented by knowledge extracted through black box techniques from the experimental data. This raises the whole modeling system to a new level of knowledge and accuracy, *Hauth (2008)*. The grey box approach is widely used in process control engineering, *Bohlin (2006)*, and there are some examples of how this approach can be used in vessel operational optimization, *Leifsson et al. (2008)*.

2. Role of modelling

When talking about ship performance, several roles of modeling can be specified. Fig. 1 describes a general representation of roles of modeling in ship performance evaluation and optimization of operations.

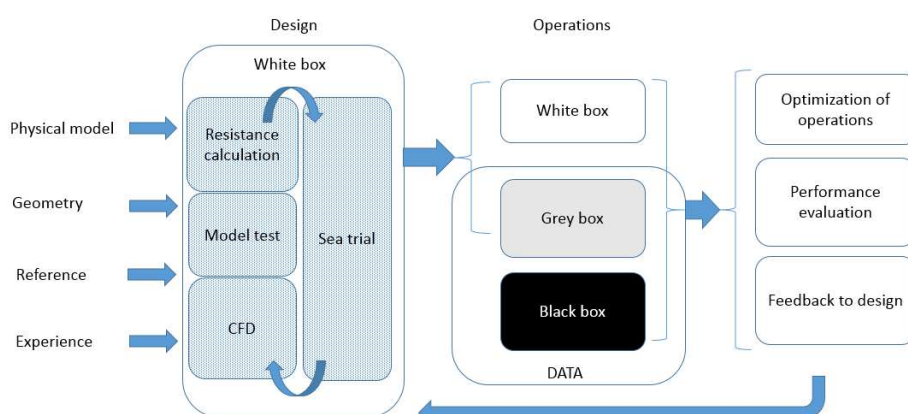


Fig. 1: Roles of modeling in ship performance evaluation.

2.1 Design stage

The central role of modeling becomes apparent at the earlier stage of the ship design. The estimation of the ship resistance is very critical and defines the needed engine power and propeller required to move the ship at the design speed. This is a well-developed field of the marine industry, *Logan*

(2011), and the role of white box modeling is significant and cannot be undervalued for ship design purpose. For example, a NAPA software very well known in shipbuilding and design community represents a complex and sophisticated white box model incorporating state-of-the-art hull surface and 3D model definition with advanced hydrodynamic, stability, and structural design software tools. NAPA is a single integrated software system that covers multiple design disciplines, one discipline being a hull form and performance component which is intended for hull design, hydrodynamic and performance optimization.

Several procedures can be used for ship performance estimation in NAPA at the design stage:

1. Holtrop method, *Holtrop (1982,1984)*
2. Combination of Taylor-Gertler and Hähnel-Labes method, *Gertler (1991), Hähnel and Labes (1964)*
3. Guldhammer-Harvald method, *Guldhammer and Harvald (1965)*
4. Todd method, *Todd (1963)*
5. Lap-Keller method, *Lap (1954), Keller (1973), Journee and Meijers (1980)*
6. Oortmerssen's method, *Oortmerssen (1971)(1978)*
7. Fisher method, *Swift et al. (1973)*

All these methods can be used for a large range of different types of vessels to estimate ship performance on the design stage. However, successful use of the methods requires a large amount of preliminary information, such as the ship hull geometry, loading conditions, as well as information about additional resistance, such as the definition of hull appendages and openings, wind drag coefficients, and water and air properties.

After the first step of the ship design process, model tests and computational fluid dynamics (CFD) simulations provide additional information about ship resistance. This information is incorporated into the white box model, which is then used to describe the ship performance. Usually this is an iterative process that targets the optimal solution for the ship hull and propeller.

The first real life data becomes involved after the sea trial after the ship has been constructed. At this point, it is not possible to use any grey or black box methods for data analysis because of the small amount of data available. Therefore, the analysis of the ship performance is usually carried out with a white box modeling approach, for example according to the standard procedures *ISO 15016* and *ITTC (2005)* or the method developed in JMU, *Orihara (2015)*.

2.2 Operations

There are three major fields where modeling can be successfully applied: hull and propeller performance monitoring, optimization of operations and feedback to design. In operations, the ship performance model is more specifically used when calculating and optimizing the voyage costs, for reporting or external charter commitment evaluations. In this usage the most common modelling approach is a white box model. It works from day one and it is easily predictable and understandable. The predictability of the model and flawless working of the model from day one is extremely important in route optimization, as here safety concerns need to be taken into account. In the worst case scenario example, a black box model without prior knowledge of e.g. 10 meter waves, could predict that they do not cause any performance decrease nor rolling motions. White and grey box models would have a pre-assumption about this built in. The verification of vessel performance is also essential for dynamic performance based revenue distributions, technical management and new development of the fleet.

2.2.1 Dynamic Performance Model

NAPA Ltd. uses Dynamic Performance Model for voyage speed profiling and route optimization purposes (Voyage Optimization). Dynamic Performance Model is a combination of physical and statistical models. The initial model uses NAPA's built-in initial performance estimation utilizing the

geometry of the vessel and supplementing information from e.g. model tests, wind tunnel tests and sea trials. The dynamic part of the model means that the parameters of subsystems are optimized with data collected onboard, so that the differences between measured and predicted values are minimized, see Fig. 2.

Once the new correction factors for the model parameters are found, they are fed to the original model resulting in more accurate predictions. This type of grey box model, which combines the physical model and statistical analysis and optimization, has benefits because it has sufficient accuracy from the beginning that improves with time as more data is collected. Compared to a purely statistical model, a grey box model predicts more reliably the uncommon conditions, like heavy storms, when the ship has not sailed in those conditions previously.

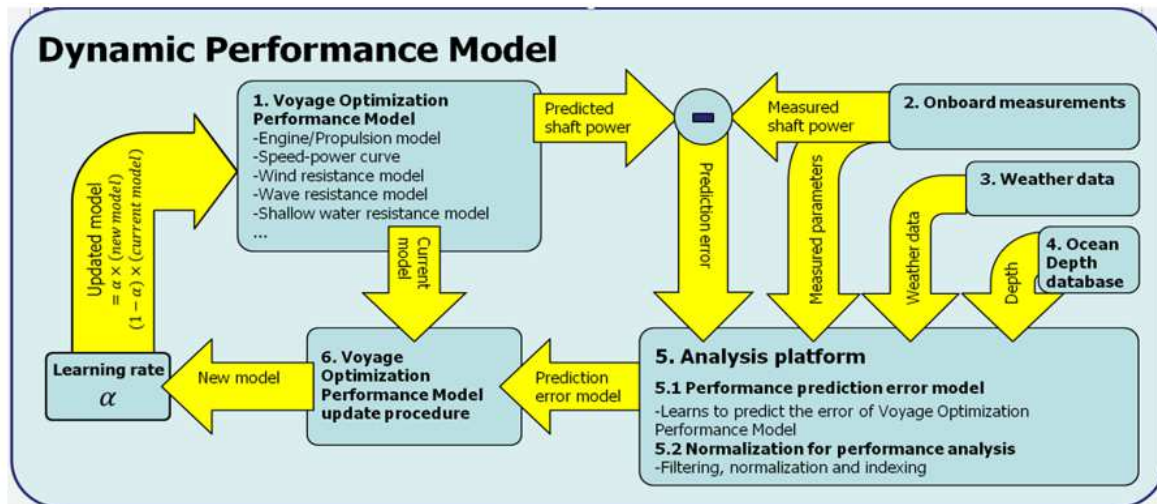


Fig. 2: Dynamic Performance Model update principles.

2.2.2 Hull and propeller performance monitoring

The only way to really know when to maintain the ship is to implement a continuous monitoring and analysis system. There is an ongoing effort for establishing a standard for this, see ISO/CD 19030-1, ISO/CD 19030-2. This standard will define how and what data should be collected from the vessels, how it should be analyzed and the outcome reported. Currently, the providers of hull and propeller condition monitoring services have different ways to analyze and report the performance decrease, making the reports hard to compare between providers.

NAPA Ltd. uses three different types of hull performance analysis which can be run simultaneously. Each one represents a different approach: white, grey and black box modeling. The main idea behind the simultaneous use of three different techniques is to increase the reliability of the analysis by cross-validating the analysis results.

The white box modeling is implemented according to the procedure developed by Japan Marine United Corporation, Orihara (2015). The black box modeling employs a multivariate adaptive regression splines model (MARS), Friedman (1991). In this approach, no assumptions are made about underlying distribution of variables or model parameters nor prior knowledge about phenomenon physics used. All possible information is coming from collected data. To control model overfitting and reduce the variance of predictions, an ensemble modeling technique is used, which employs bagging or bootstrap aggregating. This technique is a widely used and known machine learning algorithm, Hastie (2003), Breiman (1996). In practice, multiple MARS models are built, each of them using only a small random portion of data for training. Then, prediction of the output is created by aggregating over all model predictions. Basically, we assume overfitting from all models based on the training data, but that, after aggregation, the prediction will be stable and robust. This way of modeling also provides an empirical estimate of the model variance as well.

The grey modeling is implemented by using a generalized additive model (GAM), *Hastie (1986)*, in which the form of specific additive components can be defined according to the physical model, which makes this approach a grey box model. Each additive component of the model can be represented in the form of linear, polynomial, exponential, spline model or combination of different type of models. In contrary to the MARS model, the GAM model uses all the available data. The complexity of the model is controlled by adjusting the parameters of flexible components, like splines, by minimizing the model prediction error over the testing data, *Hastie (2003)*.

As for the black and grey box modeling, the role of the statistical model in ship performance evaluation at NAPA Ltd. is to describe the relationship between performance related parameters, ship operational and loading conditions, as well as environmental variables. It is very important to understand that in the case of ship performance evaluation the role of the statistical model is not predictive but rather intended for causal analysis. Of course, the model prediction accuracy is very important for the model selection and validation process but the main goal of the analysis is to find out how each specific input variable affects ship performance. Therefore, the effect of fouling is assumed to be a time effect to the model output, so the time is also used as an input variable in the modeling. It is also assumed that the effect of fouling is a slow, smooth and continued change in the propulsion power or speed, which can have discontinuity only after the ship maintenance during which the hull and propeller conditions are improved.

2.2.3 Case study

Recently, NAPA Ltd. was involved in a case where a hull performance analysis was done for a vessel exhibiting an increase in the fuel consumption of over 20% during a two years period. In the following section, we demonstrate the hull performance analysis results for this ship, which are completed with three different modeling techniques.

The data used in the analysis consists of the 5-minutes averages with information enriching metadata for each variable and covers over two years period. Before the model training, the data was filtered, but the purpose of filtering is only to remove clear outliers in the data, as well as the moments when the ship was accelerating or decelerating. The purpose of minor filtering is to acquire as much information from different influencers as possible, thus even hard weather is usually not filtered out from the data. However, such filtering rules are applied only for MARS and GAM modeling. The JMU method requires a much more careful filtering procedure and for hull performance evaluation only data from calm sea conditions are used.

Figs. 3 and 4 show the indices for speed and propulsion power change, estimated at the fixed engine rpm value over the inspected period. The analysis is done using the MARS model. This is a standard way to report the ship performance at NAPA Ltd. In the graphics, the loss indices are shown with the model partial residuals and confidence limits for the model prediction, which denote +/- one standard deviation covering about 68% of prediction variation. The model variance is assumed to be heteroscedastic and follow the normal distribution in each point of the input variable space. The vessel maintenance moment is denoted by a vertical line indicating a dramatic performance change after the dry docking.

The power loss (1) and speed loss (2) indices are calculated as the ratios:

$$I_P(t) = \frac{\hat{P}(t)}{\hat{P}_{min}}, \quad (1)$$

$$I_V(t) = \frac{\hat{V}(t)}{\hat{V}_{max}}, \quad (2)$$

where t is the time, $\hat{P}(t)$ is the propulsion power predicted by the model, \hat{P}_{min} denotes the minimum power predicted by the model over the inspected period, $\hat{V}(t)$ is the ship speed predicted by the model and \hat{V}_{max} is the maximum speed predicted by the model for the inspected period.

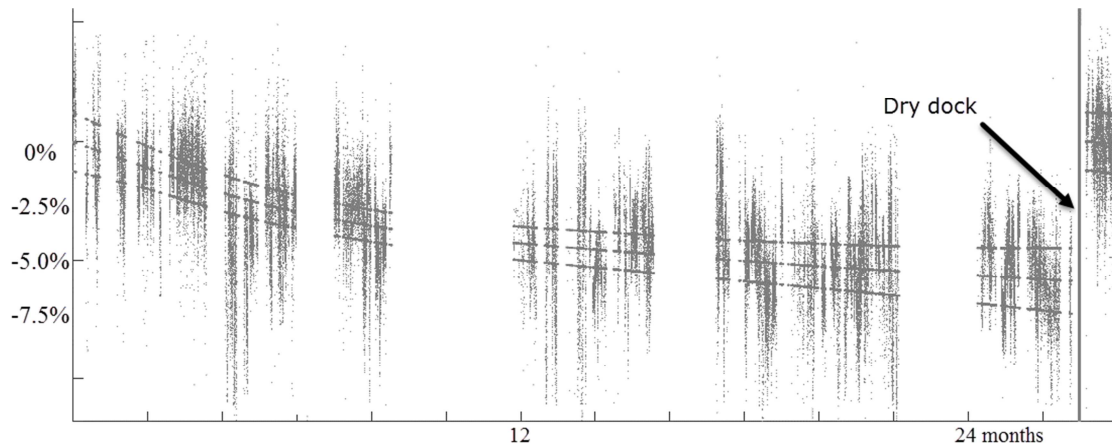


Fig. 3: Speed loss index for fixed engine rpm

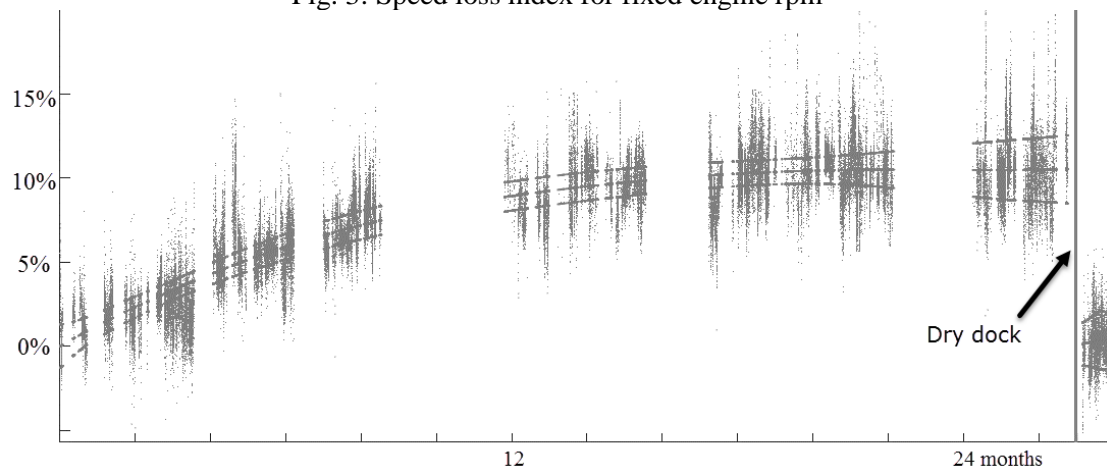


Fig. 4: Power loss index for fixed engine rpm

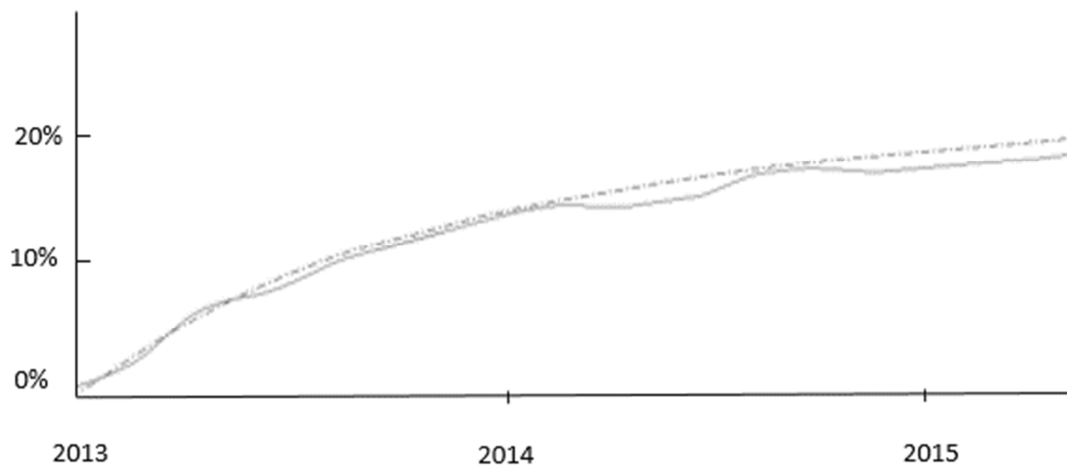


Fig. 5: Hull performance index evaluated with MARS (dash-dot) and GAM (solid)

The hull performance indices, which are evaluated by the white, grey and black box modeling techniques, are demonstrated in Figs. 5 and 6. In Fig. 5, on the same plot, the hull performance indices evaluated by the MARS and GAM are depicted showing very similar results. In Fig. 6 the same type of index is demonstrated estimated with the JMU method representing the white box modeling approach. The JMU method has very tight filtering restriction and considers the data only from laden voyages, thus there is no index estimation after the dry dock yet. It also must be mentioned that according to the JMU method the hull performance is evaluated as an average index per voyage, see

separated points in Fig. 5. The hull performance index is visualized as a second polynomial curve which is fitted into the data.

From Figs. 5 and 6 one can see that the hull performance indices estimated by the white, grey and black box models are all very similar, and they all indicate that the propulsion power increased by about 20%.

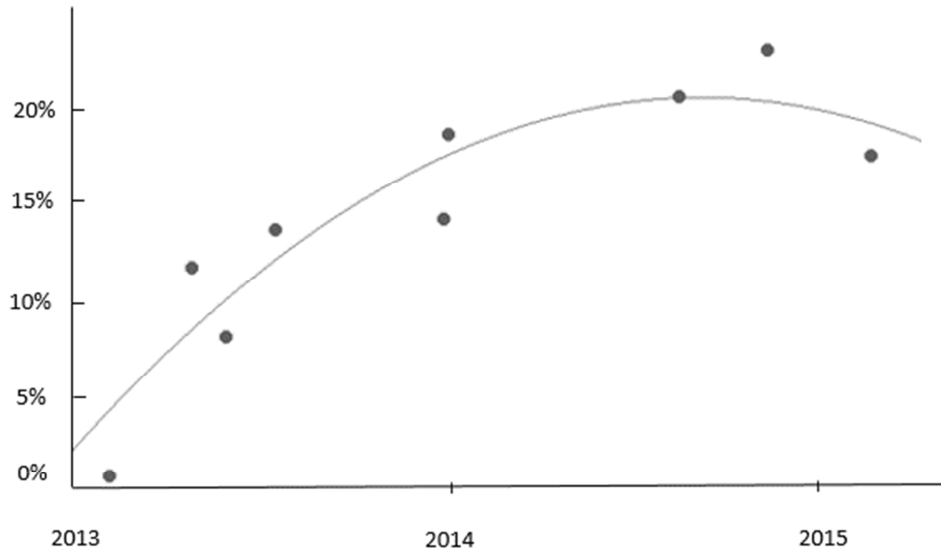


Fig. 6: Hull performance index evaluated by JMU method

3. Discussion

Although in the presented case all models demonstrate similar results for the hull performance, we can still identify differences and problems between modeling approaches. We may consider the accuracy of the white, grey and black box modeling approaches. The general idea of this is visualized in Fig. 7. It is clear that the accuracy of the white box model is constant. It cannot improve because by definition it does not receive any new data, and if we use data to improve the model it will become a grey box model.

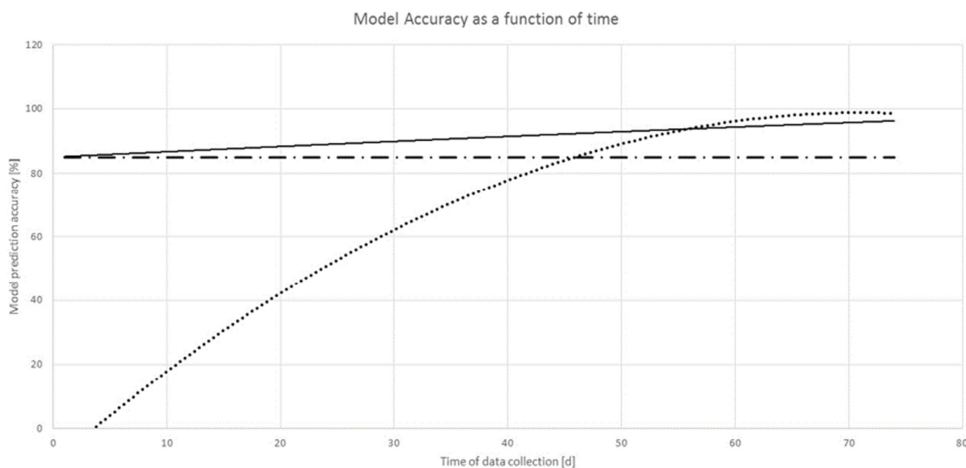


Fig. 7: Accuracy of different modeling techniques: white box (dash-dot), grey box (solid) and black box (dot) modeling

Grey box model accuracy can be improved. It starts from the accuracy of the white box model and improves it as more knowledge is extracted from the measured data. However, depending of the model structure, assumptions and dependency on the physical model, it may be too restricted to achieve

the best possible accuracy. The black box model is the most flexible model and, in principle, can show the best performance and accuracy among all these methods. However, it needs some time to learn from the data.

One of the main problems related to the white box method used for the hull performance evaluation is how the method deals with data noise. The common scenario for the white box techniques is, first, filter the data, correct measurements and perform so called data “normalization”. After that, time trends in corrected values can be assumed to be the performance changes due to hull or propeller fouling, engine aging, etc.

It appears that in the step of data filtering and further correction that data noise is not considered at all. Therefore, corrected data will include: a) variable measurement noise, b) possible errors which are related to the incorrect physical model and assumptions, c) possible errors of missed interactions in the physical model, d) possible errors of the coefficients calculated from the model tests, e) possible errors of model test scaling, etc.; refer to section 1.1. This means that the procedure of data correction will change the structure and distribution of the data noise and completely hide the phenomenon.

Furthermore, after the data is corrected, we still need to use some kind of statistical approach to reveal, quantify and demonstrate the change in the hull performance. At that stage of the hull performance evaluation, very often a linear or polynomial model is fitted to the corrected noisy data representing change in the performance. For example, in Fig. 6, a second-degree polynomial trend curve is fitted to the corrected data. It seems that the hardest task of dealing with data noise is handled by simple tools.

The situation with black and grey box modeling is different. Flexible statistical models are created to deal with the real life data with the presence of noise. The goal of the statistical modeling is to get rid of the noise and reveal the “pure” relations between variables. Thus, we may assume that these models are better tools to deal with noisy data. The statistical model deals with noise at the beginning and once the model is built we can forget about data noise and proceed with the assessment only with the modeled representation of the phenomena.

However, because statistical black or grey box models learn from data they depend highly on the quantity and quality of data. By data quality, we imply not the amount of measurement errors but rather the signal-to-noise ratio. In other words, is there enough variation in the model inputs, so their effects to the response can be recognized by the model? This problem concerns the variation of the input variables or mostly the lack of it in the case of the ship performance analysis. For example, it may happen that after we start to collect the data, the weather conditions do not vary much preventing us to adequately model the effects of the wind, waves and swell. It is possible that the ship is operated at a fixed rpm which makes it difficult to model the speed-power relationship. However, we may assume that the more data we collect on-board the more different operational and environmental conditions will be present in the data, thus helping the creation of an adequate model.

Another considerable issue is how data is collected on-board. It is clear that hull performance evaluation is a causal analysis and our primary goal is to find out the effect of time. Because the statistical model estimates all variable effects from the data there are such issues as possible multicollinearity between variables and confounding. Basically, the causal analysis requires data collected during a randomized experiment. During the experiment the model input variables should be varied according to the principles described in a theory of experimental design, *Wu and Hamada (2009)*. These principles of data collection are created precisely to prevent multicollinearity and confounding between variables. In the case of ship data those principles are often broken, especially when the data collection period is short.

For example, during the short period of data collection, the weather may change slowly from light to hard conditions, which confound the effect of the time, thus making it difficult for the model to differentiate the effects of the weather and fouling. On the other hand, the loading and floating conditions,

ships are often operated in the same manner. For example on tankers and bulkers, the ship draft and trim often correlate because one specific trim is used for the laden and the other for the ballast voyages, confounding the draft and trim.

Thus, ship data collected onboard does not necessarily follow the principle and requirements for causal analysis over short time periods. However, we may assume that the more data we collect on-board in different operational and loading conditions, as well as various environmental conditions, the more adequate and reliable model we will create.

According to the previous considerations, before the black or grey box statistical model starts producing reliable results representing the system's real behavior, we need to collect a sufficient amount of data. The questions usually asked are: "what is a sufficient amount of data?" and "how much data we need to collect so that the model produces adequate results?" When concerning ship performance modeling there is not exact answer to this question.

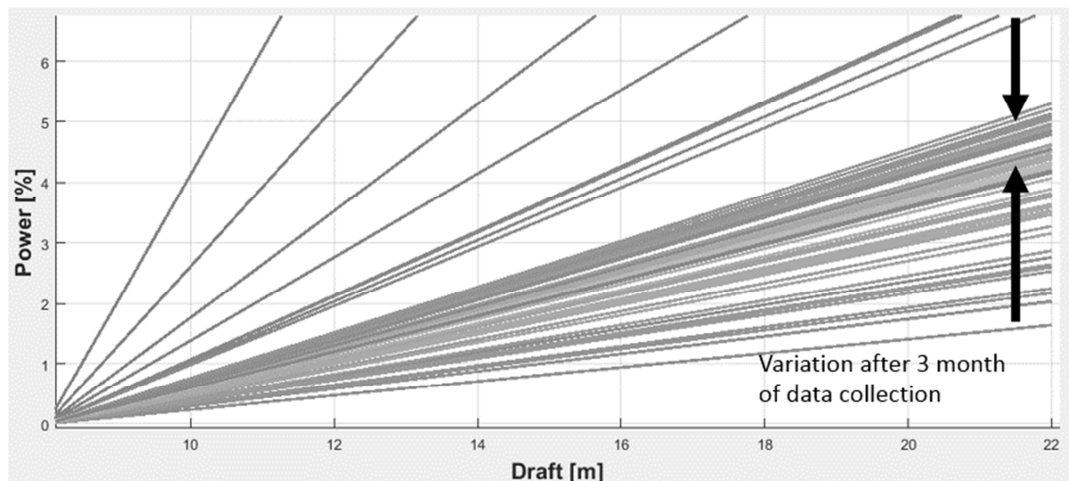


Fig. 8: Draft effect prediction variation during model training for vessel 1. When amount of data increases, prediction converges.

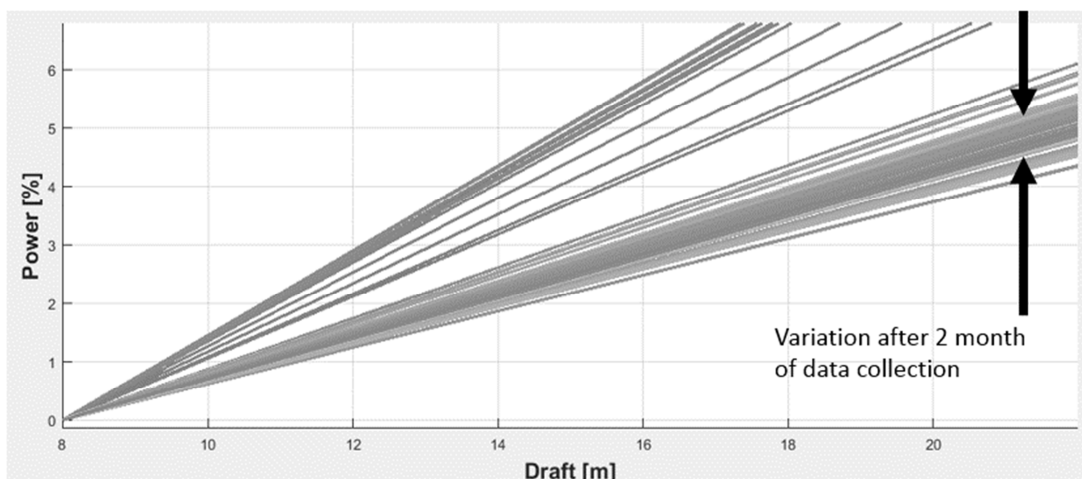


Fig. 9: Draft effect prediction variation during model training for vessel 2. When amount of data increases, prediction converges.

Based on experience we conclude that the period of data collection required for model creation may vary from few weeks to few months. Figs. 8 and 9 present the results of a test in which the convergence of the effects of the draft is inspected in relation to the amount of data used for model training. The statistical model is trained with a data set; the size of the data set is increased

sequentially according to the time. The first model is created with the data collected during the first three days, then next three days of measurements are added to the data and a new model is trained and so on. For each trained model the marginal effect of the input variable is visualized on the same plot.

In Figs. 8 and 9 convergences of the draft marginal effect to the propulsion power consumption, estimated for two sister vessels, are shown. The draft effect was estimated for similar conditions which correspond to zero-weather, deep water, the same floating condition and the same engine rpm value. The GAM model, which represents a grey box modelling approach, was used for the test. One can see from the figures that the data amount needed for the model before the draft effect becomes stable is different and with the short data collection periods it may vary a lot. For vessel #1 the effect was stabilized after 3 month of data collection, see Fig. 8. For vessel #2 the effect was stabilized after 2 months, see Fig. 9. However, after convergence the effect of the draft is approximately the same for both vessels showing an increase of the propulsion power consumption of about 5% while changing from the ballast to laden condition.

4. Conclusions

In this paper white, black and grey modeling approaches for hull performance evaluation were discussed. Each of those modeling approaches has their advantages and drawbacks. White box modeling is the only useful modeling approach for ship performance evaluation during ship design and for operational stages with relatively short data collection periods. However, sufficient onboard data measurement provides more accurate information about the ship performance and affecting factors. Empirical information about ship performance will only improve over time, thus providing a basis for more accurate and realistic models. This means that the accuracy of the ship technical performance evaluation will also improve.

An accurate model based on real measured data is necessary for accurate evaluation of hull condition, propulsion efficiency and technical evaluation of fuel saving devices. Finally, accurate modeling and performance prediction enables optimization of ship operations. Correlations may be found with statistical methods, but it is important to remember that correlation does not equal causation, *Vigen (2015)*. The best possible outcome with any of the modelling methods mentioned in this paper can be achieved only by understanding the causalities in the phenomena of ship performance.

References

- AAS-HANSEN, M. (2011), *Monitoring of Hull Condition of Ships*, M.Sc. Thesis, Norwegian University of Science and Technology, VDM Verlag Dr. Muller GmbH & Co. KG Publishers, ISBN: 978-3-639-32847-9
- BOHLIN, T. (2006), *Practical Grey-box Process Identification*, Springer-Verlag, London
- BOSE, N.; MALLOY, S. (2009), *Reliability and Accuracy of Ship Powering Performance Extrapolation*, 1st Int. Symp. on Marine Propulsors (SMP), Trondheim
- BREIMAN, L. (1996), *Bagging predictors*, Machine Learning 24 (2), pp.123-140
- FRIEDMAN, J.H. (1991), *Multivariate adaptive regression splines*, The Annals of Statistics 29/1, pp.1-141
- GERTLER, M. (1954), *Reanalysis of the Original Test Data for the Taylor Standard Series*, DTMB Report 806, Washington
- GULDHAMMER, H.E.; HARVALD, S.A. (1965), *Ship Resistance, Effect of Form and Principal Dimensions*, Akademisk Forlag, Copenhagen

- HANSEN, S. V. (2012), *Performance Monitoring of Ships*, PhD Thesis, Technical University of Denmark
- HARVALD, S.A. (1983), *Resistance and Propulsion of Ships*, John Wiley & Sons
- HASTIE, T.; TIBSHIRANI, R. (1986), *Generalized additive models*, Statistical Science 1/3, pp.297-318
- HASTIE, T.; TIBSHIRANI, R.; FRIEDMAN, J. (2003), *The Elements of Statistical Learning*, Springer, ISBN: 9780387952840
- HAUTH, J. (2008), *Grey-Box Modeling for Nonlinear Systems*, PhD Thesis, Kaiserslautern University of Technology
- HOLTROP, J. (1977), *A Statistical Analysis of performance test results*, Int. Shipbuilding Progress 24
- HOLTROP, J.; MENNEN, G.G.J. (1982), *An Approximate Power Prediction Method*, Int. Shipbuilding Progress 29 (335), pp.166-170
- HOLTROP, J. (1984), *A Statistical Re-analysis of Resistance and Propulsion Data*, Int. Shipbuilding Progress 31 (363), pp.272-276
- HÄHNEL, K.; LABES, K.H. (1964), *Systematische Widerstandversuche mit Taylor-Modellen mit einem Breiten-Tiefgangsverhältnis $B/T = 4.50$* , Institut für Schiffbau, Rostock
- INSEL, M. (2008), *Uncertainty in the analysis of speed and powering trials*, Ocean Engineering 35, pp.1183-1193
- ISO 15016, *Ships and marine technology - Guidelines for the assessment of speed and power performance by analysis of speed trial data*, Int. Standard Org.
- ISO/CD 19030-1, *Ship and marine technology – Measurements of changes in hull and propeller performance, Part 1: General Principles*, Int. Standard Org. (2015)
- ISO/CD 19030-2, *Ship and marine technology – Measurements of changes in hull and propeller performance, Part 2: Default method*, Int. Standard Org. (2015)
- ITTC (2005) – *Recommended Procedures and Guidelines, Full Scale Measurements Speed and Power Trials*, Int. Towing Tank Conf.
- JOURNEE, J.M.J.; MEIJERS, J.H.C. (1980), *Ship routing for optimum performance*, Report 0529-P, Delft University of Technology
- KELLER, W.H. (1973), *Extended Diagrams for Determining the Resistance and Required Power for Single Screw Ships*, International Periodical Press, Rotterdam
- LAP, A.J.W. (1954), *Diagrams for Determining the Resistance of Single Screw Ships*, Int. Shipbuilding Progress 1/4
- LEIFSSON, L.; SWARSDITTIR, H.; SIGURDSSON, S.; VESTEINSSON, A. (2008), *Grey-box modeling of an ocean vessel for operational optimization*, Simulation Modeling Practice and Theory 16, pp.923-932
- LJUNG, L. (2001), *Black-box Models from Inputs-output Measurements*, 18th IEEE Instrumentation and Measurements Technology Conf., Budapest

- LOGAN, K.P. (2011), *Using a Ship's Propeller for Hull Condition Monitoring*, ASNE Intelligent Ships Symp. IX
- ORIHARA, H.; YOSHIDA, H.; HIROTA, K.; YAMASAKI, K.; SAITOH, Y. (2015), *Verification of full-scale performance of eco-friendly bulk carriers under actual operating conditions by onboard performance monitoring*, Taylor & Francis Group, London, ISBN: 978-1-138-02727-5
- OORTMERSSEN, G. van (1971), *A Power Prediction Method and Its Application to Small Ships*, Int. Shipbuilding Progress 19
- OORTMERSSEN, G. van (1978), *Power Prediction Method for Motorboats*, 3th Symp. Yacht Architecture, Netherlands
- PEDERSEN, B.P.; LARSEN, J. (2009), *Prediction of Full-scale Propulsion Power Using Artificial Neural Networks*, 8th Int. Conf. Computer and IT Appl. Maritime Ind. (COMPIT), Budapest, pp. 537-550
- PEDERSEN, B.P.; LARSEN, J. (2009b), *Modeling of ship propulsion performance*, World Maritime Technology Conf. (WMTC), Mumbai
- PETERSEN, J.P.; JACOBSEN, D.J.; WINTHER, O. (2011), *A machine-learning approach to predict main energy consumption under realistic operational conditions*, 10th Int. Conf. Computer and IT Applications in the Maritime Industries (COMPIT), Berlin, pp.305-316
- PETERSEN, J.P.; JACOBSEN, D.J.; WINTHER, O. (2011b), *Statistical modelling for ship propulsion efficiency*, J. Marine Science and Technology, (DOI) 10.1007/s00773-011-0151-0
- SCHNEEKLUTH, H.; BERTRAM, V. (1998), *Ship Design for Efficiency and Economy*, Butterworth-Heinemann, Oxford
- SWIFT, P.M.; NOWACKI, H.; FISCHER, J.P. (1973), *Estimation of Great Lakes Bulk Carrier Resistance Based on Model Test Data Regression*, Marine Technology 10, pp. 364-379
- TODD, F.H. (1963), *Methodical Experiments with Models of Single Screw Merchant Ships*, Report 1712, David Taylor Model Basin
- WU, C.F.J.; HAMADA, M.S. (2009), *Experiments: Planning, Analysis, and Optimization*, 2nd Ed., Wiley, ISBN: 978-0-471-69946-0
- VIGEN, T. (2015), *Spurious Correlations*, Hachette Books, ISBN: 978-0-316-33-943-8

Practical Experiences with Vessel Performance Management and Hull Condition Monitoring

Falko Fritz, SkySails GmbH, Hamburg/Germany, falko.fritz@skysails.de

Abstract

In times of uncertain markets, shipping companies increasingly use measurement data for decision making processes. The V-PER system records data on customer vessels, transfers them to an on-shore database and offers reporting services for various stakeholders. One report is the trend report. Fuel, speed, draft and weather data are filtered and normalized to show fuel consumption trends over time. Speed normalizations are verified by conducting speed / consumption fixings on the vessels. This procedure is a solution used to overcome customer concerns connected with efficiency evaluations. In the future, further data sources are to be accessed to improve the data processing. A common understanding among all involved parties is the key to advancements in energy efficiency.

1. Introduction

The international shipping sector has gone through tremendous changes during the last decade. Unprecedented fluctuations in fuel prices, an uncertain global market, strong competition and new environmental standards require new solutions for improved decision making.

At the same time, evolving database technologies and more affordable data transfer services over satellite made it possible to access real ship data for efficiency evaluations. More and more ship owners improve their reporting structures by installing measuring devices and increasing the data flow from one manually entered dataset per vessel and day to a multitude of automatically recorded data at a much higher rate.

According to the DNV GL Energy Management Study 2015, Adams (2015), energy efficiency and bunker saving have a high importance for 76% of the shipping companies that participated in the study, not only because of the cost saving potential, but also because the ecological footprint has become an important criterion. More and more of them quantify fuel reduction targets specifically.

The Vessel Performance Manager (V-PER), produced and distributed by SkySails and LEMAG, is such a data management system. It is primarily intended for the fuel efficiency optimization on seagoing ships. In chapters 2 and 3 of this paper, an overview over the system layout and the data processing steps taken towards hull condition monitoring are given.

Throughout this paper, the term trend reporting is used for the process of documenting fuel efficiency over a period of time, usually a period of several years and including markers for dry-dock events etc. It is highly likely that hull and propeller condition are the main reasons for decreasing efficiency over time, but since some other relevant effects are very hard to detect in reality (see chapter 2.2.4, for instance), the more general term is used.

Chapter 4 lists the most common customer concerns connected with vessel performance evaluations and describes solutions that have been found suitable in practice. Chapters 5 and 6 give an outlook on future developments and conclude the paper.

2. Layout of the vessel performance management System V-PER

2.1 Meeting customer demands

Customers look for data monitoring and management solutions for a multitude of applications. In addition to hull condition monitoring, this includes e.g. daily efficiency monitoring, voyage reporting,

speed optimization, trim optimization, weather influences, charter contract compliance, claim management, greenhouse gas vetting, monitoring of main engines, auxiliaries, shaft generators, boilers, rudder movements, roll and pitch angles, and many more.

At the same time, the vessel performance management system is required to be integrated into existing communication and data handling processes, most often involving not only the customer, but also subcontractors and third company partners. In order to increase the business profitability it is important to focus on more than just technical aspects, e.g. by discussing the integration of new data sources into the customer's daily work flow.

Consequently, the number of data sources, variables, but also stakeholders and reporting formats increases with every new task. At the same time, the data transfer volume from ship to shore is still a major financial concern for many clients. As a result, an open architecture in hardware, software and reporting structure is essential for the sustainable development of performance management solutions.

2.2 Physical components of the V-PER system

The main physical components of the V-PER system are a PC, main engine fuel meters, a wind anemometer, an inertial measurement unit (IMU), an NMEA interface and a software package. Additional components are optional and recommended, but effectively the decision is made by the customer. These optional components include a torque meter, additional fuel meters for generators / boilers, and modbus interfaces for various analogue signals (e.g. rudder angle, propeller pitch, electrical generator power, etc.).

2.2.1 PC and database

The core of the V-PER system on-board is a PC certified for marine applications. It hosts the software, gathers all sensor data and hosts a small database that also stores the manual reports that were submitted by the master. A helm display connected to the PC shows the measurements and real time performance evaluations to the nautical officers. In addition, the V-PER PC is connected to the master PC. All measurements and data can also be traced here. In most cases, the master PC provides the email link used for the ship to shore communication. However, other ways of satellite communication are possible on customer demand.

2.2.2 NMEA interface

All navigational data like ship speed through water (STW), ship speed over ground (SOG), course, heading, etc. are taken from the ship's NMEA protocol.

2.2.3 Fuel meters

In addition to STW and SOG, the main engine fuel consumption rate (FCR) is the most important variable for evaluating the vessel's energy efficiency. The fuel measurement can either be installed in the supply line to the mix tank, or in the booster circulation, measuring both engine inlet and outlet.

Two types of fuel meters are in use: volumetric fuel meters and coriolis mass flow meters. Based on practical experiences, the mass flow meters have the advantage that no fuel density is needed to calculate the mass flow, and the lack of moving parts makes them more reliable in the long run. In both cases, the fuel meters measure both fuel flow and fuel temperature.

Many customers order fuel meters for the auxiliary engines and boilers in addition to the main engine fuel measurement. On the one hand, the monitoring of this equipment helps to improve its proper use and function, but also the requirements of the Energy Efficiency Operational Indicator (EEOI) or the EU's MRV regulations are a reason for this, since they include the emissions of all CO₂ sources, as defined in *IMO (2009)*.

2.2.4 Wind anemometer and IMU

The most complex set of variables to take into consideration is the weather condition. Predictions for wind force and direction, wave and swell heights and directions, as well as ocean currents can be obtained from weather services at additional costs. With or without them, an independent measurement on-board is required. The V-PER system includes an ultrasonic wind anemometer and an IMU for recording wind conditions and ship movements.

The IMU is also needed for measuring the trim and heel while on passage, so that the efficiency at different trim conditions can be evaluated.

2.2.5 Torque meter

In the general context of vessel performance monitoring and management, the torque meter is a recommended, but not strictly essential component. Since reducing fuel consumption and documenting emissions often are the main reasons for installing a system like V-PER, torque meters might not be the customer's top priority. In case of V-PER, most orders are actually placed without them. For the trend reporting this means that shaft power cannot be used as an input factor and all calculations must be based on the fuel meter readings and FCR. The downside of this method is that changes in the main engine efficiency cannot be differentiated from hull and propeller condition changes in the observed efficiency trends.

2.3 Manual entries

Some data that influence the vessel fuel consumption are usually not recorded automatically. The most important one is the vessel draft. This is particularly important on low-speed ships with large draft differences between laden and ballast, where hull friction may make up 90% of the total ship resistance according to *MAN (2012)*. On some vessels equipped with the V-PER system, the hull surface area in the water changes by more than 30% at different load states. Consequently, the influence of vessel draft is significant.

The V-PER system therefore has an option for entering vessel draft data and other information in a voyage reporting system. It is up to the customer to just send the minimum of required information for efficiency evaluations, or use the software as a full-grown voyage reporting solution with noon reporting, reports at port arrival and departure, monitoring of bunkering events, notifying of the EEOI, etc. The data structure of this application is shown in the following chapter.

2.4 Data structure

The V-PER system is a performance management solution that works bi-directionally between ship and shore, Fig. 1. It records both sensor data and manual inputs by the captain, the chief engineer or other crew members in charge. While the internal data rate of the sensors is up to 10 Hz, the on-board software writes a performance log file at a rate of one dataset per 10 minutes. This ensures that values can be observed in real time on the helm display and the connected master PC, but the data volume for satellite transfer is kept at a minimum.

The performance log files and the manual reporting files are sent to a protected on-shore database in encrypted .xml files. The database stores all data safely and generates customized reports and feeds the web portal, Fleet Online, which is accessible via PC and mobile devices. Fleet Online allows its users to access measurement data, check noon reports, and also to set alarm functions to highlight vessels on a map when the defined alarm limits are not kept.

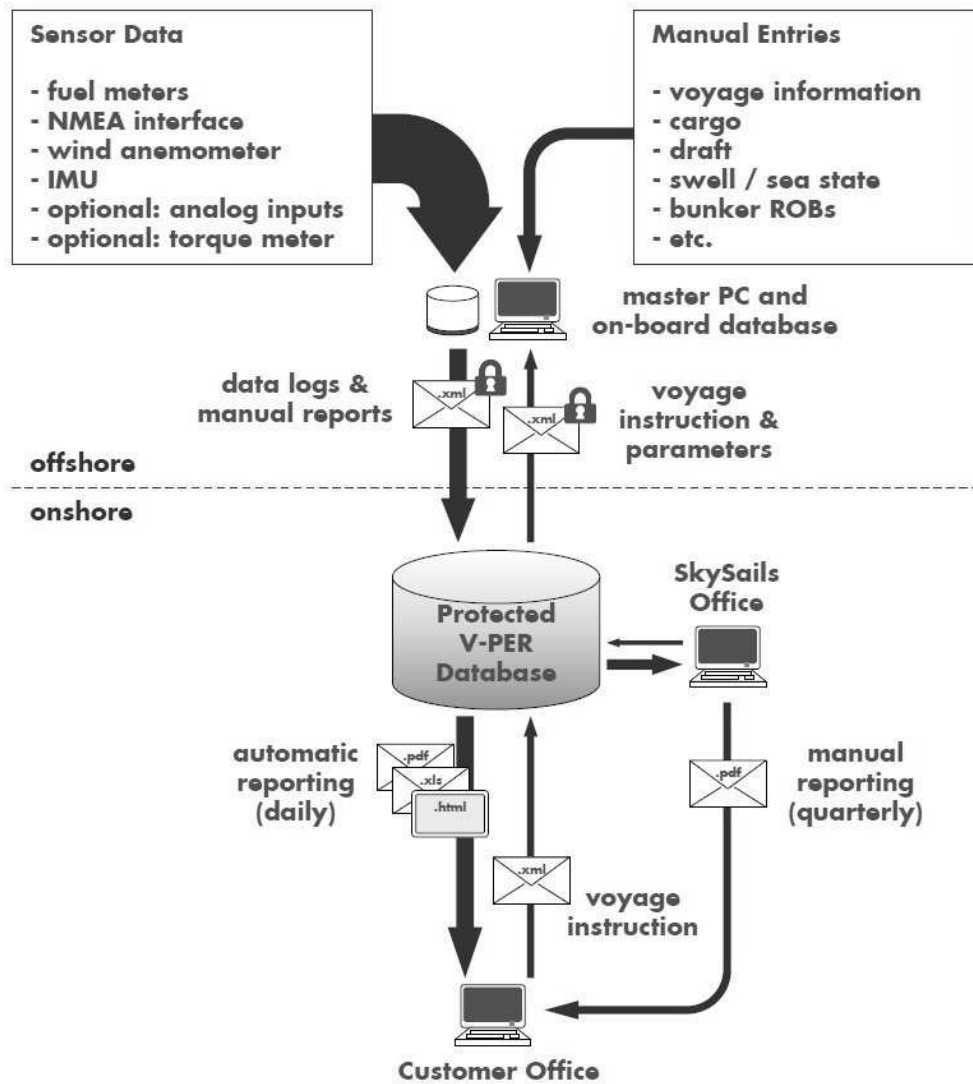


Fig. 1: simplified V-PER data structure

Some analyses however, including the trend reporting on a quarterly basis, require the control of a human operator. These are calculated and checked manually at the SkySails office and then sent to the client and designated subcontractors.

In addition to the data transfer from ship to shore, the system can also be used to send voyage instructions and software updates to the vessel. Instructions to the vessel are sent from an office tool or through the Fleet Online web interface. The customer can choose to update voyage information, instruct the ship to proceed at a certain speed or FCR, or even transmit financial parameters which the on-board software uses to estimate the most profitable ship speed under the weather conditions at hand. For this calculation, technical parameters describing the ship behaviour are generated at the SkySails office and sent to the vessel in the same way as the voyage instructions.

3. Data processing for trend reporting

A multitude of factors influences the ship speed through water at any given FCR. The V-PER system uses both filtering and normalization steps to create an accumulated set of comparable data and thereby identify an efficiency trend over time.

3.1 Data quality

When handling measurement data from ships, data quality is always a big issue. The harsh offshore environment, vibrations from heavy machinery, the risk of temporary blackouts etc. all do their share in complicating or interrupt precise measuring.

In the context of efficiency evaluations, it is important to note that while most customers focus on the measuring precision of the fuel and torque meters, the ship speed log measuring STW is a much bigger source of inaccuracy. While mass flow meters are typically precise to a fraction of a percent, the STW measurement can easily be off by several percents, or be untrustworthy altogether.

3.2 Data plausibility checks

The first step in each efficiency evaluation is therefore to check the data quality, discover implausibilities and define correction functions, if possible. For example, STW errors can be corrected to some degree if ocean current charts are available (sufficiently accurate in both time and space, e.g. provided by a weather service). The much more reliable GPS based SOG values and the surface current speeds can then be used to calculate a theoretical STW, and compare the measured STW with this result.

3.3 Data filtering

In a second step, the plausible datasets are filtered for a number of criteria, so that only data during comparable states of ship operation are taken into consideration. For the purpose of trend reporting, datasets are not used for the further analysis if

- the ship speed SOG or (corrected) STW changes by 2 knots or more during 30 minutes,
- the wind force exceeds 4 Bft,
- SOG, STW or FCR are outside the limits of normal ship operation (e.g. manoeuvring, channel or river passages), or
- the number of valid datasets is too low for particular calculations of means or quantiles.

3.4 Data normalization

All valid FCR data are then normalized to pre-defined reference conditions. The trend reports then show either the FCR in t/d or the specific fuel consumption per distance in kg/nm for the defined reference conditions. These conditions are specific for each vessel or group of sister vessels and agreed with the customer. For example, if a ship has a usual laden draft of 10 to 12 m and is operated between 11 and 15 knots, the reference condition could be set to 11 m draft and 13 knots speed. In all types of reporting, the FCR at reference conditions can be used as a recognizable key performance indicator (KPI).

The benefit of this approach is, that the results are presented in a unit the operators, technical inspectors or other stakeholders are completely familiar with, and which they can put into perspective intuitively.

While the influence of draft changes is evaluated over a longer period of time based on the standard performance log data, a special procedure, the so called speed / consumption fixing, is used to model the dependencies of FCR and STW. This procedure is as explained in the following subchapter.

3.4.1 Speed / consumption fixing

When the V-PER system is installed on a vessel, the officers are instructed to conduct one or more speed / consumption fixings, in which the ship speed is increased step by step and kept constant for a couple of minutes between each change of engine load or propeller pitch, Fig. 2.

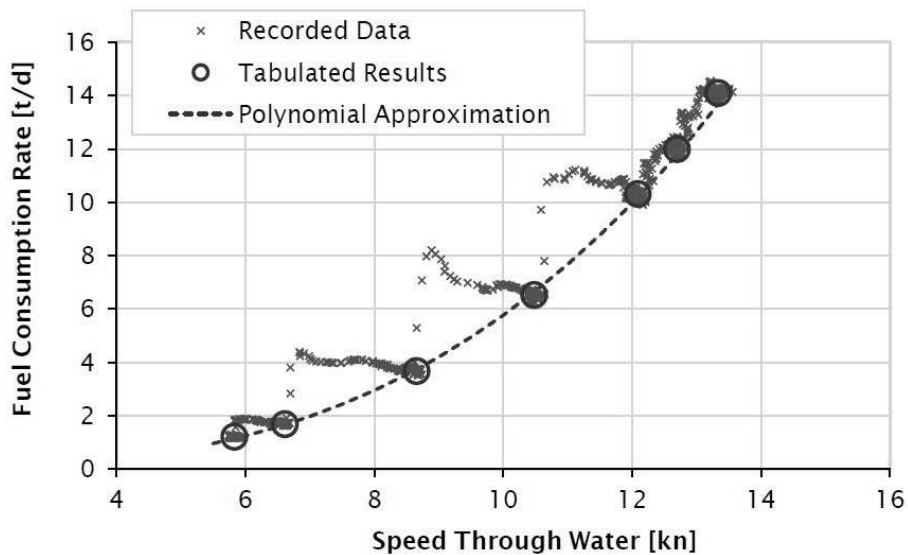


Fig. 2: Exemplary result of a speed / consumption fixing measurement

Prior to starting this procedure, the master activates a separate data log in the V-PER software on board, which writes a separate log file in 0.1 Hz, rather than 1 dataset per 10 minutes as in the usual operation. The log is sent to the onshore database automatically and evaluated in a speed / consumption fixing report. In addition, and more importantly for the trend reporting, the results are used to refine the theoretical ship model.

It is important to note that the speed / consumption fixing is only a momentary example of the ship's FCR in relation to STW at the time of its recording. Its outcome is not a general answer to how high or low the FCR is at a certain speed. Its valuable information is rather the shape and properties of the approximation curve, or whether the FCR increase can be approximated to a simple mathematical function at all.

Ideally, each ship performs a series of speed / consumption fixing procedures in different weather and load conditions and the result is an array of curves, differing in slope due to the different ship resistance in each speed run, but similar in shape, Fig. 3.

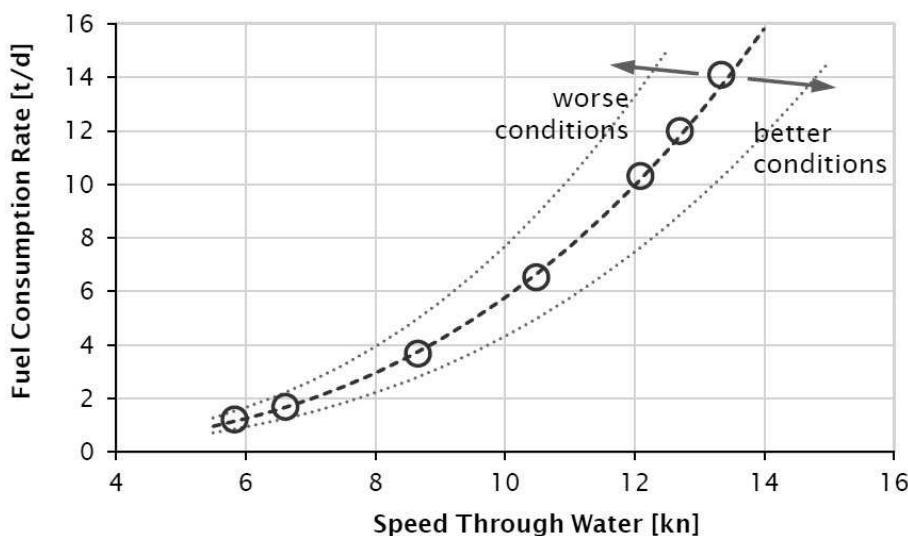


Fig.3: Array of fuel consumption curves in different conditions

This method of approximation works better for slow ship types like tankers or bulk carriers, than on faster ship types. In all cases however, carrying out one or more speed / consumption fixing procedures with the real ship as part of the V-PER commissioning improves the quality of all future data analyses. When the consumption curve array is validated in speed / consumption fixings, FCR data can be normalized to a reference speed with sufficient reliability over a certain range of speeds.

Using the actual ship for this sort of trial is of course an issue that needs to be discussed with the customer in detail. Since each speed / consumption fixing procedure requires slowing the vessel down for about half an hour, the agreement of the charter is also important. Practical experiences show that reporting the results to the customer is a vital part of creating an understanding, what the benefits of the procedure are. If done correctly, the speed / consumption fixings can often answer some customer questions very quickly, much quicker than it is possible with the general performance log data.

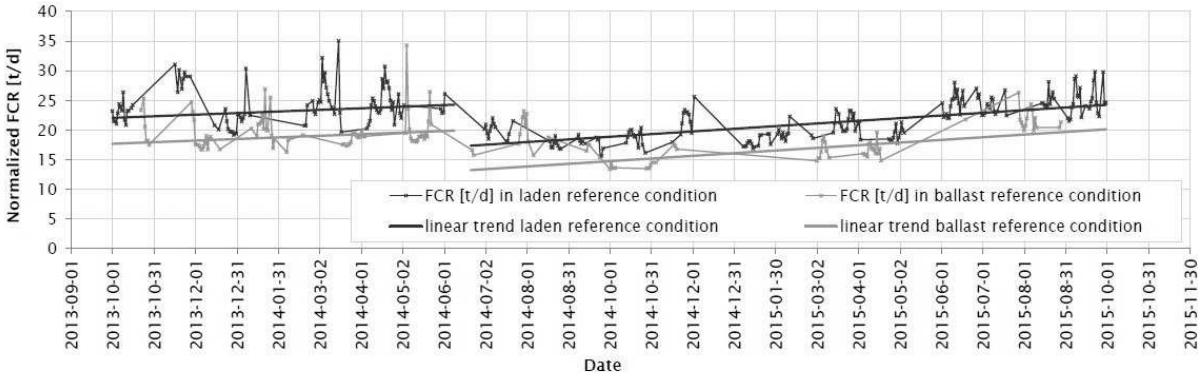
3.4.2 Draft normalization

In contrast to the speed influence on FCR, the draft influence cannot be evaluated within hours or days. Load states change from one voyage leg to the next, but each sea passage is different from the last in more than this regard. Effectively, several weeks to months of measurement data are required to evaluate the normalized FCR at different drafts.

The draft normalization is based on the theory that hull friction rises linear to the surface area in the water, which in turn is a function of general ship dimensions and draft. An empirical parameter is used to fit the theory to the measurements.

3.5 Trend reporting based on the fuel consumption rate

The result of an exemplary trend analysis is shown in Fig. 4. For this customer it was important to split the data between ballast and laden condition in order to be more comparable with the charter warranties agreed with the charterer. Linear trend lines are fitted to the data in order to visualize the efficiency trends, interrupted by a dry-dock event in June 2014. Depending on the ship type and trades, different ways of presenting the data are favourable. In the shown example, the results of ballast and laden passages differ enough to justify two separate lines in the diagram.



	Time	FCR trend	Events
Trend 1	2013-10-01 to 2014-06-09	0.26 t/d per month	Drydock 2014-06-09 to 2014-06-21
Trend 2	2014-06-21 to 2015-09-30	0.44 t/d per month	

Fig. 4: Normalized fuel consumption trends in laden and ballast condition

The comparatively high data peaks in the graphs in Fig.4 are due to the heterogeneous operation of this particular vessel. As shown in Fig.5, the recordings were taken in all kinds of sea areas, alternating between ballast and laden voyage legs of different lengths and at different speeds.

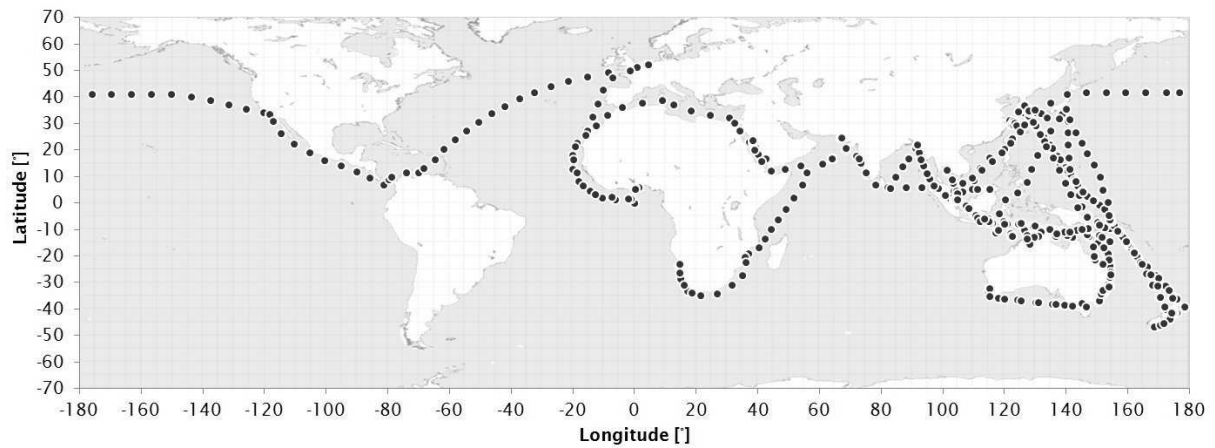


Fig.5: positions of the exemplary vessel over a two year period (2014 – 2015)

4. Overcoming customer concerns

After the dramatic increase of fuel prices in 2008 and again in 2012, it may be surprising that there are still many ships not equipped with sophisticated measuring equipment for fuel consumption or shaft power. There are numerous reasons for this. A selection of customer concerns and ways to solve them is listed below:

- Performance monitoring or management solutions do not save fuel by themselves. It is up to the recipient of the information to make use of it and optimize the ship efficiency by improved decision making. The data gathered must be analyzed and boiled down to comprehensive KPIs for easy, everyday use.
- However, limiting the information to calculated KPIs leaves the customer with the question how the KPI was calculated and how trustworthy it is. The underlying calculations must therefore not only be documented, but also explicable for stakeholders not immediately familiar with mathematical models or data analysis.
- Submitting all vessel performance data and even confidential financial information (e.g. estimated time charter equivalent values) to an equipment supplier raises the question of data protection, confidentiality and encryption. Sufficient measures must be taken to ensure customer data protection and server stability.
- The question how much cost reductions can be achieved cannot be answered directly. Only examples and experience reports from previous installations can show the financial benefits, so these must be obtained and evaluated.
- Some evaluations require measurement periods of several months or years before the results can be used for the client's benefit. This is particularly true for the trend reporting, but also for trim tables based on real ship data. A daily report showing the recorded data and daily development of KPIs is useful to offer a benefit right from the start.
- The people who buy the product are not the ones who use it. The full potential of the system can only be used if everybody involved is motivated to participate. A detailed analysis of how and by whom the provided information is to be used, and what specific needs each participant has, has to be done in close cooperation with the customer.

The precise identification of customer needs and expectations, verbalized or implied, is one of the major challenges when dealing with vessel performance monitoring or management. Based on experience, a designated person of contact on both customer and supplier side is an important step to maximize the benefit. Creating the optimum solution is an iterative process.

5. Outlook

In order to improve the quality of trend reports and other analyses, manual entries are steadily to be

replaced by measurement data in the future. An interface to the ship's loading and stability calculation program, a more widespread utilization of weather charts and the access to other data sources will permit an improved data processing. Alternative data modelling approaches, e.g. machine learning methods like neural networks or support vector machines, are also being investigated.

At the same time, more and more ship's crews, on-shore operators, inspectors, etc. familiarize themselves with the new possibilities of extended data access. Their feedback is the most productive input for the further development of the V-PER system.

6. Conclusion

Hull monitoring has to be seen as one aspect in the much larger scope of vessel performance management. Customers look for software solutions that improve the quality of both measured and manually entered data, and that take the load of evaluating large data quantities off their shoulders. Trend reporting or hull condition monitoring is one of the more complex types of analyses, mostly because so many other influences on the vessel performance have to be quantified in the process, but also due to the continuous, dependable measuring of all variables over several years.

The success is highly dependent on the communication between customers and equipment suppliers, and on the flexibility of the performance management tool to meet the demands of many stakeholders. A common understanding of the complexities of the task and the steps needed for creating solutions is essential for a seamless integration of performance indicators into the daily workflows. Specific measurement procedures on the real vessel, e.g. the speed / consumption fixings, can be a beneficial step to improve the quality of evaluations, discover irregularities, and at the same time give the customer qualified feedback before the trend report is accessible.

Vessel performance evaluations based on extensive data logs from seagoing vessels is a comparatively new field of research. The access to additional data sources, the growing expertise of people working with the data on a daily basis, and steps taken towards standardizations by authorities and organisations will pave the way for significant advancements in the years to come.

References

ADAMS, S.D. (2015), *DNV GL Energy Management Study 2015*, pp. 12-14
<https://www.dnvgl.com/maritime/energy-management-study-2015.html>, accessed February 17, 2016

IMO (2009), *Guidelines for Voluntary Use of the Ship Energy Efficiency Operational Index (EEOI)*, MEPC.1/Circ.684

MAN Diesel & Turbo (2012), *Basic Principles of Ship Propulsion*, p. 11
<https://marine.man.eu/docs/librariesprovider6/propeller-aftship/basic-principles-of-propulsion.pdf>, accessed February 25, 2014

Energy Efficiency Design Index in View of Performance Monitoring

JanWienke, Jörg Lampe, DNV GL, Hamburg/Germany, jan.wienke@dnvgl.com

Abstract

This paper presents procedure and evaluation of speed tests that are performed during newbuilding sea trials. The determined ship speed is required for the final EEDI calculation of each individual ship. The speed trials deliver absolute values. In contrast, performance monitoring is focused on relative values, meaning the variation of performance in time. Speed trials and performance monitoring are compared with special regard on accuracy. Differences and interactions are analysed.

1. Introduction

With the implementation of EEDI certification, speed trials of newbuildings have gained a new relevance. For the first time, classification societies are involved in speed tests. Sea trials are witnessed by surveyors and the results are verified by Class. Even the preceding model tests are witnessed by surveyors and checked by Class. The procedure of verification is described in the respective industry guideline by *IMO (2012)*.

In this way, the quality of speed trial data shall become more comparable in future. Procedure and evaluation of speed trials are standardized by *ISO (2015)*. Classification societies make sure that the actual procedures and evaluation are in agreement to this standard. To evaluate the results of speed trials a consideration of the uncertainties is needed. Based on this the relation to performance monitoring data can be analysed.

2. Speed trials according to ISO 15016:2015

The speed/power trials (S/P trials) are carried out as double runs, Fig. 1. Two consecutive speed runs have to be performed with the same engine setting and reciprocal heading. By considering the average of both runs the impact of current along the ship heading is cancelled. The initial heading has to be chosen so that the dominant wave system is coming from ahead (most time meaning head wind as well) and is following the ship for the reciprocal heading.

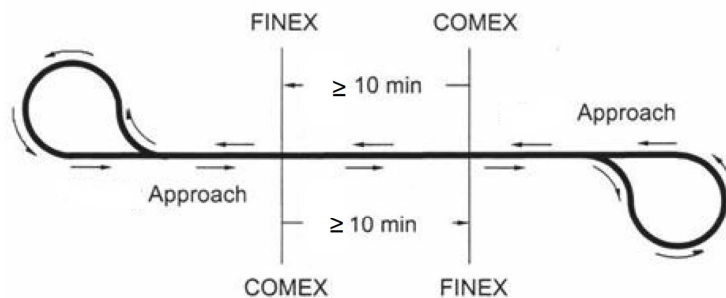


Fig. 1: Track of double run

In this way side forces are prevented and applied rudder angles can be reduced (maximum acceptable steering angle during speed run is 5°). Normally, the autopilot is switched on to keep heading. Drifting of the vessel might occur due to side current which does not affect the ship speed value since the ship speed is defined as headway distance divided by elapsed time. For a reliable current correction with double runs all runs should be evenly distributed in time. All runs have to be performed in one series one after the other. Duration of each speed run should be minimum 10 minutes.

Double runs have to be performed for minimum 3 different power settings. Power setting means constant lever setting which means usually constant shaft speed and in case of CPP constant propeller pitch as well. Lever setting must be kept constant for both runs of each double run. This means explicitly that there will be differences in shaft power between runs with the same power setting but waves and wind from ahead or astern. The three power settings should be chosen that one setting is nearby EEDI power (typically 75% MCR), one power setting is below EEDI power but above 65% MCR and the third power setting is above EEDI power.

EEDI draft is different for different ship types. Often S/P trials cannot be performed in EEDI draft, then a different draft has to be chosen (generally ballast draft). Model tests must be available for test draft and EEDI draft to calculate the transfer of results to EEDI draft.

A typical measuring set-up as applied by DNV GL for S/P trials is shown in Fig. 2. All measured data are displayed on the bridge. In this way the procedure of S/P trials can be checked, particularly it can be seen whether stable conditions are achieved for each speed run.

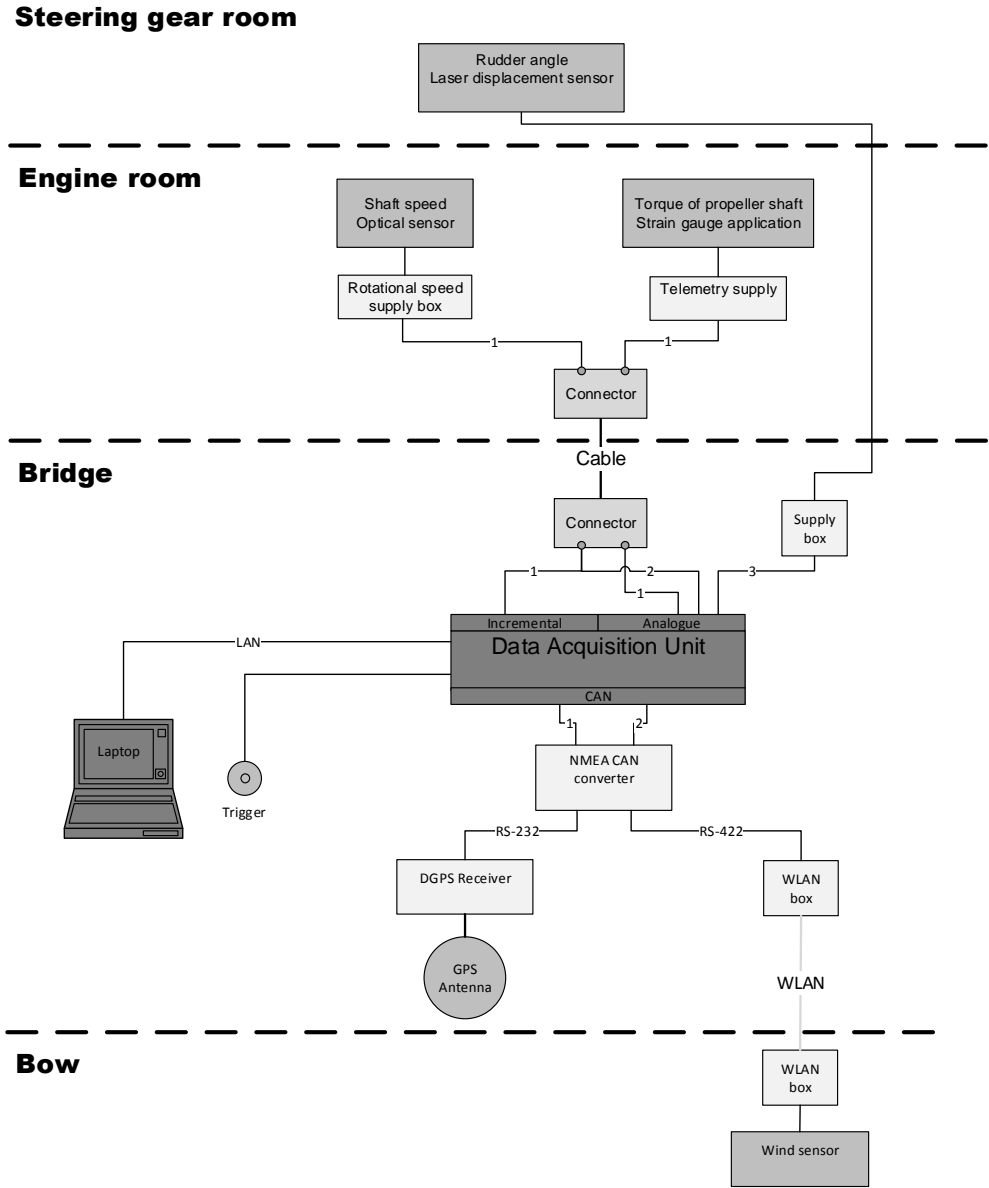


Fig. 2: DNV GL measuring set-up for S/P trials

3. Accuracy of S/P trials

ISO 15016 measurement target for an accuracy of 2% in shaft power and 0.1 kn in speed. This accuracy refers to the final values; it includes the accuracy of measurement, of correction due to the environmental conditions and of the transfer to EEDI draft.

The inaccuracy of measurements can be reduced to the uncertainty of shaft power measurement. The ship speed is measured by D-GPS which is very accurate. The speed is determined from the distance between start and stop position. The distance for speed runs of 10 minutes is above 2 nm, the accuracy of the position measurement is around 1‰ of the distance.

Usually, the dominating corrections of measured shaft power are due to sea state and wind impact. The correction methods are defined by ISO 15016:2015. Partly, these correction methods are rough application of model test experience based formula. Nevertheless, the main inaccuracy of corrections is not due to these formula or the applied coefficients but due to the values for wave height and relative wind speed. Correction values are mainly dependent on the square of wave height and wind speed meaning that the inaccuracy increases with higher waves and stronger wind.

The current correction is determined by the series of double runs. There is not a measurement uncertainty as for ship speed log measurements. The inaccuracy of speed logs already exceeds the targeted accuracy of the ship speed determination. Besides, speed logs are slightly dependent on draft and trim and therefore these devices are not suitable for S/P trials but of course standard for performance monitoring. With one double run a constant mean current can be determined. With a series of double runs a time variant current can be fitted to the measured data. This method gives reliable results as long as the current variation follows a linear and sine function. These time histories can usually be expected with regard to ocean and tidal currents. The trial area must be carefully selected to make sure that the assumptions for the current are fulfilled.

The final step of the speed trial evaluation is the transfer of the results to EEDI draft. This transfer is based on model test results. With regard to the accuracy of the ship speed results it is important to note that not the absolute model test values are relevant for the transfer but the relation of model test results for sea trial draft and EEDI draft. As long as the same model and procedure are used and the same correlation factors for the different drafts are applied a reliable relation between the results for the different drafts can be expected. For most vessels (bulk carriers, tankers) the EEDI draft agrees with the scantling draft. It is different for container vessels where the EEDI draft is decided to be 70% of the scantling draft with regard to the usual displacement of container vessels in service. It must be noted that model test basins have much experience with model test results in ballast and scantling draft. But for this 70% scantling draft experience is still missing. Experience means particularly to get results from full-scale tests to validate the prediction.

3.1. Shaft power measurements

For shaft power measurements a strain gauge application is applied. Four strain gauges are combined to a Wheatstone bridge. The arrangement of the strain gauges on the shaft might cause some measuring inaccuracy due to angular deviation but this effect is only very small.

Strain gauges change the resistance when a mechanical strain acts on the strain gauge. The sensitivity of the strain gauge is given by the gage factor k . This value is typically around 2 and must be given by the manufacturer. The accuracy of the gage factor is usually $\pm 1\%$. The resulting torque and shaft power are linearly dependent on the gage factor.

A second factor to regard is the G-modulus. This value is applied to calculate the stress from measured strain. It is a characteristic value of the shaft material. ISO 15016 states a standard value of 82,400 N/mm². The accuracy of this value is $\pm 1\%$ as well.

Inaccuracy of signal amplification can be kept small. A shunt calibration as shown in Fig. 3 can be used to check the calibration of the measuring chain. For the shunt calibration a resistance is put in parallel to one of the strain gauges and the measured signal can be related to the change in resistance.

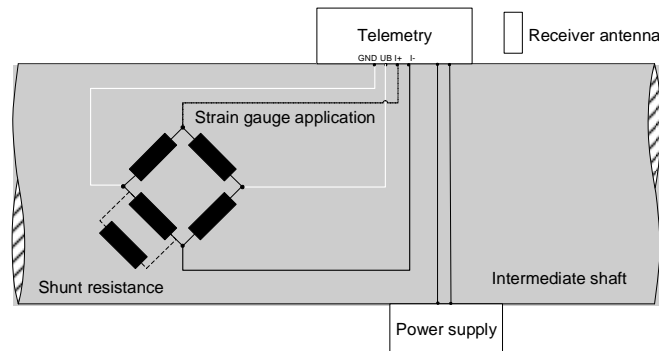


Fig. 3: Shunt calibration of strain gauge application

Finally the zero setting of the strain gauge application has to be checked. This is done by turning the shaft with the turning gear. The mean value of turning forward and reverse 360° each is the valid zero. Summing up the inaccuracies of the shaft power measurements give an uncertainty of 1.5% for the shaft power measurement which is mainly caused by inaccuracy of gage factor k and G -modulus.

The uncertainty of shaft power measurement for performance monitoring is completely different. For performance monitoring relative values are of interest and not absolute values as needed for the EEDI speed trials. Both main contributors to uncertainty are constant for each shaft power installation. Therefore, both factors do not influence the accuracy of performance monitoring as long as the same shaft power meter is applied. For performance monitoring with regard to relative values the zero setting is the most important source of inaccuracies and has to be checked regularly.

3.2. Wave correction

Usually the significant wave height and direction are determined by visual observation prior the S/P trials. The significant wave height is the mean value of the one third highest waves in a spectrum. It is the wave height that agrees with the visual impression. To avoid discussions and subjective values and to get a better accuracy DNV GL recommends the measurement of wave height. The measurement allows performing the S/P trials during night (when visual observation of wave height is impossible) and increases the maximum acceptable wave height during S/P trials.

Often a differentiation between wind waves and swell is made. This makes sense when the swell has a different direction than the wind waves. A differentiation for waves in the same direction is almost impossible for visual observation. The difference is that swell has a longer period (more than 12 seconds) whereas wind waves compose a spectrum with periods within the range between 3 seconds and 12 seconds.

For wave correction the wave height of wind waves and swell are added $\left(H = \sqrt{H_{wind}^2 + H_{swell}^2} \right)$.

DNV GL has developed a simple wave buoy that can be dropped into water before S/P trails when the vessel is stopped. For 20 minutes the buoy is drifting on the water surface and an integrated gyroscope measures the elevation. From the spectrum of measured height, the significant wave height can be calculated, Fig. 4. If needed the wave buoy is dropped into water once more after finish of speed trials. The wave buoy allows measuring the wave height with an accuracy of 10 cm. For performance monitoring this wave buoy is not suitable since the vessel must be stopped for measurement. The application of the buoy is restricted to sea trials.

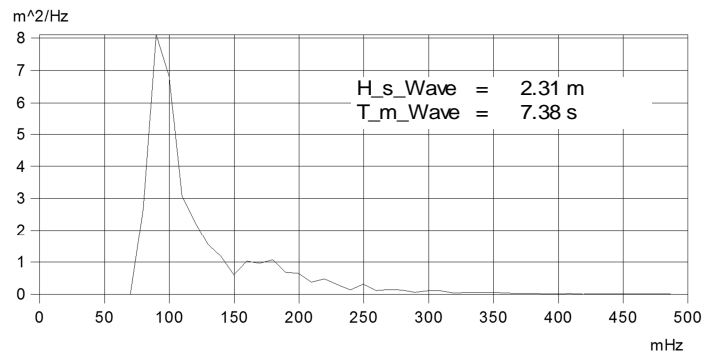


Fig. 4: Measured wave spectrum

3.3. Wind correction

The relative wind speed and direction are measured with a wind sensor on board. Commonly the ship's anemometer is used. The position of this sensor must be checked. Especially on top of the deckhouse it should have enough distance to deckhouse (placed on top of radar/lamp mast). Otherwise the wind flow around the superstructure or the radar mast itself will strongly affect the measured data. DNV GL usually installs a wind sensor on the lamp mast at the bow to measure an undisturbed wind flow, Fig. 5.

Often the true wind speeds calculated from both speed runs of a double run differ. According to ISO regulations the mean true wind value of both runs of each double run is taken to get still reliable wind data. This pragmatic procedure ignores the fact that the strong headwind is generally measured with a higher accuracy than the low relative wind when the true wind is following the vessel. A weighting of both true wind values of one double run should be considered.

Besides, the measured wind data are corrected with regard to the height of the anemometer. A power 1/7 function is assumed for the wind profile. The measured wind speed is transferred to the reference height (usually 10 m) of the wind coefficients. For performance monitoring the same transfer of the measured wind data to the reference height is required. A full-scale measurement to verify the wind profile would be useful.

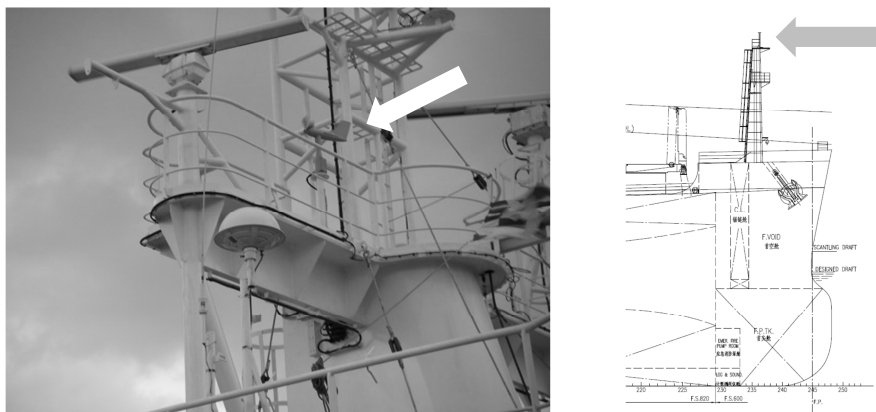


Fig.5: Position of anemometer

4. Comparison of sister vessels

S/P trials were performed on a series of container vessels. In sum, 37 vessels were investigated. Within the series the design was enlarged by 1 container row. Besides, a part of the vessels was equipped with a different main engine. The main characteristics of the series of ships are given in Table 1.

Table 1: Ship's characteristics

	Ship 1	Ship 2	Ship 3	
No.	13	18	6	
Hull	L_{pp} [m]	195.4	209.62	209.62
	B [m]	29.8	29.8	29.8
	T_A [m]	7	7	7
	T_F [m]	4.5	4.5	4.5
	Δ [t]	18570	21427	21427
	C_B	0.5558	0.582	0.582
	A_M [m ²]	163	163	163
	A_{XV} [m ²]	656	656	656
	Engine	P_{MCR} [kW]	21770	21770
n_{MCR} [min ⁻¹]		108	108	95
Propeller	Z	5	5	6
	D [m]	7	7	7.1
	P [m]	6.623	6.608	6.679
	P/D	0.946	0.944	0.941
	A_E/A_0	0.7	0.7	0.7

The S/P trials were performed and analyzed in accordance with ISO 15016:2002. The resulting ship speed was related to a shaft power of 17,500 kW and the shaft power was related to a ship speed of 22.8 knots accordingly. The results are listed in Tables 2 and 3. The complete series has a standard deviation of 1% in ship speed and 3.7% in shaft power. Dividing for the different ships (ship 1-3 as defined in table 1) gives the same result. Nevertheless, it can be seen that for ship 3 the mean ship speed is a little bit higher and the shaft power correspondingly lower. For ship 1 and 2 no significant difference appears. A further differentiation of the results was analyzed with regard to the environmental conditions during S/P trials. When only S/P trials with wind speeds of not more than 4 Bft are taken the number of ships reduces to 16. Nevertheless, the standard deviation of the results does not change significantly. This fact shows that the spreading of the results is not due to inaccuracies of the correction of data with regard to the environmental conditions. Rather there are indeed differences between the sister vessels. Reasons for the differences might be differences in coating and welding. The differences due to the measuring devices are reduced to the arrangement of the strain gauge application since for all S/P trials the same devices were used. An identical G-modulus for the shaft material can be assumed for the series of newbuildings. A graphical presentation of the results is given in Figs. 6 and 7.

The results of this investigation are in agreement with values given in literature. Krapp and Bertram (2015), state a variation of 5.6% in power and 0.5 knots in speed respectively. Before implementation of EEDI, S/P trials were often accurately performed for prototypes, meaning the first vessel of a series of sister vessels. But for the following sisters the S/P trials were reduced to one double run. These trials on sister vessels were only to check the results of the prototype and when agreement was found the result of the prototype was taken for the sister ship as well.

Table 2: Ship speed values for 17,500 kW

	Number	Min	Max	Mean	Span		Standard deviation	
					absolute	relative	absolute	relative
All Ships	37	22.520	23.358	23.003	0.838	3.64%	0.229	0.99%
All Ships < 4Bft	16	22.625	23.358	23.003	0.733	3.19%	0.235	1.02%
Ship 1	13	22.696	23.311	23.006	0.615	2.67%	0.223	0.97%
Ship 2	18	22.520	23.358	22.933	0.838	3.65%	0.222	0.97%
Ship 3	6	22.964	23.350	23.205	0.386	1.66%	0.296	1.28%

Table 3: Corrected shaft power values at 22.8 knots

	Number	Min	Max	Mean	Span		Standard deviation	
					absolute	relative	absolute	relative
All Ships	37	15931.000	18198.000	16945.243	2267.000	13.38%	633.382	3.74%
All Ships < 4Bft	16	15931.000	17941.000	16923.875	2010.000	11.88%	667.191	3.94%
Ship 1	13	15931.000	17911.000	16924.923	1980.000	11.70%	662.947	3.92%
Ship 2	18	15978.000	18198.000	17139.611	2220.000	12.95%	588.504	3.43%
Ship 3	6	15999.000	17071.000	16406.167	1072.000	6.53%	412.670	2.52%

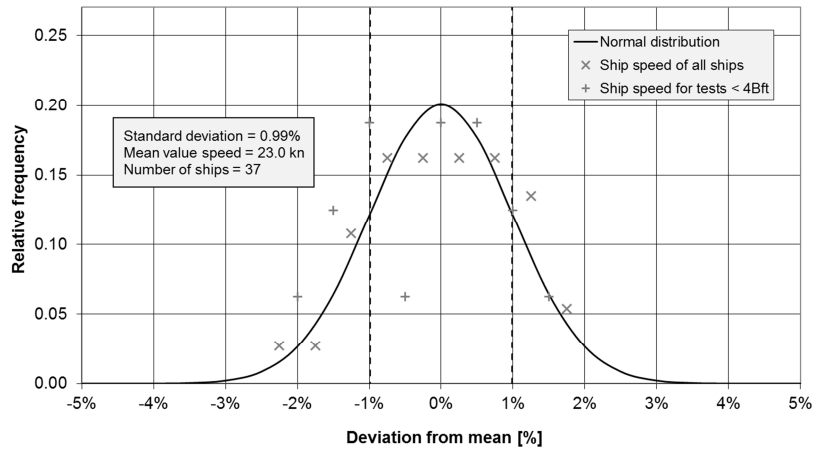


Fig. 6: Deviation of ship speed for 17,500 kW

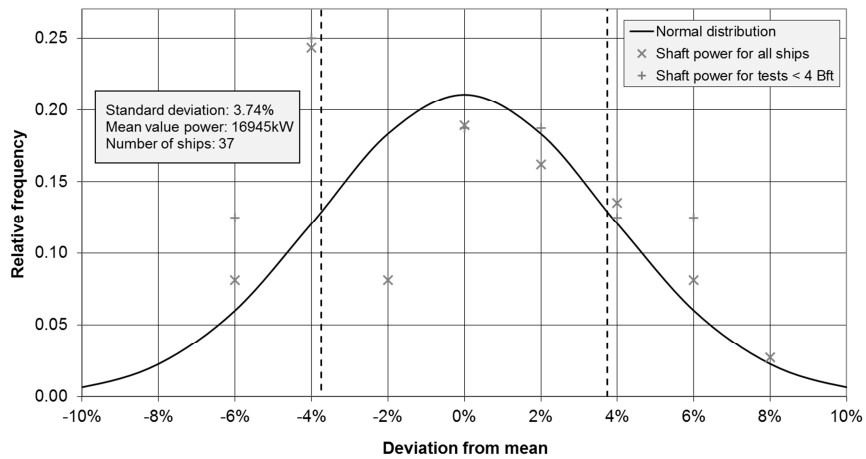


Fig.7: Deviation of corrected shaft power at 22.8 knots

IMO has decided that the EEDI is calculated for each individual vessel of a series based on the individual sea trial results. Nowadays, accurate S/P trials will be performed for all vessels under EEDI regime. The number of double runs for sister vessels is still reduced in comparison with the number of double runs required for first ships of a series but the minimum number of double runs is three which allows reliable results.

In this way, sea trials of newbuildings give an individual base for the performance monitoring of each ship, whereas model tests are a common base for the whole series. Of course, performance monitoring is focused on the change of performance of a specific vessel. Nevertheless, the comparison between sister vessels is common practise to evaluate the performance of a ship. In future, this comparison can be led back to the newbuilding sea trials.

5. Conclusions

The speed trials yield speed-power curves; that is the same in performance monitoring, except for the required accuracy. Accordingly, the procedures differ somewhat. The main difference is that speed trials give absolute values – the ship speed of the vessel for a given power with a defined accuracy - whereas performance monitoring is focused on relative comparison – the change of ship speed for a given power with time.

Speed trials yield an accurate reference curve for the performance monitoring. This curve is individually determined for each sister ship of a series and not only a common curve for the whole series as

model test curves are. EEDI requirements yield additional results for intermediate drafts. For container vessels, the relevant EEDI speed has to be determined for a draft corresponding to 70% of the deadweight. This additional information is useful for performance monitoring models. On the other hand, ship performance measurements can be used to validate model test results especially for these intermediate drafts where correlation factors are questionable due to insufficient experience.

References

IMO MEPC 64/INF.22 (2012), *First version of industry guidelines on calculation and verification of the Energy Efficiency Design Index (EEDI)*

ISO 15016:2015 (2015), *Ships and marine technology – Guidelines for the assessment of speed and power performance by analysis of speed trial data*

KRAPP, A.; BERTRAM, V. (2015), *Hull Performance Monitoring – Combining Big Data and Simulation*, COMPIT Conf., Ulrichshusen, pp.57-63

Numerical Towing Tank versus Noon Data – Powering Predictions using RANSE CFD

Lars Greitsch, MMG, Waren/Germany, greitsch@mmg-propeller.de

Tom Goedicke, MMG, Waren/Germany, goedicke@mmg-propeller.de

Robert Pfannenschmidt, MMG, Waren/Germany, pfannenschmidt@mmg-propeller.de

Abstract

Accurately predicting the powering performance of ships has gained increasing relevance in the recent years. Increasing ship dimensions and decreasing vessel speeds put model testing to its limits. The present work outlines an alternative approach combining state of the art CFD methods with sophisticated analysis of ship operational data. Noon data of a representative container vessel are evaluated using a multi-stage method. Numerical propulsion simulations have been conducted using RANSE CFD methods.

1. Introduction

Numerical approaches become increasingly important regarding propulsion test procedures. It is still too expensive and time consuming using RANSE CFD for full-scale calculations at least at industrial applications. Yet it seems to be the most appropriate method to gain full information on flow effects around a propeller working on a sea going ship.

It is common practice to use RANSE CFD for propulsion calculations in model scale as tested in a model basin. Still the uncertainty of common scaling procedures and especially the discrepancy in Reynolds number between model test and the full-scale ship makes it very difficult to optimize a propeller for the flow around a sea going ship. For this reason, the first objective of this work is to gain a good validation basis for CFD powering predictions out of noon data reports.

Using limited calculation resources CFD still offers the possibility of studying very low model scale values or in this case different model scale values to get an impression of scale effects and develop a power performance prediction, which considers this.

Mecklenburger Metallguss GmbH (MMG) started systematic investigations of such scale effects at a very early stage focused on scale influences on the open-water performance and the development of advanced scaling methods, Müller *et al.* (2009), Streckwall *et al.* (2013). This research was fundamental for propeller optimisation specialised for slow steaming container vessels, Will and Greitsch (2014). The present paper continues the full-scale oriented enhancements of propeller design methods.

2. Test Case

The study presented in this paper is based on a 5000 TEU container vessel. The particulars of the vessel are shown in Table I.

Table I: particulars of vessel

Length PP	283.00 m
Breadth	32.20 m
Design Draught	12.00 m

Database for the study is a noon report consisting of 250 data points (see Fig. 1). In addition, a well-validated numerical towing tank simulation method is used to produce model test results in two different scale ratios, Lezhnin (2014).

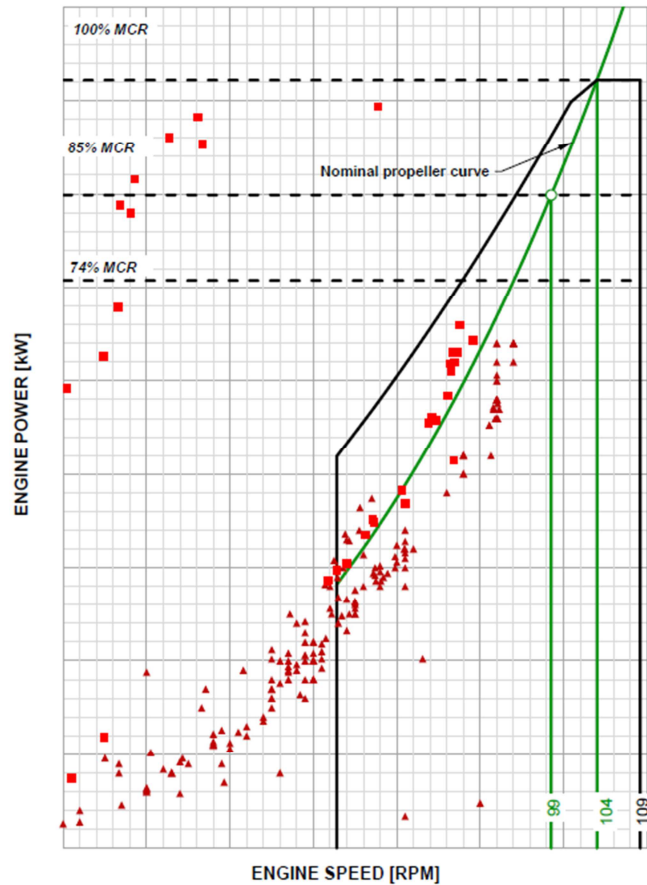


Fig. 1: Raw noon data points in engine diagram

3. Noon-Data Analysis

Noon data reports give the opportunity to gain the important information of how a full-scale powering prognosis agrees with reality. Unfortunately, it is rather difficult to extract useful data from what is plotted during vessel operation. There is a variety of uncertainties to be aware of while filtering noon reports, e.g.

- Weather reporting
- Averaging of reported variables during the voyage
- Torque measurement
- Vessel speed dependency on current

In this study, a two-step filtering method is used to find appropriate values to validate powering prognosis from numerical model tests.

3.1. Filtering Methods

3.1.1. Filtered by propeller characteristics

For filtering data points, which do not represent a good average of vessel operation during the journey it is a good option to use the propeller characteristics, Fig. 2. Data points reported during very inconsistent weather conditions will most likely not match the propeller characteristics. This first step leads to the selection of data points shown in Fig. 3. It can clearly be stated that this filter leaves a very plausible range of data, when comparing with the raw data in the engine diagram of the vessel (see Fig. 3). The speed power diagram in Fig. 3 shows filtered data and three estimated curves describing a trial prediction at design draught, 15% sea margin and 30% sea margin of a similar vessel.

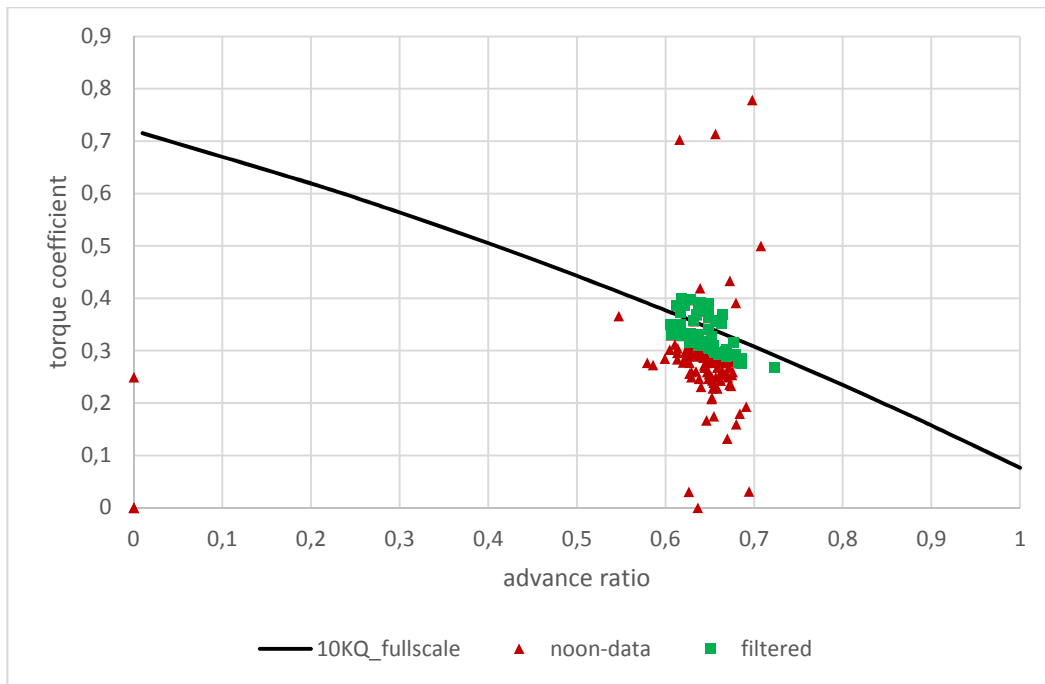


Fig. 2: Propeller open-water curve with noon data points

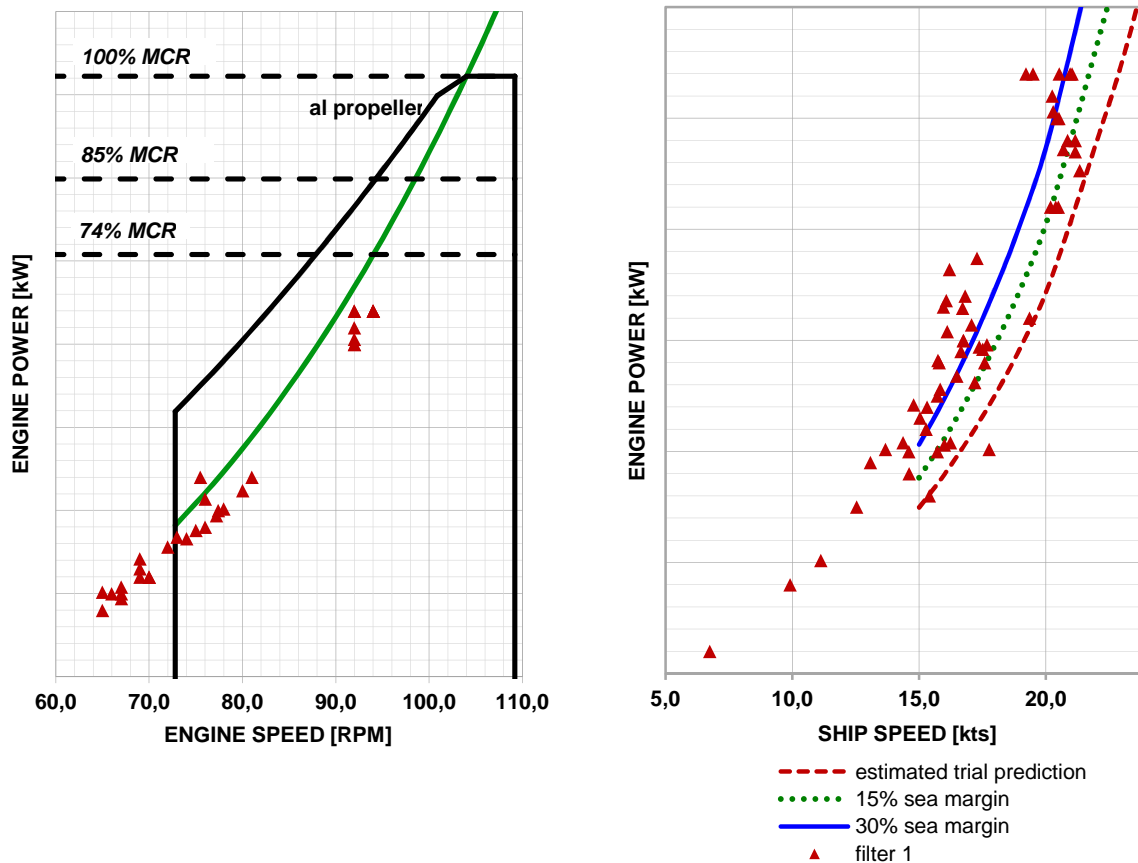


Fig. 3: Filter1: rpm-power, speed-power

3.1.2 Filtered by operation data

Second stage of data analysis is the evaluation of operational influences in the remaining data points. Obvious filter options at this stage are:

- Draught
- Trim
- Weather conditions

For the studied vessel filtered data for draughts less than design draught can be seen in Fig.4.

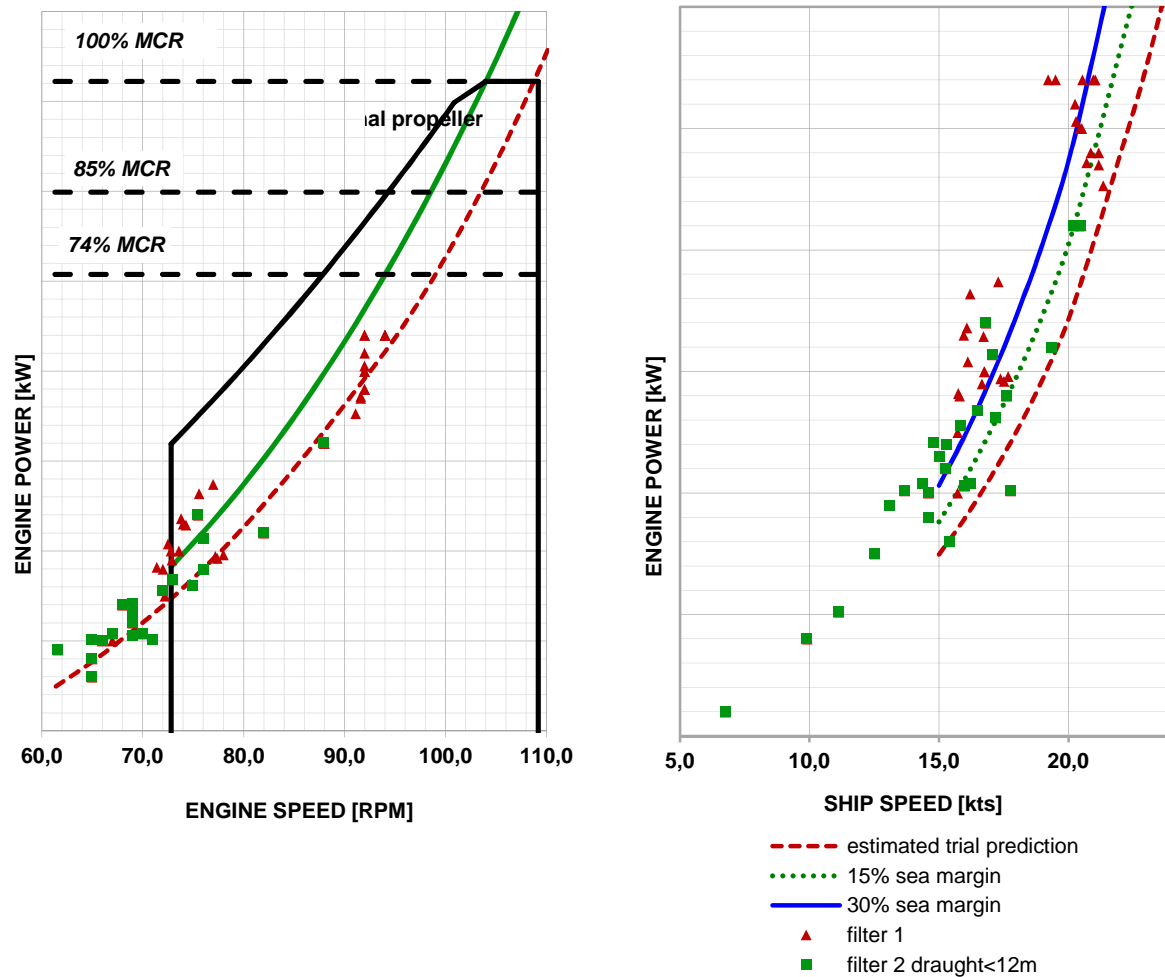


Fig. 4: Filtered by draught

4. Numerical propulsion simulation

Motivation for the numerical study was to develop an in house powering prognosis, which is as close as possible related to the operating vessel. Furthermore an objective was to find a tendency in the prognosis results due to the different scale ratios, which should give an indication on how to handle a prognosis done with model results of certain scale ratio.

4.1 Models and calculation case

For the container vessel described in Table I numerical towing tests were carried out at model scale 1:20 and 1:40, analysed regarding hull efficiency elements and full scale powering prediction using ITTC standard procedures, *ITTC (2011)*. Calculations were done using fully turbulent, unsteady RANSE CFD. As the flow around the propeller is the main point of interest for a propeller designer, ship hull and propeller geometry are completely resolved by the numerical mesh. The flow regime is defined to be fully turbulent in each of the scale ratios.

For the implementation of the rotating propeller domain into the stationary ship domain a cylinder is cut out of the ship domain to put in the separately generated propeller mesh as shown in Fig. 5. The coupling between both domains is done using the Generalized Grid Interface. An overview of the numerical setup used in this work can be seen in Table II.

Table II: Numerical setup

	Scale 1:40	Scale 1:20
Solver	Ansys CFX	
Numerical Approach	RANSE + $k-\omega$ SST turbulence model	
Grid Topology	tetrahedral mesh	
Average yPlus	100	
Number of Cells	10,000,000	3,000,000
Rotor stator interface	GGI	GGI

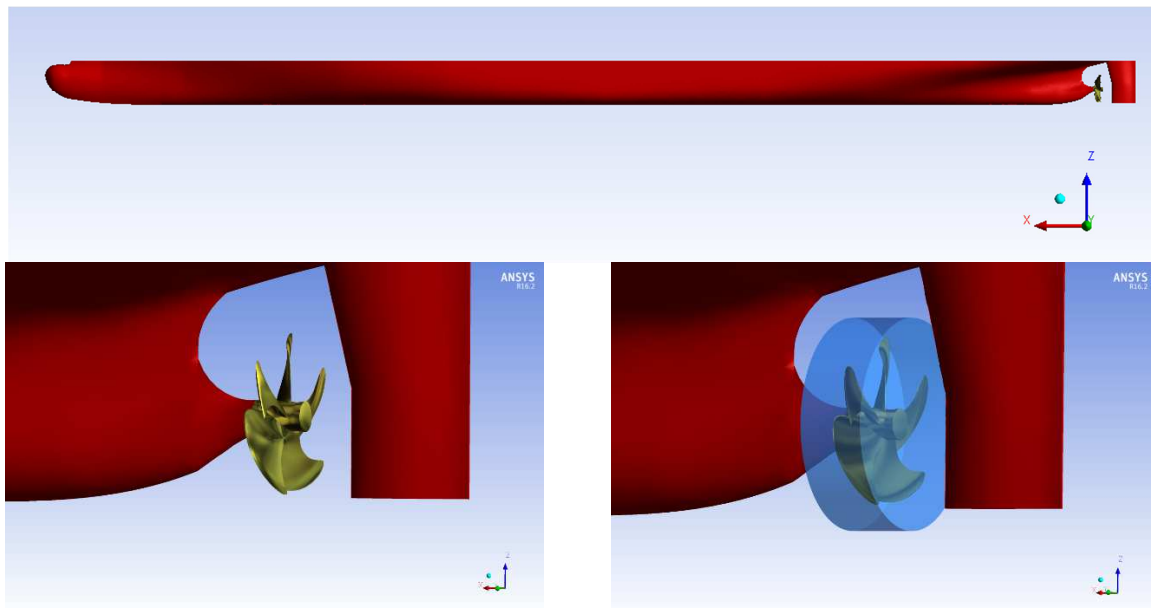


Fig. 5: Propulsion arrangement and sliding interface

4.2 Results

The first objective of this study is to show a comparison between numerically predicted powering curves and noon data reports. Looking at the ITTC prognosis based on the numerical results, Fig. 6, it can be stated that the agreement with filtered noon reports is very good. As the simulation can be compared with trial condition, the CFD prognosis describes the lowest level of the speed-power noon data. In addition, the rpm-power prediction is representing an expected trial condition quite well, which is most important at fixed pitch propeller design.

Table III shows the hull efficiency elements of both calculation cases. The values are represented in a reasonable range. Still there is a significant deviation in thrust deduction factor between the differently scaled models, which can be identified as an effect of increasing relative uncertainty in the measured or calculated forces. The calculations at scale 1:40 show an unexpected small thrust deduction factor in comparison to scale 1:20. According to empirical formulations given in *Dudszus and Danckwardt (1982)* the thrust deduction can be estimated in the range $t=0,126...0,179$. In this respect the results obtained with scale ratio 1:20 can be considered more reliable than those at scale ratio 1:40.

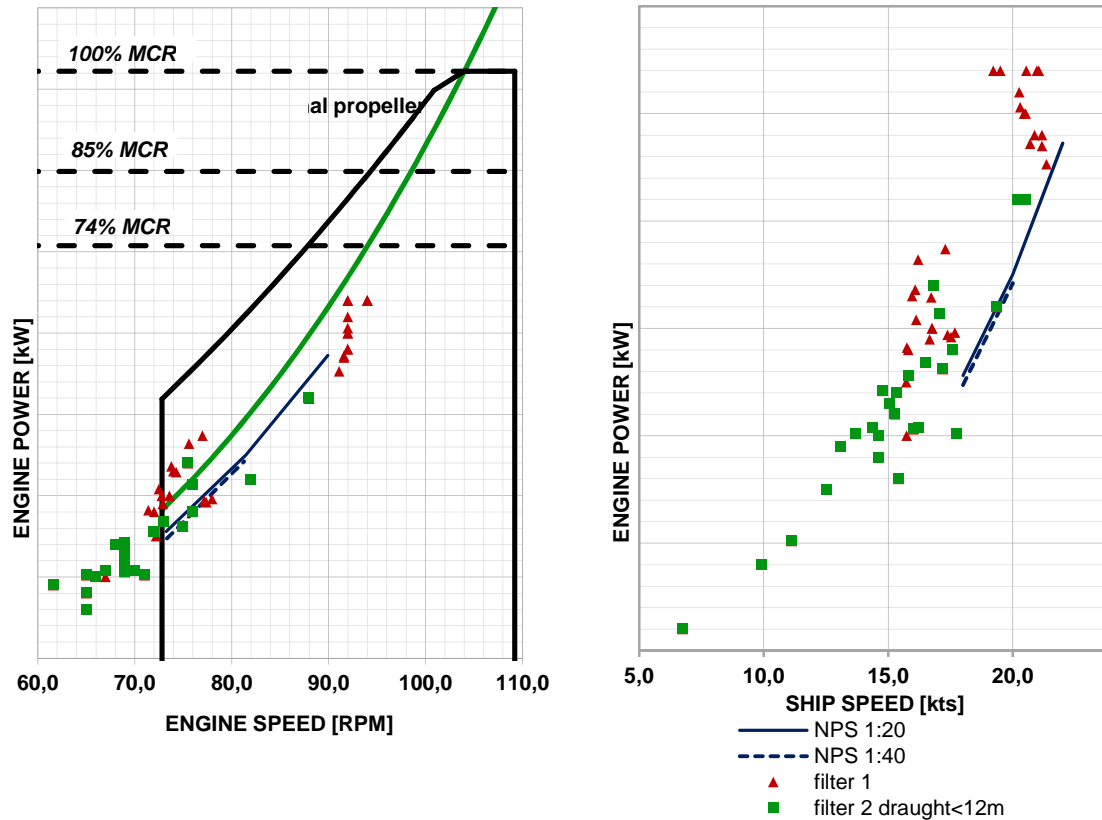


Fig. 6: CFD prediction

Another effect, which can be identified, is a shift between the relative rotational efficiency η_R and the hull efficiency η_H consisting of wake fraction and thrust deduction. The reason can be seen in scaling procedures, mainly those of propeller open-water curves and the uncertainty of thrust deduction as explained above, *Bugalski et al. (2013)*.

Table III: Hull efficiency elements for 18 knots

	Scale 1:40	Scale 1:20
wake fraction	0.18	0.203
thrust deduction	0.08	0.143
η_H	1.122	1.075
η_R	0.965	1.006
η_o	0.665	0.649
η_D	0.720	0.702

5. Conclusion

Regarding the presented noon data filtering, especially for dealing with big amounts of data, the multi-stage filtering method is a good option taking information from documented vessel operation.

The powering prognosis based on CFD calculations showed very good agreement with noon reports regarding speed-power and rpm-power, for both calculated model scales. A rather big influence of the scale ratio could be found in hull efficiencies. A tendency towards more reliable values using less scaling could be noted.

Future work will consist of performing numerical propulsion simulations in full scale to be able to verify the tendencies stated in this paper. Further investigations on reliability of prognosis methods for more sophisticated propulsion arrangements including energy saving devices will be done.

References

- BUGALSKI, T.; STRECKWALL, H.; SZANTYR, J. (2013), *Critical review of propeller performance scaling methods, based on model experiments and numerical calculations*, Polish Maritime Research Vol 20, pp.71-79
- DUDSZUS, A.; DANCKWARDT, E. (1982), *Schiffstechnik. Einführung und Grundbegriffe*, VEB Verlag Technik, Berlin
- ITTC (2011), *1978 ITTC Performance Prediction Method*
- LEZHNIN, P. (2014), *Numerical self-propulsion tests with ANSYS CFX*, ANSYS Conf. 32nd CADFEM User's Meeting, Nürnberg
- MÜLLER, S-B.; ABDEL-MAKSOUUD, M.; HILBERT, G. (2009), *Scale effects on propellers for large container vessels*, 1st Int. Symp. Marine Propulsion (SMP), Trondheim
- STRECKWALL, H.; GREITSCH, L.; SCHARF, M. (2013), *An advanced scaling procedure for marine propellers*, 3rd Int. Symp. Marine Propulsion (SMP), Launceston
- WILL, J.; GREITSCH, L. (2014), *Optimized propulsor retrofit for slow steaming for a post-panmax container vessel*, Int. Conf. Ocean, Offshore and Arctic Engineering (OMAE), San Francisco

Experiences with ISO-19030 – and Beyond

Antti Solonen, Eniram Ltd, Helsinki/Finland, antti.solonen@eniram.fi

Abstract

In this paper, we discuss our experiences with ISO-19030 hull and propeller performance monitoring methodology. In particular, we present approaches for generating speed-power reference curves using in-service data, in accordance with part 3 of the standard, and discuss the challenges faced with different vessel types. We also compare the ISO-19030 results to our own "model-based" hull performance tracking approach, where hull fouling is described by introducing a time-evolving resistance component on top of our propulsion power model. The comparison shows that the noise level is dramatically reduced compared to ISO-19030, which enables more detailed assessment of hull treatment effects. Moreover, with the model-based approach we can, for instance, track how the power consumption in calm-sea conditions at a given speed develops over time, which enables vessel comparisons and "fleet-wide" performance monitoring. We present various real-data examples with different vessel types using data collected via the Eniram platform.

1. Introduction

The ISO-19030 standard defines a practical approach for hull and propeller performance monitoring. The approach is based on calculating so called Performance Values (PVs) that track the speed loss (or power loss) compared to a reference speed-power curve. The PV time series are then used to calculate various Performance Indicators (PIs), such as dry-docking performance and maintenance effect.

One of the main aspects in implementing the standard is obtaining speed-power reference curves. The suggested methods for deriving these curves, defined in Part 2 of the standard, include a) full-scale speed trials, b) towing tank tests and c) CFD calculations. However, these approaches can be difficult to implement for many parties that offer performance monitoring solutions; e.g., data from full scale speed trials or towing tank tests might not be easily available, and performing vessel-specific CFD simulations can be a daunting task. For these reasons, Part 3 of the standard discusses alternative speed-power curve generation methods that utilize in-service data collected from the vessel. In this paper, we discuss approaches for doing the data-based speed-power curve estimation in practice. We present various real-data examples and discuss the challenges faced with different vessel types.

One benefit of the ISO-19030 approach, in addition to providing a unified methodology and measures for hull performance monitoring, is that it is rather simple and thus robust. The approach can be implemented with a modest number of input variables, and currently contains only a simple correction for wind resistance. On the other hand, the accuracy of the PVs might be limited due to a) the simplicity of the resistance correction and b) the usage of the often poor quality STW measurement as one of the primary variables. Another potential downside of the ISO-19030 approach is that the calculated PVs are not easily comparable between vessels.

In this paper, we discuss the basic principles behind our own "model-based" hull performance tracking approach, which can help in solving the aforementioned issues. In the method, we use our own propulsion power model as the reference, and describe hull fouling by introducing a time-evolving resistance component on top of the power model. The output (power loss compared to a reference model) can still be made "ISO-19030 compatible", but the noise level is dramatically reduced compared to the standard approach, which enables more detailed assessment of individual hull treatment effects. Moreover, since the fouling model is coupled tightly with the propulsion power model, we can estimate the vessel's power consumption at any conditions with and without the fouling resistance. For instance, we can track how the power consumption at calm sea conditions develops over time, which yields an interesting fouling indicator that *is* comparable between vessels, and also enables "fleet-wide" performance tracking.

The rest of the paper is organized as follows. Section 2 is devoted for the ISO-19030 approach and especially going through some techniques for generating speed-power reference curves using in-service data. Section 3 begins with a short introduction to our propulsion power model, and continues with a description of how we include the fouling resistance into the model. Section 4 concludes the paper.

2. The ISO-19030 Approach

Let us here briefly recap the ISO-19030 methodology. The focus here is on the general principles; see the original standard text for details. Implementing the ISO-19030 approach requires five main steps:

1. Obtain speed-power reference curves from sea trial data, tank test data or CFD calculations. Alternatively, estimate the reference curves based on collected in-service data. The data based method is one of the topics of this paper, and is discussed below in Section 2.1.
2. Filter the data *a*) for outliers and *b*) according to certain reference conditions (e.g. take out high winds). The filter implementation is detailed in the standard.
3. Do a wind correction to the obtained power measurements.
4. Calculate the PVs (either speed loss V_d or power loss P_d) which simply compare the obtained speed and power measurements (filtered and wind corrected) to the reference curves:

$$V_d = 100 \cdot \frac{V_m - V_e(P_m)}{V_e(P_m)} \quad \text{and} \quad P_d = 100 \cdot \frac{P_m - P_e(V_m)}{P_e(V_m)},$$

where the subscript *m* denotes a measured value and *e* denotes the expected value read from the speed-power reference curve.

5. Calculate different PIs using the PVs (dry-docking performance, in-service performance, maintenance trigger and maintenance effect).

Here, we concentrate on the first item in the above list; how to generate speed-power reference curves from in-service data. We also give some real-data examples of how the PVs look like, to get an idea about, e.g., the level of accuracy of the approach.

2.1. Obtaining speed-power reference curves from in-service data

The empirical speed-power curve generation approach outlined in Part 3 of the standard builds extensively on other parts of the standard, such as the data filtering specifications. Thus, once ISO-19030 compliant data has been gathered, it should be straightforward to apply this approach to estimate the curves.

First, one needs to monitor the vessel and gather data for a “long enough” time period so that the relevant speed levels and loading conditions are covered in the data. By loading condition, we here mean the typical draft and trim ranges that the vessel sails at. On the other hand, the data-gathering period should be as short as possible to ensure that the hull condition does not experience any dramatic changes during the period. The amount of data needed obviously depends on the vessel type; cruise vessels typically have small draft and trim effects, and even a pretty short time period might be enough to get a reliable picture of the speed-power curve. Tanker vessels typically have a small number of loading conditions, and it is still pretty straightforward to derive reference curves for each loading condition separately. With container vessels, however, the situation is obviously more complicated. Examples of the method with different vessel types are given in the subsequent sections.

The reference curve estimation is done separately for each loading condition present in the data¹. The technique itself is very simple:

¹ It is left for the “user” to define the relevant draft and trim ranges for each loading condition.

1. Gather data (vessel speed, propulsion power, wind variables).
2. Filter the data according to the ISO-19030 specifications to obtain standard weather and operating conditions (calm sea, deep water, head waves).
3. Filter the data for outliers and validate the data set according to the ISO-19030 specifications.
4. Pick the data that corresponds to the loading condition in question.
5. Fit a speed-power curve to the data.

The approach is demonstrated for a cruise vessel in Fig. 1. After successful outlier removal and filtering according to the reference conditions, one should be left with rather clean speed-power data (for the loading condition in question).

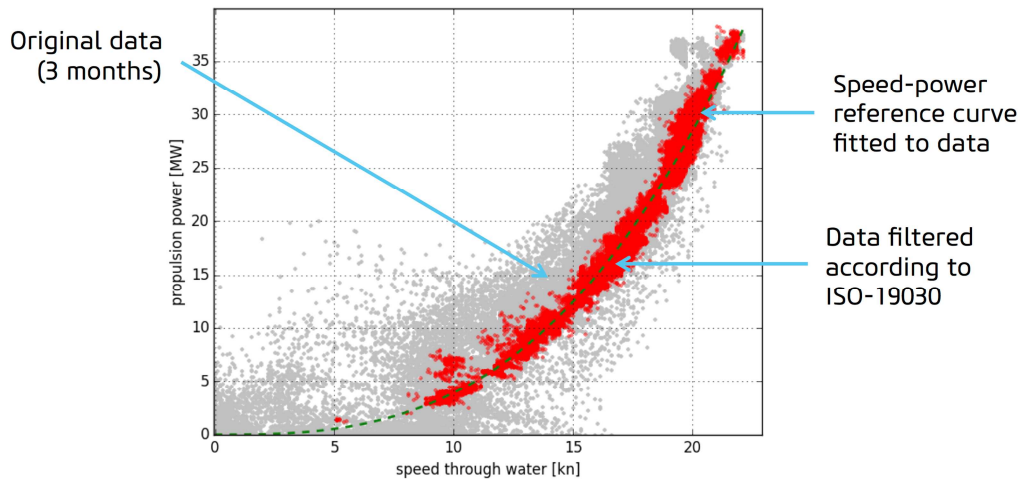


Fig. 1: Original speed-power data, the data remaining after the filtering (and wind correction), and the estimated speed-power reference curve

To implement the approach in practice, we need to define two things: 1) the mathematical form of the speed-power curve and the curve fitting technique, and 2) how to find the different loading conditions (if there is more than one) for which to estimate a curve. These things are discussed next.

2.1.1. Fitting the speed-power curve

The standard only gives some examples on how to do the curve fitting. One has freedom to use basically any approach one wishes, as long as the approach is clearly documented and the quality of the obtained curves is sufficient. Probably the simplest possible choice is to use $P = aV^3$, where a is estimated from data using linear least squares. However, for many vessels, an exponent that differs from 3 might work better, and thus a model $P = aV^b$ might be appropriate. For estimating a and b , it makes sense to linearize the model first by taking logarithms of both sides:

$$\log(P) = \log(a) + b \cdot \log(V).$$

Now, the parameters can be obtained by fitting a line in the $[\log(V), \log(P)]$ -space. This is the approach given as an example in the ISO-19030 standard text. The quality of the obtained curves can be assessed with the standard R2-value.

2.1.2. Finding the loading conditions

Here, when we talk about a loading condition, we mean a draft-trim range at which the vessel is typically operated. Thus, finding the loading conditions means finding typical clusters in the draft-trim space. If these ranges are known beforehand, these known values can obviously be used. If not, one can use data to identify the clusters.

If a vessel only has a few typical loading conditions (e.g. tanker vessels), this clustering can be done manually by just looking at the data visualized in the draft-trim coordinates. However, if the vessel experiences a wide variety of draft and trim combinations, defining the clusters by hand becomes cumbersome. To help in this, we have implemented the following “semi-automatic” clustering technique. We start by visualizing the data points in the draft-trim coordinates, and then let the user click on the figure to give some initial guesses for the cluster centres. Then, we feed the data and the initial guesses to a clustering algorithm (K-means) to automatically divide the data points into clusters. Then, we fit the speed-power reference curve to each cluster separately. The clustering and the obtained curves for a few clusters are demonstrated for a container vessel in Fig. 2.

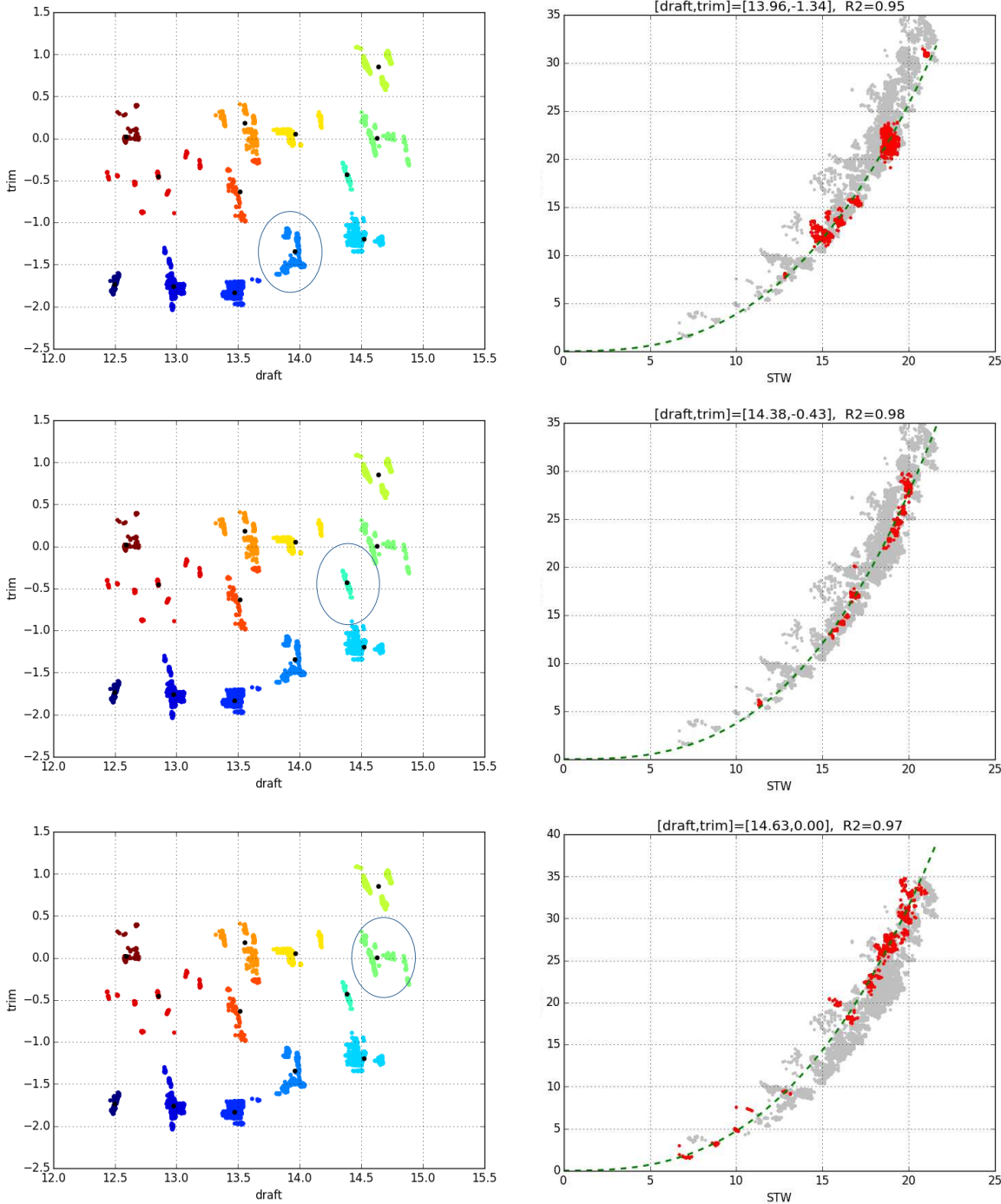


Fig. 2: Left: clusters (colored dots) and cluster centers (black dots) obtained with K-means clustering. Right: the corresponding speed-power data and the estimated reference curve.

When the ISO-19030 approach is applied in practice, we need to obtain the speed-power reference curve for any given draft and trim values. This is done in the standard by interpolating between the reference curves specified for certain draft and trim values (using, for instance, the data-based approach outlined above). Another way to account for varying trim and draft would be to include them into the reference model itself, instead of specifying reference curves separately for each range. This approach is chosen in the fouling analysis technique described in Section 3.

2.2. Example: ISO-19030 Performance Values for a Cruise Vessel

Here, we just visualize the Performance Values given by the ISO-19030 method, just to give a qualitative idea about how the time series look like, and what is the typical noise level, for instance. We choose a cruise vessel here for demonstration purposes, for which we were able to produce a good quality reference curve (the vessel is, in fact, the same that was used to demonstrate the reference curve generation in Fig. 1). The quality of the obtained propulsion power and STW data is rather good, so the example gives an indication of the “best case scenario”. The PV time series are plotted in Fig. 3. It is clear that while the method does reveal the main trends in hull performance, the noise level is such that assessing the effect of individual hull treatments is difficult.

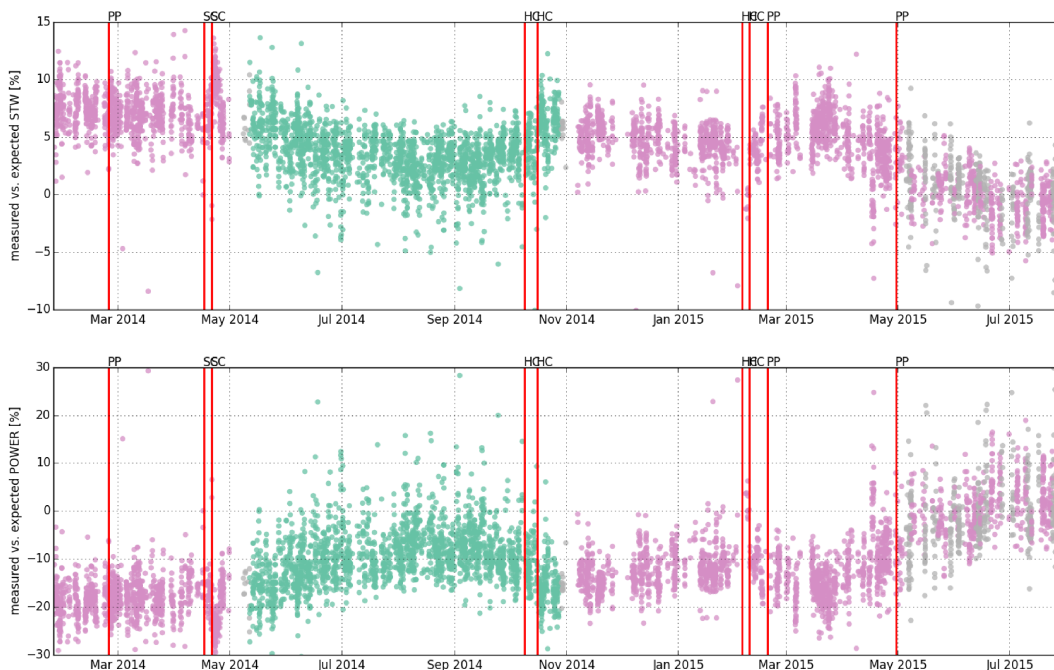


Fig. 3: Speed-loss (top) and power loss (bottom) Performance Values. Vertical lines indicate various hull treatments (PP = propeller polishing, SC = side cleaning, HC = hull cleaning). Color indicates sea area.

3. The Next-generation ENIRAM Fouling Model

At ENIRAM, we have developed a new hull and propeller performance monitoring approach, which leans heavily on our next-generation Propulsion Power Decomposition (PPD) model. The approach is designed to be “ISO-19030 compatible” in the sense that the Performance Values can be output in the same format (e.g., power loss compared to a fixed reference), and thus the same Performance Indicators can be calculated. However, the approach also includes some new ideas about how to track vessels’ performance. The main differences of the ISO-19030 and the ENIRAM approach are listed below:

- ENIRAM’s own PPD model is used to provide the “reference curve” (to calculate the expected power). This model contains a description for many different resistance components,

- as opposed to ISO-19030 that only contains a simple correction for wind resistance.
- The corrections for external factors are not done for the observed power, but the reference model itself contains the descriptions for these factors. Thus, the comparison between measured and expected values is done in the actual conditions, instead of transforming the data first towards calm-sea conditions.
- No extensive filtering to reference conditions is done, since the PPD model includes descriptions for the main resistance components.
- We can replace the noisy and problematic STW measurements with predicted STW, which dramatically reduces the noise level in the Performance Values.
- Hull/propeller fouling is modelled explicitly in the PPD model as a slowly evolving extra resistance component, which is continuously updated based on the obtained STW and power data. As a result, we can, at any time point, perform simulations at different conditions with or without the extra resistance, which allows us to, e.g., estimate the development of calm-sea propulsion power at some selected speed.

In the following sections, we discuss the above points in more detail.

3.1. Introduction to the PPD Model: the “Grey Box” Approach

For completeness, we here describe the basic principles behind our Propulsion Power Decomposition (PPD) model. The basic steps of model building are given as a flowchart in Fig. 4. First, we collect a large amount of data from various sources; most of the variables are obtained via integration to the vessel’s automation system, and some variables are measured via our own sensors installed onboard (trim, list, motion indicators). Then, we combine the mathematical propulsion power model with the measured data using Bayesian regression² and various Machine Learning techniques. This calibration step amounts to, for instance, estimating the different unknown resistance coefficients in the model. After the model has been built, we can calculate the power decomposition (which tells how different factors contribute to power consumption), hence the name Propulsion Power Decomposition.

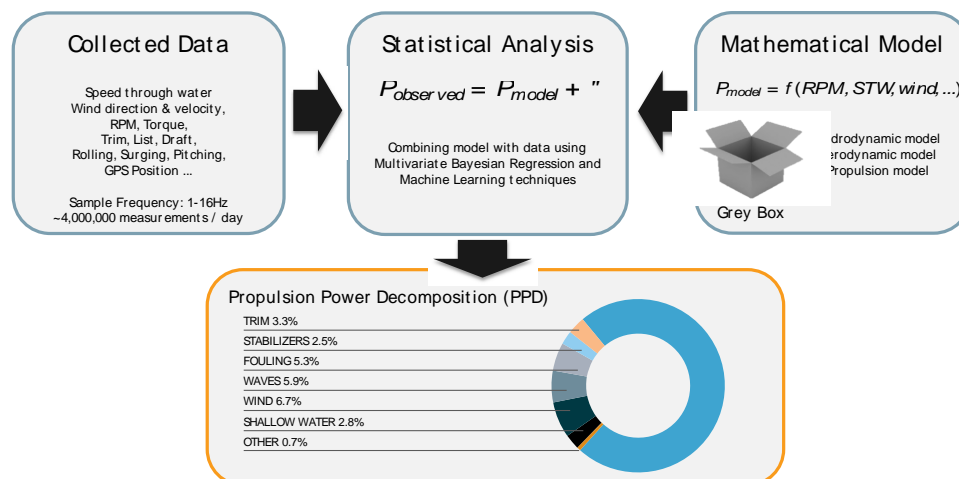


Fig. 4: Flowchart indicating the ENIRAM PPD model creation process

We categorize our modeling technique as a “Grey Box” approach, which, as the name suggests, is a hybrid between two extremes. The other extreme is the pure machine learning “Black Box” approach, where the relationship between the inputs and power consumption is learned from data, without any guidance from physics principles. At the other extreme we have the “White Box” approach, where we use only physics principles and various approximations to figure out, for instance, what the resistance coefficients are. In our “Grey Box” approach, we start from the well-known physics principles and

² See *Gelman et al. (2013)* for a classic textbook about Bayesian data analysis.

refine them with the measured data.

As a concrete example, consider modeling wind resistance. It is well known that the wind resistance is proportional to relative wind velocity squared, where the resistance coefficient depends on the relative wind angle. Many different parametric descriptions for the resistance coefficient are suggested in the literature; see for instance the widely used parameterization by Blendermann (1993), where the coefficient depends on the wind angle and various constants for which values are suggested based on the vessel type. In our approach, we acknowledge the basic fact that wind resistance is proportional to wind speed squared, but treat the resistance coefficient as an unknown function and refine our knowledge about it based on the data, starting from some reasonable “background” behavior³. In our technique, we can easily include “structural” information about the function; for instance, we know that the wind resistance coefficient is a periodic function of wind angle, and we can also force the function to be symmetric about the head wind direction (that is, wind resistance from the left and from the right are always equal)⁴. In addition, it is reasonable to assume that the function is smooth. All of these assumptions can be coded into our estimation methods, and then we let the data inform us about the rest.

An example of the wind resistance coefficient calibrated from data is given in Fig. 5. The blue envelope gives the “background” behavior (expected value \pm two standard deviations), and the black envelope illustrates the “posterior distribution”, which tells us what we can tell about the unknown function after feeding in information from the data. Note how the posterior distribution is narrow with small absolute angles (wind coming from the front) where we have plenty of data, and starts to revert back to the background behavior in regions where we have less data (relative tail wind is rarely seen). This is the core of our “Grey Box” philosophy: refine knowledge in the regions where we have data, and revert back to the “industry standard” in unobserved regions.

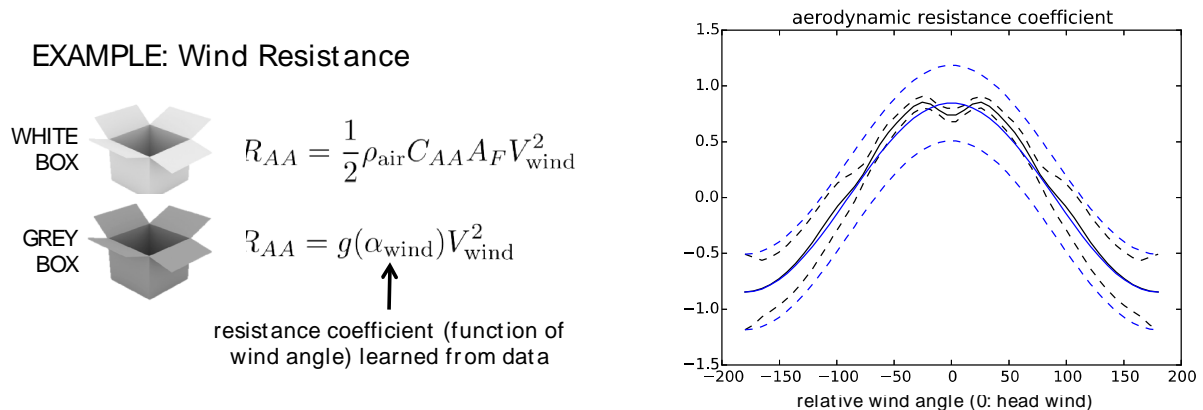


Fig. 5: Illustration of the wind resistance coefficient estimation in the “Grey Box” approach

The mathematical technique we use to express the unknown functions is called Gaussian Processes (GPs). The technique is non-parametric, i.e. we do not have to specify any parametric form for the function, but rather just give some structural information (smoothness, periodicity, etc.) about it. In the past decade, GPs have become a standard tool for non-parametric function approximation in machine learning; see *Rasmussen and Williams (2006)* for a thorough introduction into the subject.

Here, we took wind resistance as one example. Other resistance components treated similarly; frictional resistance coefficient can be set to vary smoothly as function of V (and perhaps draft and

³ In the Bayesian estimation framework this is known as prior information, and refers to the knowledge we have about the unknown before data is collected.

⁴ This is obviously a slight approximation (vessel shape can be slightly asymmetric), but imposing the symmetry constraint restricts the estimation problem nicely.

trim), and shallow water resistance can be modeled as an increasing smooth function of depth-based Froude number, for instance. The GP approach provides a nice framework for “relaxing physics”; we can let the coefficients of parametric resistance descriptions vary as a function of some other variables.

3.2. Fouling Model and Performance Monitoring

The PPD model described above can be used for performance tracking purposes. The most straightforward way to apply it in the ISO-19030 framework would be to use the model, calibrated to some time period, as the reference curve. The benefit of this is that the model contains a more comprehensive set of descriptions of different resistance components, as described above, removing, to some extent, the need for filtering the data according to the reference conditions.

However, we go one step further and implement fouling on top of the PPD model as a time varying extra resistance component. Since fouling affects the frictional resistance, we model the extra resistance to be proportional to vessel speed squared, where the resistance coefficient is allowed to vary in time. The total resistance now becomes

$$R_t^{total} = R_t^{friction} + R_t^{wind} + \dots + k_t V_t^2,$$

where the extra resistance coefficient k_t is allowed to change “slowly” in time. For instance, we can model the dynamics of k_t simply as $k_{t+1} = k_t + \epsilon_t$, where $\epsilon_t \sim N(0, \sigma_t^2)$, and thus via σ_t we can control how fast the resistance coefficient can change. Then, we can use the difference between the observed and predicted power to estimate k_t for each time step. In setting σ_t , we can use our expertise and experience about how fast hull fouling can develop; for instance, if we assume that fouling develops slowly at sea and faster at port, we can set a higher σ_t for times at port. In the future, we can also put more intelligence in how we expect fouling to change at various wash events, sea area changes, etc.

In practice, we use dynamical state space estimation (e.g., Kalman filtering) techniques to update the resistance coefficient estimates as new data is obtained; see *Särkkä (2013)* for a thorough introduction into the subject. Thus, we have, at all times, “up-to-date” power and STW prediction models available that take the current hull and propeller performance into account. This means that we can predict STW and propulsion power accurately with or without the fouling component included. To demonstrate the effect of the dynamically changing extra resistance term, we plot an example of the residuals (predicted power subtracted from the observed power) with and without the term below in Fig. 6. Note how the systematic long-time trends (these are thought to be due to fouling) in the residuals disappear after adding the extra resistance term.

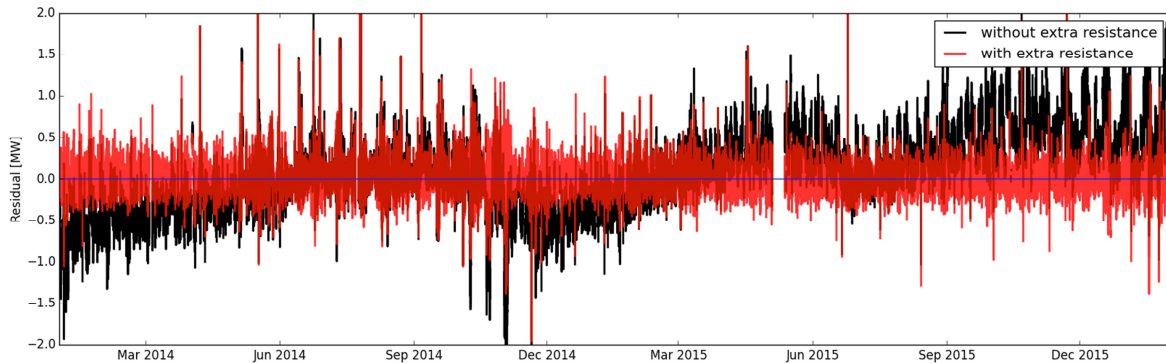


Fig. 6: Power model residuals with and without the extra resistance term

This gives a way to dramatically reduce the noise level of speed-power based performance tracking solutions. To see this, let us look again at the power loss performance values defined in ISO-19030:

$$P_d = 100 \cdot \frac{P_m - P_e(V_m)}{P_e(V_m)}.$$

As discussed and in Section 2, this is bound to give a rather noisy time series, since the noisy measured speed V_m is used as the input. However, now we can replace the measured speed with the predicted speed (with fouling component included). In addition, we can go even further and replace the measured power with the predicted power (again, with fouling component included), and write

$$P_d = 100 \cdot \frac{P_{pred} - P_e(V_{pred})}{P_e(V_{pred})},$$

where V_{pred} and P_{pred} are the predicted speed and power with the extra resistance component included, and $P_e(V)$ is the PPD model response simulated without the extra resistance term. An example of the difference between using measured and predicted quantities is given in Fig. 7. One can clearly see how the noise level is reduced, which allows for more detailed assessment of individual hull treatment effects. Note that here we calculate the power loss instead of speed loss, since that is the more natural for the PPD model (it is designed to predict power).

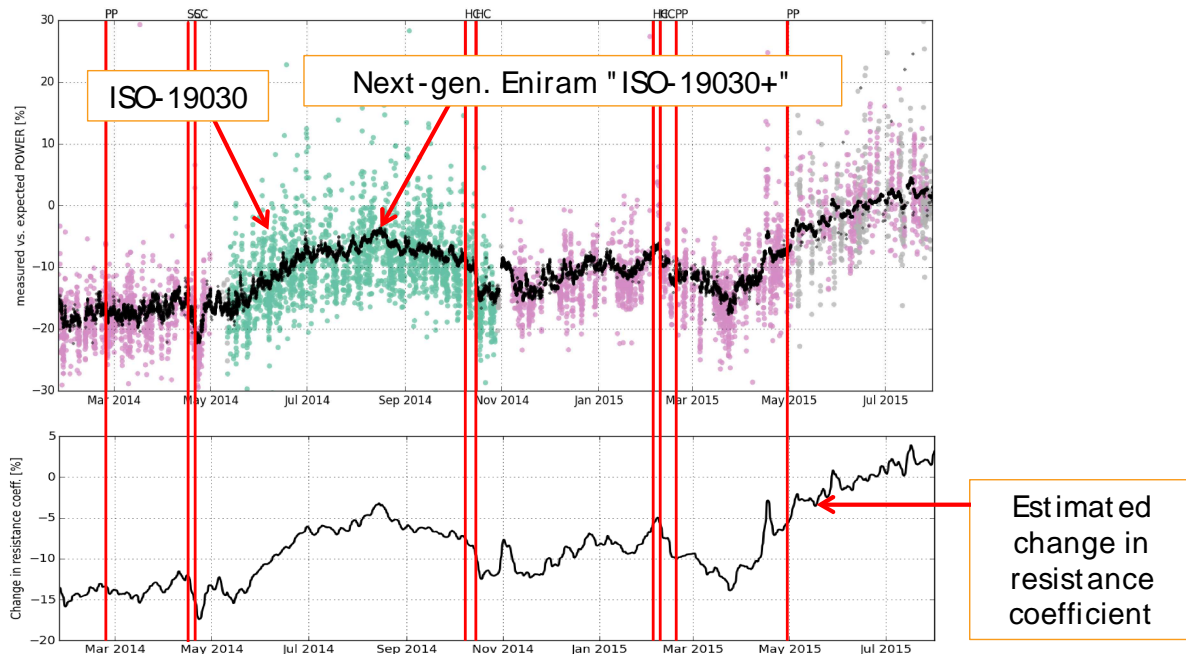


Fig. 7: Top: ISO-19030 performance values compared to the ones computed via the next-generation ENIRAM model. Bottom: estimated change in the hydrodynamic resistance coefficient due to fouling.

3.3. Tracking Calm-water Power

Another pleasant consequence of integrating the fouling model tightly with the PPD model is that we can, at any time, simulate the vessel at any condition with or without the extra resistance component included. For example, we can estimate how the calm-sea power (power consumption at calm sea conditions) at some selected speed level evolves in time. An example of such a time series is given in Fig. 8.

This approach also enables, e.g. vessel comparisons, since we can move the vessels to the same “operating point” by removing external resistance effects and the effects due to varying speed profiles. Such comparisons are hard to do with the ISO-19030 type of approach, which presents fouling as a relative difference to a reference. Moreover, a changing reference model (updated model e.g. due to a modification to the vessel) is not so much of a problem here, since we calculate physical quantity instead of a relative difference; an updated reference model would still target the same quantity.

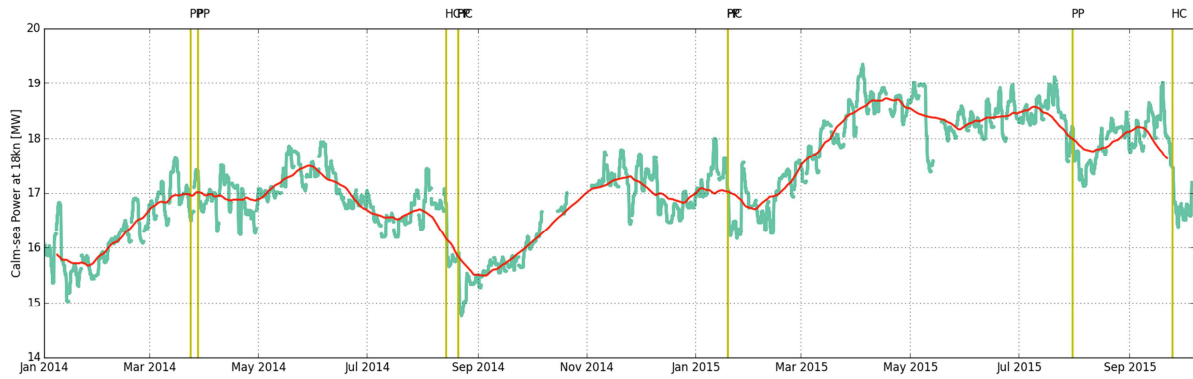


Fig. 8: Estimate of the calm-water power consumption at STW=18kn. Red line indicates the 30 day running mean, and vertical lines are different hull treatments (PP = propeller polishing, HC = hull cleaning).

In addition to vessel comparisons, one can derive interesting “fleet-level” Performance Indicators, such as the total calm-water propulsion power at some selected speed over a collection of vessels. Example illustrations of vessel comparisons and such “fleet-level” performance tracking approaches are given in Fig 9.

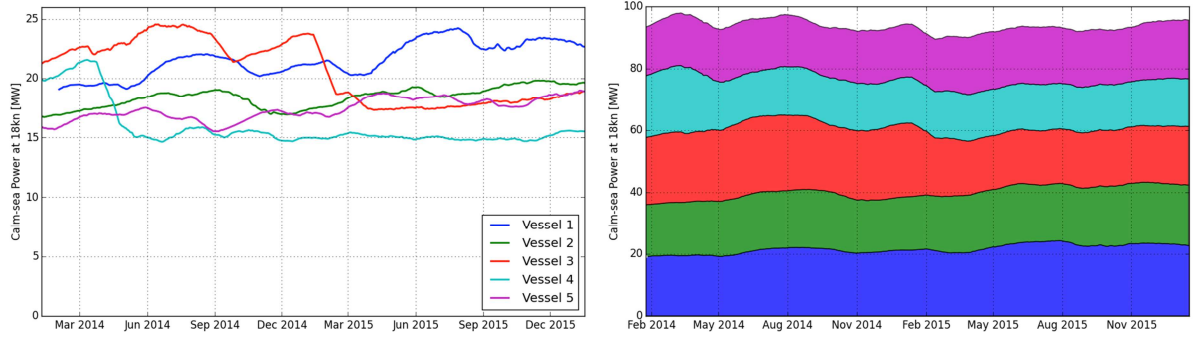


Fig. 9. Left: calm-water power at STW=18kn time series compared for 5 vessels (note the dry-dockings for vessels 3 and 4). Right: the sum of calm-sea powers over the 5 vessels.

4. Discussion and Conclusions

In this paper, we presented some practical aspects related to implementing the ISO-19030 standard for hull and propeller performance monitoring. In particular, we discussed some data-based approaches for generating the reference speed-power curves. We identified a few downsides of the ISO-19030 approach; for instance, the level of noise can be high and comparisons between vessels difficult. To address these issues, we presented our own “model-based” performance monitoring approach, where hull and propeller fouling is described with an extra resistance term included into our propulsion power prediction model. The extra resistance coefficient is allowed to evolve slowly in time, and is continuously updated as new data becomes available. The technique can be used to reduce the noise level of ISO-19030 analysis by, for instance, replacing the often poor quality STW measurement with a predicted STW produced by the propulsion power model with the extra resistance term included. In addition, since the fouling model is tightly integrated with the propulsion power model, we can, at any point in time, simulate the vessel in various conditions with or without the extra resistance component. This enables us to, for instance, track how the calm-water propulsion power at certain selected speed levels develops over time. Such indicators can be used both for comparing vessels and for tracking the performance of a whole fleet.

References

BLENDERMANN, W. (1993), *Parameter identification of wind loads on ships*, J. Wind Engineering and Industrial Aerodynamics 51, p. 339

GELMAN, A.; CARLIN, J.B.; STERN, H.S.; DUNSON, D.B.; VEHTARI, A.; RUBIN, D.B. (2013), *Bayesian Data Analysis*, 3rd Ed., Chapman & Hall, ISBN 978-1-4398-4095-5

RASMUSSEN, C.E.; WILLIAMS, C. (2006), *Gaussian Processes for Machine Learning*, MIT Press

SÄRKKÄ, S. (2013), *Bayesian Filtering and Smoothing*, Cambridge University Press

Cooperative Robotics – Technology for Future Underwater Cleaning

Angelo Odetti, CNR-ISSIA, Genova/Italy, angelo.odetti@ge.issia.cnr.it

Marco Bibuli, CNR-ISSIA, Genova/Italy, marco.bibuli@ge.issia.cnr.it

Gabriele Bruzzone, CNR-ISSIA, Genova/Italy, gabriele.bruzzone@ge.issia.cnr.it

Massimo Caccia, CNR-ISSIA, Genova/Italy, massimo.caccia@ge.issia.cnr.it

Andrea Ranieri, CNR-ISSIA, Genova/Italy, ranieri@ge.issia.cnr.it

Enrica Zereik, CNR-ISSIA, Genova/Italy, enrica.zereik@ge.issia.cnr.it

Abstract

This paper reports the description of the different types of robotic platforms currently employed in hull cleaning and ship inspection tasks, related to maintenance and classification operations. The functional requirements of the specific applications and characteristics of the different class of vehicles are presented and compared. The paper also reports the main trends in marine and maritime robotic research, with innovation transfer towards naval industry and real applications. In particular, the paper focuses on cooperative robotics bringing new ideas and concept to improve the performance, quality and safeness related to ship cleaning and inspection.

1. Introduction

In the last century, humans and goods transportation by mean of ships and vessels has surely become one of the most time and cost efficient methods.

A major enemy for the efficiency of such transportation is the cleaning status of the hull which can heavily affect the performance of the vessel in terms of fuel saving that directly turns into a cost effort. In particular, the fouling phenomenon is the main cause of ship efficiency loss; in fact fouling is the colonization of submerged surfaces by unwanted organisms such as bacteria, barnacles and algae. The increase in frictional drag caused by the development of fouling on ship hulls can reduce speed in excess of 10%. A vessel with a fouled hull burns 40% more fuel which has an impact on fuel costs and additional greenhouse gas production (estimated to be 384 million tons per year).

Side-effects of hull fouling could also be the damage of structural integrity of the ship, due to the corrosion induced by the fouling and the spread of “alien species” around the world transported by the fouled hulls, potentially threatening the balance of sensitive ecosystems.

For such reasons, periodic maintenance protocols and operations have to be developed and actuated in order to guarantee the efficient status of the ship, counteracting the invasive phenomenon of fouling. It is easy to understand that maintenance operations introduce additional costs for the ship owner:

- direct costs: as for material, devices, human personnel employed for the cleaning operations;
- indirect costs: time needed for the operation (that is equivalent to idle operational time of the ship and correspond to money loss for the ship owner), cost of certifications for the operation quality (like ISO standards) or safety level (as for instance in the case of chemical treatments that could be subject to toxicity thresholds).

Nowadays inspection and cleaning operations follow well standardized scheduling and procedures aimed at reducing the cost effort for the hull cleaning. If currently the employed methodologies for the cleaning operations rely on at-field human personnel, chemical treatments, dedicated tools and devices, the advancement in the cleaning field is heading toward the employment of innovative technologies to overcome a number of difficulties. Human personnel (divers) have to work in a very harsh environment carrying cumbersome equipment: minimizing the time and number of personnel unit to be employed in such operations has a direct relationship to cost and risk reductions. The application of chemical products for the removal of fouling and paints for the hull protection is subject to very strict

regulation because of toxicity and pollution constraints; this facts turn into high costs of the products, a need of good practice procedures for the use of toxic materials, guaranteed quality of the work to comply with regulation standards for toxic and pollutant products. Special tools and equipment is needed to execute the hull cleaning operation; this may require the formation of qualified and expert personnel as well as logistic support, such as preparation of dedicated structures or, in extreme cases, the dry-docking of the vessel.

The maritime industry is forced to follow the general trend of rationalization so as to reach a higher level of standardization of the procedures related to marine transportation that will enable higher performances according to safety and financial criteria. One way to achieve this is through the incorporation of more technological means that increase the level of automation. Robotics is an available and consolidated technology than can trigger an innovative step change in the cleaning procedures, putting as targets three main key-points: work quality, operation safeness and cost reduction.

The aim of this paper is two-fold: firstly it reports an extensive description of the actual technology available related to robotic platforms employed for hull cleaning tasks; the second goal of this paper is to propose cutting-edge methodology, frameworks and prototypes developed at research level, for a future application in real at-field hull cleaning scenarios. Furthermore, *DNV-GL (2015)* announces that since November 2015 DNV GL is accepting underwater examination of a ship's bottom by means of remotely operated underwater vehicles (ROVs); a remote means of examination – typically an ROV – may be used to carry out relevant parts of the in-water bottom survey referring to the “Rules for Classification of Ships”. This survey typically involves an overall examination of underwater hull items, i.e. the hull plating, stern frame, rudder and propeller. This news brings a disruptive methodological change into inspection and classification of ships, as well as the opening to the employment of innovative technologies for maintenance and cleaning.

Being a number of robotic and automated platform currently in use for specific cleaning operations, it is worth to have a glimpse towards latest research results, where cooperative robots and high-level autonomous systems are employed within complex marine robotic frameworks; even if a number of both technical and technological problems are still faced by researchers and engineers, some specific problems can be solved through the employment of cooperative and intelligent teams of robot. In particular, it has to be underlined that the concept of cooperation is not restricted only to robot-to-robot cooperation, but also to the strict interaction between human operator and robotic platform in situation where the human capabilities are irreplaceable.

Robots can substitute humans in various survey and maintenance tasks on-board a ship. Whether, in some cases, the employment of robotics is cost-effective, in some other it is suggested to exploit robots where direct human operations could be dangerous for the operators. On-board ships a technological aid is requested in those operations like inspections, cleaning and maintenance where humans have a physical impediment and the ship herself does not provide for adequate devices or support. Robotics is continuously evolving and has now reached a point that allows performing robotic-aided ship inspection and maintenance with quite reliable techniques. The idea of using robotics in ship inspection has started in the 80's but the necessary technological degree was reached in the last years. Consequently, a huge number of vehicles has been developed or is in the development phase for autonomous or remotely controlled (tethered or wireless) operations. Different kind of robots are able to climb the walls of the ship (both in the upper-works and in the hull), the tanks and bulkheads or the internal walls while other robots can operate in the water, air or along pre-constructed rails nearby the hull. As described in the introduction, in the last years the interest around this field of robotics has grown and the administrations are focusing on the development of this category of vehicles. For example, Singapore state has recently published a number of calls for projects concerning ship inspection crawlers and the EU has founded projects relying on the use of robotics for ship maintenance and inspection such as MINOAS, INCASS, SMARTBOT and CROCELLS.

2. Classification

With the idea of making a classification of the different systems or robots we investigated current and emerging technologies. We performed an investigation of the literature, the reports published and checked the market to identify existing and applied techniques and verify the current state of new projects.

There are many vehicles for inspections in the market; wide is the range of wall-climbing vehicles and a classification cannot stop on general characteristics. It would be difficult to identify all the existing technologies. To classify the robots for ship cleaning, maintenance and inspection it is necessary to keep in mind the requirements of a marine vehicle: they have the intrinsic characteristics of being able to survive to an immersion in water and a salty ambient. Every component on-board has therefore to be watertight and able to withstand hydrostatic pressure. Ship inspection require the vehicle to be immersed into salt water up to 25m of depth: all the electric and electronic parts require an International Protection Marking Code of up to IP68-50 and the connectors must warrant the water-tightness of all the cables and canisters. All the mechanical parts have to be protected by sealings and the materials have to be corrosion-proof or anyway require a surface treatment. Moreover this category of robots includes marine underwater vehicles that are not considered in other inspection-aimed robotics.

While wall-climbing robots for earth engineering have the main challenge of fighting gravity, *Longo and Muscato (2008)*, not all the vehicles for ship inspection need to be gravity-proof but require a system for approaching and next attaching to the hull of the ship using adhesion forces able to counteract escaping forces due to cleaning devices or other inspection elements.

We decided to classify the robots in function of their type and then functionality. We can classify the robots into two main class: Marine and Non Marine vehicles. This subdivision is based on the type of mean in which the vehicle or device moves. Marine Vehicles are able to operate in a 3D ambient in water and have the capacity of approaching and attaching to the hull with a system of attraction.



Fig. 1: Marine Vehicles

Non Marine vehicles can move in 2D ambient. Even if capable of changing the plane on which they move passing from a wall to another, they always move on a surface. They are deployed directly on the wall of the ship. It has to be considered that among Non Marine vehicles we have the category of robots built-in the vessel itself: they move on a rail but are considered 2D vehicles. Other 1D robots are not considered because not useful.



Fig. 2: Non-Marine Vehicles

The secondary classification subdivides the vehicles into categories: the system of locomotion identi-

fies every vehicle. Among the vehicles, we subdivided into: ROV, Crawlers, Hybrid, Walking, Built-in and Diver operated.

All these vehicles can have their peculiarities as it will be described later but it is necessary a first preamble for what regards the existing techniques: we define robotic-aided ship services those operations that can be performed during maintenance of the hull by using autonomous or remotely operated vehicles. Some devices, not dealing with the present thematic but representing the trait d'union with future technologies, are complex tools that are diver-operated, thus not includable in the robot category. However, recent developments in the human-robotics interaction will provide a new category of operations where humans and robots will perform underwater surveys and cleaning by means of cooperation like in case of CADDY project (described in the last section of this paper).

With this introduction, autonomous and remotely operated vehicles are those agents that can move autonomously to make the survey of a hull and those guided from remote by a pilot. They represent the subject of this survey. All the autonomous inspection robots that are present in literature or on the market can be turned to remotely operated mode. This is because human factor is quite important and the survey techniques have not reached a technological level such as to enable autonomous operations in an efficient and reliable way. So, general methodological categories can be identified for the development of standard testing requirements. Based on these main characteristics we can classify the robots in function of their type and then functionality. We will report here the classification and an example for every kind of vehicle.

3. Purposes

Different vehicles are studied for three main purposes: Cleaning, Inspection and Maintenance.

3.1. Cleaning

The main task for ships is the removal of biofouling from the ship's hull, rudders and propellers. This permit to save money in most of the cases but in other is necessary for avoiding the introduction of non-indigenous species into marine ecosystems. The International Maritime Organization (IMO) has issued the Guidelines for the control and management of ships' biofouling to minimize the transfer of invasive aquatic species, *IMO (2011)*. These invite the ship-owners to develop a biofouling management plan for the threat of invasive aquatic species introduction through ships. There are two main sources of shipping-related introduction: ballast water and vessel biofouling. IMO is also concerned about the impact of in-water cleaning on anti-fouling coatings and potential release of biocides into the environment. Therefore, the guidelines invite to develop the research into in-water cleaning technologies for biofouling removal as well as for the capture of biofouling material and other contaminants after cleaning. More than for the economic damage for the ship-owners is important to preserve the ambient. The main issue for cleaning robots is to provide removal without damaging anti-fouling coatings, *Morrisey and Woods (2015)*. Usually they are ROVs, Crawlers, or Hybrid designed to remove biofouling and collect waste in filter bags. These are tethered vehicles remotely operated by operators and the power supply comes from an external sources. Provided by cameras they use different cleaning devices: brushes, suction devices, high-pressure waterjets and cavitational jets. Usually they are heavy and have medium/big dimensions.

3.2. Inspection

The development of robots for inspection of power plants created a wide range of possibilities but the vehicles responding to ship inspection requirements constitute a smaller category. Among these, we find light and small vehicles provided by cameras but able to move in every narrow space and medium-sized vehicles provided by cameras and inspection devices necessary to assess plate thickness, coating thickness and corrosion potential.

Usually Non-Marine inspection robots are crawlers, walking or vehicles able to carry just the inspec-

tion devices. Either they can be tethered with external power supply or wireless vehicles remotely operated (with less autonomy) but an entire branch is developing for what regards autonomous inspections. Marine inspection robots are ROV or AUV provided by Sonar and visual imagery both have a key role in building maps and navigating with them

3.3. Maintenance

Maintenance vehicles are those vehicles not used for cleaning but able to realize small repairs. Used where it is difficult for humans to access, provided with cameras, are able to carry the tools necessary for repairs and to withstand the forces and counteractions generated by the operations. This class is under development and will be the future of services. Studies are providing vehicles that can realize paintings, welding, rust removal and preparation for inspections. The use of magnetic crawlers is usually the choice for these operations due to their good adhesion to the surface.

4. The vehicles

As explained in section 2 all the existing vehicles are ascribable to the following categories: Remotely Operated Vehicles (ROV), Crawlers, Hybrid and Legged. Actually, from a market analysis, it is evident that the portion of vehicles employed is quite restricted. Nowadays the most used technologies are those for hull cleaning of big ships, while inspections and maintenance vehicles are not so common. ROVs and wheeled crawlers appear to be the mostly reliable technologies but Hybrid vehicles seem to be the best configuration for future developments. Most of the other vehicles though based on solid designs are in development phase and have not yet been adopted.

4.1. ROV

A Remotely Operated Vehicle (ROV) is a tethered underwater robot provided with multiple propellers able to move with 6dof underwater. ROVs can vary in size from small vehicles with cameras for simple observation up to complex work systems, which can have several cameras and tools for hull cleaning. This kind of robot has the peculiarity of being able to move in water with the obvious advantage of quickly accessing every part of the hull of a ship. On the other hand, with ROV it is only possible to inspect or clean the immersed parts of the hull. ROVs are principally used for hull cleaning, even if some vehicles can be used for mapping the hull and assessing the intactness of active (thrusters, propellers) or passive (sea chests, rudders, fins) underwater devices. An ROV uses its vertical thrusters to approach the hull. They are a well known technology that permits to have the most commonly used vehicles for ship hull cleaning. An example of ROV is GAC EnvironHull (gac.com/siteassets/brochures/2.-shipping/environhull-19jun15.pdf). It is a big vehicle provided with 8 thrusters and cleaning devices. The solution uses adjustable pressure seawater jets rather than brushes or abrasives, resulting in minimal damage to the antifouling surface.



Fig. 3: HullWiper hull-cleaning ROV

4.2. Crawlers

Crawler is a generic term used to describe any tracked or wheeled transport system used in robotics. Even if intersecting from a mechanical point of view the main distinction does not come from the locomotion system but from the attaching system. Crawlers are subdivided into magnetic attached and suction attached. Magnetic systems are effective on ferrous hull and structures but cannot be applied to non-magnetic hulls like those of military ships (they would leave a residual and potentially detected magnetic pattern) or to ships built with aluminum or composite materials. In these cases, the suction system becomes necessary.

In magnetic applications, wheels and tracks are entirely covered by permanent magnets that ensure the attaching of the crawler to the ferrous hulls. This solution gives the possibility of resting on a surface for long periods without the need of high power supply thus permitting the possibility of autonomous surveys. In addition, these vehicles can access most of the surfaces of the ship even outside of the water. For these reasons, the magnetic systems are good for ship inspections and maintenance operations. Wheeled robots behave well on flat surfaces and permit to reach good velocities. The adoption of tracks is useful on a wider range of surfaces and to pass obstacles in an easier way.

Suction is the best solution for what regards cleaning of the hull. In fact, in most of the cases the suction device (a vortex system or the flow created by the water through the cleaning head) creates a differential of pressure sucking the vehicle to the hull. This means that the locomotion system has the only task of moving and steering the vehicle on the required surface. This is a good characteristic also because the locomotion system has low impact with the surface preventing the dispersion of fouling in the ambient. In not-magnetic solutions the tracks ensure a better traction than wheels especially on slippery surfaces. A notable example of tracked magnetic crawlers is the MicroMag inspection vehicle (www.inuktun.com/crawler-vehicles/micromag/VT100%20MicroMag.pdf), which is compact and waterproof. As most of the inspection robots, it is rapidly deployable on the magnetic surface.



Fig. 4: Versatrax 100 Micro-Mag



Fig. 5: MHC Magnetic Hull Crawler



Fig. 6: MARC, CNR-ISSIA

The MHC (www.cybernetix.fr/sites/default/files/MHCDatasheet_0.pdf) is a crawler which is able of transporting high loads and performing various surfaces on ship plates. Most of the waterproof magnetic crawlers nowadays present on the market are valid solutions for inspection on smooth surfaces. Some vehicles in development have the possibility of passing from a surface to another thanks to the geometry of the magnetic locomotion system; for example, MARC, *Bibuli et al. (2012)*, developed in the EU Project MINOAS. An example of crawler for non-ferrous hulls is the HullTimo (hulltimo-mauritius.com/pro.html) system used to clean hulls. HullTimo is a wheeled robot using rotary brush and suction systems to secure to the hull.

4.3. Hybrid

Hybrids are vehicles provided with at least two different systems of locomotion able to move in different means in the 3D space. Hybrid vehicles have the characteristics of ROVs and Crawlers together. Commonly they mix a system with 8 thrusters with a crawling device that can be a system of tracks of wheels magnetic or not. In one case, the attracting force comes from the magnets in the other

it comes from the system of propulsion or from a suction system present at the bottom of the vehicle. If magnets are present then the vertical thruster require for a rate of thrust at least necessary to separate the crawler from the surface. The existing techniques use rubber tracks and 8 thrusters; e.g. the ECA Roving BAT (www.rovinnovations.com/eca-hytec-roving-bat.html) uses the thrusters as attraction device. The vLBC uses own-patented system of vortex-based suction system to overcome ducted props or magnetic attractors (http://www.seabotix.com/products/pdf_files/vLBV950.pdf). For ferrous vessels, the hybrid vehicle with magnetic system of attraction is the universal solution allowing operating both in water and on upper-works.



Fig. 7: vLBC with vortex suction system



Fig. 8: ECA ROV BAT

4.4. Legged

Less used but interesting techniques in continuous development are those considering legged robots for inspections. Different geometries are proposed and tested, especially for civil applications. In marine applications, we can find a series of biped-type units and a series of multiple legs units. These are studied for their capacity to introduce in openings of the ship or overcoming the obstacles. Some robots use pneumatic actuators to adjust the length of the legs according to the need.

For its configuration, the legged robots require for a system of attraction that can be switched on and off at any time; two system of attraction are commonly installed on the “feet” of the legged system: Vacuum produced on cups in contact with the surface and electromagnets. Both the systems require a high and continuous power to be generated. Vacuum requires a pump installed on board or in an external position while other vacuum systems (e.g. Passive) are not reliable. The same concept for what regards electromagnets: they can be alimented by an on-board source or by tethered source.

An interesting study is carried on at DREAMS Lab, *Ravina (2016)*. The studies are oriented to the realization of a kit of low cost unsophisticated self-moving units. It is studied to realize a portable and user-friendly tool for inspectors, able to simplify and speed up the inspection visits with and automatic generation of survey reports. All projects related to this configuration are interesting but solely used in dry areas of ships.



Fig. 9: Prototype From a Kit of Self-moving units

4.5. Built-In

The last system described is quite different from the others but can be a good solution especially for farsighted ship-owners. The system is built-in the hull of a ship and is used to speed-up inspections in ballast tanks and double-bottom. The RoboShip (www.leorobotics.nl/projects/roboship) project provides an intelligent robot platform. A carriage with a robot arm constitutes the system navigating between the narrowly spaced ballast water tanks on a rail. A remote control system enables inspectors to inspect the tanks remotely thanks to a system able to determine the exact position of the robot.



Fig. 10: Built-In Robot with rail

5. Table

Table I compiles existing techniques and their main peculiarities. Every vehicle reported is a notable example of the above mentioned solutions for ship inspection, cleaning and maintenance.

6. Cooperative Robotics

Previous sections have shown how tele-operated, semi or full autonomous single robots are efficiently employed in hull cleaning operations. What are the advancements and innovations that could be transferred from research to real naval applications? Cooperative robotics appears to be the panacea to a number of naval applications; introducing more agents in the operative framework brings different advantages: 1) increasing the number of autonomous agents acts as a “force multiplier” allowing to cover wider areas or to reduce the operational time with respect to the employment of a single platform; 2) instead of a huge and complex single platform, the cooperative robotic team may be composed by smaller and simpler vehicles (simpler in terms of equipped with a reduced number of sensors or actuation systems) turning into cheaper platforms as well characterized by a simpler logistics; 3) robustness to faults given by the fact that a failure occurrence on a vehicle does not affect the functionality of the entire team and the operational goals (or at least a subset) can be still achieved by the remaining team.

The highlighted advantages are counterbalanced by a number of issues that arise when a cooperative framework is developed and brought to operational activity: 1) a reliable communication infrastructure among the agents is necessary in order to dispatch the operative information; 2) a precise sensing of the environment and of the other agents is needed to provide safe motion and actuation capabilities; 3) autonomy, self-decision making and coordination of the different agents in order to maximize the exploitation of the robotic team.

These abovementioned issues become real challenges when a cooperative robotic framework is brought from a laboratory/prototype set-up towards real application scenarios. Despite the technical and technological difficulties, many research projects have the capabilities to bring results into useful naval application in the very near future.

Table I: Robot categories and typical representatives

Vehicle	Control	Locomotion	Type of Hull	Attraction device	Purpose	Dimensions			Speed	Vision System	Sensors	State
						Length [mm]	Breadth [mm]	Height [mm]				
Versatrac 100 MicronMag	Remotely	Tracked Crawler	Magnetic	Magnetic	Inspection	400	400	300	4,55	30	Thickness	Used
Magnet Crawler II	Remotely	Tracked Crawler	Magnetic	Magnetic	Inspection	330	330	130	1,23		Thickness	R&D
Hull Crawler	Autonomous/Remote	Tracked Crawler	Magnetic	Magnetic	Inspection	254	177,8	89,9	5,8	62	Thickness	Used
Keel Crab SailOne	Remotely	Tracked Crawler	All	Suction	Cleaning (Brushes)	425	425	320	9,5		Thickness	Development
Magnetic Hull Crawler	Autonomous/Remote	Tracked Crawler	Magnetic	Magnetic	Cleaning (Waterjet)	610	460	400	60	50	Thickness Corrosion	Used
ECA ROV/BAT	Remotely	Hybrid	All	Thrust	Inspection	1105	1085	646	135		B&W and TV color Camera and Tilt	Development
VLBC	Autonomous/Remote	Hybrid	All	Suction Vortex	Inspection	650	390	500	35		Thickness	R&D
Hybrid	Autonomous/Remote	Hybrid	All	Thrust	Inspection	800	700	550			Thickness	Development (smartbot Project)
RoboShip	Remotely	Rails: Built in	All	Rail	Hull Integrity check						Thickness	Used
Hullwiper®	Remotely	ROV	All	Thrust	Inspection						Thickness	Used
CleanHull	Autonomous/Remote	ROV	All	Thrust	Cleaning (Brushes)	3000	1500	800		2000 [m ² /h]		R&D
TankBUG	Remotely	Wheeled Crawler	Magnetic	Magnetic	Cleaning(Waterjet)							Development
Hull Bio-Inspired Underwater Grooming System	Autonomous/Remote	Wheeled Crawler	All	?	Sediment removal	790	510	410	45,4	36		Development
Hulltimo	Remotely	Wheeled Crawler	All	Suction / Rotary	Inspection	700	500	400	40			Used
FleetCleaner	Remotely	Wheeled Crawler	Magnetic	Magnetic	Cleaning (Brushes)	470	430	330	20		2 cameras	R&D
Ship Inspection Robot - SIR	Autonomous/Remote	Wheeled Crawler	Magnetic	Magnetic	Cleaning (Waterjet)	1600	1600	600		1200 [m ² /h]		Used
FerroTanker-20	Remotely	Wheeled Crawler	Magnetic	Magnetic	Inspection	200	400	200			Camera	Development
MARC	Autonomous/Remote	Tracked Crawler	Magnetic	Magnetic	Inspection	700	560	345	24,5		Camera	Development
KT Self-Moving Units for Automatic Inspection	Remotely	Legged	All	Air-Suction	Inspection	490	430	180	43		Thickness	Development

6.1. MINOAS Project

MINOAS project, *Bibuli et al. (2011)*, proposed reengineering of the overall vessel-inspection methodology, by introducing an innovative system concept that incorporates state of the art technologies, but at the same time formulated a new standardization of the overall inspection process. Through holistic approach, MINOAS proposed the development of a new infrastructure that substitutes human personnel by high locomotion enabled robots and "teleports" the human inspector from the vessel's hold to a control room with virtual reality properties. The human's perceptual abilities are enhanced through the utilization of high resolution tools (e.g. sensors) and are augmented through the parallel processing property provided by MINOAS. Following the centralized control scheme adopted in similar distributed control methodologies (SCADA), the number and the sequence of the tasks required is rearranged and the overall inspection procedure is brought in alignment with the current tendency adopted in similar inspection, exploration and surveillance tasks. The proposed innovative system concept, considered the assembly of a robot fleet with advanced locomotion abilities and sets of tools that are dedicated to the tasks attached to the inspection process, the development of control techniques and algorithms that provide a semi-autonomous nature to the operation of the robot-fleet and a hierarchical controller that realize the virtual environment for the human inspector and adds newly developed toolboxes enabling on-line processing of the harvested data and operate as a Decision Support System in the aid of the inspector.

Regarding technical details, during the project a heterogeneous robotic team was developed with the aim performing inspection operations in harsh and hardly-reachable areas of ships. In particular:

- An aerial vehicle (quadcopter) was employed to perform a first and wide survey of the area to be inspected;
- One small and one bigger crawler vehicles were developed to explore, observe and perform measurements on metallic plates, reaching locations without the need of scaffolding or other particular supporting structures. The vehicles, equipped with magnetic wheels or tracks, were able to collect video data (in order to detect rusted areas or cracks on the plates) and measure the thickness of the plates by means of an ultrasonic measuring device mounted on a small robotic manipulator. The magnetic climbing robot developed by CNR is reported in Fig. 11;
- A micro-ROV (Remotely Operated Vehicle) was employed for underwater operations, in particular for the observation and measurement within water tanks without the need of removing the water from the tank itself. The micro-ROV during ballast tank survey operation is shown in Fig. 12.

Final exploitation of the project results was successfully carried out on a bulk carrier where the vehicles were deployed to evaluate their performance.



Fig. 11: The CNR magnetic crawler

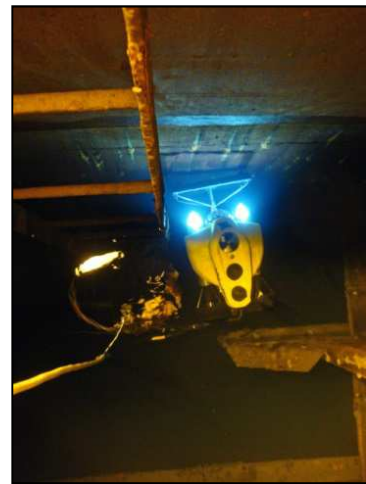


Fig. 12: Micro-ROV surveying ballast tank

6.2. CART Project

The CART project does not focus on ship inspection and cleaning, but it relates to salvage operation support; anyway, this project is a very good example on how the research in the field of cooperative robotics can provide a very useful and reliable solution to a very practical problem. The salvage operations of distressed vessels require the development and adoption of emergency towing systems (ETS), which improve the efficiency of support actions and contribute to prevent the risk of ship grounding, one of the major causes of accidents with a high environmental impact. Besides the casualties and direct costs of the ship loss, there are a number of consequences involving an immediate and long-term effect on fragile marine ecosystems, fishing, tourism and recreation, and others. The main goal of ETS is to facilitate the physical connection between the towing vessel and the distressed ship. Classical operational procedures involve the supply of a thin rope, called ‘live-line’, connected to a more robust rope or chain, which actually tows the distressed vessel.

Currently, the main ways of supplying the live-line are as follows:

- line-throwing gun: a bullet, connected to the live-line is shot from the tug to the distressed ship, where it is recovered by the crew. Then the live-line is connected to the actual towing line;
- pick-up buoy: the crew of the distressed ship fixes the live-line, or directly the messenger line, to a pick-up buoy, launched at sea before abandoning the ship.

On arrival to the site, the tug has to recover the pick-up buoy and its connected live-line, messenger and towing line, and then proceed to the towing operations. Existing emergency towing systems require a close range between the tug and the ship – this is not always possible and often very dangerous, above all for the crew on-board that, when a line-throwing gun is used, has to remain aboard the distressed vessel. Robotics can highly enhance such a procedure by designing and developing a dedicated system that could relieve humans from the execution of salvage operations. Results in this sense have already been obtained within the EU Project Cooperative Autonomous Robotic Towing system (CART), *Bibuli et al. (2014)*, whose primary goal was to develop a new safety-oriented concept and technology for salvage operations of distressed vessels at sea. The proposed concept relies on robotized unmanned marine vehicles able to semi-automatically execute the high-risk operation of linking the emergency towing system of a distressed ship and the tug.

During the project, different prototypes of autonomous semi-submersible vehicles were developed with the aim of supporting the recovery operations of distressed ships. In the CART concept, an autonomous buoy was deployed from the distressed ship, while an intelligent vehicle launched from the recovery tug-boat, was able to detect the position of the buoy, navigate around it and capture (by means of a passive hook) the messenger line connecting the buoy to the main towing line; once captured the two bound vehicle were recovered by the tug-boat that could then perform the ship towing operation.

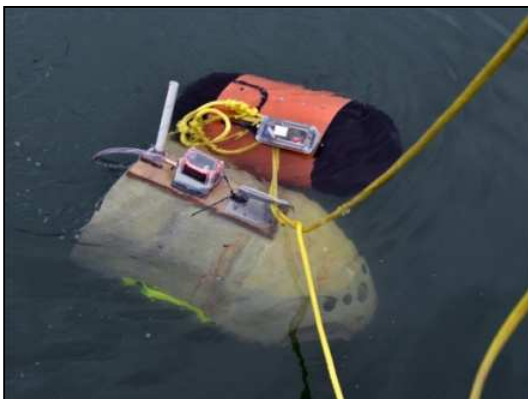


Fig. 13: The robotic platforms after the entanglement operation

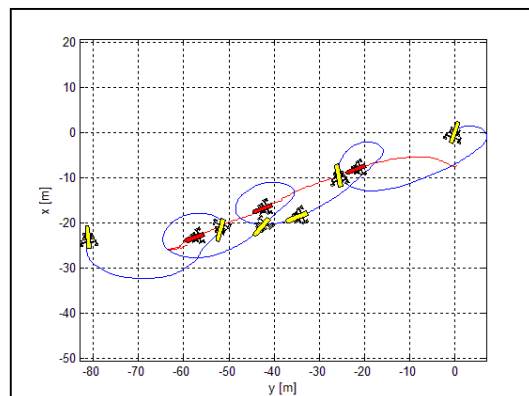


Fig. 14: Platform motion during operation

The project has highlighted a very strong effort in transferring research results related to navigation, guidance and control of robotic vehicles, as well as cooperation and coordination schemes that endowed the CART system with the autonomous capabilities to achieve the desired results. The vehicles entangled after a recovery operation are shown in Fig. 13, while the motion executed by the robotic platforms is reported in Fig. 14.

6.3. MORPH Project

Autonomous vehicles of today are not suitable for operating in challenging unstructured environments. In fact, when the terrain is rough and the environment is hostile, the vehicles can be trapped easily and valuable equipment can be lost, as witnessed in a number of occasions. The Doppler Velocity Log, a fundamental instrument in dead-reckoning navigation techniques used by underwater vehicles fails to provide reliable measurements when operated over uneven or rugged terrains. As a consequence, the vehicle ends up losing its position accuracy so that in the best of scenarios the observations cannot be geo-referenced; in the worst case scenario, the vehicle may be lost due to navigational problems.

It is for the above reasons that today, in rough and truly three-dimensional 3D terrains, only remotely controlled vehicles (ROVs) are employed. This type of vehicle is connected with a surface support ship via an umbilical cable that allows for remote control of the underwater robot and immediate access to all payload data. However (and the same happens with currently existing AUVs), accurate global positioning is virtually impossible to achieve when the ROV operates close to complex underwater terrain features (e.g. vertical walls or walls with a negative slope). As a consequence, the region being mapped scanned cannot be properly geo-referenced or be easily relocated in a subsequent dive. Moreover, the cable might be entangled with the surrounding environment, which may also lead to vehicle loss.

MORPH, *Kalwa et al. (2015)*, puts forward a new solution to overcome the above problems. To this effect, the project focuses on the development and testing of methods that will effectively enable an underwater robot to explore truly 3D environment challenging environments. For proper data geo-referencing and accurate habitat mapping in the presence of both vertical and horizontal terrain features, the navigation and scientific sensor suites of the vehicle must have the capability to adapt their geometrical formation accordingly (concept reported in Fig. 15). Explained in intuitive terms, for proper image acquisition the vehicle must have “eyes” which scan the environment for possible threats such as overhanging cliffs and optimize their location in order to optimize the observation conditions. It is obviously an advantage to “decouple and relocate these eyes” in order to observe the whole scene. This flexibility can in fact be achieved by removing any rigid links among parts of the vehicle and replace them by logic or information links. The parts of the overall supra-vehicle must be self-propelled and exhibit some intelligence and information exchange capabilities. As they stay in close proximity to each other (several meters) the capabilities of the single nodes can be limited.

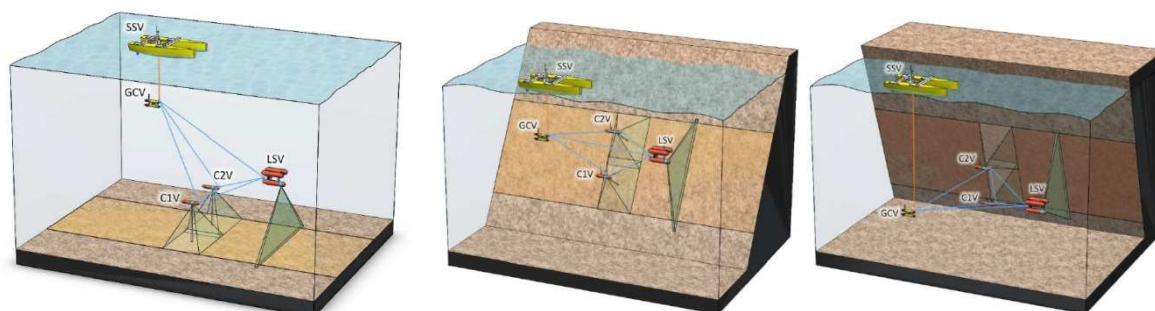


Fig. 155: MORPH concept of the variation or the robotic team formation

The project has recently ended with the successful result of allowing a heterogeneous team of both surface and underwater vehicles (equipped with different sensors such as cameras and sonars) to coordinate their motion and adapt their formation in a way to optimize the environmental observation and reconstruction. A direct follow-up of this project could be the employment of coordinated vehicles to map and reconstruct the current situation of the ship hull, in such a way to evaluate the state and plan proper action for cleaning and maintenance operations.

6.4. MARIS Project

MARIS is an Italian funded project that has the objective of developing a framework for underwater floating manipulation. In particular the project is focused on the development of two underwater robotic platforms, each one equipped with a robotic manipulator and a gripper, posing as final goal the coordinated manipulation of an object. The demonstrative scenario defined for the project is the grasping and cooperative transportation of a pipe in the underwater environment. The project poses a number of technical challenges that will allow innovative steps in the field of the underwater robotic intervention. Different issues are related to: precise navigation and control of the mobile platforms, real time communication, and artificial vision. The project can turn into a source of possible follow-up for naval applications: the possibility of autonomous underwater operations can revolutionize the methodologies nowadays employed for hull inspection, maintenance and cleaning. A pictorial representation of the operation performed by the two floating manipulation platform is represented in Fig. 16 and a real manipulation operation performed by one platform is shown in Fig. 17.



Fig. 166: MARIS operational concept



Fig. 177: Real single-platform operation

6.5. CADDY Project

The main motivation for the CADDY project is the fact that divers operate in harsh and poorly monitored environments in which the slightest unexpected disturbance, technical malfunction, or lack of attention can have catastrophic consequences. They manoeuvre in complex 3D environments and carry cumbersome equipment while performing their missions. To overcome these problems, CADDY aims to establish an innovative set-up between a diver and companion autonomous robots (underwater and surface) that exhibit cognitive behaviour through learning, interpreting, and adapting to the diver's behaviour, physical state, and actions.

The CADDY project, *Miskovic et al. (2015)*, replaces a human buddy diver with an autonomous underwater vehicle and adds a new autonomous surface vehicle to improve monitoring, assistance, and safety of the diver's mission (the concept scheme is shown in Fig. 18). The resulting system plays a threefold role similar to those that a human buddy diver should have: i) the buddy "observer" that continuously monitors the diver; ii) the buddy "slave" that is the diver's "extended hand" during underwater operations performing tasks such as "do a mosaic of that area", "take a photo of that" or "illuminate that"; and iii) the buddy "guide" that leads the diver through the underwater environment. This envisioned threefold functionality will be realized through S&T objectives which must be achieved within three core research themes: the "Seeing the Diver" research theme focuses on 3D reconstruction of the diver model (pose estimation and recognition of hand gestures) through remote

and local sensing technologies, thus enabling behaviour interpretation; the “Understanding the Diver” theme focuses on adaptive interpretation of the model and physiological measurements of the diver in order to determine the state of the diver; while the “Diver-Robot Cooperation and Control” theme is the link that enables diver interaction with underwater vehicles with rich sensory–motor skills, focusing on cooperative control and optimal formation keeping with the diver as an integral part of the formation.

At the current stage of development and with still one year until the end, the CADDY project has collected many successful results: the underwater robot is now able to detect and recognize different hand gestures performed by the diver; single or sequences of gestures are mapped into simple up to more complex actions that the robotic system has to execute to support the specific diver operation. The cooperative guidance executed by surface/underwater vehicles allows following or guiding the diver in the exploration of the underwater environment. An exemplificative of diver-robot cooperation is reported in Fig. 19.

The CADDY project represent the perfect example in which the cooperation is not intended as active coordination between different robotic platforms, but as an active support to the human operator that is still present for the in-field operations. In this view, the robotic system is intended as an “intelligent tool” that interacts with the human operator to support, execute or monitor the underwater activities.

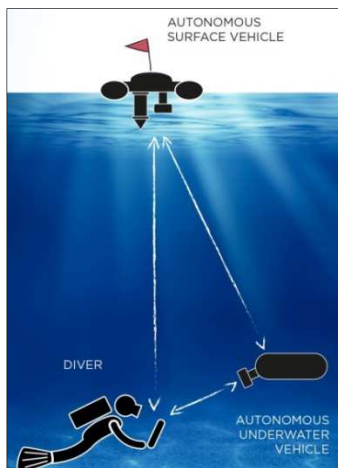


Fig. 188: CADDY concept



Fig. 199: Cooperative operation between diver and robot

7. Conclusions

Robotic technology is a consolidated reality that has rapidly taken its place in naval applications. This paper has collected, reported and proven the reliability of various types on robotic platforms currently employed in inspection, maintenance and cleaning operations. The time and cost saving combined with operation safeness has been demonstrated, so that robotic systems are quickly becoming necessary tools in naval applications. Spread of data and results regarding the performance and costs benefits derived by the exploitation of autonomous tools will generate a continuous push in robotics research and employment in real-case scenarios. Collection of reliable data about the financial and technical benefits of the robotic cleaning technology will be important for independent assessment of ship propulsion system performance. Plate thickness measurements and other data describing ship hull condition that will be collected by robot during cleaning missions could be further used by classification societies for class renewal surveys. The hull surveying using innovative robotic technology is in development phase and needs additional effort and funding to be recognized as mature technique recommended for wider use.

This paper has also reported the successful results given by knowledge transfer from research to real naval application: cooperative robotics is not a sole academic study field anymore, but a real application branch that is now being exploited. A lot of work still needs to be done before cooperative robotic

products can be put on the market, but the collected successes are boosting-up the efforts of scientists and engineers.

Acknowledgements

This research has received funding from the Italian Flagship Project RITMARE.

References

BIBULI, M.; BRUZZONE, G.; BRUZZONE, G.; CACCIA, M.; GIACOPELLI, M.; PETITTI, A.; SPIRANDELLI, E. (2012), *MARC: Magnetic Autonomous Robotic Crawler Development and Exploitation in the MINOAS Project*, 11th Conf. Computer and IT Applications in the Maritime Industries (COMPIT), Liege

BIBULI, M.; BRUZZONE, G.; CACCIA, M.; ZEREIK, E.; BRUZZONE, G.; GIACOPELLI, M.; SPIRANDELLI, E. (2014), *Final Results and Exploitation of the Cooperative Autonomous Robotic Towing System for Emergency Ship Towing Operations Support*, 13th Conf. Computer and IT Applications in the Maritime Industries (COMPIT), Redworth

BIBULI, M.; BRUZZONE, G.; CACCIA, M.; ORTIZ, A.; VOGELE, T.; EICH, M.; DRIKOS, L.; KOVEOS, Y.; KOLYVAS, E.; SPADONI, F.; VERGINE, A.; TANNEBERGER, K.; TODOROVA, A.; GAVIOTIS, I.; APOSTOLOPOULOU, V. (2011), *The MINOAS project: Marine INSpection rObotic Assistant System*, 19th IEEE Mediterranean Conf. Control and Automation (MED), Corfu

DNV-GL (2015), *In-water bottom surveys by means of remotely operated underwater vehicle (ROV) are accepted by DNV GL*, Technical and regulatory news no. 24/2015.

IMO (2011), *Guidelines for the control and management of ships' biofouling*, Annex 26, MEPC.207 (62)

KALWA, J.; PASCOAL, A.; RIDAO, P.; BIRK, A.; GLOTZBACH, T.; BRIGNONE, L.; BIBULI, M.; ALVES, J.; SILVA, M.C. (2015), *EU project MORPH: Current status after 3 years of cooperation under and above water*, 4th IFAC Workshop on Navigation, Guidance and Control of Underwater Vehicles (NGCUV), Girona

LONGO, D.; MUSCATO, G. (2008), *Adhesion techniques for climbing*, Advances in mobile robotics, pp.6-30

MISKOVIC, N.; BIBULI, M.; BIRK, A.; CACCIA, M.; EGI, M.; GRAMMER, K.; MARRONI, A.; NEASHAM, J.; PASCOAL, A.; VASILJEVIC, A.; VUKIC, Z. (2015), *Overview of the FP7 project 'CADDY – Cognitive Autonomous Diving Buddy'*, MTS/IEEE OCEANS' 15, Genova

MORRISEY, D.; WOODS, C. (2015), *In-Water Cleaning Technologies*. New Zealand: Ministry for Primary Industries

RAVINA, E. (2016), *Kit of Self-Moving Units for Automatic Inspection of Marine Structures and Plants: Low Cost Unit for Inspection of Holds*, J. Shipping and Ocean Engineering 6, pp.1-14

Impact of Hull Propeller Rudder Interaction on Ship Powering Assessment

Charles Badoe, University of Southampton, United Kingdom, ceb1r14@soton.ac.uk

Stephen Turnock, University of Southampton, United Kingdom, s.r.turnock@soton.ac.uk

Alexander Phillips, National Oceanography Centre, Southampton, United Kingdom, abp@noc.ac.uk

Abstract

It is the complex flow at the stern of a ship that controls the overall propulsive efficiency of the hull-propeller-rudder system. This work investigates the different analysis methodologies that can be applied for computing hull-propeller-rudder interaction. The sensitivity into which the interaction between the propeller and rudder downstream of a skeg is resolved as well as varying the length of the upstream skeg are also discussed including techniques to consider in such computations. Throughout the work, the importance of hull-propeller-rudder interaction for propulsive power enhancement is demonstrated. A final case study examines the performance of a twin skeg, twin screw arrangement.

1. Introduction

Increasing the energy efficiency of a ship will play an ever greater part in the design process. The design of the stern arrangement involving as it does the complex interaction between the hull wake, propeller performance and use of a rudder for vessel control is the dominant factor in determining the overall propulsive efficiency. The retrofit installation of energy saving devices or the improved optimisation of the stern arrangement during concept and detailed design phases require much higher fidelity analysis methods that have been conventionally applied.

The propulsive performance of a ship typically depends on how well the interaction between the hull, propeller and rudder is understood, assessed and modelled (Molland & Turnock, 2007). Sakamoto *et al.* (2013) state the relationship between the power delivered to the propeller in behind hull conditions P_D , the effective speed of a ship P_E , and quasi propulsive efficiency η_D , may be expressed as:

$$P_D = \frac{P_E}{\eta_D} = \frac{C_w + (1+k)C_f + \Delta C_f}{\frac{1-t}{1-w_T} \times \eta_R \times \left[\frac{J}{2\pi} \times \frac{K_T}{K_Q} \right]} \times \frac{1}{2} \rho S V_S^3 \quad (1)$$

where C_w is the ship wave-making resistance coefficient, k is the form factor of the ship, C_f is the frictional resistance coefficient, ΔC_f is the allowance correlation between model and ship, S is the wetted surface area of the ship, t is the thrust deduction fraction, which is the interaction between the hull and propeller, w_T is the wake fraction, which is the interaction between the hull and water, η_R is the relative rotative efficiency and takes account of the differences between the propeller in openwater condition and when behind the hull, ρ is the fluid density, J is the propeller advance coefficient, K_T is the propeller thrust coefficient, K_Q is the propeller torque coefficient.

$1-t$ and $1-w_T$ are interaction effects which play an important role in the overall powering of ships. For example, examination of equation (1) indicates how $1-t$ can be maximized and $1-w_T$ minimized to reduce the delivered power P_D . As hull-propeller-rudder interaction is dependent on many features, there is often scope for improvement in the overall ship powering process. The propeller performance will depend on the inflow (hull wake) which is also dependent on the hull form. The rudder also has to operate under the influence of the upstream hull and propeller.

This paper considers results on hull-propeller-rudder interaction and its impact on propulsive performance. The discussion is made based on the research results of a three year project on the 'Design Practice For The Stern Hull of Future Twin-Skeg Ships' at the University of Southampton, UK. The first part of the paper reviews approaches to hull-propeller rudder analyses, including various methodologies that have been used for such successful analyses, associated cost in

computation and the suitability for design purposes. The paper does not go into details of all approaches, but provides references for a more profound discussion.

The second part of the paper reviews a case study into the sensitivity into which the interaction between the propeller and rudder downstream of a skeg is resolved as well as varying the length of the upstream skeg. The computed results are compared to a detailed wind tunnel investigation, which measured changes in propeller thrust, torque and rudder forces. Variation of the upstream skeg length effectively varies the magnitude of the crossflow and wake at the propeller plane. A mesh sensitivity study quantifies the necessary number of mesh cells to adequately resolve the entire flow field. In addition, analysis is conducted on parameters such as propeller and rudder forces and rudder pressure distributions from the computation of the interaction between the skeg, rudder and propeller. The computational expense associated with the time resolved propeller interaction was identified as one of the major problems of the hydrodynamic analysis.

Lastly, based on the experience drawn from the above mentioned analysis, techniques to consider for hull-propeller-rudder applications such as a twin skeg, twin screw vessel are discussed, this includes the influence of small details that are easily not included in such computations, but can result in changes in flow characteristics as well as changes in propulsive power.

2. Approaches and methodologies

Flow analysis of a ship stern to gain an understanding of the interaction between the hull, propeller and rudder for performance improvement is a challenging task from a numerical point of view. The most interesting and challenging aspect of such analysis is the influence of the propeller action and the unsteady hydrodynamics of the rudder working in the propeller wake. One approach to address the problem is to adopt a direct method where the propeller and farfield domains are joined using a rotor-stator method (*Lübke, 2005*). The propeller is rotated at each time step and the interface between the two domains is achieved using a sliding mesh interface. To ensure the flow structure generated around the propeller are correctly transferred to the stationary domain, a fine mesh is required at the interface. This approach theoretically offers the highest degree of fidelity, but requires small time steps due to restrictions imposed by explicitly solving the propeller flow, thus placing a high demand on computation.

The next level of complexity involves using an indirect approach by coupling a lower fidelity propeller code (potential flow code, blade element momentum BEMt code etc.) with a CFD solver. The propeller code utilises the non-uniform inflow at the propeller plane calculated from the RANS simulation to determine the thrust and torque as well as its distribution. This is then represented in the RANS simulation by momentum source terms. Such an approach alleviates some of the time step and mesh restrictions. This has been used by *Simonsen and Stern (2003)* to simulate the manoeuvring characteristic of the Esso Osaka with a rudder. In their formulation the propeller was represented by bound vortex sheets placed at the propeller plane and free vortices shed downstream of it. BEMt was used by *Phillips et al. (2009)* amongst others to evaluate the momentum terms.

The lowest level of complexity involves the use of a prescribed body force approach where the impact of the propeller on the fluid is represented as a series of axial and tangential momentum sources. This is the simplest of the discussed methods, although more simplified first order methods also exist. For instance the approach with a uniform thrust distribution that has been used by *Phillips et al. (2010)* and which assumes a force only in the axial direction.

Badoe et al. (2014) investigated the three-way interaction between the hull, propeller and rudder by replicating experiments performed by FORCE Technology for a container ship operating at a Froude number of 0.202. The ability of three different methods were compared, namely; prescribed body force approach (RANS-HO), Two-way coupled RANS-BEMt model (RANS-BEMt) and a discretised propeller approach or direct method (AMI). This was validated against experimental data from the SIMMAN 2014 workshop on verification and validation of ship manoeuvring simulation methods,

SIMMAN (2014). Differences between the various methods were outlined quantitatively. The results demonstrated that as long as the radial variation in both axial and tangential momentum generated by the propeller are included in the computations, then the influence of the unsteady propeller flow can be ignored and a steady computation performed to evaluate the propeller influence on the hull and rudder. Below are other conclusions drawn from the study regarding the various methods:

(a) Fluid dynamic fidelity

RANS-HO assumes a constant circumferential distribution of thrust and torque, hence do not capture all aspects of hull-propeller-rudder interaction effects, especially the interaction between the hull on propeller and rudder on propeller and vice versa. The method was also poor in replicating the swirl effect which resulted in a different flow field (i.e. symmetry in the flow field).

RANS-BEMt is best suited for capturing and predicting most aspects of hull-propeller-rudder interaction effects. The method calculates the thrust and torque as part of the simulation and is able to replicate the swirl effect much better than RANS-HO.

AMI theoretically offers the highest degree of fidelity, however, it requires small time steps due to restrictions imposed by explicitly solving the propeller flow.

(b) Computational cost

RANS-HO is the least costly, can be used for quick resistance and self-propulsion estimations only if the flow field details are not of prime importance.

RANS-BEMt follows on from RANS-HO as being less costly for ship resistance and propulsion simulations with less than 0.27% of the total simulation (of 6 wall clock hours) spent on propeller modelling.

AMI is the most computationally demanding approach (typically $\geq 30\%$ of the total simulation time for similar setup with RANS-BEMt) since the full transient flow field needs to be resolved with a higher level of mesh cells in order to provide accurate estimates of resistance and propulsion parameters. The method does not only suffer from long overall simulation time, but also from increased computational time per time step.

(c) Suitability for design purposes

RANS-HO reasonably predicted the global forces compared to the experiment, but was poor in replicating the flow field as such the method may be used for initial assessment of ships resistance and propulsion where requirement for exact mirroring of the flow fields are not essential.

RANS-BEMt was able to predict the resistance and propulsion parameters much better, but the propeller influence has been averaged over one blade passage which neglects tip and hub vortices, this makes it unsuitable for cavitation analysis. The methods may, however benefit from the addition of tangential inflow conditions and coupled with the non-uniform inflow inputs may be suitable for transient manoeuvring simulations as well as resistance and powering computations.

AMI is more suitable for all the analysis described above, but requires experience in the use and distribution of high mesh cells to capture detail flow features.

3 Case studies

3.1. Skeg-rudder-propeller interaction review

As an example, a skeg-propeller-rudder interaction investigations in straight ahead condition and drift angle is presented (see *Badoe et al. 2015a* for full details of the study). An open source flow solver was used to investigate the sensitivity into which the interaction between the propeller and rudder downstream of a skeg is resolved as well as varying the length of the upstream skeg. In simulating the skeg, rudder and propeller flow, the entire flow field was considered as a result of the oblique motion and rotation induced by the propeller. A discretised propeller approach which uses the arbitrary mesh interface technique (AMI) was used to account for the action of the rotating propeller. Due to the complexity of the propeller geometry, especially around the blade tip with very small thickness, it was possible to place only two prism layers on the propeller. The surface refinement for the propeller was however increased to ensure that most of the flow features were resolved. Fig. 1 shows the different meshes generated on the propeller. Tables 1&2 show the details of the grid system along with predicted thrust and torque computed on each grid as well as viscous and pressure contributions to the total drag. Rudder lift and drag values are also presented for *Simonsen (2000)* and *Phillips et al. (2010)* who both performed similar investigations for straight ahead conditions (no applied angle of drift) using the CFDHIP-IOWA and ANSYS CFX code respectively, and using a body force propeller model with load distribution based on the *Hough and Ordway(HO) (1965)* thrust and torque distribution.

The difficulty associated with rudder drag prediction is evident in the results. This is mainly due to the difficulty associated with replicating the influence of swirl on the local incidence angle. At high thrust loadings, swirl components increases, leading to a reduction in the drag experienced by the rudder, the mechanism is illustrated in Fig. 2. *Simonsen (2000)* outlined other reasons for drag coefficient over prediction. Since the x-component of the normal to the rudder surface is large at the leading edge, the pressure contribution is dominant for the local drag coefficient in this region, therefore if the leading edge pressure and suction peaks are not adequately resolved it could lead to discrepancies in drag coefficient. Although the detail local flow features such as the tip and hub vortices (which are useful for cavitation analysis) described above will not be captured by the level of grid used, for manoeuvring performance of the rudder exact “mirroring” of the flow field is not essential as long as the required condition of flow (head) are adequately captured. *Phillips et al. (2009)* highlights the difficulties in the prediction of propeller torque and rudder forces with large uncertainties and comparison errors between calculated and experimental result unless significantly larger meshes are used. *Wang and Walters (2012)* indicated values in excess of 22M to resolve propeller forces, whilst *Date and Turnock (2002)* indicates values of 5-20M cells to fully resolve the rudder forces. However, a good level of understanding of the global forces required for rudder and propeller forces during manoeuvring may be obtained with the level of mesh resolution. Wall effects also play a defining role in rudder drag prediction as has been addressed by *Höerner (1965)* who showed that due to root vortex the drag of wall mounted experimental rudder differs from that of numerical rudder. Because the propeller was working close to the wind tunnel floor, it could have influenced the root flow, hence the root vortex and rudder drag prediction. Figs. 3&4 show the rudder forces for rudder angle $\alpha = -10.4^\circ$, -0.4° , and 9.6° . The results show improvement in the fine grid, especially for the drag coefficient.

3.1.1. Influence of propeller on rudder in straight ahead condition and at drift

The global forces for the rudder and propeller combination in isolation at straight ahead and drift angle conditions is shown in Fig. 5. Results for the straight ahead condition demonstrates that the wake field generated by the propeller compares well with experimental values of lift and drag on a rudder placed aft of the propeller at different angles of incidence. The influence of drift angle is well captured in terms of rudder lift and drag characteristics.

Table 1: Grid system used for sensitivity analysis.

Parameter	Coarse grid	Medium grid	Fine grid
BlockMesh refinement	80×18×36	113×24×51	160×36×72
Cells in rotating region	150K	300K	770K
Cells in stationary region	1.2M	2.9M	8.0M
Total no of cells (approx.)	1.4M	3.3M	8.8M
Computational expense	20-22hrs	60-65hrs	170-180hrs

NB: Computational expenses are based on parallel run of 12 partitions run on 6 core nodes for approximately 20 propeller revolutions. All times are in wall clock hours

The effect of the applied drift angle on the rudder results in a downward shift of the lift curve and does not significantly change the lift curve slope. Although not shown here, the applied drift angle resulted in an over prediction of propeller torque, since rudder forces are dependent on the inflow conditions (propeller race) which in turn are dominated by the action of the propeller, slight over-prediction in propeller force will result in an increased inflow velocity to the rudder, causing an increase in rudder force, hence the upward shift in rudder lift curve observed for the -7.5deg drift angle as compared with experiment. At $\alpha = -10^\circ$ (α_E of -23°), the predicted accuracy for rudder drag deteriorates. The reason is most likely that the rudder has stalled and the mesh count (of 3.3M) used to mirror entire flow field makes it difficult to capture the stall effect. The grid used, however is able to predict accurately the effective angle of attack (α_E) up to 18° ($\alpha = -5^\circ$). Fig 6 presents the axial velocity contours at three positions along the rudder at midchord, trailing edge and in the wake for the drift angle condition. It is interesting to note how the accelerated flow impinges on the rudder and the development of the tip vortices.

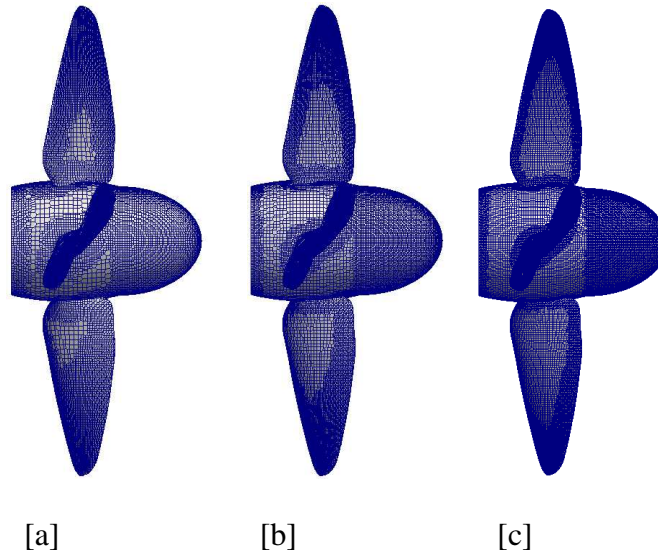


Fig.1: Mesh cut for propeller [a] coarse grid 1.4M cells [b] medium grid 3.3M cells and [c] fine grid 8.8M cells

3.1.2. Influence of skeg length on rudder-propeller performance

An upstream skeg at an angle of drift slows down the inflow to the propeller. For a rudder downstream of the propeller at drift, accurate determination of the rudder forces is influenced by the axial and tangential wake flow (Fig. 7). It can be in Fig. 8 seen that the presence of the skegs tends to reduce the lift curve slope as a result of flow straightening and there is a downward shift in the lift curve compared to the rudder and propeller alone at drift in Fig. 5. The lift curve slope, $\partial C_L / \partial \alpha$ (see Table 3) are also well predicted. The calculated drag when approaching stall was not accurately predicted due to similar reasons outlined earlier. The rudder drag at zero incidence C_{D_0} is highest for the rudder-propeller in isolation. Comparison of the plots to that of the straight ahead con-

dition in Fig 4 shows that the asymmetry in the flow results in a shift in the performance of the rudder which increases with increasing upstream skeg length. This shift may depend on the angle of drift.

Table 2: Detailed grid analysis for propeller and rudder forces, $\alpha = 10^\circ$, $\beta_R = 0^\circ$, $J = 0.36$.

Grid	Coarse grid	Medium grid	Fine grid	Simonsen (2000)	Phillips (2010)	Data
K_T	0.305	0.294	0.286			0.283
ε	+7.77%	+3.89%	+1.06%			
K_Q	0.051	0.047	0.044			0.043
ε	+18.60%	+9.30%	+2.32%			
C_L	1.350	1.280	1.220	1.270	1.360	1.251
ε	+7.96%	+2.36%	-2.44%	+1.56%	+8.76%	
$C_{D \text{ total}}$	0.190	0.170	0.148	0.070	0.187	0.109
ε	+74.3%	+55.96%	+35.78%	-93.58%	71.56	
$C_{D \text{ viscous}}$	0.075	0.072	0.069			
$C_{D \text{ pressure}}$	0.115	0.098	0.079			

At $x = 1.05$ chords, the propeller swirl dominates the flow, the rudder wake has mixed with the surrounding faster moving fluid. The overall results provide reasonable initial estimates for rudder forces at drift angle $\beta_R = -7.5^\circ$ and 0° . Overall improvements in mesh resolution around the propeller, rudder and rudder tip vortices would improve the quality of the results.

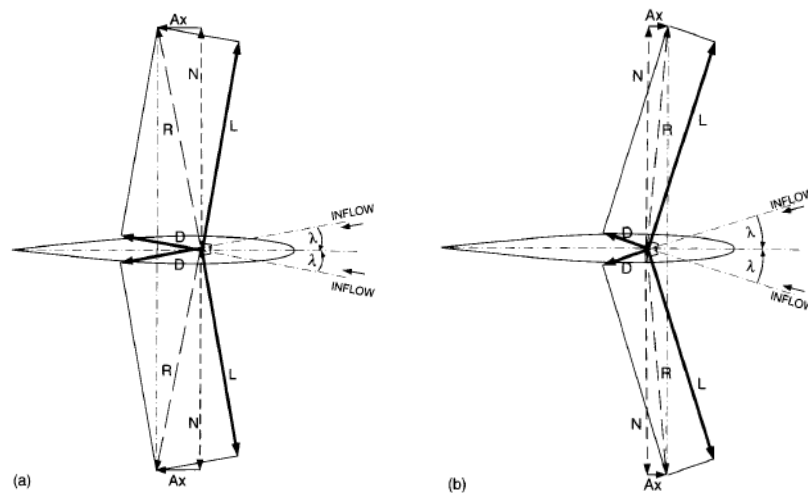


Fig.2: [a] Rudder angle zero degrees: forces due to propeller-induced incidence [b] Rudder angle zero: forces due to propeller-induced incidence - high thrust loading, source: *Molland and Turnock (2007)*.

3.1.3. Rudder pressure distribution at straight ahead and at drift conditions

The influence of the propeller and skeg on rudder at straight ahead and drift conditions are compared through chordwise pressure distribution of surface pressures for eight spanwise rudder locations from the root to tip in Fig. 9. The computed chordwise pressure distribution represented by the local pressure coefficient C_p is given by:

$$C_p = \frac{P - P_\infty}{0.5\rho U^2} \quad (2)$$

where $P - P_\infty$ is the local pressure; ρ is the density of air and U is the free stream velocity. Drift angle influence can be observed for most areas of the rudder span below the center of the slipstream (below the hub). Close to the slipstream, (span 230 & 390mm) local incidence resulted in the pressure peak increasing with increasing skeg lengths at the rudder leading edge. An area of interest was just around

the hub where the unsteadiness in the flow introduced by the hub vortex can be observed for span 530mm as a bulge in the pressure curve for the zero drift angle around the rudder trailing edge. This was not observed for the drift cases. In areas close to the tip (span 705mm-970mm) there were little or no differences in pressure curves for the drift cases. This is also seen in the streamlines passing through the short skeg at drift, Fig. 7 where most of the flow changes occur in the rudder mid span, explaining why there was little difference in pressure curves for the drift cases around the rudder tip.

Table 3: Rudder lift curve slope, $\partial C_L/\partial \alpha$, and corresponding drag at zero incidence, C_{D0} .

	C_{D0}		$\partial C_L/\partial \alpha$	
	Molland&Turnock	Calculations	Molland&Turnock	Calculations
Zero drift angle	0.016	0.02	0.132	0.129
Rudder&propeller alone	0.083	0.06	0.146	0.144
Short length skeg	0.029	0.01	0.121	0.119
Medium length skeg	0.025	0.012	0.119	0.115
Long length skeg	0.0169	0.019	0.125	0.126

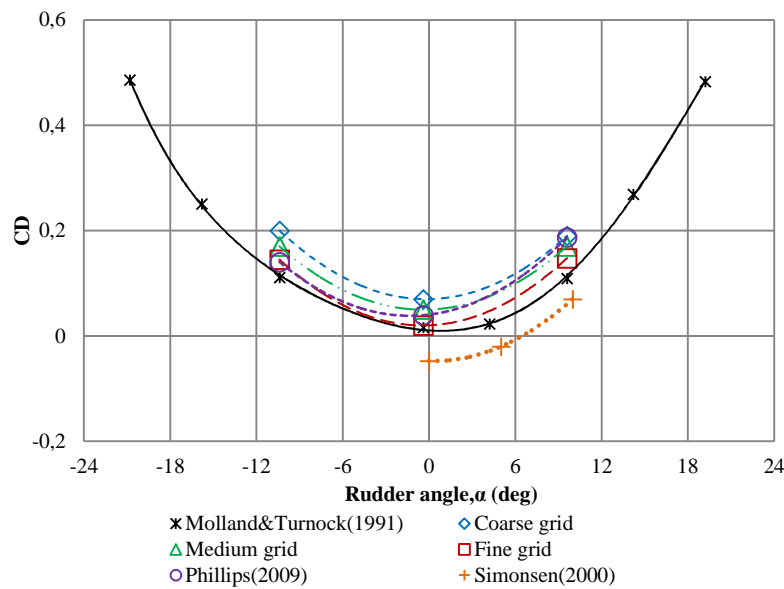


Fig.3: Rudder drag coefficient, $\beta_R = 0^\circ$, $J = 0.36$.

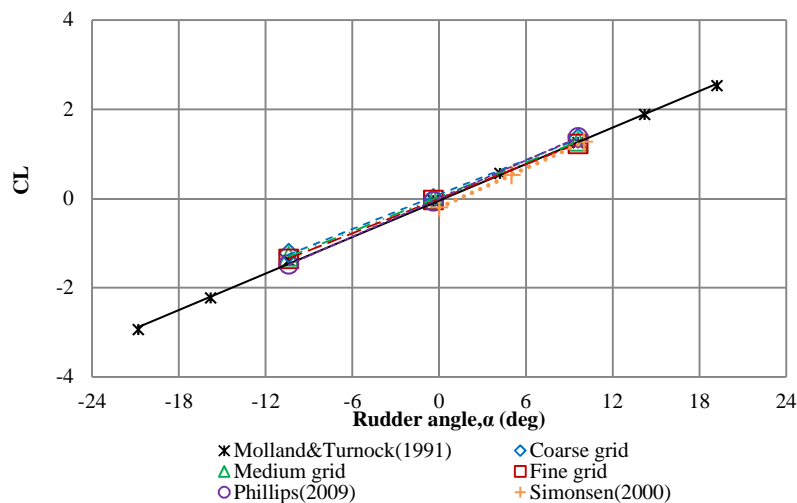


Fig.4: Rudder lift coefficient, $\beta_R = 0^\circ$, $J = 0.36$.

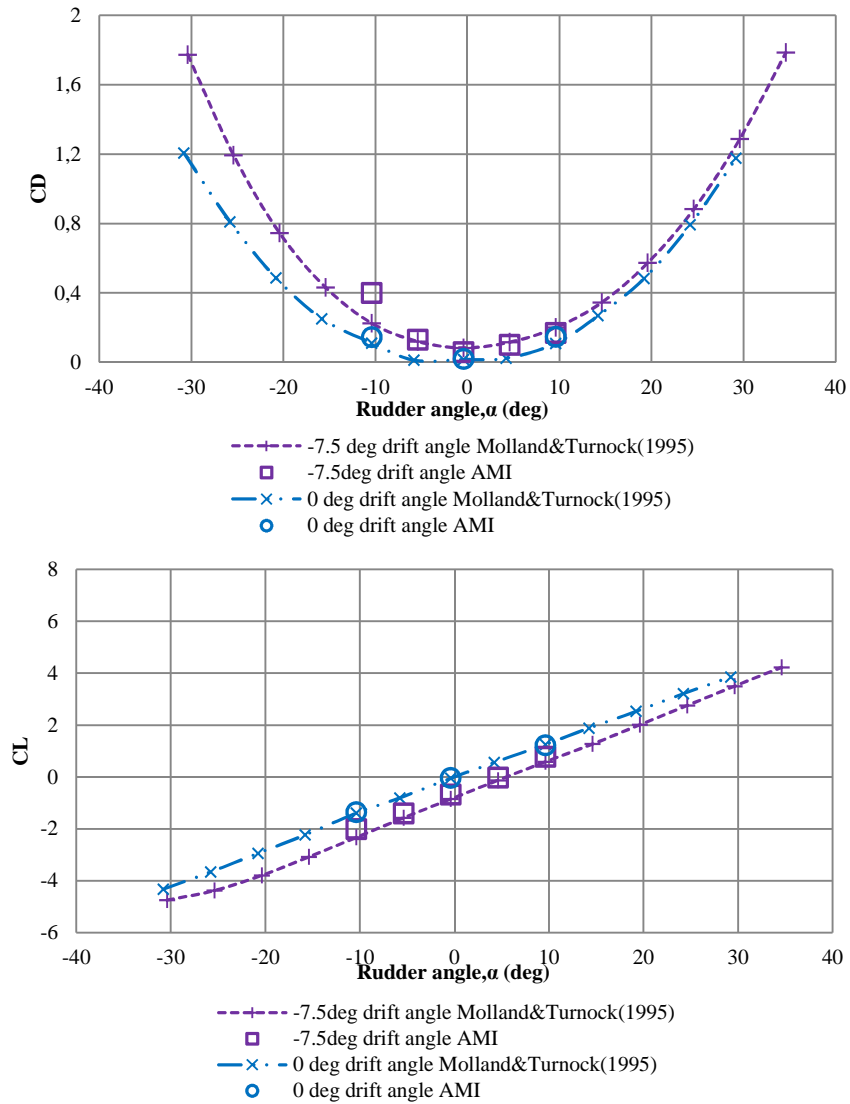


Fig.5: Effect of drift angle on the performance of a rudder and propeller combination in isolation at $J = 0.36$, $\beta_R = -7.5^\circ$ (medium grid results) and $\beta_R = 0^\circ$ (fine grid results).

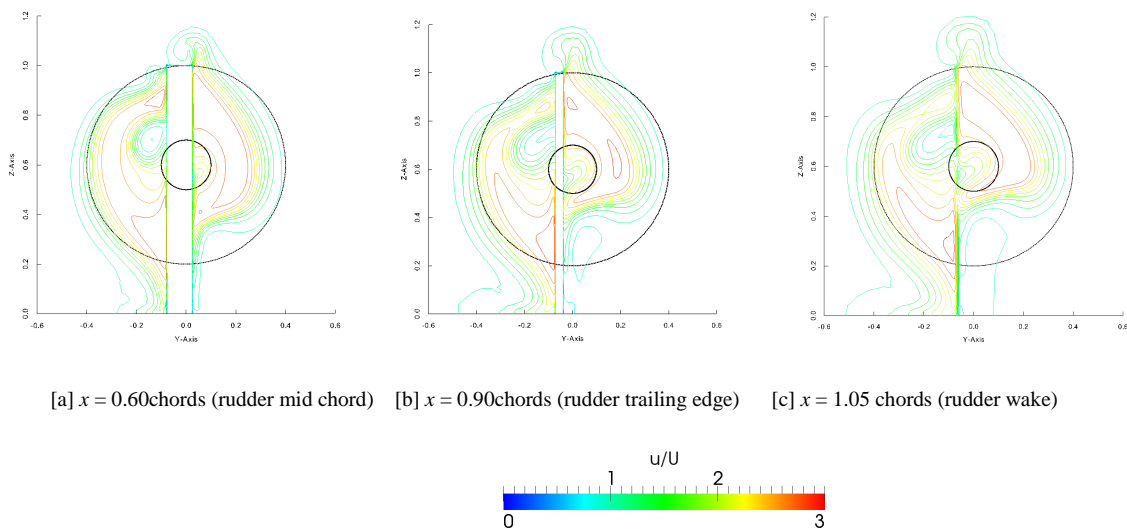


Fig.6: Axial velocity contours at different rudder x -positions, $J = 0.36$, $\beta_R = -7.5^\circ$ at $\alpha = 10^\circ$.

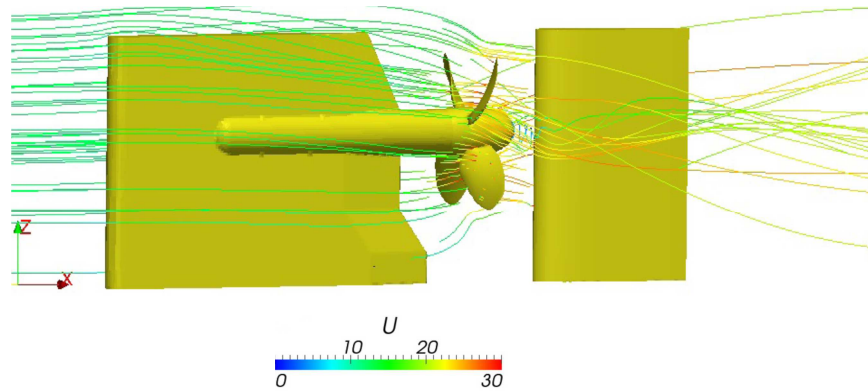


Fig.7: Streamlines passing through the shortskeg, $J = 0.36$, $\beta_R = -7.5^\circ$ at $\alpha = 10^\circ$.

3.2. Techniques to consider for effective hull-propeller-rudder computations

Various techniques to consider in ship powering based computations, including small details that can result in changes in flow characteristics as well as changes in propulsive power:

- High fidelity computations

Using Reynolds Averaged Navier Stokes solvers (RANS) to analyse hull-propeller-rudder require high fidelity computations as the boundary layer of the hull, skeg and the viscous wake needs to be captured with high level of accuracy. Here, high fidelity refers to RANS solvers which employ good grids and strong turbulence models. The skeg and hull flow may be characterised by complex vortex shedding, which may require complex grid resolution in order to understand them. *Eça et al. (2002)* showed that numerical simulation of such flows require grids with orthogonality at the ship surface where the no-slip condition is applied and high stretching of the grid towards that surface to resolve the flow in the near-wall region. The mesh in the propeller plane should be able to give circumferential distribution of the three components of the velocity as this information forms an important part of the input to the propeller. It is not always the size of the grid that determines the accuracy of the solution but its distribution so as to provide useful information of the underlying physics of the flow.

- What if the self-propelled thrust is over estimated ?

Reference is hereby made to *Badoe et al. 2015b* who focussed on calm water powering performance of a future twin skeg LNG ship specifically on the changes in propulsive power resulting from small variations in design. The influence of free surface was not included in the computations. A ‘RANS-BEMt’ approach was utilized for the self-propelled computations. The self-propulsion point was realised by manually adjusting the propeller revolutions until the self-propelled thrust (T_{sp}) equals the self-propelled drag (R_{sp}) or $T_{sp} - R_{sp} = 0$, similar to actual model test procedures. Fig. 10 shows the impact on thrust deduction when the self-propelled thrust is over-estimated. From the plot, it can be seen that a linear relation exists between self-propelled thrust prediction and its impact on thrust deduction. For example, from the results, an error of the self-propelled thrust by say 7% will result in an error in the thrust deduction by approximately 7%. It should however be pointed out that this relation has been found based on constraints placed on the hull and the use of nominal wake values as input to the propeller code.

- Tangential wake effects

A disadvantage with the equipment of skegs is that they have a high wetted surface area, hence increasing frictional resistance. But as may be seen from the streamline plot in Fig. 11, the presence of the skegs provides pre swirl to the propeller. This is advantageous for the

propeller performance as it can contribute to improving the propeller efficiency, compensating for increase in frictional resistance. Most self-propelled twin skeg computations using a body force propeller model only consider the effect of axial wake as that is the predominant component as far as most propeller straight ahead flows are concerned. Usually, an upward flow exists at the aft end which leads to an axial flow component plus a tangential flow component (Molland et al. 2011). The influence of tangential wake was studied by Badoe et al. 2015b for a twin skeg ship as shown in Fig. 12. The plots were taken at 0.18D behind the propeller plane (see Fig.13). The influence of tangential wake investigated showed that by considering the upward flow the true axial component is slightly over-predicted, both the radial and tangential components of wake are modified thus modifying the thrust deduction and hence the propulsive efficiency.

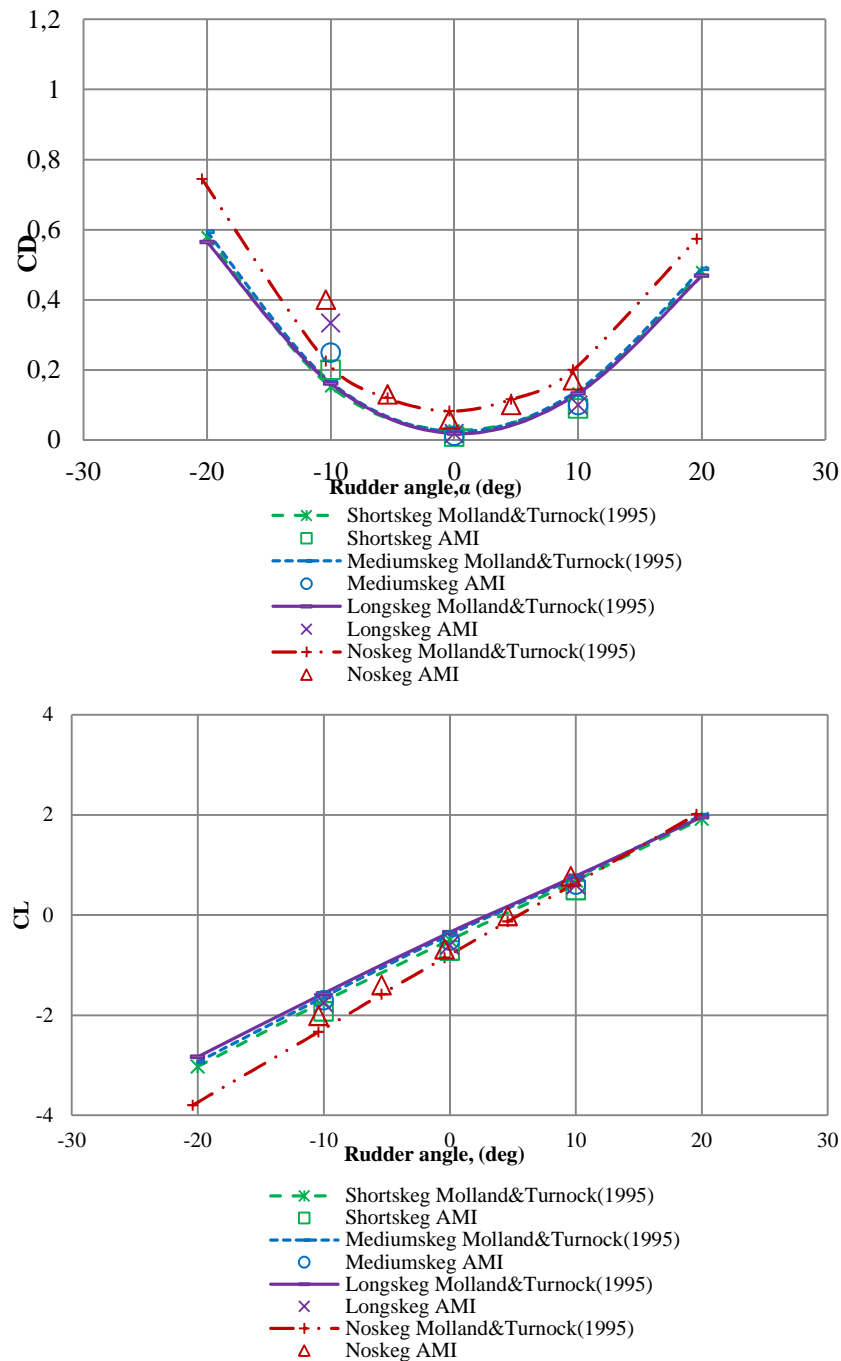


Fig. 8: Effect of drift angle rudder downstream of 3 skeg configurations at $J = 0.36$, $\beta_R = -7.5^\circ$

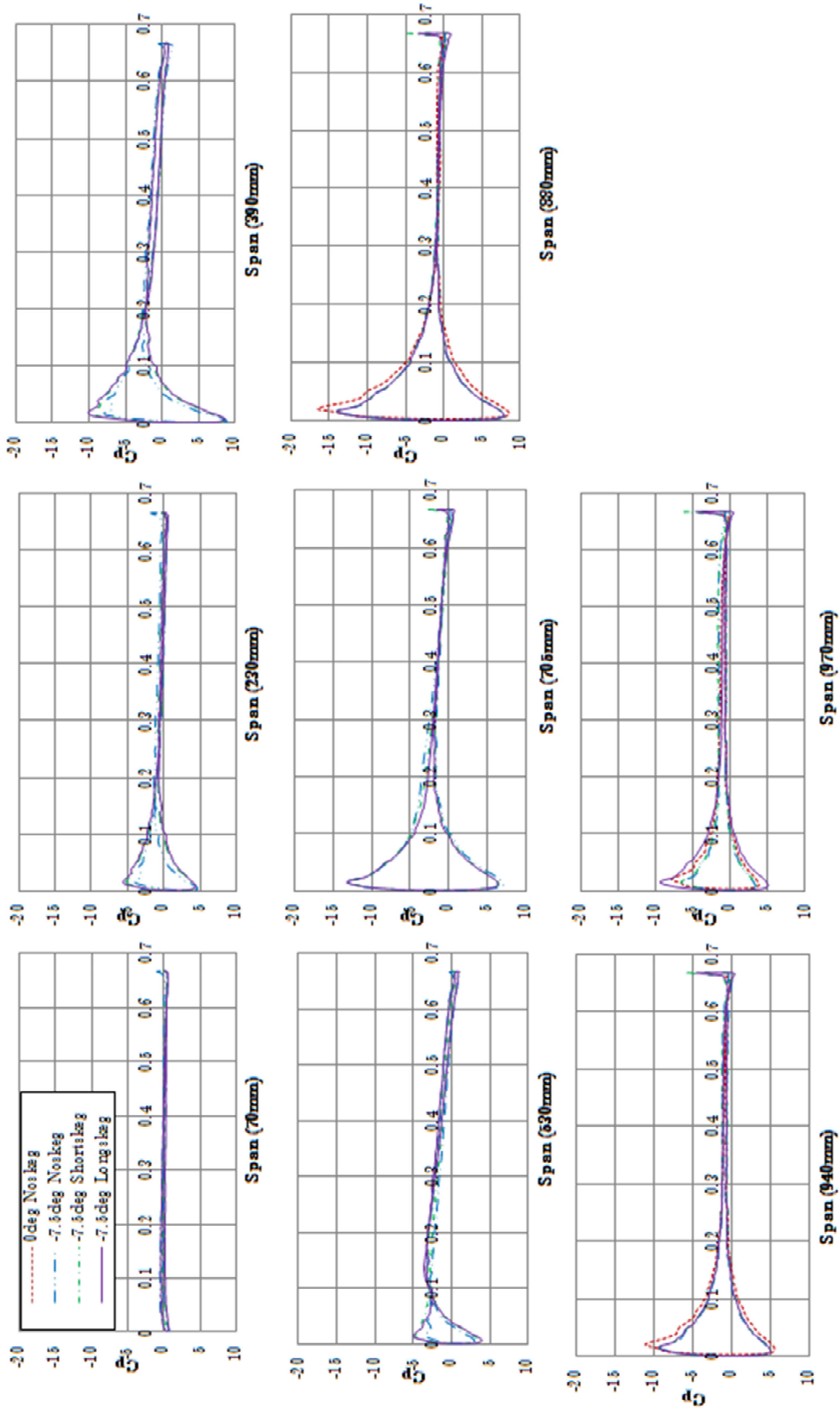


Fig. 9: Chordwise pressure distribution at various rudder spanwise positions, $J = 036$, $\beta_R = -7.5^\circ$ & 0° , $\alpha = 10^\circ$.

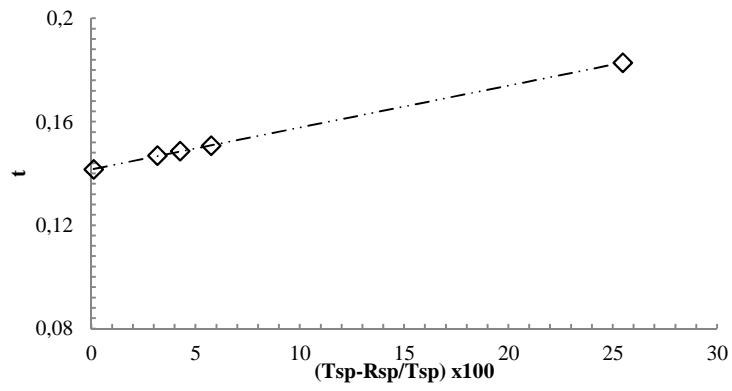


Fig. 10: Error margin in thrust deduction prediction

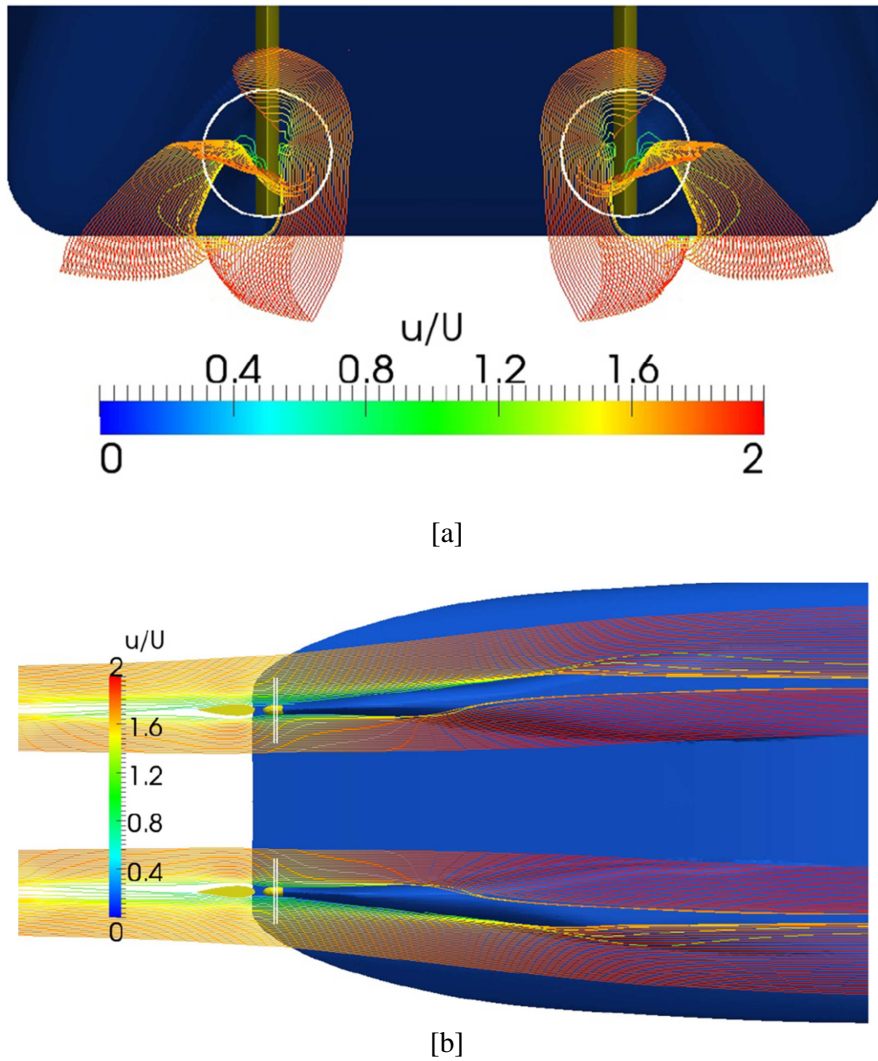


Fig. 11: Streamlines passing through twin skegs at loaded draught, $F_n = 0.197$ [a] view from stern [b] view from bottom.

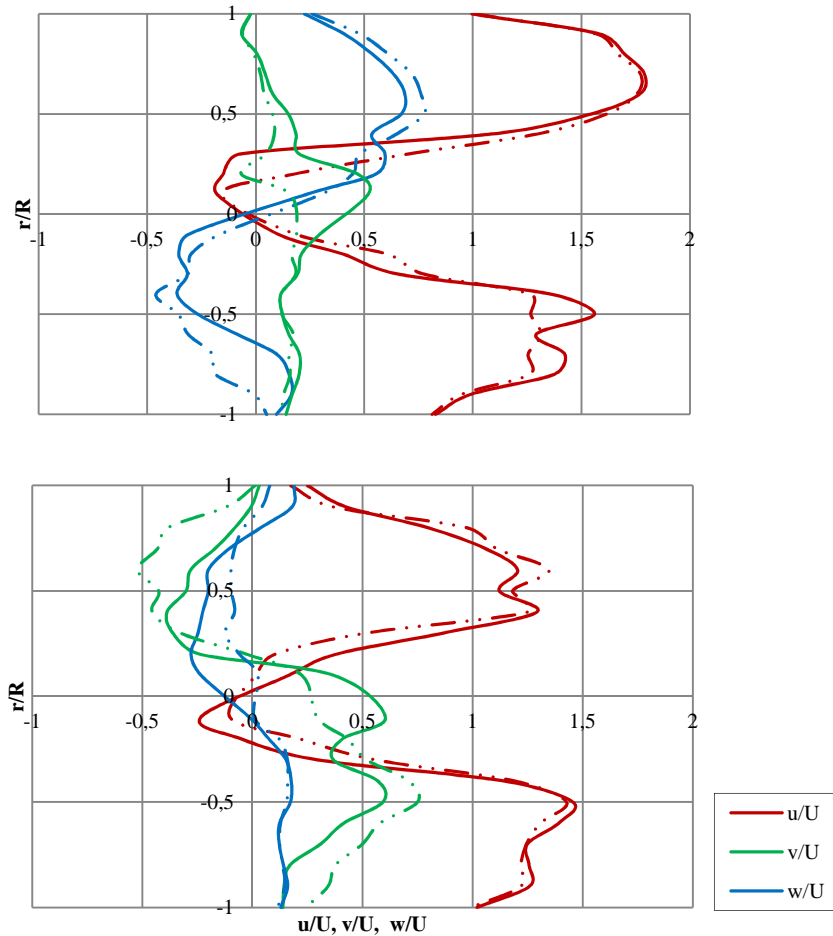


Fig. 12: Wake cut at 0.18D behind propeller plane [top] fixed z and varied y [bottom] fixed y and varied z , for loaded draught condition, port side propeller. NB: solid lines represent the addition of tangential wake effect and dotted lines represent no addition of tangential wake effect.

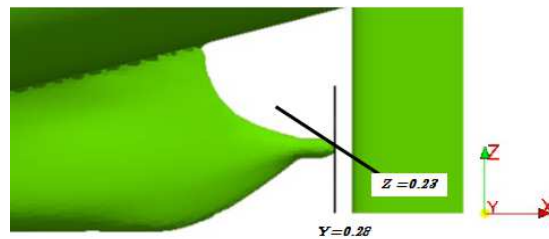


Fig. 13: Wake cut location for plots of velocity at 0.18D behind propeller plane

4 Conclusions

In the present paper, the impact of hull-propeller-rudder interaction on ship powering has been presented. Various methodologies which have been used for such successful analysis were discussed along with results into the sensitivity into which the interaction between the propeller and rudder downstream of a skeg is resolved as well as varying the length of the upstream skeg. Overall, good agreement was found between the experimental and computational results when predicting the influence of the skeg and propeller on rudder. However, it can be seen that there is a significant computational expense associated with a time resolved propeller interaction and that alternate body force based methods are likely to still be required for hull(and skeg) -propeller-rudder computations.

References

- BADDOE, C.; WINDEN, B.; LIDTKE, A.K.; PHILLIPS, A.B.; HUDSON, D.A.; TURNOCK, S.R. (2014), *Comparison of various approaches to numerical simulation of ship resistance and propulsion*, SIMMAN 2014, Lyngby
- BADDOE, C.; PHILLIPS, A.B.; TURNOCK, S.R. (2015), *Influence of drift angle on the computation of hull-propeller-rudder interaction*, J.Ocean Eng. 103, pp.64-77
- BADDOE, C. (2015), *Design practice for the stern hull of a future twin-skeg ship using a high fidelity numerical approach*, PhD Thesis, University of Southampton
- DATE, J.C.; TURNOCK, S.R. (2002), *Computational evaluation of the periodic performance of a NACA 0012 fitted with a Gurney flap*. J. Fluids Eng. 124, pp.227-234
- EÇA, L.; HOEKSTRA, M.; WINDT, J. (2002), *Practical Grid Generation Tools with Applications to Ship Hydrodynamics*, 8th Int. Conf. in Grid Generation in Computational Field Simulations, Hawaii
- HOERNER, S. F. (1965), *Fluid dynamic drag*, Midland Park, New Jersey
- HOUGH, G.R.; ORDWAY, D.E. (1965), *The generalized actuator disc*. Dev. in Theor. and Appl. Mech. 2, pp.317-336
- LÜBKE, L. (2005), *Numerical simulation of flow around the propelled KCS*, CFD Workshop Tokyo, Tokyo, pp.587-592
- MOLLAND, A.F.; TURNOCK, S.R.. (2007), *Marine rudders and control surfaces: principles, data, design and applications*, Butterworth-Heinemann, Oxford
- MOLLAND, A.F.; TURNOCK, S.R.; HUDSON, D.A. (2011), *Ship resistance and propulsion: practical estimation of ship propulsive power*, University Press, Cambridge
- PHILLIPS, A.B.; TURNOCK, S.R.; FURLONG, M.E. (2009), *Evaluation of manoeuvring coefficients of a self-propelled ship using a blade element momentum propeller model coupled to a Reynolds averaged Navier Stokes flow solver*, J. Ocean Eng. 36/15, pp.1217-1225
- PHILLIPS, A.B.; TURNOCK, S.R.; FURLONG, M.E. (2010), *Accurate capture of rudder-propeller interaction using a coupled blade element momentum-RANS approach*, Ship Technology Research 57/2, pp.128-139
- SAKAMOTO, N.; KAWANAMI, Y.; UTO, S.; SASAKI, N. (2013), *Estimation of Resistance and Self-propulsion characteristics for a Low L/B Twin-Skeg Container Ship by High-Fidelity RANS Solver*, J. Ship Research, 57/1, pp.24-41
- SIMMAN (2014), *Workshop on verification and validation of ship manoeuvring simulation methods*, Lyngby
- SIMONSEN, C. (2000), *Propeller-Rudder Interaction by RANS*, Ph.D thesis, University of Denmark
- SIMONSEN, C.; STERN, F. (2003), *Verification and Validation of RANS manoeuvring simulation of Esso Osaka: effects of drift and rudder angle on forces and moments*. J. Computers and Fluids 32, pp.1325-1356
- WANG, X.; WALTERS, K. (2012), *Computational analysis of marine propeller performance using transition-sensitive turbulence modelling*, J.Fluids Eng. 134/7, pp.071107

Fuel Saving Potentials via Measuring Propeller Thrust and Hull Resistance at Full Scale: Experience with Ships in Service

Erik van Ballegooijen, VAF Instruments, Dordrecht/Netherlands, evballegooijen@vaf.nl
Tiberiu Muntean, VAF Instruments, Dordrecht/Netherlands, tmuntean@vaf.nl

Abstract

This paper presents the possibilities offered by the full scale measurement of propeller thrust (and torque), to identify fuel saving potentials and emission reductions. Via full scale measurements of propeller thrust and torque, in relation to other parameters like ship speed, the change in propeller efficiency and the hull resistance can separately be determined over time. This for instance due to propeller or hull fouling, propeller damages and hull coatings. In addition an example will be shown of measurement results, and the possibilities of the propeller thrust and torque measurements, on a +13000 TEU container vessel in service.

1. Introduction

In general there is a large interest in the maritime world for ship propulsion efficiency. This has several reasons related to either cost savings, legislation, and/or environmental concern. An example is the focus on fuel consumption which has a direct cost relation, but has also a link to the environment when looking at green house gas emissions. In order to be able to improve on the fuel consumption and green house gas emissions, these need to be measured before any improvement actions can be verified. When looking at ship propulsion, this means to measure and quantify the present status and possible changes over time of for instance the propeller efficiency, and the total ship resistance due to propeller and hull fouling or damages.

This paper describes the way to measure the propeller efficiency over time, separate from the hull resistance, via measuring the propeller thrust, next to the common used propeller torque. If the propeller thrust is measured, the actual propeller condition can be separated from the ships hull condition. This is important for several reasons:

- a. To determine the proper timing for a hull cleaning based on the actual hull resistance without the propeller condition taken into account.
- b. To determine the actual effect of a newly applied hull coating on the ships resistance.
- c. To determine the proper timing for a propeller cleaning (this might differ from the hull cleaning timing due to measured difference in fouling condition of hull and propeller).
- d. To determine possible propeller damages, which result in a propeller performance decrease.
- e. To determine the optimal propeller efficiency conditions at several ship operational conditions (as an example to determine the effect of variable rpm versus constant rpm on propeller efficiency for a controllable pitch propeller).
- f. To determine the effect of energy saving devices (like a BCF or WED) or propeller or hull modifications (like for instance a new bulbous bow design).

VAF Instruments (the Netherlands), a well known supplier of measurement systems for the maritime market, developed the TT-Sense® thrust and torque sensor. The sensor, which is already on the market for more than three years, has been used by VAF Instruments R&D department to quantify vessel performance and to track the changes in vessel performance over time. Experience is gained until now on many types of vessels from small cargo vessels towards 14000 TEU container vessels, as well as on navy vessel shaft lines.

Once the propeller thrust and torque are known, together with several other to be measured parameters, the condition of the propeller and the ship's hull can be determined separately. In the next chapters a more detailed description is given on these type of measurements, and an example is shown of the measurement results achieved on a +13000 TEU container vessel in service.

2. Measurement layout

In order to determine via measurements the propeller and ship's hull condition, several parameters need to be taken into account and measured. In the next paragraph a general overview of these various parameters is shown. Special attention is paid to the propeller thrust measurement via the TT-Sense® sensor.

2.1. Parameters to be measured

In order to determine via measurements the propeller and ship's hull condition, several parameters need to be taken into account and measured. A typical list of to be measured parameters consists of:

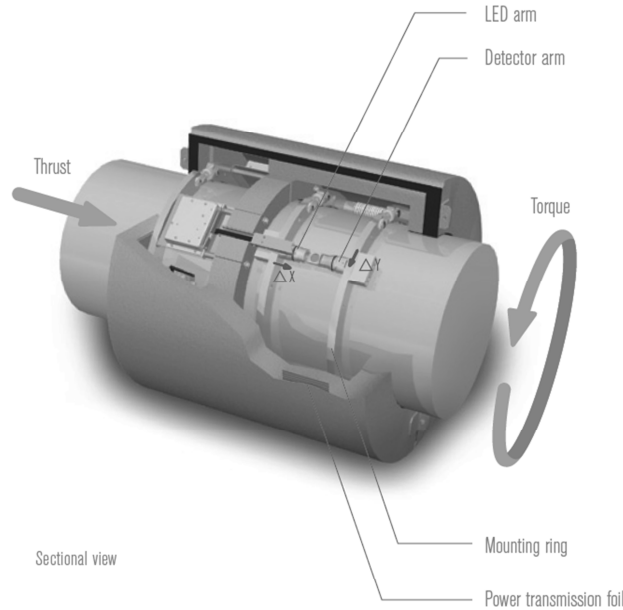
- Propeller thrust
- Propeller torque
- Propeller RPM
- Speedlog
- GPS location
- Ships draft
- Seastate
- Wind

The majority of these parameters are already measured and available on board of a ship via dedicated sensors, and or log reports. Propeller power, via torque and RPM, is nowadays a rather common measurement on board of a ship. But in order to be able to separate the propeller performance from the ship's hull performance, also the propeller thrust needs to be measured. This asks for an additional propeller thrust sensor. The TT-Sense® propeller thrust and torque sensor used in this investigation is discussed in the next paragraph.

In order to determine a trend over time of the change in propeller and ship's hull performance, the above parameters are advised to be monitored over a longer time period of typically ½ to 1 year. Additional it must be noted that the various parameters need to be monitored at their characteristic frequencies. Ships draft for instance remains constant over a longer time period compared to for instance the propeller thrust. As such the measurement frequency is different for the various parameters. In the used measurement setup all these various signals are logged digitally on a central computer on board of the ship. This collected data is then send to shore via satellite connection on a regular daily basis. This allows for a daily follow up of the propeller and ship's hull condition.

2.2. Thrust and Torque measurement sensor

In view of the propeller and ship's hull performance measurements, the propeller thrust is of special interest, as this measurement allows for a split in performance between propeller and hull. In the measurements discussed in this paper, use is made of the VAF Instruments TT-Sense® propeller thrust and torque measuring system. This TT-Sense® sensor can be mounted on propeller shafts between the propeller and the thrust bearing. When a shaft is subject to thrust and torque this results in a small compression and torsion of the shaft. The working principle of the TT-Sense® is based on measuring this shaft compression and torsion over a shaft length of typical 200 [mm]. This relative long measuring area of the shaft, compared to for instance strain gages, highly increases the measurement accuracy. LED's and extremely accurate optical sensors detect the small displacements over the shaft length, in both axial and tangential directions, corresponding to the compression (thrust) and torsion (torque) of the propeller shaft. The used optical measurement principle allows for an independent measurement of both the thrust and the torque. In Fig. 1 the general working principle of the TT-Sense® thrust and torque sensor is shown. The measured values of thrust and torque are transferred continuously from the rotating shaft to the stator part through wireless data connection with a 100 Hz transfer rate. Power transmission from the stator to the rotating shaft is performed by means of induction. The stator part consists of a power transmission coil, a data signal receiver and a control box equipped with digital or analogue output connections.



Δy and Δx are small movements of the propeller shaft surface due to strain.
 Δy is the movement in torque direction and Δx is the movement in thrust direction.

Fig.1: General working principle of the TT-Sense® Thrust and Torque sensor

3. Theoretical approach for propeller and ship’s hull performance measurement

When looking at the performance of the propeller and ship’s hull, this can be done via two ways. The first route is via the common used power / torque measurement. This provides only performance indications of the combined propeller and hull system, but not on each of them individual. The second route is via propeller thrust measurements. When applying additional propeller thrust measurements the performance evaluation of propeller and ship’s hull can be split. In the next paragraphs these two routes are explained in more detail.

3.1. Performance evaluation based on torque measurements

When measuring power / torque as input, and the ship speed as output (Fig. 2.), there can be derived a certain “efficiency” which is the conversion of propulsion power into ship speed. This is the well known speed – power relation of a ship, which can change over time due to for instance fouling of propeller or hull.

ROUTE 1:

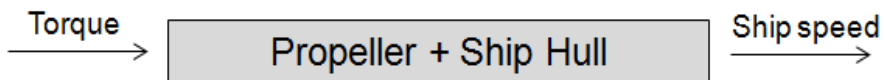


Fig.2: Performance measuring via power / torque towards ship speed

Drawback of measuring the ships performance via only power / torque is that there can be made no distinction between change in propeller performance and hull performance. As such, when a deterioration in the speed – power performance of a ship is noticed, based on a power / torque measurement, it cannot be determined if this is caused by for instance either a propeller fouling or damage, or an increased hull fouling, or a combination of both. This hampers the decision making on taking the proper action for performance improvement, i.e. should there be taken actions on the hull, or on the propeller, or both.

3.2. Performance evaluation based on thrust measurements

When taking also propeller thrust into account, as represented in Fig. 3, the route power / torque → propeller thrust → ship speed, provides two kinds of efficiencies or conversions. For the propeller this is the well known propeller efficiency, where input torque is converted into thrust at a certain RPM and water inflow velocity. For the ships hull the efficiency might be seen as the transformation of thrust towards ship speed, where the “efficiency” of this transformation is related to the hull resistance.

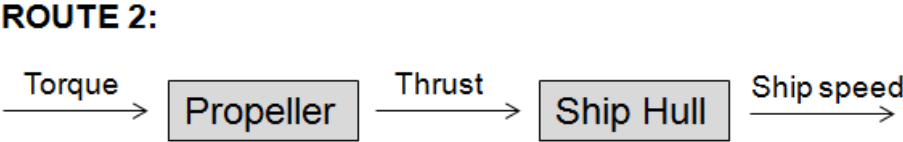


Fig.3: Performance measuring via torque and thrust towards ship speed

The advantage of measuring in addition the propeller thrust is the possibility to distinguish between propeller and hull performance. By doing so an increase in fuel consumption can be directly related to either the propeller, or the ship’s hull. This in return allows to direct the proper corrective actions to the component which actually shows the performance drop.

As will be shown in the next chapter, in which full-scale measurements are presented, the propeller performance deterioration plays, next to the hull, an important role in the total ship performance.

4. Propeller and hull performance measurements on a +13000 TEU container vessel in service

The previously described routes for total ship propulsion performance evaluation, are tested on board of several ships, making use of the VAF Instruments TT-Sense® thrust and torque sensor. In this chapter the results of one of these ships are discussed in more detail. The ship is a +13000 TEU container vessel with a fixed pitch propeller, operating on a fixed schedule between Asian and European container terminals. On this particular container vessel, the various parameters as described in paragraph 2.1 have been measured over approximately 1.5 years. As both the propeller torque and the propeller thrust have been measured, both performance evaluation methods as described in paragraph 3.1 and 3.2 have been evaluated for this ship. In the next paragraphs the various results are presented and discussed.

4.1 Performance over time based on power measurements

The first performance evaluation for this particular container vessel is based on the propeller torque measurements. This is the conventional way of analysing the total ships performance, as described in paragraph 3.1, in which no distinction between the propeller and hull performance is made.

As a first indication of the quality of the measurements, the measured speed - power curve of the vessel is shown in Fig. 4. It must be noted that for this speed - power curve it is important to use the actual speed through water (STW) instead of the speed over ground. This as there might be relevant difference between the speed over ground and the speed through water due to water current. And as the actual ships resistance depends on the actual speed of the vessel through the water, the measured speed through water is to be used. It must also be noted that in a separate study the quality of the speed through water measurement of the actual speed-log of this vessel, turned out to be of high accuracy. This very much improves the accuracy of the measured performance of the ship over time as will be shown further on.

In addition during the measurement period of 1.5 years, although this particular container vessel is sailing identical routes, there are other important parameters which vary over time. These varying parameters relate to the ships draft, sea-state, and wind, but also temporarily acceleration and

deceleration of the vessel. For all these parameters a proper filtering is applied in order to remain with the relevant measuring points which at the end serve for comparison.

As can be seen from the measured speed – power curve in Fig. 4, during the measurement period of 1.5 years there is a good correlation with model test predictions. Shown variations in the measured values are expected to be related to the actual draft differences compared to the model test draft, the influence of minor rudder steering, the actual present (low because filtered) sea-state and wind, but also due to an increase in fouling over time, which all add additional resistance.

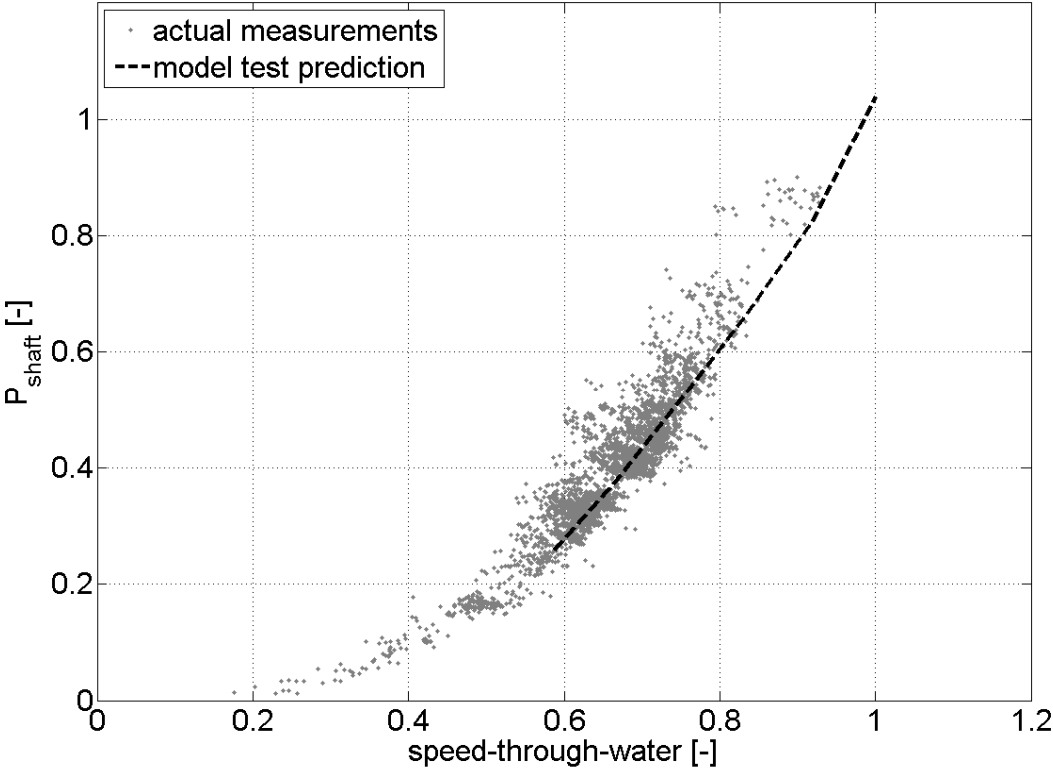


Fig.4: Speed (through water) – power curve for +13000 TEU container vessel over a 1.5 year period

The next step is to investigate how the power needed at a certain ship speed is changing over time. This in order to see if the total ship performance (propeller + hull) is deteriorating. For this the change in total “ship resistance” coefficient δ is calculated as $\delta = P_{shaft} / STW^\alpha$ in which the power factor α is determined based on the actual measurements in Fig. 4.

In this way the total “ship resistance” coefficient δ can be calculated for every measurement point, and can be plotted over time. The outcome is shown in Fig. 5, where at the start of the measurements the measured value is set to 100%. The remaining measurement values are all calculated relative to the first measured value in order to be able to show the relative change in total “ship resistance” coefficient over time.

From this figure the following conclusions can be drawn. At first it is clearly visible that the calculated total “ship resistance” coefficient has a spread. This might be explained by the earlier described variations in measured power at a certain speed through water as seen in Fig. 4. But when calculating the linear regression line over time through all the individual points, it is clearly visible that the total “ship resistance” coefficient is increasing over time. For the time frame of the measurements, the total “ship resistance” increases by +9.2%. This equals to an increase of +6.4% per year.

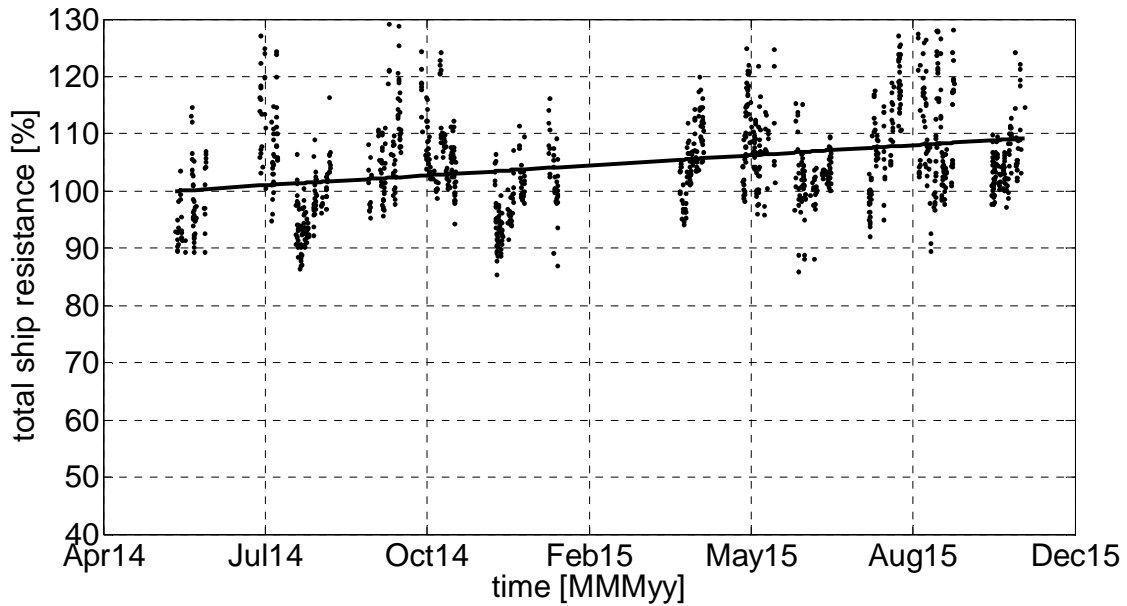


Fig.5: Total “ship resistance” coefficient δ over time, increase is 9.2% (equals 6.4% per year).

4.2 Performance over time based on thrust measurements

The second performance evaluation for this particular container vessel is based on the propeller thrust measurements, as described in paragraph 3.2. Here a clear distinction between the propeller and hull performance can be made. In the next paragraphs the separate outcome of the measured propeller performance (efficiency), and hull resistance will be shown and discussed.

4.2.1 Propeller open water curve measured at full scale

As both propeller thrust and torque are measured, together with measured speed through water and propeller RPM, it is possible to calculate for each individual measurement point the propeller open water characteristics (J , K_t , $10K_q$). Herein the J -value is determined with the wake fraction based on propulsion model tests, performed for this particular container vessel.

The +13000 TEU container vessel discussed here is equipped with a fixed pitch propeller (FPP). For this specific FPP propeller design, the propeller open water curves are determined from open water tests performed at a model test institute with the exact (scaled) geometry of the actual full scale FPP. The model scale open water curves are then the basis for the prediction of the full scale propeller performance by the model test institute.

In Fig. 6 the full-scale propeller open-water curve from model tests is shown, together with the actual measurement points via the thrust and torque measurements performed via the TT-Sense® sensor on board of the +13000 TEU container vessel. As can be seen in this Figure, the model test predictions are fairly good in line with the actual measurement points. This provides an important indication that the total set of measured parameters on board of the ship are accurate and stable in time.

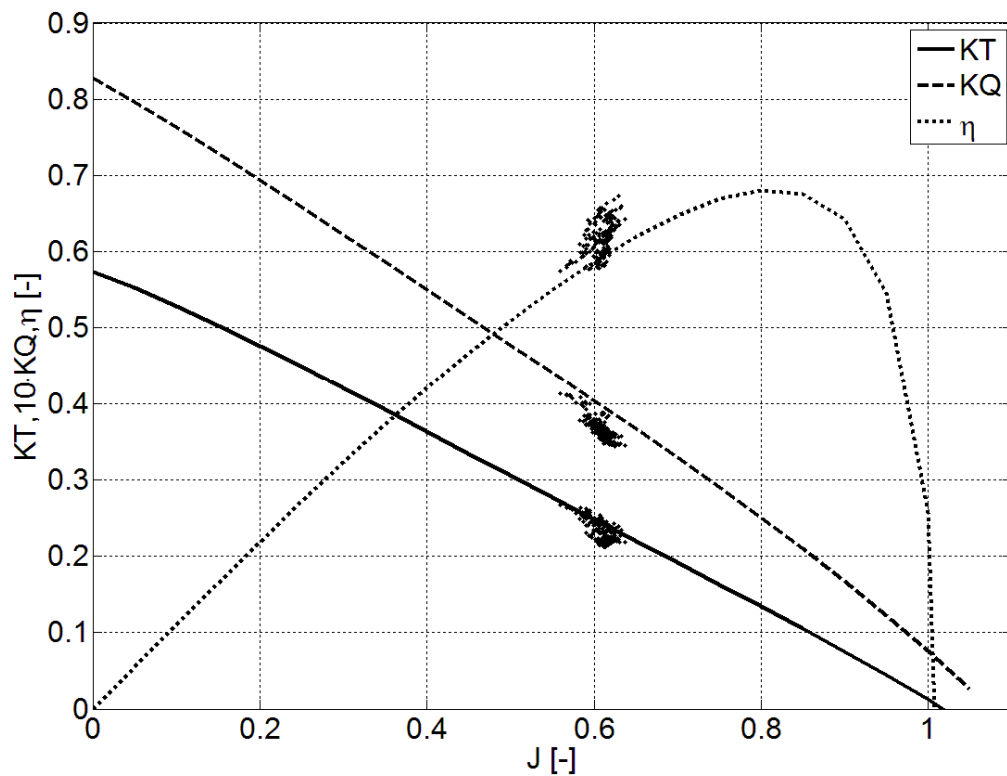


Fig.6: Propeller open-water curves: measurements at full scale with TT-Sense® (dots), versus full scale predictions based on model tests (lines).

4.2.2 Propeller efficiency over time

Since it is now possible to measure the individual propeller performance (efficiency), the next step is to evaluate this propeller performance over time. This to determine any possible propeller performance deterioration. For this, the propeller efficiency measurement points are plotted over time. The outcome is shown in Fig. 7, where at the start of the measurements the measured absolute propeller efficiency value is set to 100%. The remaining measurement values are all calculated relative to the first measured value in order to be able to show the relative change in total propeller efficiency over time.

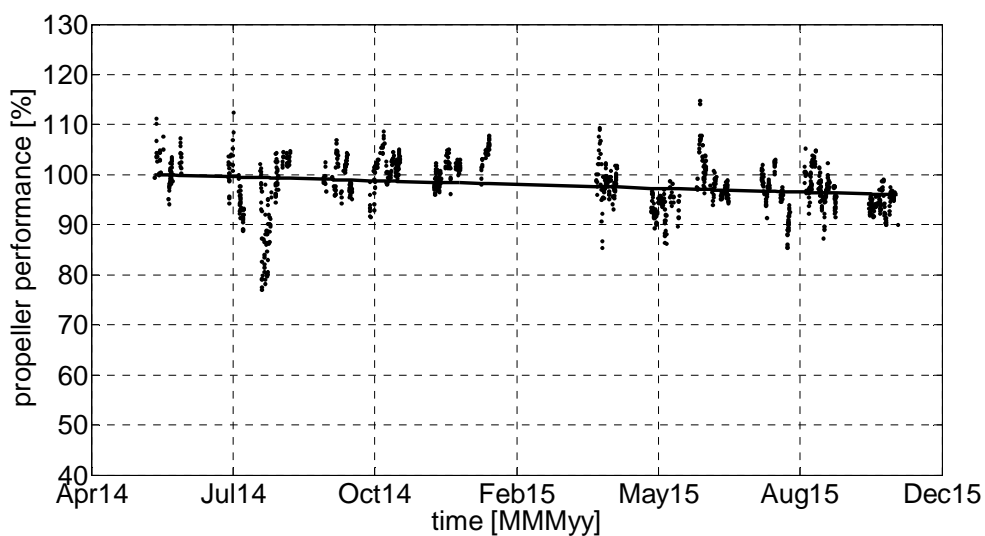


Fig.7: Propeller performance over time, decrease is 3.7% (equals 2.6% per year).

As can be seen in Fig. 7, there is a spread of the individual measured propeller performance (efficiency) points. The spread can be related to measurement accuracy of the various parameters influencing the propeller efficiency (like speed through water, thrust, torque, RPM), but also the actual propeller condition like the propeller surface fouling or damages.

When calculating the linear regression line over time through all the individual points, it is clearly visible that the propeller performance (efficiency) is decreasing over time. For the time frame of the measurements, the propeller efficiency decreases by 3.7%. This equals to a decrease of 2.6% per year.

4.2.3 Hull performance over time

Next to the propeller efficiency, also the hull resistance can be determined based on the propeller thrust measurements. The hull resistance R at a certain speed through water is proportional to the propeller thrust T as in $R = T(1-t)$. For ease of comparison, the thrust deduction factor t is taken constant for all relevant free sailing conditions, which is supported by model test results.

The measured propeller thrust is plotted against the measured speed through water in Fig. 8. This graph indicates a fairly good correlation between the full scale measurements and the model test predictions. Shown variations in the measured thrust values are among others expected to be related to the actual draft differences compared to the model test draft, the influence of minor rudder steering, and the actual present (low because filtered) sea-state and wind, which still add additional resistance. Additionally, the fouling of the hull is also playing a role during this time period.

It is commonly accepted that the total resistance is a function of vessel speed through water, as in $R = \frac{1}{2} \rho C_d A STW^2$ with ρ the water density, C_d the drag coefficient, and A the area of cross section. Since some of these parameters are sometimes difficult to reliably estimate (i.e., the C_d), a more generic modelling of the resistance is used, as in $R = C STW^\beta$ for which the parameter β is determined based on the measurements as shown in Fig. 8. Herein C is the hull resistance coefficient, which is an indication for the performance of the hull. The hull resistance coefficient C can be rewritten as: $C = T(1-t) / STW^\beta$

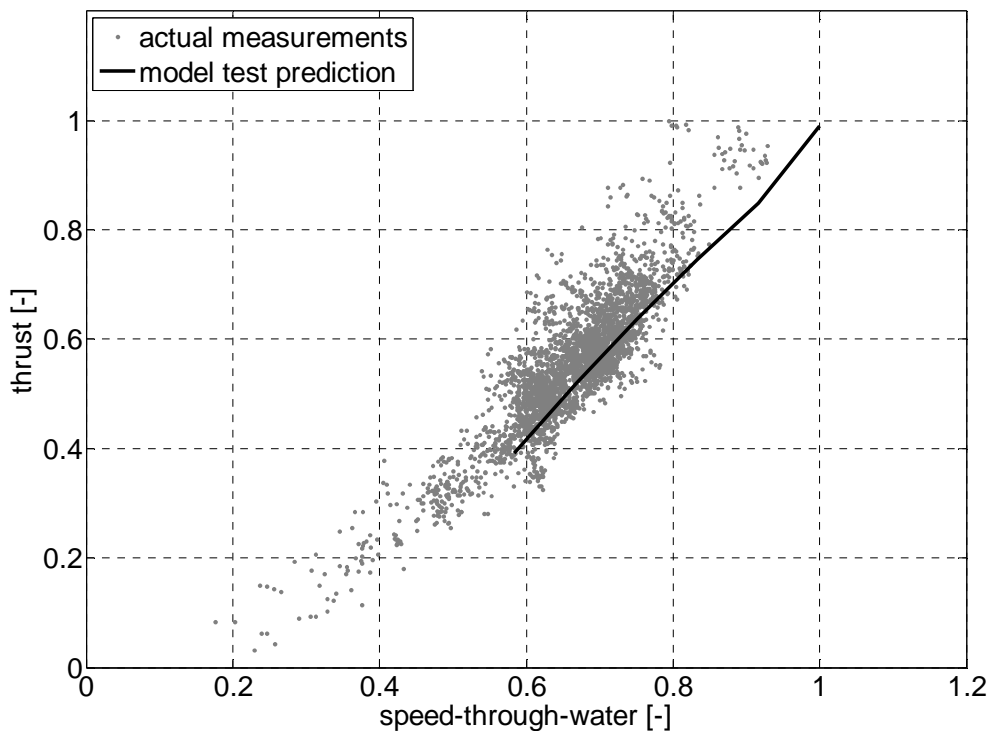


Fig.8: Thrust - speed (through water) curve for +13000 TEU container vessel over 1.5 year period

Next step is to follow the changes in the hull resistance coefficient C over time. This to determine any possible hull performance deterioration due to for instance hull fouling or hull coating deterioration. The hull resistance coefficients are plotted over time and the outcome is shown in Fig. 9. At the start of the measurements the measured absolute hull resistance coefficient value is set to 100%.

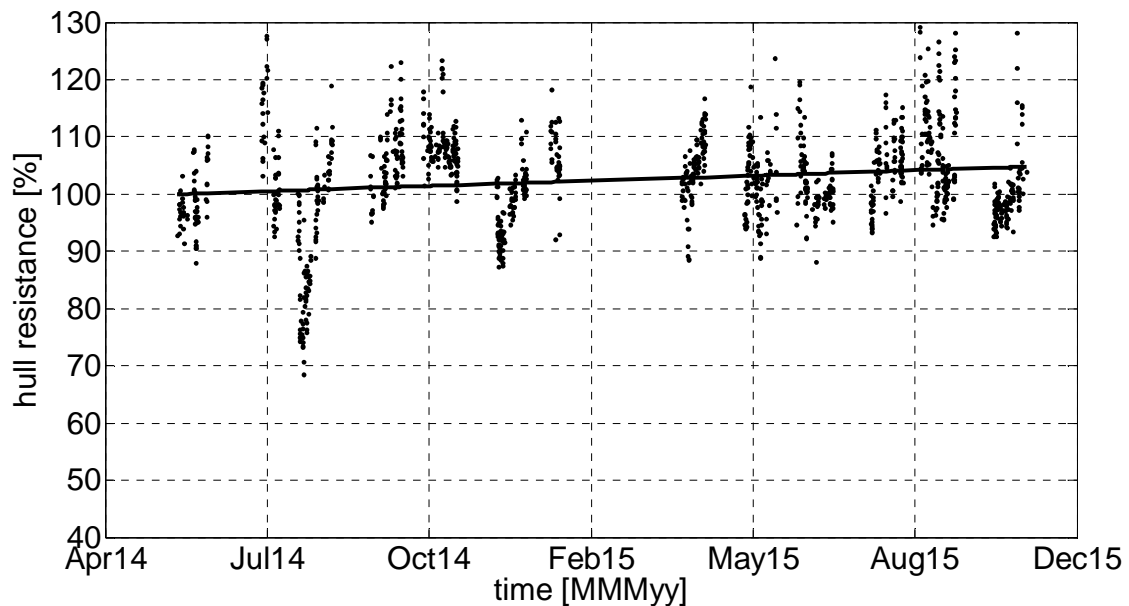


Fig.9: Hull resistance coefficient over time, total increase is 5.2%, (equals 3.6% per year)

From this figure the following conclusions can be drawn. At first it is clearly visible that the calculated hull resistance coefficient has a spread. This might be explained by the earlier described variations in measured thrust at a certain speed through water, as seen in Fig. 8, due to for instance draft differences, sea-state, wind and rudder actions, but also due to actual hull resistance variations. But when calculating the linear regression line over time through all the individual points, it is clearly visible that the hull resistance coefficient is increasing over time. The increase in hull resistance is +5.2% for the total measuring period. This equals to an increase of +3.6% per year.

4.3 Comparison ship performance evaluation via power versus thrust measurements

As shown in the previous paragraphs there are two ways used to measure the ship performance. The route via additional propeller thrust measurements allows for a split in performance between propeller and hull. But when adding both propeller and hull performance via the propeller thrust measurements, the outcome should be comparable to the total “ship resistance” measurement route via only torque measurements.

As the power (torque) is measured on board of the vessel via a different mechanism than the thrust is measured, both methods do have some independencies. Via the power measurements as described in paragraph 4.1, the total “ship resistance” increase, over the full measurement period, is +9.2%. When adding the propeller efficiency reduction of 3.7% to the hull resistance increase of +5.2%, as determined via the propeller thrust measurements in paragraph 4.2, the total “ship resistance” increase, over the full measurement period, is calculated to be +8.9%. Both measured total “ship resistance” increases are close to each other, supporting the accuracy of both measuring techniques used, and the accuracy of the individual measured propeller and hull performance.

5. Conclusions

In this paper two ways of measuring the ship propulsion performance are discussed. The first route is via measurement of the propeller power / torque. Via this route the total “ship resistance” change over

time can be determined. For the +13000 TEU container vessel described in this paper, the measured total “ship resistance” increase over the measuring period of 1.5 years equals +9.2%. But via this way only the combined effect of propeller and hull can be measured.

As such a second route is discussed in this paper, which via additional propeller thrust measurements is able to split the propeller performance (efficiency) from the hull performance (resistance). For the +13000 TEU container vessel described in this paper, the measured propeller efficiency reduction over the measuring period of 1.5 years equals 3.7%. The separately measured hull resistance increase over the same measuring period equals to +5.2%. Both efficiency reductions combined, result in a total “ship resistance” increase of +8.9%. This figure is very much comparable with the total “ship resistance” increase as measured via the power / torque measuring route, providing an indication of the achieved accuracy of the individual measured propeller efficiency and hull resistance via the thrust measuring route.

The advantage of the thrust measuring route above the power / torque measuring route is, that via thrust measurements, the individual conditions of the propeller and hull can be quantified. Based on above presented measurements, the propeller plays an important role in the total propulsion performance decrease of the vessel. Based on this the proper decisions can be made for either only a propeller cleaning or repair, or only a hull cleaning. Next to this, the effects of for instance a propeller modification, or a new hull paint can be determined much more accurate. This at the end provides better input towards a proper investment decision for propulsion energy saving measures, or green-house gas reductions.

For this specific +13000 TEU container vessel the annual fuel consumption is approximately 30.000 metric tons. The measured decrease of propeller efficiency of 3.7% , and the measured increase in hull resistance of 5.2%, result both in additional fuel consumption and green house gas emissions. The additional fuel consumption means also an additional investment in fuel, which can be weighed against the needed investment for either a propeller or a hull cleaning.

A simple calculation with an assumed fuel oil price of US\$ 200,- per metric ton, indicates that the additional investments in fuel by respectively the propeller efficiency decrease, and the hull resistance increase, are:

	Efficiency decrease	Fuel increase mton / year	Fuel increase US\$ / year
Propeller efficiency decrease	3.7%	1110	222.000,-
Hull resistance increase	5.2%	1560	312.000,-

Based on the above outcome, only a propeller cleaning, at a lower investment cost compared to a total hull cleaning or even repaint, might be an interesting alternative, given the relative high fuel saving potential of the measured propeller efficiency decrease.

By using the TT-Sense® propeller thrust measuring possibilities these distinctions between propeller and hull can be made, and provide an important input to the fuel saving and maintenance investment decisions.

References

AAS-HANSEN, M. (2010), *Monitoring of hull conditions of ships*, MSc thesis, Norwegian University of Science and Technology (NTNU), Trondheim

BOOM, van den, H.J.J.; HASSELAAR, T.W.F. (2014), *Ship Speed-Power Performance Assessment*, SNAME 2014 Annual Meeting

DINHAM-PEREN, T.A.; DAND I.W. (2010), *The need for full scale measurements*, William Froude

Conference: Advances in Theoretical and Applied Hydrodynamics - Past And Future

LOGAN, K.P. (2011), *Using a Ship's Propeller for Hull Condition Monitoring*, ASNE Intelligent Ships Symp. IX, Philadelphia

MUNTEAN, T.V. (2011), *Propeller efficiency at full scale*, PhD thesis, Technical University Eindhoven, ISBN 978-90-386-3072-4

SCHULTZ, M.P.; BENDICK, J.A.; HOLM, E.R.; HERTEL, W.M. (2011), *Economic impact of biofouling on a naval surface ship*, Biofouling Vol. 27, No. 1, January 2011, pp.87–98

Role of Reference Model in Ship Performance Management

Wojciech Górski, Enamor Ltd., Gdynia/Poland, wojciech.gorski@enamor.pl

Abstract

Ship performance monitoring received recently significant attention of ship operators and regulatory bodies. It is driven by two main aspects: economic and environmental. Therefore, despite the market fluctuations, performance monitoring remains in a focus. However, based on experience gained, it becomes obvious that simple data logging and presentation (monitoring) is insufficient. Registered data requires comprehensive analyse in order to derive meaningful information for ship officers and on-shore team. Many aspects of performance analyses require comparison with benchmark data, therefore presence of versatile reference model gains key importance. The model may be based on design data (usually developed through hydro and aero model tests and numerical analyses) or data acquired in operation. Both cases involve an issue of limited accuracy and sometimes credibility of input data. In case of data acquired during operation they may be further influenced by operational and navigational conditions which may not be fully controlled or monitored. Paper discusses a number of vital aspects of reference performance model including: purpose of the model, class of the model (white, black or grey), dimensions of the model, data sources, data pre-processing, interpolation and extrapolation methods incorporated in the model and model limitations. Efficient use of the reference model allows for transition from performance monitoring to performance management.

1. Introduction

A ship in operation can be regarded as a complex dynamic system, whose mathematical model is not known. Although at design stage a number of ship operational characteristics are determined, such information is incomplete.

This situation affects the economics of shipping. Lack of proper mathematical model significantly hinders the planning of the voyage, both in terms of selection of the correct loading condition and shipping routes. As a result, a ship can be operated in conditions significantly different from the optimum, resulting in increased fuel consumption and emissions. However increasing availability of reliable, maintenance-free measuring and recording systems allows ship performance to be better monitored. The use of thus obtained data allows to understand the characteristics of the ship and, consequently, enables building a mathematical model describing the behaviour of the ship (or selected systems) in various conditions of operation which is a necessary step in a transition from ship monitoring to performance management.

Performance management is relatively novel concept in ship operation. It is used in order to distinguish from ship operation parameters and (usually) environmental data recording (referred to as monitoring) and ability of automatic interpretation of such data into information meaningful for ship crew and owner team onshore. Based on the information involved parties may take reasonable decisions in terms of ship operation (e.g. adjustment of ship speed and trim, selection of route) and maintenance (e.g. hull cleaning).

2. Overview of the reference model

Reference model of ship performance defines desired conditions of operation. It usually describes operation of vessel of clean hull and propeller, on deep unrestricted waters without influence of wind and waves. Therefore it can be treated as a benchmark for daily ship operation. Comparison of current performance against reference model may indicate deficiencies in ship condition or her manning.

2.1. Definition and purpose

Selection of physical quantities upon which the performance model is established is essential in terms of its practical application. Prime requirement with this respect is an availability of such quantities in automatic monitoring system onboard in order to minimise manual entries which are prone to error. Furthermore a quality of measurement must be considered. Only parameters which can be monitored in continuous manner with sufficient accuracy during ship operation can be used for the purpose of setting-up reference model. It is also desirable that performance model describes trade-off between an effort and result of ship operation. An effort, in this case, can be a quantity describing costs of ship operation e.g. fuel consumption or power of prime mover. Result is described by a transport work: product of distance sailed and cargo transported by a ship.

These prerequisites are essential for practical application onboard a ship. Although the reference model can be established based on information which may not be available onboard (i.e. results of physical model tests or numerical analyses) it can be only used for daily performance benchmarking if relevant quantities are measurable in continuous and trustworthy manner. Beside the quantities constituting the reference performance model also other parameters defining conditions of operation must be recorded in order to facilitate proper selection and pre-processing of performance data. These quantities include weather (wind, wave) and sea basin (water depth) conditions as well as additional conditions of operation (e.g. trim). Therefore an application of integrated ship monitoring system with a set of error-prone sensors is fundamental in ship performance management.

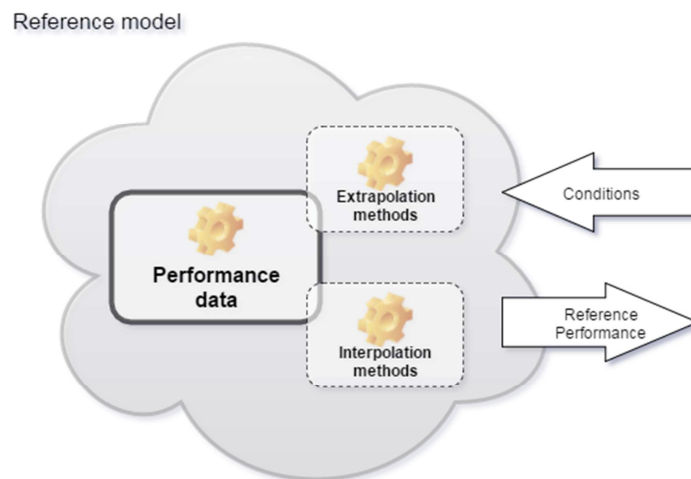


Fig. 1: Concept of reference model

It must be also noted that performance data does not fully define the reference model. The method of interpolation among model data entries and extrapolation beyond defined data range has an equal importance for the robustness of performance management, Fig. 1.

2.2 Reference model class and dimensions

Literature review allows to distinguish among three types (classes) of reference models

- Black box,
- White box
- Grey box.

Black box is a model class that does not require knowledge of the physics of an analysed system. It allows an approximation of its action solely on the basis of information about the input signals and system responses, *Pedersen and Larsen (2009)*, *Petersen et al. (2012)*. This model is the opposite

approach to the traditional models based on the generalization of experimental data (based on physical model tests or measurements at sea), often referred to in the literature as the so-called white box models. Such models include a full description of the system and do not require the adaptation (learning) of a model. Examples of such models for predicting ship power were proposed by *Harvald* (1983) and *Holtrop* (1984). Similar approach was used by *Journée and Meijers* (1980) and *Logan, et al.* (1980) for estimating ship power in real operating conditions.

As explained by *Pedersen and Larsen* (2009) white box models perform poorly in predicting the actual vessel performance under operating conditions. In turn, a black box models, because of their dependence on the scope of the data used for the learning process, are often characterized by low performance outside the scope of the input data (i.e. in extrapolation). Hence, naturally, the concept of merging of two models appeared. In the literature this class of models are referred to as a grey box, semi-natural, hybrid or semi-mechanistic models. These approaches differ in details, but they all combine a partial theoretical structure with data to complete the model. An idea of a grey box model is to combine advantages of white and black box modelling. Artificial neural network and statistical methods such *Holtrop* (1984) and *Isherwood* (1973) are popular choices for black and white parts of grey model.

Reference models can be also distinguished in terms of its dimensions:

- 0-dimensional model – reference performance is described by single value i.e. defined for one predefined combination of power, displacement and speed. Usually design parameters are used for this purpose. Use of this model allows for tracking performance changes due to aggregated influence of loading condition (mid draft and trim), speed, hull and propeller conditions and environmental conditions. While using 0-dimensional model each operation point (irrespective of actual displacement and speed) is compared with above mentioned single condition. It is the most general model and requires minimum. Although 0-dimensional model does not seem to be very practical it can be used to evaluate benefits of slow steaming.
- 1-dimensional model – reference performance is described as a function of speed only i.e. defined for one predefined displacement. A design speed-power curve (model tests and/or sea trials) can be used for this purpose. Use of this model allows for tracking performance changes due to aggregated influence of loading condition (mid draft and trim), hull and propeller conditions and environmental conditions. In order to define this model power-speed curve must be available. In case of this model each point of operation is compared with model at the same speed. This way influence of the speed on performance is not included.
- 2-dimensional model – reference performance is described as a function defined for range of speeds and loading conditions. Set of speed-power curves shall be used for this purpose. Use of this model allows for tracking performance changes due to aggregated influence of trim, hull and propeller conditions and environmental conditions. In case of 2-dimensional model each point of operation is compared with reference value determined for the same displacement (even keel) and speed. This way both speed and displacement does not influence reference performance.
- Higher-dimensional model – it may be practical to include effects of additional parameters (e.g. trim) in the reference model but it results in increased complexity and a need of using special techniques.

2.3 Data sources and pre-processing

An attempt to build the reference model shall be always preceded by evaluation of data sources upon which the model can be prepared. In general there are two types of data sources available, Fig. 2. A broad group consists of data which can be obtained with use of parametric methods used at design stage. These methods define ship by a limited number of parameters and provide a performance indication in variety of ship operational conditions including ship speed through the water, water depth, wind speed and direction, wave height, period and direction, presence of sea current etc. Although this group seems to be very versatile it should be understood that they pose serious threat

when used in nonchalant way. Major concern with respect to design methods results from their origin. They were elaborated in order to facilitate a design process i.e. provide approximation (sometimes very rough) of ship performance in certain (although very rarely explicitly given) so called “design” condition. It is usually a combination of ship displacement and speed which, at the time of concept design, is deemed to be most representative for future ship operation. For these conditions ship design is optimised and therefore methods based on generalisation of information (e.g. regression analyses of performance) fail to describe performance of vessel in off-design conditions. Even in case the method includes parameter which changes during a standard ship operation (i.e. ship draft or displacement) it does not necessarily properly reflects its impact on performance. Reason for this is quite simple but not well recognised with respect to application to operational performance. Design methods developed based on generalisation of knowledge describe performance of a vessel designed for certain conditions but fail to provide information how performance of particular vessel would change if certain condition changes. Therefore use of the method in order to determine impact of draft (displacement) would result in approximation of performance of two different vessels each designed for its own draft.

Use of methods based on generalisation of knowledge requires understanding of their applicability. They were developed for certain type of ships (i.e. type of hull form) and specific range of general particulars ratios. Some of these limitations are explicitly defined but not all. Therefore it is usually difficult to determine if certain method may be used for a specific ship without compromising data consistency.

Contrarily analytical or experimental methods based on detailed modelling of ship hull, propulsion system and environment (i.e. methods of computational fluid dynamics or physical model tests) provide very accurate approximation of performance of particular vessel. These methods may be successfully used for determination of performance in off-design conditions because a ship model is explicitly given with use of detailed geometric description. Although this class of methods also exhibit some limitations in terms of modelling (i.e. scale effect in physical model tests) but they are not significant with respect to building of reference models. Despite advantages of analytical and experimental methods their application in constituting reference model is limited. They are very time consuming and require specific skills (both in case of physical and numerical modelling). Use of the methods requires either specialised software or special laboratory conditions and therefore preparation of versatile and wide range performance model would be impractical due to relatively high costs.

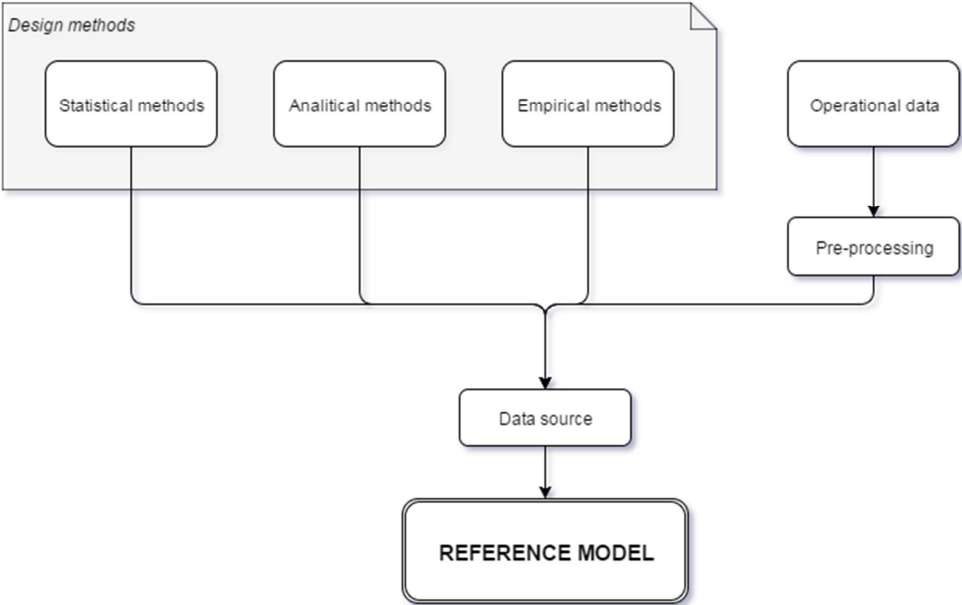


Fig. 2: Data sources for reference model preparation

In practice reference models can be set up by a combination of all mentioned methods. The preference is given to results of physical model tests (usually providing calm weather performance in two or three loading conditions) validated by sea trials and numerical results (e.g. in order to model influence of trim changes). These data are supplemented by various parametric methods in order to take into account other important factors.

There are, however, cases when such approach cannot be used especially when detailed geometrical model is not readily available or credibility of available data is questionable. High costs of numerical and physical modelling and extensive time of analyses are also serious limiting factor. Therefore building a reference model based directly on performance recorded during ship operation seems to be an interesting alternative. It is however not a new concept. An idea of using of direct performance measurements for building a reference model was introduced almost 90 years ago. Initially it was used for evaluation of ship trials by *Telfer* (1927) but capability of the method with respect to evaluation of ship performance in daily operation was also recognised, *Telfer* (1964), *Bustard* (1978). Proposed model is quite simple and therefore straightforward in application. It is based on linear approximation of a power and speed ratios in propeller slip (fixed pitch propellers) or pitch (controllable pitch propellers) domains. This method, however, contain serious limitation due to the fact that model can be created for a single loading condition. Despite its limitations this approach is widely used in performance monitoring systems, *Logan* (2011).

Essential part of setting up the reference model based on performance registration is selection of input data. It is very sensitive and crucial aspect. Selection and preparation of appropriate data directly influences quality of the reference model. However it may not be an easy task due to interference of environmental conditions and limited accuracy of registrations. Therefore in order to prepare the reference model based on current ship performance some sort of pre-processing is required. These methods involve:

- Rejecting (filtering) data registered in non-standard environmental conditions,
- Correcting registered data to the standard conditions.

In practice both of methods are used. First recorded data are filtered in order to select subset which can be successfully corrected. Extend of conditions which can be accepted for correction greatly depends on used correction method. It is sometimes difficult to precisely define these boundaries. Some existing methods do not have applicability range clearly defined. A practical solution for this problem can be based on evaluation of corrections' magnitude in comparison with uncorrected value. Large value of corrections' magnitude, exceeding e.g. 1/3 of registered value of examined parameter may indicate application of correction method beyond its applicability range. It can be further observed that application of correction method out of its range results in increased scatter of corrected data.

2.4 Interpolation and extrapolation

Reference model cannot be understood only as a set of data. The most important feature of the model is ability to adequately reassemble reference data but, at the same time, to allow for interpolation among dataset and preferably provide information also beyond the range of reference data. These features refer to approximation, interpolation and extrapolation performance respectively. These features pose currently the major challenge for existing reference models. Although approximation works well for majority of black and grey box models, it performs poorly in case of white box models. Interpolation and extrapolation performance poses even more difficulties resulting in a need of preparing separate, local models e.g. for different drafts.

Development of efficient, homogeneous model of improved interpolation and extrapolation performance was the main aim of undertaken research.

3. Upgraded grey box model

Upgraded grey box model is an attempt to overcome shortcomings of existing grey class models with respect to interpolation and extrapolation. The proposed solution provides continuous representation of fuel consumption in fair weather conditions as a function of basic ship operational parameters: speed through the water - V , average draft - T and trim - t_s .

3.1 Physical model

Fuel consumption B_{24} of ship prime movers during ship operation at steady speed, in deep waters and fair weather (i.e. without influence of wind and waves) expressed in t/day is given by a formula:

$$B_{24} = \frac{(R_R + R_F + R_{AA}) \cdot V}{\eta_D \cdot \eta_S} \cdot b \cdot \frac{24}{10^6}$$

where:

first element describes main engine power:

- R_R – hull residual resistance expressed in kN ,
 - R_F – hull frictional resistance expressed in kN ,
 - R_{AA} – ship air resistance expressed in kN ,
 - V – ship speed through the water expressed in m/s ,
 - η_D – propulsive efficiency,
 - η_S – transmission efficiency between main engine and propeller,
- and
- b – specific fuel consumption of main engine expressed in g/kWh .

Among hull resistance components only residual resistance cannot be modelled with use of approximate methods with sufficient accuracy. Remaining components are modelled as follows.

Frictional resistance is expressed as:

$$R_F = \frac{1}{2} \rho \cdot (1 + k) \cdot C_{F0} \cdot S \cdot V^2 \cdot 10^{-3} [\text{kN}]$$

where:

ρ denotes density of sea water,

k is a form factor calculated according to formula:

$$k = 18.7 \cdot \left(\frac{C_B \cdot B}{L_{PP}} \right)^2$$

Equivalent flat plate drag coefficient C_{F0} is calculated with use of ITTC-57 correlation line:

$$C_{F0} = 0.075 (\log Rn - 2)^{-2}$$

based on Reynolds number:

$$Rn = \frac{V \cdot L_{WL}}{\nu}$$

Ship wetted surface S is approximated by Mumford formula

$$S = 1.7 \cdot L \cdot T + \frac{V}{T} = 1.7 \cdot L \cdot T + C_B \cdot L \cdot B [\text{m}^2]$$

Resistance due to still air (air drag) is determined according to:

$$R_{AA} = \frac{1}{2} \cdot \rho_A \cdot C_{AA}(0) \cdot A_X \cdot V_G^2 \cdot 10^{-3} \text{ [kN]}$$

where:

A_X – ship transverse section exposed to wind (i.e. from waterline to the maximum height of the vessel) [m²]

ρ_A – mass density of air [kg/m³],

$C_{AA}(0)$ – non-dimensional air drag coefficient,

V_G – ship speed through air (speed over ground) [m/s]

3.2 Evolutionary model

In case of residual resistance application of approximate methods results in unacceptable errors. Furthermore it does not allow for modelling an influence of ship trim. Therefore residual resistance:

$$R_R = \frac{1}{2} \rho \cdot C_R \cdot S \cdot V^2 \cdot 10^{-3} \text{ [kN]}$$

is calculated based on approximation of non-dimensional residual resistance coefficient C_R with use of function of three independent variables (ship speed, draft and trim):

$$C_R = f(V, T, t_S)$$

Taking into account this representation data used for setting up the reference model can be presented as points in 4-dimensional space:

$$P_{i,j,k} = (V_i, T_j, t_{Sk}, C_R)$$

In order to carry out approximation of dataset NURBS hypersurface is used (Federici, 2009)

$$C_R = f(u, v, w) = \sum_{i=0}^U \sum_{j=0}^V \sum_{k=0}^W N_{i,p}(u_i) \cdot N_{j,q}(v_j) \cdot N_{k,r}(w_k) \cdot P_{i,j,k}$$

where:

u, v, w – are parameters in range $\langle 0,1 \rangle$ defining points locations in parametric space,

U, V, W – are indexes of control points,

p, q, r – are degrees of base functions,

N – are base functions defined by formula:

$$N_{i,p}(u) = \frac{u-u_i}{u_{i+p}-u_i} N_{i,p-1}(u) + \frac{u_{i+p+1}-u}{u_{i+p+1}-u_{i+1}} N_{i+1,p-1}(u)$$

Base functions for v and w are defined analogically.

$P_{i,j,k}$ – are control points, defining NURBS hypersurface.

Shape of the NURBS hypersurface (fig. 3) is defined over a 4x4x4 grid of control points. They are distributed uniformly, and so the parameters u, v, w take the values $\left\{0, \frac{1}{3}, \frac{2}{3}, 1\right\}$, corresponding to the operating parameters values:

$$X_i = X_{min} + i \frac{X_{max} - X_{min}}{3}$$

where

$$X_i = V, T, t_S, \text{ for } i=1,2,3$$

In order to facilitate extrapolation functionality boundary values are selected with 5% margin with respect to minimum (X_{low}) and maximum (X_{hi}) recorded value of a parameter:

$$\begin{aligned}
X_{min} &= X_{low} - 0.05 \cdot dX \\
X_{max} &= X_{hi} + 0.05 \cdot dX \\
dX &= X_{hi} - X_{low}
\end{aligned}$$

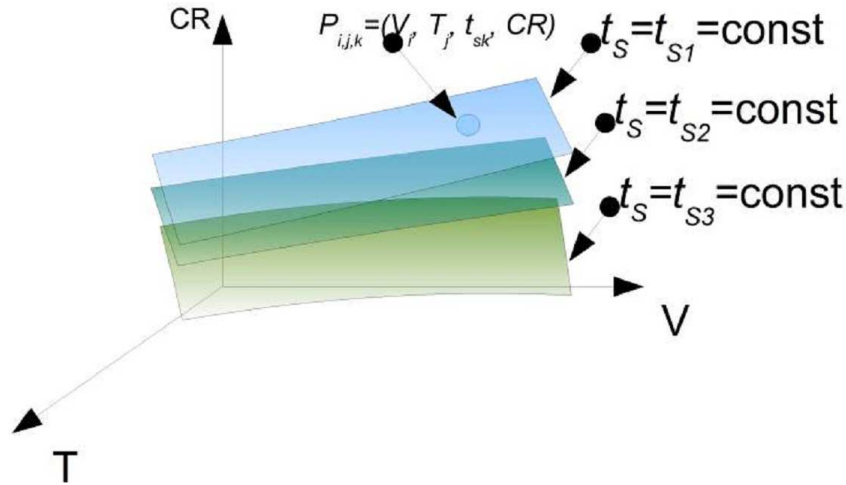


Fig. 3: Graphical representation of 4-dimensional hypersurface

Since the process of function approximation of fuel consumption is carried out in the physical parameters space of V , T , t_S , and the function of the residual resistance component is set in the u , v , w , parameter space, conversion between the two parametric spaces should be adopted. The conversion is done according to:

$$x = \frac{X - X_{min}}{X_{max} - X_{min}}$$

where:

$X = V, T, t_S$,

and

$x = u, v, w$.

3.3 Solution of approximation problem

Due to the indicated above arbitrary selection of the number and distribution of control points approximation task comes down to the selection of the fourth dimension of 64 control points of NURBS hypersurface.

The task of approximation can be treated as an optimization problem and in this particular case, as determination of minimum discrepancy between the measured values and the values of the approximating function. In practice, as the said measure a mean square error is used - hence this kind of approximation is called Least Squares Approximation. There are many methods of solution of approximation problem. Their effectiveness depends on the class of the so-called basis function. In the case when the task concerns function of several variables, which also may not be differentiable, evolutionary methods are applicable. Genetic algorithms belong to the class of these methods.

Genetic algorithms (GA) are a class of optimization methods used in solving complex multi-parametric problems. Their basic properties that make them effective tools for optimization include:

- using the simultaneous evaluation of many solutions at any stage of optimization methods, in contrast to a "step by step" (gradient-based methods), which prevents stopping at a local extremum,

- implementation of the evaluation of solutions based on calculating the value of the objective function, and not its derivatives, which allows the use of GA to optimize a wide range of functions,
- arbitrary selection of starting point.

In addition, the simple structure simplifies programming and ever increasing computing capabilities encourages finding new areas of GA application. Genetic algorithms have been applied in various fields of science to solve a number of optimization problems, in particular in case of a multidimensional space, *Michalewicz (2013), Gorski (1999)*.

Evaluation function is practically the only connection between task and algorithm in methods based on genetic algorithms. The purpose of the evaluation function is rating of individuals in the population - assigning a greater chance of survival and reproduction for "better" chromosomes. For this reason, proper definition of the evaluation function is essential for the design of optimization algorithm.

The program uses an evaluation function based on the calculation of modified root mean square error:

$$fit' = \frac{1}{\sqrt{1 + fit}}$$

where:

$$fit = \sqrt{\sum_{i=0}^n \frac{[F_i - f(\bar{x}_i)]^2}{F_i^2}}$$

and

x – denotes parameter vector,

F – denotes the measured value of optimization parameter (fuel consumption)

f – denotes value of the function describing the mathematical model (approximating function)

n – denotes the number of records stored in the data set

In this perspective, the evaluation function takes values in a (0,1) range. Values close to 0 indicate poor fit of approximating function (large error). The evaluation function tends to 1 in the case approximation error is small.

3.4 Performance in approximation problem

Analysis of approximation of fuel consumption data registered during the operation of the different ships, allows to determine the suitability of the reference model. Table I shows a summary of performed tests, illustrated by the values of selected statistical measures used to evaluate the objective function (mean value and standard deviation).

Table I: Tests of approximation performance

	Statistic measure*	Result
Ship No. 1	Average value	0.98
	Standard deviation x 100	0.12
Ship No. 2	Average value	0.75
	Standard deviation x 100	0.80
Ship No. 3	Average value	0.95
	Standard deviation x 100	0.40
* Obtained in 10 independent runs		

The average value leads to the conclusion about the usefulness of the model in terms of the quality of approximation of the input data. Considering the formulation of the objective function values close to unity indicate a good fit (small difference between the measured value and the value of the approximating function in the approximation node).

The standard deviation is used as a measure of method stability i.e. allows recognising if subsequent runs of the algorithm lead to similar solutions.

3.4 Performance in interpolation and extrapolation problem

Analysis of the results of the algorithm for proper interpolation and extrapolation is difficult due to the inability to formulate clear criteria for evaluation. In contrast to the task of approximation, where the measure of the quality of solutions is the error of fuel consumption estimation at points where the measurement was made in the operation, the criteria for assessing the quality of interpolation and extrapolation are intuitive. In both cases, it is required that the nature of approximating hypersurface did not change abruptly. The use of such generally formulated criterion is difficult in the case of operating in a 4-dimensional space due to impossibility of direct visualization of the results. Therefore, to assess the quality of interpolation and extrapolation, two-dimensional graphs were used, Fig. 4.

On graphs, drawn up separately for selected drafts - for which measurement data are available, approximating function obtained from the reference model (lines) and measurement points (circles) were illustrated. Comparison of the line with the location of the measurement points allows to formulate conclusions about the usefulness of this method in problems of extrapolation and interpolation.

Portions of curves, beyond the extreme measured values (i.e. for the trim below -1m and over 1m), are consistent with the trend set by the run of the curves within the range specified by operational data. Figure 4 allows to evaluate the quality of extrapolation in terms of speed as well. Also in this case the performance of the reference model should be assessed as correct.

The run of the curves showing the fuel consumption between points obtained from the measurements for subsequent drafts, for which the registrations were made is consistent with the distribution of input data. There were no abnormal changes of interpolating curves. They are very consistent.

4. Summary

Ship performance management is based on continuous evaluation of ship operation and its comparison with reference condition in order to optimise her efficiency. This task cannot be effectively executed without robust reference model. Presented paper discusses fundamental features of reference models and proposes an approach for building of such model. Results of the undertaken research leads to the following conclusions:

- models of grey box class offer greater flexibility in terms of building higher dimensional models, thus allow for better approximation of the reference dataset,
- use of simple physical model in a combination with genetic algorithm improves model performance with respect to interpolation and extrapolation features,
- proposed model allows for providing reference performance as a function of main operational parameters i.e. ship speed through the water, mid draft and trim.

Described reference model undergoes further development within research project co-financed by The National Centre for Research and Development (NCBR).

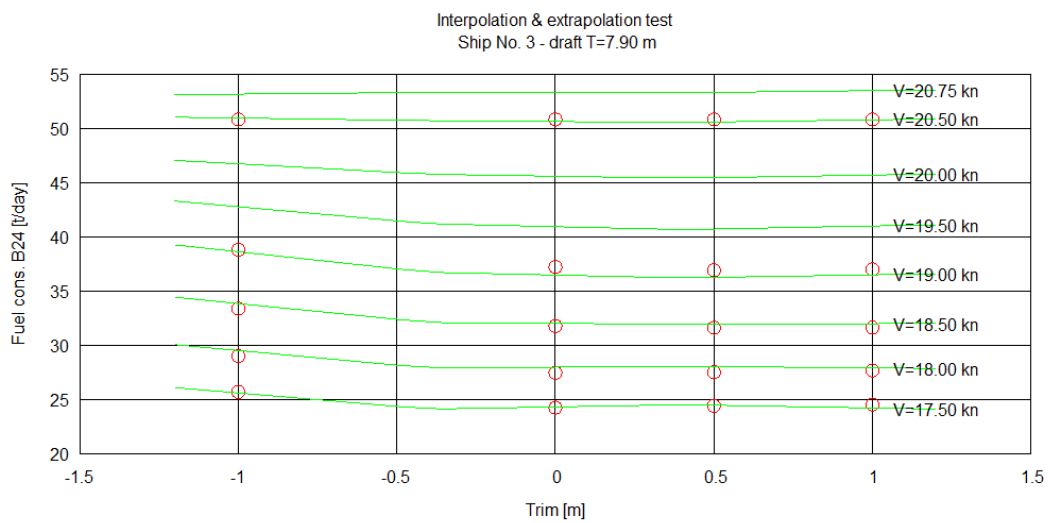
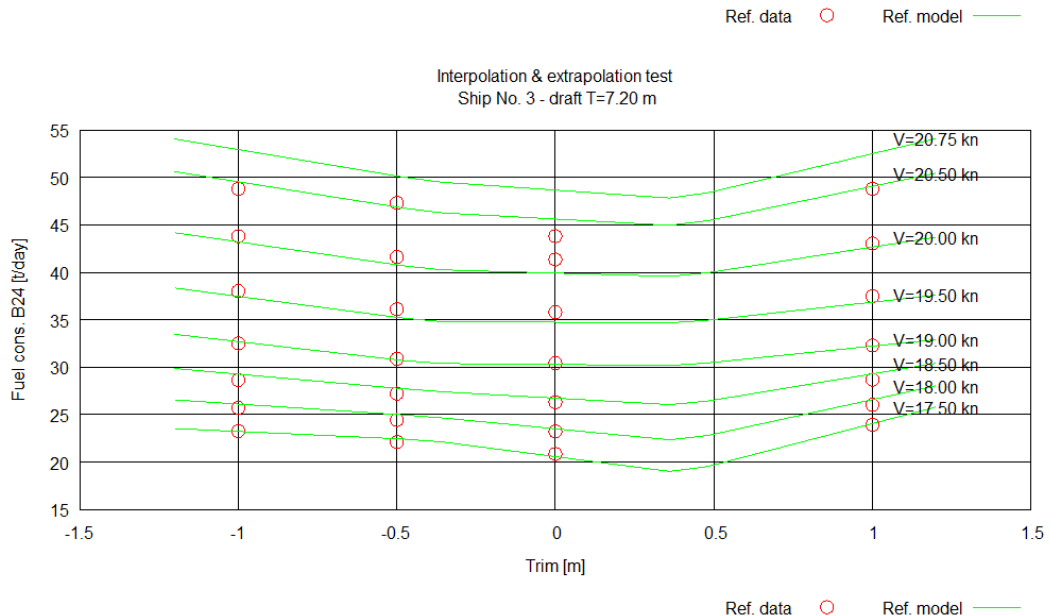
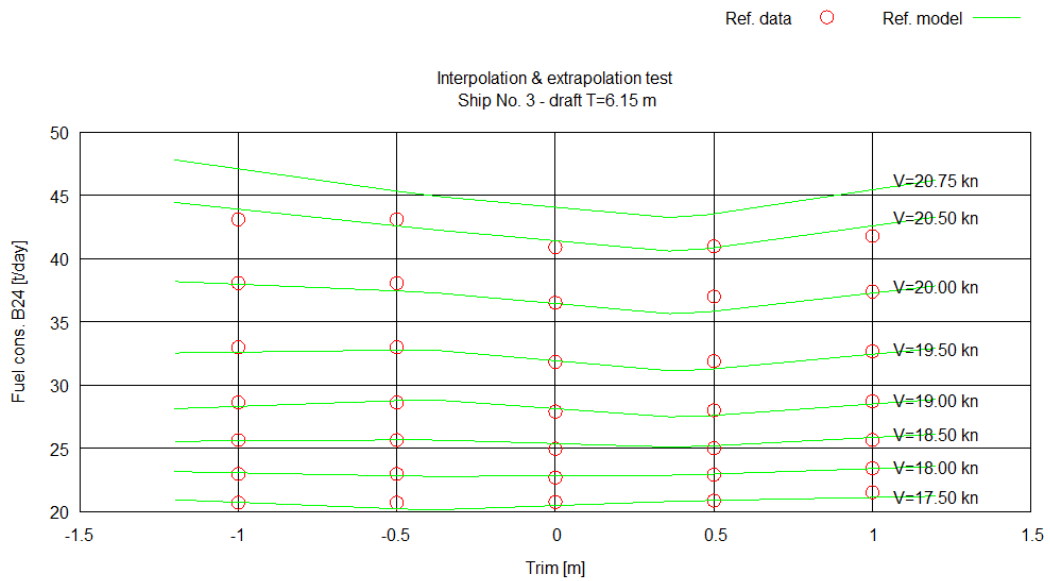


Fig. 4: Test of interpolation and extrapolation performance

References

- BUSTARD E.E. (1978), *The propeller as a power meter or speed log*, CIMarE and SNAME Joint Meeting, Toronto
- FEDERICI F. (2009), *Interpolating NURBS*, <https://www.idmarch.org/document/B-spline/459S-how/Interpolating%20NURBS%20Filippo%20Federici%20August%202023,%202009>
- GÓRSKI W. (1999), *Optymalizacja geometrii śruby napędowej na wstępnym etapie projektowania* (in Polish), Politechnika Gdańska, Wydział Oceanotechniki i Okrętownictwa, Gdańsk
- HARVALD, S.A. (1983), *Resistance and propulsion of ships*
- HOLTROP, J. (1984), *A statistical re-analysis of resistance and propulsion data*, International Shipbuilding Progress 31
- ISHERWOOD, R.M. (1973), *Wind resistance of merchant ships*, RINA Trans. Vol. 115
- JOURNÉE J.M.J.; MEIJERS J.H.C. (1980), *Ship routeing for optimum performance*, Delft University of Technology, Ship Hydromechanics Laboratory, Delft
- LOGAN, K.P. (2011), *Using a ship's propeller for hull condition monitoring*, ASNE Intelligent Ships Symposium IX, Philadelphia
- LOGAN, K.P.; REID, R.E.; WILLIAMS, V.E. (1980), *Considerations in establishing a speed performance monitoring system for merchant ships*, Int. Symp. Shipboard Energy Conservation, New York
- MICHALEWICZ, Z. (2013), *Genetic algorithms+ data structures= evolution programs*, Springer Science & Business Media
- PEDERSEN, B.P.; LARSEN, J. (2009), *Prediction of full scale propulsion power using artificial neural networks*, 8th Conf. Computer and IT Applications in the Maritime Industries (COMPIT), Budapest
- PETERSEN, J.P.; WINTHER, O.; JACOBSEN, D.J. (2012), *A machine-learning approach to predict main energy consumption under realistic operational conditions*, Ship Technology Research 59/1
- TELFER, E.V. (1927), *The practical analysis of merchant ship trials and service performance*, NEC Institute Transactions 43

Evaluation of the Fuel Saving Potential using High Resolution MetOcean Forecasts and Detailed Ship Performance Models

Andrea Orlandi, Riccardo Benedetti, Valerio Capecchi, Gianni Messeri, Albert Ortolani, Luca Rovai, Consorzio LaMMA, Florence/Italy, orlandi@lamma.rete.toscana.it
Andrea Coraddu, Damen Shipyards, Singapore, andrea.coraddu@damen.com

Abstract

A numerical simulation system composed of high resolution wind and wave forecasting models (metocean component) and of seakeeping and powering simulation models (ship performances modelling component) is used in order to estimate the fuel saving potential along routes at the Mediterranean scale. The system is applied to a ro-ro ship operated in the Central Mediterranean Sea by Forship Corsica and Sardinia Ferries, in the context of the two European projects COSMEMOS and PROFUMO. The results of several numerical simulations are analysed in order to evaluate the potential impact of the variability of meteo-marine forecasting skills on weather routing and to estimate the potential contribution to fuel savings of meteorological route optimization at the Mediterranean scale.

1. Introduction

Computer modelling and big data analysis resources are acquiring a growing role in ship energy management, *DNV-GL (2015)*, especially if integrated with in-service ship monitoring systems, e.g. *Hansen (2011)*, *Coraddu et al. (2014)*, and with other design, retrofit and operational energy efficiency measures *DNV-GL (2015, 2014a,b)*, *ABS (2014)*. The growing attention of maritime community towards energy efficiency matters is not only linked to the economic features directly connected to the fuel cost, but it is also driven by the regulations and mandatory measures adopted in recent years by the International Maritime Organization (IMO) introducing energy efficiency measures in international shipping context (Chapter 4 of MARPOL Annex VI, entered into force in January 2013, and subsequent updates coming from IMO GHG Study). In this context, we assist to a growing role of numerical modelling of ship propulsion plants and fuel consumption rates, e.g. see *Smith et al. (2013)*, and also to a renewed relevance and development of weather routing systems *Simonsen et al. (2015)*, *Chen (2008)*. Reliable weather routing techniques could have also a renewed role in guaranteeing the economical sustainability of the development and application of novel approaches to wind assisted ships *Beck et al. (1975)*, *RAE (2013)*, *Mofor et al. (2015)*, *SAIL (2015)*. The further integration with safety oriented operational guidance systems, *ADOPT (2008)*, and modern telecommunication systems could bring to the development and implementation of advanced navigation systems capable of optimally exploiting the different resources of in-service monitoring, numerical modelling, metocean observation and forecasting, positioning and telecommunication, *Kakuta (2014)*, with the final goal of reaching the best trade-off between energy efficiency and safety of navigation, for single ships and fleet management.

The work reported in the present paper has been developed in such a framework, in particular focusing on the aspects of numerical metocean forecasting and to its potential for the application to fuel saving oriented weather routing algorithms. The work has been developed in the context of the two European Projects COSMEMOS (FP7 Program, GSA, Galileo and EGNOS for Scientific Applications, concluded in May 2014) and PROFUMO (IAP Programme, ESA, Artes 20 Feasibility Studies, concluded in March 2016), both headed by Vitrociset Belgium. Both projects were aimed at improving the performances of meteo-marine forecasting systems, at the Mediterranean scale, by exploiting, through data assimilation techniques, *Kalnay (2003)*, meteo-marine data (including GNSS-based data) observed by cooperating ships and to develop innovative weather routing applications for Mediterranean navigation, based on such improved forecasts.

In the reported work, a numerical simulation system composed of high resolution wind and wave

forecasting models (metocean component) and of seakeeping and powering simulation models (ship performances modelling component) is used in order to estimate the fuel saving potential along routes at the Mediterranean scale. The system is applied by considering a detailed description of a real ro-ro ship, accounting for its performances under different conditions of engine settings and ship speed profiles along alternative routes. The numerical description of the real ro-ro ship has been tested and tuned by comparing with data from an in-service ship energy efficiency monitoring system. A huge number of voyage simulations, along routes of different length and shape, has been performed by using hourly high resolution wind and wave data produced by the daily operational metocean forecasting system of Consorzio LaMMA (Florence, Italy). Data from a wind and wave ensemble prediction system have also been used for some case studies, in order to estimate the dependence of the results on the forecast uncertainty. Part of the work has been described in recent publications *Orlandi et al. (2015a, b)*. In the present paper the main elements of the work reported in such publications are summarized in order to clarify the approaches followed in the study. The most recent part of the work, still unpublished, is then described and the first results obtained are illustrated. This last part of the work is devoted to the definition of an analysis approach aimed at estimating the fuel saving potential attainable by route optimization at the Mediterranean scale. Such a work is still not complete and hence only preliminary results and conclusions can be described here.

Such a work has been designed to be based on the analysis of the data produced by a huge number of voyage simulations, tracing back the total fuel consumption for each voyage to the different components of the ship resistance. This analysis has been considered to be capable of identifying the roles and the interplay of the several elements that characterize each voyage along different routes (route length, ship speed profile, engine settings, encountered metocean conditions). In particular the dominant contribution to the total fuel consumption, due to the calm water resistance component, must be evaluated in relation to route length and ship speed along the route, and compared with the contributions due to the encountered metocean conditions, i.e. mainly due to added resistance in waves and wind resistance. The results of such an analysis will allow to identify some strategies aimed to increase the energy efficiency during each voyage, by exploiting metocean forecasts in order to design alternative routes from the point of view of route length and route shape and considering the potential of different profiles of ship speed and engine settings along each route. The results of the present study could be useful for the implementation of more efficient optimization algorithms to be employed in weather routing algorithms, but the adopted approach could be also applied to the ship design process and to assess the potentialities of operational guidance systems, based on in-situ measurements of wind and waves.

2. Metocean forecasting

Numerical prediction of meteo-marine conditions is performed at regional operational centres by the use of a chain of numerical models. The models chain in this work is composed by a local area mesoscale meteorological model, *Pielke (2002)* and a wave model, *Komen et al. (1984)*, *Wise group (2007)*. They are run in cascade mode, i.e. the meteorological model is run first and its output provides the atmospheric forcing (namely the wind at a height of 10 meters) for the subsequent run of the wave model. Initial and boundary conditions for the operational atmospheric model runs are obtained from the outputs of lower resolution global atmospheric models, *Kalnay (2003)*. Each run of a global model is initialized by the complex process of data assimilation, *Kalnay (2003)*, that optimally blends model data of the precedent run with the huge amount of data coming from the world observing system, composed of satellites, meteorological stations, soundings and so on.

In this work data from the Consorzio LaMMA operational runs of the mesoscale meteorological model WRF, *Michalakes et al. (2004)*, with initialization and boundary conditions from the American global model (NOAA NCEP GFS), are reported. Consorzio LaMMA wave forecasts are generated by running the third generation spectral wave model Wavewatch III, *Tolman (2009)*. The resulting wind-wave forecasting operational chain is run two times a day (initialization at 00:00 and at 12:00 UC) over the whole Mediterranean Sea for the next five days at a resolution of about 12 Km, and over a nested domain covering the North Tyrrhenian and Ligurian Seas for the next three days at a resolution

of about 3 km, *LAMMA*, *Orlandi et al. (2009)*. For part of the performed studies also an approach based on a Wind-Wave Regional Ensemble Prediction System (WWR-EPS), *Kalnay (2003)*, *Alves et al. (2013)*, has been implemented, as described in *Orlandi et al. (2015a,b)*.

3. Ship performances forecasting

The set of numerical algorithms used in this work to perform detailed simulations of ship performances is called SPAR Algo (Seakeeping and Powering Along a Route Algorithm, *Orlandi (2012)*, *Orlandi and Bruzzone (2012)*). It is composed of a main procedure that drives the whole computation process along the Way Points (WP) of a given route, by extracting wind data and directional wave spectra from wind-wave forecast data files at the correct space-time positions. Such meteo-marine data are used to perform seakeeping and powering computations. The output data from SPAR Algo are, for each WP (and corresponding ship speed), the significant amplitudes of seakeeping motions along the six degrees of freedom of the ship, the main components of ship resistance and the corresponding fuel consumption rate, the RPM and power parameters characterizing the working point of the engine and propeller, together with propeller efficiency and a flag denoting eventual engine overload conditions. This last flag is used in SPAR to search for a feasible engine working point, by gradually decreasing the ship speed (involuntary speed reduction), when the engine is not capable to cope with weather at the selected ship speed. For each route, cumulative quantities are also produced, such as total voyage time and distance, and the total fuel consumption.

Seakeeping computations are performed by adopting the strip theory approximation, *Lewis (1990)*, in particular a modified version of the PDSTRIP program, *Bertram et al. (2006)* is used. Such modified version, PDSTRIP-SPC, has been developed in *Orlandi (2012)*, and allows the computation of significant responses by the use of directional wave spectra from WAVEWATCH III model. It is used to compute and archive the Response Amplitude Operators (RAO) for the seakeeping degrees of freedom and for longitudinal drift forces (i.e. the added resistance in waves operator), for the range of ship speeds of interest. Powering computations are performed by applying standard algorithms, *Carlton (2007)*, that link the total ship resistance of the ship to the propeller(s) trust, to the brake power delivered by the propulsion engine(s) and the corresponding fuel consumption rate, through the efficiencies chain and specific fuel consumption data.

Ship hull sections, loading condition and masses geometry are needed for seakeeping computations. The propeller(s) are defined through the characteristic curves for $K_T(J)$ and $K_Q(J)$, discretized on a suitable range of values of J . The engines are characterized by the layout diagram and by the specific fuel consumption map. Also shaft line efficiencies must be specified here. The total ship resistance is evaluated in terms of a decomposition in the three main components, *Lewis (1990)*:

$$R_{tot} = R_{hull} + R_{aw} + R_{wind} \quad (1)$$

Where R_{hull} is the calm-water resistance. It must be furnished to SPAR Algo as an input array of values in a suitable range of ship speeds, together with the values of hydrodynamic efficiencies. R_{aw} is the added resistance in waves and is computed in terms of the integral (numerically evaluated at each route WP):

$$R_{aw} = \int_0^\infty \int_0^{2\pi} RAO_{aw} S_\zeta d\theta_r d\omega \quad (2)$$

where RAO_{aw} is the added resistance operator computed in terms of the longitudinal component of the drift force, *Lewis (1990)*, *Faltinsen (1998)*, by PSTRIP-SPC (based on the Böse approach: *Böse (1970)*, *Graf et al. (2007)*, on the same direction (θ_r , ship-wave relative), frequency (ω) grid on which the directional wave spectrum S_ζ is computed by the wave forecasting model, *Orlandi (2012)*, *Orlandi and Bruzzone (2011)*, *Coraddu et al. (2013)*). In order to speed-up the computation, all the needed RAOs (for motions and drift forces) are computed off-line and archived in a suitable range of

speeds, generating a seakeeping dataset. The wind resistance R_{wind} is computed in terms of the formula:

$$R_{wind} = K\rho_{air}A_{TX}U_{wir}^2 \cos \theta_{wir} \quad (3)$$

where the longitudinal wind resistance coefficient K is given as an input array of its values for a suitable set of values of the relative wind angle θ_{wir} . U_{wir} is the relative wind speed, ρ_{air} is the air density and A_{TX} is the transverse projected area of vessel.

4. The tuning of the ro-ro ship numerical model and first assessment results

In the study a real ship has been simulated, it is a ro-ro ship operated in the Central Mediterranean Sea by Forship Corsica and Sardinia Ferries, partner in both COSMEMOS and PROFUMO Projects. A considerable body of data have been made available by the technical office of the company allowing to construct and tune a detailed model of the ro-ro ship. Such data have been used, in a first phase, for the generation of most of the input datasets needed to feed the SPAR Algo. The principal particulars of the ship are summarized in Table I for the full load condition, i.e. the loading condition selected for performing all numerical simulations reported in this paper.

Table I: Principal particulars of the real ro-ro ship simulated with SPAR

Item	Symbol	Value
Full load displacement	Δ	15466 t
Length between the perpendiculars	L_{PP}	160m
Beam	B	25m
Mean Draft	T	6.7m
Vertical center of gravity	VGC	11.2m

The ship propulsion plant is composed of four Wärtsilä 12V46C engines, with 11700 kW of power each, with two shaft lines, each equipped with a 4 blades CPP propeller.

A complete dataset of seakeeping RAOs has been generated and archived for SPAR Algo runs, by using PSTRIP-SPC program, for ship speeds in the range 10-28 knots.

In a second phase, a considerable amount of data recorded in navigation during the years 2012 and 2013 have been used to perform a tuning and validation of the numerical model of the ship. They consisted in two datasets, one coming from the ship log-book and the other coming from an in-service monitoring system. The first dataset has been collected by manual recordings by the ship personnel and regarded cumulative quantities of total fuel consumption, total voyage times and rough reference to the encountered meteo conditions (Beaufort scale level). The use of these data for our analyses has been straightforward, but they did not allowed detailed voyage analyses and had to be considered as affected by a higher level of uncertainty, being manually recorded. The in-service data have been recorded by a totally automated process and allowed more detailed voyage analyses, but required more intensive and complex data processing activities. These data regarded fuel consumption rates recorded during each voyage at a high sampling rate, together with ship speed and other ship motion data. In a first phase of model tuning, these automatically recorded fuel consumption rate data versus ship speed have been processed in order to evaluate the calm water resistance for ship speeds in the range 10-28 knots, *Orlandi (2014,2015a)*. Such a processing required identifying the fuel consumption rate values corresponding to calm water conditions at each speed and to invert the powering algorithms in SPAR, to pass from the identified calm water fuel consumption rate to the corresponding calm water resistance at the same speed. The resulting estimated calm water resistance is shown in Fig. 1 (left panel, blue line).

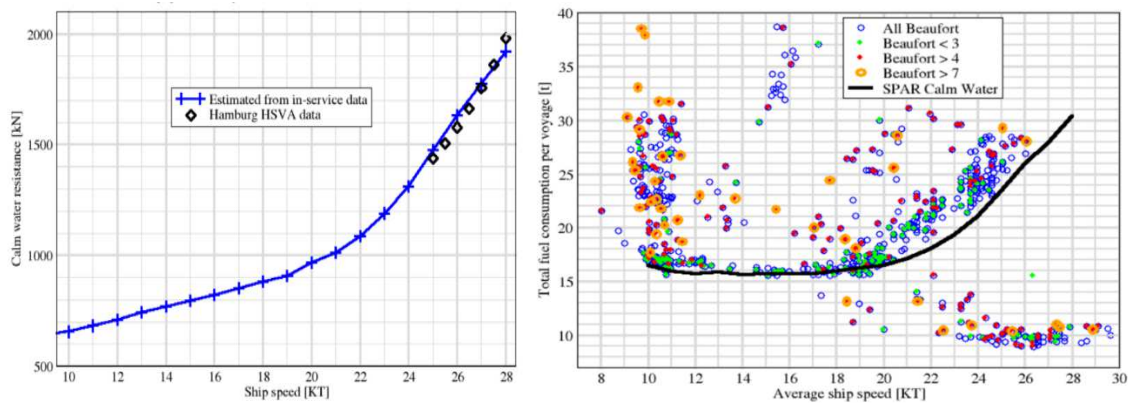


Fig. 1: Left: the blue line is the estimated calm water resistance, black diamonds denote experimental measurements on a scale model of the ship, from HSVA (1999). Right: Total fuel consumption in tonnes versus average ship speed in knots from log-book data for the ro-ro ship voyages on the line Savona-Bastia.

In Fig. 1 left panel, data measured on a scale model at the Hamburg Ship Model Basin are reported (black diamonds), denoting good correspondence with the estimated calm water resistance.

After this first calm water resistance tuning, some real voyages performed by the ro-ro ship in the Leghorn-Bastia line have been simulated with SPAR and the values of the total fuel consumption have been compared with the available measured data from the ship's log book, finding good accordance *Orlandi et al. (2015b)*. During this phase a global analysis of the manually recorded log-book data has been performed, finding a general good accordance with in-service automatically recorded data. An interesting feature emerged plotting the total fuel consumption in each voyage as a function of the corresponding average ship speed. To illustrate this, the resulting distribution of the average speed, total fuel data, for each recorded voyage, are reported in Figure 1(right panel), considering only the voyages from Savona to Bastia, with different colours depending on the corresponding wind Beaufort scale level. We notice an evident tendency of the data recorded in more calm conditions (green dots, Beaufort<3) to lie along the back curve, corresponding to the total fuel consumption computed at the various speeds by SPAR Algo for calm water conditions along the shortest route (represented as route 00 in Figure 4, left panel). In such a computation the fuel consumption rate value is evaluated utilizing the calm water resistance of Fig. 1 left panel (plus the wind resistance due to ship speed). The relevant feature emerging from Fig. 1 right panel is that, in the range of speeds from about 10 knots to about 19 knots, the total fuel consumption grows very slowly as a function of the average ship speed, while for higher speeds it increases more steeply. The presence of analogous plateaus in the same range of speeds emerged also along all the other lines covered by the ro-ro ship service, but with different values correspondingly to the differing shortest port-to-port distances of each line. Moreover, an exactly corresponding structure of the data emerged also from the automatically recorded data. It must be pointed out that the presence of such a behaviour with a plateau in the speed range 10-20 knots is peculiar of the studied ship and is due to the fact that in the range 10-19 knots the dependence of the fuel consumption rate for calm water conditions (i.e. that emerging from the resistance of Figure 1 left panel) is roughly linear. Physically this causes that, in such a speed range, the increase in fuel rate is balanced by the decrease of the total voyage time due to the corresponding increase in ship speed. From Figure 1 right panel other features emerge, one of them is that, at the same speed, there is also a spreading of the total fuel consumption values, that extend mainly towards higher values, with respect to the calm water total fuel consumption. Such a spreading is in many cases due to the added resistance from wind and waves, combined with eventual greater lengths of the selected route, that especially in heavy weather conditions, have been varied by the ship master w.r.t. the shortest one, usually adopted in calm conditions. It must be pointed out that a fraction of the available data are quite noisy and appear not totally reliable, with too high or too low total fuel consumption values, apparently not explained by the corresponding ship speed or by the corresponding Beaufort grade. Such data could be affected by unexplained recording errors and should be filtered out or better investigated.

An analysis of both log-book data and automatically recorded data allowed to estimate that the increase in total fuel consumption, w.r.t. the calm water one, due the encountered meteo-marine conditions may range from a few points of percentage to 20-30% and in extraordinary cases also more. A certain number of voyages among those recorded in such two datasets have also been simulated by the SPAR Algo, by using wind and wave data from Consorzio LaMMA forecast models. The comparison of such simulated and corresponding observed data allowed to estimate a good reliability of the SPAR algorithms in simulating the considered ro-ro ship powering and seakeeping performances in real voyages, *Orlandi et al. 2015b*.

In order to collect a huge dataset of simulated data, needed for the SPAR Algo verification and validation activities and also needed to perform the fuel saving potential estimation, several systematic runs of SPAR simulations of the ro-ro ship on several routes have been performed. These simulated voyages had no real corresponding voyage and have been performed also along lines not covered by the real ro-ro ship. These totally numerical runs allowed analysing many details of the single voyages and of the overall ship seakeeping and powering performances. As an example Fig. 2 shows scatter plots of the added resistance in waves versus the corresponding significant wave height, computed by SPAR Algo at 18 and 22 knots (red triangles and green squares resp.) along a huge ensemble of voyages along the Leghorn-Bastia line, in several meteo-marine conditions described by Consorzio LaMMA wind and wave models forecast. The data have been partitioned considering different mean wave directions relative to ship heading. In particular four conditions are reported: following waves (top left), stern quartering waves (top right), beam waves (bottom left), head waves (bottom right). Also quadratic interpolation curves are shown superimposed to the scatter of computed data (18 KT continuous, 22 KT dashed). Note that the spreading of such data around the quadratic interpolation curve is due to the variability of the directional wave spectra accounted for in SPAR Algo. Also such spreading has a quadratic dependence on significant wave height.

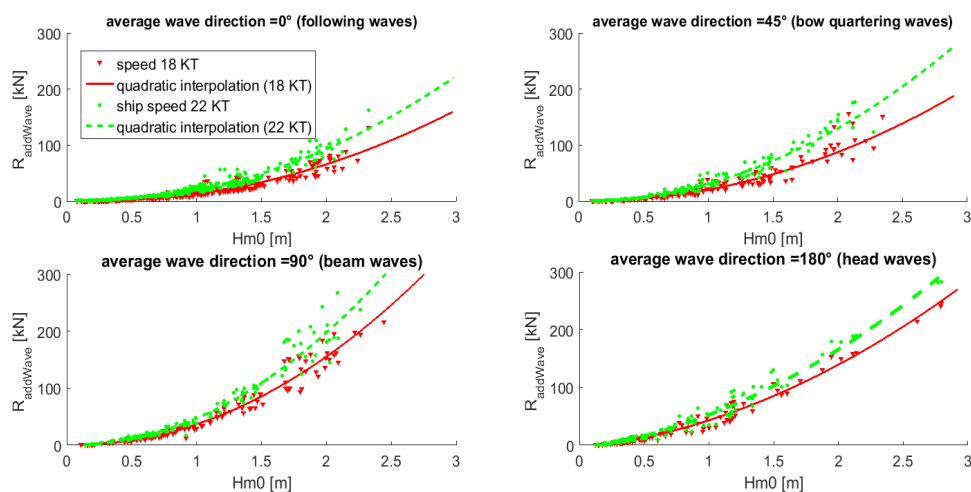


Fig. 2: Scatter plots of added resistance in waves computed by SPAR versus significant wave height the speeds of 18 knots (red) and 22 knots (green), also quadratic interpolations are shown. The data have been partitioned for different wave directions relative to ship heading.

The effects of forecast uncertainty onto the total fuel consumption estimation have been investigated by applying an ensemble forecasting technique on some voyage simulations in the line from Genoa to La Valletta, as described in *Orlandi et al. (2015a, b)*. From several of these simulations emerged that the fuel estimations along the different routes may have a not negligible spreading, but that this does not hampers the possibility of performing a reliable minimal fuel route selection.

5. Fuel saving potential at the Mediterranean scale

In order to estimate the fuel saving potential that could be achieved by weather routing techniques exploiting to the metocean conditions variability along Mediterranean routes, an approach is being

developed based on the huge amount of data that can be numerically generated by the integrated use of the two metocean forecasting and ship simulation components of the system described above. In particular some Mediterranean lines have been selected, considering different ranges of total distance. Fig. 3 shows the shortest (left panel) and short-intermediate length (right panel) lines. The shortest line is the one from Savona to Bastia and it is really served by the studied ro-ro ship. Due to this it has also been used in the phases of algorithms validation as described above. It must be pointed out that the alternative routes selected as northward variations (N1, N2) and southward variations (S1, S2), w.r.t. the shortest direct route 00, are very similar to the ones adopted in real voyages of the ro-ro ship. The short-intermediate line is from Genoa to La Valetta (Malta) and it is not served by real voyages of the ro-ro ship. Also for this line the 00 direct route is the shortest one, and the other eastward (E01, E02, E1, E2) and westward (O1) variations are all of different and greater length.

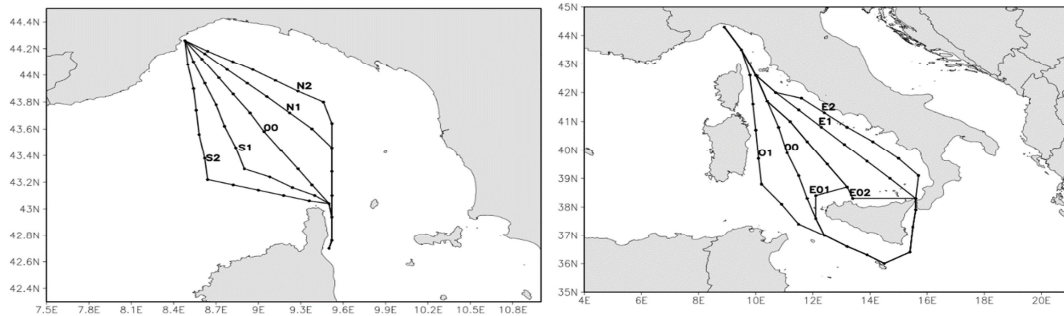


Fig. 3: Alternative routes adopted for numerical simulations along the two short-medium lines: Savona-Bastia line (left panel), Genoa-La Valetta line (right panel).

The lengths in nautical miles (NM) and the corresponding fuel consumption in fair weather conditions are reported in Table II, for someone of the studied ship speed values in knots (KT). Such fair weather fuel consumption values have been computed by considering only the tuned calm water resistance, *Orlandi et al. (2015a)* and the wind resistance caused by the relative wind due to the ship speed.

Table II: Length and total fair weather fuel consumption computed by SPAR Algo for the ro-ro ship for the two short-medium lines.

Route	Route length [NM]	Fair weather fuel cons speed 18 KT	Fair weather fuel cons. speed 24 KT
Savona-Bastia N2	117.1	16.3	21.8
N1	111.7	15.5	20.7
00	106.4	14.8	19.7
S1	111.7	15.5	20.7
S2	122.7	17.0	22.6
		11 KT	18 KT
Genoa-LaValletta O1	610.6	82.1	83.1
00	585.2	78.7	79.6
E01	650.8	87.6	88.4
E02	685.2	92.2	93.3
E1	641.1	86.3	87.2
E2	663.4	89.2	90.2

In Fig. 4 the selected medium-long and long Mediterranean lines are shown. In particular the lines connecting Port Said Cagliari (top panel) and Gibraltar (bottom panel) have been considered due to their relevance in the Mediterranean shipping activity, also due to the connection of such lines with the global shipping traffic through the Suez Canal and the Gibraltar Strait.

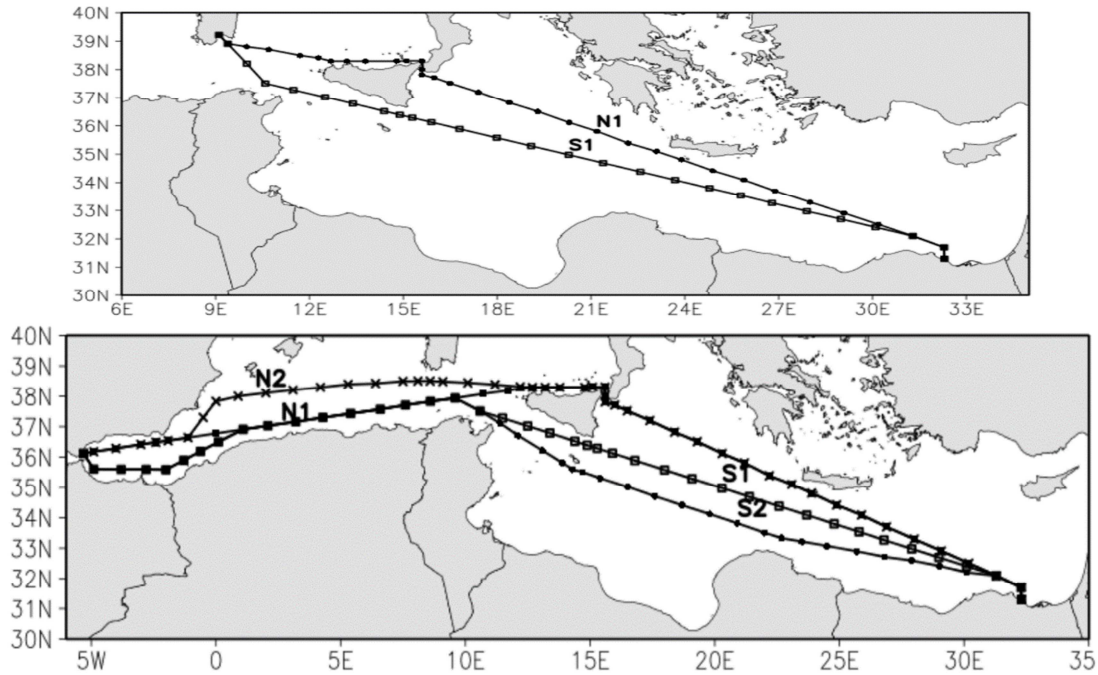


Fig. 4: Alternative routes adopted for numerical simulations along the two medium-long lines: Port Said-Cagliari line (top panel), Port Said-Gibraltar line (bottom panel).

The lengths and the corresponding fuel consumption in fair weather conditions are reported in Table II, as for the short routes of Fig. 3. It must be pointed out that while for the short-medium routes we defined a shortest route 00 and other varied longer routes, for the medium-long routes we have no shortest route and the northward (N1, N2) and southward (S1, S2) alternative routes are of nearly equal length. The selected four routes connecting Port Said with Gibraltar have been constructed by joining common legs.

Table III: Length and total fair weather fuel consumption computed by SPAR Algo for the ro-ro ship for the two medium-long lines.

Route	Route length [NM]	Fair weather fuel cons. [t] Ship speed 20 KT
Port Said-Cagliari N1	1274.3	180.3
S1	1275.4	180.5
Port Said-Gibraltar N2	1988.1	281.3
N1	1963.3	277.8
S1	1962.9	277.8
S2	1983.0	280.6

Several simulations of the ro-ro ship have been performed along the two short-medium routes, by making it to travel every day for a long period of time, with the same departure time each day. The simulations have been performed, by using wind wave data from Consorzio LaMMA, with constant speed (for several values in the range 11-24 knots) and with varied speed profiles, with 4 engines active and with 2 engines active. In Figure 5 an example of the results obtained is shown. In particular the results obtained along the Savona-Bastia route, with time of departure 18:30 UTC for every day of October 2015, steaming at constant speed of 18 knots, with 4 engines active, are shown.

In October 2015 several days were characterized by relatively calm conditions in the area traversed by the Savona-Bastia line. In the calmest days, as e.g. 08 October, the fuel consumption along the five routes is near to the fair weather values reported in Table II and the spacing among the respective values are determined by the calm water resistance component and by the respective route lengths.

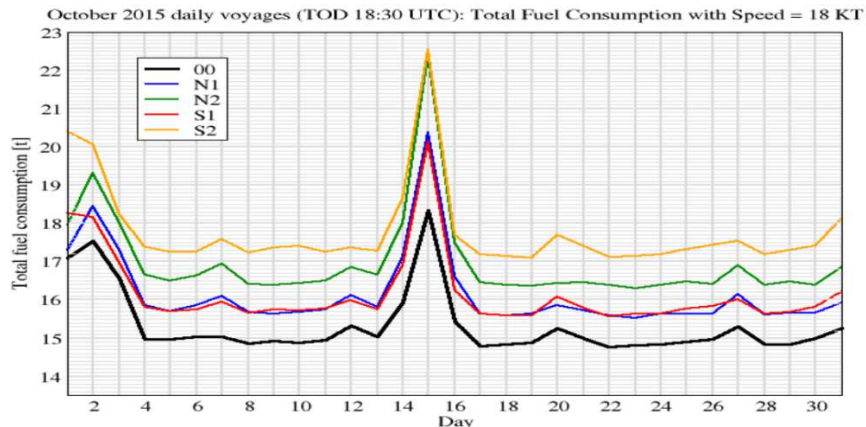


Fig. 5: Total fuel consumption computed by SPAR along the 5 alternative routes in the line Savona-Bastia, for daily voyages with departure time on 18:30 UTC each day of October 2015, steaming at 18 knots, with 4 engines active.

In dates with low-intermediate meteo-marine conditions the absolute values of the fuel consumption along the 5 alternative routes increase of quantities amounting up to some points of percentage, due to the encountered meteo-marine conditions. The two routes of almost equal length, N1 and S1, present fuel consumption with inversions in the ordering of the respective values, while the longest routes, N2 and S2, present an invariable ordering, and the shortest route 00 is always the least consuming one. This is due to the fact that, for short lines, with low-intermediate meteo-marine conditions, the differences among the meteo related added fuel consumption are frequently not sufficient to counterbalance the increase in fuel consumption due to the increase of length of the varied routes. In these cases fuel savings of few points of percentage can be expected mainly by varying very slightly w.r.t. the shortest route and by searching for optimal speed and engine setting profiles. In the first and middle days of October 2015 significant heavy weather conditions generated relevant increases of fuel consumption along all the alternative routes. In the days around 15 October the environmental conditions have been characterized by a space-time scale that affected all the routes in almost the same way, with the result of no significant variation of the ordering of the respective values. In the first four days of the month significant variations of the ordering emerged, the shortest route remained the least consuming, but N1 and S1 could become interesting because characterized fuel consumption values similar to route 00, but being also longer than it, hence they could be characterized by the possibility to exploit better seakeeping conditions. In order to better investigate these days, further simulations with varied time of departure have been performed. As an example, in Figure 6 some of the results are shown with plots of the total fuel consumption along the 5 alternative routes from Savona to Bastia, computed with meteo-marine data for 03 October, with varied UTC time of departure: 00:00, 01:00, 02:00, ..., 05:00. The data shown refer to simulations performed with constant ship speed of 18 knots (left panel) and 24 knots (right panel). It is interesting that, due to the encountered heavy weather, at 18 knots with departure time on 00, 01, 02 UTC, the shortest route is no more the least consuming one. In such cases the least consuming routes are S2 and S1 that interchange in such role, while at 24 knots something similar happens with time of departure on 01 and 02 UTC, while departing on 00 UTC, S1 and S2 are not the least consuming but they are very near to route 00. The differences between these two cases are not only linked to the different fuel rates as implied by the significantly differing ship speeds. They are also related to differences in the evolution of the encountered meteo-marine conditions, caused by the speed related differing voyage timing. Moreover, the relatively rapid variations of the ordering of the fuel consumption along the alternatives are due to the rapid evolution of the intense meteo-marine conditions. These were characterized by a deep and small scale low pressure system rapidly crossing the Ligurian Gulf from South-West to North-East, generating strong spatial gradients and rapid time variations of the intense wind and wave fields in the area. The ordering of the computed fuel values gradually returns to the normal one, determined by the routes length ordering, while the low pressure system gradually leaves the area and enters the Italian peninsula. These results demonstrate that, in some cases also the time of departure may be a relevant optimization parameter.

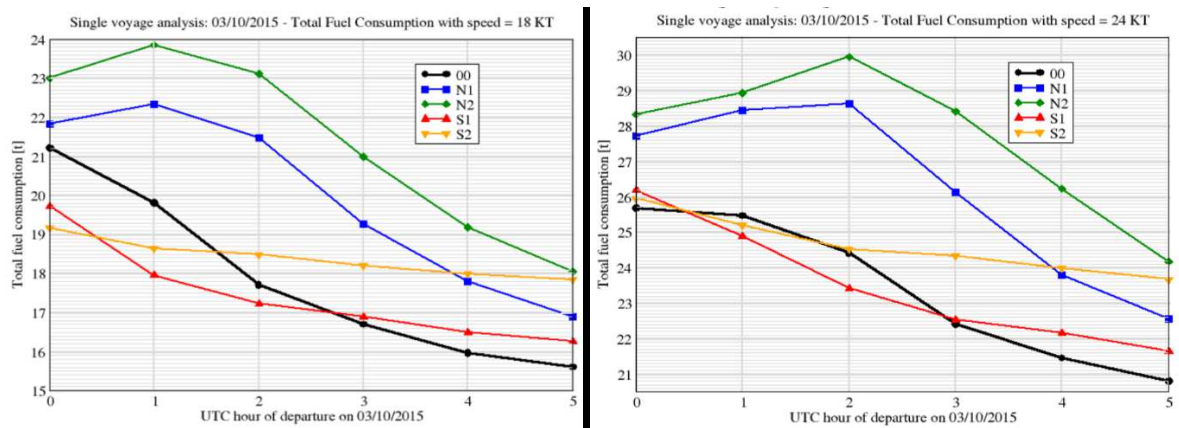


Fig. 6: Total fuel consumption of the ro-ro ship computed by SPAR Algo versus UTC time of departure: 00, 01, 02, ..., 05. The data have been computed along the 5 alternative routes from Savona to Bastia for the day 03 October 2015, with constant ship speed: 18 knots (left panel) and 24 knots (right panel).

Results analogous to those reported in Fig. 5 have been obtained also along the Genoa-La Valletta line. Due to the longer distances and to the consequent wider meteo-marine conditions variability, the fuel saving potentiality is higher, but still the direct shortest route is frequently the least consuming one. In Figure 7, the results obtained by simulating the ro-ro ship at quite a low constant speed of 11 knots (thick lines), in the Genoa-La Valletta line are shown. The simulations have also been performed with two different speed profiles (thin continuous and dashed lines) with few first (profile a) and few last (profile b) way points with a speed of 13 knots, and all the other way points with a speed of 10 knots, so as to have an average speed of 11 knots. All these data have been computed with 4 engines active. The dotted lines report also the results obtained along routes 00, O1 and E1, with 2 engines active at a constant speed of 11 knots. From these data emerges that, at slow speed, the use of only 2 engines allows fuel savings of some points of percentage. The application of a varied speed profile may allow further fuel savings of some points of percentage, but this is weather dependent, hence obviously the two tested profiles are useful only in some days in the simulation period shown. It must be pointed out that also the amount of fuel savings due to the use of only two engines is weather dependent. Such savings are possible only at low speeds and with low-intermediate meteo-marine conditions. The increase of total resistance due to higher speed and to heavier weather generates a higher load on the engines, bringing them to work less efficiently unless switching to four engines. The best application of such routing elements requires an optimization process that is better performed by a software capable of numerically finding the optimal combination of speed and engine setting profiles in a totally time and weather dependent approach.

The SPAR simulations of the ro-ro ship performed along the medium-long routes from Port Said to Cagliari and Gibraltar gave similar results, with additional meteo related fuel consumption up to 10-20%, but with more recurring fuel differences among the routes of some points of percentage. Hence the fuel saving potential is greater and more stable for longer routes and this is due to the higher variability of the encountered meteo marine conditions, implied by the greater spatial distances and to longer voyage times. The short-medium routes of Fig. 3 imply voyage times of around 7 hours and 30 hours respectively, while the medium-long routes of Fig. 4 imply voyage times from three to more than four days. A relevant feature is that in these latter cases it is possible to define routes of very similar length, but with significant geographic differences, as for the considered routes passing North or South of Sicily. As an example, Table IV shows the results obtained by simulating the ro-ro ship on the Port Said-Gibraltar line.

The data shown refer to voyages with departure both from Gibraltar and from Port Said. They have been simulated with the same constant speed of 20 knots and the same time of departure on 14/02/2016 at 12:00 UTC. Obviously in the two simulated voyages the encountered meteo-marine conditions are significantly different, with consequent significant differences in total fuel consump-

tion. It is evident considering Figs. 8 and 9, where, for both voyages, the computed fuel rate along the routes is shown (continuous lines) together with the corresponding values of the encountered significant wave height (dashed lines) as a function of the distance along each respective route.

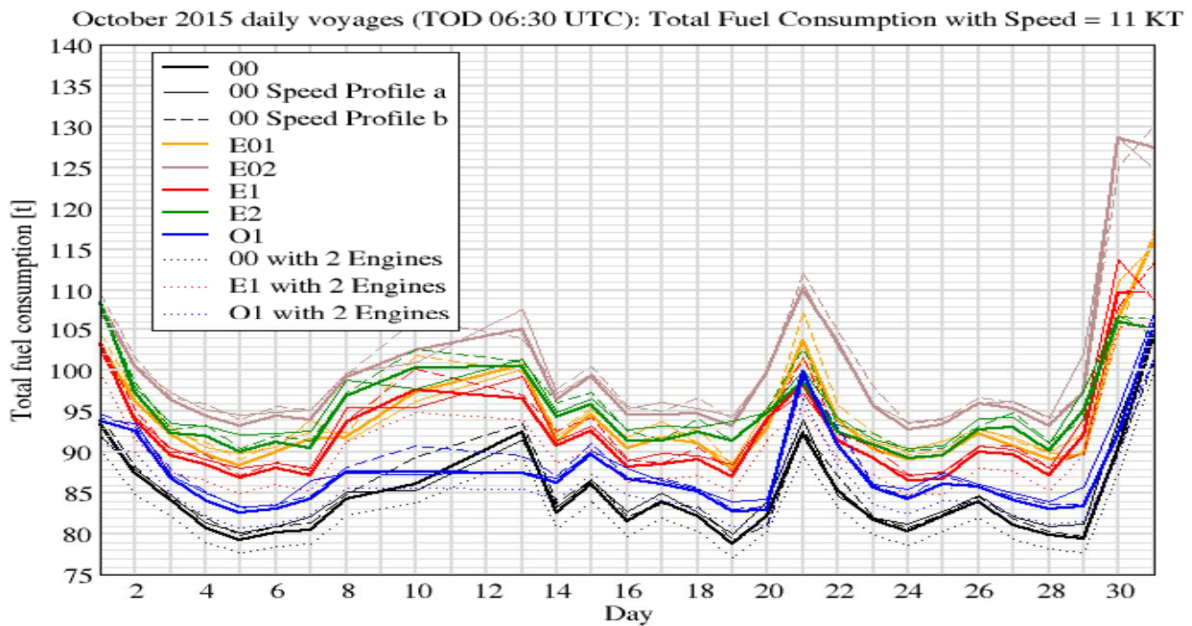


Fig. 7: Total fuel consumption computed by SPAR along the 5 alternative routes in the line Genoa-La Valletta line, for daily voyages with departure time on 06:30 UTC each day of October 2015, steaming at 11 knots, with 4 engines active (thick lines) and 2 engines active (dotted lines for routes 00, O1 and E1). Thin continuous and dashed lines report the results obtained with varied speed profiles for all the routes.

Table IV: Total fuel consumption computed by SPAR for the ro-ro ship for the simulated voyages Port Said-Gibraltar and Gibraltar-Port Said at constant speed of 20 knots, with metocean data forecasted by Consorzio LaMMA with initialization on 14/02/2016 at 12:00 UTC

Route	Fuel consumption [t] TOD: 14/02/2016 at 12 UTC Ship speed 20 KT	Route	Fuel consumption [t] TOD: 14/02/2016 at 12 UTC Ship speed 20 KT
Port Said-Gibraltar N2	309.0	Gibraltar-Port Said N2	353.8
N1	304.6	N1	345.0
S1	311.6	S1	351.8
S2	314.9	S2	350.5

In analysing these fuel consumption data it is worth remembering that the N and S routes have similar length in couples. What emerges is that in the voyage from Port Said to Gibraltar both the North routes are less consuming than the corresponding South routes, and N1 is better than N2 mainly because it is shorted. In the opposite direction voyage, all three routes N2, S1, S2 imply a similar total fuel consumption (but for differing causes due to length and meteo conditions), while route N1 emerges as significantly the better and less consuming one. It must be noticed that nevertheless S1 has the same length of N1 it implies a significantly fuel consumption, nearly equal to that of the longer N2 and S2.

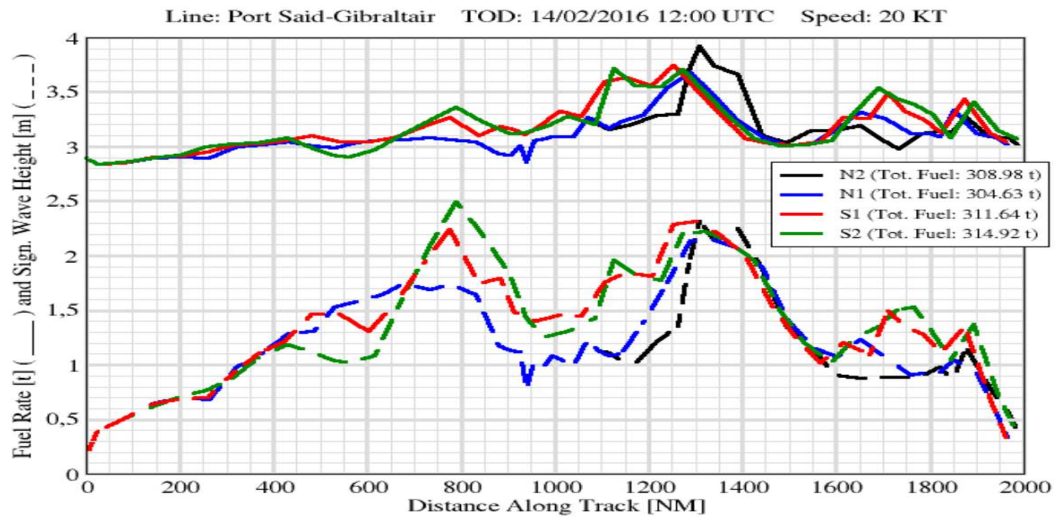


Fig. 8: Fuel rate [t] of the ro-ro ship (continuous lines) computed by SPAR and corresponding value of the significant wave height [m] (dashed lines) for the voyage from Port Said to Gibraltar, at constant speed of 20 KT, with departure time on 14/02/2016 at 12:00 UTC.

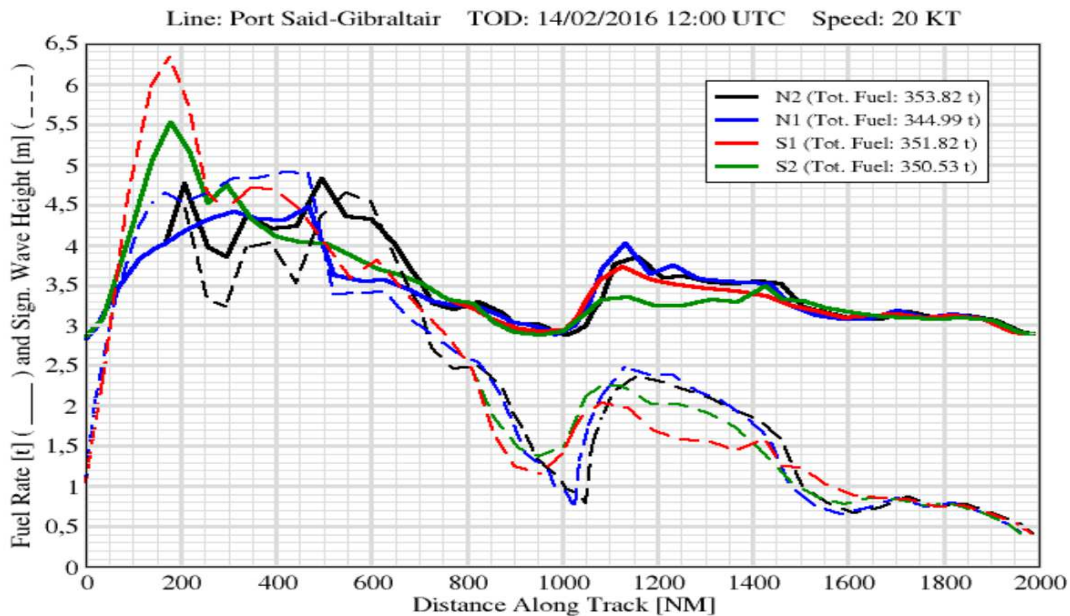


Fig. 9: Fuel rate [t] of the ro-ro ship (continuous lines) computed by SPAR and corresponding value of the significant wave height [m] (thin dashed lines) for the voyage from Gibraltar to Port Said, at constant speed of 20 KT, with departure time on 14/02/2016 at 12:00 UTC.

6. Conclusions

In the present work a computational suite resulting from the integration of meteo-marine forecasting models with algorithms for the detailed simulation of seakeeping and powering performance of ships in realistic meteo-marine conditions is described. The various computational parts have been tuned and verified by means of comparisons with data regarding a real ro-ro ship. By exploiting such data and by performing several simulations along Mediterranean routes of different length and geographic extension, a first assessment of the fuel saving potential has been performed in the perspective of implementing novel weather routing algorithms tuned to the Mediterranean scale. The first results obtained by processing the huge amount of data have shown that a potential of some points of percentage is available for fuel savings in many meteo-marine conditions of intermediate intensity. In cases of heavier weather the fuel saving potential may be also greater. The more promising situations are those characterized by the availability of more than one equivalently shortest route, but traversing

significantly different geographic areas (as in the cases where a significant navigational obstacle, e.g. as a big island, is present obliging to pass over it through one or the other of its sides). When only one shortest direct route is available, the fuel saving potential must be searched by exploiting other internal degrees of freedom as the possibility of adopting varied speed profiles and different engine or propeller pitch settings, dynamically depending on the encountered meteo-marine conditions. Some testing on these alternatives has shown that their addition may allow a greater fuel saving potential. Other tests demonstrated that also the time of departure could be varied to exploit the time variability of meteocean conditions in order to save fuel.

In the performed tests a small number of simply varied routes have been tested, but in further developments numerical optimization algorithms will be employed, so as to be capable of systematically testing a significantly wider set of more complex routes, speed-propulsion profiles and time windows. Due to project constraints, the study has been based only on a single real ro-ro ship. It has been simulated also un long routes, for which it was not well fitted, being characterized by a high speed potential, but also by high values of fuel consumption. For a more sound analysis the study need to be extended to a number of different ship types, covering a wide spectrum of different trades.

References

ABS (2014), *Ship energy efficiency measures advisory. Status and guidance*, American Bureau of Shipping

ADOPT (2008), *Final Report of ADOPT (Advanced Decision Support System for Ship Design, Operation and Training) Project*, EU FP6 2007-2008

ALVES, J.M.G.M.; WITTMANN, P.; SESTAK, M.; SCHAUER, J.; STRIPLING, S.; BERNIER, N. B.; MCLEAN, J.; CHAO, Y.; CHAWLA, A.; TOLMAN, H.; NELSON, G.; KLOTZ, S. (2013), *The NCEP-FNMOC Combined Wave Ensemble Product Expanding Benefits of Interagency Probabilistic Forecasts to the Oceanic Environment*, Bulletin of the American Meteorological Society, BAMS, December

BECK, R.F.; WOODWARD, J.B.; SCHER, R.; CARY, C.M. (1975), *Feasibility of sailing ships for the American merchant marine*, Report No. 168, Dept NAME, University of Michigan

BERTRAM, V.; VELO B.; SÖDING H. (2006). Program PDSTRIP: public domain strip method. Software documentation

BÖSE, P. (1970). *Eine einfache Methode zur Berechnung der Widerstandserhöhung eines Schiffes im Seegang*, Ship Technology Research 17

CARLTON, J.S. (2007), *Marine propellers and propulsion*, Elsevier, ISBN: 978-0-7506-8150-6

CORADDU, A.; FIGARI, M.; SAVIO, S.; VILLA, D.; ORLANDI, A. (2013), *Integration of seakeeping and powering computational techniques with meteo-marine forecasting data for in-service ship energy assessment*, Sustainable Maritime Transportation and Exploitation of Sea Resources, Guedes Soares & Lopez Peña (eds), Taylor& Francis Group, London, ISBN 978-1-138-00124-4

CORADDU, A.; ONETO, L.; BALDI, F.; ANGUIA, D.; (2014), *Ship energy efficiency forecast based on sensors data collection: improving numerical models through data analytics*, IEEE Oceans, Genova

CHEN, H. (2008), *Voyage optimization supersedes weather routing*, Jeppesen Marine

DNV-GL (2015), *Energy management study 2015*, DNV GL, Hovik

- DNV-GL (2014a), *The future of shipping, a broader view*, DNV GL, Hovik
- DNV-GL (2014b), *Next generation energy management*, DNV GL, Hovik
- FALTINSEN, O.M. (1998), *Sea loads on ships and offshore structures*, Cambridge University Press
- HANSEN, S.V. (2011), *Performance monitoring of ships*, PhD thesis, Technical University of Denmark (DTU), Lyngby
- HJORTH SIMONSEN, M., LARSSON, E.; MAO, W. AND RINGSBERG, J. (2015) *State-of-the-art within ship weather routing*, ASME 34th Int. Conf. Ocean, Offshore and Arctic Engineering (OMAE), St John's
- HSVA (1999), *Model test for a 2-screw passenger Ro-Ro vessel*, Report WP 3/99, The Hamburg Ship Model Basin, Hamburg
- KAKUTA, R. (2013), *How ICT can assist energy efficient fleet operations - How broadband changes quality of weather routing*, Digital Ship Singapore
- KALNAY, E. (2003), *Atmospheric Modeling, Data Assimilation and Predictability*, Cambridge University Press
- KOMEN, G.J.; CAVALERI, L.; DONELAN, M.; HASSELMAN, K.; HASSELMAN, S.; JANSSEN, P.A.E.M. (1994), *Dynamics and modelling of ocean waves*, Cambridge University Press
- LAMMA, *meteo-marine models web pages*: www.lamma.rete.toscana.it/mare/modelli/vento-e-mare
- LEWIS, E.V. (1990), *Principles of naval architecture: volume III*, SNAME
- MOFOR, L.; NUTTALL, P.; NEWELL, A.; (2015), *Renewable energy options for shipping*, Int. Renewable Energy Agency (IRENA), Innovation and Technology Centre
- ORLANDI, A.; BRANDINI C.; PASI F.; TADDEI S.; DORONZO B.; BRUGNONI G.; ROSSINI G.; BENEDETTI R.; GOZZINI B.; ORTOLANI, A.; VACCARI F.P.; et al. (2009), *Implementation of a meteo marine forecasting chain and comparison between modelled and observed data in the Ligurian and Tyrrhenian seas*, Volume sulle attività di ricerca scientifica e tecnologica del CNR nell'ambito del mare e delle sue risorse, CNR, Rome
- ORLANDI, A.; PASI, F.; CAPECCHI, V.; CORADDU, A.; VILLA, D. (2015a), *Powering and seakeeping forecasting for energy efficiency: assessment of the fuel savings potential for weather routing by in-service data and ensemble prediction techniques*, 16th Int. Congress of the Int. Maritime Association of the Mediterranean (IMAM), Pula
- ORLANDI, A.; CAPECCHI, V.; ROVAI, L.; BENEDETTI, R.; ROMANELLI, S.; ORTOLANI, A.; CORADDU, A.; VILLA, D. (2015b), *Ship performances forecasting at the Mediterranean scale: evaluation of the impact of meteocean forecasts on fuel savings for energy efficiency and weather routing*, 18th Int. Conf. Ships and Shipping Research (NAV), Lecco
- ORLANDI, A.; BRUZZONE, D. (2012). *Numerical weather and wave prediction models for weather routing, operation planning and ship design: The relevance of multimodal wave spectra*, Sustainable Maritime Transportation and Exploitation of Sea Resources, Taylor& Francis Group, London
- ORLANDI, A. (2012). *Integration of meteo-marine forecast data with ship seakeeping and powering computational techniques*, PhD Thesis, University of Genoa

PIELKE, S.R. (2002), *Mesoscale meteorological modelling*, Academic Press

RAE (2013), *Future ship powering options. Exploring alternative methods of ship propulsion*, Royal Academy of Engineering (RAE)

SAIL (2015), *Final Report. Roadmap for sail transport: Engineering*, SAIL Project, EU Interreg IVB

SMITH, T.; O'KEEFE, E.; ALDOUS, L.; AGNOLUCCI, P. (2013), *Assessment of shipping's efficiency using satellite AIS data*, UCL Energy Institute

TOLMAN, H.L. (2009), *User manual and system documentation of WAVEWATCH III version 3.14*, NOAA NWS NCEP MMAB Technical Note 276

WISE GROUP, CAVALERI, L.; et al. (2007), *Wave modelling. The state of the art*, Progress in Oceanography 75/4, pp.603-674

Acquisition and Integration of Meaningful Performance Data on Board - Challenges and Experiences

Michael vom Baur, Hoppe Marine GmbH, Hamburg/Germany, m.vombaur@hoppe-marine.com

Abstract

This paper focuses on collecting, integrating and pre-processing data for performance monitoring purposes on existing vessels, where sensors and systems were often not designed to share information to "third parties". Challenges range from judging the reliability and uncertainty of existing sensors on board and understanding individual manufacturer interpretations of different communication protocols to ensuring that any data transmitted to shore still contains consistent and meaningful information. The latter can be provided by intelligent plausibility checking and pre-processing. Practical experiences from numerous on-board installations and examples are discussed.

1. Introduction to Performance Monitoring: Purpose and Key Success Factors

The drastic increase of bunker fuel prices starting in 2007, with peak values exceeding US\$ 750 / ton for Heavy Fuel Oil (HFO), triggered a closer focus on vessel performance in the international shipping community. Several strategies to reduce fuel cost, which became the by far dominating part of the total operation costs, have been established in the past years, ranging from operational measures such as slow steaming, trim and route optimization to conversion investments to optimize in particular container vessels to new operation conditions, e.g. de-rating of main engine, new propeller and bulbous bow, retrofitting of roll damping devices (e.g. the FLUME[®] Roll Damping System) to enable higher and more flexible cargo intake. However, the first step was to create a basis for better understanding of how the ship performs at sea and how much fuel it consumes under certain loading and operational conditions.

The measuring, reporting and systematic analysis of various performance parameters is nowadays summarized under the term "Performance Monitoring" (PMO). As Lord Kelvin said: If you cannot measure it, you cannot improve it (and I may humbly add: cannot prove it). Thus meaningful PMO today is a mandatory pre-requisite for

- creating a knowledge base for the optimization of fuel consumption
- complying with more and more challenging reporting requests of charterers, which in some cases already includes the request for justification of the voyage fuel balance, the judgment how the crew has used optimization potentials during the charter period as well as quality ranking benchmarks for future charter ship selection
- rejection of charterer's fuel claims (in time charter)
- proof of function of retrofitted propulsion improving devices ("before / after"), also in context with loan financing of such devices and conversions
- monitoring of the hull fouling condition for decision when to clean / paint next time, also pre-requisite for performance based contracts with paint suppliers (important in particular for ships operating with dominating frictional resistance such as tankers, bulkers and container vessels in slow steaming condition)
- enabling fleet performance improvement by transparent competition between the crews of sister vessels
- integrating ship performance information in operators' fleet monitoring centers as well as in future "big-data" strategies

Monitoring the performance of a vessel is not a new invention. Dedicated inspectors and fleet managers have done this in the past as well, mainly by analyzing manual "noon reports" collected from the ship. However, everyone who has been involved in such type of analysis knows that this can only be a rather vague picture of the reality, which often resembles a cloud of scattered points in a

diagram where a (e.g. speed-power-) curve would be expected. This is obviously due to the relatively high uncertainty of manual readings in combination with the low observation frequency (typically 1 x / day) but may, as a general indication, still be acceptable for some purposes. However, trying to identify e.g. fuel consumption differences due to trim optimization by comparing noon reports is equivalent to the attempt of finding a needle in a haystack.

Aldous et al. (2013) clearly demonstrated how automatic, higher frequency (every hour or below) data acquisition can reduce the overall uncertainty of PMO and thus enable a much higher resolution performance picture.

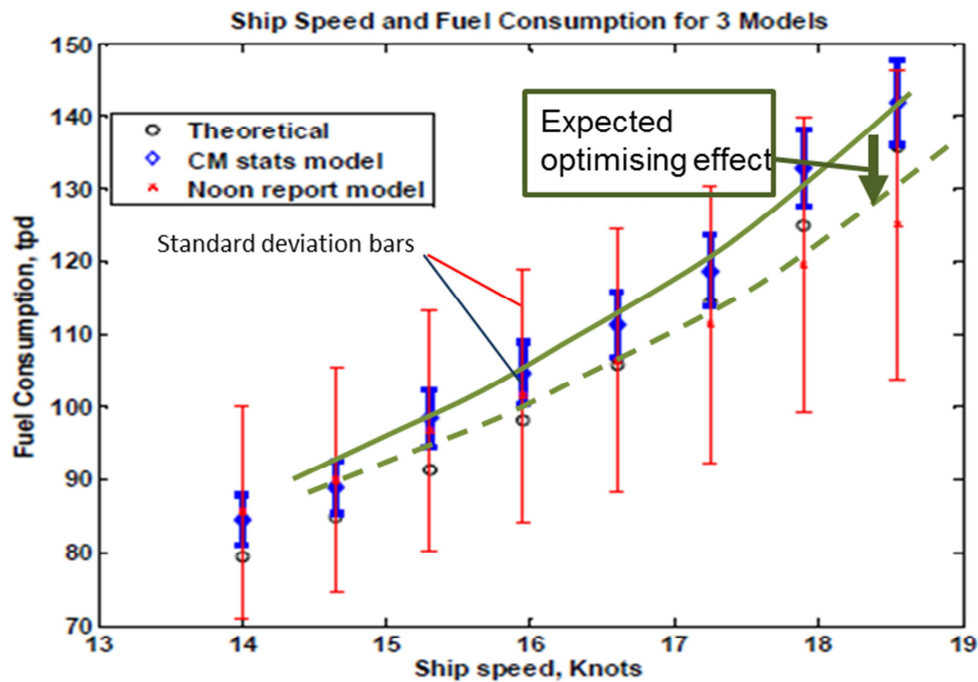


Fig. 1: Challenge in determining trim optimization results via noon data, *Aldous et al. (2013)*

But even automatic recorded performance data bear considerable sources of uncertainty, caused by e.g. the measuring methods as well as quality and actual condition of the sensors and by the consistency and synchronicity of stored data (sources of uncertainty were considered by *Aldous et al. (2014)*).

The increasing challenge to provide precise performance analyses, which use may even have commercial or legal impact (evident e.g. for performance based hull coating contracts, charterer's fuel claims or ship benchmarking), was the impetus to develop the ISO 19030 standard, intended to give methodical guidance and uncertainty information for measuring changes in hull and propeller performance. This voluntary standard (currently at DIS ballot stage) allows several PMO approaches and comparison of uncertainties to be expected for the different methods and will most likely be quoted as a basis for onboard measurements in most commercial agreements based on ship performance. The ISO 19030 default method defines parameters to be measured and recorded at least once every 15 s,

- primary parameters: time and date, speed through water (STW), propeller shaft torque and propeller shaft revolutions or fuel flow
- secondary parameters: speed over ground (SOG), ship heading, water depth, rudder angle, relative wind speed & direction, draught fore & aft (static), dynamic trim, seawater temperature

Primary and secondary parameters shall be stored in packages under a common time stamp. The secondary parameters, which could also be augmented by information like ship roll and pitch angles etc., are recorded with the intention to enable filtering data according to ISO 19030 reference conditions to enable a comparison of “apples with apples”. Thus their consistency and completeness is of same importance for a precise PMO analysis as the one of the recorded primary parameters.

When considering all mentioned parameters and the related measuring methods and sensors available, it becomes obvious that the quality of data recorded on board is key for meaningful PMO analyses. Such analyses are very much governed by the “GIGO-Principle” (“Garbage in = Garbage out”): even the most sophisticated and glossy performance analysis software will deliver unreliable and misleading results, if the data acquired on board are of minor quality, fragmentary and / or inconsistent. The impact of low-quality on-board data is, until today, often underestimated, since systematic PMO is a relatively new task with still only limited experience from operation practice. However, with growing experience it becomes evident that a strong focus must be on acquisition and integration of meaningful performance data on board.

Although bunker prices are almost back to pre-2005-levels (far below US\$ 200 / ton HFO), PMO has meanwhile become an important element in most leading ship operators’ activities and plans.

2. Data Acquisition Sources on Board

Typical sources for the acquisition of primary and secondary ISO 19030 parameters and further key data on board are as follows:

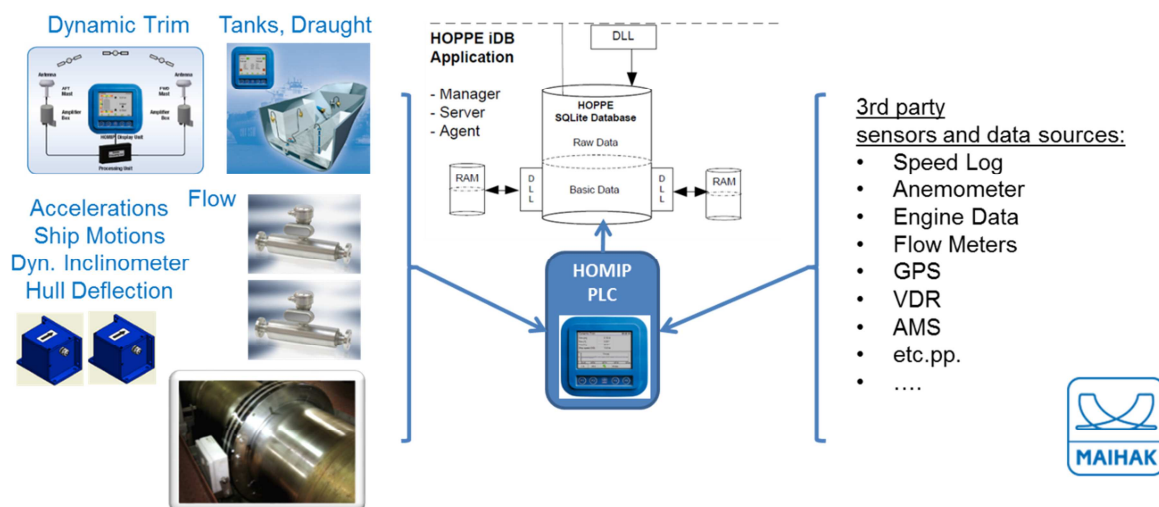


Fig. 2: Typical data sources onboard, *Maihak (Hoppe Marine)*

- direct acquisition sources
 - Shaft Power Meter: torque, rpm (e.g. via Hoppe MAIHAK)
 - Flow meters (Coriolis or volume counter type)
 - GPS (time, position, SOG)
 - Dynamic trim (e.g. via Hoppe Marine TRIMCON),
 - Ship motion data (e.g. via Hoppe Marine HOSIM)
 - Individual nautical instruments (e.g. STW, anemometer, depth sounder, (wave) radar)
- bundled sources (e.g. via AMS, VDR or ECDIS)
 - Nautical data
 - Draught indication fore and aft
 - Tank content data (mass of liquid in tank) Main and Auxiliary Engine data

- Cargo Data via loading computer
- Further sources depending on operator request.

The state of the art of measuring the above mentioned parameters and therewith the uncertainty of the measuring methods differs considerably. The weakest parameter in the chain is certainly the speed measurement (STW), done mostly today with Doppler logs, which do not often have sufficient precision and reliability. These devices have been used on board for many years, but have often not been considered as a key measuring system and thus did not receive the necessary attention and maintenance by the crew, because speed over ground (SOG) as displayed by the GPS appeared to be the much more stable parameter. On the other hand, a precise STW measurement is a must for comparative PMO analyses.

All involved sensors have individual characteristics and uncertainties, which depend on their measuring method, sensor design, long-term stability, their sensitivity and robustness against external environment changes, age (e.g. mechanical wear) and actual maintenance status.

For automatic PMO data acquisition the considered sources must be able to export analog or binary signals, which will be digitized via I/O units and communicated to the “data collector” via defined and described interfaces using standardized protocols. Typical interfaces are RS485, RS422, CAN Bus, Ethernet and Maker Bus Standards (e.g. Hoppe Marine HOBUS). Typical Protocols are e.g. NMEA183, MODBUS TCP/IP, MODBUS RTU, UDP, OPC UA or Maker Bus protocols.

The parameters to be measured have individual and different physical characteristics, which may require different sampling frequencies in order to provide the required accuracy and catch possible dynamic effects. While for example the shaft revolutions can physically not significantly fluctuate in 10 s intervals, the rudder angle or motion parameters can change a lot in the same interval and therefore should be acquired in higher frequency. However, all data must finally arrive in the database in “slices” (data sets) with a common time stamp, which are based on signals acquired in different frequencies. It is evident that certain pre-processing operations are necessary to generate such data sets and to achieve full data integration.

Last but not least, the data sets have to be compressed and stored on board, to enable efficient shore transmission whenever connected in feasible time slots at reasonable telecommunication costs.

3. Challenges and Typical Headaches

Collecting data on board appears almost trivial, even when looking at the respective single line diagram. However, the devil is in the details. Since data acquisition almost always goes down to PLC level, programming and interface / communication handling is on machine code level, which is mostly not very user friendly. Furthermore the support by the OEMs is not always sufficient, on older vessels sometimes even no longer available. The fact that typically some dozens or (including engine data) up to some hundreds of signals are acquired, recorded and processed, illustrates the magnitude of the challenge, which often demands “detective talents” from the project engineers.

A particular challenge is the implementation of stable data acquisition on existing ships. Data sources such as sensors and meters on older vessels may lack precision and have not been designed share data with other systems.

Frequently observed problems include:

- Different OEMs have different interpretations of data bus protocols.
- There is no standard for signal names (e.g. for the so-called “friendly names” /describing names) and makers are often neither disciplined nor consistent in using such names.



Fig. 3: The often experienced reality of gathering data onboard

- Sensors or meters do not have appropriate interfaces to be integrated in a data bus communication system, upgrades or exchanges become necessary.
- The ship's main automation system does not support modern interfaces and bus technologies, it is often not well documented, respectively has insufficiently documented deviations between the ships of a series, even within one system generation.
- Software and interface description of older systems are sometimes no longer officially supported by the makers, staff with the necessary know-how regarding older versions no longer available for answers and consulting.
- Sensors or meters are found not well maintained or have already reached the end of their lifecycle and are thus no reliable data sources (data interruption due to mechanical and electrical failures).
- Volume type flow meters are often worn out and no longer properly calibrated after years of operation.
- Some flow meters do not distinguish between forward and backward flow and can thus send misleading results in case of pulsation in the fuel cycle (in particular if the flow meter location was not selected with necessary care).
- For older tank and draught sensors deviations or data interruptions due to electric or pneumatic problems may occur.
- Shaft power meters (in particular of strain gauge type) have drifted over the years and can hardly be re-calibrated.
- Doppler logs (STW) have sometimes been mounted by the yard in zones with instable flow, etc.

Many of the above listed problems have the potential to create totally misleading results or even jeopardize the entire PMO efforts. Frequent temporary recording interruptions of certain parameters may create difficulties in the later analysis tools, they have to be identified, properly dealt with and checked for completeness and plausibility on board.

Considering the above said it becomes evident that reliable data acquisition and integration on board is a necessary pre-requisite and key for meaningful PMO analyses. At this time the reality regarding standardization of protocols is poor and thus the data integrator will have most of the burden in project implementation, which requires a respective strategy and a lot of experience.

4. Strategy for Plausible and Consistent Data

Under the brand “Maihak”, Hoppe Marine has developed a reliable and flexible data acquisition, pre-processing and storage concept which can integrate all kind of data sources. In a first step the digitized Basic Signals from the sources are acquired by a PLC based system (HOMIP) which is independent of frequent operation system software changes on PC level. The recorded data (“Basic Data”) is made available for further processing and integration. On HOMIP level also several computed values as well as standardized reports can be visualized via a webserver tool.

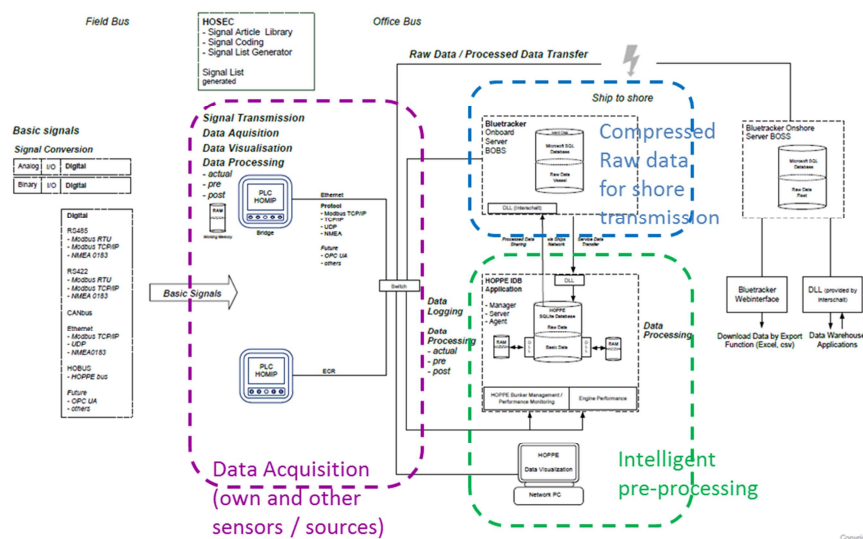


Fig. 4: Possible data acquisition, pre-processing and storage concept, *Maihak (Hoppe Marine)*

During the second step the Basic Data will be checked for completeness and (optionally) for physical plausibility, consolidated and compiled in data sets with common time stamp and compressed for shore transmission, before they are stored as “Raw Data” in a PC-based proprietary data base (Maihak / Hoppe iDBS). From this data base the time stamped data sets can be transmitted at any time when connected to an identical data base in the operator’s office ashore, where they are then available for display (e.g. on user defined dash boards) and analysis tools.

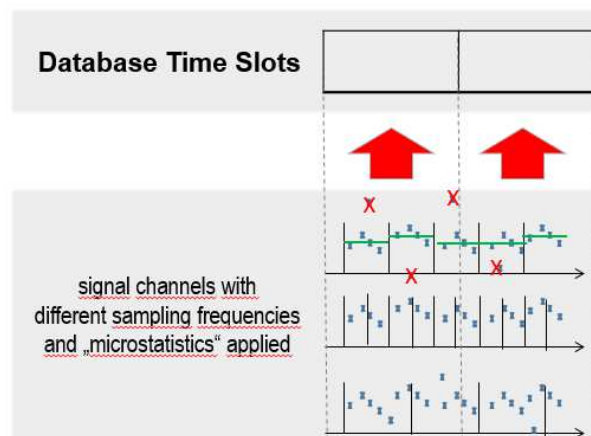


Fig. 5: Intelligent pre-processing, *Maihak (Hoppe Marine)*

The “intelligent pre-processing” which can be applied in the second step aims to provide “cleaner” and physically plausible Raw Data, by intelligent, parameter-individual aggregation for short time windows (“micro-statistics”), in line with the physical characteristics of the signal, and by removing outliers which violate the physical continuum characteristics of the respective parameter. This pre-processing does not correct measured data but supports the necessary averaging processes when consolidating data with different sampling frequencies.

In the later analysis, process ISO 19030 recommends to use only comparable Raw Data obtained by filtering according to reference conditions (e.g. regarding weather) rather than trying to apply correction computations in order to normalize all Raw Data to reference conditions. This approach will reduce the volume of eligible data and therewith the sample sizes considerably but does not add new uncertainties created by the theoretical correction methods (e.g. for ship resistance in sea state). When acquiring data automatically with reasonable frequencies, there will be sufficient data available anyway.

5. Highlights and References

Hoppe Marine (former Hoppe Bordmesstechnik) has long experience with measuring speed (STW, Pitot Tube sensor) and shaft power (strain gauges and Maihak vibrating string) at sea. Hoppe’s first modern automatic PMO system was implemented on a 2.500 TEU container vessel in September 2011. Since then nearly 100 ships have been equipped with different expansion levels of PMO systems under the Hoppe-Brand Maihak, integrating so far up to around 300 signals per vessel from sources such as individual sensors (Hoppe Marine / Maihak and external make), AMS, VDR, loading computer and motion reference units. The recorded results have been carefully evaluated and have formed the know-how basis for further developments.

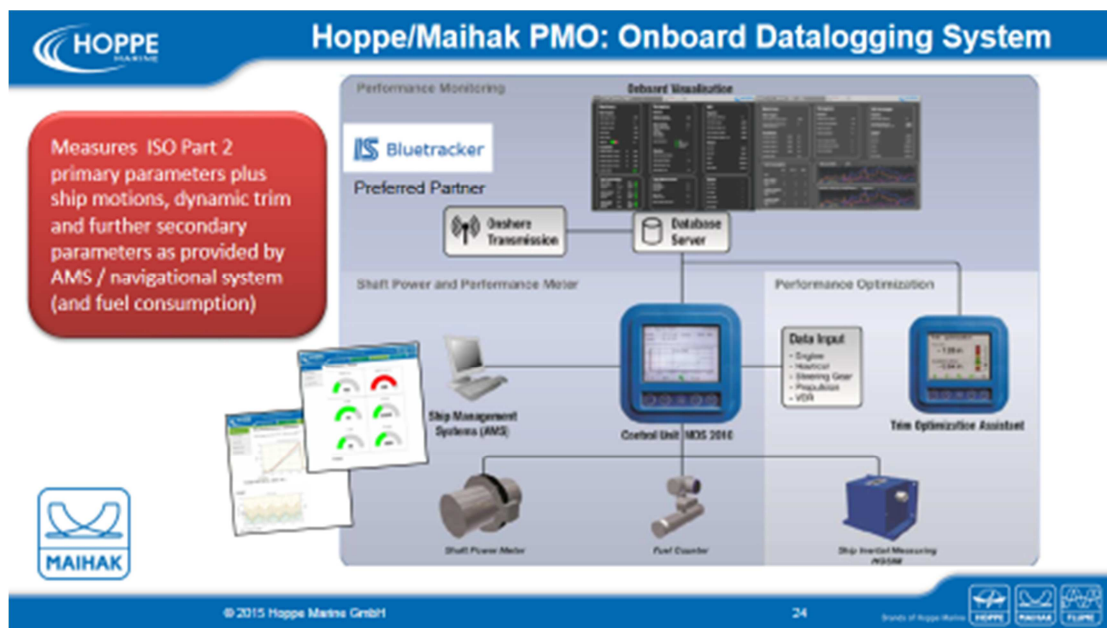


Fig. 6: Typical Maihak (Hoppe Marine) PMO setup

One of the important findings derived from long-term comparative analyses of STW and SOG with statistical methods for different vessels was that Doppler Type Speed Logs can have dynamic errors which are speed dependent (see Fig.7). Based on this recognition the quality of the STW measuring can be assessed and checked in regard of vessel individual characteristics and possibly recommendable corrections on board. Acknowledging that the STW measurement is the weakest part in the measuring chain, such plausibility checks are an important contribution to enhance precision.

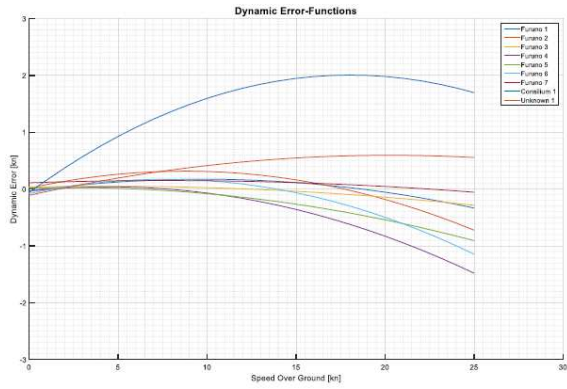


Fig. 7: Dynamic STW error [kn]

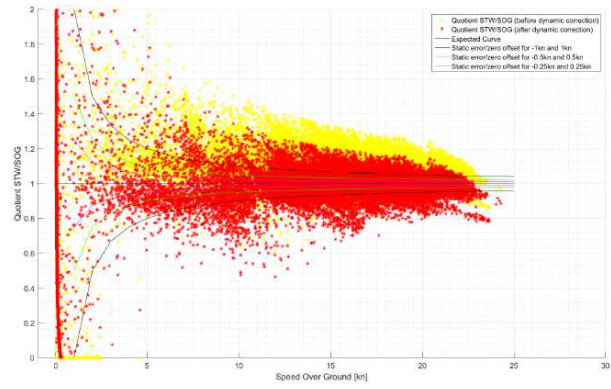


Fig. 8: Corrected and uncorrected quotient of STW/SOG with static error

Further regular checks when assessing automatically recorded performance data should be done with the shaft power meter. The “zero rpm”-torque values, which are sampled during port periods, should be observed over time; eventual deviations are a hint for recalibration need. In addition the possible individual offset of the sensor should be assessed, by using the linear relation between rpm and square root of torque. Additional validations e.g. of flow-meter data are also strongly recommended.

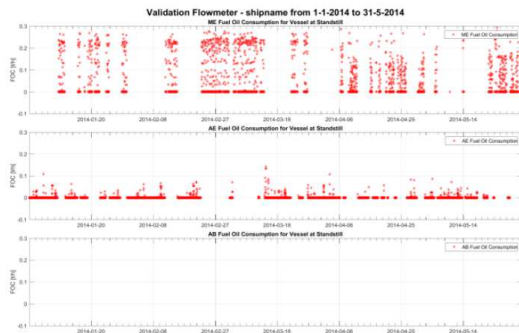


Fig. 9: Validation of flow-meter data at zero flow

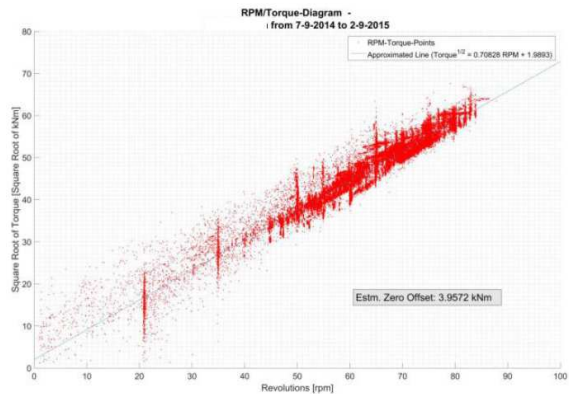


Fig. 10: Estimating torque meter zero offset

Polar diagram type plots of data cross checks between parameters such as e.g. voyage specific fuel oil consumption (FOC) against wind encounter angle and speed can help to identify systematic weaknesses such as anemometers in partial wind shadow for certain encounter angles (see Fig 11).

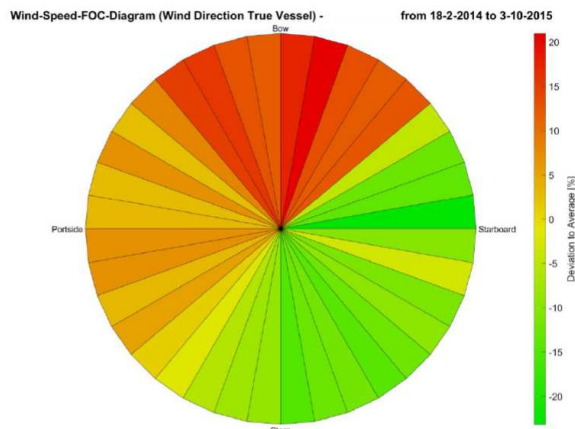


Fig. 11: Plot of voyage specific FOC against wind encounter angle

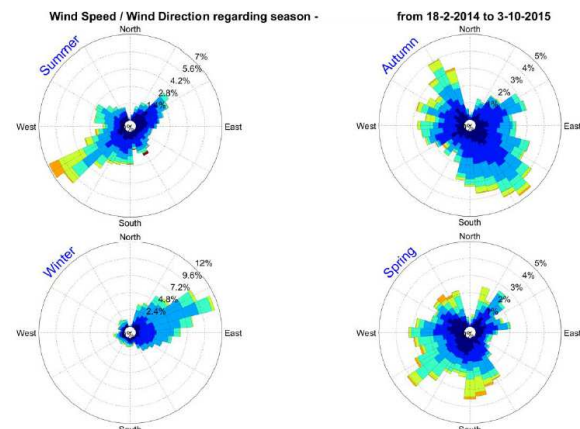


Fig. 12: Plot of experienced wind by seasons (for specific vessel)

6. Conclusions

Collecting, integrating, pre-processing and storing data for Performance Monitoring (PMO) purposes on existing vessels is the opposite of trivial and requires solid knowledge about ship operation and theory, sensors, IT interface and database technologies. The challenges range from judging the reliability and uncertainty of existing sensors on board and understanding older automations systems or individual manufacturer interpretations of different communication protocols to ensure that any data transmitted to shore is as complete as possible and contains consistent, plausible and meaningful information. Frequently incomplete data sets can create not only “empty” diagrams and dashboards, but may as well jeopardize entire long term analyses.

It can be concluded that data acquisition and integration on board could be a headache for the crew, it should better be projected and implemented by an experienced specialist entity.

Applying intelligent pre-storage pre-processing but also regular longer term plausibility analyses can significantly reduce uncertainties and thus enhance understanding of the operational processes and the quality of data. This is key to meaningful PMO.

References

ALDOUS, L.; SMITH, T.; BUCKNALL, R. (2013), *Noon report data uncertainty*, Low Carbon Shipping Conference, London

ALDOUS, L.; SMITH, T.; BUCKNALL, R.; THOMPSON, P. (2014), *Uncertainty Analysis in Ship Performance Monitoring*, Ocean Engineering 110, pp.29-38

ISO 19030 1-3, *Measurement of changes in hull and propeller performance*, Int. Standard Org.

Advances in Measurements of Hull Performance: Implications for Buyers and Sellers of Performance Enhancing Technologies and Solutions

Geir Axel Oftedahl, Jotun A/S, Sandefjord/Norway, geir.axel.oftedahl@jotun.no

Abstract

Over the last several years a wide range of new and innovative technologies and solutions has been brought to market with the promise of substantial improvements in hull performance and thereby improved ship efficiency. Potential buyers have largely found themselves unable to accurately and reliably determine their individual contributions, however. The resulting ambiguity has slowed down investments in technologies and solutions that actually deliver. At the same time it has resulted in needless spending on many that never will. Current advances in sensor technologies, on board ICT infrastructure as well as analysis methods are making it increasingly possible to isolate and measure the energy efficiency contributions from individual technologies and solutions. When published, ISO 19030 will make it easier to rely upon and compare the output from such measurements. This paper will explore the profound implications of such advances for both buyers and seller of technologies and solutions that promises improvements in hull performance.

1. Backdrop

If left unchecked, bio-fouling and mechanical damage on underwater hulls would literally result in the shipping industry grinding to a halt. Within a few weeks or months in service most ships would double the amount of energy consumed in order to maintain speed. Bunker costs would become prohibitively high and Green House Gas emissions per unit of cargo transported would skyrocket.

For centuries the solution has been to apply underwater hull coatings with some form of antifouling properties at every dry-docking. Today there are many different antifouling technologies – some more and some less effective at protecting underwater hulls from bio-fouling over the course of the dry-docking interval.

However, a number of factors beyond bio-fouling and mechanical damages affect the energy efficiency of ships and buyers of antifouling coatings have found it difficult to accurately and reliably measure good versus bad underwater hull performance and to quantify impact on the energy efficiency of the ship in question. The market for coatings with antifouling properties has therefore largely driven by a focus on per liter cost, rather than the effectiveness, of the coatings.

As a result, today hull performance is a ship efficiency killer. According to the Clean Shipping Coalition in MEPC 63-4-8, poor hull and propeller performance accounts for around 1/10 of world fleet energy cost and GHG emissions. This indicates an astonishing improvement potential; 1/10 of world fleet energy costs and GHG emissions translate into billions of dollars in extra cost per year and an increase of around 0.3% in man-made GHG emissions.

Current advances in sensor technologies, on board ICT infrastructure and analysis methods are making it increasingly possible to isolate, measure and monitor the energy efficiency contributions from individual technologies and solutions – including those influencing hull performance. When published, ISO 19030 will make it easier for the various stakeholders to rely upon and compare the output from such measurements.

This paper will explore 3 profound implications of such advances for both buyers and sellers of technologies and solutions that promise improvements in hull performance.

2. Implications of advances in measurements of hull performance

Advances in measurements of hull performance should make it possible for buyers and sellers of technologies and solutions that promise improvements in hull performance to:

- make better decisions
- make quicker decisions
- better align stakeholder interests

2.1. Better decisions

For decision makers, reliable and comparable measurement output will make it easier to learn from the past and thereby make better decisions for tomorrow.

Consider the real-life example in Fig. 1. The figure shows actual hull and propeller performance over three separate five year dry-docking intervals on the same vessel in the same trade, but with different hull coating solutions.

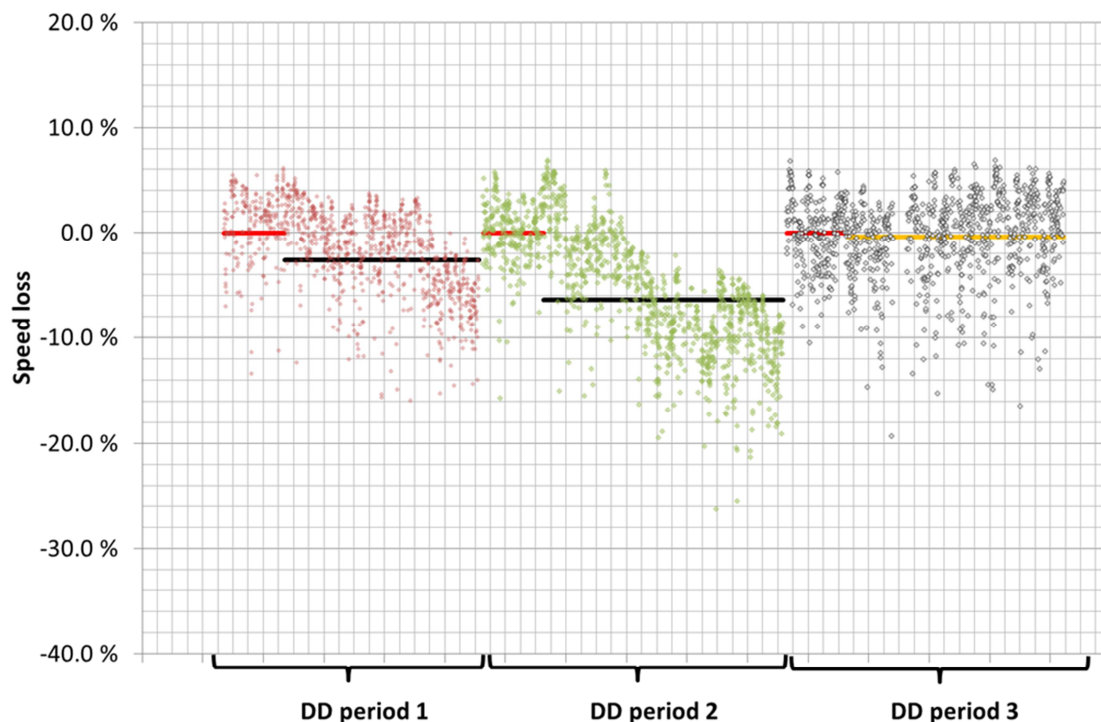


Fig. 1: Change in hull performance on same vessel in same trade over 3 full dry docking intervals with different hull coating solutions

In the middle dry-docking interval the development in hull performance is very similar to what was found to be market average in MEPC 63-4-8. In this interval there is a 6.4% speed loss or a 19% increase in power needed to maintain the same speed - on average over the four years following the benchmark period. Note that the ship needs 38% more power at the end of the period to maintain the same speed. In the first of the three dry-docking intervals the development in hull performance is somewhat better. In this interval there is a 2.7% speed loss or an 8% increase in power needed - on average over the four years following the benchmark period. In the last of the three dry-docking intervals the development in hull performance is indicative of what is possible with today's hull antifouling technologies: virtually no performance loss over the full period. On this particular vessel the hull coating in question is Jotun's SeaQuantumX200.

The difference between market average and best performance is around 18% in the power required to maintain the same speed over the last 4 years of the dry-docking interval. On the 54k dwt bulk carrier in question, at a bunker price of \$350 per ton, this difference would translate into a \$1.8 million difference in fuel cost and a 16 000 ton difference in CO₂ emissions.

2.1.1. Buyer decisions: Opportunities and pitfalls

For buyers of technologies and solutions that promise improvements in hull performance the opportunities arising from such advances in measurements in terms of better decisions are obvious. Given reliable and comparable measurements of what has been the actual impact of these technologies and solutions on hull performance in the past, buyers can better predict what will be the impact on hull performance in the future and what will be the return on investments in the given technology or solution.

But there are also some pitfalls. The impact of a given technology and solution on hull performance is often both situation specific and, even given an identical situation, probabilistic. A technology or solution may, for example, perform well on a vessel in a given trade, and then fail completely on the same vessel in a different trade. Furthermore, the same technology or solution may also perform quite differently on the same vessel in the same trade – e.g. on account of variability in either manufacturing and/or application.

Buyers should therefore consider both the relevance and the size of the sample before using measurements of past hull performance for predictive purposes. For example, an average from measurements of hull performance on 10 randomly picked vessels in a relevant trade offers a much better basis for a prediction than measurements of hull performance on a single – potentially hand-picked - vessel in a different trade.

2.1.2. Seller decisions: Opportunities and pitfalls.

Also for sellers of technologies and solutions that promise improvements in hull performance there are several opportunities arising from such advances in measurements.

Given reliable and comparable measurements of the actual impact of different technologies and solutions on hull performance it is much easier to decide on an appropriate positioning of own technologies and solutions in terms of price-performance. Note also that, over time, an increased level of transparency should serve to eliminate much of the marketing mumbo-jumbo that is so prevalent, and a source of great confusion, in the market today. This should make it easier to successfully market appropriately positioned technologies and solutions.

Finally, and perhaps most importantly, reliable and comparable measurements of the actual impact of different technologies and solutions on hull performance is likely to provide valuable insights to sellers' respective R&D departments.

But the same pitfalls apply for sellers as for buyers. Also sellers must consider both the relevance and the size of the sample before using measurements of past hull performance for predictive purposes.

2.2. Make quicker decisions

For decision makers, reliable and comparable measurement output will, when delivered in a timely fashion, also allow for quicker decisions on unplanned maintenance and repair of the underwater hull. Such a capability can prove very valuable.

Consider again the middle interval from the real life example provided in Fig. 1.

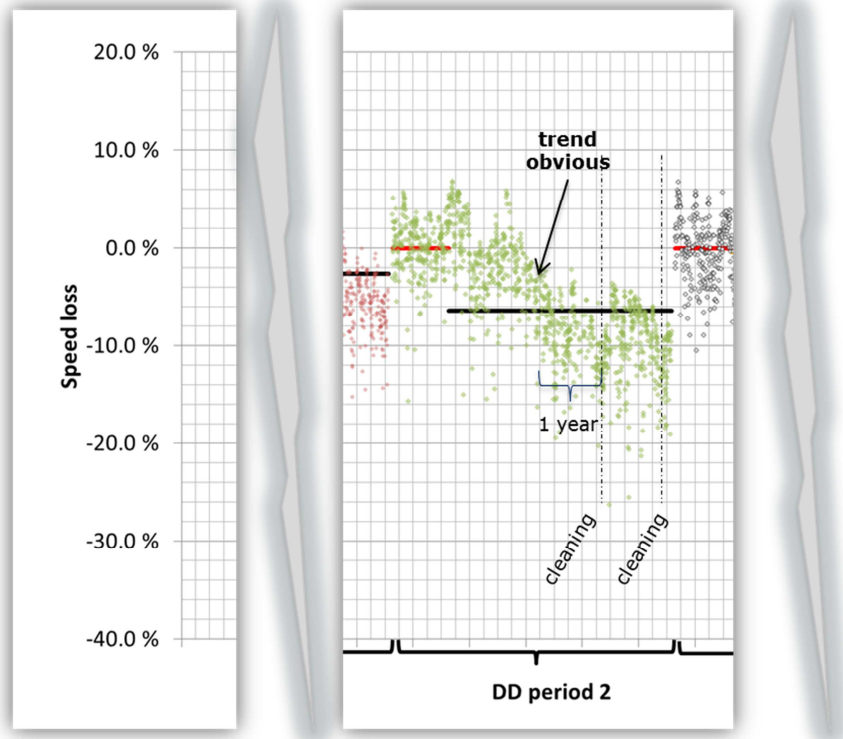


Fig. 2: The potential for quicker decisions on unplanned maintenance and repair

After around 3.5 years into the dry-docking interval the underwater hull on the vessel was cleaned. This resulted in an immediate improvement in speed of around 6% or conversely an 18% reduction in the power needed to maintain speed. Note that the hull was cleaned a second time around 4.5 years into the dry-docking interval.

On this vessel, at the time, performance data was collected and stored but changes in hull performance was not monitored continuously. As can be seen from the data, if changes in hull performance had been continuously monitored it would have been possible to identify a negative trend at a much earlier stage. 2.5 years into the dry docking interval this negative trend would have been impossible to miss.

Regular cleaning of the underwater hull from around 2.5 years and onwards would not have eliminated the problem but would have served to improve hull performance over the remainder of the dry docking interval considerably. A reasonable estimate is that the vessel, given cleaning every 6 months or so (for a total of 5 cleanings), would have been able to end up with an average over the period speed loss of around 4% rather than 6.4% (based on 2 cleanings).

On the 54k dwt bulk carrier in question, at a bunker price of \$350 per ton, this difference would translate into a \$0.7 million difference in fuel cost and a 6 000 ton difference in CO₂ emissions. The direct cost of the 3 additional underwater hull cleanings would typically be around \$0.1 million – leaving a \$0.6 million net gain.

Also here there are some pitfalls. There is a lot of scatter in raw performance data – reflecting uncertainties in sensor data as well as variability in environmental (e.g. weather & wind) and operational conditions (e.g. speed and displacement). Depending on the method used to measure and monitor hull performance, this can result in quite a lot of uncertainty – in particular over short time intervals. On the other hand, the cost of wrongfully identifying a loss in hull performance does not have to be very high. The cost of a dive inspection to confirm that there is a problem, for example, is quite moderate.

2.3. Better align stakeholder interests

Advances in measurements of hull performance should make it possible to better align various stakeholder interests. Such advances will make it possible for buyers and sellers of technologies and solutions that promise improvements in hull performance to commercially contract on the actual performance improvement delivered thus ensuring a mutual interest in achieving same. Furthermore, such advances will make it possible to align the interest of the buyer and seller on the one hand with the interest of 3rd parties such as the owner in a New Build situation or the charterer in a Time Charter situation on the other.

2.3.1. Aligning interests of buyers and sellers

Advances in measurements of hull performance will make it possible for buyers and sellers of technologies and solutions that promise improvements in hull performance to commercially contract on the actual performance improvement delivered.

If appropriately calibrated, such a contract will create a strong incentive for the sellers to not promise more than they are confident they will be able to deliver. For buyers then, it will be much easier to trust sellers' promises and as such easier to justify an investment in a technology or solution that promises the right level of improvement.

If appropriately structured, such a contract can also create strong incentives for the buyers and sellers to work more closely together to ensure the promised level of hull performance is actually delivered. For example, sellers can be incentivized to ensure they have the best information available when specifying the technology or solution for the vessel in question and buyers can be incentivized to provide same.

2.3.2. Aligning interests of buyers, sellers and owners in NB situations

Advances in measurements of hull performance will make it possible to be much more precise in the specification of hull coatings in new-build contracts. New-build contracts today typically specify based on a very broad categorization of technology and lifetime, e.g. "SPC, 60 months". The problem with being more specific has been that different suppliers use different technologies to deliver the same level of performance. Furthermore that even given much narrower categorization of technology (e.g. Silyl Acrylate, 60 months), there can be a substantial performance differential between two different products.

Reliable and comparable measurement output will make it possible to specify the level of performance rather than technology. Sellers can be requested to provide either documentation that the technology or solution specified will deliver on the promised level of hull performance or, to the same effect, an appropriately structured and calibrated performance guarantee.

In the event that sellers are requested to provide documentation, the same pitfalls as outlined under 2.1.1. apply and both buyers and owners should therefore consider both the relevance and the size of the sample before accepting measurements of past hull performance as adequate documentation of performance.

2.3.3. Aligning interests of buyers, sellers and charters in TC situations

Finally, advances in measurements of hull performance will make it much easier than it is today for charter owners and charterers to contract on improved speed-consumption and thereby creating incentives for delivering on same.

Changes in hull performance over time have a considerable impact on speed-consumption and charter owners are, as they should be, reluctant to promise charterers more efficient tonnage without being in

real control of same. Given reliable and comparable measurements of what have been the actual impact of a given technology or solution on hull performance in the past, charter owner can better predict what will be the impact on hull performance in the future. Reliable and comparable measurement output will, when delivered in a timely fashion, also allow for quicker decisions on unplanned but needed maintenance and repair of the underwater hull –reducing the risk of claims. Finally, charter owners will even be able to further limit their risk with back-to-back guarantees from the sellers of the technologies or solutions.

3. Summary

Advances in measurements of hull performance will make it possible for buyers and sellers of technologies and solutions that promise improvements in hull performance to make better and quicker decisions. It will also make it easier for both to better align interested with 3rd parties. Advances in measurements of hull performance should therefor contribute to the realization of the great improvement potential within hull and propeller performance and as such to have a measurable impact on world fleet energy cost and GHG emissions.

References

IMO Marine Environment Protection Committee, “MEPC63/4/8, December 23rd, 2011.

Baseline Propeller Roughness Condition Assessment and its Impact on Fuel Efficiency

Crystal Lutkenhouse, Brian Brady, Jamaal Delbridge, Elizabeth Haslbeck, Eric Holm, Dana Lynn, Thad Michael, Angela Ross, David Stamper, Carol Tseng, Anthony Webb,
NSWC-CD, Bethesda/USA, elizabeth.haslbeck@navy.mil

This paper is provided for information only and does not constitute a commitment on behalf of the United States Government to provide additional information on the program and/or sale of the equipment or system.

Abstract

Roughness on a ship's propeller(s), due to the presence of fouling, for example, increases frictional resistance requiring the impacted vessel to use more power and fuel in order to reach a given speed. We developed methods for assessing the fouling or roughness condition of in-service propellers, calculating the effect of this roughness on propeller performance, and estimating ship fuel penalties associated with the roughness. Results indicate where technology changes can be made in order to save fuel and enhance fleet operational effectiveness. Modifications to the timing and frequency of cleanings and/or the use of propeller coatings are likely to be effective.

1. Introduction

Fouling on ship hulls and propellers increases drag and frictional resistance. In order to overcome these effects ships must use more power and therefore fuel in order to reach a given speed, *Woods Hole Oceanographic Institution (1952), Townsin (2003), Schultz (2007), Schultz et al. (2010)*. The US Navy (Navy) currently uses a combination of antifouling coatings and condition-based cleanings to mitigate the effects of hull roughness due to fouling on ship performance, *Naval Ships' Technical Manual (2006)*. By contrast, the propellers of Navy vessels are not protected from fouling and the control of roughness is instead accomplished by means of relatively frequent cleanings approximately twice per year, *Schultz et al. (2011)*. The unprotected surfaces of propellers develop two forms of roughness – mineral deposits (also known as cathodic chalk or calcareous deposits) and biofouling. On ships fitted with cathodic protection systems, designed to mitigate corrosion of uncoated areas of ship hulls by cathodically polarizing exposed metal using an external current, *Carlton (1994)*, mineral deposits develop relatively quickly on uncoated propeller blade surfaces. Biofouling accumulates on uncoated propellers, whether a ship is fitted with cathodic protection or not. Biofouling primarily develops when ships are in port, inactive, or not moving, and includes both soft and hard forms. For the purposes of this paper, fouling includes biofouling (primarily hard fouling as the type contributing to roughness and drag since soft fouling tends to quickly slough during underway periods) in combination with cathodic chalk.

The impact of propeller roughness on ship propulsion has primarily been quantified through a combination of modeling and direct measure (for example, power trials). Roughness due to cathodic chalk is typically quantified using the Rubert scale, and has been related to power, Table 1, using models based on blade strip theory, *Svenson and Medhurst (1984), Townsin et al. (1985)*. Reciprocal run power trials have been used to quantitatively measure the impact of hull and propeller roughness on power. Hundley and Tsai conducted series of power trials on Navy Knox Class (FF 1052) frigates, *Hundley and Tsai (1992)*. In order to account for the contribution of propeller fouling alone, a series of power trials were conducted before and after propeller cleaning, *Hundley and Tsai (1992)*. As an example, power trials of USS Whipple (FF 1062) indicated a 29% improvement in rate of fuel use over the associated class standard data from the sister ship USS Meyerkord (FF 1058), and the improvement was attributed to propeller cleaning alone.

In order to lower costs and improve operational capability, ship owners are motivated to search for tools and technologies to reduce the negative impacts of propeller fouling. However, in order to justi-

fy transition to alternative solutions, ship owners must be able to compare projected impacts to current (or baseline) conditions. In this study we sought to conduct a comprehensive survey of Navy ship propellers in order to quantify the baseline roughness condition. Concurrently, we sought to close gaps and address weaknesses associated with the techniques used to quantify propeller roughness and its impact on ship powering. Key improvements included making advances in the application of blade strip theory to account for both forms of fouling (cathodic chalk and biofouling) and developing a means by which to account for the variation in type, size, and distribution of fouling on ship propellers. We also developed accurate fuel efficiency estimates while accounting for ship activity, electric load, plant alignment, and propeller pitch. We sought to obtain a baseline estimate of the impact of propeller fouling on ship performance without relying on expensive, time consuming, and disruptive reciprocal run power trials.

Table 1: Rubert roughness (no biofouling) and relationship to power and fuel consumption, *Svensen and Medhurst (1984)*

Rubert Rating	Increase in power @ 20 knots
A	0%
B	0%
C	1.7%
D	2.9%
E	4.9%
F	5.7%

2. Methods

Multiple propeller inspections (57 inspections of 40 ships) of several Navy vessel classes were performed between March, 2012 and September, 2013. Destroyer- (DDG) and Cruiser- (CG) class vessels, plus several Landing Ship Dock (LSD, LHD, LHA – together referred to as L-ship classes) class vessels (as opportunities arose), were targeted for data collection because they represent a large proportion of the fleet in terms of the number of vessels (82 total DDGs and CGs) and fleet propulsive fuel use. The type of ship activity targeted was primarily associated with “full deployments”, meaning the ship departed its home port for at least four months and travelled to foreign ports. As often as possible, inspections were conducted just before or just after ship full deployments. A subset of inspections was associated with non-deployment activity [referred to as short operations (short ops)]. The number of these was limited. Navy ship propellers tend to be cleaned by divers about twice per year, *Schultz et al. (2011)*, and capturing the benefit of this practice was an important component of the work. Therefore, the occurrence of propeller cleanings was also tracked as comprehensively as possible, including cleanings that occurred while a ship was deployed.

In-water inspections were carried out using either divers or unmanned remotely operated vehicles (ROV; VideoRay Pro3). Because propeller blade faces were to be evaluated for both the coverage of cathodic chalk deposits and coverage and type of biofouling, a combination of close-up video (nominally 10 cm x 15 cm view) and still photographs were required to document fouling type, size, and coverage. Roughness ratings associated with cathodic chalk were assigned to blades either directly by divers using a Rubert Comparator Gauge or estimated from the video captured by the ROV.

The effects of surface roughness on propeller performance, and thus vessel fuel efficiency, vary as a function of where on the propeller blade the roughness occurs, the associated increase in velocity due to shaft rotation, and the increase in moment arm with radius, *Gaudet et al. (1973)*, *Townsin et al. (1985)*. In order to develop the most accurate data set and to account for these effects, an inspection pattern, Fig. 1, was established to associate biofouling and cathodic chalk roughness to location on the blade. Images were recorded for each of nine sections on both the suction (forward looking) and pressure (aft looking) blade faces beginning at the propeller leading edge near the hub and running to the tip, down the trailing edge, and back up through the middle of the blade face, Fig. 1.

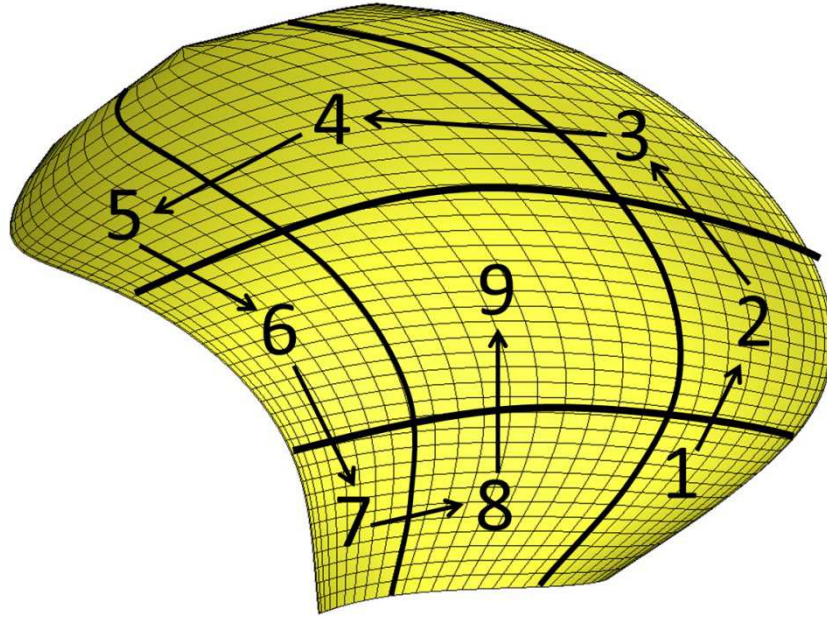


Fig. 1: Inspection pattern for a blade face showing the 9 regions of the blade where coverage of fouling was assessed, overlaid on the DDG 51 (Flight I) propeller computational grid (thin lines)

2.1 Analysis of Video and Photographs

Because variation in fouling condition among blades was less than expected, a total of eight blade faces per inspection event per ship were inspected - both faces of each of two blades, on each of two propellers. Blade areas that appeared free of biofouling were assumed to be covered with at least a thin layer of cathodic chalk and were therefore scored as Rubert roughness rating “D”. Blade areas that were covered by obvious white cathodic chalk were associated with Rubert roughness rating “F”. These ratings were confirmed by divers. Percent cover ratings were associated with three types of hard biofouling – barnacles, tubeworms, and bivalves. Estimates of the height were determined from video and still photographs. Because it was sometimes difficult to detect the smallest forms, and because the practice is regularly applied in the quantification of wave height, the average height of the largest 30% of individuals was recorded. Observed remnants of hard biofouling, such as barnacle and bivalve bases, were scored as “tubeworm” as the most hydrodynamically-similar category. Encrusting and arborescent bryozoa were also scored as “tubeworms” due to their form and size. The total score of Rubert D, Rubert F, barnacles, tubeworms, and bivalves necessarily summed to 100% for the hydrodynamically-relevant calculations. Soft biofouling forms were also scored, however these scores were not included in the drag analysis since soft biofouling forms were observed to detach from propeller blade surfaces during underway periods. Although soft biofouling had little to no effect on propeller roughness and thus vessel fuel efficiency (due to the inability to remain adhered while underway), it did occasionally obscure our view of underlying hard fouling and thus interfered with accurate assessment of hard biofouling coverage in a subset of inspections. The longer the ship had stayed idle the greater the interference. For pre-deployment inspections where soft biofouling was abundant, and where post-deployment coverages of hard biofouling were observed, hard biofouling and cathodic chalk coverage (Rubert F) were estimated.

2.2 Ranking of Propeller Roughness by Relative Roughness Units (RRU)

A means by which to group propellers of like roughness condition was developed. This allowed the selection of the most useful data sets for detailed hydrodynamic and fuel penalty analysis. A method by which to apply a relative roughness unit (RRU) to express propeller roughness was devised. RRU (Eq. 1) accounts for biofouling height and coverage, and location of the biofouling in each of the nine regions of the blade face and for each face of the blade. Roughness due to cathodic chalk was not included in the calculation of RRU. For each region i on each propeller face f , a mean value for the

height (\bar{H}_{if}) and coverage (\bar{C}_{if}) of biofouling was calculated across all the blades inspected. The RRU was calculated by multiplying these values by a radial weighting factor W_i representing the specific effect of biofouling location on the propeller on powering impacts, and summing over all regions and blade faces.

$$RRU = \sum_f \sum_i (1000 \times \bar{H}_{if} \times \bar{C}_{if} \times W_i) \quad (1)$$

2.2.1 Derivation of the Radial Weighting Factor W_i

For a propeller, the relevant velocity for calculation of drag is the local relative velocity which is the vector sum of ship speed and rotational speed at the local radius. In our case, we used the propeller-specific advance ratio at 100% pitch with two shafts driving. By that, we were able to associate the relative velocities to blade location corresponding to the three radial bands in the inspection plan, Fig. 1. This is verified by comparison to the relative velocities from the propeller performance software PSF-10, *Greeley and Kerwin (1981)*, calculated at a similar condition. PSF-10 (more completely addressed in the next section) predicts surface velocities and propeller thrust and torque based on inviscid theory with corrections for viscous drag added through empirical drag coefficients at each radius. Relative velocities for the three radial locations, calculated as above, compare favorably to the surface velocities at several chord-wise locations predicted by PSF-10.

Power is directly related to torque, and torque is proportional to the product of drag and radius. To predict the effect of roughness on power (as opposed to drag), for each radial location we derived an appropriate weighting factor for power (a weighting factor for each radial location - see Fig. 1; radially from blade root to tip, the locations regions 1, 7, 8, regions 2, 6, 9, and regions 3, 4, 5 respectively).

2.3 Calculation of the Fuel Penalty Due to Roughness

2.3.1 Summary of the Approach

Fuel penalties due to propeller roughness were calculated following a two-step process – first a relationship between roughness and drag was established, and then that drag was associated with a fuel penalty. The reader may find the provided outline of the process, Fig. 2, helpful as each component of the process is further described.

In summary, drag coefficients for specific regions of the blade were determined from the inspection data. These coefficients were then used in a corrective tool to compute the change in thrust, torque, and efficiency of the propeller as a function of fouling. These results were combined with a powering analysis and the ship's operating profile (speed vs. time) to estimate the fuel penalty due to the added propeller roughness. Penalties were expressed as a fraction of the value of fuel use with clean propellers. Penalties associated with biofouling roughness alone, as opposed to total roughness (due to both biofouling and cathodic chalk), were also calculated.

The propeller performance was computed using PSF-10. The surface velocities were computed on a grid of 70 points in the chord-wise direction (35 per side) and 51 points in the span-wise direction. Figure 1 shows the computational grid for the DDG 51 Flight I propeller. The DDG 51 Flight I or Flight IIa propellers were used for computations as appropriate to the ship inspected. Roughness analyses of CG propellers were treated according to the DDG 51 Flight IIa propeller model with the nine inspection regions overlaid. No L-ship data were analyzed using this technique. For integrating the added forces due to roughness and fouling, the velocity at each PSF-10 point was used with the fouling inspection data for the region in which it lies. The velocity was assumed to be constant over the area surrounding the point and these velocities were assumed to be the viscous boundary layer edge velocities in calculations requiring such a velocity.

Added forces due to cathodic chalk (Rubert roughness) and biofouling were computed, resolved into thrust and torque components, and summed over the blade. When inspection data for multiple blades were available, they were averaged. The forces were then multiplied by the number of blades and applied to the open water thrust and torque of the unfouled propeller to create a fouled open-water curve for each pitch setting.

2.3.2 Computation of Drag Due to Cathodic Chalk or Rubert Roughness

Roughness due to cathodic chalk was modeled primarily following the method used by *Townsin et al. (1985)*. To compute a change in drag due to roughness, the drag of a smooth blade, computed by the same means, is subtracted from the drag of the rough blade. The baseline roughness used for this analysis corresponded to a freshly cleaned propeller blade surface which is routinely reported by divers as Rubert A. The incremental drag coefficients are used with the local velocity vector, the area around the PSF-10 point, and the area coverage fraction to compute the force vector for each point due to roughness. This method was repeated and integrated for each region of the blade (Fig. 3), and each Rubert roughness rating (either D or F) observed in that region. The results of the method described above were compared with those of *Townsin et al. (1985)* and the methods show good agreement.

2.3.3 Computation of Drag due to Biofouling Roughness

Gowing (2012) collected drag data for barnacles, tubeworms, and oysters. Models of the three types of organisms were mounted on a flat surface and subjected to hydrodynamic flow in multiple orientations in order to measure the drag due to oncoming flow from each direction. These data were analyzed to determine average lift and drag coefficients for all rotational orientations in both uniform and boundary layer flow, Table 2. Averaging across all rotational orientations is equivalent to assuming that the orientation of the organisms will be random with respect to flow. The dimensionless drag coefficients were computed as a function of drag, fluid density, inflow velocity, and basal area of the organism. Calculations for propeller blades estimated a local characteristic velocity ratio following the method used by *Gowing (personal communication in 2014)* to predict the drag of fouling organisms in ship hull boundary layers. The boundary layer thickness at each PSF-10 point was a function of the local distance from the leading edge of the blade and the local Reynolds number on the blade. The ratio of the characteristic velocity and edge velocity corresponded with water tunnel measurements. When this ratio at a PSF-10 point was less than unity, the boundary layer data from the water tunnel measurements were used. When using the boundary layer data, a characteristic velocity for the organism was computed using the observed height data from the biofouling inspection region containing the PSF-10 point. The drag coefficient was multiplied by the square of the ratio of the velocities for organisms in the boundary layer.

Neighboring organisms can significantly impact the hydrodynamic forces on each other, *Hoerner (1965)*, and the effect is a function of the spacing-to-diameter (s/d) ratio. The height-to-diameter ratios of the organisms, calculated by *Gowing (2012)*, were used to determine the average diameters of the observed organisms from the height observations in the biofouling inspection region containing the PSF-10 point. The equivalent diameter of each type of organism was used to compute an average basal area. The equivalent number of organisms was then calculated from this average basal area, the coverage (as a proportion) of the organism in question, and the total area associated with the PSF-10 point. A minimum spacing ratio value of 1.1 was allowed because if the spacing were smaller the organisms would be touching and this method would not be appropriate. A drag reduction factor was then computed based on data for cylinder rows, *Aiba et al. (1981)*, which showed that drag reduction is similar for the third and fourth cylinders in a row. Based on these data, and that of others including *Igarashi (1986)*, it was assumed that the average drag reduction for all organisms is approximately equal to that for the third and subsequent organisms. The interpolation assumes that the drag returns to the isolated value once the s/d ratio reaches 100. The drag coefficient was multiplied by this reduction factor.

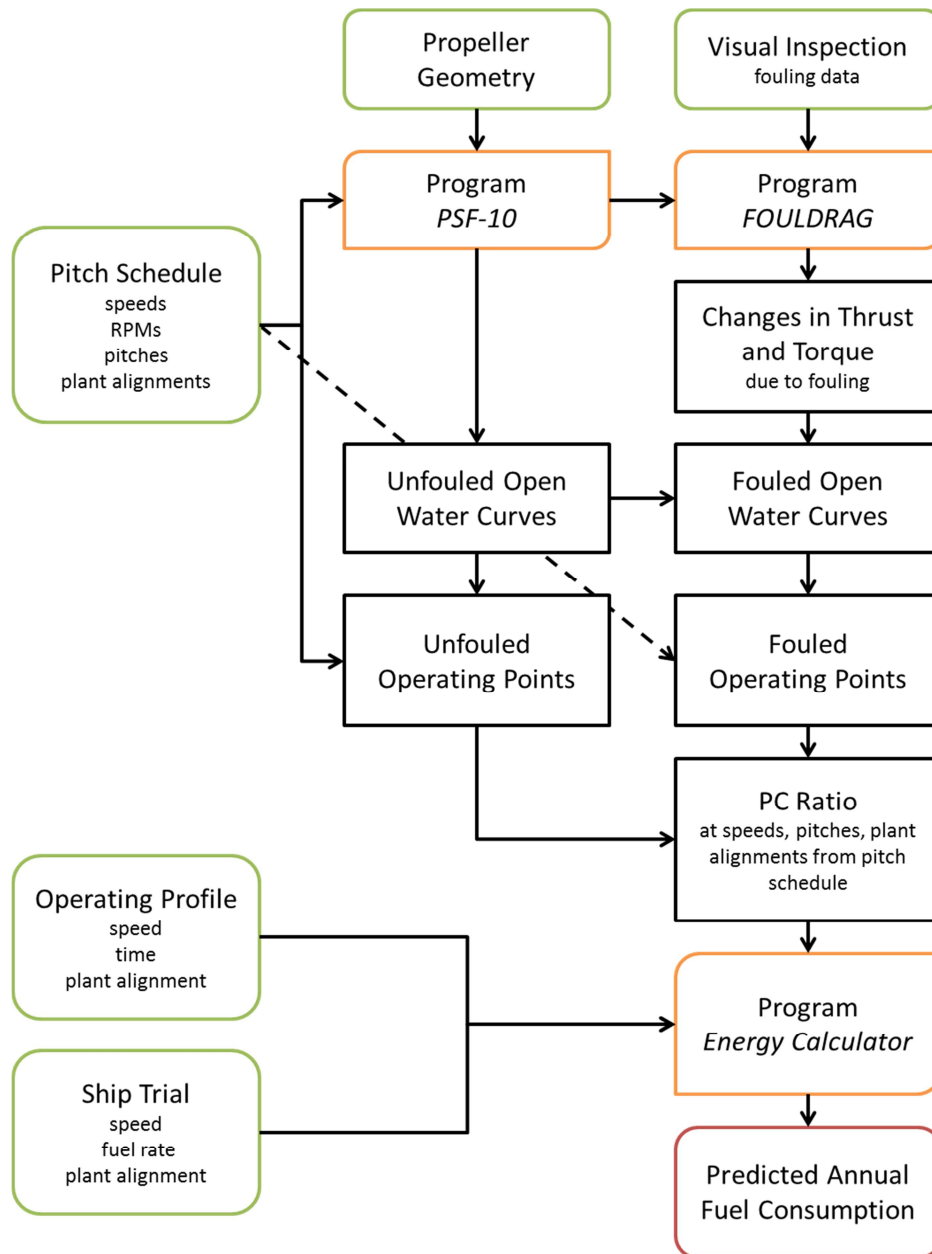


Fig. 2: Process for predicting annual fuel consumption based on propeller roughness condition

Table 2: Measured drag coefficients of several examples of fouling organisms, *Gowing (2012)*

Organism	Drag Coefficient	
	with boundary layer	No boundary layer
Barnacle 1	0.1019	0.1991
Barnacle 2	0.1520	0.2112
Tubeworm 1	0.0773	0.0989
Tubeworm 2	0.0708	0.0993

Finally, the drag coefficients adjusted for the boundary layer were used with the reduction factor due to interference, local velocity vector, the area of the region associated with the PSF-10 point, and the area coverage fraction to compute the force vector for each PSF-10 point due to a given type of biofouling. This method was repeated for each PSF-10 point, and each type of biofouling observed in that region (the nine blade regions in Fig. 1).

2.3.4 Roughness Effects on Propeller Efficiency – Calculating Propulsive Coefficient (PC) Ratio

A standard powering analysis approach was used to predict the operating point [the revolutions per minute (RPM) that the propeller will have to spin to push the ship, together with the thrust and torque produced at a given ship speed and propeller pitch] of the fouled propeller at each speed associated with the operating profile for each possible machinery plant alignment condition, Table 3, at that speed. This operating point was compared with the unfouled operating point to compute the PC Ratio, the ratio of the fouled propeller efficiency (or power) to the unfouled propeller efficiency (or power). Since DDGs and CGs are fitted with variable pitch propellers, we accounted for reduced pitches at low speeds by following the class-specific ship pitch schedule for a given speed and plant alignment.

Table 3: Possible machinery plant alignments - DDGs

Machinery Plant Alignments	Description
In Port	Shore power. No ship fuel is being consumed.
At Anchor	Generators only. Propulsion engines secured.
Trail Shaft	One propeller shaft rotating under power. Other shaft & propeller dragging/trailing (added resistance).
Split Plant	One propulsion engine operating on each shaft.
Full Plant	All 4 engines operating. Minimum service generators (at least 2) operating to satisfy electric load.
Full Plant, All-On	Condition I - all propulsion engines and generators operating regardless of power required.

2.3.5 Calculating the Fuel Penalty

PC ratios were integrated into a Navy ship-specific calculation tool (Energy Calculator) to estimate annual fuel consumption for the ships of interest. This tool was developed by the Advanced Machinery Systems Integration Branch [Naval Surface Warfare Center, Philadelphia Division (NSWCPD), Code 326], and employs a variety of ship-specific parameters and an annual ship operational profile as input data to generate an annual fuel consumption value. Similar tools can be developed for specific ship classes when the below factors are considered:

- shaft horsepower (SHP) or effective horsepower (EHP) and propulsive coefficient required to attain a particular speed
- efficiency losses through the propulsion train to attain the brake horsepower (BHP) required by the main propulsion engines to make a particular speed
- operational profile which defines the machinery plant alignment, taking into consideration how the engine power may be split among the engines as required by operations
- engine specific fuel consumption (SFC) (based on an equation which uses R_{power} and R_{speed} as independent variables) at each point of the operational profile (that is, ship speed and machinery plant alignment; the propulsion fuel burned at each point can be calculated by multiplying the SFC by the engine BHP and the time spent at that point.)
- fuel consumption by the ship service generator, accounting for:
 - average electric load applied throughout the operational profile – static and dynamic periods
 - variation in loads due to electrical distribution system losses and generator efficiency losses
 - generator engine power or BHP required to satisfy the electrical load
 - BHP split across the number of generator engines
 - number of generator engines required to satisfy the electric load
 - ship operating doctrines regarding the balance between electric load/generator
 - engine speed ratio [should be assumed to always be 1.0 (for a steady state analysis)]

Based on the maximum engine power available, the propeller speed (as RPM), and the maximum engine speed (as RPM), we estimated engine power and engine speed ratios. The power ratio, SFC, and fuel burned at each point of the operational profile were calculated as described for the propulsion engines. The propulsion fuel burned and the ship service generator fuel burned were summed at each point of the operational profile (that is, ship speed and machinery plant alignment), to obtain the total fuel burned at each point. The totals at each point were summed to obtain the overall annual fuel burned.

The PC ratios developed for each of the 11 ships from this study selected for full analysis were used to calculate the change in fuel use (propeller roughness - fouled) over baseline (propeller roughness - Rubert A). PC ratios represent the effect of propeller fouling on ship powering requirements. Specifically, the PC ratios are the unfouled power to fouled power ratio at each speed. Each PC ratio data set included ratios for full plant, split plant, and trail shaft. PC ratios were also considered in the context of ship operational profiles and ship trial information in order to predict annual fuel consumption by ships in a similar propeller condition. We used a US Navy resource for tracking ship operational schedule to characterize the duration and frequency of deployments and other active periods for the subject ships. These data were used to calculate new ship powering requirements using the powering condition derived from a series of power trials as the “unfouled DDG 51 Flight IIA baseline”. Initially, an unfouled (propeller roughness - Rubert A) DDG 51 Flight IIA annual fuel consumption calculation was performed using the Energy Calculator and the baseline powering. Then, for each set of PC ratios, new powering and propeller speed calculations were made. Each of these new data sets sequentially replaced the baseline powering and propeller speed data in the Energy Calculator and new annual fuel consumption calculations were made.

3 Results and Discussion

3.1 Propeller Fouling

During the portion of the project where inspections were being executed (March, 2012, through October, 2013), 57 inspections were performed on propellers of 40 different ships at 5 US Navy bases including those on the East Coast [Norfolk (Virginia), Mayport (Florida)] and those on the West Coast and Pacific [Pearl Harbor (Hawaii), San Diego (California), Everett (Washington)]. Propellers of 25 DDGs and 10 CGs were inspected, as were 5 amphibious warfare ships (3 LSDs, 1 LHA, and 1 LHD), which were vessels of opportunity while DDGs or CGs were also being inspected.

Complete, full deployments (deployments which were initiated and completed between January, 2012 and December, 2013, and where ships departed their home ports for at least four months and traveled to foreign ports) were recorded for DDGs and CGs, as were “incomplete deployments” for these same ships, which began before January, 2012, or ended after December, 2013. Approximately two-thirds of all DDGs and CGs participating in complete, full deployments during the period of interest were inspected. Complete and incomplete deployments associated with the several inspected L-class ships were also tracked.

Ship operational tracking data suggested that deployment operations were comprised of underway periods combined with inactive periods or “stops” (presumed to be port calls) of up to a week in duration. One week long inactive periods were typical and were determined to be low risk for biofouling (see below).

Of the 57 inspections that were performed, 36 inspections were comprehensively scored for cathodic chalk and biofouling. Nine additional inspections were subjected to a cursory examination for a total of 45 inspections that were scored for cathodic chalk and biofouling. 12 of the 45 inspections were conducted prior to vessel activity/pre-deployment. 32 inspections were conducted after an underway period/post-deployment. One inspection (USS Gettysburg, CG 64) was not associated with any type of underway period.

Not all inspections were comprehensively scored for fouling because a cursory review was often deemed sufficient. Cursory review was carried out in situations where:

- Ships were cleaned within days to a few weeks of activity, especially when previously inspected (and scored) ships had experienced a similar pattern of operations.
- Inspections were conducted prior to ship activity, with the intent of inspecting the propellers after the ship's return to port. However, in some cases the propellers were cleaned before the post-deployment inspection was, or would have been, performed.
- Ships had a mid-deployment propeller cleaning.
- There was no opportunity to conduct a post-activity inspection after having conducted a pre-activity inspection because of the lack of availability of equipment or divers, or due to schedule conflicts. The value of pre-activity inspections alone in some cases was limited. Comprehensive scoring of pre-deployment or pre-activity video was, therefore, performed only on a subset of these ships.

3.1.1 Cathodic Chalk

Propeller surface areas that appeared free of both heavy mineral deposits (white cathodic chalk) and hard biofouling took on the appearance of "bare metal". However, because mineral deposits have anecdotally been determined to develop relatively quickly (within weeks), areas that appeared to be bare metal were assumed to have accumulated some level of cathodic chalk and were therefore scored as Rubert D, rather than Rubert A. Obvious cathodic chalk was scored as Rubert F.

All but one inspection revealed at least some coverage of cathodic chalk on nearly all blade faces inspected. Propellers essentially free of both cathodic chalk and hard biofouling were only observed on one vessel, USS Peleliu (LHA 5).

3.1.2 Biofouling

We observed no hard biofouling on 19 propeller inspections. Hard biofouling or remnants of hard biofouling were observed in 26 of the 45 inspections, of which 14 revealed more than 1% of a blade surface covered by hard biofouling. Soft biofouling occurred on propellers of 8 of the 13 vessels that were inspected before commencing operations. No soft biofouling was observed on the propellers of ships that had recently been underway. A small subset of inspection results can be found in Table 4.

The Relative Roughness Unit (RRU) metric (see Equation 1) generally reflected the level and type of biofouling observed on propellers. For propellers that supported no biofouling, RRU ranged from 0 to 6, while trace levels of biofouling generated values between 12 and 53. Propellers with more obvious hard biofouling typically expressed RRU values greater than 200. RRUs of between about 250 and 500 were associated with less than 1% hard fouling, between about 2,000 and 52,000 1-5% hard fouling, and greater than 228,000 more than 5% hard fouling. For the 45 inspections for which biofouling was either comprehensively scored or estimated, RRUs ranged from 0 to approximately 750,000.

3.1.3 Change in Fouling While Underway

The propellers of several vessels were inspected both before and after deployments or shorter operational periods. These inspection pairs allowed us to determine the extent to which fouling, both biofouling and cathodic chalk, changed while ships were underway. Inspection results suggest that hydrodynamic forces or cavitation erosion were severe enough to remove some hard biofouling and cathodic chalk (Table 5; Figs. 3 and 4). In every case where soft biofouling was present prior to deployment, it was completely removed by the time the ship returned. Hard biofouling present prior to deployment became damaged and killed, but not completely removed (proportions of shell/baseplates left behind). In a subset of inspection pairs we observed a reduction in coverage of thick accumulations of cathodic chalk, which presented itself as areas of essentially bare metal. However, this effect

was limited [Table 5, Rubert F (%)]. In all cases, changes in fouling as a function of having been underway resulted in lower RRU scores. However, biofouling observed after underway periods remained sufficient to generate fuel penalties. Thus, ships that commence operations with biofouling on their propellers will experience a fuel penalty throughout those operations.

3.2 Propeller Fouling and Fuel Consumption

Propeller inspections were ranked by their resulting RRU values, and then divided into larger groups of comparable RRU scores reflecting increasing severity of biofouling. These groupings were then used to choose 11 inspections or ships for a full analysis of hydrodynamic impact and fuel use. For several RRU groups more than one ship/inspection was chosen for the full analysis, in order to capture the possible effects of perceived differences in the type or location of the biofouling observed. We estimated the baseline annual fuel use for a ship with “clean” propellers assuming a propeller roughness equivalent to Rubert A. Based on our ship-specific data and following the method described above, we were able to calculate annual underway fuel use (per ship, including hotel load) as well as annual fuel use (per ship) for propulsion. These values were used to calculate fuel penalties, due to propeller fouling, for each RRU group.

Table 4: Comparison of fouling scores for pairs of pre- and post-underway inspections. Note that CG 73 was only underway for a short period between inspections. All other inspection pairs represent vessels on full deployments.

Ship	Underway (mo)	Rubert F (%)		Hard Biofouling (%)		Soft Biofouling – not slime (%)		RRU (Eq. 1)	
		Pre	Post	Pre	Post	Pre	Post	Pre	Post
DDG 93 USS Chung-Hoon	< 5	40-70, 70-100	40-70, 70-100	1-5	1-5	0	0	36,072	15,534
CG 73 USS Port Royal	< 5	70-100	70-100	1 to >10	1-10	1-5	0	741,000	40,865
DDG 81 USS W. Churchill	> 5	70-100	0-100	0.1-1	0	50-100	0	15	0
DDG 98 USS F. Sherman	> 5	70-100	70-100	0.1-1	0.1-1	10-20	0	480	288
DDG 109 USS J. Dunham	> 5	70-100	70-100	1-2	0.1-1	20-40	0	23,040	258
CG 66 USS Hue City	< 5	70-100	70-100	0	0	0	0	0	0
CG 53 USS Mobile Bay	> 5	40-70, 70-100	40-70, 70-100	trace	0	0	0	21	6

The fuel penalty associated with propeller fouling increased with increasing RRU, Fig. 5. Fouling resulting only in Rubert roughness (cathodic chalk, RRU group 0-10) generated a fuel penalty of 0.7% of underway fuel or 1.3% of propulsion fuel. This penalty compares favorably to the predictions made by *Townsin et al. (1985)* for the effects of Rubert roughness.

Table 5. Representative examples of inspection results.

Ship and Inspection Date	Pre v. Post Active ¹	Pierside During	Rubert F (%) ²	Hard Biofouling (%)							Soft Fouling (slime, soft %)	Notes	
				0	trace	0.1-1	1-2	2-5	5-10	>10			Type ³
DDG 93 (2/13) <i>USS Chung-Hoon</i>	PRE D	Dec-Mar	40-70, 70-100			X	X	X				5-15 0%	Light slime with abundant tubeworms.
DDG 58 (6/12) <i>USS Laboon</i>	PRE D	Jun	40-70	X								50-90 0-20%	Port prop only. Trace of encrusting bryozoans among tunicates.
CG 73 (6/12) <i>USS Port Royal</i>	PRE SO	Feb-Mar, May-Jun	70-100						X	X		70-80 1-5%	Mature tubeworms (~10%) plus other hard fouling. Heavy slime and some tunicates.
DDG 93 (10/13) <i>USS Chung-Hoon</i>	PO D	----	40-70, 70-100				X	X				0%	Heavier biofouling (10-15%) at some prop roots. Average <5% overall.
DDG 60 (6/13) <i>USS P. Hamilton</i>	PO D	----	0-40, 70-100	X								0%	Port blade supported chalk and TWs, with more near base. Stbd blade supported less chalk, with TWs.
CG 65 (8/12) <i>USS Chosin</i>	PO SO	----	70-100			X	X	X				0%	Stbd and port similar, but biofouling on port blades slightly heavier.

¹Pre-deployment (PRE D), Pre-short ops (PRE SO), Post-deployment (PO D), Post-short ops (PO SO)

²Balance appeared clean and was scored as Rubert D, as described in text

³Arborescent bryozoan (ArB), Barnacles (B), Barnacle bases (Bb), Barnacles and bases (B/b), bivalves (BiV), encrusting bryozoan (EncB), Tubeworms (TW), Tubeworm bases (TWb), Tubeworms and bases (TW/b)

Fuel penalties doubled with the occurrence of even trace amounts of biofouling. For RRU between 10 and 10,000, fuel penalties were comparable at 1.3% to 1.6% of underway fuel or 2.4% to 2.9% of propulsion fuel, and were associated with less than 1% hard fouling. Biofouling producing RRU values between nominally 10,000 and 40,000 demonstrated much larger fuel penalties, and were primarily associated with up to 10% coverage by hard fouling comprised of primarily barnacles and tube-worms and their bases. The highest penalty was associated with heavier coverages of barnacles, tube-worms, and their bases. For example, we estimated that USS Porter (DDG 78), operating with propellers exhibiting an RRU of approximately 228,000, suffered a penalty of 14.3% of her propulsion fuel.

By using the RRU 0-10 group as a basis for comparison, we were able to estimate the fuel penalty costs associated strictly with biofouling, Fig. 5. The proportion of the fuel penalty due to biofouling increased with RRU. For RRU between 10-100, approximately 45% of the fuel penalty was due to the presence of biofouling. For the highest RRU group, however, biofouling generated 91% of the fuel penalty.

3.3 Extrapolating to the DDG and CG Fleet

We calculated fleet-wide fuel penalties for all propeller fouling and for hard biofouling only, Table 6, by assuming that the typical activity level of the fleet could be represented by the annual underway fuel use for the entire CG/DDG fleet, and that the proportion of ships in the fleet of a particular fouling condition matched that of the ships included in this study. We calculated annual underway fuel use as the average of fleet fuel use for fiscal years 2012-2014. By using the annual fleet underway fuel use as the metric for activity, it was not necessary to know the exact size of the CG/DDG fleet, the exact number of CG or DDG operational in any given year, or the exact nature of those operations. By contrast with the previous section, these fuel use figures represent underway fuel use (and not propulsion fuel use). Therefore we based our calculations in Table 6 on the Average % Penalty for underway fuel.

The proportion of the CG/DDG fleet falling into each RRU group was calculated from CGs and DDGs for which we had carried out inspections immediately after deployment. Because propeller fouling decreases over the course of operations, RRU at the end of a period of activity represents a conservative estimate of the propeller condition during that activity, and of its corresponding impact on fuel use. We chose to focus on deployments only, and not include data from short operations, as post-deployment inspections covered a substantial proportion of all CG and DDG deployments over the period of the project and are an unbiased sample of propeller condition of deployed ships. In contrast, inspections carried out after periods of short operations were occasionally scheduled to examine particular hypotheses regarding the effects on roughness of the length of time between propeller cleaning and commencement of activity, and thus (and given their relatively small number) do not represent an unbiased sample of propeller condition. Based on these considerations, we included 19 ships/inspections in our calculations of the fleet fuel penalty, covering the full range of RRU groups observed.

The inspection data suggest that most (58%) of the CG and DDG in the fleet operate while on deployment with propellers fouled only with cathodic chalk. An additional 21% of vessels likely operate with trace levels of biofouling on their propellers. A non-negligible proportion (5%) of the fleet, is however, probably deployed with heavily fouled propellers including abundant hard biofouling. The fleet-wide fuel penalty due to all fouling (both cathodic chalk and biofouling) is approximately 1.4% of underway fuel use (and 2.5% of propulsion fuel use). Half of this penalty (49.6%) is attributable to the effects of hard biofouling. Ships operating with heavy accumulations of biofouling on their propellers likely make up only a small proportion of the active CG/DDG fleet. Despite this, excess fuel use represents 31% of the total fuel penalty associated with propeller roughness of the entire CG/DDG fleet. Our estimate of the volume of the fuel penalty currently incurred by CG and DDG is comparable to the annual underway fuel use (propulsion fuel and hotel load) for a single CG or DDG. If the Navy could maintain all CG and DDG propellers free of cathodic chalk and biofouling, sufficient fuel would be saved to operate a single CG or DDG for one year.

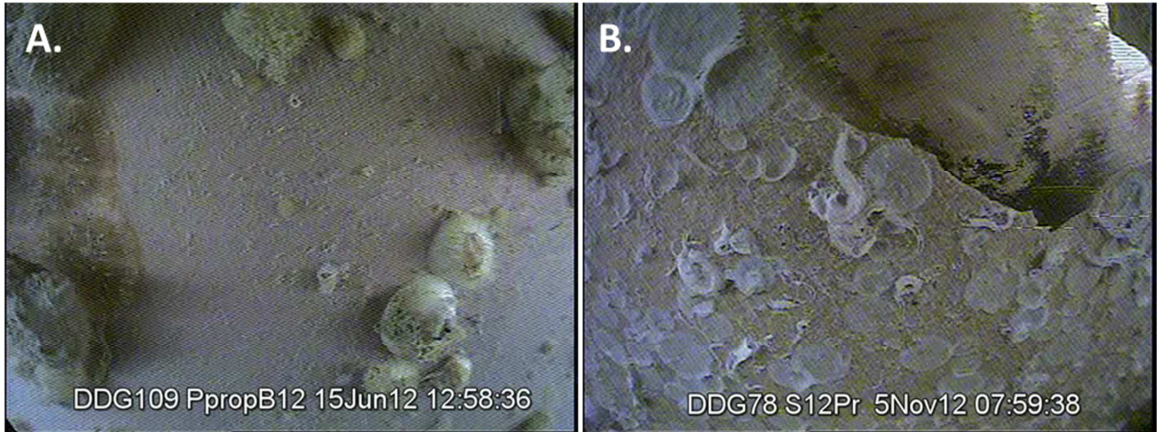


Fig: 3. A. Hard biofouling (barnacles) and soft biofouling (tunicates) on a propeller inspected before deployment. B. Barnacle bases (round, white, raised material), semi-intact tubeworm shells, and loss of cathodic chalk observed on a propeller inspected after deployment. These images were from different vessels.

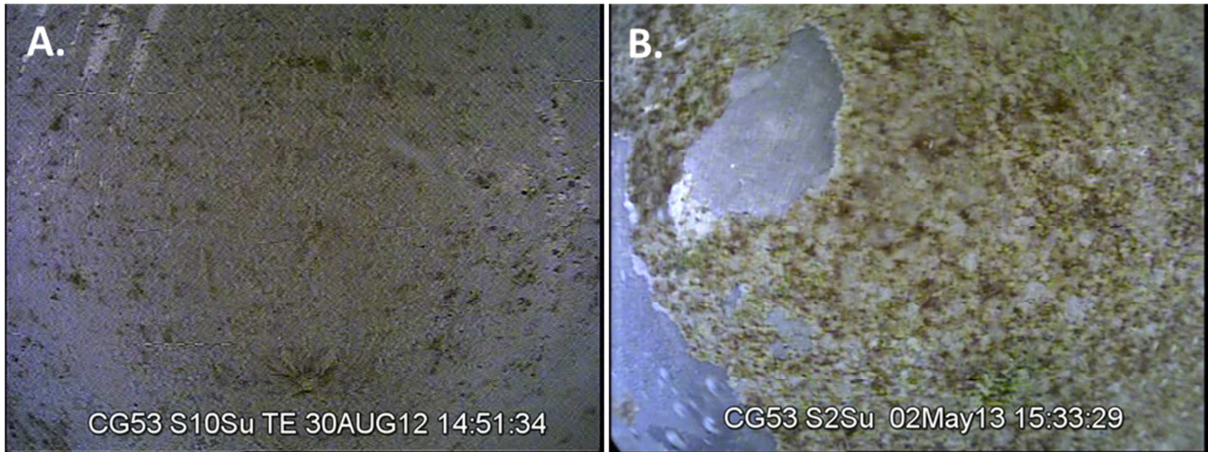


Fig: 4. Condition of the suction (forward) face of the starboard prop on USS Mobile Bay (CG 53), before (A.) and after (B.) deployment. Note loss of small patches of cathodic chalk, visible as exposed metal in (B.) during deployment.

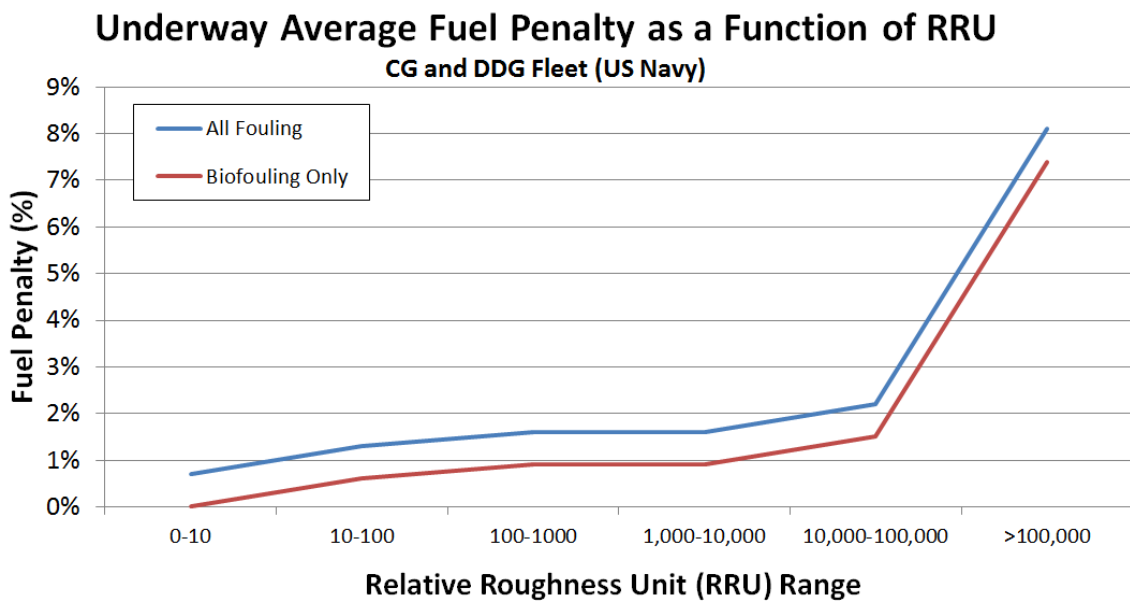


Fig. 5: Underway average fuel penalty as a function of RRU

Table 6. Estimated annual propeller fouling penalty for the CG and DDG fleet. Assumptions for these calculations are described in the text. Fuel penalties (as a percentage) for each RRU class are given for underway fuel use (as opposed to propulsion fuel use), in order to enable calculation of penalty volume and cost/value from i-ENCON underway fuel use records.

RRU Group	# Ships in Study in Class	% Ships in Study in Class	Average % Fuel Penalty		Average % Fuel Penalty		Proportional Penalty		Fleetwide Fuel Penalty		Annual Fuel Penalty @	
			Underway, All Fouling	Underway, Biofouling	Underway, All Fouling	Underway, Biofouling	Proportional Penalty ¹	Proportional Penalty ²	Proportional Penalty ³	Fleetwide Fuel Penalty (bbl/yr) ⁴	Fleetwide Fuel Penalty (bbl/yr) ⁵	Annual Fuel Penalty @ \$150/bbl ⁶
0-10	11	58%	0.70%	0%	0.0041	0.0041	0	22,622	0	0	\$3,393,298	0
10-100	4	21%	1.30%	0.60%	0.0027	0.00126	0.00126	15,277	7,051	7,051	\$2,291,578	\$1,057,651
100-1000	2	11%	1.60%	0.90%	0.0017	0.00095	0.00095	9,401	5,288	5,288	\$1,410,202	\$793,238
1,000-10,000 ⁸	0	0%	1.60%	0.90%	0	0	0	0	0	0	0	0
10,000-100,000	1	5%	2.20%	1.50%	0.0012	0.00079	0.00079	6,463	4,407	4,407	\$969,514	\$661,032
>100,000	1	5%	8.10%	7.40%	0.0043	0.0039	0.0039	23,797	21,741	21,741	\$3,569,573	\$3,261,092
Totals					0.0139*	0.0069*	0.0069*	77,561	38,487	38,487	\$11,634,165	\$5,773,013

¹ % fuel penalty due only to hard biofouling, equal to % fuel penalty for all fouling minus the % fuel penalty for the 0-10 RRU group, which is due strictly to cathodic chalk

² % of ships in study in class multiplied by % fuel penalty (all fouling), expressed as a proportion (rounded). This represents the proportion of underway fuel (fleetwide) used to counteract the effects of all fouling, for the particular RRU group

³ % of ships in study in class multiplied by % fuel penalty (hard biofouling only), expressed as a proportion (rounded). This represents the proportion of underway fuel (fleetwide) used to counteract the effects of biofouling, for the particular RRU group

⁴ Proportional fuel penalty (all fouling) multiplied by 5,582,049 bbl, the average annual underway fuel use for the entire CG/DDG fleet for FY12 – FY14 (rounded)

⁵ Proportional fuel penalty (hard biofouling only) multiplied by 5,582,049 bbl, the average annual underway fuel use for the entire CG/DDG fleet for FY12 – FY14 (rounded)

⁶ Value of the fleetwide annual fuel penalty due to all fouling (rounded)

⁷ Value of the fleetwide annual fuel penalty due to hard biofouling only (rounded)

⁸ No study vessels in this RRU group met the requirements for inclusion in the calculation of the fleet-wide CG/DDG fuel penalty (see text)

* Values represent the *proportional* fleetwide underway fuel penalty due to all fouling or hard biofouling alone

3.4.2 Cost-Effectiveness of Propeller Cleaning

Our data suggested a propeller cleaning can improve vessel fuel efficiency during subsequent operations, if it is carried out within approximately 21 to 28 days of commencement of those operations. The cost-effectiveness of propeller cleanings can be related to RRU group (that is, extent of biofouling) and accounts for the associated fuel penalty, the cost of cleaning, and vessel operational profile. Our analysis of rate of accumulation of biofouling and cost-effectiveness of cleaning suggested cases where propeller cleaning would be unlikely to generate a net benefit due to fuel savings:

- propellers fouled only with cathodic chalk
- ships that have been pierside for an insufficient number of days to accumulate significant biofouling and only short underway periods planned after cleaning
- mid-deployment cleanings when a propeller cleaning was conducted close to departure date
- ships that will be pierside for lengthy periods after cleaning but before operations (of any length)

4. Conclusions

We carried out 57 inspections of the propellers of 40 US Navy vessels in order to quantify the baseline roughness (or fouling) condition of propellers across the fleet. Inspections included 25 DDG-class vessels, 10 CG-class vessels, and 5 L-ships of various types. Inspections focused on CG- and DDG-class vessels due to their high numbers and fuel use relative to the rest of the fleet. Inspections covered 57% to 65% of the deployment activity of these classes over the duration of the project. Inspection data were incorporated into an improved model of propeller performance that accounted for variation in roughness across the blade face. We then used propeller performance data to calculate fuel penalties based on actual ship operational profiles, including speed-time profile and machinery plant alignment, in order to give the most accurate assessment of propeller roughness on fuel penalty possible from data taken from in-water inspections alone.

- Most propellers (60% of inspections) were fouled with only cathodic chalk or chalk and trace levels of encrusting organisms. However, 20% of inspections revealed the presence of hard biofouling organisms at coverages of greater than 5%.
- We estimate the annual fuel penalty incurred by CG- and DDG-class vessels, due to propeller fouling (including both cathodic chalk and biofouling), as 1.4% of underway fuel use, or 2.5% of propulsion fuel use.
- Half of this fuel penalty is attributable to the effects of biofouling. Although propellers supporting relatively heavy encrustations (> 5% cover) of biofouling are likely to be uncommon in the fleet, we estimate they account for approximately 40% of the total fuel penalty, and 68% of the fuel penalty due to biofouling alone.
- Inspections of propellers carried out before and after underway periods indicated that ship operations reduced the severity of fouling by both cathodic chalk (minimal) and hard biofouling (primarily height) organisms. However, neither type of fouling is likely to be completely removed from propeller surfaces simply by operating the ship – heavily fouled propellers retained substantial levels of fouling even after more than five months of being underway.

Our inspection data also enabled us to examine the time course of accumulation of biofouling to propeller blades and the timing of propeller cleanings, and thereby develop an understanding of the cost-effectiveness of the Navy's current propeller maintenance strategy.

- Propeller cleaning is generally a cost-effective means of improving ship fuel economy, particularly when coverage of hard biofouling is greater than 1%. For propellers in this condition, cleaning is beneficial for vessels with missions as short as 20 days in length.
- Significant hard biofouling roughness begins to develop on propeller blades after about 30 days of pierside time. In contrast, cathodic chalk appears to form relatively quickly and consistently, although we do not understand the exact time course of formation of this type of fouling.

- Analysis of the length of pierside time between propeller cleaning and operations suggests that, for the CG and DDG fleet, 33% to 50% of cleanings are executed in such a way that time (approximately 28 days) is available for hard biofouling to begin to develop on blade surfaces. Affected vessels will incur a fuel penalty that could be recovered (or avoided) through improved timing of the cleaning effort.
- Roughness associated with cathodic chalk accounts for about 50% of the fuel penalty associated with propeller fouling. Cathodic chalk can be removed by in-water propeller cleanings, but the effect is likely short-lived as the mineral deposits re-form relatively quickly. Cleanings alone will not be a cost-effective means by which to mitigate this form of this type of roughness.
- Based on the rates of biofouling accumulation we observed, previous research on the formation of cathodic chalk, and the analysis of cost-effectiveness of propeller cleaning, we can identify cleaning scenarios that are unlikely to either generate a net benefit or fuel savings. These include cleaning of any propeller fouled only with cathodic chalk, propeller cleanings carried out after less than 21 to 28 days pierside with only short underway periods (< 30 to 45 days in length) planned after cleaning, mid-deployment cleanings when a propeller cleaning was conducted < 21 to 28 days before departure (exception – extended pierside interval while deployed), and cleanings accomplished on ships that are planned to remain pierside for more than 30 to 45 days after cleaning.

5. Recommendations

- A decision matrix would aid the maintenance community in determining if a propeller cleaning is justified to realize fuel savings. Factors to consider should tie the projected date of the cleaning to the date of commencement of the next underway period, duration of the next underway period, cost of cleaning, and the date of the next opportunity to clean.
- A propeller cleaning < 21 to 28 days prior to departure should be the goal for all deploying (Navy) vessels. The actual target time frame could be adjustable taking into account the location of the home port and seasonality of the time pierside, to the extent that local biofouling conditions are well known.
- More attention should be paid to propeller condition in advance of short operations, particularly when a ship has been pierside for more than one to two months. When propellers are very heavily fouled (RRU > 100,000), cleaning before departure on even very short operations is cost-effective.
- Propeller cleanings not associated with fuel savings (see above) should be tracked in order to determine their relevance and justify their cost. If not associated with maintenance needs, these cleanings should be eliminated.
- The rate at which cathodic chalk develops, under relevant environmental conditions, should be examined in order to determine the extent to which excess fuel costs associated this form of fouling can be recouped by cleaning.
- For some classes of ships, propeller coatings have been shown to be effective in controlling the accumulation of both cathodic chalk and biofouling, *Haslbeck et al. (2014)*. In order to transition these coatings to the entire US Navy fleet, they will have to be improved.
- Sufficiently durable, cleanable, cavitation-resistant coatings that are not designed to control biofouling may mitigate the development of cathodic chalk which accounts for approximately half of the fleet's fuel penalty due to propeller roughness. When a combination of coatings that are effective at reliably controlling cathodic chalk, and cleanings that are effective at controlling hard biofouling, are demonstrated and transitioned, the propulsive fuel savings associated with smooth propellers would double over that arising from control of biofouling alone.

References

ABIA, S.; TSUCHIDA, H.; OTA, T. (1981), *Heat transfer around a tube in a bank*, Bull. JSME 24, pp.380-387

- CARLTON, J. (1994), *Marine Propellers and Propulsion*, Butterworth-Heinemann, Oxford
- GAUDET, L.; WINTER, K.G. (1973), *Measurements of the drag of some characteristic aircraft excrescences immersed in turbulent boundary layers*, Royal Aircraft Establishment, Technical Memorandum Aero 1538
- GOWING, S. (2012), *Flow-generated forces on hull fouling organisms and hydrodynamic self-cleaning of fouling-release coatings*, 16th Int. Congress on Marine Corrosion and Fouling, Seattle
- GREELEY, D.S.; KERWIN, J.E. (1982), Numerical methods for propeller design and analysis in steady flow, Soc. Nav. Arch. Mar. Eng. Trans. 90, pp.415-453
- HASLBECK, E.G. (2016), *Unpublished data for baseline fouling condition of CG and DDG vessels*, See also, in part, *Schultz et al. (2011)*.
- HASLBECK, E.G.; STEINBERG, M.; HOLM, E.; LYNN, D.; CURRAN, J.; LUTKENHOUSE, C.; MICHAEL, T.; TSENG, C. (2014), *Performance of fouling-release coatings on US Navy Ship Propellers*, 16th Int. Congress on Marine Corrosion and Fouling, Seattle
- HOERNER, S.F. (1965), *Fluid Dynamic Drag*, Bakersfield
- HUNDLEY, L.L.; TSAI, S.J. (1992), *The use of propulsion shaft torque and speed measurements to improve the life cycle performance of U.S. Naval Ships*, Naval Engineers J. 104(6), pp.43-57
- IGARASHI, T. (1986), *Characteristics of the flow around four circular cylinders*, Bull. JSME 29, pp.751-757
- KAN, S.; SHIBA, H.; TSCHUCHIDA, K.; YOKOO, K. (1958), *Effect of fouling of a ship's hull and propeller upon propulsive performance*, Int. Shipbuilding Progress 5, pp.15-34
- NAVAL SHIPS' TECHNICAL MANUAL (2006), *Chapter 081 – Waterborne Underwater Hull Cleaning of Navy Ships*, Publication #S9086-CQ-STM-010/CH-081, Revision 5
- OFFICE OF THE CHIEF OF NAVAL OPERATIONS (2010), *A navy energy vision for the 21st century*, Naval Sea Systems Command, Washington DC
- SCHULTZ, M.P. (2007), *Effects of coating roughness and biofouling on ship resistance and powering*, Biofouling 23, pp.331-341
- SCHULTZ, M.P.; BENDICK, J.A.; HOLM, E.R.; HERTEL, W.M. (2011), *Economic impact of biofouling on a naval surface ship*, Biofouling 27, pp.87-98
- SVENSEN, T.; MEDHURST, J. (1984), *A simplified method for the assessment of propeller roughness*, Mar. Technol. 21, pp.41-48
- TOWNSIN, R.L. (2003), *The ship hull fouling penalty*, Biofouling 19 (Supplement), pp.9-15
- TOWNSIN, R.L.; SPENCER, D.S.; MOSAAD, M.; PATIENCE, G. (1985), *Rough propeller penalties*, Soc. Nav. Arch. Mar. Eng. Trans. 93, pp.165-187
- WOODS HOLE OCEANOGRAPHIC INSTITUTION (1952), *Marine fouling and its prevention*, United States Naval Institute, Annapolis

NAT 5000 - Nakashima Advanced Virtual Tank 5000

Kenichi Fukuda, Yoshihisa Okada, Kenta Katayama, Akinori Okazaki, Masatoshi Nakazaki
Nakashima Propeller, Okayama/Japan, k-fukuda@nakashima.co.jp

Abstract

The conventional approach to evaluate propulsion performances has been based on model tests with extrapolation to full scale. However, there are some drawbacks for model tests to evaluate ship performances in actual sea. For instance, results from model tests cannot be reproduced easily due to unknown factors. In addition, the effect of minor modifications of propulsion systems or additional appendages such as ECO-Cap or Ultimate Rudder cannot be evaluated with model tests due to scale sizes. Recently, CFD has evolved as a serious alternative. In this paper, the model test for propulsion systems and CFD simulations are compared in terms of accuracy. The test case is the bulk carrier of 208000DWT. Adjusting the Reynolds number to the full scale ship yielded more accurate estimates for propeller performance than based on model test. This is particularly important for propulsion improving devices

1. Introduction

Nowadays, the situations of maritime industries strongly require eco-ship because of environmental and economical issues. The expected tighter regulations and predicted increasing fuel price make maritime industries put on higher pressure regarding productions of further fuel efficiency ships with low costs. Shipyards are considering an optimization of ship from design and cost points of views in order to produce better eco-ship. In the past decade, one of the most useful tools for design optimization is thought to be CFD (computer fluid dynamics) simulations due to a high-speed computer available with relatively low cost. Consequently, CFD can provide the way as a cost and time effective method for optimizing the ship design in the early phase of addressing scale effects, compared with a conventional model test. Currently, full-scale effects for ship resistance, propeller performance and propeller-hull interaction can be extrapolated from the model test results. The method of the model test has long time history and various kinds of data collection available, resulting in accurate full-scale performance prediction. However, the model test has time and cost consuming from preparation to obtaining final results. This situation leads that new types of propulsion or appendages for ESD (energy saving device) cannot easily be developed with model tests due to limited model test facilities. In addition, the limited Reynolds number in model tests makes precise estimation for total hull performance obscure.

As for general CFD approach, body force propeller model is used to evaluate hull resistance and propulsive efficiency. However, when more precise estimation is required especially for total hull performance, geometry information should be used. This is because this information can be useful to solve the interaction effects of hull, propeller and appendage. Therefore, new advanced CFD approach, which is taken account of geometry information, should be considered and applied to total performance estimates or small ESD performance estimates in terms of accuracy. This leads that the future of CFD simulation should be established as self-completion method and then be achieved to full-scale performance estimates with accuracy.

In the previous research, Kawamura *et al.* (2013) has already employed CFD simulation to evaluate the effect of ESD called as PBCF (propeller boss cap fins). As for propulsion systems, in earlier studies, propeller performance has been discussed and evaluated by conducting rotated propellers with CFD simulation, Shen *et al.* (1997), Funeo (2002). Funeo (2002) addressed that the simultaneously CFD approach for hull, rudder and propeller in a ship could be obtained better view of performance estimations. A comprehensive CFD simulation, which total stern design for hull, rudder and propulsion is considered, is believed to apply an optimization for ship design in near future.

Nakashima propeller is establishing to employ an advanced CFD simulation as optimization hydrodynamic propulsion system design. Not only propeller performances and cavitation conditions but also ESD performances can be evaluated using the advanced CFD simulation. *Himei and Yamaguchi (2015)* attempted the propulsion performance estimates for surface piercing propeller with the CFD simulation. *Hasuike et al. (2015)* compared the pressure fluctuation calculated for 20 propellers with experimental results and revealed that the CFD simulation attained adequate level for a practical use. *Okazaki et al. (2015)* estimated the effect of ECO-Cap using CFD and explained that pressure distribution behind the cap was a key of efficiency for it. In this paper, the results from Nakashima propeller advanced CFD simulation are introduced. The bulk carrier of 208000DWT is used as the case study. The ship resistance and self-propulsion factors are estimated by Nakashima advanced CFD simulation and compared with the model test. Efficiency of Ultimate Rudder evaluated by the advanced CFD simulations is presented to explore the application of this method to business adaptability.

2. Strong points for CFD simulation

Currently procedure for design of propulsion is showed schematically in Fig. 1. In the final stage, the extrapolation to full-scale performance has been required in the model test due to constrained model size related to Reynolds number. As previously mentioned, the results from model tests have been accumulated in a very long time and full-scale performance can be predicted with accuracy. However, as for this model test method, it takes a long time to obtain the final outcome of propulsion performance, while CFD simulation can produce the result with relatively short period. For instance, model test always requires manufacturing a model ship and propeller. In addition, propulsion performance estimates with an unusual hull dimension cannot be easily obtained with confidence because this method is based on an empirical approach. CFD simulation basically can be calculated directly to full-scale with adjusting Reynolds number. To achieve this, CFD simulation based on model should be compared with sea trial and then Reynolds number is adjusted. Consequently, the effect of Reynolds number can be minimalized.

In recent years, developments of new energy saving devices are required and the evaluations of the efficiency of propulsion systems in total (hull, propeller and ESD etc.) are very important. These evaluations are urgently required for a ship design. CFD simulation can be compensated the results from the model test and evaluated the efficiency together with the model test. Fig. 2 indicates the concept of self-completion for CFD simulation. Once CFD simulation is established the relation with the model test or checked the validity using with various kinds of actual ship results, CFD simulation can deliver quick performance results with accuracy. Furthermore, in the near future, an estimation of ship performance at sea will become more important than ever. In this situation, the results from model test cannot be produced easily due to wave effects (weather effects), while theoretically CFD simulation can be calculated with these effects.

Strong points of CFD simulation compared with model tests are:

- Analytical and human error can be eliminated easily
- Reproducing (robust) results can be obtained easily
- Water flow information around hull and propulsion can be obtained with visualization
- Lead-time can be shorten due to the time of CFD simulation
- CFD simulation can be low cost
- Scale effect do not need to be considered
- Wall effect do not need to be considered
- Parameter survey for developing products can be carried out in short period
- CFD simulation can be carried out from first stage to final stage at one facility

The above can be very useful for developing high-efficiency propulsion with low cost and short lead-time. Therefore, outcome from CFD simulation need to be verified with available data such as the model test and after obtaining confidence with CFD simulation, it can be used as an alternative way of

model test. In addition, it is very important for CFD simulation to understand the obtained values of meaning. This means CFD simulation is not result of calculation but result of design. Consequently, to achieve the scenario in Fig.2, CFD simulation should be carried out the place where the knowledge of hull, propulsion and appendage, and geometry information for them are accumulated. Such place can be produced with reliable and accuracy. Nakashima propeller is accumulating geometry data for many kinds of propeller and can design not only propeller but also ESD.

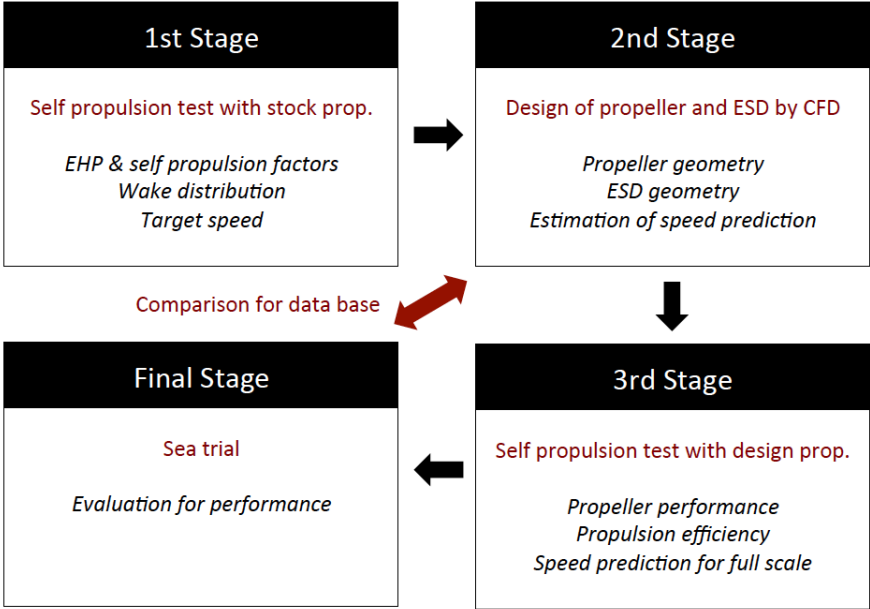


Fig.1: General procedure for design of propulsion system

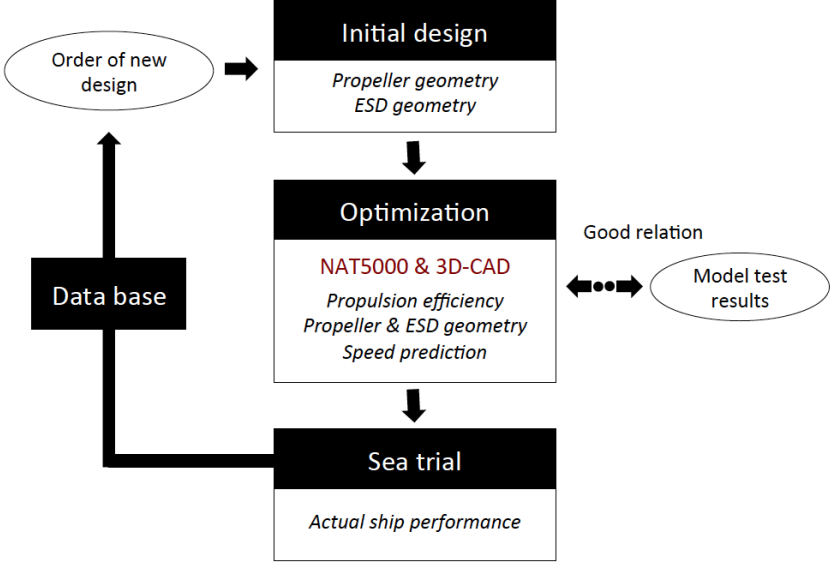


Fig. 2: Optimization propulsion design for NAT5000

3. About NAT5000 – Nakashima Advanced Virtual Tank 5000

In this study, the CFD approach was carried out with SOFTWARE CRADLE SCRYU/Tetra Ver.10, a commercial CFD code based on a finite volume method with unstructured grid. The Shear Stress Transport k- ω model was applied to the turbulence model of CFD simulation. Non-uniform wake flow was simulated around a propeller. A rotating propeller simulation in the wake was used with the sliding mesh methodology.

A full hull body submerged under the design load water line was modeled. The rotation was introduced to simulate the propeller rotation condition. Fig. 3 shows the present computational domain and the surface mesh around the hull with a propeller and rudder. Fig. 4 shows that the computational domain for propeller analysis is composed of inner rotational part including the propeller and the outer stationary parts. Constant velocity and zero pressure were prescribed at the inlet and the outlet boundary, respectively. The numerical mesh was an unstructured grid, and basic cells were tetrahedral and prismatic cell were applied to near the surface for resolving the boundary layer. The first layer thickness of the prism layer was set to a non-dimensional wall distance for a wall-bounded flow $y^+=1$. The total number of meshes was about 45 million.

A symmetry condition (double-body model) at a still water surface was implemented in this study. The wave resistance coefficient cannot be calculated in this study and the values were obtained from the resistance test. CFD simulations of the resistance, self-propulsion and propeller open water tests were performed to analyse the self-propulsive performance at the thrust identity condition as used in the self-propulsion test. At the self-propulsion point, the total resistance of the ship including an additional towing force (e.g. Skin friction correction) was balanced by the delivered thrust from the propeller. The required propeller thrust was obtained by interpolating the three different rotating results for the propeller.

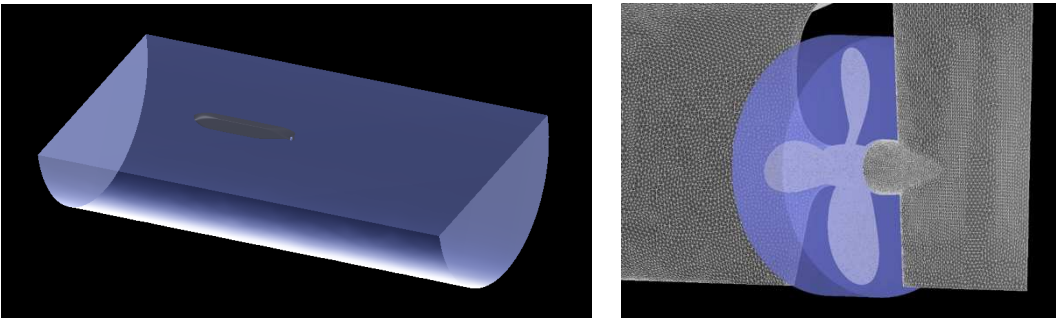


Fig.3: Analysis model of CFD simulation for hull, propeller and rudder

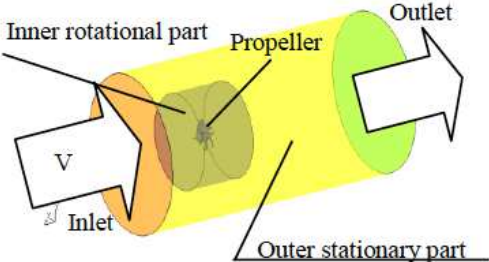


Fig.4: Analysis model of CFD simulation for propeller

4. Case study for NAT5000

4.1 Hull, propeller and Ultimate Rudder

208000DWT bulk carrier was used for Nakashima advanced CFD simulation as a case study. The effect of Ultimate Rudder was compared with normal rudder and evaluated with CFD simulation. Four-blade propeller was installed in this bulk carrier. The image of the hull and propeller are shown in Figs. 5 and 6. The information of the hull dimension and propeller particular are summarized in Table 1. Fig. 7 shows the rudder profiles for CFD simulation.



Fig. 5: Hull profile of 208000DWT bulk carrier

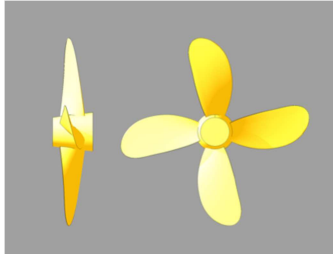


Fig. 6: Propeller Profile

Table 1: Hull dimension and propeller particulars

Hull dimension		Propeller particulars	
	Actual / Model	Number of blades	4
Lpp (m)	295 / 6.54	Dia. (m) Actual/Model	8.8 / 0.195
B (m)	50 / 1.1085	Pitch ratio	0.75
d (m)	16.1 / 0.3569	Boss ratio	0.18
Cb (-)	0.839	Exp. area ratio	0.4

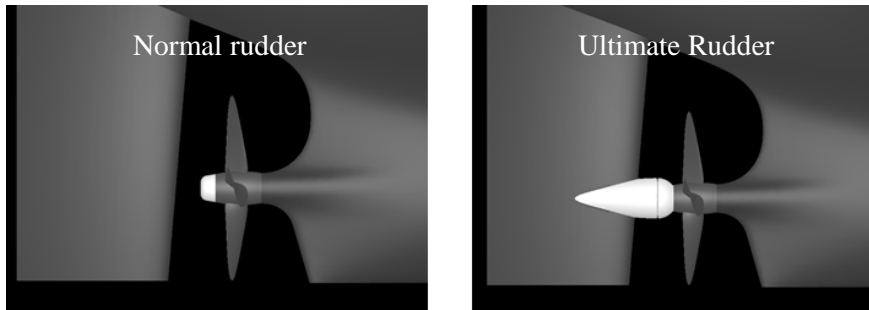


Fig. 7: Rudder profile

4.2 Calculation results for NAT5000

Fig. 8 shows the comparison of the model test and CFD simulation in axial and tangential wake distribution at the towed condition. The pattern of wake in both model test and CFD simulation were almost similar. This leads us to evaluate the propeller cavitation pattern with accuracy and then design high efficiency propeller with reducing a blade area of propeller. In addition, these conditions of CFD simulation can be achieved enough level to analyse for the development of the rudder bulb because this CFD simulation can capture a slow velocity area such as around boss.

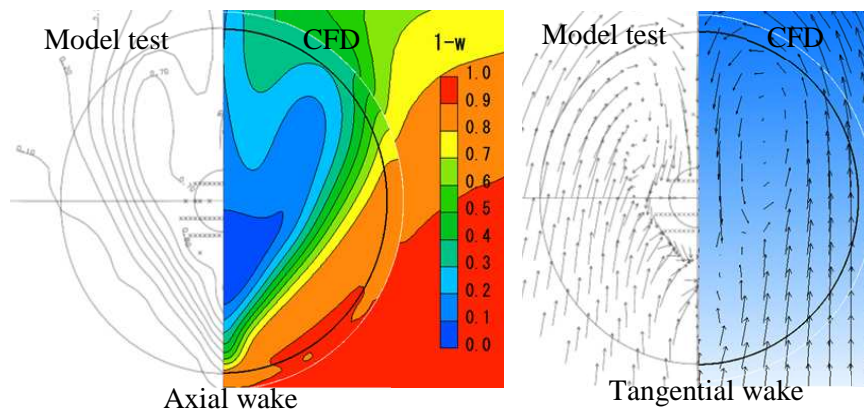


Fig. 8: Comparison of Wake Distribution between Model test and CFD simulation

Fig. 9 shows the propeller open characteristics from this CFD simulation. The results were compared with model test (Fig. 9). The propeller open water efficiency (η_o) from this CFD simulation and

model test agreed well accordingly to the values of advance coefficient (J) although the calculated values for thrust coefficient (K_T) and torque coefficient (K_Q) from this CFD simulation were slightly lower than these from model test. These results indicated the value obtained from CFD simulation could be used as estimation of self-propulsion factors.

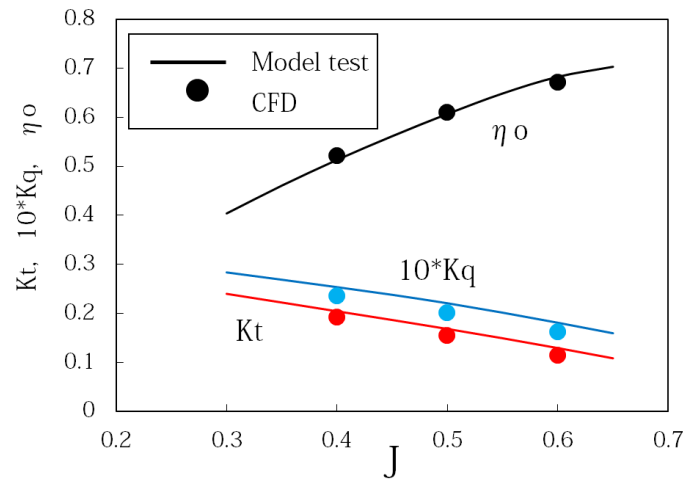


Fig. 9: Comparison of propeller open-water characteristics

Self-propulsion factors from this CFD simulation were carried out to compare with the model test and evaluate the effect of Ultimate Rudder. $1-t$, $1-w$, η_r and η_h were calculated for normal rudder and Ultimate Rudder. To analyze this CFD data obtained from normal and Ultimate Rudder, self-propulsion factors (η_r and η_h) for Ultimate Rudder from CFD simulation and model test results were divided by those from the normal rudder at the both results. Fig. 10 shows the comparison of η_r and $\eta_r \times \eta_h$ from CFD simulation and the model test. These results unveiled the efficiency for Ultimate Rudder, although the amount of increase was slightly different. The same trends of this CFD simulation and the model test can lead us to use the evaluation of propulsion systems with confidence. Fig. 11 shows the comparison of power curve for CFD simulation and the model test. Self-completion CFD results were compatible with the results from the model test. Both results showed the effect of Ultimate Rudder compared with normal rudder. The degree of improvement for both results showed similar. Therefore, this CFD approach can be used as a tool for evaluation of efficiency of propulsion systems.

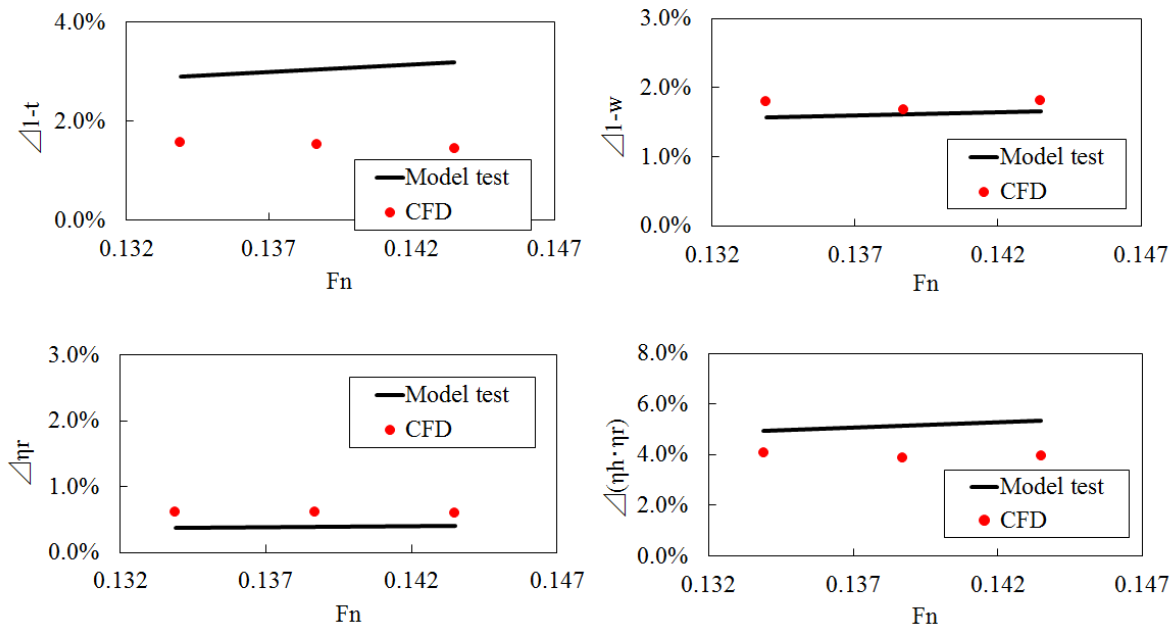


Fig. 10: Comparison of self-propulsion factor

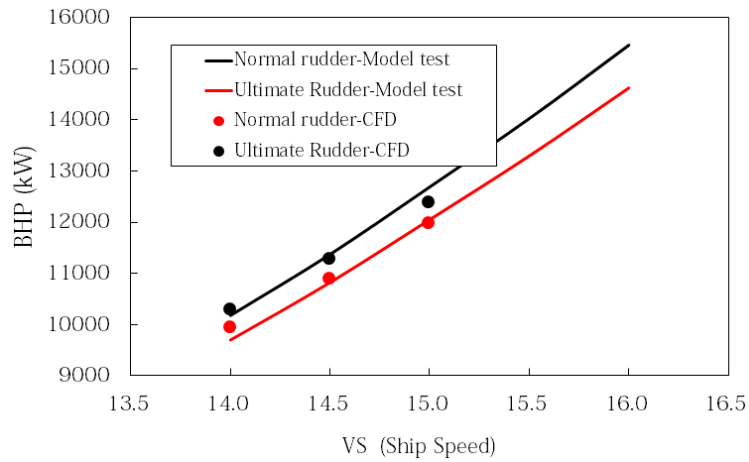


Fig.11: Comparison of power curve for NAT5000 and model test

Fig. 12 shows vortex behaviour behind the normal and Ultimate Rudder and turbulent energy obtained by this CFD simulation. Vortex behaviour was represented by Q-function, which meant the second invariants of the velocity gradient tensor. This simulation could be easily seen the volume of vortex and the location of energy loss. In addition, this visualization corresponded reasonably well with the result of self-factors results. Therefore, design developer can modify easily shapes in a computer and evaluate the phenomena for optimization using this analysis.

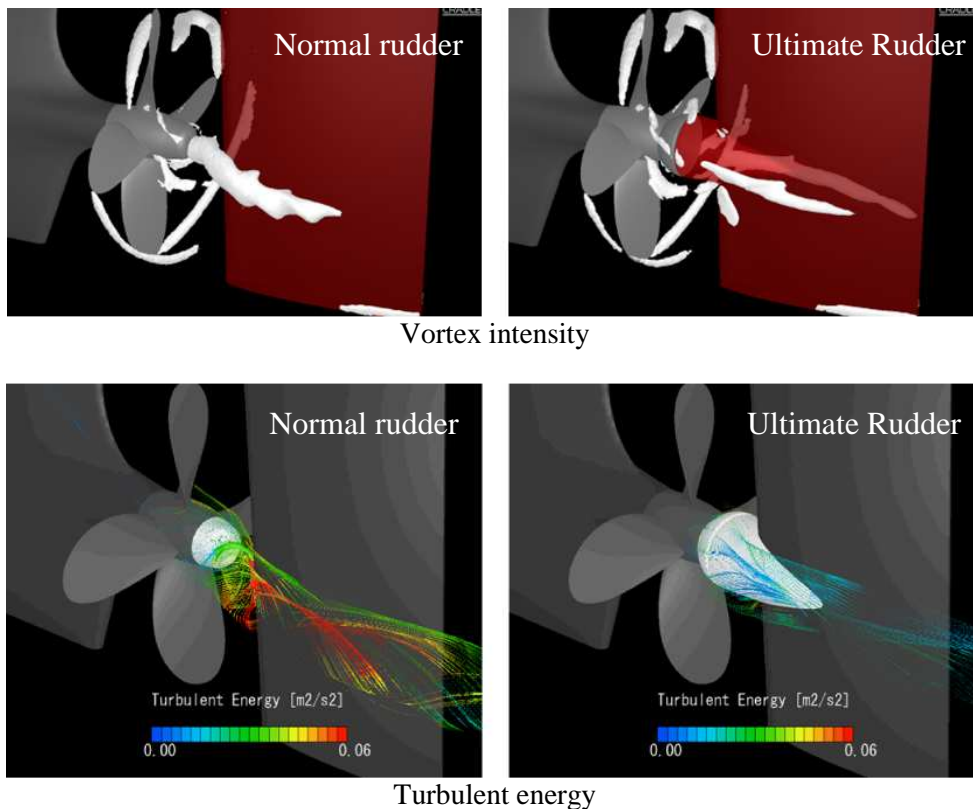


Fig.12 Comparison of the vortex intensity and turbulent energy

5. Conclusions

As shown above, authors developed the CFD simulation and compared the CFD results with model test. It was found that this CFD simulation could produce resistance, self-propulsion factors and wake distribution, and the results obtained are compatible with model test. This means that this CFD simulation is ready to apply for an evaluation of propulsion efficiency. In addition, visualization of

phenomena can help us to find the place where should be modified. By using this CFD simulation, an optimizing design point can be found in short time compared with model test. The optimizing design point means not only from one device but also from total propulsion system. This is very important for ship owner to comply with various maritime regulations. In addition, the optimizing design for propulsion development is required the result with short analytical time for the cost. Therefore, for the first stage establishment of the relation between CFD simulation and model test is required with a number of experiences. Combining CFD data with model test can be evaluated the efficiency of propulsion in total effectively in terms of time and cost.

Key finding in this paper were:

- The tendency of improvement of self-propulsion factors for Ultimate Rudder was estimated by Nakashima advanced CFD simulation.
- The effects of Ultimate Rudder were confirmed by Nakashima advanced CFD simulation as visualized flows.
- Decrease of the turbulent energy for Ultimate Rudder was confirmed by Nakashima advanced CFD simulation.
- The improvement of self-propulsion factors for Ultimate Rudder was confirmed by Nakashima advanced CFD simulation and model test.

References

FUNENO, I. (2002), *Analysis of unsteady viscous flows around a highly skewed propeller*, The Kansai Society of Naval Architects, Japan, pp.39-45

HIMEI, K.; YAMAGUCHI H. (2015), *Numerical study on performance of surface piercing propeller using RANS approach*, 13th Int. Conf. on Fast Sea Transportation, Washington

HASUIKE, N.; KAJIHAMA, T.; FUKUDA, K. (2015), *Numerical simulation of pressure fluctuation induced by cavitating propellers in wake flow*, 18th Numerical Towing Tank Symposium, Cortona

KAWAMURA, T.; OUCHI, K.; TAKEUCHI, S. (2013), *Model and full scale CFD analysis of propeller boss cap fins (PBCF)*, 3rd Symp. on Marine Propulsors (SMP), Launceston, pp.486-493

OKAZAKI, M.; KAJIHAMA, T.; KATAYAMA, K.; OKADA, Y. (2015), *Scale effect analysis of ECO-Cap by CFD*, 18th Numerical Towing Tank Symposium, Cortona

SHEN, C. et al. (1997), *Unsteady multigrid method for simulating 3-D incompressible Navier-Stokes flows on dynamic relative motion grids*, AIAA 97-0446

Observational Study on Powers Estimated by Shaft Torque and Fuel Consumption

Yakabe Fumi, Japan Ship Technology Research Association, Tokyo/Japan, yakabe@jstra.jp

Abstract

This paper provides the complete version of the observational study of the onboard power estimation, which is done on the basis of operation monitoring records provided by shipowners in Japan. The first version was presented in November 2014 at ISO/TC8/SC2/WG7 Busan meeting to compare brake power to shaft power during voyages. Samples from various ship types are added in this version. It will give a clearer observational view on the power estimation techniques.

1. Introduction

Among issues related to ship performance, power estimation is one of intricate problems. Output from the main engine is an essential parameter in the monitoring and control of ship performance, and to complicate matters further, power as the engine output during the voyage is not directly measurable but conceptually calculable. Ship performance has been apparently a major concern for ship owners, operators, naval architects and suppliers, and accordingly there are technologies and techniques developed by the industry to estimate output of the engine during voyages against its complexity.

Recently, ship performance becomes more a matter of public concerns, since monitoring and control of ship performance would also enable carbon dioxide emission control effectively. Accordingly there are more increasing recognition of the complexity of the ship performance and demand for universal or harmonized standard methods and procedures which would give clear and impartial explanation about ship performance. Power estimation technologies and techniques which are embedded in the evaluation of ship performance also come into focus.

ISO/DIS 19030 family “Ships and marine technology — Measurement of changes in hull and propeller performance —” which is developed by ISO/TC8/SC2/WG7 infuses two types of power estimation technologies and techniques, namely, shaft power method and brake power method, into its scheme for measuring changes in hull and propeller performance.

Shaft power is calculated from the main shaft torque and revolution during the voyage. There are some techniques used for the torque meter and revolution counter. Shear modulus of the main shaft and measurement of shaft strain are components required for the calculation of the shaft torque. ITTC defines shaft power as “net power supplied by the propulsion machinery to the propulsion shafting before passing through all speed-reducing and other transmission devices and after power for all attached auxiliaries has been taken off”.

Brake power of the marine engine is calculated at the test bench in the manufacturer with the hydraulic dynamometer, before the engine is delivered to the ship. Brake power is defined by ITTC as “power delivered by the out-put coupling of the propulsion machinery before passing through any speed reducing and transmission devices and with all continuously operating engine auxiliaries in use.” Brake power is normally considered as a reliable source for the engine output, as measurement precision of brake power is high due to simple mechanism of hydraulic dynamometers. Brake power is dedicatedly measured at the test bench, but the engine in unchanged condition requires the equal amount of fuel in order to produce the power wherever as it did at the bench test. This is the idea behind for estimating the power by fuel consumption on board. In order to obtain the accurate brake power on board, it is important to ensure that the engine has been in good condition and precise technique is used to calculate the brake power. The details of the technique to estimate the brake power during the voyage is provided by Part 2 of ISO/DIS 19030 as the default method.

As each method for power estimation is yielded from individual idea and different sources for measurement, powers as results of those methods are not comparable values to each other. There were intensive discussion among ISO/TC8/SC2/WG7 experts how the standard provides power estimation. In November 2014 at Busan meeting, author presented comparison of shaft power and brake power calculated from fuel consumption to show that the difference between their accuracies means little in terms of the evaluation of changes in a ship's performance. Later, it was endorsed by the uncertainty analysis over the whole measurement of changes in hull and propeller performance, which is addressed in ISO/DIS 19030 family. This paper provides the complete set of the observation of onboard power estimation and evaluation of ship performance using two different powers.

2. Observation of onboard power estimation

Detailed observations are carried out on 7 container ships, 4 tankers and 7 vehicle carriers in this study.

2.1. Ship information

Table 1 shows ships observed in this study. All ships are fitted with the automatic continuous monitoring system which collects data normally once every hour.

2.2. Acquisition of data and information used for the calculation

During the observation period, the automatic continuous monitoring system on each ship collects data normally once every hour on:

- speed through water;
- shaft power (P_s);
- fuel flow;
- fuel temperature;
- wind speed; and
- water depth.

Displacements are manually recorded at every port of departure.

Shop test reports provide curves to calculate brake power from fuel consumption (P_b). Fuel consumption is calculated from the fuel flow and temperature and corrected according to ISO 3046-1 to be equivalent to the shop test condition. The procedure for estimating brake power is defined in Annex C to Part 2 of ISO/DIS 19030 and it is trailed by this study.

2.3. Environmental and operational condition

Extreme conditions in the environment and operation are filtered out from records, according to criteria below.

- Vessel speed through water is between 50% and 110% of design speed
- Shaft power is between 30% and 100% of Maximum Continuous Rating
- Displacement is within $\pm 5\%$ of the displacement values for the available speed-power curves
- Wind speed is 0 – 7.9 m/s (between BF 0 and BF 4)
- water depth is greater than the values obtained from the formula: $h = 2.75 V^2/g$, if it is available (V : vessel speed through water, g : gravitational acceleration)

2.4. Shaft power and brake power

Time series of shaft and brake power under the condition described in 2.3 appears with a certain gap between shaft and brake power, and the trend over a period of time appears nearly close to each other. The gap could be explained by the different mechanisms of each power, which is intrinsically inevitable. The sources of friction with the main shaft between the out-put coupling of the engine and the shaft power meter, for example thrust bearing and reduction gear, would induce the gap. However,

this would provide only partial explanation, when the relation between shaft and brake power figures out how their gap exists. Fig.1 shows all 18 ships' relation between shaft and brake power. In most of ships, data points show their direct linear relationship, while there are noisy diagrams reflecting weak correlation between shaft and brake power. They would only drop a vague hint to the question whether if the gap between shaft and brake power would have an effect on the evaluation of changes in a ship's performance.

3. Observation of changes in a ship's performance using shaft power and brake power

In order to illustrate how the gap between shaft and brake power would affect the evaluation of changes in a ship's performance, further calculation is carried out in this study.

3.1. Calculation of speed loss

ISO/DIS 19030 employs the tactic of speed loss in order to quantify changes in a ship's performance in her history. Percentage speed loss is "the relative difference in per cent between the measured vessel speed through water and an expected speed through water" (ISO/DIS 19030-2 paragraph 5.3.6.1) and defined as:

$$Vd = \frac{Vm - Ve}{Ve} \times 100 \text{ [%]}$$

Vd : Percentage speed loss [%]

Vm : measured vessel speed through water [knot]

Ve : expected speed through water [knot]

Expected speed through water is obtained from estimated power from measurements on board and speed-power curves provided at design and/or sea trial. Percentage speed loss is averaged over a period of time, and averages of speed loss are comparable figures for the same period of time. This study follows the calculation defined in ISO/DIS 19030. Two expected speeds are acquired from two powers, using the same curve. Percentage speed loss calculated by shaft power is:

$$Vd(Ps) = \frac{Vm - Ve(Ps)}{Ve(Ps)} \times 100 \text{ [%]}$$

and, percentage loss calculated by brake power is:

$$Vd(Pb) = \frac{Vm - Ve(Pb)}{Ve(Pb)} \times 100 \text{ [%]}$$

3.2. Calculation of changes in hull and propeller performance

In this study, all records of percentage speed loss for a ship during the observation period are divided in non-overlapping periods of 3 months and averaged for each 3 month. Due to the limitation by data availability, 3 month blocks are arranged where data is available and so blocks are not continuous. Blocks which only contain less than ten sets of data are omitted, as it is assumed that they would not produce a statistically representative value. The same records are also split and averaged for 6 months and 12 months. It is presumed that the difference between averages of percentage speed loss in two periods would express the change in the ship's performance, and this study examines how the gap between two powers affects the ship's change. There are six types of change in ship performance calculated from a ship's record in this study:

$k_{3(Ps)}$: the ship's change calculated by shaft power, which is the difference between averages of percentage speed loss in two 3 month periods

$k_{3(Pb)}$: the ship's change calculated by brake power, which is the difference between averages of percentage speed loss in two 3 month periods

- $k_{6(Ps)}$: the ship's change calculated by shaft power, which is the difference between averages of percentage speed loss in two 6 month periods
- $k_{6(Pb)}$: the ship's change calculated by brake power, which is the difference between averages of percentage speed loss in two 6 month periods
- $k_{12(Ps)}$: the ship's change calculated by shaft power, which is the difference between averages of percentage speed loss in two 12 month periods
- $k_{12(Pb)}$: the ship's change calculated by brake power, which is the difference between averages of percentage speed loss in two 12 month periods

This study would not investigate the cause of changes nor give any reason behind the change. The duration over a change (duration between two averaged periods) and status of the ship between two periods are important issues in the evaluation of the change in a ship's performance, however, this study approaches the evaluation of ship performance for effects of the gap between two powers on the evaluation, and does not evaluate the ship performance itself. Accordingly, any result of changes would not be explained in this study.

Changes are calculated as many as possible from all 18 ships, but no quantified change is obtained from 3 ships (ship B, S, and T) because of the limitation by data availability. Table 2 shows the number of changes calculated, and they are samples for the comparison of a ship's change reckoned from shaft power and brake power. Accordingly, the total number of data points contained in each calculated change varies from 24 (3 months) to 4,468 (12 months) and their averages are shown in the last column. Since all data blocks are made only where data is available in this study, density of data points is found comparatively high in 3 month comparison (186 data points/month in average) and low in 12 months (104 data points/month in average).

Figs. 2~4 illustrates the relation between a ship's change calculated by two different power, which is the difference between averages of percentage speed loss in two periods (3, 6, 12 months), and histogram of the difference from $k_{x(Ps)}$ to $k_{x(Pb)}$ shown as the residual. Samples appear to fit the line well, and histograms of residuals would suggest that the residuals are normally distributed. The normal probability plot of the residuals in Figs. 5~6 is approximately linear supporting the condition that the residuals are normally distributed, especially where an amount of residuals exists and so a statistical approach is appropriate. Fig. 7 indicates that residuals for the change between two 12 month periods appear closer Student's t-distribution rather than normal distribution, as its sample size is smaller than 100.

Table 3 digests the difference of between a ship's change calculated by shaft power and brake power. The mean of residuals calculated in this study is less than 0.1 %, and at the 95% confidence level, the true mean of residuals is in the range of $\pm 0.10\sim 0.38$ % from the sample mean. The variance of the range apparently depends on the sample size, and in this study it should be noted that data density which contributes accuracy of the representative value for each period also would be a component of variance.

4. Conclusion

The relationship between powers estimated by shaft torque and fuel consumption is observed on 18 ships, for the total period of more than 48 years, in this study. In many cases, there appears a gap between shaft and brake power, and also correlation between them is not always significant. However, in terms of evaluation of changes in the performance of a ship, effects of the gap between shaft and brake powers are obviously narrowed and it is likely to be negligible. This study would provide a snapshot of empirical comparison of two power estimation techniques, while it is self-evident that inevitable errors are included in the process of this study and influence the result. It could be elaborated by the future experience on the evaluation of ship performance and power estimation technologies and techniques.

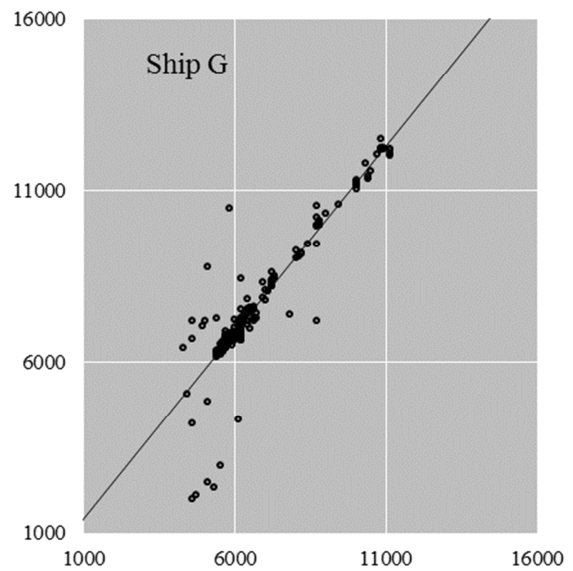
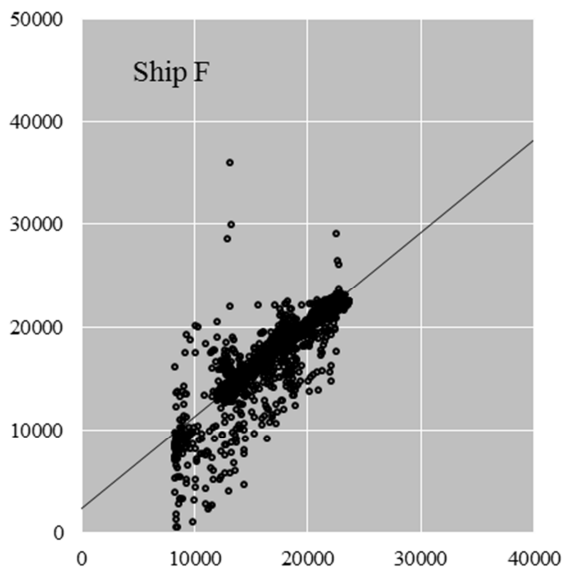
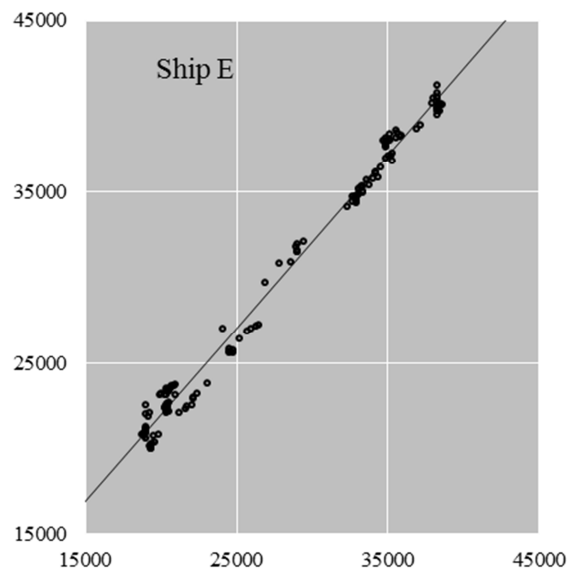
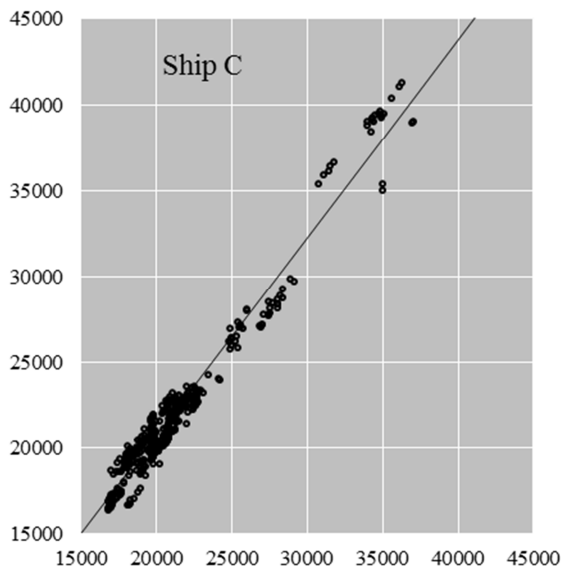
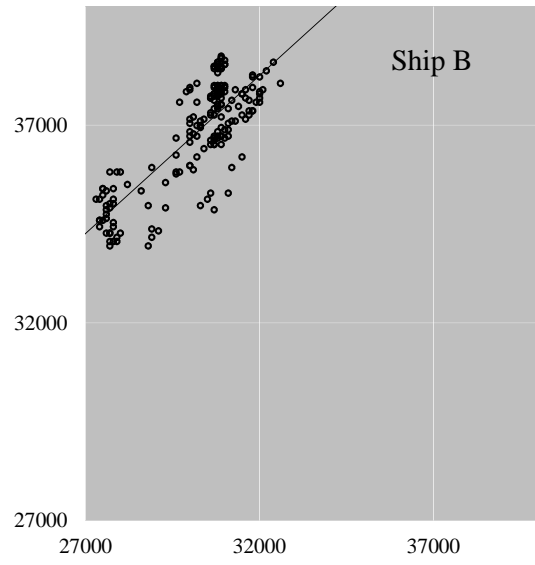
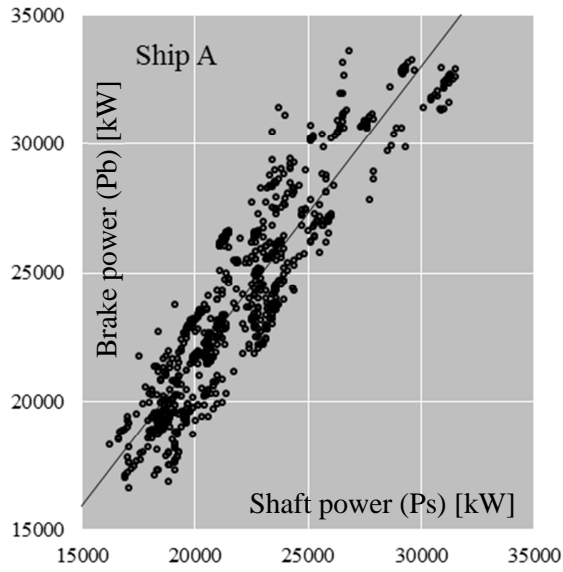


Fig.1: Relation between shaft and brake power

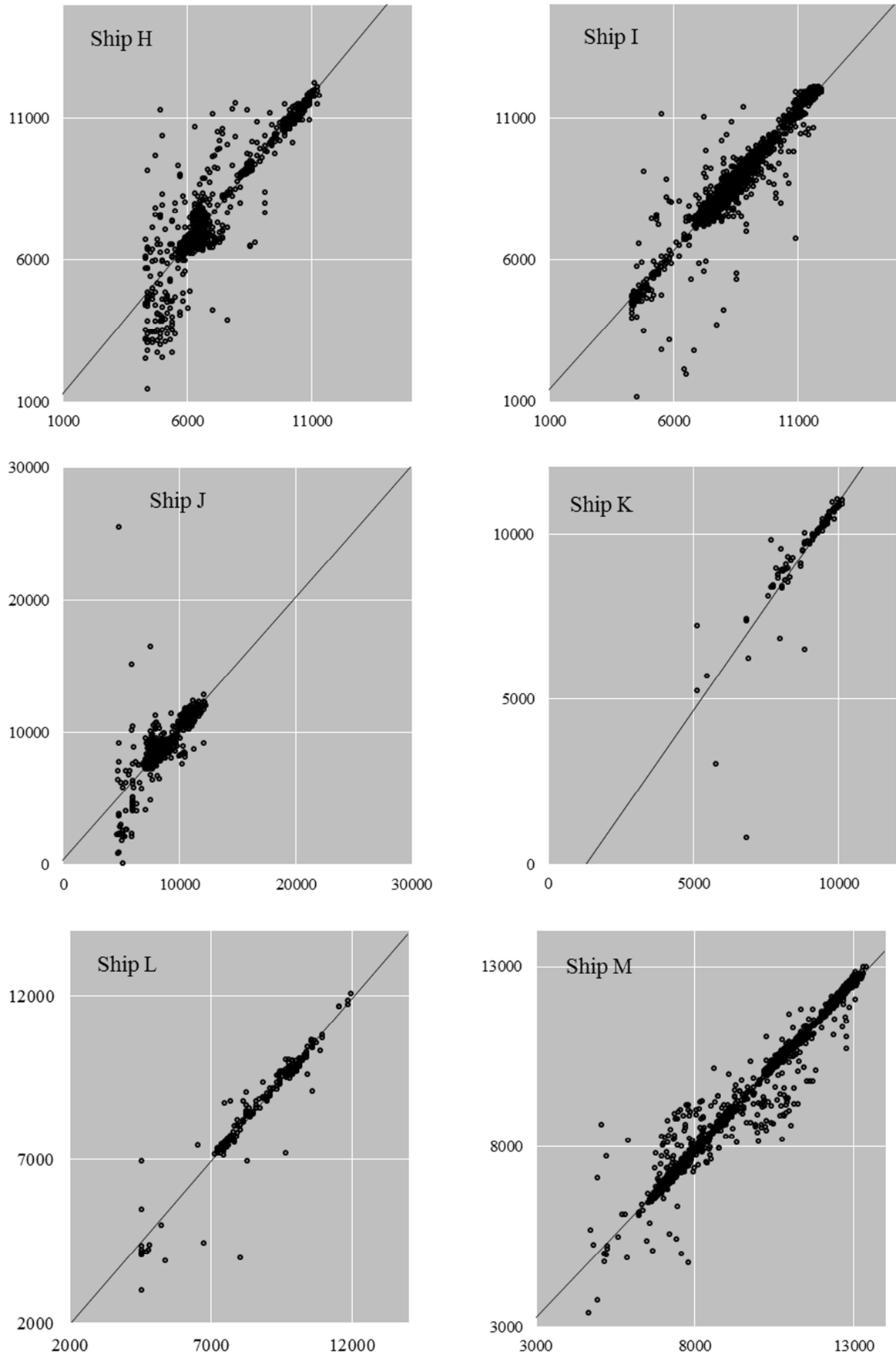


Fig.1: Relation between shaft and brake power (Continued)

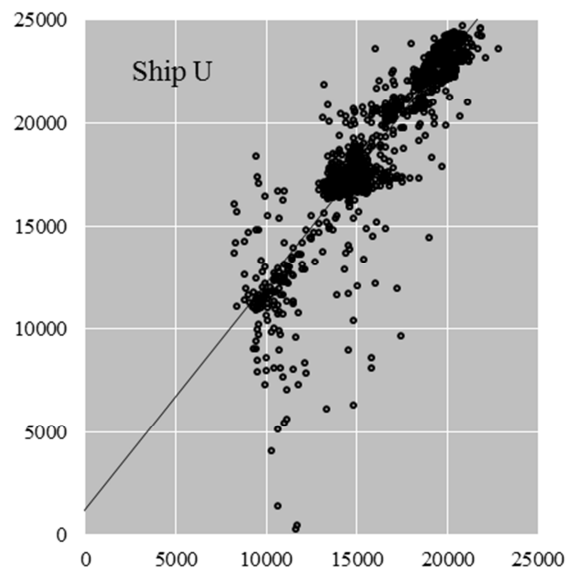
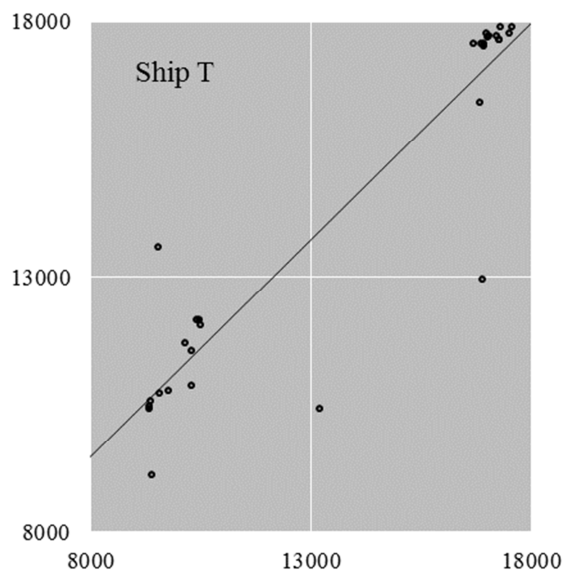
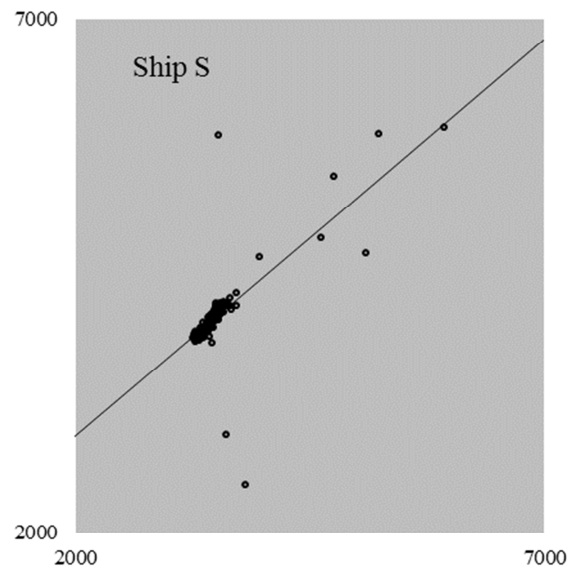
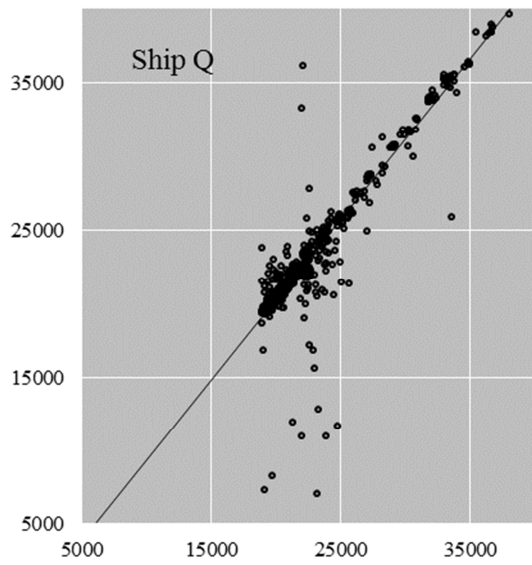
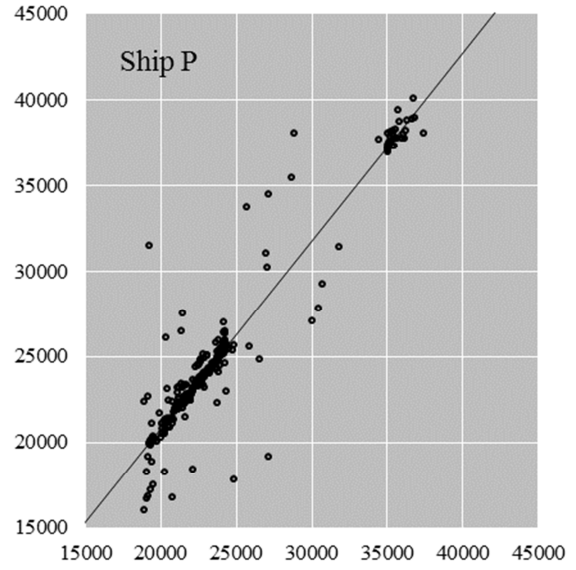
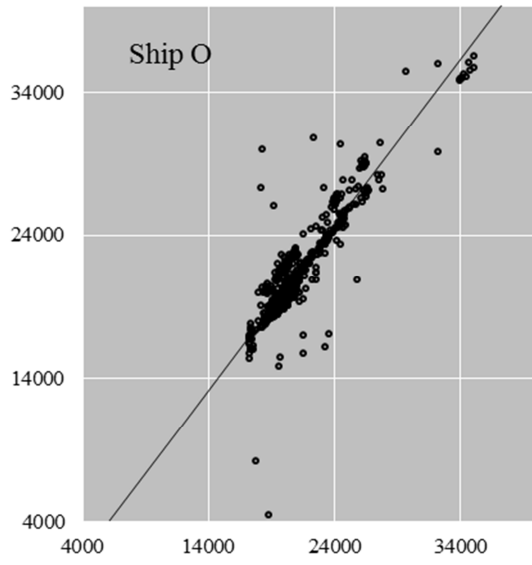


Fig.1: Relation between shaft and brake power (Continued)

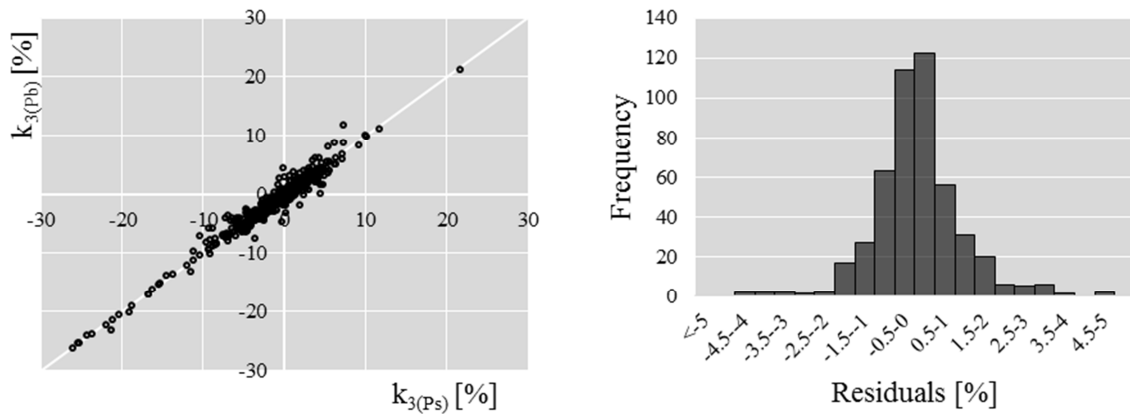


Fig.2: Relation between a the ship's change calculated by two different power, which is the difference between averages of percentage speed loss in two 3 month periods, and histogram of residuals

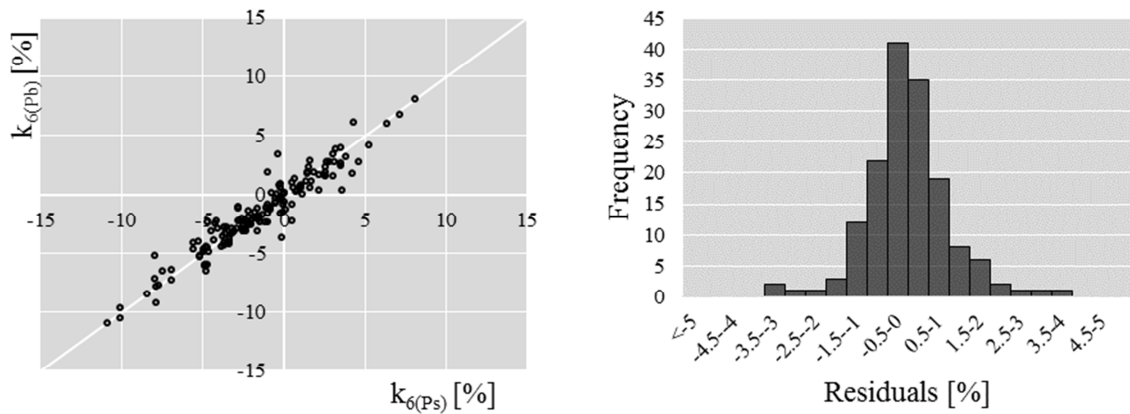


Fig.3: Relation between a the ship's change calculated by two different power, which is the difference between averages of percentage speed loss in two 6 month periods, and histogram of residuals

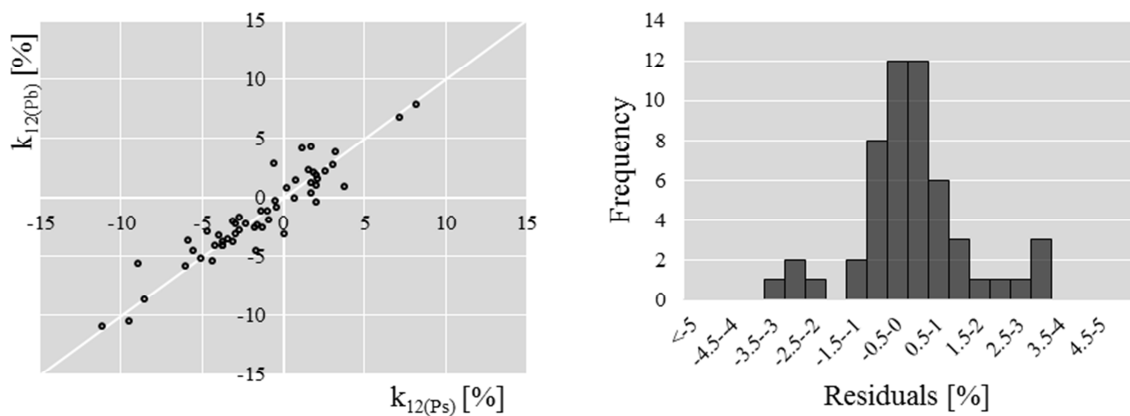


Fig.4: Relation between a the ship's change calculated by two different power, which is the difference between averages of percentage speed loss in two 12 month periods, and histogram of residuals

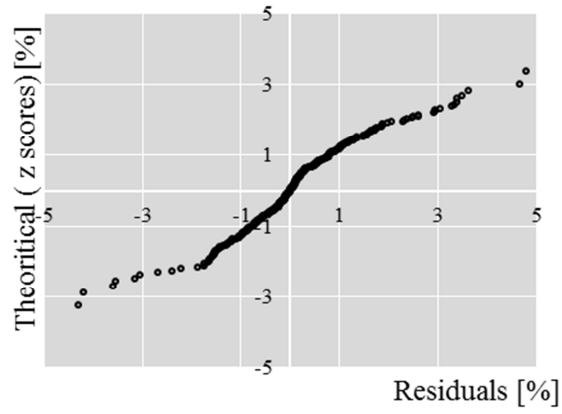


Fig.5: Normal probability plot of residuals illustrated in Fig.2

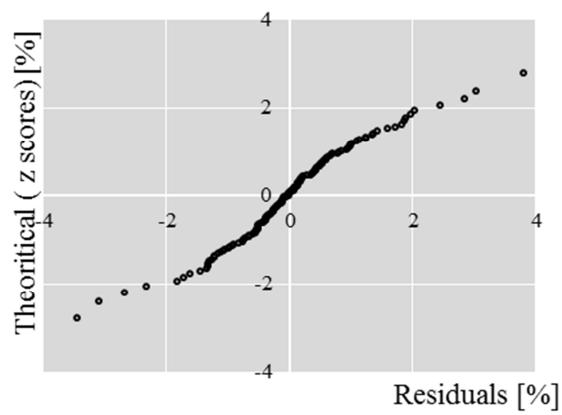


Fig.6: Normal probability plot of residuals illustrated in Fig.3

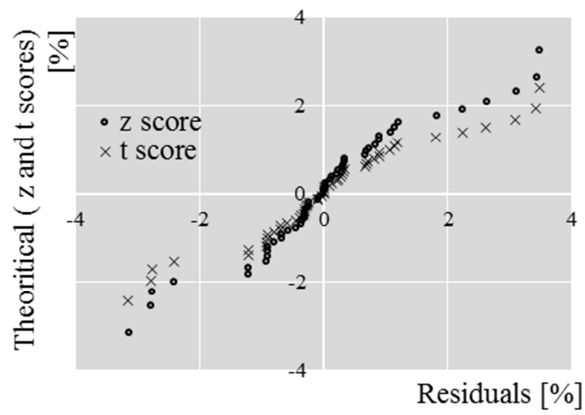


Fig.7: Normal probability plot of residuals illustrated in Fig.4

Table 1: Ship information

Ship	Type	Size	Ship route	Period (yy/mm/dd)
A	Container	6,000 TEU	Asia – North America (West coast)	08/12/21 – 14/6/30
B	Container	6,000 TEU	Asia – North America (West coast)/ Asia – Europe	09/11/5 - 14/6/30
C	Container	6,000 TEU	Asia – Europe/ Asia – North America (West coast)	08/12/01 - 14/6/30
E	Container	6,000 TEU	Asia – Europe/ Asia – North America (West coast)	10/1/01 - 14/6/30
F	VLCC ¹	310k DWT	Japan – Persian Gulf	09/4/22 - 14/8/31
G	PCC ²	6,400 Cars	Asia – Europe/ Asia – North America (West coast)	12/6/24 - 14/8/31
H	PCC	6,400 Cars	Asia – Europe/ Asia – North America (West coast)t)	12/4/5 - 14/8/31
I	PCC	6,400 Cars	Asia – Europe/ Asia – North America (West coast)	09/1/22 – 14/8/31
J	PCC	6,400 Cars	Asia – Europe/ Asia – North America (West coast)	12/4/5 – 14/8/31
K	PCC	6,400 Cars	Asia – Europe/ Asia – North America (West coast)	10/6/25 – 14/8/31
L	PCC	6,400 Cars	Asia – Europe/ Asia – North America (West coast)	12/3/18 – 14/8/31
M	PCC	6,400 Cars	Asia – Europe/ Asia – North America (West coast)	12/5/1 – 14/8/31
O	Container	8,000 TEU	Japan – Europe	12/12/4 - 14/9/9
P	Container	8,000 TEU	Japan – Europe	13/3/25 - 14/9/9
Q	Container	8,000 TEU	Japan – Europe	13/4/10 - 14/9/9
S	MR ³	50k DWT	Asia – Europe/ Asia – North America (West coast)	13/9/24 – 14/9/9
T	VLCC	310k DWT	Japan – Persian Gulf	13/1/26 – 14/9/9
U	VLCC	305k DWT	Japan – Persian Gulf	12/9/12 – 14/9/9

Table 2: Number of calculated changes

Length of averaged period	Total	Container ship	Tanker	Vehicle carrier	Number of data points included in a calculated change (Average)
3 months	479	76	186	217	558
6 months	155	39	48	68	884
12 months	53	17	16	25	1,253

¹ Very Large Crude Carrier² Pure Car Carrier³ Medium Range Product Carrier

Table 3: Interval estimation of the true mean of residuals

	3 months	6 months	12 months
Sample size	479	155	53
Sample mean	0.076 %	-0.0015 %	0.072 %
Unbiased estimate of variance	1.17 % ²	1.050 % ²	1.86 % ²
Sample standard deviation	1.08 %	1.024 %	1.36 %
Distribution of samples	Normal	Normal	Student's t
Degree of freedom	-	-	52
Sample error at the 95% confidence level	0.10 %	0.16 %	0.38 %
Upper confidence bound	0.18 %	0.16 %	0.45 %
Lower confidence bound	-0.024 %	-0.16 %	-0.31 %
Confidence interval	-0.024 ~ 0.18 %	-0.16 ~ 0.16 %	-0.31 ~ 0.45 %

Acknowledgements

I would like to express my gratitude to all experts of ISO/TC8/SC2/WG7 and its Japanese mirror group who encouraged me to get involved in this issue, and supported me by providing strong hints and excellent materials.

References

ISO (2015), *Ships and marine technology — Measurement of changes in hull and propeller performance — Part 1: General principle*, ISO/DIS 19030-1:2015

ISO (2015), *Ships and marine technology — Measurement of changes in hull and propeller performance — Part 2: Default method*, ISO/DIS 19030-2:2015

ISO (2015), *Ships and marine technology — Measurement of changes in hull and propeller performance — Part 3: Alternative methods*, ISO/DIS 19030-3:2015

ITTC (2005), *Analysis of Speed/Power Trial Data*, ITTC – Recommended Procedures and Guidelines 7.5-04-01-01.2

MAN (2011), *Basic Principles of Ship Design*, Denmark

A Statistical Study of Propulsion Performance of Ships and the Effect of Dry Dockings, Hull Cleanings and Propeller Polishes on Performance

Ditte Gundermann, Tobias Dirksen,

Propulsion Dynamics Europe, Copenhagen/Denmark, dgu@propulsiondynamics.com

Abstract

A statistical study of the propulsion of vessels and of the effects of different hull and propeller treatments on the performance is presented. The analysis is based on data of more than one thousand maintenance events and several hundred vessels, which have been monitored by the CASPER® Service. The study shows that most vessels have added resistances in the range between 10 and 40 percent, with development rates between 0.3 and 1.5 percent per month. It is found that dry dockings in average reduce the level of added resistance by 2/3 of the pre-dock level. Combined hull cleaning/propeller polishes were found to give a higher relative saving than individual hull cleaning and propeller polishes as expected. Hull cleanings and propeller polishes were found to give approximately the same relative saving, presumably because hull cleanings are often only carried out on the vertical sides.

1. Introduction

The aim of this study is to obtain better reference values for evaluation of vessels propulsion performance and of the possible results of future husbandry treatments. The analysis is based on data from several hundred ships (bulk carriers, tankers and container ships) and more than one thousand husbandry events (dry dockings, hull cleanings and propeller polishes) carried out on these ships. The performance of the ships has been monitored by the CASPER® Service, utilizing manually and/or automatically collected data, and is quantified in terms of the “added resistance”, which is defined as the percent increase in resistance, at design draft and design speed, compared to the corresponding clean, smooth hull and propeller resistance at sea trials ($\Delta R/R_{\text{trial}}$).

2. Levels of added resistance

Fig. 1 shows the distribution of added resistance for 210 vessels. The values range between a few percent and up to more than 80 percent, but the most typical values are between 10 and 40 percent.

Fig. 2 shows the average level of added resistance of the same vessels sorted according to their age. The effect of the usual 5-year dry-docking intervals is evident from the bar-plot as a clear reduction in added resistance around 5, 10, 15 and 20 years. It is also seen that the level of added resistance generally starts at a low to intermediate level at the beginning of a dry-docking period and increases towards the end of the period. There are some deviations from the trend especially in the third and fifth dry-docking period, which could be a result of the management strategies with regard to propeller and hull treatment. The result of the second and the fourth dry-docking after delivery is on average better than the first and the third, probably due to the fact that often only a partial hull blast is applied at the first and the third dry-docking while a full blast is more often carried out at the second and fourth dry-docking after delivery.

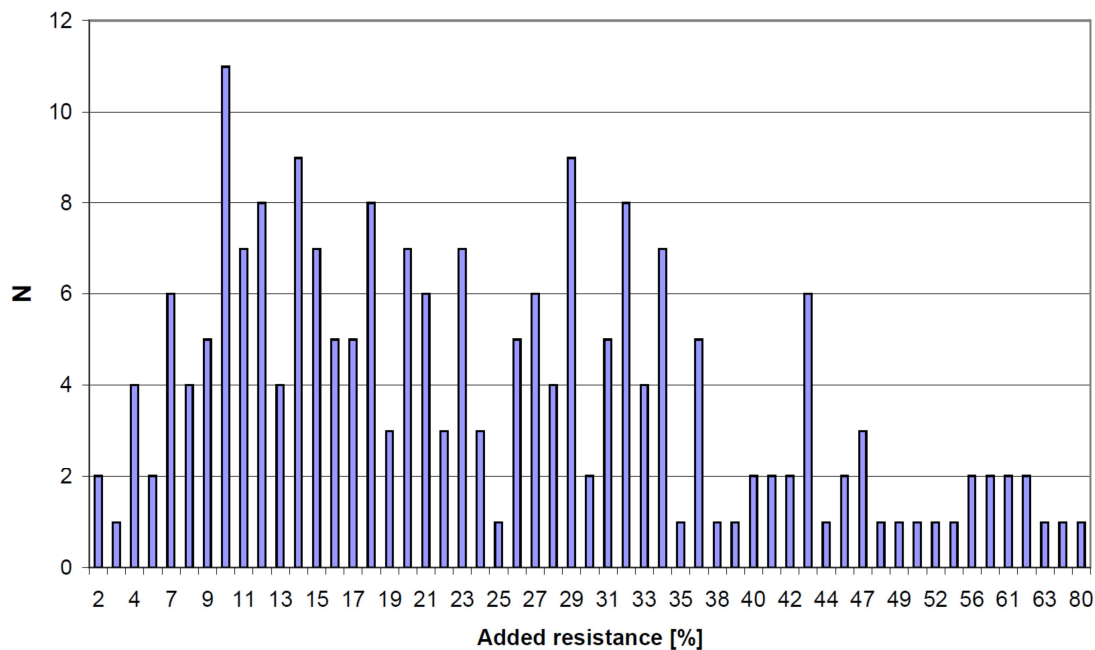


Fig. 1: Distribution of level of added resistance of 210 vessels. N refers to number of ships.

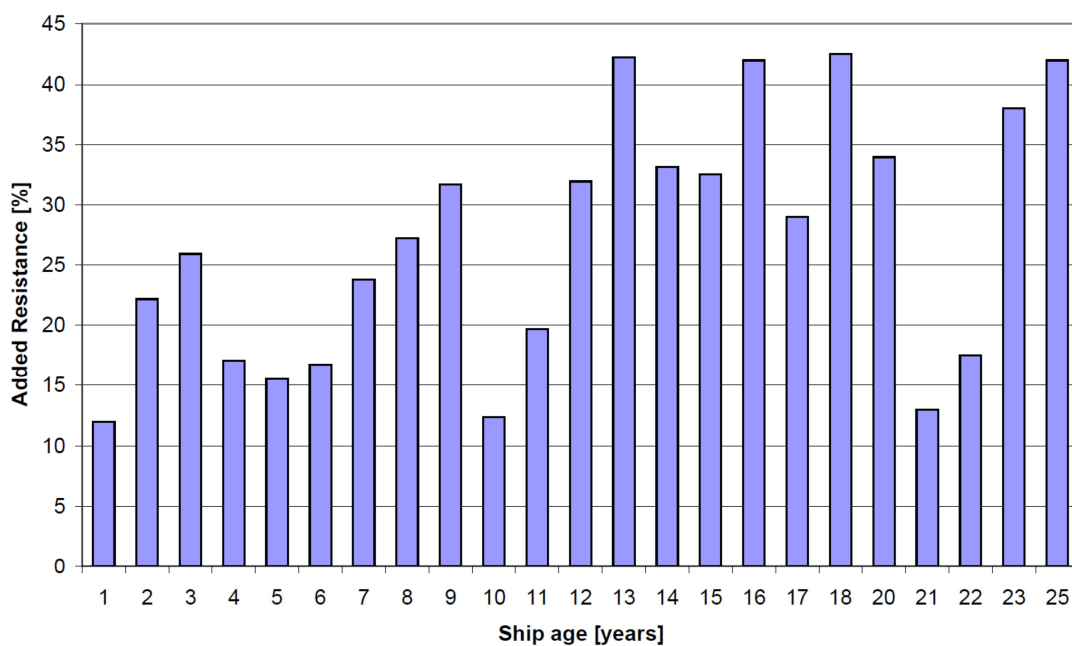


Fig. 2: Average levels of added resistance versus ship age

Fig. 3 shows the average level of added resistance in each inter-docking period. The general level increases with ship age, which may be a result of an increase in permanent resistance with ship age. The apparent decrease in average level for vessels older than 20 years compared to vessels younger than 20 years may be a result of the rather comprehensive maintenance work, which often is carried out in connection with the fourth Special Class Survey.

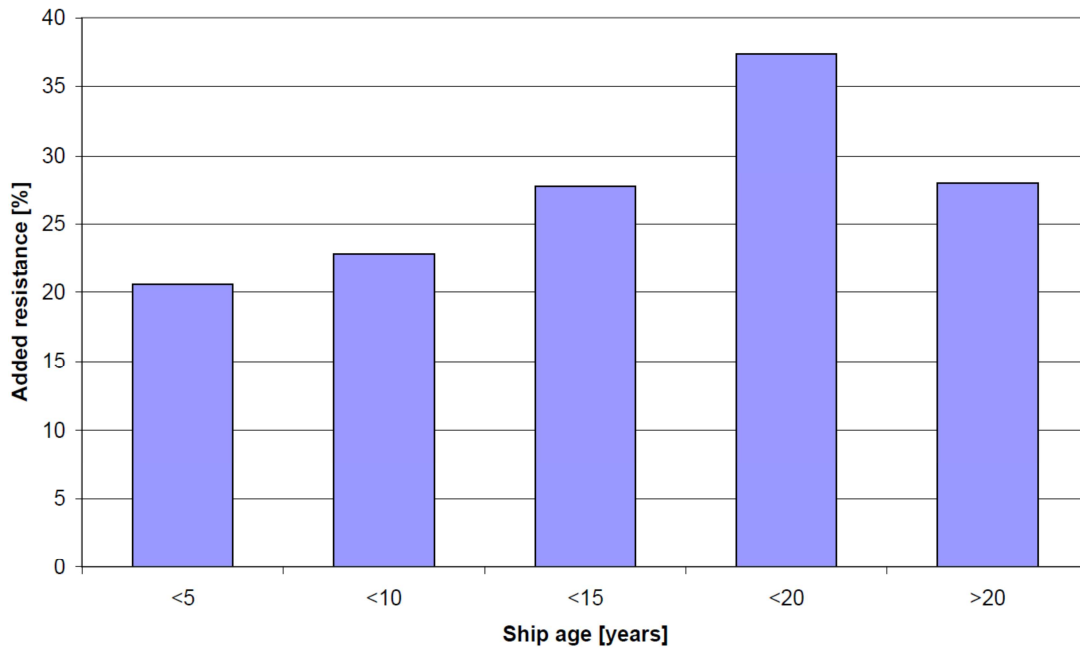


Fig. 3: Average levels of added resistance for 5-year periods corresponding to usual docking periods

3. Development rate of the added resistance

It is assumed that under normal conditions and when no husbandry is carried out, the level of the added resistance (F_b) develops as the second part of an S-shaped growth curve (Fig. 4), described by

$$F_b = A \cdot \tanh(B \cdot t),$$

where A is the asymptotic amplitude, B is a growth rate, and t is time.

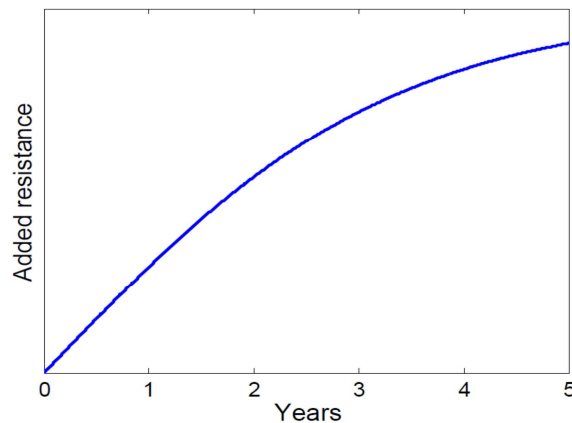


Fig. 4: The normal development of the added resistance over a dry-docking period given that no intermediate husbandry actions are taking place

This means that the rate of increase of added resistance (the slope of the curve) for a specific ship in principle should be larger at the beginning of a dry-docking period and smaller at the end, provided that no discontinuities appears during this period.

Fig. 5 shows a histogram of development rates of the 210 ships with all different types of hull coating systems. It is seen that the main peak lies around a development rate of 0.5 percent per month, but a secondary peak is also seen around 1.2 percent per month. The development rate lies mainly between 0.3 and 1.5 percent per month.

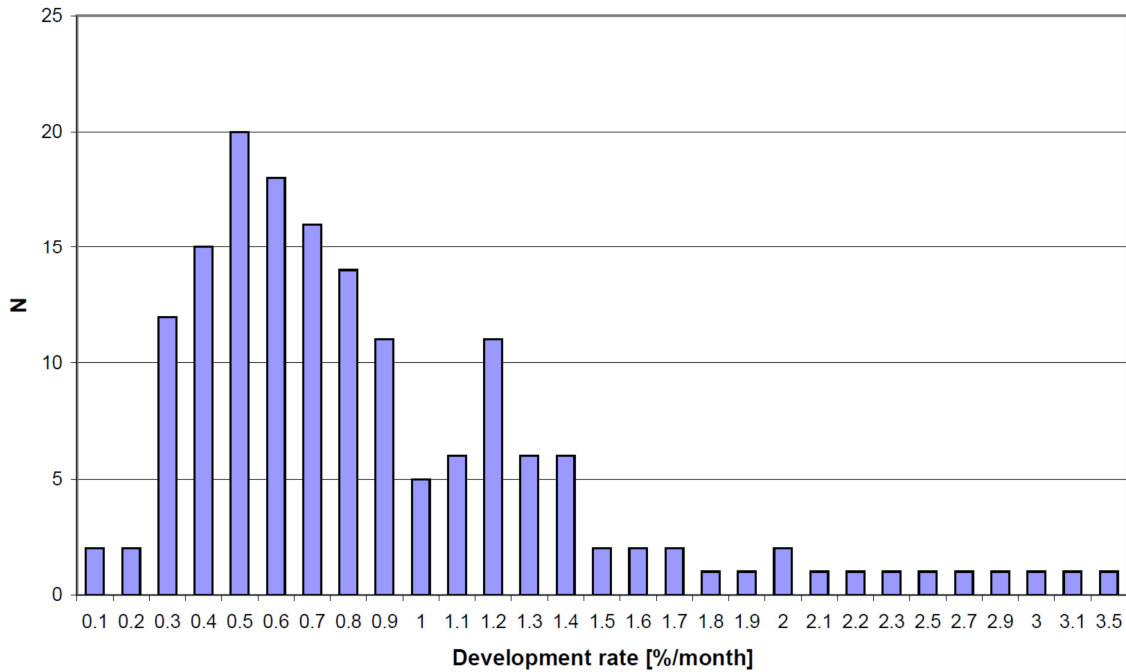


Fig. 5: Distribution of development rates

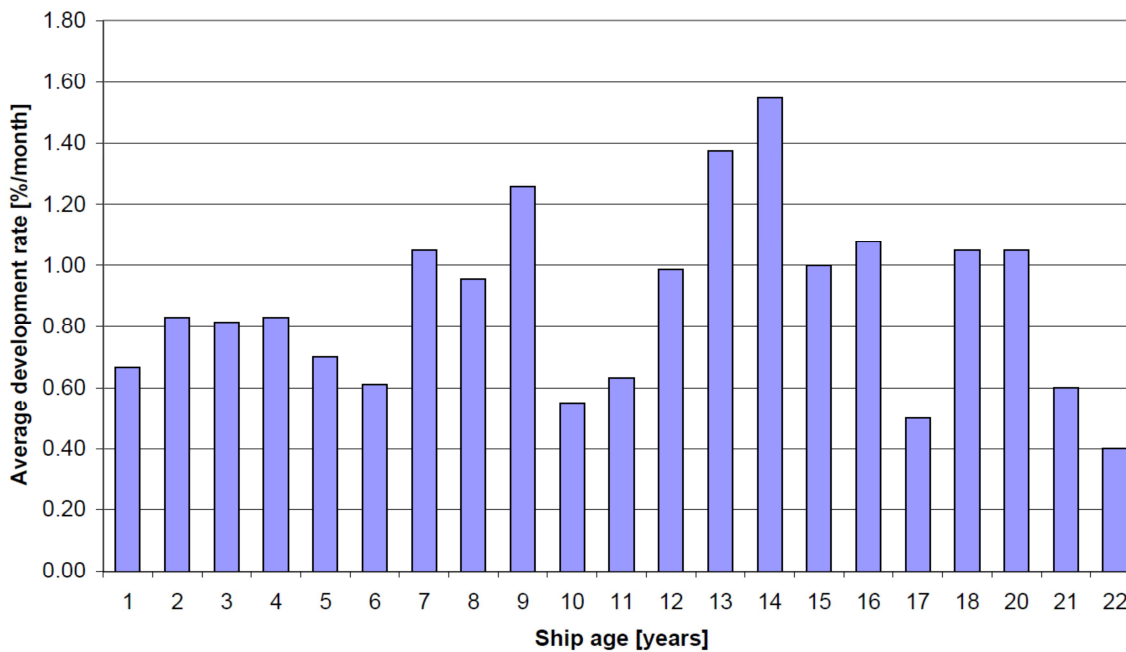


Fig. 6: Average development rate versus ship age

The average development rate is plotted against ship age in Fig. 6. It looks like the average development rate increases towards the end of the docking periods. This is further illustrated in Fig. 7, which shows the average development rate versus years out of dock. The increase in development rate at the end of the docking periods reflects a reduction of the anti-fouling or foul release efficiency of the coating. This does however not contradict the asymptotic behavior of the development of added resistance (Fig. 4), which only describes the development, when no actions causing a discontinuity of the curve are taking place. In practice the anti fouling or foul release coating of a ship may be affected by many kinds of events, such as hull cleanings or long idle periods. Hull cleanings may, if not carried out in due time, damage the coating, so that the development rate is increased though the added resistance is reduced. Fig. 7 shows average development rates with no accounts taken for hull cleanings, propeller polishes or other events.

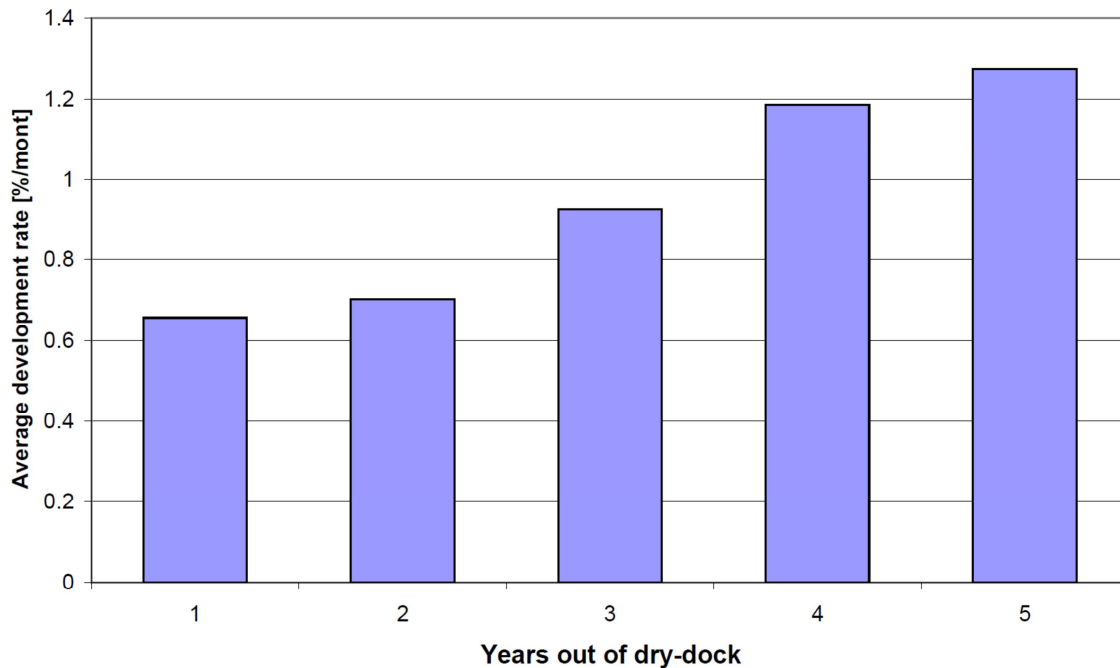


Fig. 7: Average development rate versus years out of dock

4. Effects of hull and propeller treatments

The study of the effects of hull and propeller treatments are based on 1391 treatments/events comprised of 237 dry dockings, 127 hull cleanings and 445 propeller polishes.

It should be stressed that the study does not take a number of important parameters into account. Some of these parameters are:

- type of hull treatment and preparation in dry dock
- type of coating systems applied
- quality of the dry-docking treatment
- length of the dry-docking intervals
- number of hull and propeller cleanings in the dry-docking intervals
- the frequency, scope and quality of in-water hull and propeller cleanings
- ship operation conditions (speed, loading, operation areas, idle periods, temperature, port stays, etc).

It is well-known that these parameters have a great influence on the marine fouling and therefore also on the propulsion performance and on the procedures for hull and propeller maintenance. This again will influence the results of the various husbandry actions. The results of this study show therefore only general tendencies, which may not necessarily apply to the individual ship or the individual maintenance action.

4.1. Dry dockings

The 237 dry docking results are plotted in Fig. 8 versus the level of added resistance entering dock. The data show relatively large scatter illustrating the difficulty in predicting the result of a dry docking. The large variation is probably due mainly to differences in treatments (full blast/spot blast) and coating types. Often a spot blast is carried out after 5 years and a full blast after 10 years.

A linear regression line through the points is also shown (solid line) in Fig. 8. The dotted line shows the level of added resistance before dry docking. The reduction in the level of added resistance due the docking can be read on the y-axis as the difference between the two lines. The regression suggests that the level of added resistance is reduced by almost 2/3 due to a dry docking. Note, that points above the dotted line represents a negative change ($F_b^{\text{After}} > F_b^{\text{Before}}$) in added resistance. These cases are rare and include only ships with relatively low pre-dock levels and only marginally worse levels after docking. However, several cases have been seen where vessels leaving dock with a higher result than expected have reduced their added resistance significantly by an in-water propeller polishing soon after dry-dock, suggesting poor propeller treatment in dock or possible accumulation of dust and paint spray on the propeller in dock.

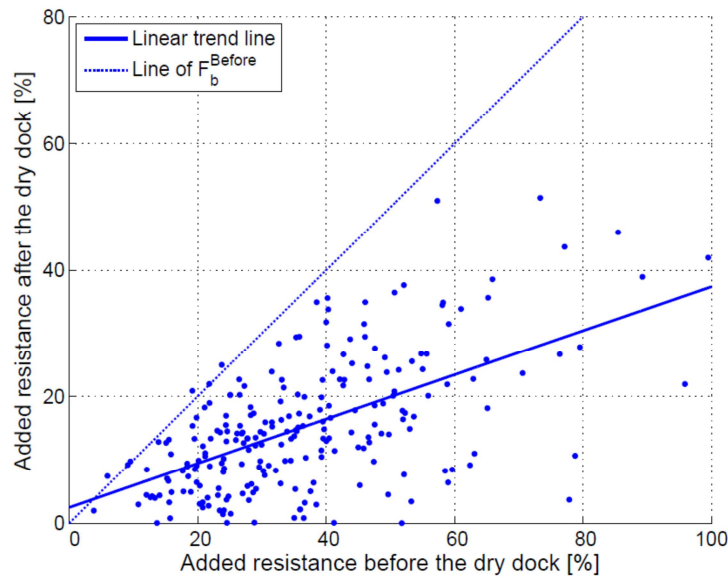


Fig. 8: The points show level of added resistance after a dry docking versus the level of added resistance before the dry docking. The solid line shows a linear regression given by $F_b = 0.018 + 0.37F_b^{\text{Before}}$. The dotted line is a guideline showing the level of added resistance before dry docking.

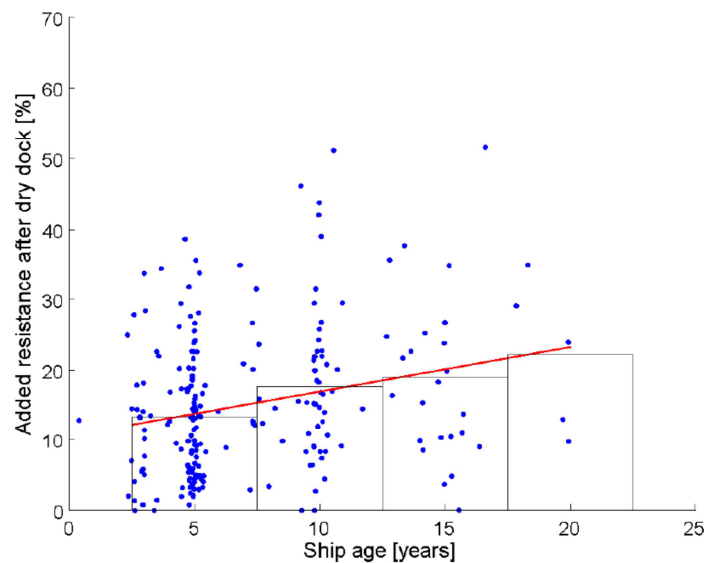


Fig. 9: The added resistance after dry docking versus ship age. The line shows a linear regression given by $F_b^{\text{After}} = 0.108 + 0.0064t$, where t is the ship age in years. The bars show mean values in the given periods (2.5 to 7.5 years, 7.5 to 12.5, 12.5 to 17.5 years and 17.5 to 22.5 years.).

The relation between the level of added resistance right after a dry-docking and the ship age is examined in Fig. 9, which shows the level of added resistance right after a dry docking as a function of ship age. The bars show the average levels in the given periods. It can be seen that the added resistance after a dry docking appears to increase with ship age although large scatter is seen in the data. This is consistent with the hypothesis that ships develop a permanent resistance over time. A linear fit is also shown in the figure.

4.2. Hull cleanings

Data are available from 127 independent hull cleanings, including divers-with-brushes and robotic cleaners, where the hull cleanings are not performed jointly with a propeller polish or a dry docking. The level of added resistance after a hull cleaning is plotted versus the level of added resistance before the hull cleaning in Fig. 10 together with a linear regression line through the data. Again a guide-line showing the pre-cleaning level (dotted line) is also shown. The regression gives a reduction in added resistance of around $\frac{1}{4}$ of the pre-cleaning result. A couple of points lie above the dotted line representing increased levels of added resistance after the cleaning. Since it seems unlikely that a cleaning would increase the level of added resistance, these cases may reflect inaccurate data.

The relation between the reduction in added resistance due to a hull cleaning and the time since the latest hull cleaning/dry dock is examined in Fig. 11. No clear relation can however be seen, presumably because there are so many variables as mentioned earlier.

Similarly, it has been investigated whether there is a correlation between the effect of a hull cleaning and the ship age, the time out of dock, the number of hull cleanings, the ship dimension, the ship type, and the development rate before the hull cleaning, but no significant correlations have been found.

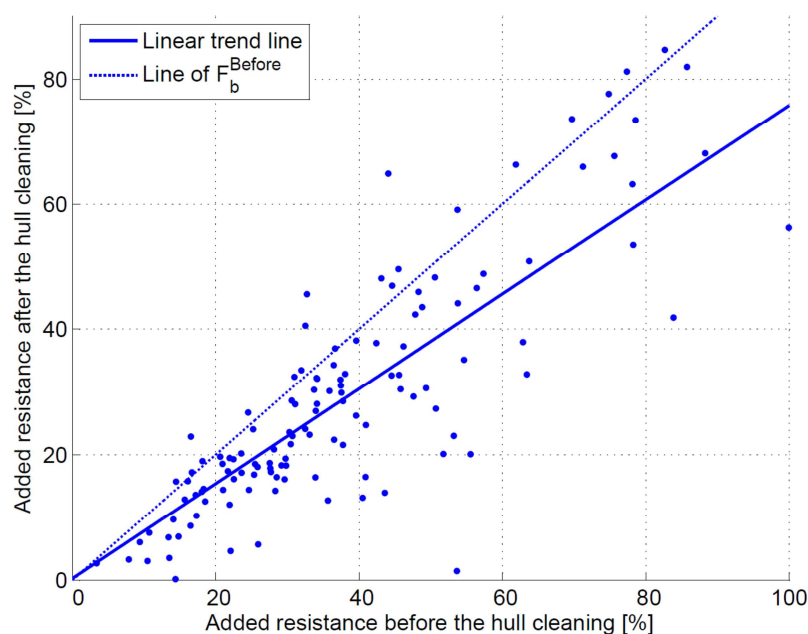


Fig. 10. The points show levels of added resistance after hull cleaning versus the level of added resistance before the cleaning. The solid line shows a linear regression given by $F_b^{\text{After}} = 0.0027 + 0.755 F_b^{\text{Before}}$. The dotted line is a guideline showing the level of added resistance before hull cleaning.

It would be interesting also to investigate whether there is a correlation between the effect of a hull cleaning and the increase of added resistance since the latest hull cleaning. However, too little data on this are available. It requires that the vessels have been in the program for a long time and that propeller polishes are not done in-between the hull cleanings. The latter is rarely the case.

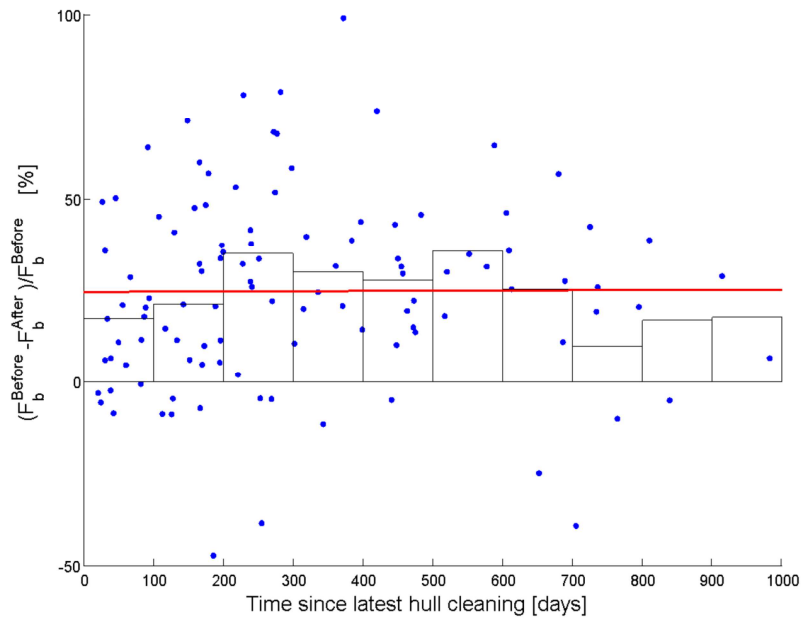


Fig. 11: Reduction in added resistance in percent versus time since latest hull cleaning. The bars show the average value in intervals of 100. The curve shows a linear regression. No correlation is seen.

4.3. Propeller polishes

Data on 445 independent propeller polishes are available, including normal polishing methods and “super-polishing”. Again, the added resistance after a propeller polish is shown (Fig. 12) versus the added resistance before the polishing with a linear regression line (solid), and a line showing the level of added resistance before the polishing for (dotted). Again, a number of cases are seen where $F_b^{After} > F_b^{Before}$. These may be caused by poor polishes or be a result of poor data. The regression suggests a reduction in added resistance of little more than 1/5 due to a propeller polish.

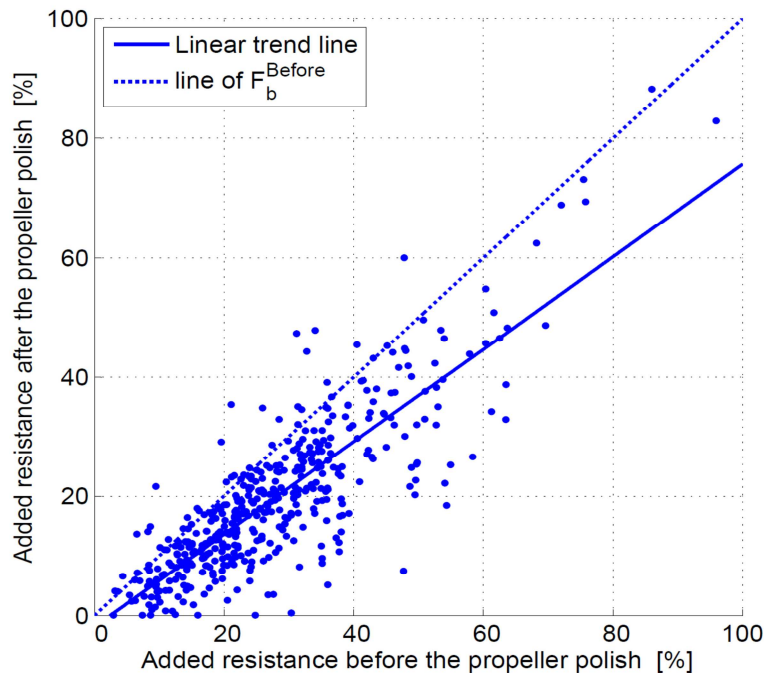


Fig.12: Points show levels of added resistance after propeller polishes versus the level of added resistance before. The solid line shows a linear regression given by $F_b^{After} = -0.019 + 0.776 F_b^{Before}$. The dotted line is a guideline showing the level of added resistance before dry docking.

A number of other correlations have been examined, but none of these have been found to be significant.

4.4. Combined hull and propeller cleanings

Data on 394 combined events are available. Fig. 13 shows a plot of added resistance values after a combined hull and propeller cleaning versus the added resistance before the cleaning, with a linear regression line (solid). The regression line gives a reduction in added resistance of little more than 1/3 of the pre-cleaning level by a combined hull cleaning and propeller polish.

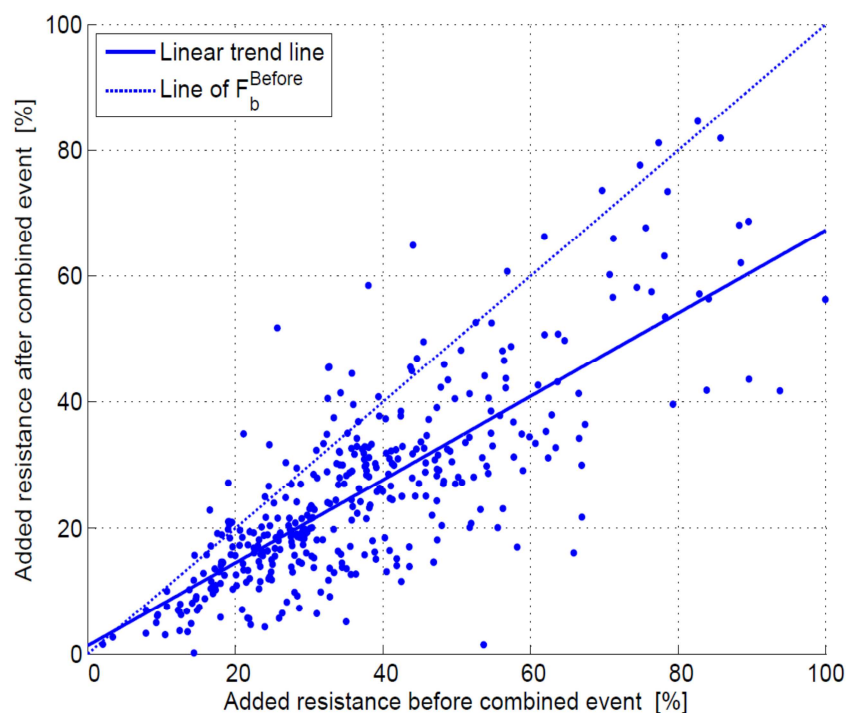


Fig. 13: Points show levels of added resistance after combined hull and propeller cleanings versus level of added resistance before the cleanings. The solid line is a linear regression line given by $F_b^{\text{After}} = -0.013 + 0.660F_b^{\text{Before}}$. The dotted line shows the level of added resistance before the cleaning.

5. Conclusion

The concept of added resistance allows for a direct comparison of the propulsion performance, and hence of the hull and propeller condition, between different vessels and different vessel types. The present study shows that the added resistance typically lies between 10 and 40 percent. The average level of added resistance is found to increase with ship age. Typical development rates lie between 0.3 and 1.5 percent per month, and the average development rate was found to increase with time out of dock.

The level of added resistance is reduced by hull and propeller treatments, but the data indicate an underlying permanent resistance which increases with ship age. Fig. 14 shows the regressions of the four different maintenance treatments. It can be seen that dry dockings give the best result, and that combined hull and propeller cleanings give somewhat better results than independent hull cleanings or propeller polishes. Taking the statistical uncertainty into account, hull cleanings and propeller polishes give equal results.

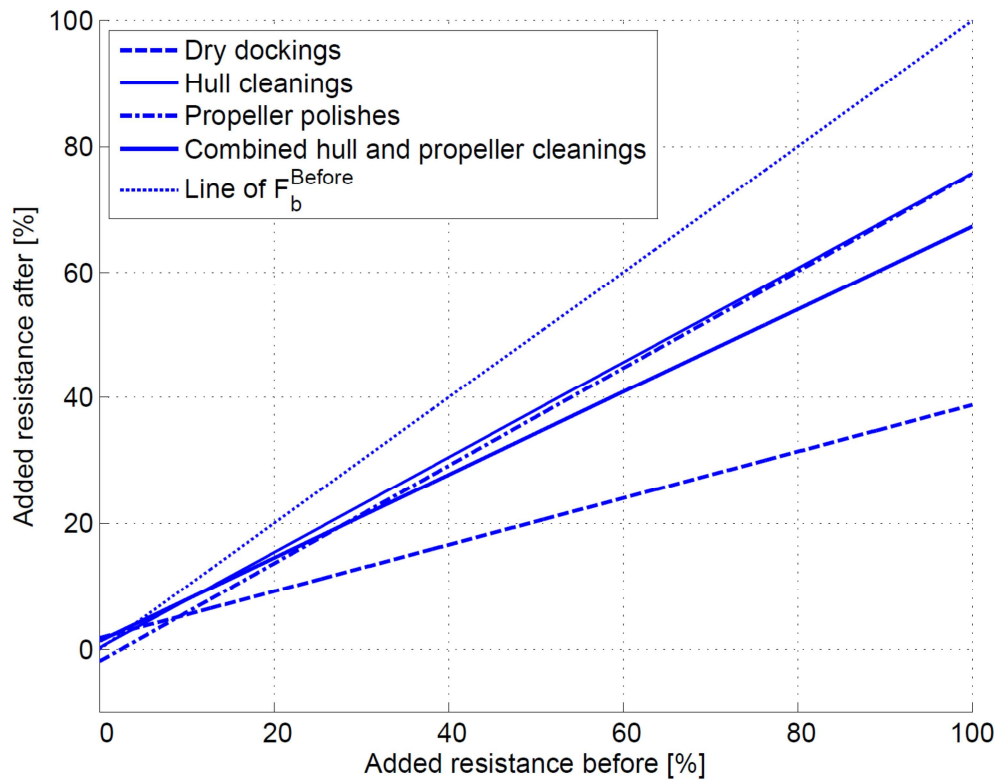


Fig. 14: Collection of the four regression lines for dry dockings, hull cleanings, propeller polishes and combined hull and propeller cleanings

ISO 19030 – Motivation, Scope and Development

Svend Søyland, Nordic Energy Research, Oslo/Norway, svend.soyland@nordicenergy.org
Geir Axel Oftedahl, Jotun A/S, Sandefjord/Norway, geir.axel.oftedahl@jotun.no

Abstract

This paper describes the history of ISO 19030 for hull and propeller performance assessment for ships in service. It outlines initial motivation, purpose and implementation of the standard. The standard is intended to serve the wider community as well as support shipping operators and suppliers in better business practice.

1. Why ISO 19030 is needed?

Today hull and propeller performance is a ship efficiency killer. According to the Clean Shipping Coalition in MEPC 63-4-8, poor hull and propeller performance accounts for around 1/10 of world fleet energy cost and GHG emissions. This points to a considerable improvement potential; 1/10 of world fleet energy costs and GHG emissions translates into billions of dollars in extra cost per year and around a 0.3% increase in man-made GHG emissions. The culprits are a combination biofouling and mechanical damages. Most vessels leave the new build yard or subsequent dry-docking with their hull and propeller in a fairly good condition. Then on account of a combination of biofouling and mechanical damage, hull and propeller performance begins to deteriorate.

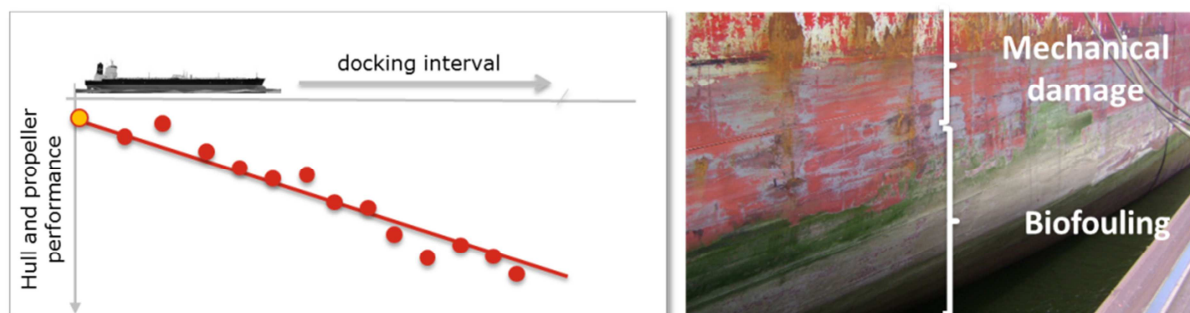


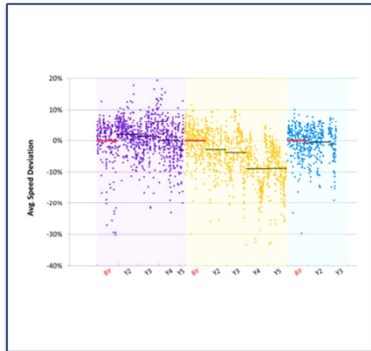
Fig. 1: Hull and propeller performance

There are technologies and solutions on the market that can protect the hull and maintain good performance over the full duration of the docking interval - why then is hull and propeller performance still so poor?

In the past the problem has been a lack of measurability. If one cannot measure it, one cannot manage it. Now a multitude of measurement methods are being introduced in the market; some quite good, some really bad, most of them proprietary (black box) and many using their own yardsticks. It is becoming challenging, however, even for the most resourceful to determine which of these methods can be relied upon and which cannot. Moreover, the measurement methods have different and incompatible yard sticks resulting in the measurement output serving to confuse rather than inform.

This standard is intended for all stakeholders that are striving to apply a rigorous, yet practical way of measuring the changes in hull and propeller performance. It could be ship-owners and operators, companies offering performance monitoring, shipbuilders and companies offering hull and propeller maintenance and coatings. ISO 19030 will make it easier for decision makers to learn from the past and thereby make better informed decisions for tomorrow. It will also provide much needed transparency for buyers and sellers of technologies and services intended to improve hull and propeller performance. Finally, it will make it easier for the same buyers and sellers to enter into performance based-contracts and thereby better align incentives.

Allow learning from the past to make better decisions for tomorrow



Provide needed transparency for buyers and sellers of fuel saving tech.



Enable performance based contracting and better alignment of incentives

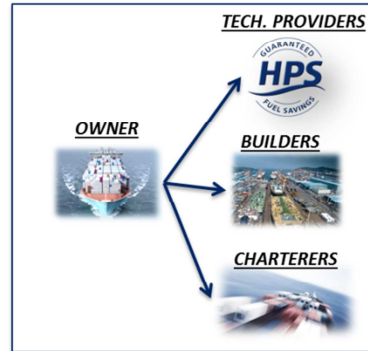


Fig. 2: Why ISO 19030 is needed

2. What ISO 19030 cover

ISO 19030 outlines general principles of, and defines both a default as well as alternative methods for, measurement of changes in hull and propeller performance. The standard defines sensor requirements, measurement procedures, including various filters and corrections, as well as how to calculate a set of four performance indicators for hull and propeller related maintenance, repair and retrofit activities.

One of the performance indicators is “In-service performance”. In-service performance refers to the average change in hull and propeller performance over the dry-docking interval. Performance over the first year following the docking is compared with performance over whatever remains of the docking interval – typically two to four years. This performance indicator is useful for determining the effectiveness of the underwater hull and propeller solution – for example the hull coating system used.

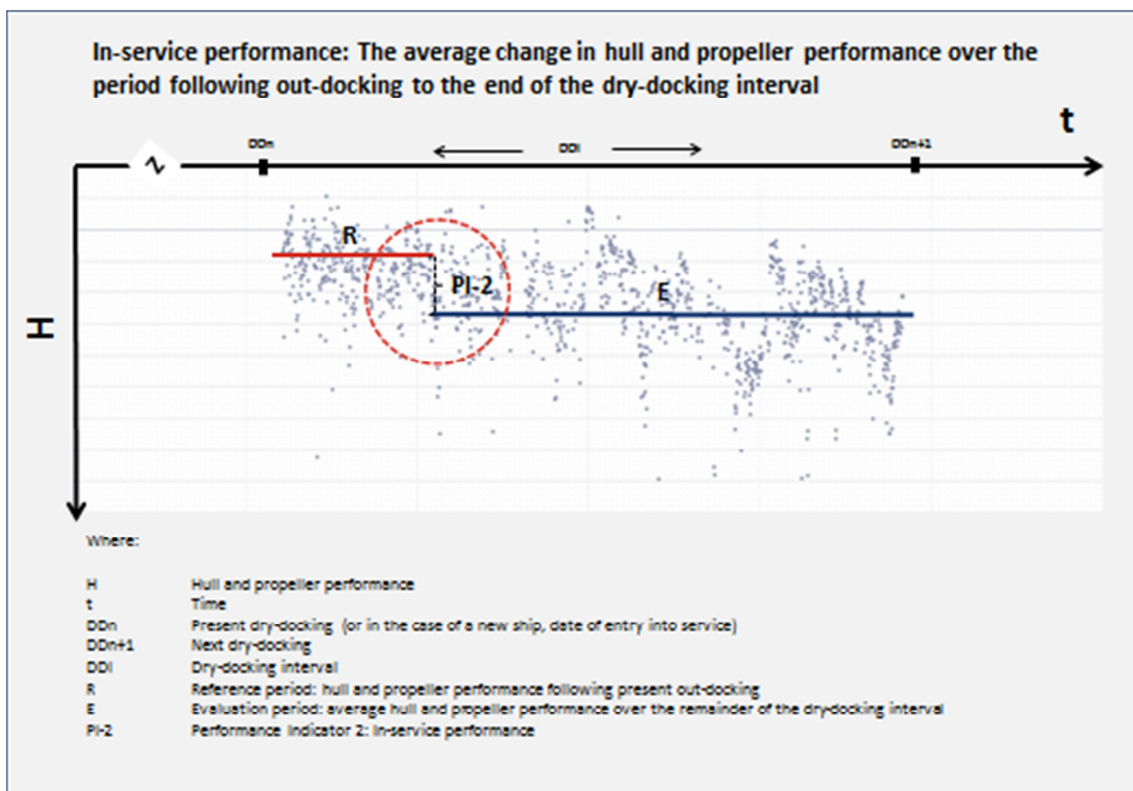


Fig. 3: Performance indicators in ISO 19030 – In-service performance

The three additional performance indicators are “Dry docking performance”, “Maintenance trigger” and “Maintenance effect”:

- Dry docking performance: Hull and propeller following the present out-docking is compared with the average performance from previous out dockings. This provides useful information on the effectiveness of the docking.
- Maintenance trigger: Hull and propeller performance at the start of the dry-docking interval is compared with a moving average at a point in time. Useful for determining when hull and propeller maintenance is needed – including propeller polishing or hull cleanings.
- Maintenance effect: Hull and propeller performance in the period preceding the maintenance event is compared with performance after. This provides useful information for determining the effectiveness of the event.

ISO 19030 is fairly all-encompassing. It covers what sensors are required, how these are to be maintained, step-by-step procedures for filtering and correcting the data, and finally how the individual performance calculators are to be calculated.

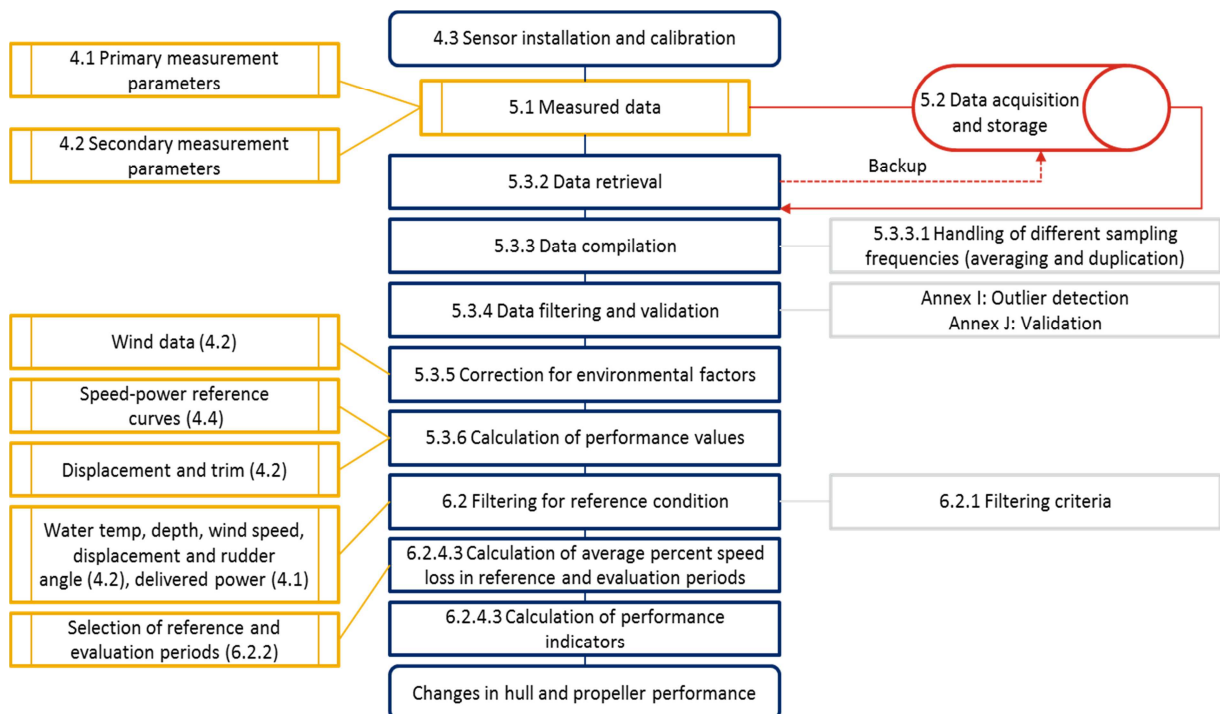


Fig. 4: ISO 19030 scope

The standard is organized into three parts:

- ISO 19030-1 outlines general principles for how to measure changes in hull and propeller performance and defines the 4 performance indicators for hull and propeller maintenance, repair and retrofit activities.
- ISO 19030-2 defines the default method for measuring changes in hull and propeller performance. It also provides guidance on the expected accuracy of each performance indicator.
- ISO 19030-3 outlines alternatives to the default method. Some will result in lower overall accuracy but increase applicability of the standard. Others may result in same or higher overall accuracy but include elements which are not fully validated in commercial shipping.

Descriptions and explanations are outlined in ISO 19030-1. Methodological alternatives that are state-of-the-art and mature are addressed in ISO 19030-2. Alternatives that are state of the art but not fully

mature have either been included in ISO 19030-3 or will be addressed in future revisions of the standard. Alternatives that give the same overall accuracy are included as options in ISO 19030-2. Finally, alternatives that yield lower overall accuracy but increase applicability of the standard are covered in ISO 19030-3.

3. How ISO 19030 has been developed

The process towards developing the ISO19030 started when the Environmental NGO Bellona Foundation and Jotun A/S had informal discussions on how to improve energy efficiency within the maritime sector. Bellona Foundation looked for a robust and verifiable way to reduce CO₂ emissions, whereas Jotun A/S saw the need for a more transparent approach to verify a myriad of performance claims on hull and propeller maintenance.

A series of workshops held in accordance with Chatham House Rules involved a steadily increasing number of stakeholders and paved the way for a common understanding among performance monitoring companies, measurement manufacturers, ship maintenance system providers, classification societies, shipbuilders and ship-owners and their associations. Bellona Foundation and Jotun subsequently held a side-event at IMO-MEPC meetings and presented the embryo for a reliable and transparent hull and performance standard at several maritime conferences.

Work on the ISO-Standard was initiated in June 2013 when Working Group 7 under SC2 TC8 was formed. Svend Søyland from Nordic Energy Research serves as the Convener of the working group and Geir Axel Oftedahl from Jotun has the role as Project Manager. A series of Working Group meetings were held; Oslo (June 2013), Tokyo (November 2013), Hamburg (July 2014), Pusan (November 2014), San Ramon (February 2015) and Copenhagen (September 2015). More than 50 experts and observers, representing ship owners, shipping associations, new build yards, coatings manufacturers, performance monitoring companies, academic institutions, class societies and NGOS participated in the ISO working group that reached consensus on ISO 19030 standard. Additional industry stakeholders have been consulted and involved as a part of this extensive process. World-class experts shared their deep expertise in a truly collaborative effort and put aside their professional ties. A determination to find workable compromises was the hallmark of the drafting process. Representatives that in other contexts would be fierce competitors share expertise, policies and performance data etc. This was a larger than usual Working Group under the ISO-system and the by far largest with the Ship Technology section. The drafting process uncovered a need to address both the most rigorous methods available and the most commonly used approaches used. This led to the division into three parts.

A Committee Draft of part 1 and 2 (CD) was submitted in March 2015. A Ballot among P-members was concluded in May 2015 with sound support. The target date for submitting a Draft International Standard (DIS) of all three parts was December 2015. An ISO-Ballot was concluded in March 2016 and it is expected the Standard will achieve final approval and official publication by June 2016. The Working Group (WG7) will remain operational in order to prepare future revisions and refining the standard.

The preparation for the Standard was followed with great interest for both trade journals and all relevant stakeholders. Many stakeholders are in the process of incorporating the standard in their daily operations and prepare contracts that use the ISO-standards as a point of departure. Ship owner associations are drafting guiding documents and ISO 19030 may also become the bedrock for a carbon offset/crediting scheme incentivising greenhouse gas emission reductions.

4. Frequently asked questions related to ISO 19030

This standard aims at comparing the change of hull and propeller performance of one ship over time compared only to its own performance. Sister ships are regarded to have inherently different performance profiles based on trade and areas of operation. The standard is not developed as a tool to rank

ships or classes of ships. The standard measures relative and not absolute performance. The Working Group acknowledged that “speciality” ships such as offshore service vessels, towing ships, barges etc. and ships with irregular trading patterns are less likely to yield benefits of ISO 19030.

The focus of this standard is limited to hull and propeller performance and do not cover the overall performance of the ship. Covering overall ship performance would be a more challenging task as it includes engine train performance, quality of fuel, wind resistance as well as other drivers of energy efficiency used on board a ship. This first iteration of the hull and propeller performance standard covers fixed single or twin pitch propellers.

In order to include e.g. variable pitch propeller(s) the methodology would have to be developed further. Variable pitch propeller(s) introduce added complications that the first version of this standard was unable to accommodate. Support for variable pitch propellers will - if justified - be included in later revisions of the standard.

The default method (part II) lays out how ship owners and operators can achieve the most accurate measurement of changes in hull and propeller performance. The default method is based on the application of measurement equipment, information, procedures and methodologies that are generally available and internationally recognized. This will evolve over time and revisions of the standard will accommodate improved approaches.

A number of ships will not be equipped with the measurement equipment, information, procedures and methodologies which is required to meet the default method. Part 3 outlines alternatives to the default method for measuring changes in hull and propeller performance and defines the effects these alternatives will have on overall accuracy. Part 3 introduce proxies or alternative measurements and outlines how they will affect the overall accuracy. The more alternatives introduced combined with changes in data collection frequency and evaluation periods will subsequently decrease the accuracy. For some applications a lower accuracy may still be acceptable to the user of the standard. The selection of acceptable measurement criteria will depend on the specifics of the vessel, operations, and anticipated use of the performance indicators.

Continuous monitoring provides more data points to allow greater accuracy during shorter evaluation periods and reduce human error and filter out various conditions (for instance transient conditions and bad weather). Continuous monitoring is a requirement of the default method. Noon reporting is still a common practice on many vessels. Noon reporting is therefor an option in part 3.

Part 2 have minimum requirements outlining instrument specification, maintenance and calibration procedures. The alternative method in Part 3 offers several proxy options with alternative measurements. The accuracy of a measurement is determined by both its’ trueness and precision (ISO 5725). Trueness refers to the closeness of the mean of the measurement results to the actual (true) value and precision refers to the closeness of agreement within individual results. Precision is a function of both repeatability and reproducibility, where reproducibility refers to the variation arising using the same measurement process among different instruments and operators, and over longer time periods. Measurement procedures have a considerable impact on the reproducibility of, and therefore on the accuracy of, the performance indicators.

The ISO standard filters and corrects for wind based on on-board wind measurements. Annex C in Part 1 explains how calculations of true wind speed and direction. Salinity is rarely measured on-board vessels. Seawater temperature is used to filter out icy water conditions since the ISO standard cannot take into account the ice conditions directly (less than 2 degrees Celsius). For the time being, waves are not measured and not filtered out directly. However, wind generated waves will indirectly be filtered out by filtering for wind. Further revisions of the standard may take into account waves directly, but at the time of this version of the standard, accuracy of wave measurements are not considered adequate.

The basis for accuracy in this ISO standard is Consistent with ISO 5725-1 Accuracy (trueness and precision) of measurement methods and results. Three important sources of uncertainty influencing the accuracy of the performance indicators are:

1. measurement uncertainty (e.g. related to a sensor's accuracy - both uncertainty that might be observed in a laboratory test in ideal conditions, and any additional uncertainty that might be related to a sensor's installation, maintenance and operation by an operator);
2. uncertainty introduced through the use of a sample, an average or aggregate values of a parameter when that parameter is variable with time (e.g. using an average of the wind speed over a period of time);
3. uncertainty introduced through the use of equations that necessarily simplify relationships in order to manage the complexity, or because of imperfect information (e.g. use of sea trial data for draught corrections, or the approximation in the Admiralty formula if used to normalize data measured at a specific draught to a reference draught).

Bearing in mind that this standard is measuring relative changes in performance, differing response from speed measured by speed logs and GPS readings it is not a concern as long as it is constant. Sensor drift will on the other hand need to be monitored and trigger calibration. The standard assumes that instruments are calibrated according to manufacturers' specifications. Users of this standard may use fixed speed rather than power as a constant. Power increase will be computed from speed loss using the speed reference curves.

References

CSC (2011), *A transparent and reliable hull and propeller performance standard*, Submitted by Clean Shipping Coalition to MEPC63/4/8

IMO (2014), *Third IMO Greenhouse Gas Study 2014*, IMO, London

<http://www.imo.org/en/OurWork/Environment/PollutionPrevention/AirPollution/Pages/GHG-Emissions.aspx>

Predicting the Impact of Fouling Control Coatings on Ship Powering Requirements and Operational Efficiency

Barry Kidd, AkzoNobel/International Paint Ltd., UK, barry.kidd@akzonobel.com

Alistair A. Finnie, AkzoNobel/International Paint Ltd., UK, alistair.finnie@akzonobel.com

Haoliang Chen, AkzoNobel/International Paint Ltd., Singapore, haoliang.chen@akzonobel.com

Abstract

New ship powering prediction models are presented which combine an assessment of total roughness (comprising micro, macro and fouling roughness components) with CFD modelling of total resistance for different hull forms. The model is directly applicable for most commercial vessel types and operational profiles, and the modelled outputs include quantitative analyses of powering requirements, fuel consumption, cost / benefits and consequent environmental emissions over a full drydock cycle for relevant potential fouling control coating choices. The impact of sub-optimal fouling control coating choice on vessel performance is well recognised and so the ability of ship owners and operators to make informed coating selection choices is of critical importance.

1. Introduction

AkzoNobel through its marine coatings business, International Paint, has a long history of providing effective fouling control solutions and services to the marine industry, *Kidd et al. (2013)*. Given the operational pressures that ship operators face in today's increasingly competitive market it is clearly important for budget holders to make an informed choice of fouling control coating for their ships. When a ship operator makes an investment in a fouling control coating, the expectation is that the coating will provide reliable and consistent performance. In simple terms, a successful fouling control coating is one that provides fouling protection and minimises any frictional resistance and powering increase over the entire drydock cycle. Before making a decision, evidence of historical performance is usually reviewed, normally derived from past experience of hull coatings used on similar ships with similar speed ranges and operational profiles. Very often this information is presented as observations of coating performance over time and is, where possible, supported by data for in-service ship performance. Whilst this type of historical evidence is important, it does not always provide the ship operator with sufficient detail to perform a reliable cost benefit analysis of the different coating options for their specific ships.

Fouling control coating choice is one of the key variables influencing ship efficiency, *Finnie and Williams (2010)*. The frictional resistance of the underwater hull surface of a ship can contribute between 50-85% of the total resistance experienced, *Lewis (1988)*. Maintaining a smooth and clean hull condition is important and selecting the optimal fouling control coating can help maximise ship operational efficiency over a drydock cycle. However, as even the best fouling control coating is unlikely to prevent all fouling on all ship types under all conceivable operational profiles it is advantageous to explicitly consider the potential risk of fouling when selecting a fouling control coating.

No ship's hull is hydrodynamically smooth and naval architects have long recognised the general impact of surface roughness on vessel powering requirements, *Lackenby (1962)*. Work by *Townsin et al. (1980,1986)* to quantify the impact of Average Hull Roughness (AHR) was particularly valuable. This approach was accepted by the International Towing Tank Conference, *ITTC (1990)*, and is still commonly used to predict the powering penalties associated with changes in hull and coating roughness over a drydock cycle relative to a hypothetical hydrodynamically smooth surface. Building on this seminal work, *O'Leary and Anderson (2003)* introduced the Hull Roughness Penalty Calculator, a software model that predicts ship powering as a function of the predicted increase in underwater hull roughness combined with the risk of fouling associated with different fouling control coating types over a drydock cycle.

More recently, Schultz (2007), Schultz et al. (2011) provided fresh insight into how fouling control coatings and the impact of biofouling may affect the performance of naval ships. Building on this work, Stenson et al. (2013,2014) reviewed the impact of micro and macro physical roughness and developed a revised approach to predicting the impact of hull roughness on the frictional resistance of ships. The impact of antifouling coatings on ship resistance and powering has also been discussed by Demirel et al. (2013,2014), who highlighted a new CFD model which enables prediction of the effect of antifouling coatings on frictional resistance.

These previous approaches provide valuable insights into the potential performance implications of different hull and coating conditions and are useful as general guides. In today’s increasingly competitive market, vessel operators require clearer guidance on the potential performance benefits of fouling control coatings for their specific vessels so that they can make the optimal coating choices. Delivering this expectation requires the development of new fouling control coating performance models which can only be developed from a substantial database of in-service coatings performance, such as AkzoNobel’s Dataplan® system. In conjunction with this, it is important to correlate Data-plan® with the operational profile of the vessels to further enrich our understanding of the key operational variables which impact on the in-service performance of coatings.

The work presented in this paper describes the development of a new model to predict the impact of fouling control coating choice on ship operational efficiency which aims to provide reliable comparative powering requirement, fuel consumption, cost / benefit and environmental impact analyses for potential fouling control coating choices over the full drydock cycle.

2. Prediction of total roughness change over a drydock cycle

2.1. A new total roughness model

Any approach to model the impact of the fouling control coating choice on vessel operational efficiency should ideally encompass a detailed understanding of the impact of vessel operational profile on the performance of the coating. If settlement and growth of biofouling on the coating occurs, this will influence the frictional resistance of the hull, as will the micro and macro roughness characteristics of the hull. In order to take these factors into account, a new total roughness model has been developed which, by analogy, considers the effect of the biofouling as “fouling roughness”. This is then combined with the micro and macro roughness in order to provide a measure of the “total roughness” of the hull, Fig. 1.

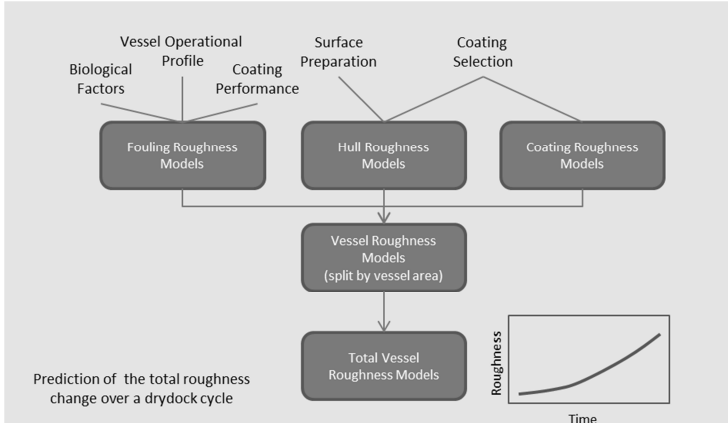


Fig. 1: Overview of the new total vessel roughness model

It is important to realise that “fouling roughness” as used in this model does not relate to the physical surface roughness of the fouling as measured directly, for example via profilometry. Instead, by “fouling roughness” we mean the equivalent sand-grain roughness (k_s) that would give rise to the same frictional resistance as the particular type and extent of fouling that is present. This approach is

in line with Schultz’s work on ship powering requirements and by using Townsin’s standard correlations with AHR we can also express the micro and macro roughness in terms of k_s and so readily combine the three parameters to quantify the total roughness.

Additionally, it is common practice to apply different fouling control coatings to different vessel areas. For example, for economic or performance reasons, different coatings will often be applied to the underwater vertical sides and the flat bottom, or boot-top areas. This complexity is dealt with by new vessel roughness models that have the ability to take into account the individual and collective contributions of different coating choices on different areas of the vessel.

The development of new hull roughness and coating roughness models have been explored by *Stenson et al. (2013,2014)*, who proposed an updated model for predicting the average hull roughness (AHR) of ships. This updated model considers the impact of micro and macro roughness elements on the ship’s hull separately. In general the macro elements relate to the underlying substrate roughness or hull roughness and the micro elements relate to the coating roughness. While this new model offered an improvement on previous approaches, the impact of the “fouling roughness” must be included to deliver a more comprehensive and reliable total roughness model.

2.2 The development of fouling roughness models

A necessary first step in the development of any new fouling roughness model involves a review of the impact that vessel operational profiles have on fouling control coating performance. All of the detailed ship operational profile information used in this study was generated by Intertrac®, a proprietary software platform developed by AkzoNobel that interrogates satellite and terrestrial AIS data and captures date and time stamped information regarding a vessel’s position, speed, bearing and draught, etc. for all time points from 2009 onwards when satellite AIS data became available. This allows a detailed picture to be derived of any individual vessel’s trading route, activity, speed distribution and where and when the vessel was static. Intertrac® also makes use of the concept of multiple separate marine eco-regions, *Sherman (2005)*, and characterises the relative risk of fouling, taking into account the amount of time the vessel spends in each eco-region and further adjusted for the seasonal variation in the fouling challenge.

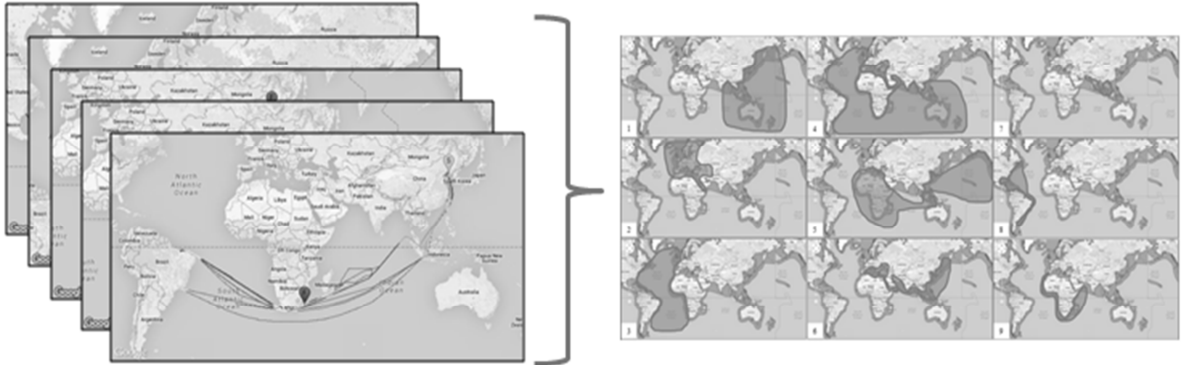


Fig. 2: Grouping vessel operational profiles into example representative aggregated trading routes

By repeating this process for multiple ships it is possible to reduce the complexity of the overall dataset by identifying common trading patterns and operational profiles for the world fleet and grouping these vessels together into aggregated trading routes, Fig. 2. There are approximately 100,000 vessels in the world commercial shipping fleet, *IMO (2009)*. While it is possible in principle to perform this analysis for all these vessels, it is more practical to use a representative sub-set of vessels. Therefore in this work we have made use of the dataset of the several thousand vessels coated with AkzoNobel’s International Paint fouling control products since 2009.

In this initial phase of development, nine aggregated routes were selected, comprising a variety of common intercontinental and coastal trading routes. Although it would be possible to identify many more aggregated routes, this represents a pragmatic approach and the selected routes reflect the operational profiles for the majority of world commercial shipping fleet, *UNCTAD (2015)*.

Having performed this grouping exercise we can now consider the relationship between the different environmental and fouling challenges prevalent within each aggregated trading route and the performance of different fouling control coating products. The source of fouling control coating performance information used in this work is AkzoNobel’s extensive database of drydock and in-water inspections of fouling control coatings applied to each vessel. The key output from this review is the development of a coating performance index related to each aggregated trading route and each fouling control coating product for each area of the underwater hull of the vessel, e.g. the flat bottom, vertical sides or boot-top areas, Fig. 3.

The coating performance index provides valuable information regarding the expected relative performance of different fouling control coating options for a vessel with a particular trading route and operational profile. As stated earlier, even the best fouling control coatings are unlikely to prevent all fouling, on all ship types under all conceivable operational profiles. This is reflected in the fact that the absolute in-service performance of a fouling control coating is often strongly influenced by the operational profile of the vessel to which it is applied. In general terms it has been recognised for many years that risk of fouling is greater for vessel operating at slower speeds, with longer static periods, longer drydock cycles, exposed to warmer sea temperatures and operating in coastal trading routes, *Visscher (1927)*. In reality, any fouling control product applied to a range of vessels is therefore likely exhibit a range of fouling control performance profiles across the fleet. The coatings performance index therefore takes this actual range of performance into account rather than simply relying on a nominal “best case” performance profile.

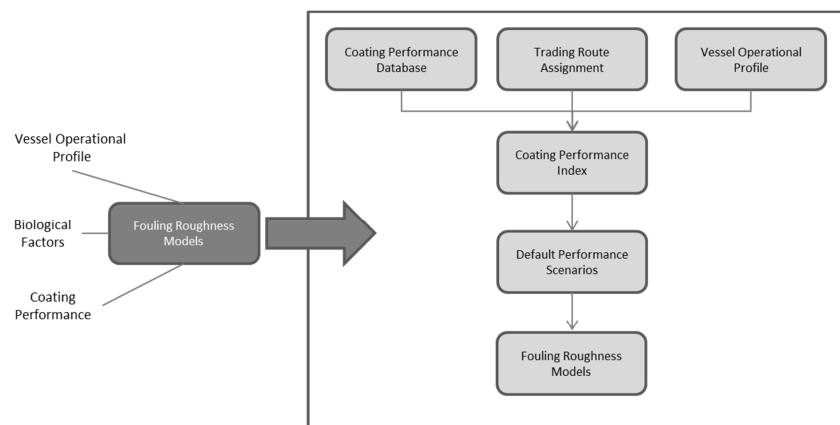


Fig. 3: Overview of the development of the fouling roughness models

The coating performance index is additionally sub-divided into a series of “performance scenarios”. These performance scenarios are based on an expected statistical distribution of real life in-service coating performance, allowing a more realistic assessment to be made of the range of performance that may be delivered by each potential coating choice. The three default performance scenarios in the model are:

- 1) a performance profile reflecting the high performance level achieved on the majority of vessels (typically 70% or more);
- 2) a lower performance profile, reflecting the lower performance level achieved on a subset of vessels (typically 20% or less);
- 3) a third performance profile, reflecting the significantly poorer performance level that is achieved on a very small subset of vessels (typically 10% or less).

It is expected that these default scenarios will be relevant to most combinations of coating choice and operational profile, but the fouling roughness models have built-in flexibility to introduce alternative performance scenarios as required. However, as the first default scenario reflects the high level of performance that will be achieved on the vast majority of vessels, it is expected that this scenario will have the greatest relevance to ship owners and operators.

The default performance scenarios are translated into an equivalent sand-grain roughness (k_s) scale to derive the fouling roughness models. This builds on the approach of *Schultz (2007)* and *Schultz et al. (2011)* and utilises a new empirical polynomial expression which is derived from the correlation of coating performance index with the equivalent sand-grain roughness for each fouling type and extent.

It will be realised that biofouling growth is generally a progressive phenomenon and so a key next step in the model is to take account of how the “fouling roughness” will change over the relevant drydock cycle. One of the major factors influencing how the fouling roughness changes over a drydock cycle is vessel activity. In this model vessel activity is determined using Intertrac® software platform and is taken to be the total percentage of time during a given period when a ship is travelling at a speed over ground of >3 knots. Through interrogation of the Dataplan® database, the fouling control coating performance can be correlated with vessel activity in order to derive a vessel activity factor. Specific vessel activity factors can be generated as required representing appropriate sub categories of the world’s commercial shipping fleet such as specific ship types (e.g. bulkers, tankers, container vessels, etc.), particular aggregated trading routes, Fig. 2, and/or particular fouling control coating choices etc. By bringing these factors together a theoretical fouling roughness prediction can be derived for each performance scenario over the drydock cycle.

As shown in Fig. 1, the modelled fouling roughness is then combined with the modelled hull and coating roughness values in order to provide a total vessel roughness.

3 Correlation of total roughness, total ship resistance and powering requirements

The powering requirements for a vessel are intimately linked to the resistance of the ship’s hull to movement through the water. This resistance comprises a number of key components, the most important of which are the frictional resistance, wave resistance and pressure resistance. Generally, the frictional resistance is much larger than the wave resistance and typically comprises 50-85% of the total ship resistance for most commercial ships at normal operating speeds, *Lewis (1988)*. As the frictional resistance is induced by shear stress over the surface of a hull, a key factor affecting the total resistance is the roughness of the hull. The higher the hull roughness, the higher the frictional resistance and the higher the power required to maintain a ships speed. As a result, more fuel will be burned and more greenhouse gas (GHG) will be emitted, *Armstrong (2013)*.

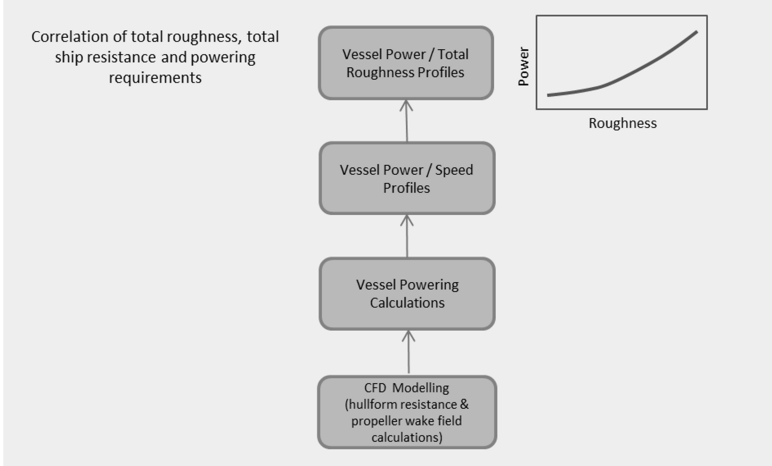


Fig. 4: Overview of the ship powering requirement model

The approach used to predict the impact of changes in total vessel roughness over the drydock cycle has been described in Section 2. As illustrated in Fig. 4, the total vessel roughness model can now be further expanded to provide an overall model of ship powering requirements.

This work initially focussed on the development of vessel powering requirement models for representative hull forms including bulkers, tankers, and container ships which reflect over 85% of the world's commercial fleet, *UNCTAD (2015)*. Given that the predicted powering requirements for these hull forms are directly related to their shape and size, typical small, medium and large examples of each within the commercial fleet were selected, Table 1.

Table 1: Modelled hull form characteristics

Hull form Type	Hull form Parameters	Small Size	Medium Size	Large Size
Bulkер	Length between perpendiculars (m)	160	194.5	290
	Breadth moulded (m)	31	32.26	15
	Design draught moulded (m)	11.6	13.3	18.3
	Displacement volume moulded (m ³)	44985	71716	204693
	Displacement mass (T)	46109	73509	209810
	Wetted surface area (m ²)	7402	10278	20894
	Block coefficient	0.78	0.86	0.86
Tanker	Length between perpendiculars (m)	160	255	324
	Breadth moulded (m)	31	50	60
	Design draught moulded (m)	11.6	17	21.5
	Displacement volume moulded (m ³)	44985	178793	344440
	Displacement mass (T)	46109	183263	353051
	Wetted surface area (m ²)	7402	18534	28874
	Block coefficient	0.78	0.82	0.82
Container	Length between perpendiculars (m)	100	220	319
	Breadth moulded (m)	13.35	32.2	48.2
	Design draught moulded (m)	5.7	10.5	13
	Displacement volume moulded (m ³)	6073	48169	119847
	Displacement mass (T)	6224	49373	122843
	Wetted surface area (m ²)	2172	8820	17203
	Block coefficient	0.8	0.65	0.6

3.1 CFD Calculations of Total Ship Resistance

Because of the impracticality of performing routine full-scale ship trials, model-scale tests, such as towing tank trials are commonly employed to generate information on the form drag and understand the impact of hull design and operational parameters on powering requirements. However, even such model-scale tests are often difficult, expensive, time consuming and practically challenging, especially when multiple parameters are being varied. Increasingly such model-scale testing is often supplemented by Computational Fluid Dynamics (CFD) modelling in order to characterise the nature of the flow of seawater over a ship's hull and provide calculations of the boundary layer conditions.

In this study, CFD modelling was performed via MARIN's proprietary PARNASSOS CFD software, *Hoekstra and Eca (1998,1999)*. This was used for each representative hull form and size at a range of speeds to calculate the local skin frictional resistance over the hull form resulting from total roughnesses, expressed as the equivalent sand grain roughness, ranging from 0 μm , representing the hypothetical hydrodynamically smooth surface, up to 1000 μm , representing roughness that would result from presence of significant hard shelled animal fouling and weed, *Schultz (2007)*. Examples of typical outputs of the modelling are shown in Fig. 5.

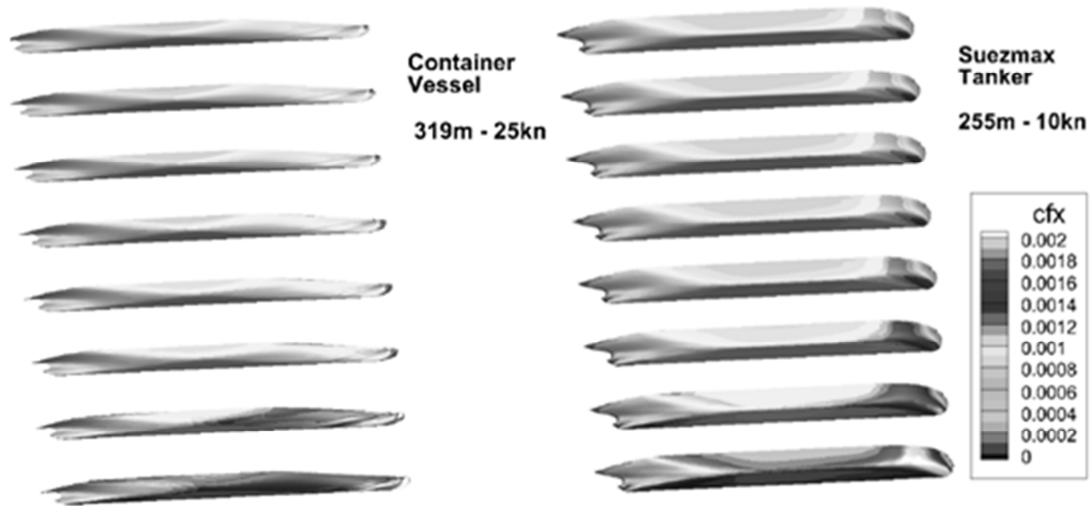


Fig. 5: Local skin friction coefficient (c_{fx}) maps for a large containership at 25 kn (left) and a medium sized tanker at 10 kn (right); total roughness ranges from 0 (top) to 1000 μm (bottom).

In addition to using CFD to calculate the effect of total roughness and vessel speed for the different hull forms, CFD has also been used to calculate the effect of the wake field on propeller efficiency. A higher roughness increases the boundary layer thickness and leads to a higher wake fraction in the propeller plane. Due to this, the propeller encounters water with a lower velocity and subsequently the propeller loading becomes higher. A higher loading can lead to a lower efficiency. Thus it would be generally expected that as well as leading to a higher frictional resistance of the hull, an increase in roughness would also be expected to lead to lower propeller efficiency, *Carlton (2007)*.

The results of the CFD calculations are in line with general expectations, but also indicate that the impact of roughness on the wake fraction is also different for each hull form and depends on vessel size and speed; see Fig. 6 for a typical example.

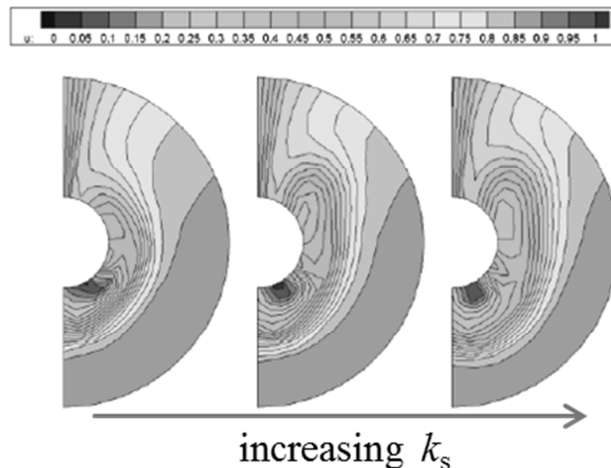


Fig. 6: Calculated wake fields for a typical large bulk carrier hull form (Capesize) at 14.5 knots and equivalent sand-grain roughness 30 μm (left), 75 μm (middle), 300 μm (right)

A fully comprehensive programme of work would require an impractical amount of computing resource and time in order to model all possible draft conditions for each roughness and speed scenario for each representative hull form and size. Therefore in this initial study only the fully laden condition or maximum design draft is modelled. Further work to model a more extensive range of draft conditions is expected to follow at some future point.

3.2 Calculating Vessel Powering Requirements, Fuel Oil Consumption and Emissions

MARIN's DESP software package was used to compute the powering requirement for each hull form for the hypothetical hydrodynamically smooth condition and the selected range of total vessel roughness, expressed as an equivalent sand-grain roughness. DESP predicts the resistance and propulsion characteristics of displacement ships and makes use of the Holtrop-Mennen approach, *Holtrop and Mennen (1982)*, *Holtrop (1984)*. After selection of the propeller type and dimensions, the required thrust is modelled using the calculated resistance and a statistically determined thrust deduction. The effective wake fraction and relative rotative efficiency are also determined and together with the calculated open-water efficiency of the selected propeller the overall powering requirements are calculated for each relevant operational profile.

A series of speed/power curves for each hull form and size are then generated at a series of total vessel roughness from $k_s = 0$ to $1000 \mu\text{m}$. As illustrated in Fig. 7, the relationship between total vessel roughness and power requirement for any particular hull form at any particular speed can then be readily derived.

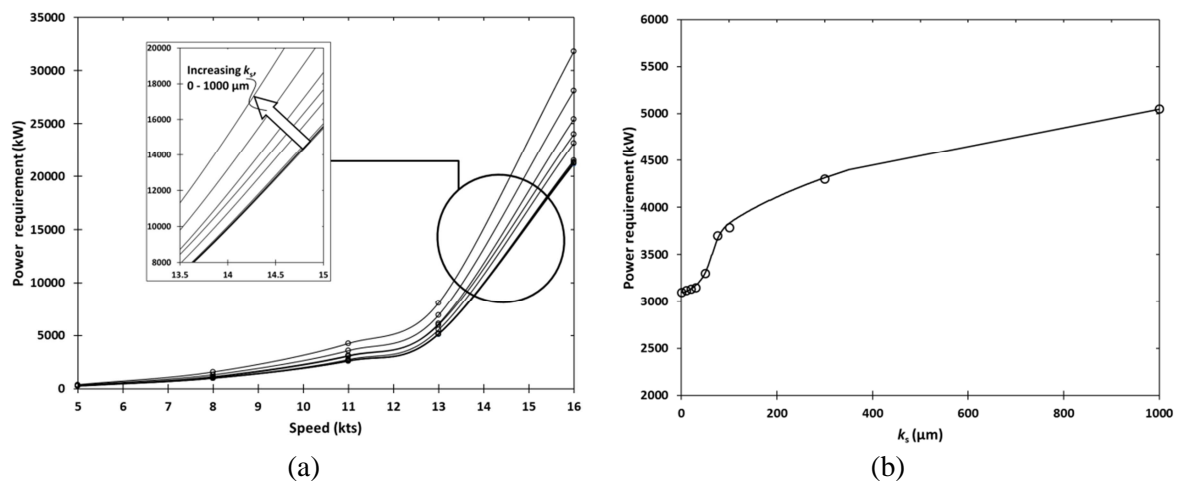


Fig. 7: (a) Representative speed/power profile for a 60k DWT bulk carrier hull form for a range of total vessel roughness from 0 to $1000 \mu\text{m}$ and (b) derived relationship between total vessel roughness and required power at 12 knots

The impact of the predicted vessel powering requirement on fuel oil consumption (FOC) can be determined relative to an appropriate reference consumption. This is achieved by making the common assumption that the required vessel power and FOC are directly proportional to each other, *Lu et al. (2013)*. Typically the reference FOC is based on the actual FOC from a ship in-service with known hull condition. Alternatively, if suitable in-service reference data is unavailable for the particular vessel in question, an FOC prediction can be made relative to the actual FOC for a related vessel.

The total cumulative CO_2 emissions are calculated from the FOC in MT/day based on the assumption that every tonne of fuel consumed typically generates 3.2 tonnes of CO_2 , in line with IMO guidance, *IMO (2014)*.

4. Putting the models into practise

As illustrated in Fig. 8, the new models discussed above predict the impact of fouling control coating choice on ship powering requirements for various ship types, sizes and operational profiles. These models can be considered to follow a “bottom-up” approach, i.e. they make use of observations of past fouling control coating performance to make future predictions of vessel powering requirements. As outlined in Section 3, the underlying model is based on data for only a limited set of representative hull forms and sizes. When using the model to predict powering requirements for vessels that do not

exactly correspond with any of these particular vessel characteristics, the model will default to the closest fit based primarily on the vessel's length between perpendiculars, DWT and block coefficient.

Among the typical outputs that are generated from these models for each potential coating selection and substrate preparation choice are predictions of ship powering requirements, fuel oil consumption and cost, and GHG emissions over the full drydock cycle. A key benefit of this new approach is the ability of the model to take into account the application of different fouling control coatings to different areas of same vessel. Additionally the model is also able to take into account the impact of surface preparation (for example spot blasting versus full blast prior to painting) and hull cleaning choices on vessel powering requirements.

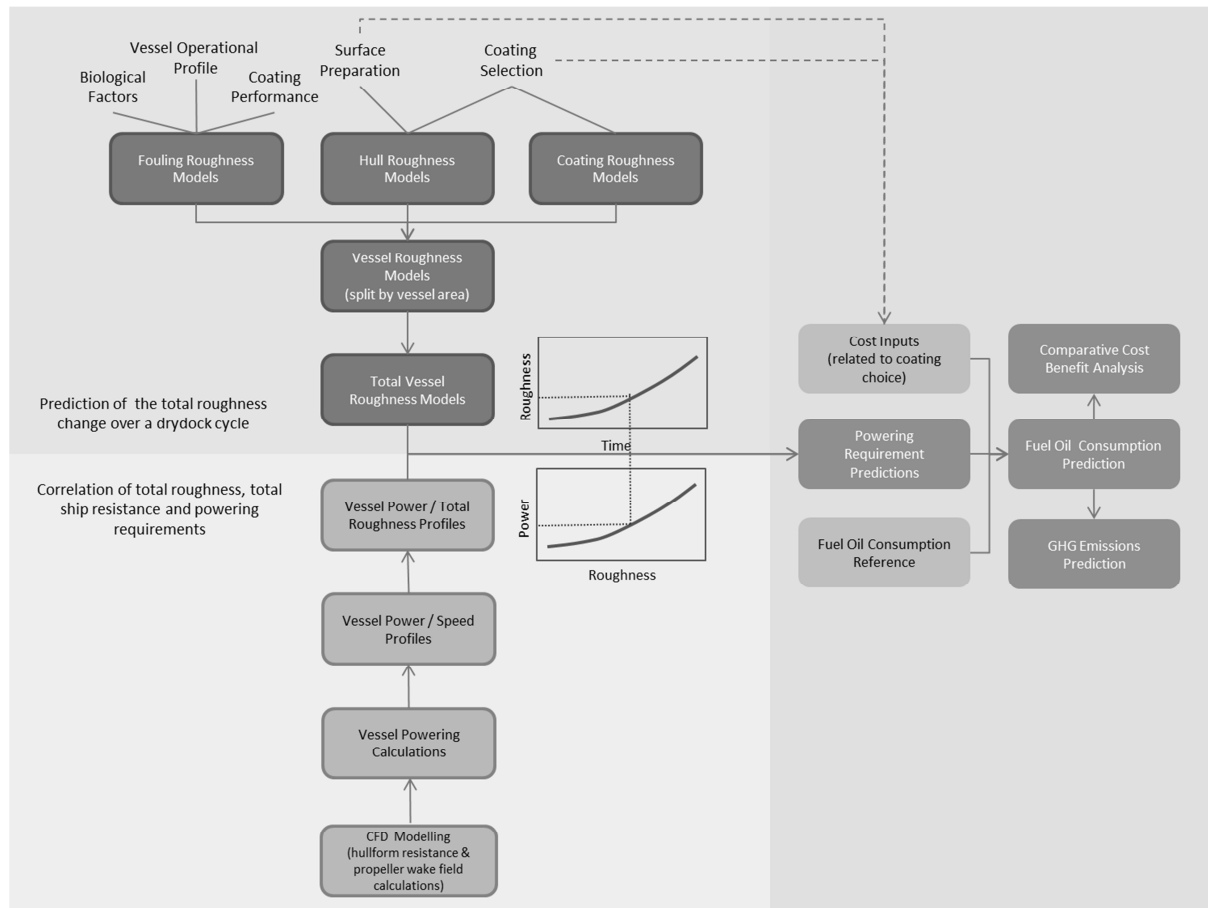


Fig. 8: Overview of the new vessel powering requirement models showing required inputs, key processes and typical outputs

As highlighted earlier, no currently available fouling control coating is likely to equally prevent all fouling on all ship types under all conceivable operational profiles. The new model therefore explicitly considers the potential risk of fouling for each fouling control coating option that is being considered for a particular vessel with a particular expected operational profile. The adopted approach considers the three default performance scenarios outline in section 2.2 in order to establish the potential risk of fouling and compares the relative difference in the percentage increase in powering requirement for each scenario. In this way a comprehensive and transparent overview of the predicted risk of fouling can be generated for each scenario and coating choice under consideration, see Fig. 9(a), where a new build 115k DWT tanker is assumed to operate on a worldwide trading route at 85% activity, an average speed of 13 knots and with a drydock cycle of 60 months).

Another important benefit of these new models is the ability to simultaneously compare the percentage increase in required power for several different fouling control coating options. In the illustrative case shown in Fig. 9(b), selection of the example foul release coating (FRC) product is predicted to

deliver a significantly reduced percentage increase in power requirement over the dry-dock cycle in comparison to the example SPC and CDP products. This reflects the ability of this particular FRC to generally provide superior fouling control performance over the drydock cycle than this particular SPC, which in turn provides better fouling control performance than the particular CDP.

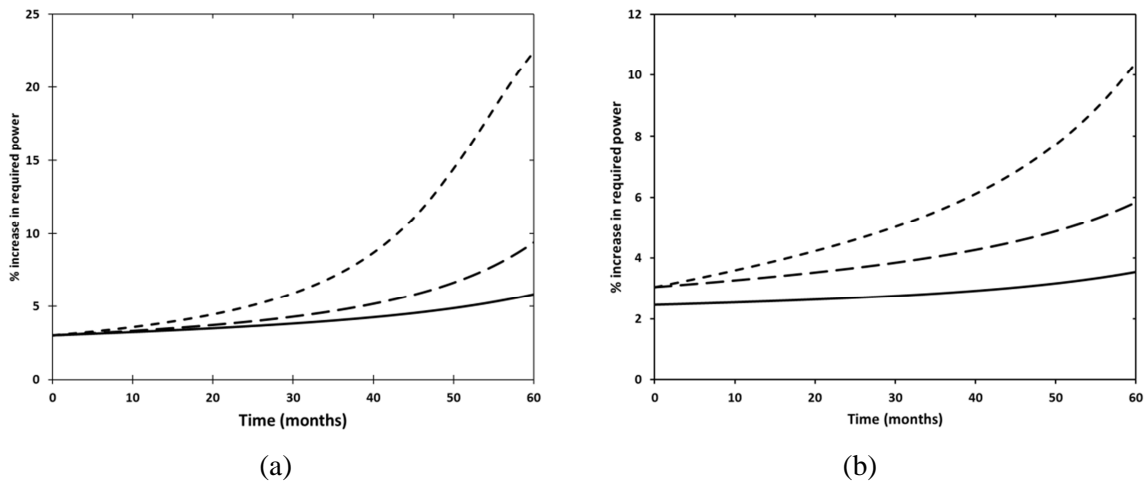


Fig. 9: Predicted % increase in required power for a new build 115k DWT tanker with (a) an example SPC coating applied to the entire underwater area for default performance scenario 1 (solid line), 2 (long dashes) and 3 (short dashes); and (b) example FRC (solid line), example SPC (long dashes), and example CDP (short dashes) applied to the entire underwater area for default scenario 1.

As described by *Stenson et al. (2014)*, the extent of substrate preparation (i.e. extent of blasting) is chief amongst several parameters that dictate the expected macro roughness of the hull following maintenance and repair and coating re-application operations. Specifically, macro roughness is minimised when the hull has been fully blasted prior to re-coating but is significantly increased when only spot blasting is performed. The impact of different hull preparation options from a fully blasted condition through varying degrees of spot blasting on the predicted powering requirements can also be performed. The models allow the effect of hull preparation to be explicitly reviewed so that the impact of surface preparation and coating selection can be considered both separately and in combination as part of an overall cost benefit analysis.

However, it is no surprise that the results of such a cost benefit analysis are also highly dependent on several other factors, most notably the cost of the relevant fouling control coatings to be applied to the different vessel areas (including the costs of the required primers and tie-coats etc.), the cost of substrate preparation (blasting/spot blasting), the total roughness model appropriate to the selected fouling control coatings, the vessel's hull form and size, the vessel operational profile (activity, average speed and trading route), vessel fuel costs and the expected baseline FOC for the vessel when it enters service. Commercially, an additionally important factor is the breakeven or payback period over which the costs of any particular investment become outweighed by the financial benefits of that choice. A number of approaches can be adopted to perform a cost benefit analysis, but perhaps the most insightful approach is one that considers a comparison of the available fouling control coatings choices. As an illustration, Figure 10 highlights the total accumulated costs over a 60 month drydock cycle for the example fouling control coating products discussed above applied to 13k TEU/142k DWT containership a trans-Pacific route with 80% activity and an average speed of 18 knots.

In this case, the example CDP product is used as the reference fouling control coating: typically the example SPC and FRC products will exhibit superior fouling control performance in comparison to the example CDP product, although the overall initial investment costs for the example CDP will be less. As can be seen from Fig. 10, the breakeven point or payback period at which the additional investment cost of selecting the example SPC or FRC product is outweighed by the reduced

operational costs that accrue from the reduced FOC is less than 2 years for this particular vessel. Additionally, the financial benefit of selecting this example FRC product in preference to these SPC and CDP products is approximately \$1.5 million and \$3 million respectively over the drydock cycle. Obviously, the actual cost benefit will vary significantly depending on the vessel type and operational profile, the specific coating options under consideration and the projected fuel price over the drydock cycle. In each case this approach will allow particular fouling control coating options to be readily ranked and the associated costs and/or benefits to be directly quantified.

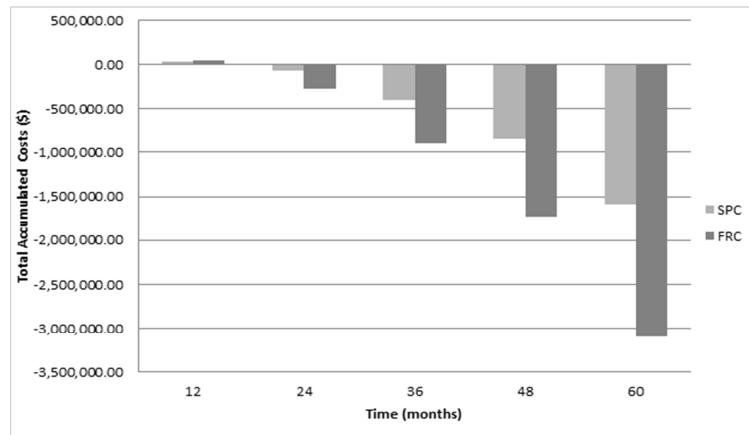


Fig. 10: Total accumulated additional costs (\$) over a 60 month drydock cycle for the example SPC and FRC products relative to the example CDP product when applied to the entire underwater area of 13k TEU/142k DWT containership

It should be noted that the example above is for a relatively fast vessel. As could be expected, the model indicates that the predicted return on investment from the selection of a high performance FRC may be less pronounced for slower vessels with lower FOC, such as tankers and bulkers.

Understanding the validity of these new “bottom up” empirical models is a critical step in developing confidence in the accuracy of the predictions to reflect what happens during the real in-service drydock cycle for any relevant vessel. In collaboration with University College London and several commercial ship operators, work is underway to compare the predicted powering requirements with real in-service data for, in the first instance, more than 80 vessels. At this point in time, collation and analysis of the datasets is not yet complete and it is too early to draw definitive conclusions. However, early results indicate that the model predictions generally correlate well with reality. As an example, the modelled percent increase in required power under the 3 default performance scenarios versus the determined percentage power increase in for a 52k DWT/4250 TEU containership is shown in Fig. 11.

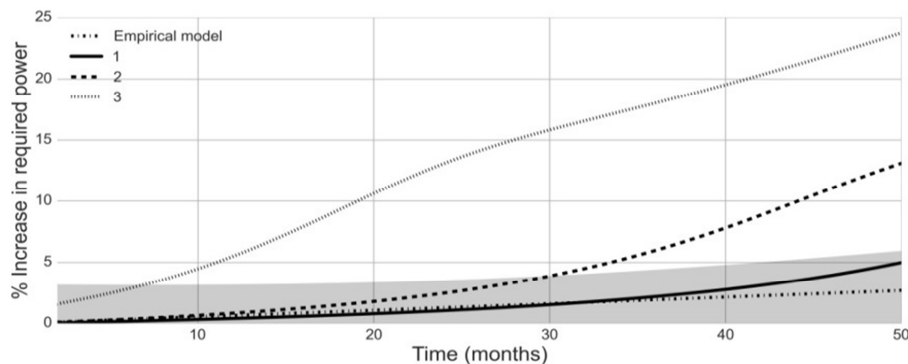


Fig. 11: Predicted % increase in required power for a 52k DWT / 4250 TEU containership coated with example FRC coating applied to the entire underwater area default performance scenarios 1 (solid line), 2 (dashes) and 3 (grey dots), overlaid with the percentage power increase determined from the empirical model from the real in-service vessel data (black dots) and the 95% confidence interval for the empirical model (grey shading)

In this example the vessel was operating on a trans-Pacific trading route with 63% activity and an average speed of 17.3 knots and a drydock cycle of 50 months. As can be seen, the modelled power increase not only falls comfortably within the 95% confidence interval for the determined power increase, it is almost coincident with the average trend line.

These initial results support the general validity of the new approach and further testing will continue with the aim of establishing an enhanced dataset of in-service data and demonstrating the utility of the model for a full range of ship types and operational profiles.

5. Conclusion

The impact of sub-optimal fouling control coating choice on vessel performance is well recognised. Ship owners and operators are sometimes sceptical about comparative fouling control coating performance claims, perhaps in part because it is often not clear on what basis the comparisons have been made. As such, there is a genuine need for more accurate and transparent prediction approaches to be developed. In response to this, new models have been developed for predicting the impact of fouling control coating choices on ship powering requirements and operational efficiency which incorporate a number of refinements and improvements over previous models.

These models can be broken down into two main component sub-sections: firstly, models for how the total roughness of the vessel changes over a drydock cycle for each coating option in response to the ship's operational profile; and secondly, models to correlate the total vessel roughness to total ship resistance and powering requirements. The model for the total roughness change makes use of a new total roughness treatment that takes account of the micro and macro roughness of the hull and the impact of biofouling (if any), characterised as the "fouling roughness". The total roughness model also takes account of the effect of substrate preparation and coating application choices on surface roughness and builds on an enhanced understanding of the impact of vessel operational profile including, hull cleaning events, on coating performance. The correlation of total roughness, total ship resistance and powering requirements is based on new CFD resistance and wake field flow models for different representative hull forms, incorporation of these CFD models in optimised ship powering requirement calculations, derivation of speed / power curves as a function of total roughness, and an enhanced understanding of how ship powering requirements is influenced by the total roughness.

The key outputs of these new models include predictions of vessel powering requirement, fuel oil consumption, fuel oil cost, GHG emission predictions and full cost benefit analyses over the full drydock cycle for each potential fouling control coating choice. The overall approach can be considered to follow a "bottom-up" approach as observations of past fouling control coating performance are used to make future predictions of vessel powering requirements. The approach also offers many new insights regarding vessel operational profiles and allows the optimal fouling control choices and hull preparation scenarios to be identified for each individual vessel (or fleet of vessels), operational profile and budget. Additionally, as this new model adopts a more holistic approach than most previous general models used by the shipping industry, then it seems reasonable to suggest that it should therefore provide more valid (i.e. accurate and reliable) predictions than previous models.

Initial work to assess the accuracy and reliability of the new models is underway and a substantial dataset comparing model predictions to the actual in-service performance of a wide range of commercial ships is currently being generated. In contrast to the bottom up modelling approach, this work can be considered as using a "top down" approach whereby vessel powering trends are derived from real in-service data collected from vessels where the fouling control coating performance and hull preparation history is known.

These new models are already being used commercially by AkzoNobel through the Intertrac@Vision software platform. The stated intention of Intertrac@Vision is to allow ship owners and operators to make informed decisions regarding fouling control coating selection from both an economic and environmental perspective, *NN (2015)*. As the library of real life vessel performance data expands to

encompass a fuller range of vessel types, operational profiles and fouling control options we anticipate that further refinements and improvements will be made as the models continue to evolve.

Acknowledgements

The authors would like to acknowledge and thank the following for their contributions to the developing of the powering predictions models: Joy Klinkenberg and Klaas Kooiker of MARIN for CFD modelling and vessel powering requirement calculations; Tristan Smith and Eoin O’Keeffe of University College London for analysing in-service vessel performance data, the development of “top-down” vessel performance models and validation of the powering predictions models.

References

- ARMSTRONG, V.N. (2013), *Vessel optimisation for low carbon shipping*, Ocean Eng. 73, pp.195-207
- CARLTON, J.S. (2007), *Marine Propellers and Propulsion*, Butterworth-Heinemann, Oxford
- DEMIREL, Y.K.; KHORASANCHI, M.; TURAN, O.; INCECIK, A. (2013), *On the importance of antifouling coatings regarding ship resistance and powering*, 3rd Int. Conf. Technologies, Operations, Logistics and Modelling for Low Carbon Shipping, London
- DEMIREL, Y.K.; KHORASANCHI, M.; TURAN, O.; INCECIK, A. (2014), *Prediction of the effect of hull fouling on ship resistance using CFD*, 17th Int. Congress Marine Corrosion and Fouling, Singapore
- HOEKSTRA, M.; ECA, L. (1998), *PARNASSOS: An efficient method for ship stern flow calculation*, 3rd Osaka Coll. Advanced Appl. of CFD to Ship Flow and Hull Form Design, Osaka, pp.331-357
- HOEKSTRA, M.; ECA, L. (1999), *An example of error quantification of ship-related CFD-results*, 7th Int. Conf. Numerical Ship Hydrodynamics, Nantes
- IMO (2009), *Second IMO greenhouse gas study*, Int. Maritime Org., London, pp.33-34
- IMO (2014), *Third IMO greenhouse gas study*, Int. Maritime Org., London, p.327
- ITTC (1990), *Report on the powering performance committee*, 19th Int. Towing Tank Conf., Madrid, pp.235-287
- FINNIE, A.A.; WILLIAMS, D.N. (2010), *Paint and coatings technology for the control of marine fouling*, Biofouling (Eds. Durr and Thomason), John Wiley & Sons, Chichester, pp.185-206
- KIDD, B.; FINNIE, A.A.; STENSON, P.A. (2013), *Low friction fouling control coatings: an International Paint perspective*, J. Japan Inst. Marine Eng. (JIME) 48, pp.34-41
- HOLTROP, J. (1984), *A statistical re-analysis of resistance and propulsion data*, Int. Shipbuilding Progress 31, pp.272-276
- HOLTROP, J.; MENNEN, G.G.J. (1982), *An approximate power prediction method*, Int. Shipbuilding Progress 29, pp.166-170
- LACKENBY, H. (1962), *Resistance of ships, with special reference to skin friction and hull surface condition*, Proc. Inst. Mech. Eng. 176, pp.981-1014

LU, R.; TURAN, O.; BOULOUGOURIS, E. (2013), *Voyage optimisation: prediction of ship specific fuel consumption for energy efficient shipping*, 3rd Int. Conf. Technologies, Operations, Logistics and Modelling for Low Carbon Shipping, London

NN (2015), *In focus: Intertrac®Vision*, Dockyard Magazine, December, pp.32-33

O'LEARY, C.; ANDERSON, C.D. (2003), *A new hull roughness penalty calculator*, The Economic Importance of Hull Condition: A Collection of Technical Papers Reprinted by International Marine Coatings, pp.59-67

SCHULTZ, M.P. (2007), *Effects of coating roughness and biofouling on ship resistance and powering*, Biofouling 23, pp.331-341

SCHULTZ, M.P.; BENDICK, J.A.; HOLM, E.R.; HERTEL, W.M. (2011), *Economic impact of biofouling on a naval surface ship*, Biofouling 27, pp.87-98

SHERMAN, K.; SISSEWINE, M.; CHRISTENSEN, V.; DUDA, A.; HEMPEL, G.; IBE, C.; LEVIN, S.; LLUCH-BELDA, D.; MATISHOV, G.; McGLADE, J.; O'TOOLE, M.; SEITZINGER, S.; SERRA, R.; SKJOLDAL, H.R.; TANG, Q.; THULIN, J.; VANDEWEERD, V.; ZWANENBURG, K. (2005), *A global movement toward an ecosystem approach to management of marine resources*, Marine Ecology Progress Series 300, pp.275–279

STENSON, P.A.; KIDD, B.; FINNIE, A.A. (2013), *Measurement and impact of surface topology and hydrodynamic drag of fouling control coatings*, 3rd Int. Conf. Advanced Model Measurement Technology for the EU Maritime Industry, Gdansk

STENSON, P.A.; KIDD, B. (2014), *Understanding the impact of coating and hull roughness on frictional resistance*, 17th Int. Congress Marine Corrosion and Fouling, Singapore

STENSON, P.A.; KIDD, B.; CHEN, H.L.; FINNIE, A.A.; RAMSDEN, R. (2014), *Predicting the impact of hull roughness on the frictional resistance of ships*, Int. Conf. Computational and Experimental Marine Hydrodynamics (MARHY), Chennai

TOWNSIN, R.L.; BYRNE, D.; MILNE, A.; SVENSEN, T.E. (1981), *Speed, Power and Roughness: The Economics of Outer Bottom Maintenance*, Trans. RINA 122

TOWNSIN, R.L.; BYRNE, D.; SVENSEN, T.E.; MILNE, A. (1986), *Fuel economy due to improvements in ship hull surface condition*, Int. Shipbuilding Progress 33

UNCTAD (2015), *Review of maritime transport 2014*, United Nations, New York and Geneva, ISBN 978-92-1-112892-5

VISSCHER, P.J. (1927), *Nature and extent of fouling of ships' bottoms*, Bulletin of the United State Bureau of Fisheries, Part II, Document 1031, pp.193-252

Automated Hull Surface Preparation and Paint Application and the Potential Influence on Ship Performance

Niels Hentschel, H-PMC GmbH, Hamburg/Germany, hentschel@h-pmc.com

Christoph Rühr, H-PMC GmbH, Hamburg/Germany, ruehr@h-pmc.com

Niklas v. Meyerinck, H-PMC GmbH, Hamburg/Germany, meyerinck@h-pmc.com

Abstract

This paper summarizes the current standards in the surface preparation and coating of cargo vessels as manual processes. Furthermore a newly developed hull ultra-high pressure water blasting and paint application system is introduced. The results of this automated process are described using typical quality standards, showing, that the main benefits among others is a significant reduction in the surface roughness. The potential benefits for resistance reduction, resulting from a smoother coating surface applied by this automated process are presented.

1. Introduction

Despite the decreasing oil price, the focus of the shipping companies is still the optimisation of the vessel's performance. Measures, such as flow optimisation, downsizing of the propulsion systems or the introduction of software-based power management systems are just a part of the main measures. Due to the large ship's wetted surface area and the related friction resistance, the improvement of the hull's coating roughness is indeed an effective and efficient method.

This paper shows the up-to-date possibilities of an automated coating process, offers an overview of the used methods and presents results of automated surface preparation and coating going beyond the quality standards, which were possible until now.

2. State of the art

The main world-wide standard for the reconditioning or renewal of hull coatings is the manually performed grit blasting in combination with manually applied recoating. Grit blasting is becoming more and more of an environmental issue and potential residues of e.g. grit on the treated surface provide an unfavourable base for recoating. Additionally the manual application of paint proposes a challenge on maintaining a consistent coating layer thickness. This all may result in an uneven coating with areas of under- and over coating as well as flaws, residues and inclusions in the coating itself. This again may result in bad corrosion protection, weak adhesion of the coating itself and an increased surface roughness leading to increased frictional resistance.

Occasionally semi-automated proceedings, using ultra high pressure water jetting attached to telescopic booms or magnetically operated tool heads for surface preparation may be found at some ship yards however fully automated paint application was up to now not available.

3. Automated surface preparation and coating application

The surfaces investigated in this paper were treated with the Hubert Palfinger Technologies HTC System, which performs a fully automated surface preparation using ultra high pressure water jetting and an also fully automated airless paint application process.

Following the outline of the ship's main deck, a track is installed on the dock's floor, on which the system moves and operates fully self-sustained. All units such as paint pump and mixing unit, ultra-high pressure generator, control stand etc. are situated on the chassis. A hydraulic telescopic boom with the ultra-high pressure (UHP) water jetting tool, as well as the paint application head is moving up and down at a grid tower.



Fig. 1: Automated Hull Treatment Carriere (HTC), left to right: washing, ultra-high pressure water jetting, recoating

The distance of the tool heads to the ship's hull is constantly monitored and automatically adjusted. The limited degrees of freedom, which result from moving along the rail track, ensure a precise repositioning for consecutive work steps.

With this setup, various scopes of work can be performed. Low pressure washing will remove any mud, dirt and marine fouling. During the so called sweeping process the surface of the existing coating can be roughened or layer wise be removed. For UHP jetting full blast and also spot treatment is available. In case of spot treatment, the position of the blasted areas are stored, so they can be automatically be re-approached for coating.

For coating, any multi-component paint system with wet film thickness of up to 1.000 μm per run can be applied. The system's performance speed varies, depending on the surface to be treated and the paint system to be applied.

The water used for blasting is vacuumed directly of the surface, collected and filtered for environment friendly disposal. Due to the water temperature in the UHP jetting tool of 70°C, the hull surface remains nearly dry after treatment. The flash-rust contamination can be delayed significantly.

4. Scope of investigation

For the purpose of this paper, various investigations of the past years have been evaluated. In order to gain detailed information of the prepared surface and the paint application, first test steel samples have been manufactured. These coated samples were blasted and recoated with the HTC systems. For comparison, identical samples have been treated using conventional methods of grit blasting and manual recoating. These samples then have been examined by the SGS Fresenius institute to gain, among others, information on surface roughness and -cleanliness of the blasted / prepared surface, paint layer structure and paint surface roughness.

In the next step the treatment and application under yard condition has been tested at a test wall at Blohm & Voss in Hamburg / Germany. Again, data regarding particulars and quality of the water blasted surface, as well as on the applied coating has been collected. Finally full operation on a 295 m Tankship was performed, gathering information on the process itself and the suitability of the system for yard operation.

5. Blasting and surface preparation

The blasting was performed with a maximum pressure of 3000 bar (approx. 43,000 psi) and a tool head speed of up to 144m/h along the surface. Any coating or rust was stripped of the surface to the bare steel. Microscopic investigations performed by the SGS Fresenius institute reveal a surface cleanliness exceeding WA 2,5 according to EN ISO 8501 1-5 after 24h.

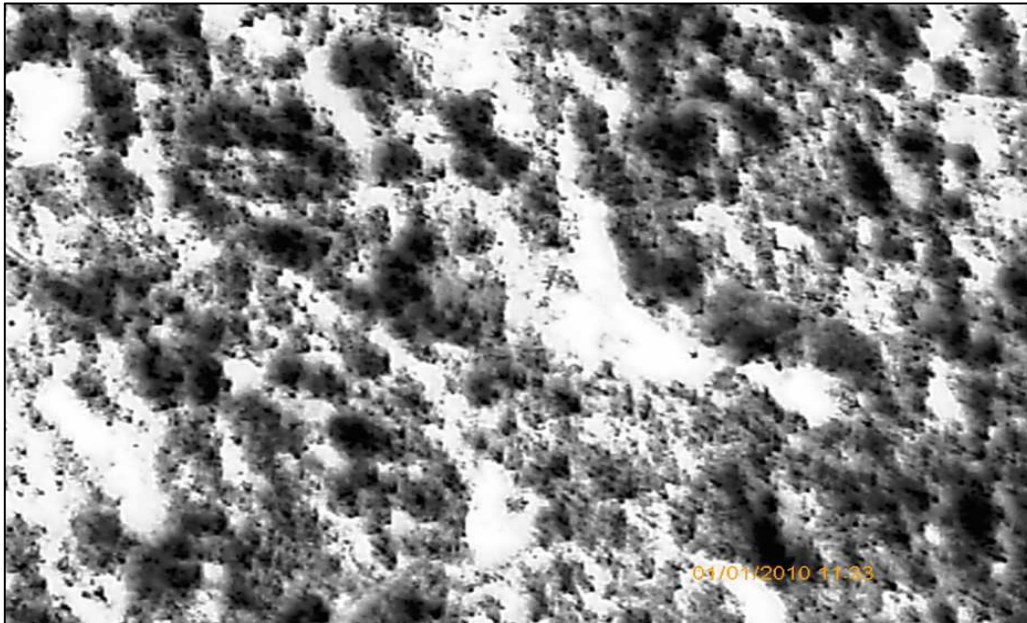


Fig. 2: Purity of the water-jetted surfaces in the test after 24h, cleanliness exceeding WA 2.5 according to EN ISO 8501 1-5, approx 300x magnification

Due to the high kinetic energy of the water particles impacting the surface at constantly 90° angle microspores within the steel surface were opened, adding additional micro profile to the original surface, which favours the adherence of the later applied coating. Other than that no additional roughness is gained. The blasting result and quality was maintained consistent for all treated areas. All surfaces were dry immediately after blasting and thus remained without any rust for over 48h.

6. Recoating

For the purpose of this investigation a typical four layer JOTUN coating system was applied consisting of one layer Jotamastic 80, one layer Safeguard Universal ES, one layer SeaQuantum classic and one final layer of SeaQuantum X200, Table I.

Table I: Overview JOTUN applied coating system

Coating step	Target DFT	Achieved DFT (mean value)
Jotamastic 80	150 µm	143 µm
Safeguard Universal ES	150 µm	168 µm
SeaQuantum Classic	100 µm	76 µm
SeaQuantum X200	100 µm	84 µm
Total	500 µm	471 µm

In order to investigate the regularity of the applied coating a measurement series of 30 values distributed throughout the surface was performed, the results illustrated in Fig. 3. A typical coating layer distribution is shown in Fig. 4. With the consistent process parameters angle (90°), distance to the surface and processing speed, the coating results are of very homogenous and of high quality. Overspray rates of 5% were achieved.

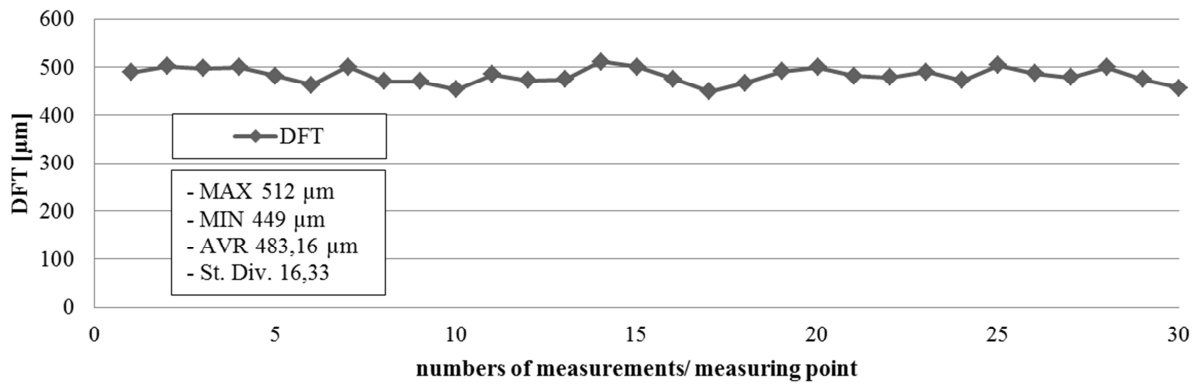


Fig. 3: DFT readings of automatic applied coating

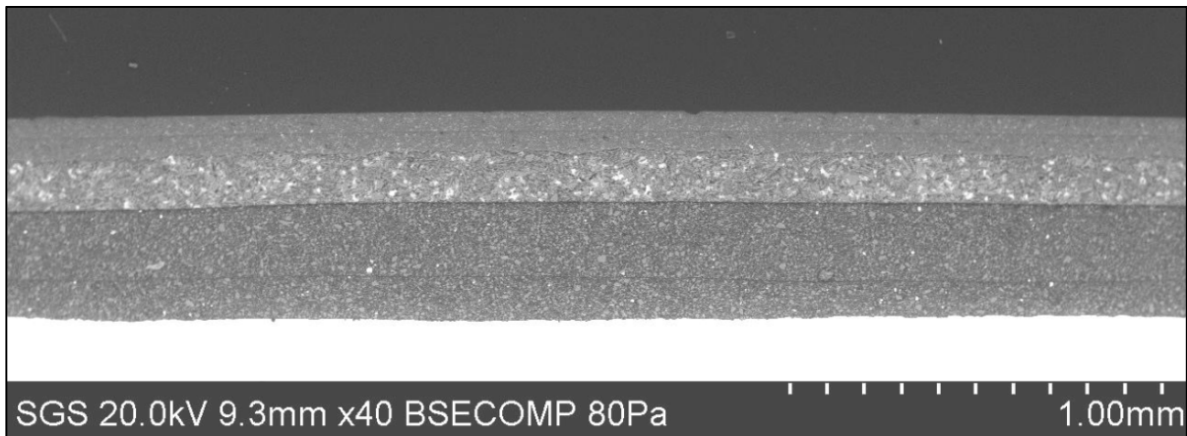


Fig. 4: Typical cross section of coating layer applied by the HTC (Note: The shown cross section does not represent the coating build up described previously)

7. Surface quality

In order to investigate the effects of a smooth coating, the surface roughness was measured. The following subsections give an overview of the current standards for surface roughness measurements and present the achieved results.

7.1. Measuring surface roughness

The first values representing the roughness taken from the fully coated surface were the R_z values. R_z is a commonly used in the painting and coating industry. This value represents the surface profile over a one-directional distance of 12.5 mm and within this averaging five min-max peaks ($R_{z1} - R_{z5}$). For the HTC coated test surfaces the R_z value was taken at three different locations. The obtained values are listed in Table II.

Table II: Measured R_z on fully coated test wall

Pos:	R_z
1	16.74 µm
2	22.00 µm
3	15.51 µm

However, with respect to ship hull resistance the value R_z does not have any major relevance resp. is not applicable at all but rather the MHR / AHR values gained from the R_{150} value. R_{150} (also in µm) is averaging one min-max peak within a one directional distance of 50 mm, as shown Fig. 5.

The ship's hull is divided into 100 to 120 patches. Per each patch approx. 10 to 15 R_{150} values are gathered and averaged, leading to the mean hull roughness (MHR) for this patch, which again averaged over all patches along the ship's hull leads to the average hull roughness (AHR). Although the characters of the R_Z and R_{150} (resp. MHR/AHR) are very similar, the data ascertainment differs. This makes it impossible to transfer R_Z into R_{150} and vice versa. Fig. 5 lists the obtained MHR values for a patch pattern adopted to the evaluated test wall. For the test wall a value of $AHR=65 \mu m$ was determined.

	Mock-Up			
1	28	134	96	23
2	90	21	108	
3	29	100	23	
	01	02	03	04

Fig. 5: MHR [μm] values of the test wall

The cause for the large discrepancy of the values in close vicinity (of up to 600%) is so unknown. As there are about an equal number of very high and very low values, a measuring error can be ruled out. The chart in Fig. 6 sets the found AHR into context.

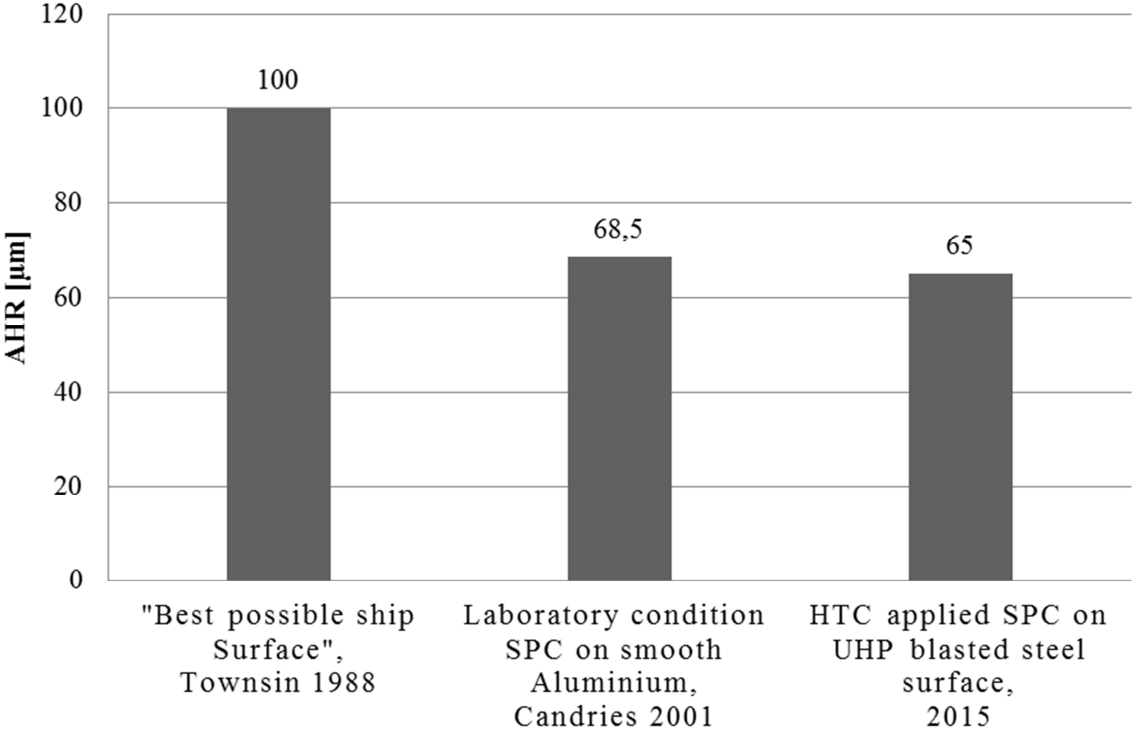


Fig. 6: Different surface roughness values with HTC results, *Townsin (1988), Candries (2001)*

Although, different coating systems were applied, it was possible to obtain a surface roughness under ship yard conditions comparable to results under laboratory conditions.

7.2. Influence of coating surface roughness on frictional hull resistance

A ship's hull over all resistance can be represented by the following equation (not taking into account appendices, air drag, etc.):

$$R = 0.5 \cdot \rho_w \cdot A \cdot U^2 \cdot C_T$$

With: R overall hull resistance [N]
 ρ_w density of water [kg/m³]
 A wetted surface area [m²]
 U ships speed [m/s]
 C_T total resistance coefficient, $C_T = C_t + C_f$ [-]
 C_t towing / wave coefficient [-]
 C_f frictional coefficient [-]

A typical distribution for seagoing ships of wave-to-frictional resistance is 1:2. To evaluate the influence of the surface roughness on the friction coefficient, Fig. 7 is considered. Furthermore a typical C_f value for a 250 m container vessel can be determined at around $C_f=0.0015$. Averaging the characteristics from Fig. 7, a reduction of C_f for a roughness reduction from 300 μm to 200 μm of $\Delta C_f \approx 0.0001$ can be estimated.

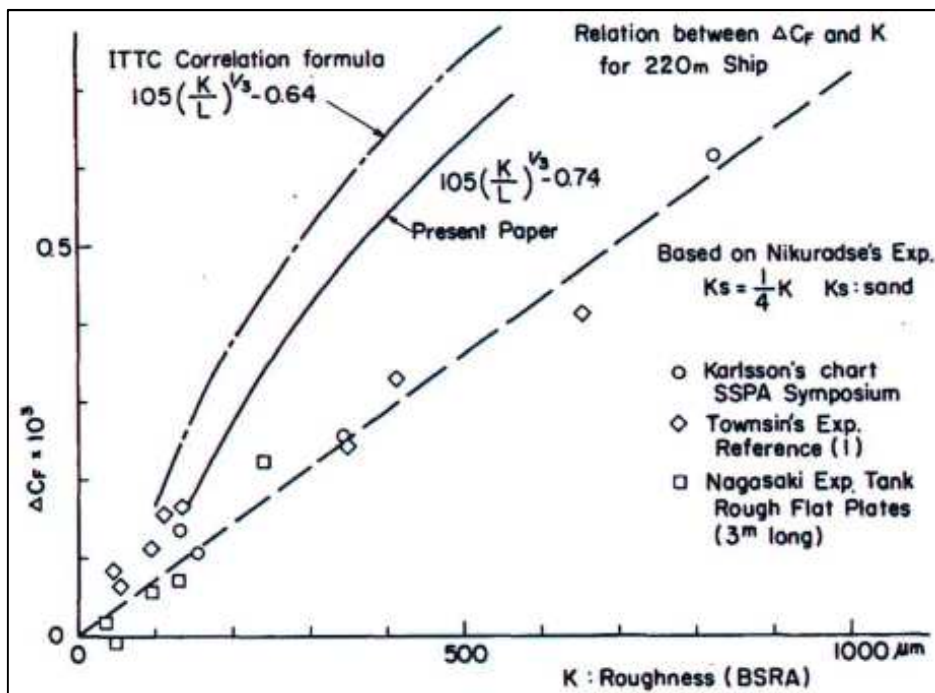


Fig. 7: Influence of surface roughness on the frictional coefficient, Townsin (1988)

Considering $C_f=0.0015$ and the relation of wave- to frictional resistance of 1:2 the following overall reduction of C_T resulting from the above mentioned hull surface roughness reduction can be calculated:

$$C_{Tr} = C_t + C_f = 0.00225$$

$$C_{Ts} = C_t + C_f - \Delta C_t = 0.00215$$

With C_{Tr} total resistance coefficient (ship with rough hull coating surface) [-]
 C_{Ts} total resistance coefficient (ship with smooth hull coating surface) [-]

In conclusion the reduction of the overall hull surface roughness by 100 μm could lead to an overall resistance reduction of approximately 4.5%. A plausible value for the average hull roughness for recoated hulls, using the standard methods of Grit blasting and manual recoating could be around AHR=150 μm . This now put into relation with the results obtained by the HTC of AHR=65 μm this leads to a theoretical potential overall resistance reduction of approx. 3.8%.

8. Discussion and further investigation

The previous chapters show the big potential of resistance- and as a direct consequence fuel reduction as a result of hull surface roughness reduction. However, the above listed calculations are mainly based on general assumption and leave out further relevant considerations. For example the influence of growth and fouling is neglected. Additionally up to now, the reasons for the huge deviation of the values measured for the MHR remain unknown. A possible explanation could be more significant imperfections in the steals surface profile beneath the coating, which remained unchanged during the UHP blasting. Other methods of measuring the surface roughness as optical scanning of negative surface moulds instead of the used surface touching measuring devices are in discussion.

This again leads to the question, of how big the potential influence of a smoothly coated surface on a rather rough structured ship's hull surface could be in general. Never the less, the fact, that repeatedly MHR values around 20 μm were achieved by the automated HTC coating system, which are way smoother than the overall AHR, leads to the assumption that surface roughness could be significantly reduced way below an average of 65 μm . After all it is very possible to artificially worsen the measured results of a good smooth coating by having imperfection on the surface below the coatings but not possible to artificially improve the quality of a rather rough coating on a smooth surface below.

To gather closer inside on the influence of a smooth hull's surface on the ship's resistance and performance and to obtain deeper, more reliable results investigations on a full size 4045 TEU Panmax container vessel are planned. On the vessel a modern performance monitoring system is installed and data over the past year have been gathered. The intention is to treat the hull with the HTC system and collect data on the following ships performance. Although this approach appears to be straight forward, still various problems and uncertainties have to be ruled out. For example will not only be the hull renewed put also re propeller due to previous damages. Ways of separating the effects of the repaired prop from the benefits obtained by a smooth hull surface have to be found. Additionally, besides the hull's roughness a very huge number of other influences have an effect on the ships performance. Finding comparable conditions will be a challenge, respectively ways of comparing different conditions will have to be found.

References

TOWNSIN, R. L. et al. (1981) *Estimating the Technical and Economic Penalties of Hull and Propeller Roughness*, SNAME Trans. 89, pp.295-318

CANDRIES, M. (2001), *Drag, Boundary-Layer and Roughness Characteristics of Marine Surfaces Coated with Antifouling's*, PHD Thesis, University of Newcastle

Monitoring, Reporting, Verifying and Optimizing Ship Propulsive Performance: A Support System to Ship Management Focused on Energy Efficiency

Giovanni Cusano, CETENA SpA, Genova/Italy, cusano@cetena.it
Mauro Garbarino, CETENA SpA, Genova/Italy, garbarino@cetena.it
Stefano Qualich, CETENA SpA, Genova/Italy, qualich@cetena.it
Giuseppe Stranieri, CETENA SpA, Genova/Italy, stranieri@cetena.it

Abstract

Minimizing pollutant emissions, lowering fuel consumption and improving ship propulsive efficiency are cross-linked targets for both ship owners/operators and regulatory authorities. The one way to assess target approaching is to monitor and verify ship performances by means of unmanned systems; apart from improving design of ships and propulsive plants, the most efficient way to reduce fuel consumption and pollutant emissions is to act on ship operational management strategies. The Performance Monitoring (PM) system equipped with the Optimum Trim Estimator (OTE) module fulfils mentioned needs, allowing the energy managers to evaluate the effectiveness of both adopted strategies and retrofits.

1. Introduction

Current available technology allows to measure a number of data on board ships, from navigation conditions to propulsive performances to fuel consumption. The automated and unmanned Performance Monitoring (PM) system has been developed by CETENA to continuously monitor all parameters on board and to provide customized information on ship propulsive performances. The benefits of this system rely on both the normative and the economical perspectives.

According to the incoming MRV EU regulation, CO₂ emissions by ships will have to be monitored and reported to the Authorities according to an affordable and verifiable methodology: the use of the PM system to monitor fuel consumption or even directly CO₂ and other pollutant emissions by proper sensors complies with such duties.

On the economical side, it's a matter of facts that minimisation of fuel consumption is one top priority of ship owners and operators. Several actions aimed at reducing ship propulsive fuel consumption can be taken, both acting on ship operational management strategies and performing retrofit interventions: hull cleaning, silicon painting, reblading can lead to high percentages of fuel saving.

The PM system and its data analysis software allow to evaluate ship propulsive performances along ship life, by building and comparing the speed-power and speed-consumption curves referred to different operational management strategies and to different configurations of hull, propeller and whole propulsive system, in particular before and after a retrofit intervention.

Real cases referred to silicon painting / reblading / engine overhaul retrofits of Ro-Pax ships have been analysed. Focus is made on the detected and assessed propulsive performance improvement gained, both from shaft power and from fuel consumption points of view, singling out contributions by the mentioned actions.

Performance improvement during ship operation can be achieved by using the additional Optimum Trim Estimator (OTE) module, which provides the ship Master with real time information on the optimum dynamic trim to be adopted as a function of actual ship speed and displacement. Following suggestions provided by this Decision Support System, the on board personnel is induced to adopt actions aimed at restoring the optimum trim condition: up to a 2-4% reduction of fuel consumption, depending on ship type, can be achieved.

2. Overview on MRV regulation

European Union (EU) regulation 2015/757 on the Monitoring, Reporting and Verification (MRV) of carbon dioxide (CO₂) emissions from maritime transport entered into force on July 1st, 2015 having been adopted by European Council (EC) and Parliament.

The main scopes of this regulation are to quantify CO₂ emissions from maritime transport, to obtain an accurate archive of them by a method based on data that are already taken under control or even already monitored on board ships and to establish CO₂ reduction targets. Other greenhouse gas emissions are not considered by the MRV.

The EU method to calculate CO₂ emissions consists in 3 phases:

- Implement the MRV scheme to establish the nature and quantity of CO₂ emissions from maritime transport.
- Establish an agreed global energy efficiency standard as part of the regulation.
- Identify whether the efficiency standards are achieving the EU's desired absolute CO₂ emissions reductions and determine what else should be done, e.g. introduction of a Market Based Measure (MBM).

EU MRV regulation is mandatory for vessels greater than 5,000 GT (with some exceptions) that navigate into, out of and between EU ports and will require annual reporting of CO₂ emissions of these ships. Moreover, it requires per-voyage monitoring of CO₂ emissions (except those ships that undertake more than 300 voyages within the reporting period or if all their voyages during the period either start or end at a port under the jurisdiction of an EU member state), as well as other parameters including energy efficiency metrics and quantities of cargo carried.

Stating that, each shipowner has to produce a monitoring plan and each year must provide the Authorities with an emissions report regarding the previous year and with the evaluation of the technical efficiency of the ship: all data will be aggregated annually and reported for all voyages conducted into, out of and between EU ports.

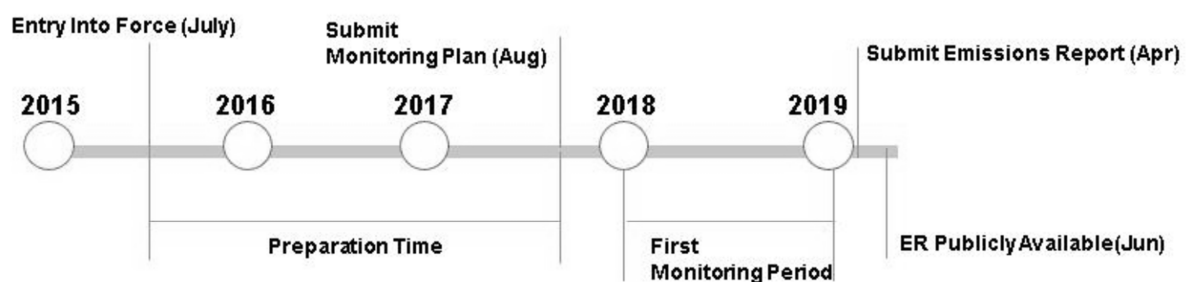


Fig. 1: EU MRV Regulation timeline

Ship owners are allowed to choose one or more of four methods for monitoring fuel consumption in each combustion source being monitored:

- The use of Bunker Fuel Delivery Notes and periodic stocktakes of fuel tanks (except for those vessels where cargo is used as fuel, as LNG carriers);
- Bunker fuel tank monitoring;
- Flow meters for applicable combustion processes (if fuel consumption is measured in units of volume, the density of that fuel also needs to be determined, through either the bunker delivery note or on-board measurement systems or a company's independent fuel analysis);
- Direct emission measurements.

In above mentioned ways, CO₂ emissions are calculated by considering fuel consumption and using appropriate emissions factors for the used fuel type, or by direct emissions monitoring, with a back-calculation of the fuel consumption using the relevant emissions factor. Moreover, a combination of these methods is also permitted if it would improve the accuracy of the CO₂ emission measurement for a given combustion source.

The MRV regulation hasn't to be considered only as a duty for ship owners, but as an opportunity especially for those owning significant fleets. CO₂ emissions are linked to fuel consumption: having at disposal fuel consumption data monitored according to fixed procedures can be of utmost importance to improve fleet efficiency.

Comparing consumptions of sister ships on different routes or of different ships on the same route or of the same ship operated by different crews can lead to considerations on operational management strategies and to improve the whole fleet efficiency. With this aim in mind, it is more effective for ship owners to fulfil MRV duties by means of an automated system which monitors and analyses ship data, rather than with manual procedures.

3. PM (Performance Monitoring) system

The installation on board of an unmanned monitoring system, Fig. 2, able to acquire, store and analyse all significant data relevant to the ship propulsive efficiency allows to identify the main causes leading to excessive propulsive consumptions and to adopt the proper countermeasures. This can be done by comparing the actual performance against the reference curves, related to:

- cleaned propeller and hull, to single out performance decreasing due to propeller/hull fouling;
- engine SFOC in overhauled conditions, to evaluate progressive loose of engines efficiency;
- optimum dynamic trim reference curve as a function of speed and displacement, to identify the power lost while navigating with a non-optimal trim for actual speed and displacement.

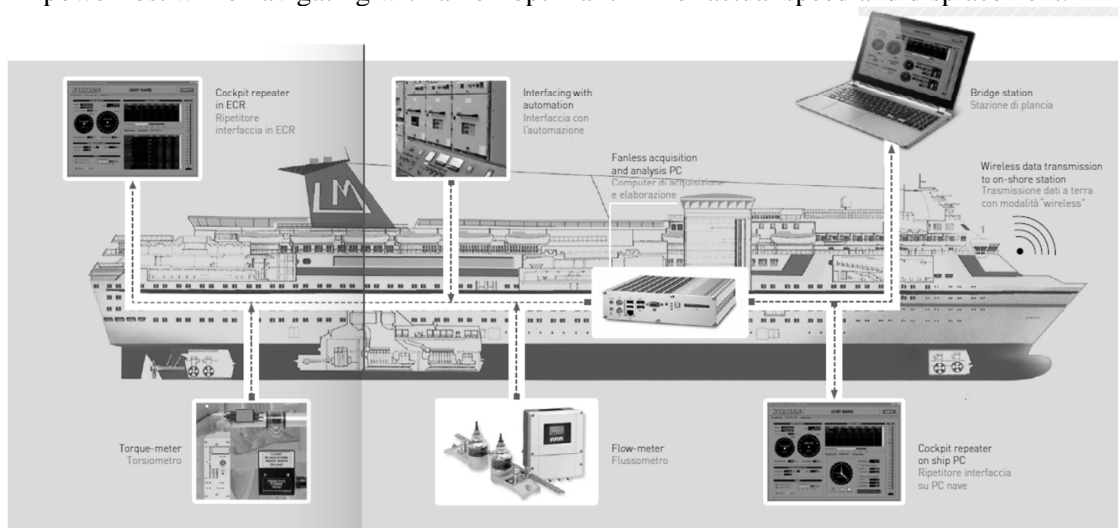


Fig. 2: Typical “Performance Monitoring” system lay-out

A number of information items are needed to be measured, concerning both the operative conditions:

- time and location;
- ship speed, course and heading;
- propulsive chain operating conditions (propeller rpm and pitch);
- propulsive power at shaft lines by means of torquemeters;
- environmental conditions (wind, sea state, sea current, ...);
- ship loading conditions (draft, trim, displacement);

- anti-roll stabilizer fin status (on/off) from automation system;
- rudder angle;
- ship operating status (navigation, maneuver, docking/anchor) by means of a dedicated signal or by a proper association of ship automation signals;
- other data of interest for specific tailored purposes.

and the thermodynamic / energy generation aspect:

- fuel flow to Main Engines and Diesel Generators;
- status of MMEE and DDGG;
- electric power generated by DDGG;
- electric power generated by Shaft Generator.

In some cases all data are available on the ship automation system and can be acquired simply by connecting PM system to it; in most cases, the PM has to be connected to a number of onboard systems and/or of specifically installed sensors (torquemeters, flowmeters, anemometer, etc).

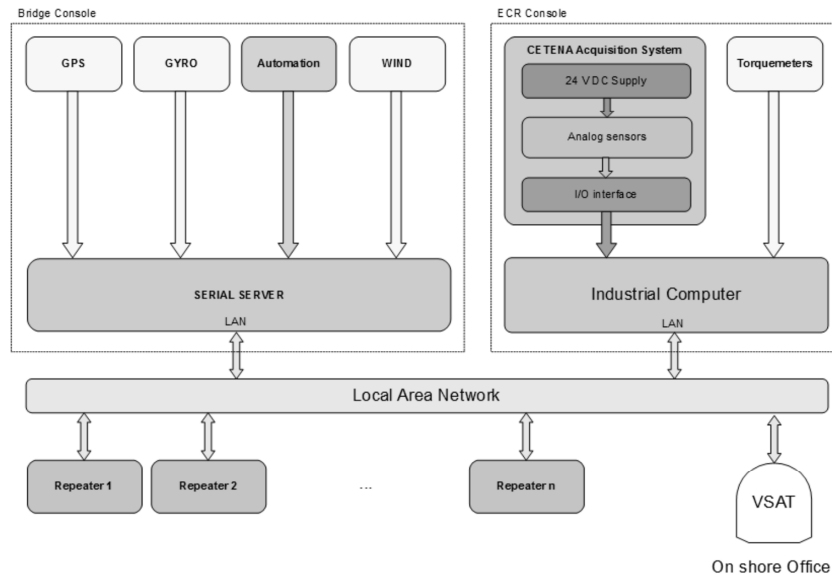


Fig. 3: Typical “Performance Monitoring” system block diagram

The PM system developed by CETENA, Fig. 3, basically consists of:

- a rugged and affordable industrial controller and (if needed) a serial server, added to ship LAN, acquiring signals from ship systems and from analogue/digital signals acquisition hardware;
- dedicated hardware to acquire signals from specifically installed sensors;
- “Data Collector” unmanned software installed on the controller for acquisition, analysis, recording and storage of all data and for preparation of properly customized voyage reports;
- “Repeater” visualization software (Fig. 4) installed on on-board PCs and if requested on on-shore ship owner’s PC, to provide ship Master/Officers and Energy Managers with real time data collected on board.

The Repeater SW also provides an interface to manually input some data which could be not available from the onboard systems: fuel type and characteristics, cargo on board (number of passengers/cars/trucks/TEUs), sea state conditions during the trip, crew identification, and so on, Fig. 5. In this way all information needed to comply with MRV needs and to compare ship performances and operational management strategies are automatically saved in the same voyage file.

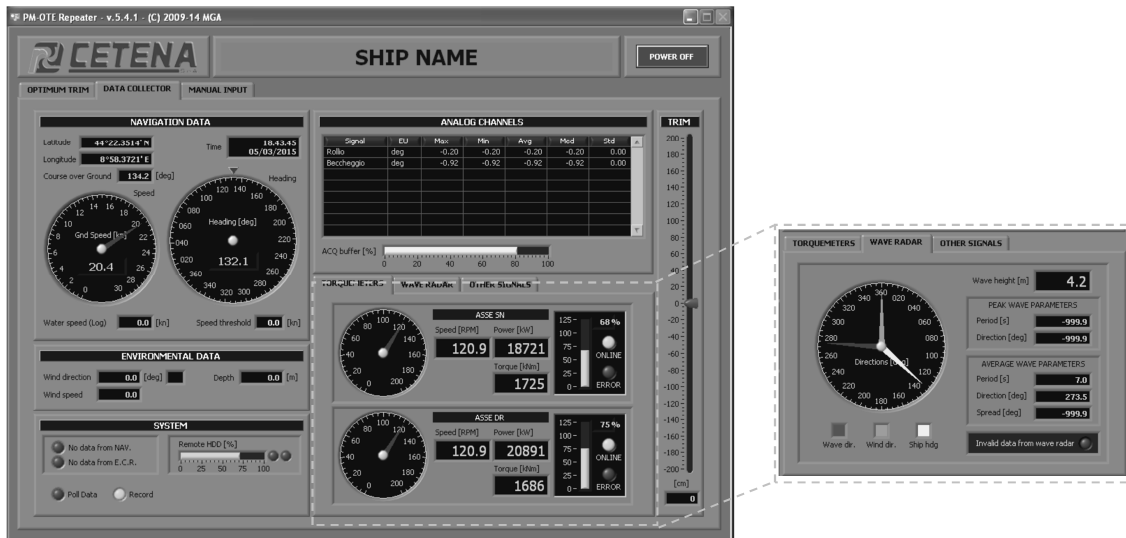


Fig. 4: “Performance Monitoring” system: onboard cockpit



Fig. 5: “Performance Monitoring” system: manual input

3.1. Data storage and report for MRV purposes

Stating the MRV regulation requires to report CO₂ emissions for each voyage, the “Data Collector” software recognizes - on the basis of GPS coordinates, ship speed and (if available) engine status - if and in which harbour the ship is standing. For each port-to-port voyage it creates a file with all data recorded during the trip and a specific report on the voyage complying with MRV regulation: both of them are saved on the controller - at disposal of the onboard personnel and of the authorities requiring them - and automatically transferred to an FTP server on-shore or forwarded by e-mail to the Shipowner technical office for further analysis.

4. OTE (Optimum Trim Estimator) module

One of the most efficient ways to reduce fuel consumption during navigation is to adopt the optimum dynamic trim, i.e. that trim which minimizes ship drag at actual speed and displacement conditions. To this perspective it has to be noted that the dynamic trim has to be measured in real time - by means of high precision inclinometers installed on stiff structural parts of the ship and accurately calibrated - rather than the static trim, due to effects of ship speed and of hull girder deflection while navigating in variable deep water.

Dynamic trim values are monitored by PM system and analysed by the additional module “Optimum Trim Estimator” (OTE). On the basis of actual speed and displacement, OTE evaluates the optimum dynamic trim to minimize propulsive power, compares the actual dynamic trim against it and estimates the percentage of exceeding power due to the actual/optimum trim gap. All those values are recorded by PM in voyage files and put at Energy Manager’s disposal to check how ship was operated and how much fuel would have been possible to be saved by acting on trim.

OTE module (Fig. 6) provides a significant added value to PM system: it in fact shows in real time in a user-friendly graphical interface how much the actual ship propulsive performances are far from optimal ones. Knowing that, the on board personnel can adopt proper countermeasures to restore the optimum trim condition, thus reducing/minimizing the fuel consumption.

Furthermore, by using day-by-day the OTE module, ship Master and Officers can better understand the optimum static/dynamic trim dependence on ship speed. Cargo and ballast can thus be distributed on board before the departure looking at the expected trim relevant to the foreseen voyage speed and displacement: the close-to-optimum trim achieved will then be tuned during navigation following OTE module indications.

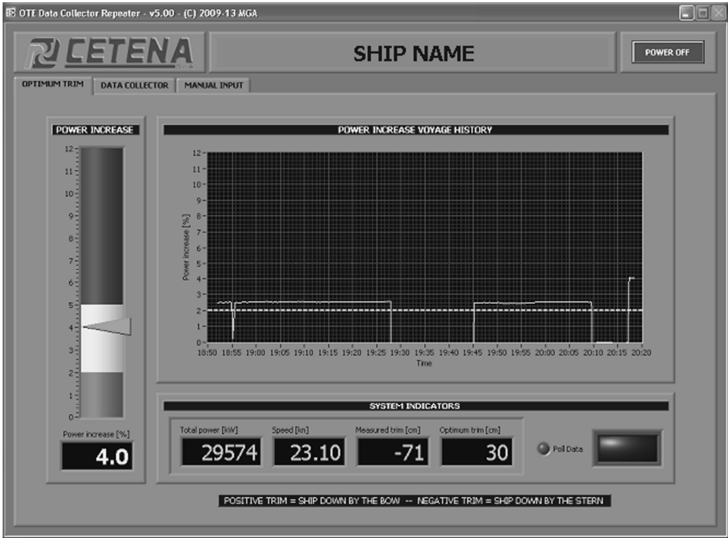


Fig. 6: "Optimum Trim Estimator" module inside the "PM" system

4.1. Generating Optimum Trim surface

Optimum trim surface as a function of speed and displacement constitute the added value in the OTE module: hydrodynamic skills are needed to compute it. In order to take into consideration the whole propulsive behaviour of the ship, optimum trim/speed curves are built by analysing results by tank tests performed for several displacements and trims and calibrated against sea trials. Afterwards, curves can be updated by analysing data acquired by PM during navigation, thus tuning them against the real operative use of the ship.

In case tank test / sea trials data would not be available, curves (Fig. 7) can be defined by analysing:

- dedicated runs performed with cleaned hull/propeller, in favorable environmental conditions;
- data registered by PM during ship operation, correcting measured values against environmental conditions and elapsed time from the last hull and/or propeller cleaning.

Mentioned approaches are to be preferred to auto-learning ones, since all measured data are affected by the environmental conditions encountered during navigation (sea state, wind, current) and it can't be completely affordable to automatically single out the effect of trim optimisation (leading to 2% to 4% reduction of fuel consumption) when superimposed to effects of environmental conditions -

sometimes even not accurately measured - influencing the fuel consumption up to 20%. Furthermore, during tank test / sea trials a wider range of trims and displacement can be investigated: curves can be built also for unusual operative conditions, for which the auto-learning tool could not have at disposal a significant amount of data to be sufficiently trained.

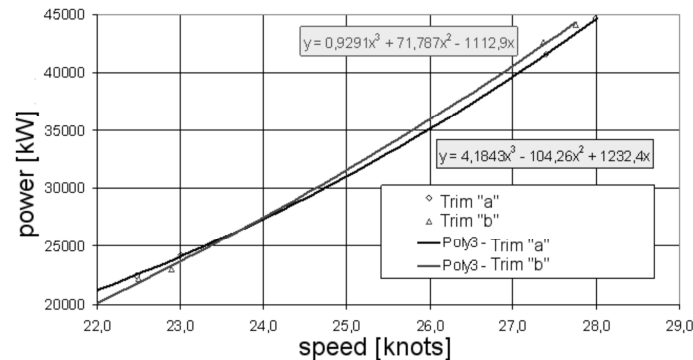


Fig. 7: Power/speed curves for one displacement, two trims (dedicated sea trials)

This way, for each displacement and each speed the optimum dynamic trim is evaluated, as well as the extra power needed to perform the same speed with trims far from the optimum one, Fig. 8. This information is used by OTE to indicate - and by PM to store in the voyage file - the value of power which could be saved by adopting the optimum trim rather the actual one.

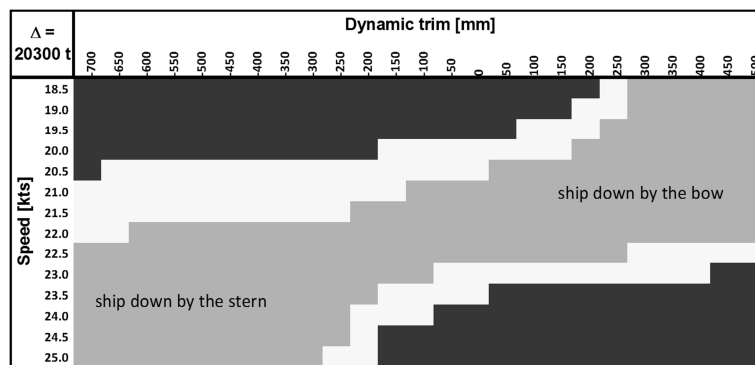


Fig. 8: Extra power spent depending on speed and trim

5. PMDA (Performance Monitoring Data Analysis) software

A proper tool for offline data post-processing has been developed to analyse the large amount of data recorded by PM&OTE system: a fast analysis of ship propulsive performances along its operational life allows to critically compare operational management strategies and to assess benefit of retrofit interventions. The tool is characterised by the following main features:

- voyage(s) selection;
- plot of voyage(s) route and of recorded signals time histories;
- statistical data resume (max, min, mean, standard deviation, etc) of signals recorded;
- filtering of voyage(s) data among main ship operating parameters (sea area, speed, power, wind/sea state, engine status, stabilizer fin status, etc ...) and/or among time: data analysis can be focused on most significant voyages, having ship performance not (or not too much) to be influenced by encountered conditions;
- set-up of a customized report file summarizing all info recorded during voyage(s) or during a considered period of ship operation (week, month...).

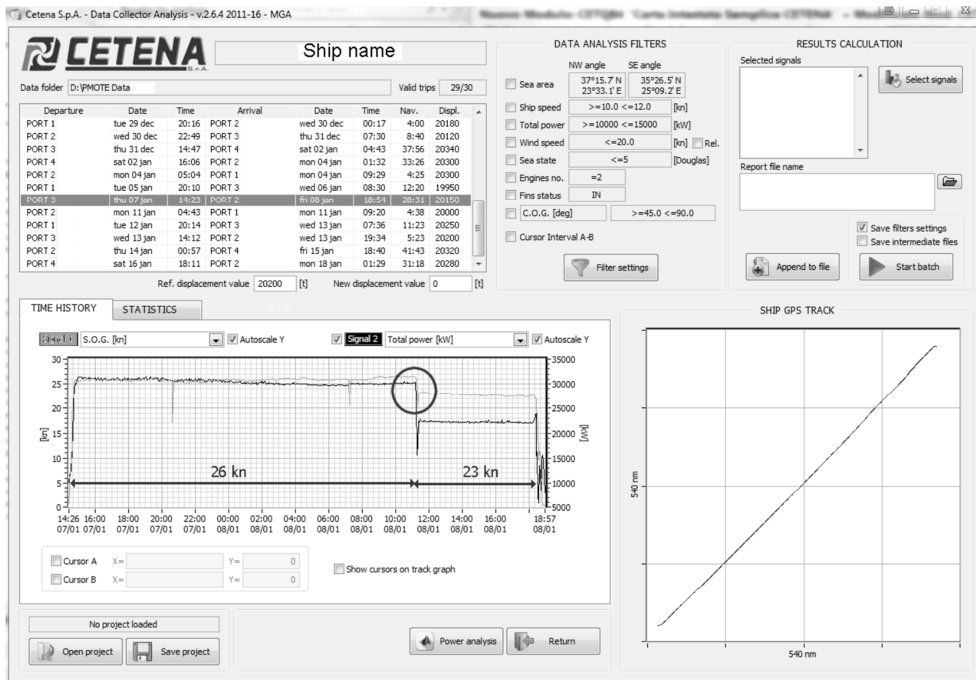


Fig. 9: PMDA software: analysis of operational management strategies

In the example shown, Fig. 9, a non-efficient operational management of a Ro-Ro ship has been detected over a voyage about 28 hours long. The ship was operated at about 26 knots for 20 hours, afterwards speed decreased to 23 knots for 8 hours in order to get in time at destination port. Despite over a so long trip some time margin is acceptable and has to be taken into account in order not to arrive late even in case of unexpected events, the high-speed operation was too extended and resulted too expensive in terms of fuel consumption.

By seeing at operational data recorded by PM, the Energy Manager ashore can judge whether ship are correctly managed or if there are some ways to save money without significant efforts: in this case, reducing speed for the first voyage part would have lead to fuel savings without affecting schedule.

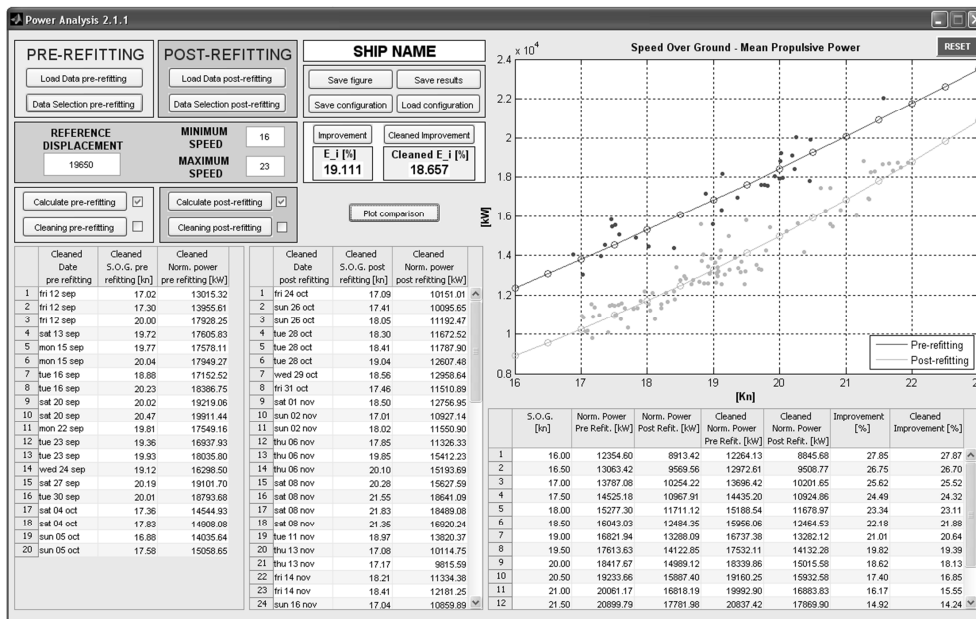


Fig. 10: PMDA software: assessment of retrofit effectiveness

5.1. Building and comparing speed-power curves

Retrofit effectiveness as well as effects by improved operational management strategies can be simply evaluated by comparing ship speed/power and/or speed/consumption curves before and after the considered intervention. Ship performance data have to be filtered among main ship operating parameters and mainly against environmental conditions, excluding voyages too much influenced by them. Once having corrected power data by means of the Admiralty's formula to refer all of them to a reference displacement, polynomial curves fitting data scatters are built, for pre- and post-intervention conditions, Fig. 10. The statistical approach adopted allows to "clean" curves from external uncontrollable effects.

The performance improvement due to retrofit or the efficiency gain due to a more efficient ship management is calculated as a percentage of the propulsive power at fixed speed. An Efficiency Index "E_I" is calculating by weighted-averaging the performance improvement at the various speed steps considered. This approach has been applied to a number of situations, as explained hereafter.

6. Common interventions to improve ship propulsive efficiency

Following the change of world economical scenario and the subsequent variation of priorities by freighters – no more leaded by high speed transport but by maximum loading coefficient of cargo ships – a number of ship owners decided to make significant retrofit interventions on ships to improve performance efficiency.

As a matter of fact, ships designed for a cruise speed of 25 and more knots were being operated slow-steamed at 20-22 knots to fulfil the new freight schedule. This induced to re-design and change propellers, optimising blade dimension and shape to achieve the highest efficiency at the new cruise speed: the efficiency gained and the fuel saved were calculated to be so significant that a return of investment was foreseen in a few years. Despite in the last year the fuel oil cost dramatically decreased, such interventions are still performed by ship owners, even if the RoI time is longer.

Together with reblading, several other interventions are commonly performed during dry-dock: hull and propeller cleaning, application of silicon-based paintings, engine overhaul and so on. It hence comes of interest to single out contributions to improvement of performance efficiency by each action, to assess the actual RoI of them: acquiring information on their influence on degradation of ship propulsive performance with time leads to a better schedule of ship hull and propulsive plant maintenance.

6.1. Test case #1: assessment of reblading and hull cleaning effects

In the first test case taken under consideration, two sister Ro-Pax ferries were re-bladed. One of them was undergone dry-dock a few months before, thus being characterized by almost cleaned hull before the reblading intervention; the sister ship had instead dirty hull, having had the hull cleaned more than two years before. The PM system was installed on board both ships to record ship performance data over a period of 2 month before entering dry-dock (one cleaned, one fouled hulls and old propellers) and 2 months after dry-dock (both cleaned hulls and new propellers).

The above described methodology was adopted, excluding from the analysis those legs in which propulsive performances were affected by adverse weather conditions, i.e. rough sea and/or strong wind and referring all data to a unique displacement value.

While after reblading the two sister ships were obviously characterized by the same speed/power curve, before it a significant difference was found between them: the effect of hull/propeller fouling on ship propulsive efficiency clearly arose, Fig. 11.

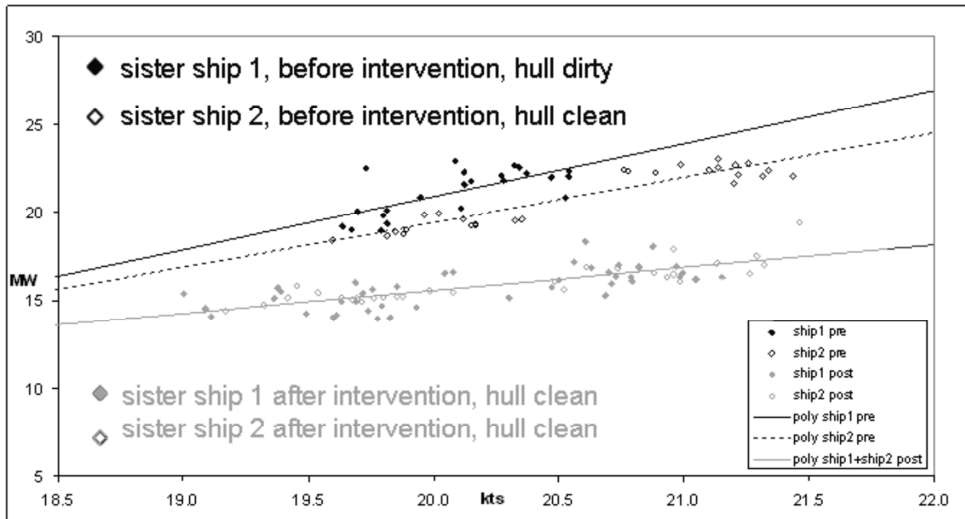


Fig. 11: Effect of hull/propeller fouling on propulsive performance

It was found that – in the speed range around the new cruise speed of 20 knots – ships with new propellers saved about 20% of power to achieve the same speed, taking as a reference the cleaned hull performances. On the other side, the effect of hull/propeller fouling on ship propulsive performances was detected to be around 6%.

Apart from the assessment of reblading effectiveness – which confirmed the expected benefit – the information about fouling effect was very useful to ship owner. Having quantified it, the time interval between hull/propeller cleanings was reviewed on the basis of the dry-dock intervention cost and of the efficiency gain and subsequent money saving achievable by hull cleaning.

6.2. Test case #2: assessment of reblading and engine overhaul effects

The second test case concerns a Ro-Pax ferry onto which a monitoring campaign was performed to evaluate the effectiveness of both reblading and engine overhauling: one of four main engines was in fact overhauled just before the campaign beginning. During the 1 month monitored period before dry-docking, all four engines were used, while afterwards the ship was able to navigate at the same speed with only two engines running.

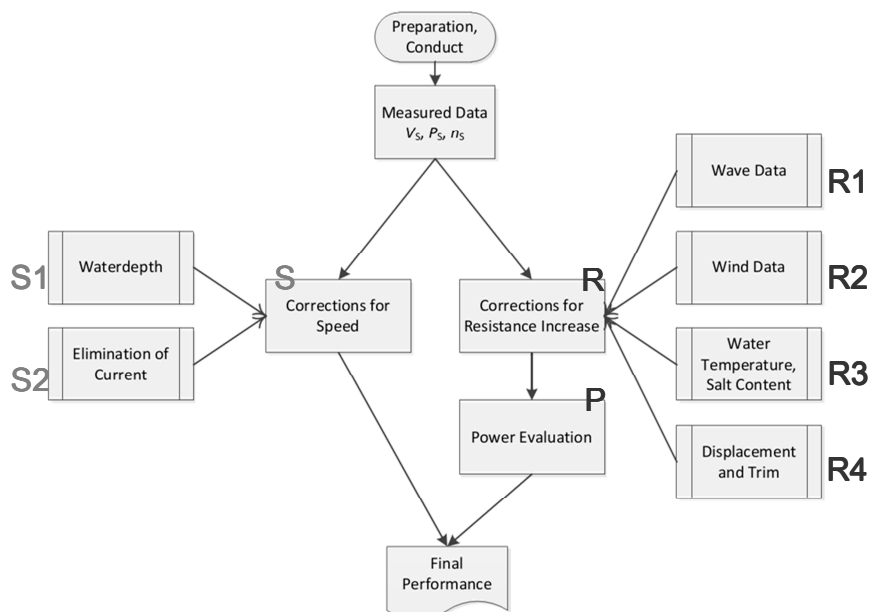


Fig. 12: ITTC speed/power correction procedure flowchart

In this case - in addition to disregard recorded data characterised by adverse weather conditions - average values of ship speed and power over considered legs were corrected according to *ITTC (2012)* procedures, Fig. 12, to evaluate ship performance in 'no wind and no wave' conditions.

A proper procedure to correct fuel consumption was developed, Fig. 13, and applied to values measured by onboard flowmeters and recorded by PM system:

- fuel leakage by each engine was measured during dedicated sea trials before and after the reblading, with engines running at different rpm and loads: average leakage values at different engine rpm were then subtracted from measured consumption values;
- power/consumption curves relevant to engines running on board before/after the dry-dock were built on the basis of measured power and “consumption minus leakage” values;
- corrected fuel consumption was afterwards determined by entering with the ITTC corrected power rather than the measured one in the mentioned curves.
-

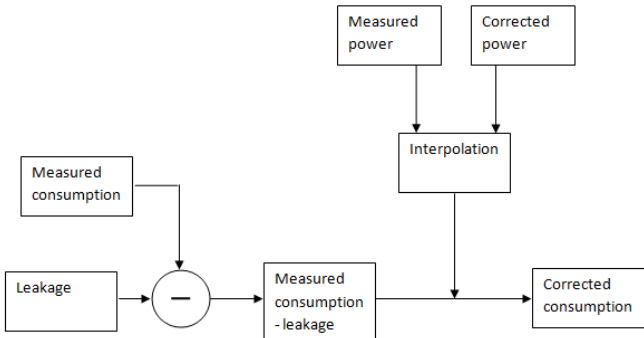


Fig. 13: Fuel consumption correction procedure flowchart

Speed/power curves fitting the scatter of points acquired during the campaign and ITTC-corrected were obtained, Fig. 14, and revealed that the efficiency improvement before/after retrofit referred to power resulted in about 9% at contractual speed in commercial service.

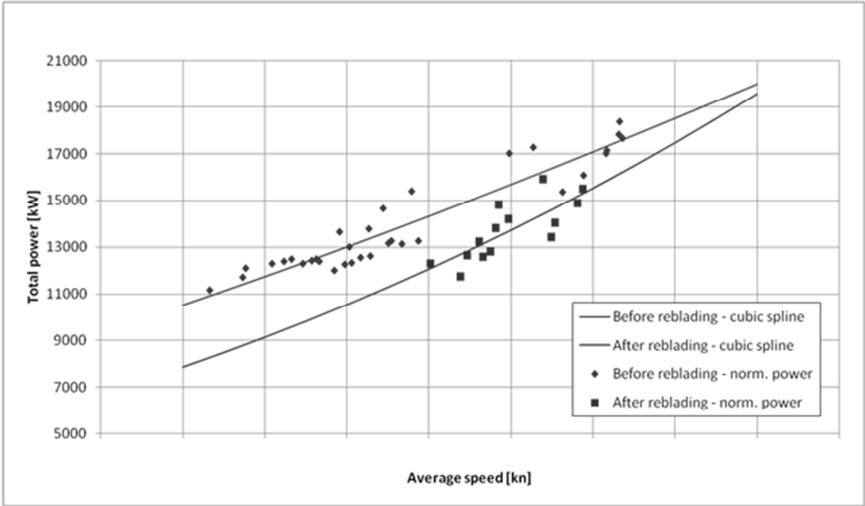


Fig. 14: Speed/power curves before and after retrofit

Speed/consumption curves were also built to fit the scatter of points acquired during the campaign and corrected by previously described procedure (Fig. 15): the efficiency improvement before/after retrofit referred to fuel consumption resulted in about 14% at contractual speed in commercial service.

Some considerations apply to fuel consumption curves and explain the 9% to 14% increase in efficiency gain with respect to power curves:

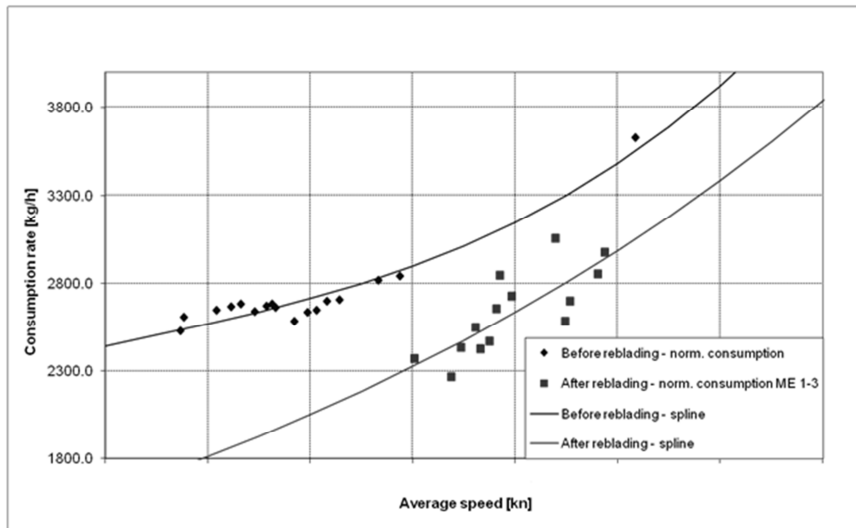


Fig. 15: Speed/consumption curves before and after retrofit

- after reblading only two engines were used, among which the overhauled one (ME n°3): 50% of power delivered was generated by an efficient engine, against the 25% before reblading when all 4 engines were running;
- after reblading engines were running in minimum SFOC zone (around 80% load), whilst before they were running at inefficient rpm values (around 45% load, high SFOC);
- the arched shape of speed/consumption curves is due to SFOC variation with engine load, which is higher at low loads (before reblading) rather than at optimal loads (after reblading).

In order to single out the effect of engine overhauling from the optimization of engine running loads, dedicated sea trials runs were performed - according to *ITTC (2012)* - before and after reblading: in this second phase it was possible to operate the ship with and without the overhauled engine running. The efficiency improvement referred to fuel consumption in sea trials resulted in about 14% with ME 1-3 running and about 11% with ME 2-4, Fig. 16. The effect of engine overhauling was thus found to be significant on fuel consumption, resulting to be around 3%.

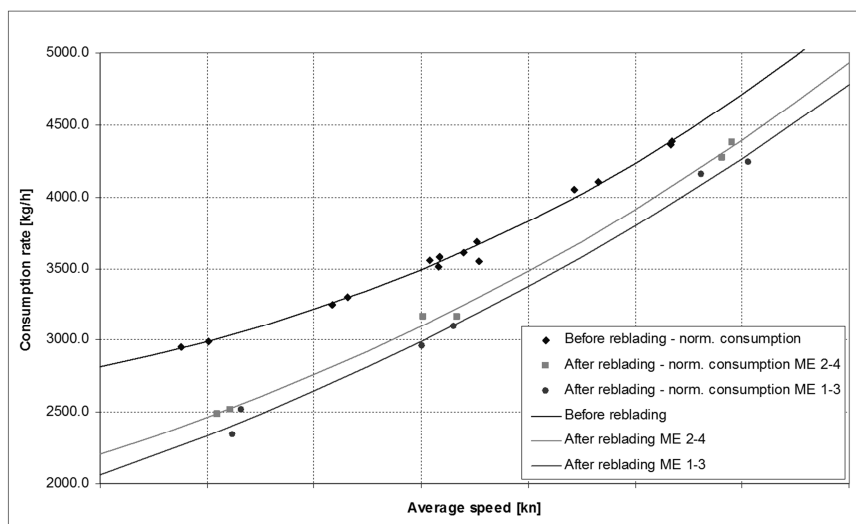


Fig. 16: Effect of engine overhaul on fuel consumption

As in the hull fouling case, this analysis provides Energy Managers with useful information to better schedule ME overhauling according to cost/benefit considerations.

8. Conclusions

Taking under control ship propulsive performance and operational management strategies is having a growing importance in the maritime world. From both the regulation point of view – with the incoming MRV EU regulation forcing to monitor and report CO2 emissions by ships – and the energy efficiency one, the installation on board ships of unmanned Performance Monitoring systems can provide the ship owner with significant added values:

- compliance with EU regulations;
- compliance with IMO SEEMP guidelines;
- fuel consumption and emissions reduction by improving energy efficiency (optimum trim and in general operational management strategies);
- assessment of retrofit and maintenance actions effectiveness (new propellers, silicon paints, hull appendages, engine overhauling, etc);
- acquisition of information to better schedule ship and plants maintenance;
- control of crews and reporting of vessel performance and management to onshore team;
- fuel and money saving.

The installation of the PM system on board Ro-Ro ships and Ro-Pax ferries and the analysis of propulsive performance data described in the present paper demonstrated how this approach to ship management can lead Energy managers to acquire useful information regarding both operational management strategies adopted by crews and effectiveness of retrofit and maintenance interventions.

References

- ITTC (2012a), *Preparation and Conduct of Speed/Power trials*, ITTC Recommended Procedures and Guidelines 7.5-04-01-01.1
- ITTC (2012b), *Analysis of Speed/Power trial data*, ITTC Recommended Procedures and Guidelines 7.5-04-01-01.2

Continuous Estimate of Hull and Propeller Performance Using Auto-Logged Data

Sigurdur Jonsson, Marorka, Reykjavik/Iceland, sigurdur.jonsson@marorka.com
Helgi Fridriksson, Marorka, Reykjavik/Iceland, helgi.fridriksson@marorka.com

Abstract

Energy performance management is one of the key levers for competitive operations in the maritime industry. One area of importance is the awareness of hull and propeller conditions and the deterioration of performance, based on changed conditions. This paper demonstrates a methodology for monitoring both the hull and propeller conditions on short time-scales, along with an evaluation of the effectiveness of maintenance events. Deducing the change in propulsion power on short-time scales requires effective use of the available data, by normalising for external conditions and quantifying of the confidence in the estimates.

1. Introduction

Trading and shipping of merchandise have been continuously increasing over the past decades, shaping the economic growth of the period. From the year 1990, seaborne trade has increased by 250%, compared to the year 1990, illustrating the importance of seaborne trade to the world economy, *Hoffman et al. (2015)*. At the same time, oil prices have increased considerably, only to fall dramatically at the end of the period, remaining at a similar level today as in the 1990's. The most significant change during this period is the increased environmental awareness, translating in an enhanced regulatory framework and taxation for all transport, which has now begun to affect the maritime industry. This has been encapsulated in work carried out within the IPCC and UNFCCC, leading to the Kyoto Protocol, where greenhouse gas emission quotas were established, and the Paris Agreement, where all agreeing parties committed to limiting the global warming to less than two degrees Celsius. As a result of these increased regulations and heightened sensitivity to oil prices, there has been a significant increase in the number of vendors for performance monitoring systems in the maritime industry. These systems focus on various areas of performance management, with applications ranging from automatic logging and reporting to model-based decision support solutions, such as trim optimisation and weather routing. One important aspect of performance monitoring is tracking of the underwater condition of both the hull and propellers, which changes over time. This is a composition of two elements, permanent roughness and temporary roughness. According to *Carlton (2012)*, the temporary roughness is caused by marine fouling, while the permanent fouling is the amount of unevenness in the steel, ranging from a variety of variables, such as:

- Corrosion
- Mechanical damage
- Deterioration of the paint film
- A build-up of old coatings
- Rough coating caused by poor application
- Cold flow, resulting from a too short drying period prior to immersion
- Scoring of the paint film, due to scrubbing while removing fouling
- Poor cleaning prior to repainting

While the permanent roughness is clearly important, the marine fouling is more manageable from a ship-operators point of view. The amount of marine fouling, or the rate of surface growth, depends both on the condition of waters where a vessel is operated and the vessel's operational profile. This accumulated surface growth will, over time, increase the skin friction and, therefore, the vessel's total resistance through water. In the maritime industry, this increased frictional resistance is often cited in terms of an annual speed drop, commonly ranging from 1-5%. Therefore, considerable gains in fuel consumption can be achieved annually by proper maintenance of the hull and propeller, *Carlton*

(2012), Molland *et al.* (2011). As a result, considerable efforts have been put into the development of antifouling technology and its application, Molland *et al.* (2011). When investing in an application of antifouling technology, often at a considerable cost, there needs to be a way to monitor the fleet performance, as well as the potential gains from the antifouling measures. This requirement initiated the work being carried out on the expected ISO standard on hull and propeller performance. At the same time, the need for increased temporal resolution of operational data for analysis of hull and propeller performance has been identified, Aldous *et al.* (2015). In spite of the emergence of a variety of performance monitoring systems and extensive collaborative work on standardising analytical methods for the maritime industry, there is still no standard way of evaluating the performance degradation in service while accounting for different operational conditions, such as variations in speed, weather and ocean waves. When analysing short-term performance degradation and effectiveness of maintenance events, often based on limited available data, a reliable estimate of the confidence in the results is a prerequisite for rational decision making by ship owners and operators.

In this paper, a method is presented that accounts for both the sensor uncertainty and the model uncertainty on the estimated performance drop. To illustrate the method, two test cases were selected; one from a single, general cargo vessel where cleaning events have been reported, and one where two sister vessels, with no registered events, are compared. Using auto-logged data, filtered in alignment with the upcoming ISO standard, and normalising external effects, the outcome is a useful and reliable estimate of the time-dependent underwater hull and propeller condition.

2. Data collection

The data used in the analysis, presented in this paper, was collected using the Marorka Onboard system, transferred on-shore to the Marorka Online servers and imported to the data analysis tools via the Marorka Online OData API. The information collected for each of the vessels used in the analysis in this paper is highlighted in Fig. 1.

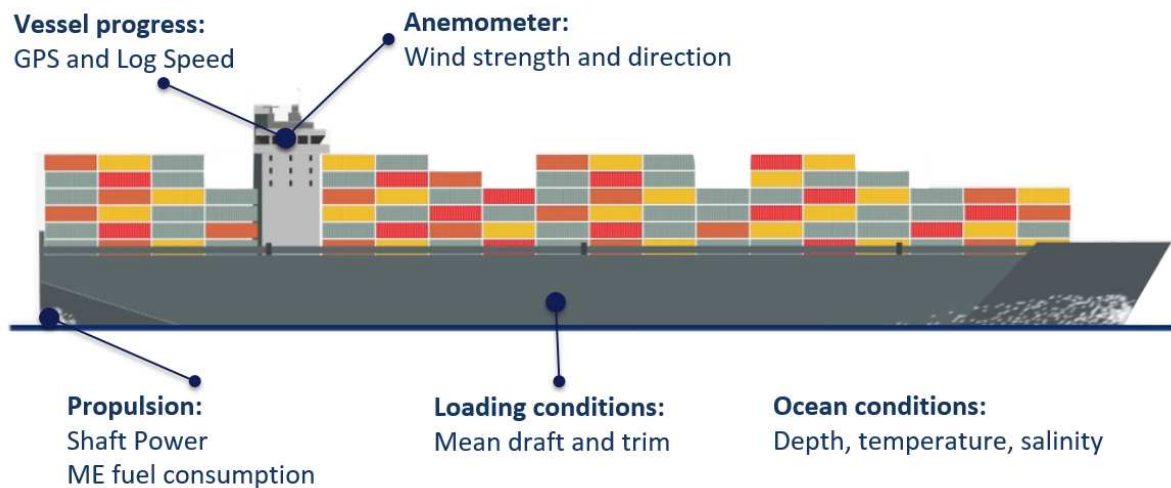


Fig. 1: Information collected for the analysis presented in the paper.

2.1. Marorka Onboard system

The Marorka Onboard system consists of a Marorka Maren Server, Marorka Workstations and DAQ units. An example of a Marorka Onboard system setup is displayed in Fig. 2. The Marorka Maren Server connects to a wide range of sensors and third-party systems (e.g. Alarm and Monitoring Systems) and supports several standard protocols including NMEA, OPC, Modbus, as well as many proprietary (file, serial or network based) forms of data exchange. Data is stored in the Maren Server in 15 s aggregates.

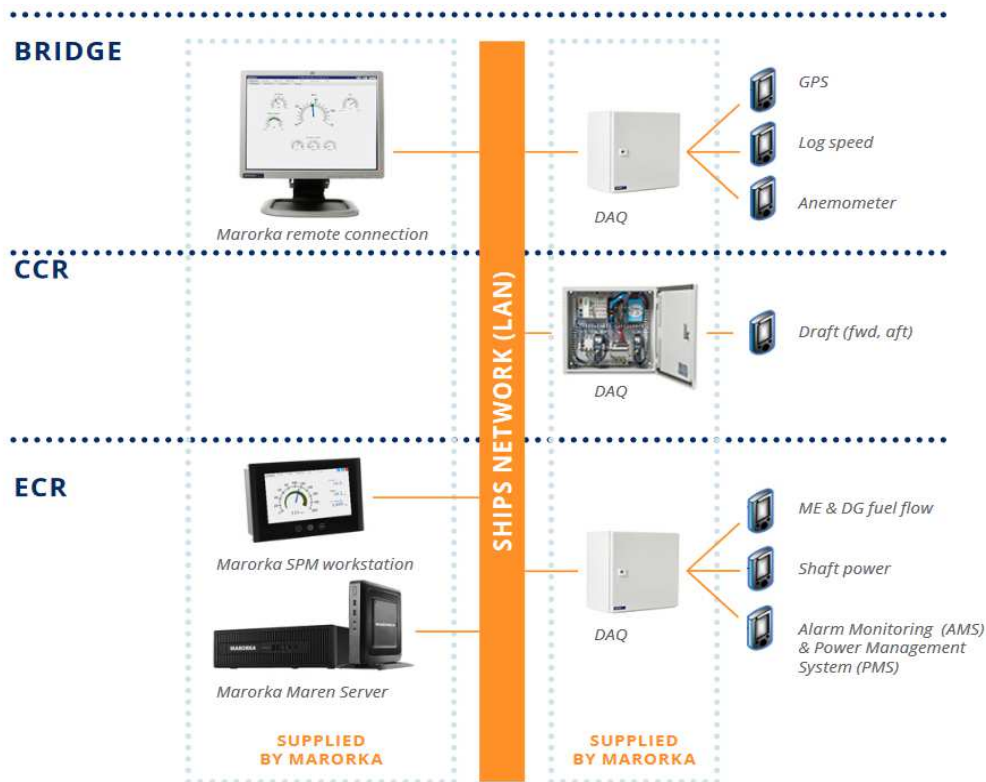


Fig. 2: An example of the Marorka Onboard system setup

2.2. Marorka Online system

Marorka Online collects operational data from Marorka Onboard, in data bundles which are received every 15 minutes. In the Marorka Online system, the information is processed and delivered in the form of interactive reports, such as fleet performance indicators for propulsion, trim, fuel use, emission and more. In the Marorka Online server, data quality is monitored by cross-validation of signals, as well as standard filters for frozen sensors or out-of-bounds values. Apart from accessing the interactive reports via the Marorka Online web-interface, the data for each vessel can be accessed from the Marorka Online servers via the OData API. This enables easy data export for any special reporting or third-party business application. The data used for the test cases, presented in this paper, was extracted from the Marorka Online servers via the OData API.

2.3 Test cases

In order to test the proposed method, a selection of test cases was needed. For the purpose of this demonstration, two cases were selected; one where a single general cargo vessel is tracked over a period extending roughly one year, and another where a pair of sister vessels are compared, over a period of 1½ years.

2.3.1 Test case 1: 50.000 DWT general cargo vessel

The first test case considers a single, 50.000 DWT, general cargo vessel, equipped with sensors connected to the Marorka system. The following signals were collected for the analysis:

- Loading condition: Draft fore and aft
- Vessel progress: Speed through water and GPS speed
- Anemometer: Relative wind speed and direction
- Propulsion power: Shaft RPM and shaft power
- Fuel consumption: Main engine fuel oil mass flow

The data collection covered just over one year, during which the vessel has had two propeller cleaning events. It is of practical interest to estimate the increase in resistance, due to temporary roughness, and the resulting speed drop between events. It is also beneficial to be able to quantify the effectiveness of each event, in terms of reduced resistance. This added information will assist ship owners and operators in deciding on what type of anti-fouling treatment or cleaning event to invest in.

2.3.2 Test case 2: A pair of sister vessels

The second test case considers a pair of 13.000 TEU container vessels. The vessels are identical sister vessels and share the same hull structure, engine specifications and all other particulars. There is, however, a difference in the initial anti-fouling treatment.

The vessels are equipped with the Marorka system, and the signals collected are identical to those in Test case 1. Data for these sister vessels was collected in parallel for the same 1½ year interval, during which, no hull or propeller maintenance events were scheduled for either vessel.

The main objective of the comparison of the sister vessels was to identify which one was experiencing a larger added resistance, due to temporary roughness, and which one would benefit more from a maintenance event. In general, estimates of excess resistance and the associated uncertainty may enable ship-operators to rationally schedule maintenance events for their fleet.

3. Data pre-processing and analysis

Once data has been collected, it must be pre-processed, by applying pre-defined filters to the data-set, before being used for analysis. Vessels operating under real conditions seldom experience the exact same conditions. However, in order to accurately evaluate the increase in temporary roughness, two comparable operational points, only differing in time, must be compared. There are both operational- and external effects that, in combination, influence the given speed-power relationship of a vessel. The operational conditions include the vessel speed, loading conditions and trim, while the external effects include weather factors, ocean waves and currents. Additionally, the external factors include the ocean conditions, such as depth, salinity and temperature. The level of filtering depends heavily on the analysis method and its robustness.

One of the problems when discussing the estimation of hull and propeller roughness is the lack of approved methods, or industry standard. This has resulted in extensive data collection periods and aggressive filtering of the data, to obtain comparable operational-points. The intention has been to address this problem with the issuing of the expected ISO standard. Even with an expected standard to be released, there is no standard way of reflecting the impact of sensor accuracy on the estimated result. When physical models are applied to normalise for external effects and loading conditions, the uncertainty in the models also need to be considered in the final result.

3.1 Proposed method

Both the aforementioned effects, operational and external, can be taken into account with physical resistance models, which need to be calibrated for each vessel. Along with these physical resistance models, modern statistical techniques allow us to estimate the performance degradation, originating from short data collection periods, while accounting for measurement noise and model uncertainty. This has enabled us to considerably shorten the data collection period, as the analysis provides a probability distribution of the estimate, allowing a construction of confidence intervals, which reflect the amount and quality of the underlying data.

3.2 Data pre-processing

For a reliable evaluation of a change in performance, a robust filtering of data points is required. Data points from manoeuvring and transient states are removed, along with frozen signal values and other

clear outlier points. Additionally, the data points fulfilling any of the following conditions are eliminated

- Shallow water, i.e. depth below 100 m.
- True wind greater than 5 BF.
- Difference between the speed log and GPS speed exceeding 1.0 knot.

The aggressive wind filter is unnecessary, as wind models are able to normalize for larger values, but for the sake of this test, a more aggressive filter was used. In order to ensure that all manoeuvring states are removed, log speeds below 10 knots were removed. The shaft power values were limited to the operating range of the engines, i.e., not vastly exceeding the MCR values of the engine. The fuel consumption readings were also filtered to remove obvious outliers, based on SFOC values. Finally, the trim of each vessel was limited to the densest operating range, which was close to even-keel.

4. Results & Discussion

After pre-processing the data, the analysis was performed, making use of the physical resistance models calibrated for the vessels. The resistance models account for the effects of external conditions on the vessels' resistance, as well as the calm-water propulsive-power requirements. The model also estimates the effect of different loading conditions on the required propulsive-power. Using the initial condition of each vessel as a base for the analysis, the results display the development the normalised speed-power relationship over time, along with the estimated uncertainty.

4.1. Test Case 1

The results for the single, general cargo vessel, or Test case 1, are provided in Fig. 3. As stated previously, there are two propeller cleaning events registered for the vessel during the one year and two months' period.

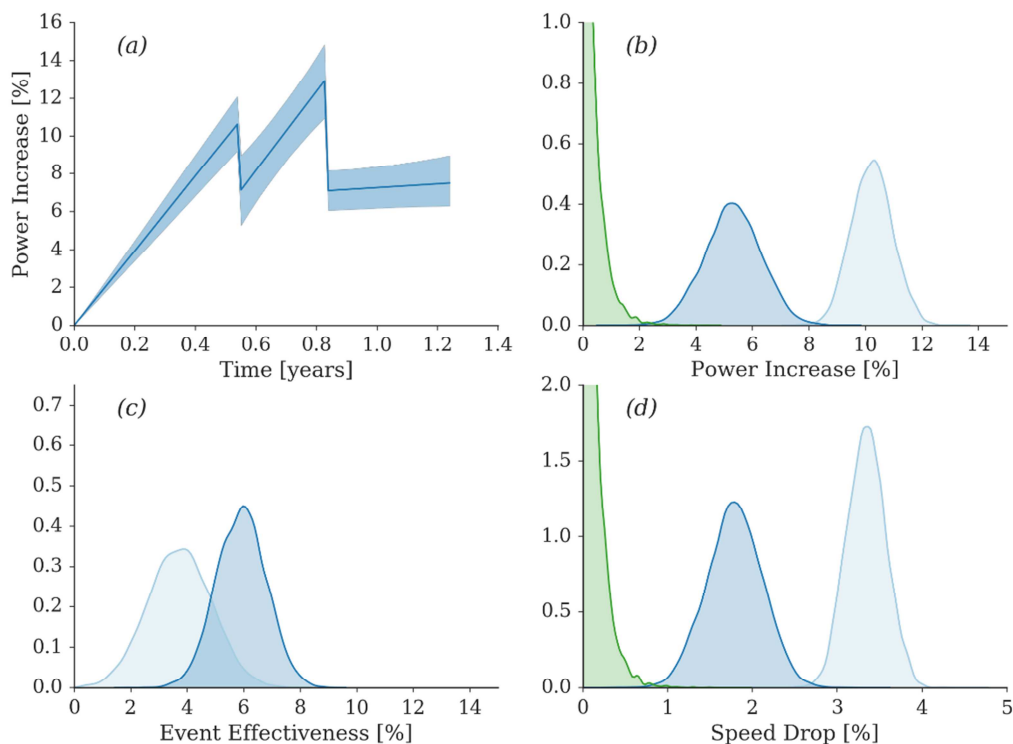


Fig. 3: The time evolution of performance-drop for test case 1. (a): Increase in required power relative to the initial point, with confidence intervals (95%). (b): Increase in required power between events. (c): Estimated effectiveness of the two cleaning events. (d): Resulting speed-drop between events.

Fig. 3(a) depicts the development of the vessel's temporary roughness, represented as a relative power increase. The first event is registered roughly six months after the start of data collection and the second event around ten months after the data collection started, or four months after the first one.

Fig. 3(b) shows the probability distribution of the relative power increase, corresponding to the trends in Fig.3(a). The first 6 months of the data collection period show an increase of the required relative, normalised power of around 10%, followed by similar rate of increase after the first scheduled event. The accumulated increase during the second four-month period is around 5%. The third, and final period of the data collection shows, however, an insignificant increase in temporary resistance. The speed-drop corresponding to the three periods is shown in Fig.3(d), where in the first period a speed-drop between 3% and 4% was demonstrated, the second period showed around 2% speed-drop and in the third period, the speed-drop was below 1%.

When reviewing Fig.3(a), it can be seen that the initial uncertainty estimate of the power increase is low but increases with time. This is because in the method the power requirement relative to the initial time is estimated, while the density and quality of data in each time period also affects the uncertainty assessment.

Fig. 3(c) shows a distribution of the estimated effectiveness of each of the maintenance events; that is the decrease in required power. Both registered maintenance events are propeller cleaning events, and show an effectiveness of 3% and 6% respectively.

4.2. Test Case 2

The sister vessels from Test case 2 were monitored during a 1 ½ year period. However, as neither vessel had any registered maintenance events, only a comparison of the relative power increase, and the resulting speed-drop is considered.

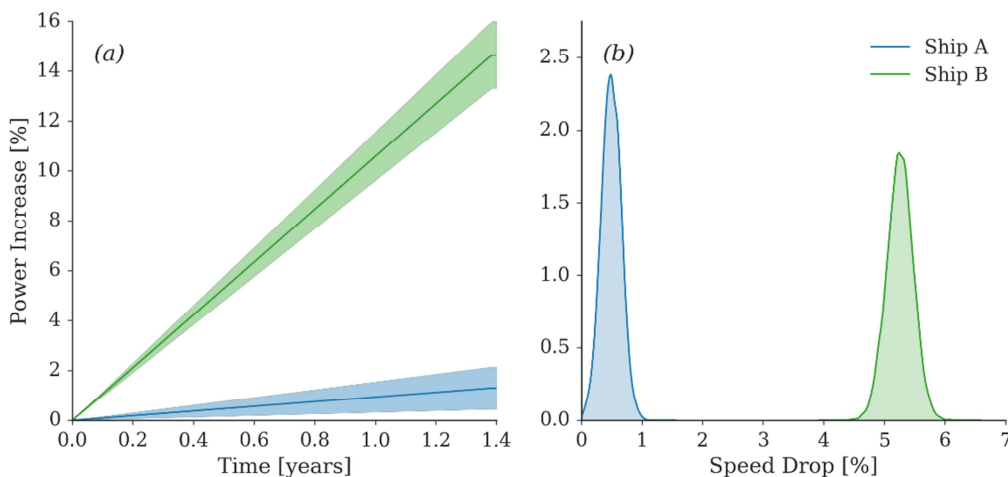


Fig. 4: Increase in power for a 13,000 TEU container ship. (a) Shows the power increase relative to the initial point, with 95% confidence intervals. (b) Shows the probability distribution in speed drop.

Fig. 4(a) shows the results of the relative power increase for both vessels. During the 1½ year data collection period, there is a considerable difference between the increase in temporary roughness between the vessels. Vessel A demonstrates a relative power increase of around 1%, and a corresponding speed-drop below 1% over the period, as shown in Fig. 4(b). Vessel B, however, shows a relative power increase of around 14-15%, and a corresponding speed-drop ranging from 4.5% to 6%.

It is worth noting that there was a difference in the initial anti-fouling measures applied on the vessels, so a slight difference was to be expected. It might, however, be argued that the demonstrated

difference is somewhat larger than anticipated from only a difference in the initial anti-fouling measures. This might reward a closer analysis of the underlying reasons for the noted difference, such as the operational profiles of each vessel. Whatever the additional reasons, these results clearly highlight the importance of applying appropriate anti-fouling measures during construction and dry-docking. A rough estimation of the savings made, by applying the more effective anti-fouling measures in this case, is around \$500,000, over the entire period. This estimation does not consider the difference in cost of the different measures, only the potential savings.

5. Conclusions

The method applied and presented in this paper provides a way to estimate the combined deterioration of the hull and propeller during service, while accounting for uncertainties in both sensors and the underlying physical model. The method is capable of normalising for external conditions and is not reliant on a specified reference period, as it uses the entire period for inference of the performance drop. The final outcome is not only an estimate of the resistance evolution, but also quantification of the confidence in the estimate. A method which introduces an assessment of the certainty can be highly valuable when the estimate is used to support decision of hull and propeller maintenance, which may be very costly.

The advantage of the procedure is the ability to observe short-term changes in performance, giving operators the opportunity to react early to potential performance problems. It enables fleet managers to rationally schedule maintenance events, based on the estimated temporary roughness, scheduling of individual vessels, as well as estimated cost.

The method can also be used to evaluate and compare the efficiency of different cleaning events, as well as comparing the effectiveness of different anti-fouling solutions. Using the same approach, a comparison of dry-docking events, different treatments applied during dry-docking or even different locations for dry-docking can be made.

The intentions behind the introduction of the presented method are not to try to replace the expected ISO standard, but rather serve as a complement to that effort, focusing on short-term, in-service changes. Due to the nature of the data collection on-board vessels in service, there is a need to effectively use the limited amount of data, on shorter time scales. This implies that it is necessary to effectively normalise for external conditions, and to be able to quantify the uncertainty of the estimate. By doing this successfully, ship operators can schedule maintenance of their fleet effectively, in a data-driven manner.

References

- ALDOUS, L.; SMITH, T.; BUCKNALL, R.; THOMPSON, P. (2015), *Uncertainty Analysis in Ship Performance Monitoring*, Ocean Engineering, Elsevier, pp 1-10. doi:10.1016/j.oceaneng.2015.05.043
- CARLTON, J. (2012), *Marine Propellers and Propulsion, Third edition*. Butterworth-Heinemann
- Historic Paris Agreement on Climate Change: *195 Nations Set Path to Keep Temperature Rise Well Below 2 Degrees Celsius*. (12.12.2015). <http://newsroom.unfccc.int/unfccc-newsroom/finale-cop21/>
- HOFFMAN, J.; ASARIOTIS, R.; BENAMARA, H.; PREMTI, A.; SANCHEZ, R.; VALENTINE, V.; WILMSMEIER, G.; YOUSSEF, F. (2015), *Review of Maritime Transport 2015*, United Nations Publication
- Kyoto Protocol. http://unfccc.int/kyoto_protocol/items/2830.php
- MOLLAND, A.F.; TURNOCK, S.R.; HUDSON, D.A. (2011), *Ship Resistance and Propulsion: Practical Estimation of Propulsive Power*, Cambridge University Press

Performance Monitoring and Hull Performance: A Ship Manager's View

Cezary Afeltowicz, E.R. Schiffahrt, Hamburg/Germany, cezary.afeltowicz@er-ship.com

Abstract

Performance monitoring and hull performance are major factors for successful overall "performance". In order to survive in the highly competitive market, it is essential for a ship manager to meet customer needs in terms of energy efficiency. However, ship performance from a ship manager's view is much more than energy efficiency. In modern ship management there are simultaneously different demands and requirements from the object "ship" as multiple stakeholders are present, sometimes even with contradicting expectations. A successful ship manager is able to provide an optimum solution to each single stakeholder, without causing impairment to the interests of others.

1. Introduction modern Ship Management

1.1. Brief presentation E.R. Schiffahrt

E.R. Schiffahrt (ERS) is a ship management company with activities in container and bulk segments. Currently it manages more than 90 vessels in service. The dry bulk division of E.R. Schiffahrt consists of 20 handymax, supramax, kamsarmax and capesize vessels, aggregating about 2.2 million dwt. The container fleet of E.R. Schiffahrt consists of more than 70 container vessels in service, aggregating about 450,000 TEU. The vessels are chartered by liner and bulk shipping companies. ERS aims to be one of the best ship management companies in the shipping industry. To assure this ambitious target, the manifold interest of the diverse group of interest must be bore in mind, harmonized in coexistence and settled to a matched optimum. There are currently about 3500 crew members at sea and employees ashore, working as a team who are dedicated to securing safety, reliability and performance for the benefit of customers and business partners worldwide.

1.2. Safety, quality, compliance and environment

The modern safety and quality management system is geared to the following four criteria and forms the framework for the work of every employee:

- Safety of crew, ships, environment and cargo
- Compliance with national and international regulations and legislation
- Ensuring consistently high quality
- Optimal economic efficiency

High safety standards ensure that any threats and risks to crew, ships, environment, cargo, and thereby for the customers, are kept as low as possible. Compliance with national and international rules and regulations is an essential basis for doing so. A stringent quality management system is necessary to ensure the consistently high quality of services and identifying new potential for optimization.

An adequate risk management system is required. In the interest of the customers and partners all activities are to be monitored by means of an operations management system to ensure implementation of improvements with a maximum operating efficiency. Moreover the modern ship manager must comply with a risk management monitoring system and must minimize risks and implement measures on a continuous improving basis.

All company employees are constantly working to improve and enhance the high quality standards and to harness further potential to optimize quality and safety.

Ensuring compliance with national and international regulations and legislation appropriate certification must be provided. In this example case, ERS is certified by DNV GL in accordance with the International Safety Management code to BS OHSAS 18001:2007, DIN EN ISO 9001:2008, ISO 14001:2004 and ISO 50001.

Last but not least, optimal economic efficiency must be provided by all means focusing customers' benefits, the monitoring of new developments, innovations and management and ship operation methods need adaptation on a continuous basis. Support of third parties is often necessary. Classification societies are helpful and able to credit and value such remarkable efforts, e.g. DNV GL "Modification Excellence Award" where E.R. Schiffahrt was the first company which received this award which was presented by DNV GL at the end of November 2014. The classification society herewith confirmed energy savings of 15 percent as well as improved cargo capacities for a series of retrofitted 13100 TEU vessels. The measures include new bulbous bows, energy efficient propellers, engine modifications and cargo boosting.

2. Performance factors in a modern ship management

Modern ship management shall provide first-class and flexible services in the appointed segments. The reliable ship management shall offer customized arrangements to ensure excellent results in shipping for the customers and all business partners.

The performance factors in a modern ship management company are multilayer and need to cover diversified expectations with long term benefits for:

- Ship owner:
 - Keep the value of the vessel
 - Costs reduction
 - Earnings optimization
 - Maximization of vessel's life-time while keeping high quality standards
- Charterer:
 - Fuel costs awareness (= monitoring)
 - Fuel performance optimization (= modifications)
 - 24/7 operational availability, constancy in schedule
 - Energy, emissions and earnings efficiency
- Ship manager:
 - Operational expenses (OPEX) fidelity
 - Conformity with regulations
 - Prevention of off-hire and detentions by PSC
 - Development of excellence and good reputation
- Crew:
 - Maintenance and workload optimization
 - Increase of crew's know-how, experience and quality
 - High level of accommodation and recreation facilities on board
 - High identification grade with vessel, owner, charterers and ship manager

The settlement of the performance factors must be implemented within the management structures and operational processes within the management company. The highest standards of quality, precision, safety and economic efficiency are to be guaranteed by all dedicated employees on shore and at sea. The following key sentences could be considered as guidelines for a modern ship management company in order to cover the performance factors for all stakeholders.

2.1. Customer's success to be top priority

The tailor-made solutions and service are to be provided by:

- Focus on long-term and strategic partnerships
- Customer requirements are the key
- Cost efficiency program
- Technical reliability
- Operational flexibility
- Customized services to ensure required and wanted results

2.2. Continuous and dedicated customers care

Customers' relations and operation are to be kept on highest possible level provided by:

- Daily exchange with brokers and customers to identify customers' needs and create individual employment charter concepts
- Regular customer calls for a face-to-face dialogue
- Coordination of the worldwide broker network
- Matching customer needs with technical requirements for dry-docking, maintenance & repair
- Project department for specific tasks, business development and fleet-wide innovation

2.3. Technical Fleet Management is to be excellent

Technical Fleet Management is to be paradigm for efficiency and reliability provided by:

- Professional and interdisciplinary fleet management to ensure sound operations
- Support for the existing fleet teams by specialized technical and nautical teams
- Special expertise in energy efficiency, dry-docking, propulsion and vessel-IT

2.4. Fuel Cost Awareness

Fuel cost awareness and energy efficiency are additional values for the customer and excellent "unique selling proposition" (USP) if managed properly. They are specific, measureable and easy comparable to the competitors. Focus on fuel efficiency is to be provided by:

- Real-time Vessel Performance Monitoring Center (VPMC) with 24/7 real-time recommendations to crew on board for operation optimization
- Continuously consultancy to customers (Charterers, Owners) for vessels in service regarding possible cost efficiently measures e.g. hull and propeller cleanings in service (via VPMC)
- Close cooperation with liners, manufacturers and research institutes for innovative optimization concepts to reduce fuel consumption
- Fleet/vessels to be optimized for super slow steaming
- Further savings through individual weather routing, trim optimization and low friction paint

2.5. Fuel Performance Optimization

Fuel performance optimization by major modifications is a further key factor for USP for the end customer. This can be provided by:

- Retrofitting of propeller
- Energy Saving Propeller Cap (ESCAP)
- Bulbous bow optimization
- Design optimizations on hull to propeller (Mewis-duct) and propeller to ruder (Rudder bulb)
- Full Blasting and Low Friction Paint application
- Retrofitting of main engines
- Frequency controlled sea-water pumps and Engine Room fans
- Turbocharger cut-out
- Know-how available to customers

2.6. Earnings Efficiency Optimization

Performance optimization for a holistic and modern ship manager is not limited to fuel cost awareness and fuel performance optimization. Further efficiency improvements way beyond direct fuel savings shall be considered. This could be provided by major and minor modifications as:

- New Panama Canal adjustment
- Cargo Capacity Boost via Draft increase and/or Wheel House Elevation increase
- Reefer Boost on existing vessel
- Increased cargo and trade flexibility (Air Draft reduction for e.g. Bayonne Bridge)
- Route Specific Container Stowage
- Shore Power connection (Cold Ironing)
- Major modification regarding compliance with new rules and regulations (e.g. Emission Control Areas -SECA-, Ballast Water Management –BWM- etc.)/ consultancy with customers
- Additional innovations for customer benefits

2.7. Crewing Policy

Crewing policy in a modern ship management company must be considered focusing on high quality crewing as always reliable people on board are the linchpin for successful use of energy and earnings efficiency measures on board. Without smart people on board smart solutions will be ineffective. Innovative and efficient crewing policy can be provided by:

- Tailor-made crewing arrangements for the customers
- Close link between ship and shore for an efficient cooperation and communication
- Highly skilled crews
- Continuous practical crew training courses and regular on-shore seminars worldwide e.g.:
 - Regular Fleet Officer meetings, Group Presentation/Briefings and individual briefings
 - Simulator trainings on-shore and on board trainings
 - Trainings at manufacturer’s sites

Please keep in mind that crew training is all about knowledge, awareness and dedication and this should be an essential part of company’s crewing management policy. Although all the different performance factors are of significant importance for a successful ship manager, the further elaboration within this paper will focus on energy efficiency performance.

3. Energy Efficiency improvement

The conditions for a good propulsion performance (= energy efficiency) of a vessel underlie permanent changes and are to be classified as a dynamic process. In the shipping business it is generally not common (and not possible) to respond and act on each technical variation and innovation. The most of those innovations are accompanied by high financial burden and off-hire or stay on a shipyard, but both are not available for a ship without certain restrictions. Manufacturers announced innovations in terms of fuel-oil-saving-rates which are rather difficult to be specified and verified as those are depending on a wide range of simultaneously appeared and varying parameters. Furthermore it would be obligatory to have time- and cost consuming tools for data collection and analysis in order to verify such promises substantive. Just as an example the most fuel oil consumption affecting parameter “speed profile” has changed in the last years significantly.

3.1. Speed-/consumption-profiles today and in the past

In the past decade, vessels were designed for higher speeds than nowadays required. Hull and propulsion set-up (main engine and propeller) were designed even to keep the maximal possible speed. Increased fuel oil prices and overcapacity of tonnage turned the trend to slow and super slow steaming, where the designed operational points of the propulsion systems reach technical limits.

The vessels are operating down up to 10% of the maximum continuous rating of main engine on long-term usage, which is not only out of operational point but also very burden to the engine components. Furthermore it requires also particular operational procedures. The current operational points are far beyond the designed operational speed, so the vessels are generating massive overconsumption versus vessels designed for the slow-steaming speed. Fig.1 shows the change of speed profile over last six years on example for 10 year old Post-Panmax vessels.

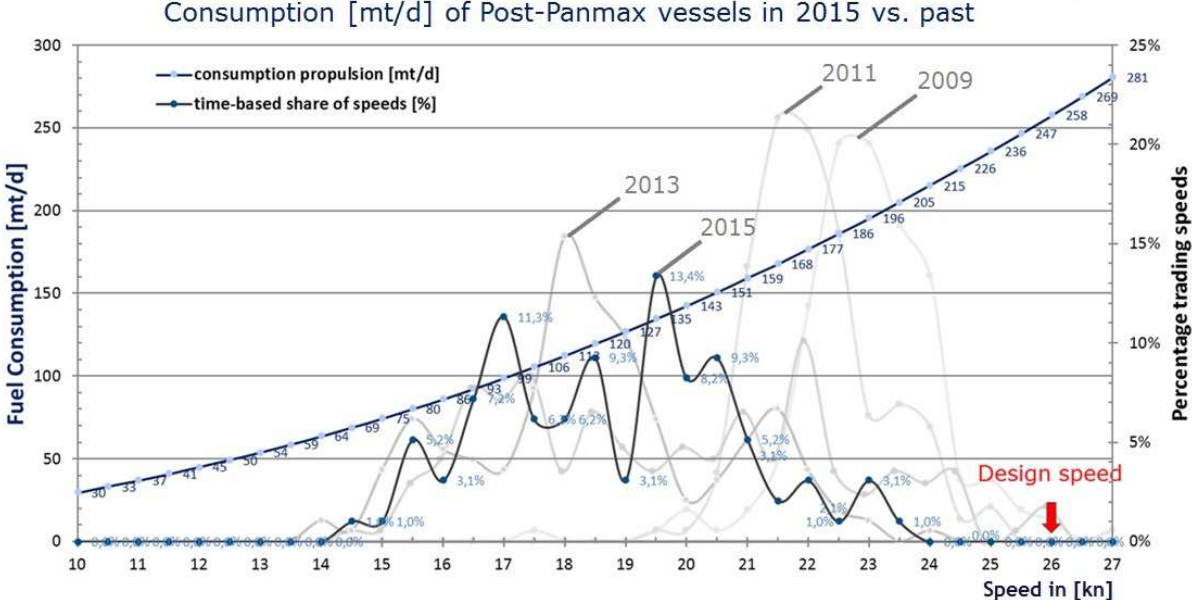


Fig.1: Speed-/Consumption profile of Post-Panmax vessels since 2009

The speed profile changes since 2009 are clearly visible. The average speeds were going down year by year, since late 2014 a slightly increase of speed range can be observed which is obviously an effect of the strong dropped fuel oil prices. Generally deduction is, that the vessels designed and build for the maximum speed (in this case for 26kn), are operating far below this point. The maximum speed point is not reached/ desired nowadays at all. The only conclusion from the discrepancy of design operational point and actual operating speed range is that the vessels are sailing in very disadvantageous speeds generating overconsumption over their whole operational range.

3.2. Energy Efficiency adjustments according to operational requirements

Before improvements can be implemented, sources of overconsumption need to be identified. Overconsumption can be a result of non-optimized design reasons, as machinery or hull or non-optimized operational reasons, which could be related to charterer’s reasons (scheduling, waiting times etc.) and to owner/ship manager reasons (voyage execution, trim, maintenance etc.).

Identified the overconsumption wide range of modifications (= energy efficiency optimization) are possible (see 2.5.). However depending upon the kind of modification investment costs could be very high, so the target to increase the energy (and earnings) efficiency must be well adjusted to the financial situation of the vessel and in reasonable terms of return of investment.

Considering the cost relation between the charter rates and the bunker prices, an Energy Efficiency improvement of 10% (= lower bunker costs of 10%) could be equivalent up to 25-30% of the charter rate. In such cases it is recommended to present these numbers to charterers who could support financially as he is directly benefiting and seeing the positive impact on his fuel oil bill. On the other hand the Owner and/or Ship manager could take modification costs on their own account in order to present (for the charterer) a better vessel, which could result in higher charter rates.

Using the example E.R. Schiffahrt, more than 300 energy and earning improvement modifications were carried out since 2013. There are about 35 Propellers and 45 ESCAP changes and more than 30 bulbous bows were replaced in order to improve the energy efficiency. All energy and efficiency increasing modifications, as listed under 2.5. and 2.6., were carried out by the company. Because of the complexity and high amount of work, such projects cannot be managed by technical departments taking care of daily business on the optimal way. Therefore in 2014 a self-contained department was created within the Technical Fleet Management of E.R. Schiffahrt, where such modifications and propulsion improvement projects are evaluated, planned and carried out by BestShip (www.bestship.com) experts also for outside third parties.

In view of fuel cost awareness a Vessel Performance Monitoring Center (VPMC) has been established within the performance department of E.R. Schiffahrt. On large flat-screen monitors the collected data from the vessels can be monitored, evaluated and communicated back to the vessels. This issue is the topic of the next chapter.

3.3. Vessel Performance Monitoring

Performance monitoring and in line with that fuel consumption monitoring are the key factors for additional value for the customer, but those are also of significant values for the ship manager. According to the motto “If you can’t measure it, you can’t manage it” appropriate data collecting tools are an essential first step for profound performance monitoring and analysis. The main goal of an efficient performance monitoring system must be the degree of transparency allowing the charterer to rely on lowest possible bunker costs and a good carbon footprint, the owner a careful use of their asset and ship managers on optimal balance to prove on high quality at reasonable operational expenses.

The collecting data from the vessels can be generally provided by two ways:

- Automatically collected data (sensors, mass flow meters and further measuring devices)
- Manually collected data from various sources and reports

3.3.1. FuelSafe¹- Automatically collected data

One of the central benefits of automatically collected data is that reading, compiling and transmitting the measured results is not increasing crew’s workload. With a continuous flow of a few hundred measured signals per ship, from shaft power meter, weather and nautical data, tank sensor readings, mass flow meters in the fuel lines of the main and auxiliary engines and the boiler, enabling plausibility checks in all directions with a wide and flexibly variety of criteria. The system can precisely calculate how much of every metric ton of bunker has been converted into how many kilowatts of propulsion energy, electrical energy and thermal energy.

The comparative instalment costs of automatic collected data systems versus manually collected data are high, but the potentials of optimization and savings are incomparable higher and the return of investment is expected to be below in one year. In doing so, the savings of bunker are considered here only. Additional to this there are operational expenses savings as parallel runs of auxiliary engines on low load (Fig. 2), lubrication pumps (Fig. 3), air compressors, engine room fans and so forth can be avoided resulting in reduction of running hours and herewith with significant lowering of maintenance costs and times.

Furthermore monitoring, evaluation and controlling of all operational subjects can be helpful in prediction of fuel consumptions for future voyages or charter descriptions. Foresight of irregularities on the machinery and equipment and herewith proactive intervention before machinery/equipment

¹ FuelSafe®- the new performance monitoring system from E.R. Schiffahrt developed in collaboration with well-known maritime partners. FuelSafe hardware and software is developed and adapted to ship manager needs in a way that no-one has achieved in the industry up to now.

failures is a further benefit of substantial data acquisition by automatically generated, collected and evaluated performance monitoring systems.

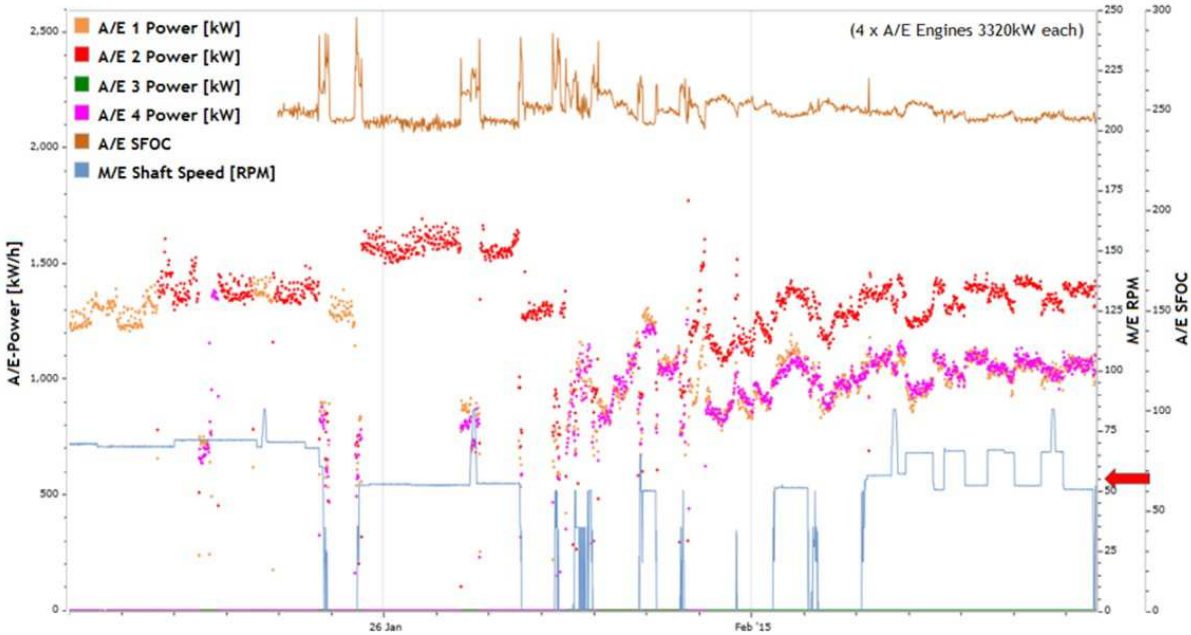


Fig. 2: FuelSafe indication of simultaneous operation of auxiliary engines at low loads (<30% MCR)

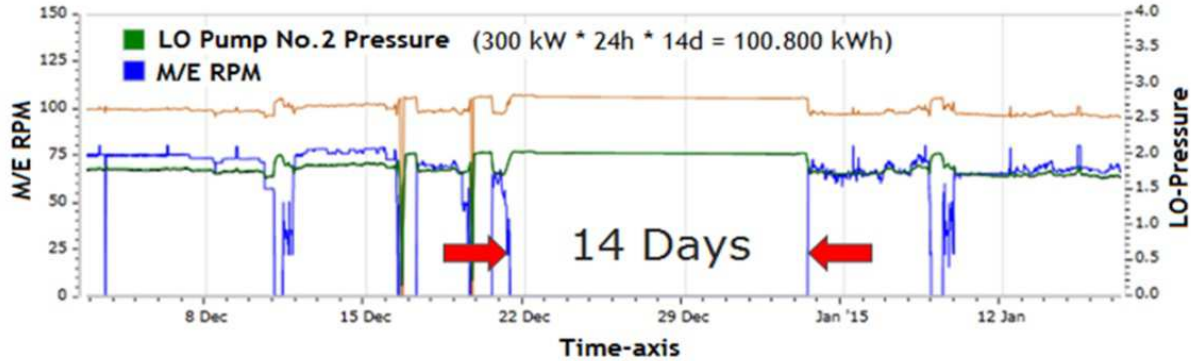


Fig. 3: FuelSafe indication of permanently operation of LO Pump during 14 days of lay-up

Voyage planning and voyage conduction with constant speed is a further remarkable playground for high bunker cost savings (Fig. 4). Last but not least, in-depth look back in the past is always possible allowing follow-up, checking and improvement of processes as well as availability of comprehensive data basis for any kind of discussions regarding speed-consumption questions for any voyage, see passage or time intervals.

Current planning of E.R. Schiffahrt’s fleet see around 40% of the container fleet equipped with FuelSafe by end of 2016. Whereas FuelSafe soft- and hardware is available on board and ashore, the own data server is ashore only. The secondly automatically collected 200-300 signals are sent to office in 5min-data packages. Live evaluation on board and in Vessel Performance Monitoring Center are the key-factors in development of FuelSafe.

Automatic monitoring via own created Key Performance Indicators (KPI) allows evaluation of Curves, Specific Consumption factors, Trim, Hull condition, Speed-Consumption, Fuel balance etc.. Comparison to benchmark, own reference curves and benchmarking, verification and plausibility checks between vessels at different times, voyages, sections with a wide range of filtering are possible as well. These KPIs are weighted, traffic light visualized and betokened on the vessel on a world map.

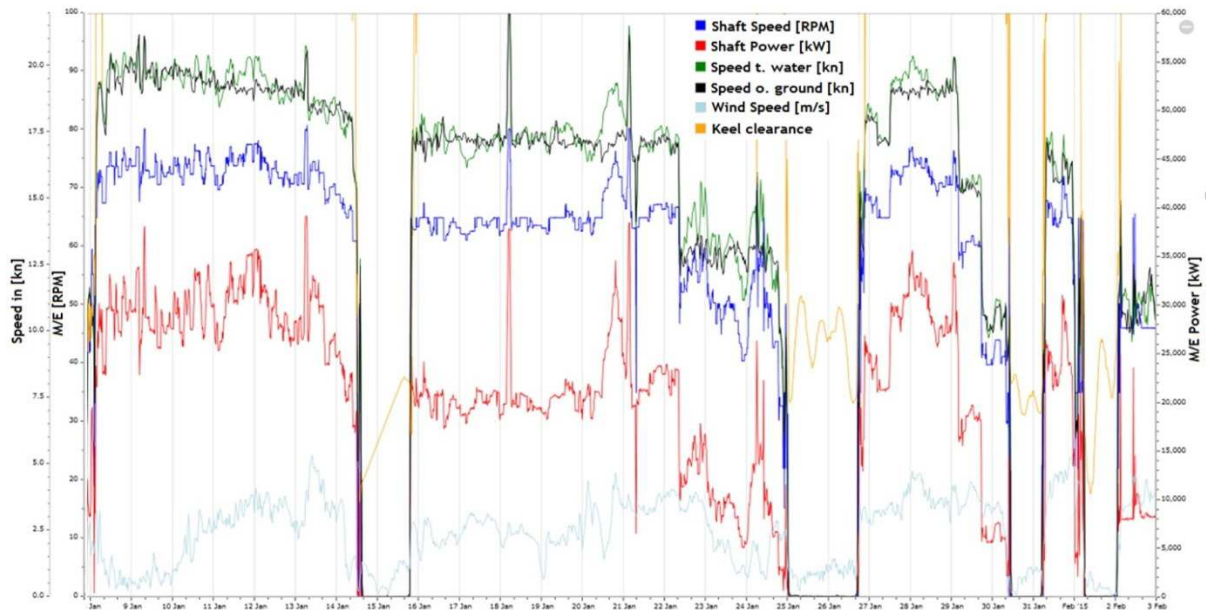


Fig. 4: FuelSafe indication of voyage conduction with inconstant speeds

3.3.2. FuelSafe_light - manually collected data

The second way to get an overview about vessels performance is manually collecting data via noon-reporting and comparison of these with sea-trail reference curves or benchmark vessels. Although the workload on board and ashore is surpassing higher, the data coverage and data correctness will not achieve the data quality generated by automatically performance monitoring systems. Noon-reporting (NR) is the first approach for ship performance monitoring within tight budget constraints. A further benefit is the coverage over the whole fleet providing some transparency for the customers over all vessels of the managed fleet. For essential demand of data collection for example as ISO 50001 (energy management) or for MRV of EU ETS (Monitoring, reporting and verification of European Union Emissions Trading System) NR should be sufficient if premeditated properly.

FuelSafe_light monitoring ...example COC / SCOC

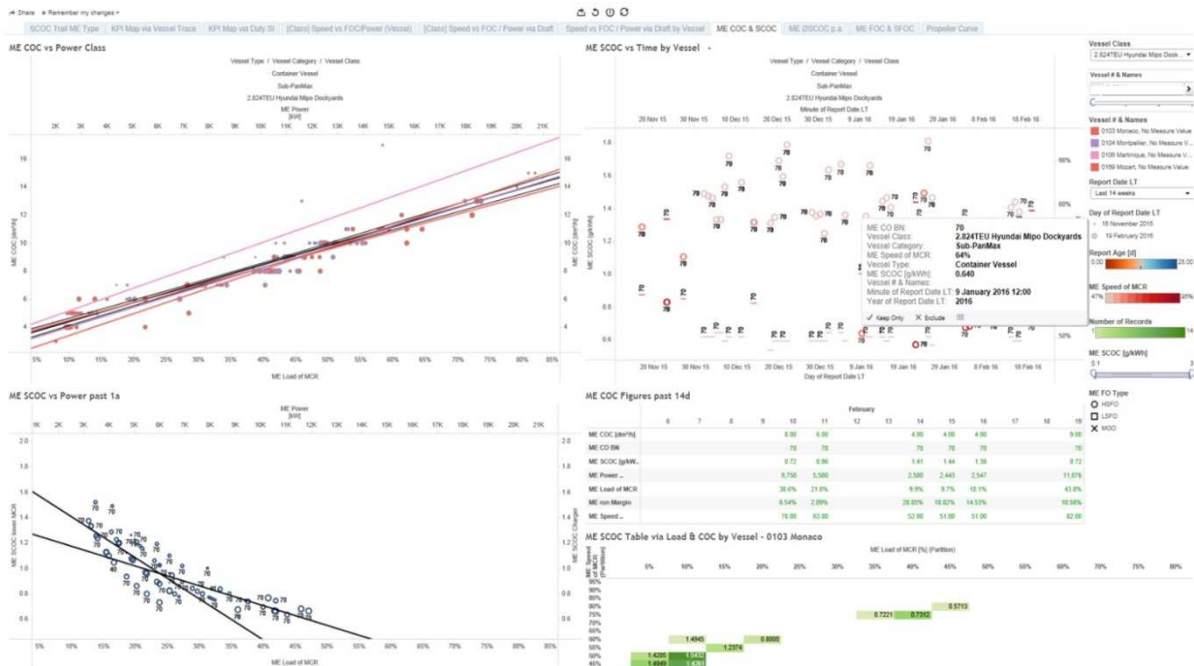


Fig. 5: FuelSafe_light display of reporting, Cylinder Oil Cons. (COC), Specific COC and more...

Using the example E.R. Schiffahrt FuelSafe_light noon-reporting system has been implemented, however transmission, output to office, data collection ashore and their storage, evaluation and monitoring are working on automated systems. Data collection and input on board are semi-manually via a software-module developed in collaboration with well-known maritime partner. Plausibility checks and warnings within the software are controlled via own defined KPIs carried out automatically before transmission to shore.

On shore evaluation is flexible and individual adjustable/programmable. Analysis, monitoring and communication with the vessels are performed by assigned nautical, performance and propulsion experts within ERS Vessel Performance Monitoring Center (VPMC). Various tailor-made analyses and analytics are provided as main engine specific/ fuel/cylinder oil consumption, comparison to accurate benchmarks, own references, between vessels, with filtering at different time intervals, voyages, considering trim, hull condition monitoring, speed-consumption and so forth, Figs. 5 and 6.

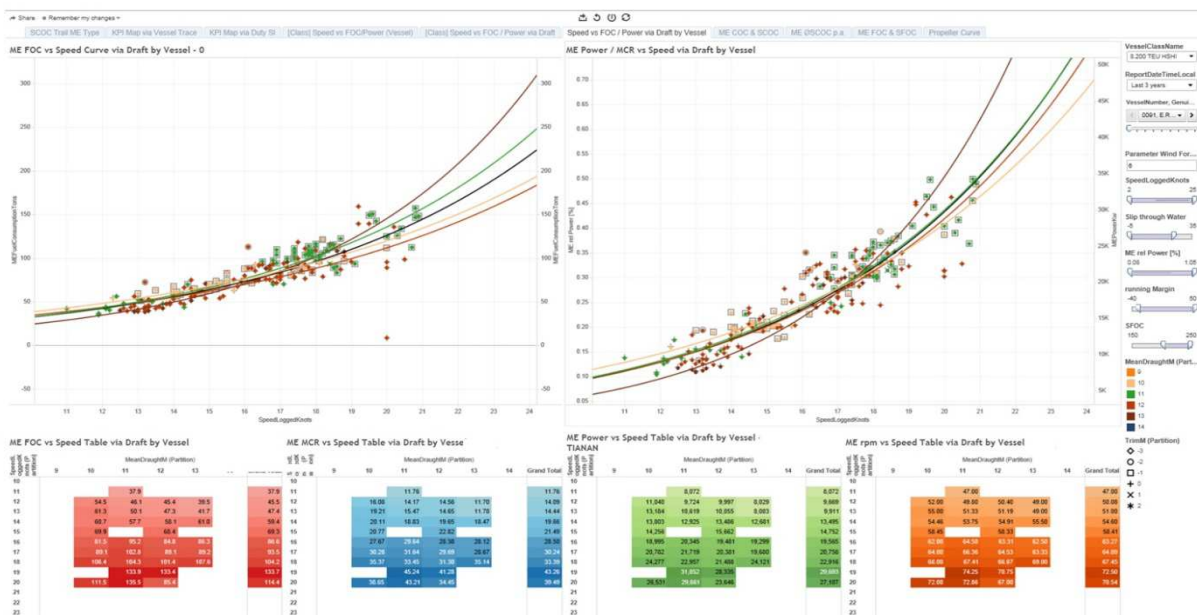


Fig.6 FuelSafe_light display Fuel Oil Consumption vs. Speed and Drafts for a series of vessels



Fig. 7 FuelSafe_light display of KPIs on world map filtered by superintendent

Unchanged to FuelSafe also FuelSafe-light KPIs are weighted, traffic light visualized and betokened on the vessel on a world map. Additionally alternatively filtering by series of vessels, charterers or by the managed fleet team or individual superintendent is possible, Fig. 7.

3. Summary and Outlook

Looking at the development of ship performance analysis in the last couple of years preferable automatic data collecting and evaluating systems will be used. The increasing demands of requirement of live-streaming analysis and interaction by on-going varying ship draft, loading, weather, water depth, propulsion, charterers schedule and another specified inputs cannot be covered by manually generated noon-reporting.

However the automatic systems will be used checking the performance via KPIs and giving feedback to crew on board or ashore, the human factor seems still to have the most important impact regarding energy efficiency. Assuming to have the best possible equipment on board and to have the most efficient procedures for voyage planning written down there will be only very limited effect on bunker saving side if the people will be not properly trained, aware and willing to carry out their task with most available and by itself emerged motivation. Repeating the phrase:

“Without smart people on board smart solutions will be ineffective”

is to be said again only high quality crewing as always reliable people on board are the linchpin for successful use of energy and earnings efficiency measures on board. Crew training is all about knowledge, awareness and dedication. This must be an essential part of company's crewing management policy in order to be a successful ship manager, who provides the maximum energy and earnings efficiency, proper asset management and all attainable benefits for the involved stakeholders of the subject SHIP.

The key performance initiator is our colleague on board!

References

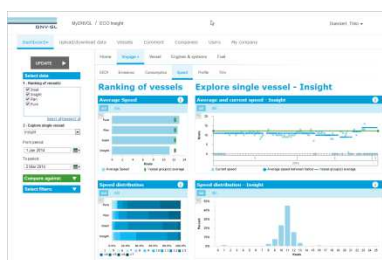
- AFELTOWICZ, C. (2008), *Wirtschaftlichkeit und Wirkungsweise silikonbasierter Antifouling bei Seeschiffen*, CT Salzwasser-Verlag
- ELJARDT, G. (2014), *Efficiency increasing retrofit solutions*, STG Sprechtag Intelligente Nachrüstung von Schiffen
- EETVELDE, L. van (2015), *Slow Steaming, Super Slow Steaming*, 10th Vessel Efficiency & Fuel Management, London
- HARVALD, S.A. (1983), *Resistance and Propulsion of Ships*, John Wiley & Sons
- KUDRITZKI, J. (2013), *E.R. Schifffahrt's Energy Efficiency*, Ship Efficiency Conf. Hamburg
- KUDRITZKI, J. (2015), *How to save 20% of your vessel's energy & emissions*, 10th Vessel Efficiency & Fuel Management Summit, London
- SCHNEEKLUTH H.; BERTRAM, V. (1998), *Ship Design for Efficiency and Economy*, Butterworth-Heinemann

Index by Authors

Afeltowicz	339	Lutkenhouse	245
Ando	96	Lynn	245
Badoe	178	Messeri	215
Ballegooijen	192	Meyerinck	312
Baur, vom	230	Michael	245
Benedetti	215	Muntean	192
Bertram	5,14,41,62	Nakazaki	263
Bibuli	163	Odetti	163
Bos	106	Oftedahl	239,292
Brady	245	Okada	263
Bruzzzone	163	Okazaki	263
Caccia	163	Oliveira	82
Capecchi	215	Orihara	70
Coraddu	215	Orlandi	215
Cusano	319	Ortolani	215
Chen	298	Pakkanen	115
Del Toro	29	Paraeli	62
Delbridge	245	Pfannenschmidt	145
Deng	29	Phillips	178
Dirksen	282	Qualich	319
Dücker	23	Queutey	29
Finnie	298	Ranieri	163
Fridriksson	332	Ross	245
Fritz	128	Rovai	215
Fukuda	263	Rühr	312
Garbarino	319	Salo	115
Goedicke	145	Schmode	23
Gonzalez	49	Solonen	152
Gorski	203	Soyland	292
Granhag	82	Stamper	245
Greitsch	145	Stranieri	319
Guilmineau	29	Tseng	245
Gundermann	282	Tullberg	23
Hagestuen	49	Turnock	178
Haranen	115	Visonneau	29
Haslbeck	245	Webb	245
Hentschel	312	Wienke	137
Herradon	14	Yakabe	271
Holm	245	Yonezawa	96
Ishiguro	70	Yoshida	70
Jonsson	332	Zareik	163
Kakuta	96		
Kariranta	115		
Katayama	263		
Kidd	298		
Krapp	41,62		
Lampe	137		
Lund	49		

2nd Hull Performance & Insight Conference (HullPIC)

Castle Ulrichshusen / Germany, 27-29 March 2017



Topics: ISO 19030 and beyond / sensor technology / information fusion / big data / uncertainty analysis / hydrodynamic models / business models / cleaning technology / coating technology / ESDs

Organiser: Volker Bertram (Tutech Innovation (TU Hamburg))
Geir Axel Oftedahl (Jotun)

Advisory Committee:

Michael vom Baur	Hoppe Marine	Tsuyoshi Ishiguro	JMUC	Hideaki Saito	JSTRA
Torsten Büssow	DNV GL	Jeppe S. Juhl	BIMCO	Svend Soyland	Nordic Energy Research
Erik Hagestuen	Kyma	Andreas Krapp	Jotun	Geoff Swain	FIT
Simon Hayes	BMT Smart	Jussi Pyörre	Eniram	Diego M. Yebra	Hempel
Esa Henttinen	NAPA				

Venue: The conference will be held at Castle Ulrichshusen in Germany

Format: Papers to the above topics are invited and will be selected by a selection committee. Papers may have up to 15 pages. The proceedings will be made freely available to the general public.

Deadlines: anytime Optional "early warning" of interest to submit paper
01.12.2016 Submission of abstracts
10.02.2017 Payment due for authors
10.02.2017 Final papers due

Fees: **600 €** – early registration (by 10.2.2017)
700 € – late registration

Fees are subject to VAT (reverse charge mechanism in Europe)
Fees include proceedings, lunches, coffee breaks and conference dinner

Sponsors: Jotun, DNV GL, Hoppe Marine, Propulsion Dynamics Inc.

Information: www.HullPIC.info
volker.bertram@dnvgl.com